THÈSE PRÉPARÉE ET PRÉSENTÉE EN COTUTELLE INTERNATIONALE À

**L'UNIVERSITÉ DE PAU ET DES PAYS DE L'ADOUR (UPPA)**

**ET**

**UNIVERSIDAD DEL PAÍS VASCO/EUSKAL HERRIKO UNIBERTSITATEA (UPV-EHU)**

Pour obtenir le grade de

**DOCTEUR**

SPÉCIALITÉ : Chimie analytique

**Par Nagore GRIJALBA MARIJUAN**

# WINE COUNTERFEITING: DEVELOPMENT OF FAST, NON-DESTRUCTIVE AND MULTIFACTORIAL LASER-BASED SPECTROCHEMICAL METHODS FOR AUTHENTICATION OF BOTTLED WINE

Soutenue prevue le 8 Novembre 2017

MEMBRES DU JURY

***RAPPORTEURS***

| | |
|---|---|
| V. Kanický | Professeur (Université de Masaryk, République Tchèque) |
| P. Simon | Directeur de Recherche (CEMHTI-CNRS UPR3079, France) |

***EXAMINATEURS***

| | |
|---|---|
| O. Donard | Directeur de Recherche (UMR 5254 CNRS-UPPA, France) |
| B. Fernández | Ingénieur de Recherche (Universidad de Oviedo, Espagne) |
| M. Maguregui | Maître de Conférence (Université du Pays Basque, Espagne) |
| F. Claverie | Ingénieur de Recherche (UMR 5254 CNRS-UPPA, France) |

***DIRECTEURS***

| | |
|---|---|
| C. Pécheyran | Ingénieur de Recherche (UMR 5254 CNRS-UPPA, France) |
| N. Unceta | Maître de Conférence (Université du Pays Basque, Espagne) |

***INVITÉS***

| | |
|---|---|
| B. Medina | Consultant et Conseiller scientifique (SECF, France) |
| R. Barrio | Professeur (Université du Pays Basque, Espagne) |

# Wine Counterfeiting:

# Development of fast, non-destructive and multifactorial laser-based spectrochemical methods for authentication of bottled wine

This Doctoral Thesis has been carried out in the Department of Analytical Chemistry at the University of the Basque Country, UPV/EHU (Faculty of Pharmacy, Vitoria-Gasteiz, Spain)

and

The *Laboratoire de Chimie Analytique, Bio-inorganique et Environnement* of the *Université de Pau et des Pays de l'Adour* (IPREM-LCABIE UMR 5254 CNRS-UPPA, Pau, France)

NAGORE GRIJALBA MARIJUAN
November 2017

(c)2017 NAGORE GRIJABA MARIJUAN

*"Science and everyday life cannot and should not be separated"*

Rosalind Franklin

*"Don' be afraid of hard work. Nothing worthwhile comes easily. Do not let others discourage or tell you that you cannot do it. In my day, I was told women did not go into chemistry. I saw no reason why we couln't"*

Gertrude Elion

*"After you see something works, then you realize that it's not so complicated after all."*

J. Franklin Hyde

**Acknowledgments**

*Nire gurasoei*

*eta denboraldi honetan nire bizitzaren parte izan diren guztiei*

A heartfelt thanks to all the persons I have met throughout this pleasant period of my life and who have conveyed me the felling that in all reaches of the earth there are people who deserve to be known. I would like not to do particular mentions, it would be remiss of me if I forgot some of you. Thus, include yourself, you are of course in my list.

Gracias Eskerrik asko Gràcies Merci Grazie Obrigada Dziękuję

## Acknowledgments

**Acknowledgments**

First, I would like to thank the University of the Basque Country (UPV/EHU) for the predoctoral fellowship which enabled the development of this co-supervised thesis between the Department of Analytical Chemistry (Faculty of Pharmacy) and the Laboratoire de Chimie Analytique, Bio-Inorganique et Environnement (LCABIE-IPREM) of the Université de Pau et des Pays de l'Adour.

I would like to thank Ramón Barrio and Arantxa Goicolea for giving me the chance to be part of their research group since many years ago and for all their encouraging words during this period. Similarly, I would also want to thank Olivier Donard and then Ryszard Lobinski, who accepted me for two years in the *Institute des Sciences Analytiques et Physico-Chimiques pour l'Environnment et les Matériaux* (IPREM).

My sincere thanks to my supervisors for accompanying me in this endeavor. On the one hand, Nora Unceta for introducing me in the research and of course, for all the time dedicated to this project, her advices and her meticulous corrections. On the other hand, Christophe Pécheyran since without him none of this would have been possible. Thanks for teaching me the "art" of laser ablation, your support and transmitting me all your knowledge, I hope to have proven to be worthy of it.

But my thanks, of course, also go to Bernard Médina who has followed my work over these years and has offered me the opportunity to present it at international conferences, as well as for helping me joining forces with other groups and enterprises in this area. It has been a real pleasure to be able to count on him for his support and expert advice.

Finally, I would also like to thank the evaluators for agreeing to judge my work: Viktor Kanický and Patrick Simon. Equally, thanks to members of the jury: Olivier Donard, Fanny Claverie, Maite Maguregui and Beatriz Fernández. I am honoured and privileged to have you in such important day that marks the end and the beginning of one stage of my life.

Sincerely, thanks to all of you for making this work possible.

## Acknowledgments

# TABLE OF CONTENTS

List of figures…… I

List of tables……..…XI

List of acronyms……..…XV

Summary, Résumé, Resumen……XIX

**Chapter 1. Wine authentication methods – A review 1**

**1. The origin of the *wine culture*……..3**

**2. Wine adulteration and frauds: historical examples…….6**

**3. Wine fraud financial impact on figures and actions taken……..7**

*Current situation of Spanish wine sector*…….……9

*Current situation of French wine sector*……11

**4. Wine authentication methods.....15**

4.1 Invasive verification methods…….....17

4.1.1 Mass spectrometry for elemental analysis……17

4.1.2 Mass spectrometry for molecular analysis……..……...19

4.1.3 Spectroscopy…….……20

4.1.3.1 Nuclear Magnetic Resonance (NMR)……..20

4.1.3.2 Molecular spectroscopic techniques…….……21

4.1.4 Other…….…21

4.1.4.1 Sensory analysis……...……21

4.1.4.2 DNA analysis…….…22

4.2 Quasi non-invasive verification methods…….……..22

4.2.1 Wine analysis through the packaging……...……..23

4.2.1.1 Radioactivity…….....23

4.2.1.2 Molecular spectroscopic techniques……...…….23

4.2.1.3 Nuclear Magnetic Resonance (NMR)…….…….24

4.2.1.4 Other……...…..…24

4.2.2 Packaging analysis……..……24

4.2.2.1 How the glass could help in wine authentication?.....26

4.2.2.2 How the paper and the ink could help in wine authentication?.....26

4.2.2.3 How the capsule could help in wine authentication?.....27

**5. Chemometrics in analytical chemistry…….....28**

**6. Conclusions and future trends……30**

**7. Bibliography……..……..31**

**Chapter 2. Objectives, Objectifs, Objetivos 43**

**Chapter 3. Instrumentation 57**

**1. Laser ablation coupled to inductively coupled plasma mass spectrometry (LA-ICPMS) for the analysis of trace elements in solid samples……...59**

1.1 Inductively Coupled Plasma Mass Spectrometry (ICPMS)……..….59

1.1.1 Basic concepts of Inductively Coupled Plasma Mass Spectrometry (ICPMS).59

1.1.2 ICPMS process description…….....60

1.1.2.1 Sample introduction system……...……61

1.1.2.2 Ionization source and sample ionization……..……..62

1.1.2.3 Interface…….62

1.1.2.4 Quadrupole mass filter……..…..63

1.1.2.5 Ion detector……63

1.1.3 Advantages and limitations of ICPMS…….……64

1.1.4 Spectral and non-spectral interferences in ICPMS……..65

1.2 Laser ablation…….68

1.2.1 Basic concepts of laser ablation……...….68

1.2.2 Laser ablation: an alternative to liquid sample introduction and microchemistry……...……..69

1.2.3 Laser technology and laser ablation systems……...….70

1.2.4 Limitations and drawbacks of LA-ICPMS…….…77

1.2.5 Femtosecond laser ablation system used in this work: ALFAMET……79

1.2.5.1 Industrial design and creation…….79

1.2.5.2 Technical characteristics……...…..80

1.2.5.3 System components…….81

1.2.6 Applications of LA-ICPMS…….84

1.2.6.1 Biology and environment……...…….84

1.2.6.2 Health and medicine……....84

1.2.6.3 Geochemistry…….……85

1.2.6.4 Forensic science……..85

1.2.6.5 Archaeology……..……..85

1.2.6.6 Material science.....85

**Table of contents**

**2. Optical spectroscopy……...……86**

2.1 Scattering spectroscopy: Raman spectroscopy……..87

2.1.1 Basic concepts of Raman spectroscopy…….87

2.1.2 Raman spectroscopy technology……...……89

2.1.3 Raman spectroscopy system……..91

2.1.3.1 Excitation source……..……91

2.1.3.2 Sample illumination and light collection optics…….……..92

2.1.3.3 Wavelength selector…….….92

2.1.3.4 Detection and computer control/processing system……....93

2.1.4 Applications…….…..94

2.1.4.1 Pharmaceutical industry……...94

2.1.4.2 Bioscience and medical diagnosis……...…….94

2.1.4.3 Food and agricultural industries…….……..94

2.1.4.4 Environmental applications……..95

2.1.4.5 Forensic science……95

2.2 Absorption spectroscopy: Infrared spectroscopy……...……97

2.2.1 Basic concepts of Infrared spectroscopy…….……..97

2.2.2 Infrared spectroscopy technology……...……100

2.2.3 Infrared spectroscopy system…….….101

2.2.3.1 Source of Infrared emission……...…..102

2.2.3.2 Interferometer…….……..102

2.2.3.3 Detector and signal processor……..104

2.2.4 Applications……...……..104

2.2.4.1 Biological applications…….……104

2.2.4.2 Disease diagnosis…….……104

2.2.4.3 Clinical chemistry……...……105

2.2.4.4 Pharmaceutical industry……...….105

2.2.4.5 Food and agricultural industries……...…105

2.2.4.6 Environmental applications……..……106

2.2.4.7 Forensic science……...……106

**3. Bibliography……107**

**REVIEW: Laser bidezko ablazioaren gaur egungo egoera eta aplikazioak……..……121**

(State-of-the-art of laser ablation and its applications)

**Chapter 4. Development of a new ablation cell adjustable to different bottle shapes 143**

**1. Ablation cells for laser ablation-inductively coupled plasma mass spectrometry…….145**

**2. Design and development of new ablation cell adjustable to different bottle shapes….153**

2.1 1st design……..…154

2.2 2nd design……...……..157

2.3 3rd design: final design……158

**3. Bibliography……..…161**

**Chapter 5. Analysis of packaging for wine authentication – Part 1: Elemental analysis of glass by femtosecond laser ablation coupled to ICPMS 165**

**General introduction: what is glass?.....167**

**1. Introduction……...……..172**

**2. Material and methods…….……174**

2.1 Description of the sample set……...……174

2.2 Instrumentation…….……175

2.3 Ablation parameters and data acquisition…….……176

2.4 Minimally invasive analysis……..178

2.5 Data pre-processing…….……...178

**3. Results and discussion……...……..181**

3.1 Optimization of the ablation strategy……181

3.2 Analytical performance of the fsLA-ICPMS method……..….181

3.2.1 Long-term reproducibility……..…….181

3.2.2 In-day repeatability……...……..182

3.2.3 Homogeneity……..…….183

3.2.4 Linearity……..184

3.2.5 Limits of detection……...……...184

3.3 Casework glass sample set……185

3.3.1 Casework 1: genuine vs. counterfeited bottles……....187

3.3.2 Casework 2: collection of a bottles series from the same wine cellar…….190

3.3.3 Casework 3: collection of worldwide bottles.....210

3.3.3.1 Classification of green wine bottles……..211

*Worldwide green bottles*……....211

*European green bottles*……..214

3.3.3.2 Classification of transparent wine bottles……..215

**4. Conclusions……..217**

**5. Bibliography……..…220**

**Chapter 6. Analysis of packaging for wine authentication – Part 2.1: Elemental analysis of label paper and ink by femtosecond laser ablation coupled to ICPMS 227**

**General introduction: what are paper and ink?.....229**

**1. Introduction……237**

**2. Materials and methods……239**

2.1 Description of the sample set……239

2.2 Instrumentation……240

2.3 Ablation parameters and data acquisition……241

2.4 Data pre-processing……243

2.5 Synthesis of matrix-matched standards……243

**3. Results and discussion……246**

3.1 Optimization of the ablation strategy……246

3.2 Development of homemade matrix-matched standards for ink quantification……251

3.2.1 Synthesis process of homemade matrix-matched standard……251

3.2.2 Quality assessment of homemade matrix-matched standards: imaging of paper edge……257

3.2.3 Quantification of label paper and label printed ink……260

3.3 Analytical performance of the fsLA-ICPMS method……262

3.3.1 Long-term reproducibility……262

3.3.2 In-day repeatability……264

3.3.3 Homogeneity……264

3.3.4 Spectral interferences……265

3.4 Minimally invasive analysis……266

3.5 Casework paper and ink sample set……267

3.5.1 Casework 1: genuine vs. counterfeited bottles……267

*Label matrix*……267

*Black ink*……269

3.5.2 Casework 2: collection of a bottle series for the same wine cellar……272

*Label matrix*……272

*Black ink*……274

*Red ink*……277

3.5.3 Casework 3: collection of worldwide bottles……279

*Label matrix*……279

*Black ink*……283

**4. Conclusions……285**

**5. Bibliography……289**

**Chapter 7. Analysis of packaging for wine authentication – Part 2.2: Molecular analysis of paper and ink by Raman and Infrared spectroscopy 297**

**1. Introduction……299**

**2. Materials and methods……300**

2.1 Description of the sample set……...300

2.2 Instrumentation and methods……...…301

**3. Results and discussion……302**

3.1 Casework 1: *in situ* and non-destructive analysis of genuine and counterfeited bottles……302

3.1.1 Analysis of label matrix……..…303

*Peer 1: S205 (France) vs. S206 (China)*……..….303

*Peer 2: S207 (France) vs. S208 (China)*……....307

*Peer 3: S209 (France) vs. S210 (France)*……..309

*Peer 4: S211 (France) vs. S212 (China)*……..309

3.1.2 Analysis of ink matrix……312

*Red ink*……312

*Black ink*……313

3.2 Casework 2: *in situ* and non-destructive analysis of a bottle series from the same winery ……...316

3.2.1 Analysis of label matrix……....316

3.2.2 Analysis of ink matrix……...…318

*Red ink*……318

**4. Conclusions……322**

**5. Bibliography……324**

**Chapter 8. General conclusions and perspectives 329**

**Annexes 349**

**Annex I. Preliminary analysis of capsules for wine authentication……349**

**Annex II. Scientific achievements……...363**

**Annex III. Supplementary information……375**

## LIST OF FIGURES

### Chapter 1. Introduction

**Figure 1:** Vintage and wine making scene depicted on the walls of the tomb of Nachkt, 1550-1295 BC……..4

**Figure 2:** Vine and wine production expansion through centuries. Adapted from Coralie Martin's doctoral thesis……..5

**Figure 3:** Area under vines according to continent/country and year (Source: OIV, 2017)…….8

**Figure 4:** Area under vines in Spain……..9

**Figure 5**: French wine production from 2000-2012 (Source: OIV, 2016)……..…11

**Figure 6:** Area under vines in France……..12

**Figure 7:** Scope of counterfeiting (Source: CNAOC)……13

**Figure 8:** Inductively Coupled Plasma based mass spectrometry technique for trace element and isotope analysis in wine**.** The sample is atomised in a high-temperature argon plasma and the elemental ions are detected based on their mass-to-charge ratios (m/z). This analytical technique can be coupled to chromatographic separation techniques depending on the nature of the analyte and the target of the analysis……18

**Figure 9:** Chromatography coupled to mass spectrometry techniques for molecular analysis in wine. Firstly, analytes are separated in the chromatographic column. After, they are ionized in the interface and finally, detected according to m/z ratio……20

**Figure 10:** Common workflow in analytical chemistry studies……..28

**Figure 11:** PCA compresses the information given in a data matrix into uncorrelated PC and projects it down on different dimensions……29

## Chapter 3. Instrumentation

**Figure 1:** Approximate detection capabilities of the ICPMS (Source: PerkinElmer, Inc.)…..…60

**Figure 2:** Inductively Coupled Plasma Mass Spectrometer diagram……..60

**Figure 3:** Principles of sample introduction in ICPMS……...61

**Figure 4:** Nebulization process scheme (pneumatic concentric nebulizer)……61

**Figure 5:** Sample ionization process……...……62

**Figure 6:** Quadrupole mass filter scheme……....63

**Figure 7:** Discrete dynode detector operating scheme……64

**Figure 8:** Laser ablation (LA) sample introduction system coupled to ICPMS…….69

**Figure 9:** Setup of a simple laser cavity composed by highly reflecting curve mirror, the gain medium and a partially transmissive flat mirror.……..71

**Figure 10:** CPA process in ultra-short laser systems……...…73

**Figure 11:** Laser-matter interactions in both long and ultra-short pulse lasers (Clark-MXR, Inc.). Images show fs- and ns- ablation of polished brass. The ablation crater produced by the nanosecond laser shows a clear melting ring whereas femtosecond laser produced crater is neat and clean……...73

**Figure 12:** Laser induced aerosol behavior according to particle size. Adapted from Horn et al (49)...……...75

**Figure 13:** Evolution of tested laser ablation systems for LA-ICPMS between 1985 and 2015. Adapted from (47) and (56)……..76

**Figure 14:** Elemental and isotopic fractionation sources during LA-ICPMS measurements….78

**Figure 15:** Front and back views of ALFAMET laser ablation device……...80

**Figure 16:** ALFAMET laser optics…….81

**Figure 17:** Schematic representation of the galvanometric scanner……82

**Figure 18:** Light-matter interaction types in Optical Spectroscopy……86

**Figure 19:** The different possibilities of light scattering in Raman spectroscopy: Rayleigh scattering (no exchange of energy: incident and scattered photons have the same energy), Stokes Raman scattering (atom or molecule absorbs energy: scattered photon has less energy than the incident photon) and anti-Stokes Raman scattering (atom or molecule loses energy: scattered photon has more energy than the incident photon)……..……88

**Figure 20**: Types of Molecular Vibration……98

**Figure 21:** Infrared Spectroscopy reflection methods……...100

**Figure 22:** A schematic representation of an interferometer used in FT-IR spectrometers..…103

**REVIEW: Laser bidezko ablazioaren egungo egoera eta aplikazioak**
(State-of-the-art of laser ablation and its applications)

**1. irudia:** Akoplamendu induktibozko plasma-masa espektrometroari loturiko laser bidezko ablazioaren (LA-ICPMS) eskema……..122

**2. irudia:** Laser-materia interakzioa a) nanosegundo laser bidezko ablazioan eta b) femtosegundo laser bidezko ablazioan (Clark-MXR, Inc.-ren baimenarekin erabilitako irudiak).....126

**3. irudia:** Aingira (*Anguilla anguilla, L.*) otolitoen kokalekua eta bizi-zikloa……..128

**4. irudia:** Aingira (*Anguilla anguilla, L.*, Adour ibaia, Frantzia) otolito baten gainazalean egindako ablazio zuzena fsLA-ICPMS bidez eta lortutako seinaleak: Sr:Ca (marra beltza, ur gazian igarotako aldia) eta Ba:Ca (marra grisa, ur gezan igarotako aldia) ratioen eboluzio jarraiak aingira nomada batek izandako migrazioa erakusten du……...128

**5. irudia:** Bizkar-hegatsaren lehenengo hezurraren kokalekua eta zeharkako ebakiduraren argazkia……...129

**6. irudia:** LA-ICP-MS bidez mapping-a egiteko jarraitu beharreko prozedura……130

**7. irudia:** Petrolioaren ablazioaren eskema Ricard eta lankideek diseinatutako ablazio gelaxkan [65]……131

**8. irudia:** Laser izpiak tiro-aztarnaren gain eragin eta materia erauzten du. Ondoren, ICPMS detektagailuan denborarekin aldakorra den seinalearen erregistroa lortzen da. Sb, Ba eta Pb elementuen seinaleen aldi bereko erregistroak partikula tiro-aztarna bati dagokiola baieztatzen du……133

**9. irudia:** Uranioaren konposizio isotopikoa erabileraren arabera……134

**Chapter 4. Development of a new ablation cell adjustable to different bottle shapes**

**Figure 1:** Design of an ablation cell: factors to take into account ……...…….146

**Figure 2:** Schema of two volume closed cell. Adapted from Müller et al (20)…….....148

**Figure 3:** Sketch of the experimental setup for the direct atmospheric sampling for LA-ICPMS. The sample is place in a holder under ambient conditions. A transport tube, which is directly placed as closed as possible to the sample surface, is connected to the diaphragm pump. During laser ablation, the laser-induced aerosol is sucked into the system and carried to the gas exchange device and further to the ICPMS by the pump……...…151

**Figure 4:** Assembled portable laser ablation sample device (A) and details of the LA module (B). Figure extracted from Glaus et al……152

**Figure 5:** Prototype of the ablation cell adjustable to bottle shape……...…153

**Figure 6:** Upper, bottom, lateral and cross sections of the new ablation cell……154

**Figure 7:** Poly (lactic acid) polymer chain……....…155

**Figure 8:** 1st design of the ablation cell: 1) upper, 2) bottom and 3) lateral views……155

**Figure 9:** Laser beam focusing and effective working distance in air……...…156

**Figure 10:** Metallic holder for bottles……157

**Figure 11:** 2nd design of the ablation cell: 1) upper, 2) bottom and 3) lateral views……..…157

**Figure 12:** Final design of the ablation cell and its inclusion on the laser ablation system..…159

## Chapter 5. Analysis of packaging for wine authentication – Part 1: Elemental analysis of glass by femtosecond laser ablation coupled to ICPMS

**Figure 1:** The blow and blow process employed in the manufacturing process of glass bottles. Molten 'gobs' of glass are delivered into a blank mould. A puff of compressed air blows the glass down into the base of the mould to form the neck of the bottle. This is after transferred to a second mould in which the bottle is blown to its final form……..168

**Figure 2:** Histograms showing the distribution of refractive index values for flat glasses from FBI for the periods of a) 1964 to 1979 and b) 1980 to 1997…….170

**Figure 3:** Scheme for the forensic analysis of glass and current main analytical techniques for its elemental analysis……..171

**Figure 4:** A typical laser ablation signal for selected isotopes for a bottle glass analysis……178

**Figure 5:** Line ablation strategy on glass surface (500 x 100 µm) which is almost invisible to naked eye……....178

**Figure 6:** Construction of calibration curves by ablating CRM NIST 612 and 610…….180

**Figure 7:** Biplot (PC1 vs PC2) representing French original bottles (in blue) and Chinese counterfeited bottles (in green) with the loadings (variables) responsible of such discrimination…….188

**Figure 8:** Clustering of original French bottles (in blue) and counterfeited Chinese bottles (in green). Dendrogram showing dissimilarity (Euclidian distance) and Ward agglomeration method……189

**Figure 9:** PCA (PC1 vs. PC2) for the 34 samples coming from the same winery but different vintage……...…….191

**Figure 10:** Distribution of the selected variables in PC1 and PC2. A, B, C and D (in blue) indicate the quadrants for a better comprehension of the variables having influence in each sample group……..192

**Figure 11:** Individual charts for each isotope and vintage. Lineal tendency line shows how elemental ratios change in function of production time…….195

**Figure 12**: Change of the intensity of green color from the ancient bottles (light green) to newest bottles (dark green)…….....193

**Figure 13:** PCA (PC1 vs PC2) and loadings of the transparent and green bottles……210

**Figure 14:** Biplot (PC1 vs. PC2) representing Asian (in blue), European (in green) and American (in pink) bottles with the loadings (variables) responsible of such discrimination…….212

**Figure 15:** Cooman's plot obtained from SIMCA modelling with its corresponding classification table……..……213

**Figure 16:** Discrimination power of each variable used in the SIMCA modelling……...…213

**Figure 17:** Biplot (PC1 vs. PC2) representing European green bottles and the corresponding loadings……...…214

**Figure 18:** A) PCA (PC1 vs. PC2) of the European transparent bottles and B) corresponding loadings for distinguishable each group (Portugal/Spain vs. France)……...….216

**Chapter 6. Analysis of packaging for wine authentication – Part 2.1: Elemental analysis of label matrix and ink by femtosecond laser ablation coupled to ICPMS**

**Figure 1:** Overview of the papermaking process……...…230

**Figure 2:** Analysis methods for paper and printed ink……..…232

**Figure 3:** A typical laser ablation signal for selected isotopes for paper and ink analysis……243

**Figure 4:** Different cases of paper and ink ablation depending on the spot density……..246

**Figure 5:** Optimization of the OSD value for the matrix ablation of paper and ink…….247

**Figure 6:** Gradually increased number of pulses per spot and consequent paper piercing…...247

**Figure 7:** Ablation profile of 30 OSD and 5 pulses per sport matrix (4 replicates)……..…248

**Figure 8:** Depth of ablated matrix (500 x 500 µm, 30 OSD) as a function the number of pulses per spot……...249

**Figure 9:** Images of optical microscopy (x40) of paper edges showing the absorption of the ink when different types of glossy papers have been used……...…249

**Figure 10:** Number of pulses per spots versus the signal intensity of Cu63 (cps) when different types of papers have been employed for printing (office paper and 5 glossy papers)……...250

**Figure 11:** Deposition of 5µL of blue and black ink on A) Whatman filter paper (0.1 µm, 47 mm Ø) from Durapore ® and B) common office paper (2500xDIN A4, 210x297 mm, 109 ± 3 µm thickness, 80 g/m$^2$) from InapaTecno……...…252

**Figure 12:** Proportionality of ink deposition at each printout……...253

**Figure 13:** Printing homogeneity test on common office paper (2500xDIN A4, 210x297 mm, 109 ± 3 µm thickness, 80 g/m$^2$) from InapaTecno with transparency of 0%, 50%, 80%, 90%, 95% and 98%. Magenta color was used for this test……..254

**Figure 14:** Printed spot distribution and frequency for the transparencies of 90%, 95% and 98%.....255

**Figure 15:** Solution printing strategy based on the RGB color model……..256

**Figure 16:** Image plots of paper edge for several isotopes in standards 1 and 3 with color scale of cps……...…258

**Figure 17:** Scheme of suggested hypothesis for solution surface deposition based on subsequent tidelines formation and cellulose degradation……....259

**Figure 18:** Developed calibration model for ink quantification……261

**Figure 19:** Typical examples of obtained calibration curves for light, middle and heavy isotopes……...…262

**Figure 20:** Ablation matrix (500 x 500 µm) on A) label matrix and B) black ink……266

**Figure 21:** Biplot (PC1 vs PC2) representing French original bottles (in blue) and Chinese counterfeited bottles (in green) with the loadings (variables) responsible of such discrimination (label paper)……268

**Figure 22:** Clustering of original French bottles (in blue) and counterfeited Chinese bottles (in green). Dendrogram showing dissimilarity (Euclidian distance) and Ward agglomeration method (label paper)……...……269

**Figure 23:** Biplot (PC1 vs PC2) representing French original bottles (in blue) and Chinese counterfeited bottles (in green) with the loadings (variables) responsible of such discrimination (black ink)……...……270

**Figure 24:** Clustering of genuine French bottles (in blue) and counterfeited Chinese bottles (in green). Dendrogram showing dissimilarity (Euclidian distance) and Ward agglomeration method (black ink)……..271

**Figure 25:** PCA (PC1 vs. PC2) for the 34 samples coming from the same winery but different vintage (label paper)……...273

**Figure 26:** Distribution of the selected variables in PC1 and PC2 for samples of same winery but different vintage (label paper)……..274

**Figure 27:** PCA (PC1 vs. PC2) for the 34 samples coming from the same winery but different vintage (black ink)……..275

**Figure 28:** Distribution of the selected variables in PC1 and PC2 for samples of same winery but different vintage (black ink)…….276

**Figure 29:** PCA (PC1 vs. PC2) for the 34 samples coming from the same winery but different vintage (red ink)……..…277

**Figure 30**: Distribution of the selected variables in PC1 and PC2 for samples of same winery but different vintage (red ink)……..…278

**Figure 31:** PCA (PC1 vs. PC2) for the European, American and Asian bottles (label paper)..280

**Figure 32:** Distribution of the selected variables in PC1 and PC2 for label paper of worldwide bottles…….281

**Figure 33:** Cooman's plot obtained from SIMCA modelling with its corresponding classification table……..282

**Figure 34:** PCA (PC1 vs. PC2) for the European, American and Asian bottles (black ink)….283

**Figure 35:** Distribution of the selected variables in PC1 and PC2 for black ink of worldwide bottles……...…..284

**Chapter 7. Analysis of packaging for wine authentication – Part 2.2: Molecular analysis of paper and ink by Raman spectroscopy and Infrared spectroscopy**

**Figure 1:** Analyzed matrix: A) label matrix, B) red ink and C) black ink observed with the long-distance lens of x50 (Renishaw RA100 spectrometer, Gloucestershire, UK)……...303

**Figure 2:** Raman spectra of sample S205 (red) and S206 (blue) label. PP = Polypropylene, C = Calcite and R =Rutile…….304

**Figure 3:** DRIFT spectra of sample S205 (red) and S206 (blue) label. C=O = Carbonyl, C = Calcite, PP = Polypropylene and C-Halide = Carbon-halide bond vibration. The bands not market in the DRIFT spectra are assigned to PP……305

**Figure 4:** Raman spectra of sample S207 (red) and S208 (blue) label. PP = Polypropylene, C = Calcite and R = Rutile……307

**Figure 5** DRIFT spectra of sample S207 (red) and S208 (blue) label. PP = Polypropylene, C = Calcite, aromatic C=C stretching (C=C), C-O bands and C-Halide band. The bands not market in the DRIFT spectra are assigned to PP. At the top of the Figure a zoom of the 1850-1650 $cm^{-1}$ area showing the position of calcite band at 1796 $cm^{-1}$ and C=O bands (1735 $cm^{-1}$ for S207 label and 1750 and 1720 $cm^{-1}$) are observable……308

**Figure 6:** Raman spectra of the label for pair S209 (red)-S210 (blue). PP = Polypropylene and C = Calcite. Bands not marked in the spectra are assigned to PP…….…….309

**Figure 7** DRIFT spectra of sample S209 (red) and S210 (blue) label. C=O = Carbonyl, C = Calcite, PP = Polypropylene.The bands not market in the DRIFT spectra are assigned to PP..309

**Figure 8:** Raman spectra of the label for pair S211 (red) -S212 (blue). PS = Polystyrene, C = Calcite and R = Rutile……310

**Figure 9:** DRIFT spectra of sample S211 (red) and S212 (blue) label. C=O = Carbonyl, C = Calcite, PS = Polystyrene, K = Kaolinite……...311

**Figure 10:** Raman spectrum of red pigment of bottle S209. PP = Polypropylene, C = Calcite, R = Rutile, Ri = Red ink……312

**Figure 11:** Representative Raman spectrum acquired on the black pigment of bottle S211 (red) and Raman spectrum of Cu phthalocyanine blue pigment standard (blue)……...314

**Figure 12:** Representative Raman spectrum acquired on black pigment of bottle S210 (red) and Raman spectrum of ultramarine blue pigment standard (blue)……..…315

**Figure 13:** Raman spectra of label of vintages 1969 in blue (oxidized cellulose), 1974 in red (partially oxidized cellulose) and 1998 in green (non-oxidized cellulose)……317

**Figure 14:** Representative Raman spectrum of calcium carbonate (C) filled polystyrene (PS) label of the 2009 vintage……...…318

**Figure 15:** Representative Raman spectra of red inks from groups 1 (sample 1969), 2 (sample 1993) and 3 (sample 2004)…….…319

**Figure 16:** Representative Raman spectra of red ink from group 4 (2010 vintage)……..….321

## LIST OF TABLES

### Chapter 1. Introduction

**Table 1** Analytical techniques used for wine verification. Adapted table from Luykx et al. Favorable (+), moderate (+/-) and unfavorable (-)……...17

### Chapter 3. Instrumentation

**Table 1**: Figure of merits for ICPMS……...65

**Table 2**: Some common Plasma/Matrix/Solvent-Related polyatomic spectral interferences in ICPMS ……66

**Table 3**: Performance comparison of ICPMS and LA-ICPMS**.** Adapted from Becker et al (30)……...70

**Table 4:** Key developments in the history of laser ablation systems for LA-ICPMS. Adapted from Sylvester et al……...72

**Table 5**: Comparison of analytical performances of ns-LA and fs-LA systems for LA-ICPMS measurements……...75

**Table 6:** Technical characteristic of ALFAMET ablation system……...81

**Table 7:** Schematic representation of the galvanometric scanner……...…83

**Table 8:** Common laser sources in Raman spectroscopy……92

**Table 9:** Infrared Spectral Ranges……...…97

**Table 10:** FT-IR sources……102

**REVIEW: Laser bidezko ablazioaren egungo egoera eta aplikazioak**

(State-of-the-art of laser ablation and its applications)

**1. taula:**. ICPMS eta LA-ICPMS tekniken konparazioa……...…124

**2. taula:** Lagin solidoen analisirako teknika desberdinen konparaketa……..…125

## Chapter 4. Development of a new ablation cell adjustable to different bottle shapes

**Table 1:** Closed laser ablation cells and aerosol transport characteristic simulations in the literature……...…147

**Table 2:** Open laser ablation cells in the literature and their main characteristics……149

**Table 3:** Open and non-contact ablation cells in the literature and their main characteristics..149

**Table 4**: Comparison of the performance of conventional and laboratory designed cells……160

## Chapter 5. Analysis of packaging for wine authentication – Part 1: Elemental analysis of glass by femtosecond laser ablation coupled to ICPMS

**Table 1:** Main components of glass according to their principal manufacturing function……167

**Table 2:** Batches of bottles analyzed in this work……174

**Table 3:** Distribution of 3rd batch of bottles according to their origin (continent) and color…174

**Table 4:** Operating conditions of fsLA-ICPMS system for glass analysis……177

**Table 5:** Final isotopes list and reproducibility of the Element/Si ratio in a reference bottle (n = 9 sessions) during 3 years……..….182

**Table 6:** Reproducibility of selected isotopes within a single bottle (n = 3 bottles, 30 replicates per bottle) and within a lot of bottles belonging to a same winery and vintage (n = 20 bottles, 3 replicates per bottle)….....183

**Table 7:** Limits of Detections for the selected isotopes calculated by the 3σ criterion…….185

**Table 8**: Proximity matrix (Euclidian distance) of the original French bottles (in blue) and counterfeited Chinese bottles (in green)…….190

## Chapter 6. Analysis of packaging for wine authentication – Part 2.1: Elemental analysis of label matrix and ink by femtosecond laser ablation coupled to ICPMS

**Table 1:** Experimental conditions of main applications of LA-ICPMS to the analysis of paper……...233

**Table 2:** Experimental conditions of main applications of LA-ICPMS to the analysis of ink……...236

**Table 3:** Batches of bottles analyzed in this work……..…239

**Table 4:** Distribution of 3rd batch of bottles according to their origin (continent/country)…...240

**Table 5:** Operating conditions of fsLA-ICPMS system for paper and ink analysis……..242

**Table 6:** Operating conditions for the microwave digestor……...244

**Table 7:** Operating condition for ICPMS instrument……...245

**Table 8:** Final elemental list and reproducibility of each isotope measured in a reference bottle (n=9 sessions) during 3 years……..…263

**Table 9:** Reproducibility of selected isotopes within a single bottle (n=3 bottles, 15 replicates per bottle) and within a batch of bottles belonging to the same winery and vintage (n=20 bottles, 3 replicates per bottle)……265

**Table 10:** Potential spectral interferences due to the composition of paper matrix……..266

## Chapter 7. Analysis of packaging for wine authentication – Part 2.2: Molecular analysis of paper and ink by Raman spectroscopy and Infrared spectroscopy

**Table 1:** Peer-correlated samples used in this work……..303

**Table 2:** Raman bands of polypropylene identified in the Raman spectra of sample S205 and S206……...…….304

**Table 3:** IR bands of polypropylene identified in the DRIFT Raman spectra of sample S205 and S206…….....305

**Table 4:** Average areas of carbonyl band normalized against PP band for S205, S206, S207 and S208 samples……..…305

**Table 5:** Chemical structure of the BON red mono-azo lake pigment PR57:1 and the identified Raman bands…….....313

**Table 6:** Chemical structure of the Cu phthalocyanine pigment PB15 and the identified Raman bands …….….314

**Table 7:** Chemical structure of the ultramarine blue pigment PB29 and the identified Raman bands……...316

**Table 8:** Raman bands of the cellulose identified in the spectra acquired for the sample 1998. Bands have been assigned according to the work carried out by Willey and Atalla……..…317

**Table 9:** Chemical structure of the Napthol AS pigment PR112 and the identified Raman bands……...319

**Table 10:** Chemical structure of the B-Napthol lake red pigment PR53:1 and the identifed Raman bands……..320

## LIST OF ACRONYMS

| | |
|---|---|
| **IPR** | Intellectual Property Right |
| **DOP** | Denominación de Origen Protegida<br>(Protected Designation of Origin) |
| **DO** | Denominación de Origen<br>(Designation of Origin) |
| **DOCa** | Denominación de Origen Calificada<br>(Designation of Qualified Origin) |
| **BOE** | Boletín Oficial del Estado<br>(Official State Gazette) |
| **GDP** | Gross Domestic Product |
| **FranceAgriMer** | Establissement National des Produits de l'Agriculture et de la Mer<br>(National Establishment of Agricultural and Marine Products) |
| **VQPRD** | Vins de Qualité Produits dans des Regions Determines<br>(Quality Wines Produce in Determined Regions) |
| **AOC** | Appellation d'Origine Controllée<br>(Controlled Designation of Origin) |
| **AO-VDQS** | Appellation d'Origine-Vin de Qualité Supérieure<br>(Designation of Origin-Superior Quality Wine) |
| **INAO** | Institut National des Appelations d'Origine<br>(French Institute for Appellation of Origin) |
| **IGP** | Indication Géographique Protegée<br>(Protected Geographical Indication) |
| **AOP** | Appellation d'Origine Protegée<br>(Protected Designation of Origin) |
| **CNCCEF** | Comité National des Conseillers du Commerce Extérieur de la France<br>(French Foreign Trade Advisors) |
| **GI** | Geographical Indication |
| **WTO** | World Trade Organization |
| **EUIPO** | European Union Intellectual Property Office |
| **OIV** | Organisation International de la Vigne et du Vin<br>(International Organization of Vine and Wine) |
| **EFOW** | European Federation of Origin Wines |
| **CNAOC** | Confédération Nationale des producteurs de vins et eaux de vie de vin à Appellations d'Origine Contrôlées<br>(National Confederation of Wine Producers and Wine Spirits with Controlled Appellations of Origin) |
| **FEDERDOC** | Confederazione Nazionale di Consorzi Volontari per la Tutela delle Denominazioni Italiane di Origine<br>(National Confederation of Volunteer Consorts for the Protection of Italian Wines) |
| **CECRV** | Conferencia Española de Consejos Reguladores Vitivinícolas<br>(Spanish Conference of Wine Regulatory Councils) |
| **IVDP** | Instituto dos Vinhos do Douro e Porto<br>(Douro and Porto Wines Institute) |
| **HNT** | Hegyközségek Nemzeti Tanácsa<br>(National Council of Wine) |
| **CMO** | Common Market Organization |
| **CAP** | Common Agricultural Policy |
| **ICP** | Inductively Coupled Plasma |
| **ICPMS** | Inductively Coupled Plasma Mass Spectrometry |
| **IRMS** | Isotope Ratio Mass Spectrometry |
| **GC-MS** | Gas Chromatography – Mass Spectromety |

| | |
|---|---|
| **HPLC-MS** | High Performance Liquid Chromatrography – Mass Spectrometry |
| **NMR** | Nuclear Magnetic Resonance |
| **PCR** | Polymerase Chain Reaction |
| **Q MS** | Single Quadrupole Mass Spectrometry |
| **TIMS** | Thermal Ionization Mass Spectrometry |
| **SFMS** | Sector Field Mass Spectrometry |
| **MCMS** | Multicollector Sector Field Mass Spectrometry |
| **m/z** | Mass-to-charge ratio |
| **LC-MS** | Liquid Chromatography – Mass Spectrometry |
| **ESI** | Electrospray Ionization |
| **APCI** | Atmospheric Pressure Chemical Ionization |
| **APPI** | Atmospheric Pressure Photoionization |
| **SACI** | Surface Activated Chemical Ionization |
| **MALDI** | Matrix Assisted Laser Desorption Ionization |
| **FTIR** | Fourier Transform Infrared Spectroscopy |
| **NIR** | Near Infrared |
| **IR** | Infrared |
| **ISO** | International Organization for Standardization |
| **SSR** | Simple Sequence Repeat |
| **SORS** | Offset Raman Spectroscopy |
| **PIXE** | Particle Induced X-ray Emission spectroscopy |
| **XRF** | X-ray Fluorescence |
| **LA** | Laser Ablation |
| **FEVE** | European Container Glass Federation |
| **TLC** | Thin Layer Chromatography |
| **PE** | Polyethylene |
| **PET** | Polyethlyne Terephthalate |
| **PVC** | Polyvinyl Chloride |
| **PCA** | Principal Component Analysis |
| **PC** | Principal Component |
| **AHC** | Agglomerative Hierarchical Clustering |
| **SIMCA** | Soft Independent Modelling of Class Analogy |
| **EDA** | Exploratory Data Analysis |
| **PLS** | Partial Least Squares |
| **ppt** | Parts Per Trillion |
| **LD** | Limit of Detection |
| **RF** | Radiofrequency |
| **DRC** | Dynamic Reaction Cell |
| **CEM** | Channel Electron Multiplier |
| **CRM** | Certified Reference Material |
| **LASER** | Ligth Amplification by the Stimulated Emission of Radiation |
| **Nd:YAG** | Neodymium-doped Yttrium Aluminum Garnet |
| **Yb-KGW** | Potassium Gadolinium tungsten doped Ytterbium-$KGd(WO_4)_2$ |
| **CPA** | Chirped Pulse Amplification |
| **ns** | Nanosecond |
| **fs** | Femtosecond |
| **UV** | Ultraviolet |
| **Vis** | Visible |
| **ALFAMET** | Ablation Laser Femtoseconde pour l'Analyse de Métaux Traces |
| **CDD** | Charge Coupled Device |
| **FT-Raman** | Fourier Transformed Raman spectroscopy |
| **RRS** | Resonance Raman Spectroscopy |
| **SERS** | Surface Enhanced Raman spectroscopy |
| **CARS** | Coherent anti-Stokes Raman scattering |

| | |
|---|---|
| **SNR** | Signal-to-Noise Ratio |
| **PMT** | Photomultiplier Tubes |
| **PDA** | Photodiode Array |
| **FIR** | Far Infrared |
| **ATR** | Attenuated Total Reflectance |
| **DTGS** | Deuterated Tryglicine Sulfate |
| **TGS** | Triglycine Sulfate |
| **CSF** | Cerebrospinal Fluid |
| **HEAD** | High Efficiency Aerosol Dispersion |
| **VOLM** | Volume Optional and Low Memory |
| **Q-GED** | Gas Exchange Device |
| **FDM** | Fused Deposition Modelling |
| **PLA** | Poly (Lactic Acid) |
| **PS** | Polystyrene |
| **PE** | Polyethylene |
| **THF** | Tetrahydrofuran |
| **CFD** | Computational Fluid Dynamics |
| **ASTM** | American Society of Testing and Materials |
| **FBI** | Federal Bureau of Investigation |
| **RI** | Refractive Index |
| **SEM-EDX** | Scanning Electron Microscopy Energy Dispersive X-ray spectrometry |
| **NAA** | Neutron Activation Analysis |
| **LIBS** | Laser Induced Breakdown Spectroscopy |
| **PTR-MS** | Proton Transfer Reaction Mass Spectrometry |
| **NIST** | National Institute of Standards and Technology |
| **DRC** | Dynamic Reaction Cell |
| **TRA** | Time Resolved Analysis |
| **RSD** | Relative Standard Deviation |
| **GEOREM** | Geological and Environmental Reference Materials |
| **AAS** | Atomic Absorption Spectroscopy |
| **DART-MS** | Direct Analysis in Real Time Mass SpectrometryCE |
| **CE** | Capillary Electrophoresis |
| **SEC** | Surface Elemental Concentration |
| **PTFE** | Polytetrafluoroethylene |
| **OSD** | Optimal Spot Density |
| **RGB** | Red Green Blue |
| **TOC** | Total Organic Carbon |
| **SNS** | Surface Normalized Signal |
| **SNC** | Surface Normalized Concentratio |
| **DRIFT** | Diffuse Reflectance Infrared Fourier Transform spectroscopy |
| **TC** | Thermoelectric Cooled |
| **FWHM** | Full Width at Half Maximum |
| **PDA** | Personal Digital Assistant |
| **PP** | Polypropylene |
| **CI** | Carbonyl Index |
| **DBDPO** | Decabromodiphenyl oxide |
| **PS** | Polystyrene |

**Summary**

The interest of humans in the viticulture and the geography of wine is as old as the history of humankind. Indeed, it is well known from ancient civilization the influence of the "*terroir*", that is the combination of factors including soil and climate, on the characteristic of wine produced within an area giving to the wine its distinctive character. Most of wines have a name associated with the place where the grapes were grown, producing a unique wine made from a particular grape variety. However, far from today's global wine manufacturing, it is believed that first men discovered the wine by chance when the sweet juice of crushed grapes became into an alcoholic beverage. The oldest evidence of wine dated back to the year 7500 BC and its geographical study has its roots in the Greek and Roman civilizations. Nowadays, the wine production and trade are globally extended, with most of the countries of the world producing wine. The scientific advances and the standardized wine making procedures guarantee that the resulting product meets uniform standards in terms of quality and flavor, contributing to the smooth character and complex bouquet of wine.

The great wines are a prime target for counterfeiters because of their brand value and excise duty of final price, mostly originating from the Asian market. China has surpassed France as the largest consumer of red wine in the world. This booming consumption has made wine counterfeits grow at the same pace as their sales. According to the National Committee of Foreign Trade Advisers of France (*Comité National des Conseillers du Commerce Extérieur de la France*, CNCCEF) the wine fraud is not just a matter of a few bottles but also includes an entire clandestine industry. According to the Wine and Spirits Commission of the CNCCEF, there is at least one bottle of forged wine for each bottle of original French wine in China. Although China is not the only supplier of counterfeited wines, the rapid growth of the wine market in this country and the absence of laws protecting intellectual property have triggered the counterfeit market.

Counterfeiting and piracy are illicit activities linked to intellectual property rights (IPR) infringement which could affect the health and safety of consumers due to the possibility of contamination or the use of poor-quality ingredients; accordingly, the need to protect consumers and safeguard intellectual assets has become an enforcement priority for Member States and other non-governmental institutions. However, there is still no comprehensive picture of its criminal dimension in the EU in relation to the scope and impact. Many attempts have been carried out to quantify the scale of counterfeiting and its consequences for businesses but there is not still a consensual and consistent methodology for collecting and analyzing the data. According to the European Union Intellectual Property Office, it is estimated that the legitimate industries losses approximately €1.3 billion of revenue annually due to the presence of counterfeit spirits (€740 million) and wine (€530 million) in the EU market, 3.3% of the sector's sales which means direct employment losses of approximately 4,800 jobs. Indeed, it is estimated that the quality of

approximately the 10% of the European wine is lower than the specified in the label. Wine fraud may be categorized in several forms and anti-counterfeiting measures have shown lack of effectiveness. Invasive techniques are mainly used for this purpose, based on liquid sampling, requiring opening the bottle, which can be fateful when it comes to great value wines. Therefore, there is an emerging need of objective, reliable, non-destructive and fast analysis tools for wine authentication and traceability, making international trade more transparent.

Among centuries, wine fraud has always existed and forgers are constantly in search of new ways of counterfeiting wine. There is no doubt that counterfeited wine will continue to haunt the market and consequently, winemakers and wineries will must adapt to the various forms of fraud, mainly by resorting to modern technology. The wine industry provides relatively little information about the effects of counterfeiting on their firm to avoid scaring customers and losing their investment. In consequence, they invest considerable sums of money to counter the threat from piracy. In fact, several wineries are already laser-engraving their bottles with unique serial number, adding tracer elements on their tagged inks, using tamperproof capsule seals or experimenting with hologrammed or bar-coded stickers placed half on the bottle-half on the capsule, that serve as identification tag and will shred if removed. However, the various strategies developed to prevent counterfeiting have been, in some cases, ineffective. Up to day, the unique techniques able to guarantee the authenticity of a wine are based on the organoleptic and/or chemical analysis. Nonetheless, the invasive and destructive nature of these techniques leads to a devaluation of the wine, which implies the need for new fast non-invasive tools.

The research work described in this Doctoral Thesis aims to develop a new diagnostic tool based on the direct and non-invasive (i.e. not visible by the naked eye) analysis of the chemical fingerprint (elemental and molecular) of the packaging: glass, paper, ink and capsule. Thus, femtosecond laser ablation coupled to inductively coupled plasma mass spectrometry (ICPMS) was used for trace element characterization and and Raman and Infrared spectroscopies were used for molecular characterization.

Firstly, glass is defined as an inorganic product of fusion that has cooled to a rigid condition without crystallization. Most of the container glass manufactured around the world is soda-lime glass and consists mainly of geologically derived raw materials and recycled broken glass, or *cullet.* Each of these raw materials contains impurities that cannot be easily controlled by manufactures and consequently can produce measurable variations either in the chemical, optical and physical properties of the final glass product. Therefore, for discrimination purposes, the elements of interest in glass are not the major components but rather the trace and ultra-trace, frequently unintended components, which inherently make glass sources distinguishable.

Secondly, any written document paper whose source or authenticity is doubtful could be considered as a *questioned* document. Generally, questioned documents consist of handwritten, typed or printed information on paper. The analysis of questioned documents involves different types of analyses including comparison of the ink and printing procedure as well as physical and chemical characterization of the paper itself. In wine counterfeiting, the relabeling of inferior and cheaper wines to more expensive brands is another common type of wine fraud. In particular, rare, expensive and cult wines characterize this type of fraud. Even the main components of the paper are similar, there can still be variations in the trace elemental composition. Because the paper is produced from natural materials and recycled consumer waste, it is possible to characterize it through its trace elements, which can be different from one manufacturer to another. Therefore, the variability in paper manufacture makes it possible to identify a great variety of subtle distinctions that give each batch of paper or each sheet of paper a unique chemical fingerprint. On the other hand, the chemical composition of the inks undergoes continuous changes due to manufacturers' urge for innovation and the inorganic/organic portions of the ink can be a valuable tool for the characterization and discrimination of printing inks.

Finally, regarding capsule manufacture, lead was firstly used due to its malleability and resistance to corrosion. Nevertheless, lead capsules were phased out due to environmental and health related problems. Nowadays, the use of aluminium is widespread and tin capsules have replaced lead capsules for expensive wines. In some cases, polyethylene, polyethylene terephthalate (PET) or polyvinyl chloride (PVC) can be also employed for partial or entire capsule manufacturing. Therefore, the composition of the alloy is specific and cannot easily be imitated as well as the inks employed to color the capsules, which could be useful for counterfeiting detection.

In the first stage of this work, a new ablation cell adjustable to different bottle shapes was developed. During the LA-ICPMS measurements, the ablation cell housing the samples plays a very important role, as it must allow a quantitative and rapid transport of the laser-induced aerosol to the ICP source. However, when considering large-sized samples like wine a bottle, the conventional cells' dimension is a deal breaker, since they accept only samples of few cubic centimetres. With the aim of a direct analysis of wine bottles, a new open ablation cell adjustable to different bottle curvatures was designed and constructed. A 3D printer was used to create the ablation cell using poly-lactic acid (PLA) polymer as construction material, as conventional high precision micromachining was not feasible for such a complex prototype.

In the second part, a minimally invasive (< 0.5 mm) ablation strategy, which causes no apparent damage to the surface of the bottle, was optimized for the analysis of the glass. Certified glass standards were used for the quantification of trace elements on the samples. The developed method was applied for the analysis of authentic and genuine bottles and bottles of different origin and vintage. The following procedure was used for this purpose: i) selection of the elemental menu and optimization the ablation strategy, ii) evaluation of the analytical method in terms of limits of detection, long-term reproducibility and homogeneity within a bottle and within a batch of bottles and iii) application of statistical methods. The statistical processing of data, based on multivariate analysis, allowed to establish and prioritize the most important variables for the identification of counterfeited bottles and as well as to distinguish the chemical signature of bottles according to their origin country. Finally, the study of a series of bottles from the same winery, which comprises the period from 1969 to 2010, showed that the amount of trace elements in the glass constitute a chemical imprint which allows to distinguish among the bottles.

In the third part of this work, a novel ablation strategy was developed for the analysis of paper and ink, avoiding the perforation of the label. Moreover, owing to the lack of certified reference materials, matrix-matched standards were synthesized as external calibrators using a commercially available inkjet printer and their suitability was assessed. The purpose of the methodology was to perform a quantitative and comparative analysis of label and ink. The developed characterization methodology was successfully applied to a large number of bottles. Statistical data processing based on multivariate analysis draw clear distinction between genuine and counterfeited bottles by isolating and prioritizing the most important trace elements. In addition, it was also possible to distinguish the chemical signature of bottles according to their origin country and vintage. The study the series of bottles from the same wine cellar comprising the vintages from 1969 to 2010 also showed that the amount of trace elements found on paper allows to clearly identifying the vintage of a given bottle. In addition, a brief study was carried out on capsules to assess the feasibility of their analysis to discriminate between authentic and fraudulent wine bottles and bottles of different origin, being the obtained results highly encouraging.

Finally, in order to complement the results obtained with the fsLA-ICPMS, a new unambiguous diagnostic tool based on Raman and Infrared spectroscopies was developed for the direct and qualitative molecular characterization of label paper and ink. Both analytical techniques are non-destructive and do not require previous sample preparation. In addition, the spectra are specific and can be used for comparison purposes. A direct, fast and reproducible analytical method was developed for the comparison of the label paper and the inks, which was successfully applied to a selected number of genuine and counterfeited bottles and a series of bottles belonging to a concrete winery, comprising the vintages from 1969 to 2010. The obtained results pointed out

that both techniques are complementary and useful for identifying counterfeits but due to the availability of such unique samples, they were not applied to a large number of samples, which avoided assessing their discrimination power. Moreover, although comparison of spectra is enough to discriminate among samples, a step forward has been done to identify the basis composition of the paper label and the inks.

L’intérêt des Hommes pour la viticulture et la géographie du vin est aussi ancien que l’histoire de l’humanité. Il est bien connu que le « terroir », à savoir la combinaison de facteurs tels que le sol et le climat, a de l’influence sur les caractéristiques du vin produit dans une zone lui donnant son caractère distinctif. La plupart des vins ont un nom associé à l'endroit où les raisins ont été cultivés, ceux-ci produisant un vin unique, caractéristique d'un cépage particulier. Cependant, loin de la fabrication mondiale actuelle de vin, il est dit que les premiers hommes ont découvert le vin par hasard lorsque le jus sucré de raisins écrasés est devenu une boisson alcoolisée. La plus ancienne preuve d’existence du vin remonte à l'année 7500 av. J.C. et son étude géographique a débuté dans les civilisations grecques et romaines. De nos jours, la production et le commerce de vin sont globalement étendus, la plupart des pays du monde produisant du vin. Les progrès scientifiques et les procédures normalisées pour la vinification garantissent la conformité aux normes en termes de qualité et de goût.

Les grands vins représentent une cible privilégiée pour les faussaires en raison de la valeur de leur marque et des coûts des droits d’accises. La contrefaçon s’intensifie et se développe en grande partie en Asie. La Chine a dépassé la France et est devenue le plus grand consommateur de vin rouge au monde. Cette consommation en plein essor a fait que les contrefaçons de vin augmentent au même rythme que leurs ventes. Selon le Comité National des Conseillers en Commerce Extérieur de France (CNCCEF), la fraude sur le vin ne concerne pas uniquement quelques bouteilles contrefaites, mais elle couvre également toute une industrie clandestine. Selon la commission des vins et spiritueux du Comité National des Conseillers du Commerce Extérieur de la France, il existe au moins une bouteille de vin contrefaite en Chine pour chaque bouteille de vin d’origine française. Bien que la Chine ne soit pas le seul fournisseur de vins contrefaits, la croissance rapide du marché du vin dans ce pays ainsi que l'absence de lois protégeant la propriété intellectuelle ont déclenché le marché de la contrefaçon.

La contrefaçon et le piratage sont des activités illégales liées à la violation des droits de propriété intellectuelle (DPI) qui peuvent affecter la santé et la sécurité des consommateurs en raison de la possibilité de contamination ou de l'utilisation de d’ingrédients de mauvaises qualité ; par conséquent, la nécessité de protéger les consommateurs et les DPI est devenue une priorité pour les États membres et les autres institutions non gouvernementales. Cependant, il n'y a toujours pas de représentation exhaustive de sa dimension criminelle dans l'UE en ce qui concerne la portée et l'impact. De nombreuses tentatives ont été menées pour quantifier l'ampleur de la contrefaçon et ses conséquences pour les entreprises, mais il n'existe pas encore une méthodologie consensuelle et cohérente pour collecter et analyser des données. L'office de la propriété intellectuelle de l'Union européenne estime que les industries légitimes perdent environ 1,3 milliard d'euros de recettes annuelles en raison de la présence de contrefaçon de spiritueux (740

millions d'euros) et de vin (530 millions d'euros) sur le marché de l'UE. Cela correspond à 3,3% des ventes dans ce secteur, soit une perte directe d'environ 4 800 emplois. Il est estimé qu'environ 10% du vin européen a une qualité inférieure à celle indiquée sur l'étiquette. La fraude au vin peut être classée en différentes catégories et les mesures anti-contrefaçon ont montré un manque d'efficacité. Des techniques invasives sont principalement utilisées pour effectuer les contrôles d'authenticité des vins. Ces techniques, basées sur l'échantillonnage du liquide, nécessitent alors l'ouverture de la bouteille. Cela peut être regrettable quand il s'agit de vins de grande valeur. Il y a par conséquent un besoin de faire émerger des outils d'analyse fiables, rapides et non destructifs pour l'authentification et la traçabilité du vin afin que le commerce international devienne plus transparent.

Au cours des siècles, la contrefaçon du vin a toujours existé et les faussaires sont constamment à la recherche de nouvelles formes de contrefaçon. Il ne fait aucun doute que le marché du vin contrefait continuera à se développer et, par conséquent, les vignerons et les caves à vin devront s'adapter aux différentes formes de fraude, principalement ayant recours aux nouvelles technologies avancées. L'industrie du vin fournit relativement peu d'informations sur les effets de la contrefaçon sur leur entreprise pour éviter d'effrayer les clients et de perdre leur investissement. En conséquence, ils investissent des sommes d'argent considérables pour contrer la menace du piratage. En fait, plusieurs caves à vin enregistrent déjà leurs bouteilles avec un numéro de série unique gravé par laser, ajoutent des éléments traceurs dans l'encre de l'étiquette, utilisent des joints de capsules inviolables ou encore expérimentent les hologrammes ou les codes-barres placés au niveau du centre du capsule de la bouteille. Ce dernier sert d'étiquette d'identification et se déchire lorsqu'il est enlevé. Cependant, les différentes stratégies développées pour lutter contre la contrefaçon se sont avérées inefficaces dans certains cas. A ce jour, les seules techniques capables de garantir l'authenticité d'un vin sont basées sur l'analyse organoleptique et/ou chimique. Néanmoins, la nature invasive et destructrice de ces techniques conduit à une dévaluation du vin, ce qui implique la nécessité de développer de nouveaux outils non invasifs et rapides.

Le travail de recherche décrit dans cette thèse de doctorat vise à développer un nouvel outil de diagnostic basé sur l'analyse directe et non invasive (c'est à dire quasi invisible à l'œil nu) de la signature chimique (élémentaire et moléculaire) de ce qui constitue l'emballage d'une bouteille de vin : le verre, le papier, les encres et la capsule. Ainsi, l'ablation laser femtoseconde couplée à une détection par spectrométrie à plasma induit (ICPMS) a été mise en œuvre pour la caractérisation des éléments traces et les spectroscopies Raman et Infrarouge pour la caractérisation moléculaire.

Tout d'abord, le verre est défini comme un produit inorganique de fusion qui, en refroidissant, a atteint l'état solide sans cristalliser. La plupart du verre utilisé pour l'emballage est fabriqué principalement à partir de matières premières d'origine géologique naturelle et de verre recyclé. Chacune de ces matières premières contient des impuretés difficiles à contrôler et, par conséquent, peuvent produire des variations significatives des propriétés chimiques, optiques et physiques du produit final. Ainsi, dans un but d'identification, les éléments d'intérêt dans le verre ne sont pas les composés principaux, mais plutôt les composants en état de trace et d'ultra-trace, qui sont fréquemment présents involontairement, et qui rendent les sources du verre distinguables.

D'une autre côté, toute étiquette dont la source ou l'authenticité est douteuse peut être considéré comme une étiquette d'origine suspecte. Généralement, les étiquettes suspectes se composent d'informations manuscrites, dactylographiées ou imprimées sur papier. L'étude des étiquettes suspectes implique différents types d'analyses, incluant la comparaison de l'encre et la procédure d'impression ainsi que la caractérisation physique et chimique du papier lui-même. Le ré-étiquetage des vins de bas de gamme à des marques plus coûteuses est un autre type commun de fraude. Plus précisément, c'est pour les vins rares, coûteux et cultes que ce type de fraude est le plus souvent rencontré. Même si les composés principaux du document sont similaires, il peut y avoir des variations dans la composition des traces élémentaires. Étant donné que le papier est fabriqué à partir de matériaux naturels et de déchets de consommation recyclés, il est possible de le caractériser à travers les éléments trace, qui peuvent être différents d'un fabricant à l'autre. Par conséquent, la variabilité du papier manufacturé permet d'identifier une large variété de distinctions subtiles qui confèrent à chaque lot de papier ou à chaque feuille de papier une empreinte chimique unique. D'autre part, la composition chimique des encres subit des changements continus en raison de l'incitation des fabricants pour l'innovation. Les fractions inorganiques/organiques de l'encre peuvent constituer un outil précieux pour la caractérisation et la discrimination des encres d'impression.

Enfin, en ce qui concerne la fabrication des capsules, le plomb a d'abord été utilisé pour sa malléabilité et sa résistance à la corrosion. Néanmoins, les capsules en plomb ont été éliminées en raison de problèmes environnementaux et liés à la santé. De nos jours, l'utilisation de l'aluminium est répandue et les capsules d'étain ont remplacé les capsules de plomb pour les vins coûteux. Dans certains cas, le polyéthylène, le polyéthylène téréphtalate (PET) ou le chlorure de polyvinyle (PVC) peuvent également être utilisés pour la fabrication partielle ou totale de capsules. Ainsi, la composition de l'alliage est spécifique et ne peut pas être facilement imitée. C'est le cas également des encres utilisées pour colorer les capsules. Ceci pourrait alors être utile pour la détection de contrefaçon.

En première étape de ce travail, une nouvelle cellule d'ablation adaptable à différentes formes de bouteilles a été développée. Au cours des analyses par LA-ICPMS, la cellule d'ablation dans laquelle sont placés les échantillons joue un rôle très important, car elle doit permettre un transport quantitatif et rapide de l'aérosol induit par le laser vers la source ICP. Cependant, pour les échantillons de grande taille, tels que les bouteilles de vin, le volume des cellules d'ablation conventionnelles est rédhibitoire car elles n'acceptent que des échantillons de quelques centimètres cube. Afin d'effectuer l'analyse directe des bouteilles de vin, une nouvelle cellule d'ablation ouverte et ajustable à différentes courbures de bouteilles a été réalisé. Une imprimante 3D a été utilisée pour créer un prototype de cellule d'ablation en utilisant un polymère d'acide poly-lactique (PLA) comme matériau de construction, la fabrication de cette pièce complexe étant techniquement irréalisable au moyen des machines-outils de micro-usinage conventionnelles.

Dans une deuxième étape, cette cellule a été appliquée à l'analyse directe de l'emballage, notamment du verre, du papier et des encres. Une stratégie d'ablation quasi non invasive (<0,5 mm), infligeant des dommages à la surface de la bouteille invisibles à l'œil nu, a été optimisée pour l'analyse du verre. Des étalons de verres certifiés en éléments traces ont été utilisés pour la quantification. La méthode développée a été appliquée à l'analyse de bouteilles authentiques issues de différents millésimes et pour l'analyse de bouteilles contrefaites. Pour ce faire, la procédure suivante a été appliquée: i) sélection des éléments à mesurer et optimisation de la stratégie d'ablation, ii) évaluation de la méthode analytique en terme de limites de détection, de reproductibilité sur le long terme, de variabilité des mesures sur un lot de bouteilles identiques, et de variabilité spatiale sur une bouteille et iii) application de méthodes statistiques. Le traitement statistique des données, basé sur l'analyse multivariée, a permis d'une part d'établir et de hiérarchiser les variables les plus importantes pour identifier les bouteilles contrefaites et d'autre part de distinguer la signature chimique des bouteilles selon leur origine géographique. Enfin, l'étude des millésimes d'un même château sur une période de 1969 à 2010, a également permis de montrer que les teneurs en traces élémentaires dans le verre constituaientt une empreinte chimique permettant de distinguer les bouteilles entre elles.

Dans la troisième partie de ce travail, une nouvelle stratégie d'ablation a été développée pour l'analyse du papier et de l'encre, en évitant la perforation de l'étiquette. L'analyse du papier et des encres, en raison du manque de matériaux de référence certifiés représente un véritable challenge analytique. Nous avons donc développé nos propres étalons de papier par impression jet d'encre à partir de solutions dopées permettant une analyse quantitative et comparative du papier et des encres des étiquettes. Cette méthodologie a été appliquée avec succès à un grand nombre de bouteille parmi lesquelles des bouteilles authentiques d'origine contrôlée et des bouteilles

contrefaites. Le traitement statistique des données a permis d'établir une distinction claire entre les bouteilles authentiques et contrefaites. Il a été également possible de distinguer la signature chimique des bouteilles selon leur pays d'origine. L'étude de la collection d'un château sur les millésimes allant de 1969 à 2010 a également montré que les teneurs en éléments traces du papier permettait d'identifier clairement le millésime des bouteilles. En outre, une étude succincte a été réalisée sur les capsules pour évaluer la faisabilité de leur analyse afin de différencier les bouteilles authentiques et contrefaites, ainsi que les bouteilles d'origine différente. Certains premiers résultats sont, en aucun doute, prometteurs.

Enfin, un nouvel outil de diagnostic basé sur la spectroscopie Raman et la spectroscopie Infrarouge a également été développé pour l'analyse moléculaire qualitative et directe du papier et des encres afin de compléter les résultats obtenus avec la technique fsLA-ICPMS. Ces deux techniques d'analyse sont non destructives et ne nécessitent pas de préparation préalable des échantillons. De plus, les spectres obtenues sont spécifiques et peuvent être utilisés à des fins de comparaison. Une méthode analytique directe, rapide et reproductible a été développée pour comparer le papier de l'étiquette et les encres. Cette méthode a été appliquée avec succès à un certain nombre de bouteilles authentiques et contrefaites ainsi qu'à la collection des millésimes de 1969 à 2010 du château étudié précédemment. Les résultats obtenus ont montré que les deux techniques sont complémentaires et utiles pour distinguer les bouteilles authentiques des bouteilles contrefaites et pour établir une date approximative de la mise en bouteille. Cependant, en raison de la faible disponibilité de ces échantillons uniques, la méthode ne peut pas être appliquée à un grand nombre d'échantillons afin d'évaluer son pouvoir de discrimination. De plus, bien que l'étude des spectres soit habituellement suffisante pour comparer les échantillons entre eux, nous sommes allés au delà d'une simple étude comparative en identifiant les principaux composés de l'étiquette papier et des encres.

**Resumen**

El interés que han suscitado la viticultura y la geografía del vino en el ser humano es tan antiguo como su propia historia. Desde las civilizaciones antiguas es bien conocida la influencia del "*terroir*" en las características del vino producido dentro de una determinada área, el cual da al vino su carácter distintivo. La mayoría de los vinos están asociados al lugar donde se cultivaron las uvas, produciendo un vino único hecho de una variedad de uva particular. Sin embargo, lejos de la actual producción global de vino, se cree que el vino fue descubierto por casualidad cuando el mosto de uvas fermentó y se transformó en una bebida alcohólica. La evidencia más antigua de vino se remonta al año 7500 a.C. y su estudio geográfico tiene sus raíces en las civilizaciones griega y romana. Hoy en día, la producción y el comercio del vino son actividades globales, puesto que la mayoría de los países del mundo producen vino. Los avances científicos y los procedimientos normalizados para la elaboración del vino garantizan que éste cumpla con las normas en cuanto a calidad y sabor.

Los vinos de alta gama y elevado valor económico, y aquellos de menor valor pero que se producen a gran escala, están particularmente expuestos a su falsificación, principalmente con el origen en el mercado asiático. China ha sobrepasado a Francia como el mayor consumidor de vino tinto del mundo. Este consumo floreciente ha hecho que las falsificaciones de vino crezcan al mismo ritmo que su venta. Según el Comité Nacional de Consejeros de Comercio Exterior de Francia (*Comité National des Conseillers du Commerce Extérieur de la France*, CNCCEF) el fraude de vinos no es solo cuestión de unas pocas redes de falsificación, sino que abarca toda una industria clandestina. Según la Comisión de Vinos y Bebidas Espirituosas del CNCCEF, en China, por cada botella de vino francés original, al menos hay una botella de vino falsificada. Aunque China no es la única proveedora de vinos falsificados, el rápido crecimiento del mercado del vino en este país y la ausencia de leyes que protejan la propiedad intelectual han disparado el mercado de las falsificaciones.

La falsificación y la piratería son actividades ilícitas relacionadas con la infracción de los Derechos de Propiedad Intelectual (DPI) que pueden afectar a la salud y la seguridad de los consumidores debido a la posibilidad de contaminación o el uso de sustancias nocivas. En consecuencia, la necesidad de proteger a los consumidores y salvaguardar los DPIs se ha convertido en una prioridad para los Estados miembros y otras instituciones no gubernamentales. Sin embargo, todavía no existe un panorama completo de su dimensión en la UE en relación con el alcance y el impacto, ya que a día de hoy se carece de una metodología consensuada que permita recopilar y analizar los datos. Según un informe de la Oficina de Propiedad Intelectual de la Unión Europea, las repercusiones directas del fraude de vino suponen la pérdida de aproximadamente 1.300 millones de euros de ingresos anuales debido a la presencia de bebidas espirituosas (740 millones de euros) y vinos (530 millones de euros) falsos en el mercado de la UE, lo que

representa el 3.3% de las ventas del sector y se traduce en la reducción de 23.400 puestos de trabajo y de 1.2 billones en ingresos públicos. Además, se estima que el 10% de los vinos europeos son de una calidad inferior a la indicada en la etiqueta. El fraude en el vino puede darse de diferentes formas y las medidas anti-falsificación existentes han demostrado ser ineficaces. Actualmente, las técnicas para la verificación de vino se basan en el muestreo del propio líquido. Por lo tanto, se trata de técnicas invasivas que requieren la apertura de la botella, lo que resulta inviable cuando se trata de vinos de gran valor. En consecuencia, se requieren herramientas analíticas objetivas, fiables, no-destructivas y rápidas que garanticen la autenticidad y trazabilidad del vino para un comercio internacional más transparente.

El fraude del vino ha existido siempre y los falsificadores están constantemente en busca de nuevas formas de falsificación. Por ello, no cabe duda de que el vino falsificado continuará siendo un problema para los viticultores y las bodegas, que deberán adaptarse a las diversas formas de fraude, principalmente recurriendo a la tecnología moderna. La industria vitivinícola proporciona relativamente poca información sobre los efectos de la falsificación en sus respectivas empresas para evitar consecuencias negativas, por ejemplo, la pérdida de clientes e inversiones. En consecuencia, invierten considerables sumas de dinero para contrarrestar la amenaza de la piratería. De hecho, varias bodegas graban con láser las botellas con un número de serie único, añadiendo elementos trazadores en la tinta de etiquetas, usando cápsulas a prueba de manipulaciones o experimentando con hologramas o con código de barras colocados entre el cuello de la botella y la cápsula que se rompen si se retiran y que sirven a su vez como etiqueta de identificación. Hasta la actualidad, las distintas estrategias desarrolladas para evitar la falsificación han resultado, en algunos casos, ineficaces. A día de hoy, las únicas técnicas que pueden garantizar la autenticidad de un vino son el análisis organoléptico y/o químico. Sin embargo, el carácter invasivo y destructivo de estas técnicas conlleva una devaluación del vino, de lo que se deduce la necesidad de nuevas herramientas de análisis rápidas y no invasivas.

Con este objetivo se plantea la presente Tesis Doctoral, que pretende avanzar en el desarrollo de una herramienta analítica que permita certificar la autenticidad de un vino de forma inequívoca mediante técnicas analíticas no invasivas (es decir, prácticamente inapreciable a simple vista) como son la ablación laser con plasma de acoplamiento inductivo-espectrometría de masas (LA-ICPMS) y las espectroscopias Raman e Infrarroja, que permiten el análisis de una muestra sólida sin necesidad de procesarla y sin inducir degradación o alteración apreciable alguna. Mediante la metodología desarrollada se pretende establecer el perfil elemental y molecular del vidrio, el papel, la tinta y la cápsula de las botellas de vino.

Por un lado, el vidrio común o vidrio de soda-cálcica es un material obtenido por la fusión de compuestos inorgánicos a altas temperaturas, y que ha sido enfriado adquiriendo un estado rígido, no cristalino. La mayor parte del vidrio destinado para la elaboración de envases se fabrica principalmente a partir de materias primas de origen geológico natural y de vidrio reciclado. Cada una de estas materias primas contiene impurezas que difícilmente se pueden controlar y, por lo tanto, pueden producir variaciones medibles en las propiedades químicas, ópticas y físicas del producto final. Consecuentemente, el análisis de impurezas presentes a nivel de trazas en las materias primas emerge como una alternativa útil para la discriminación.

Por otro lado, cualquier documento escrito cuya fuente o autenticidad sea dudosa podría considerarse un documento cuestionado. Generalmente, los documentos cuestionados consisten en información manuscrita, mecanografiada o impresa en papel. Por lo tanto, el análisis elemental de tinta y papel resulta de interés para la determinación de la autenticidad de documentos, la identificación del origen, el estudio comparativo entre dos documentos diferentes, e incluso para su datación. El análisis de los documentos cuestionados implica diferentes tipos de análisis, incluyendo comparaciones de la tinta empleada y el procedimiento de impresión, así como la caracterización física y química del papel en sí. En la falsificación de vino, el re-etiquetado de vinos de inferior gama a marcas más caras es otro tipo común de fraude. Concretamente, es en los vinos raros, caros y de culto donde con mayor frecuencia se da este tipo de fraude. En primer lugar, el avance en el control de calidad de la manufactura del papel ha minimizado la variabilidad de las propiedades físicas y ópticas de estos materiales, lo cual limita la posibilidad de discriminación entre documentos y hace necesario su análisis químico. Debido a que el papel se produce a partir de materias primas naturales y papel reciclado, este puede ser diferente de un fabricante a otro o incluso podría haber distinciones sutiles que dieran a cada lote de papel una huella química única. En segundo lugar, la composición química y formulación de las tintas sufre continuos cambios como consecuencia del interés de mejora e innovación de los fabricantes y la determinación de los compuestos orgánicos e inorgánicos surge como una valiosa herramienta para la caracterización y discriminación de tintas de impresión.

Finalmente, en cuanto a las cápsulas, el plomo se utilizó antiguamente como material de fabricación debido a su maleabilidad y resistencia a la corrosión. Sin embargo, estudios publicados a este respecto destacaron el peligro del plomo para el medioambiente y su riesgo para la salud, lo que dio lugar a la sustitución del plomo por otros materiales más inocuos. Hoy en día, la utilización de las cápsulas de estaño es la práctica más extendida en los vinos de alta gama, mientras que las cápsulas de aluminio con polietileno son más utilizadas en los vinos de menor calidad. En algunos casos, también se emplean otros compuestos como el polietileno, el tereftalato de polietileno (PET) o el cloruro de polivinilo (PVC) para la fabricación parcial o total de

cápsulas. Por lo tanto, la composición de la aleación es específica y difícilmente imitable, así como las tintas empleadas para colorear las cápsulas, lo que podría ser útil para la detección de la falsificación, haciendo de ésta una potencial fuente de información para la detección de falsificaciones.

En la primera etapa de este trabajo se diseñó y fabricó una nueva cámara de ablación adaptable a las diferentes formas de las botellas. Durante las mediciones LA-ICPMS, la cámara de ablación juega un papel muy importante, ya que debe permitir un transporte cuantitativo y rápido del aerosol inducido por láser a la fuente ICP. Sin embargo, el tamaño de la muestra es un factor limitante para el análisis de algunas de ellas. Por lo tanto, la necesidad de encontrar alternativas viables para la ablación directa de cualquier muestra, independientemente de su tamaño, fomentó el desarrollo de nuevos diseños. En consecuencia, con el objetivo de realizar el análisis directo de las botellas de vino, se diseñó y construyó una nueva cámara de ablación abierta. Su fabricación se llevó a cabo mediante impresión 3D ya que sus características no son alcanzables mediante técnicas de micro-mecanizado convencional de alta precisión, empleando ácido poliláctico (PLA) como material.

En la segunda parte del trabajo, se optimizó una estrategia de ablación no invasiva (< 0.5 mm) para el análisis del vidrio y se utilizaron estándares de vidrio certificados en su contenido de elementos traza para el análisis cuantitativo de las muestras. El método desarrollado se aplicó a botellas auténticas de origen controlado y sus falsificaciones y botellas de diferente origen y cosecha. Para ello se utilizó el siguiente procedimiento: i) selección de los elementos a monitorizar y optimización una estrategia de ablación, ii) evaluación del método analítico en términos de límites de detección, reproducibilidad a largo plazo y homogeneidad tanto en una botella como en un lote de botellas y iii) aplicación de métodos estadísticos. Del procesamiento estadístico de los datos, basado en el análisis multivariante, se pretende establecer un patrón de análisis que permita identificar las botellas falsificadas y aislar y priorizar las variables más importantes a considerar para la determinación de su origen geográfico. Además, el análisis de una serie de botellas pertenecientes a una misma bodega, y que comprende los años 1969-2010, mostró que la cantidad de elementos traza constituye una huella química que permite distinguir entre las botellas de diferente año.

En la tercera parte de este trabajo, se desarrolló una nueva estrategia de ablación para el análisis de papel y tinta, evitando la perforación de la etiqueta. Además, debido a la falta de materiales de referencia certificados, se sintetizaron nuevos estándares *"matrix-matching"* utilizando para ello una impresora de inyección de tinta y se evaluó su idoneidad. El propósito de la metodología desarrollada era su aplicación para el análisis cuantitativo y la comparación de etiquetas de papel y tinta impresa. Por ello, igual que en el caso de análisis del vidrio, el método desarrollado se

aplicó con éxito a botellas auténticas de origen controlado y sus falsificaciones y botellas de diferente origen y cosecha. El posterior procesamiento estadístico de datos permitió establecer una clara distinción entre botellas originales y falsificadas, aislando y priorizando los elementos traza más importantes. Además, también fue posible distinguir la firma química de las botellas de acuerdo con su país de origen y cosecha. Adicionalmente, se realizó un pequeño estudio en las cápsulas para evaluar la viabilidad de su análisis con el fin de discriminar entre botellas originales y falsificadas, así como de distinto origen, obteniendo unos primeros resultados sin duda prometedores.

Finalmente, se desarrolló una nueva herramienta diagnóstica complementaria basada en las espectroscopias Raman e Infrarrojo para la caracterización molecular directa y cualitativa del papel y de la tinta, cuyo objetivo es complementar los resultados previamente obtenidos por fsLA-ICPMS. Ambas técnicas analíticas son no destructivas y no requieren preparación previa de la muestra. Además, debido a que los espectros son específicos de cada compuesto, éstos se pueden utilizar con fines de comparación. Se desarrolló un método analítico directo, rápido, reproducible para la comparación del papel de la etiqueta y de las tintas, y se aplicó con éxito a un número seleccionado de botellas originales y falsificadas, así como a una serie de botellas pertenecientes a una determinada bodega y que comprenden los años de 1969 a 2010. Los resultados obtenidos indicaron que ambas técnicas son complementarias y de gran utilidad para discernir entre botellas originales y falsas, así como para establecer una fecha aproximada de embotellamiento. Sin embargo, debido a la reducida disponibilidad de tales muestras únicas, la metodología no se pudo aplicar a un gran número de muestras para evaluar su poder de discriminación. Asimismo, y a pesar de que la comparación de los espectros resulta suficiente para discriminar entre las muestras, se ha llevado a cabo la identificación de los principales componentes tanto de la etiqueta como de las tintas.

# CHAPTER 1:

# Wine authentication methods – A review

## 1. The origin of the *wine culture*

Viticulture is one of the oldest agricultural activities of humans as grape growing has always had an important role in the life and trade of people from ancient civilizations to the modern world. In fact, it is said that the knowledge of grape and wine is as old as the cultural history of mankind (1). Early cultures had already become aware of the influence of geography upon the characteristics of wine produced within an area and an understanding of differences in wine coming from various regions. Up until today, grape growing and wine production are valuable economic activities and have important consequences on culture, socio-economic development and the resulting landscapes of regions. The distribution of vineyards and wine elaboration are located in certain areas where the "*terroir*" or the combination of factors including soil, climate and sunlight gives wine grapes their distinctive character (2). Most wines of the world have a name associated with the geographical region in which the grapes grow and each geographical location has a millenary history of producing a unique wine made from a particular grape variety (3, 4).

Far from actual industrial processes and current knowledge, the first men found that crushed grapes became over time into a new beverage: the conversion of the sweetie taste of the grapes' juice into an alcoholic beverage. It could be that first wine was discovered by chance, when someone tasted the fermented juice of wild grapes that had been collected and stored in vessels. Indeed, the discovery of fermentation is a step important in the evolution of humanity. In fact, the evolution of winemaking from periodic event to a common cultural activity means the development of a settled lifestyle (5).

Wine has an archeological record dating back of more than 7500 years. The earliest suspect wine residues come from a pottery jar (3500 B.C.) found in a Neolithic village in the Zagros Mountains in Iran. Most research believes that winemaking was evolved in southern Caucasia which includes parts of the present-day northwestern Turkey, northern Iraq, Azerbaijan and Georgia. Quevri pottery is another evidence of early winemaking. It is an egg-shaped vessel unique to Georgia, dating back over 8000 years predating Greco-Roman traditions of winemaking. These vessels, usually coated with bee wax lignin inside and a lime encasement outside, were buried in the ground and used for wine fermentation and storage, Being totally immersed in the earth gave it naturally stable temperature (6). Older precedents of fermented beverage which were produced in China as early as 7000 B.C. have also been exposed but they seem to have been produced from rice, honey and fruit. The Egyptians were also important in the early production of wine as the first unequivocal evidence of intentional winemaking was the finding of wine presses from the reign of Pharaoh Udimu as early as the First Dynasty (3100-2890 B.C.).

Figure 1 shows how advanced was grape growing and wine making by the illustration of grape growth on a pergola, the grape harvest and treading, the straining of the juice and the storage of the wine in amphorae.

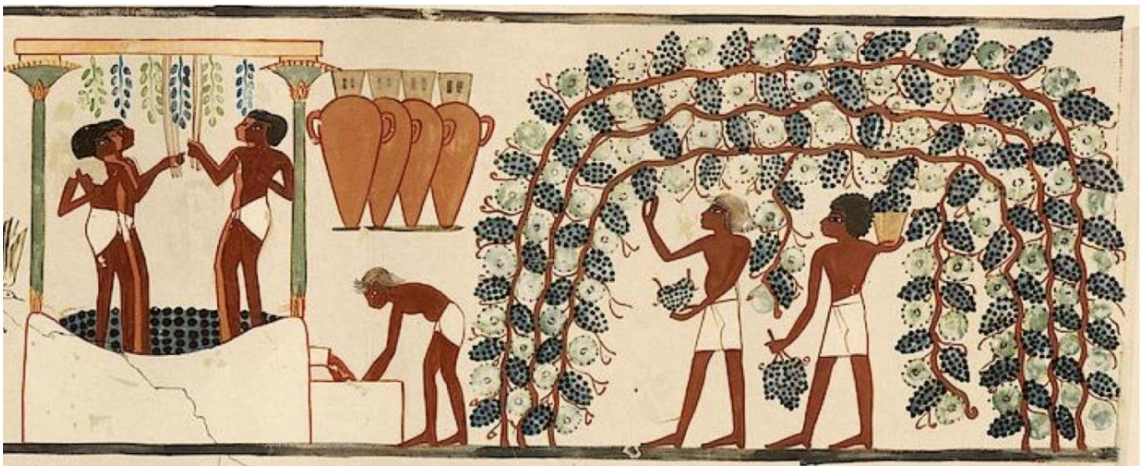

**Figure 1** Vintage and wine making scene depicted on the walls of the tomb of Nachkt, 1550-1295 B.

The geographical study of grapes and wine has its roots in the Greek and Roman civilizations. There are a great number of remaining wine amphorae and vessels which show the importance of wine in the daily life of people in the ancient world. This wine value was reflected in their spiritual lives with the creation of the Greek God Dionysus and the Roman God Bacchus representing the god of wine. But it was during the Roman era when wine became popular throughout society as Romans exported wine and wine-making to the rest of Europe.

After the fall of Rome, wine continued to be produced in the Byzantine Empire in the eastern Mediterranean. It spread eastward to Central Asia along the Silk Route and it was known in China by the 8$^{th}$ century. Meanwhile, waves of Slavs, Franks, Vandals, Goths and Huns invaded Europe for land and puissance, which destabilized the economic situation. Therefore, during this period, viticulture was primarily encouraged to monasteries because of the need of wine in the Christian sacraments. During the 15$^{th}$ and 16$^{th}$ centuries the characteristics of some wine regions were valued by the increasingly skilled wine drinkers. However, wines began to gain their modern expression during the 17$^{th}$ century when the use of sulfur in barrel treatment was introduced as biocide which greatly increased the likelihood of producing better quality wines and extending their aging potential. By the 18$^{th}$ century the wine trade soared, especially in France, where Bordeaux became one of the most renowned producers of fine wines. Thereby, the growth of distinctive strains of wine grapes led to the production of regional wines with recognizable characteristics.

Wine-making occurred out of Europe too, for example: viticulture in Chile goes back to 16th century, in South Africa to 17th century, in United States to 18th century and in Australia to 19th century. Despite the increasing success of the industry, a phylloxera epidemic destroyed the old European vineyards, which involved a huge ecological disaster that affected wine production for decades. Fortunately, the plague was overcome by grafting cuttings of European varietal vines onto disease-resistant American rootstock (7, 8).

Nowadays, wine manufacture is a global industry, with most of the countries of the world producing wine. The uninterrupted technological advances have enabled machines that can harvest large areas increasing the production of wine and modern science developments have guaranteed that the resulting product meets uniform standards in terms of quality and flavor. With mechanization, cylindrical glass bottles became the standard container for both wine maturation and transport, allowing bottles to be laid on their sides. The reintroduction of cork for bottle closure, due to its impermeability and hermeticism, isolates wine from external liquid contamination and oxygen. Thus, its nature contributes to the development of a smooth character and complex bouquet. Figure 2 shows the growth of winemaking through centuries and countries.

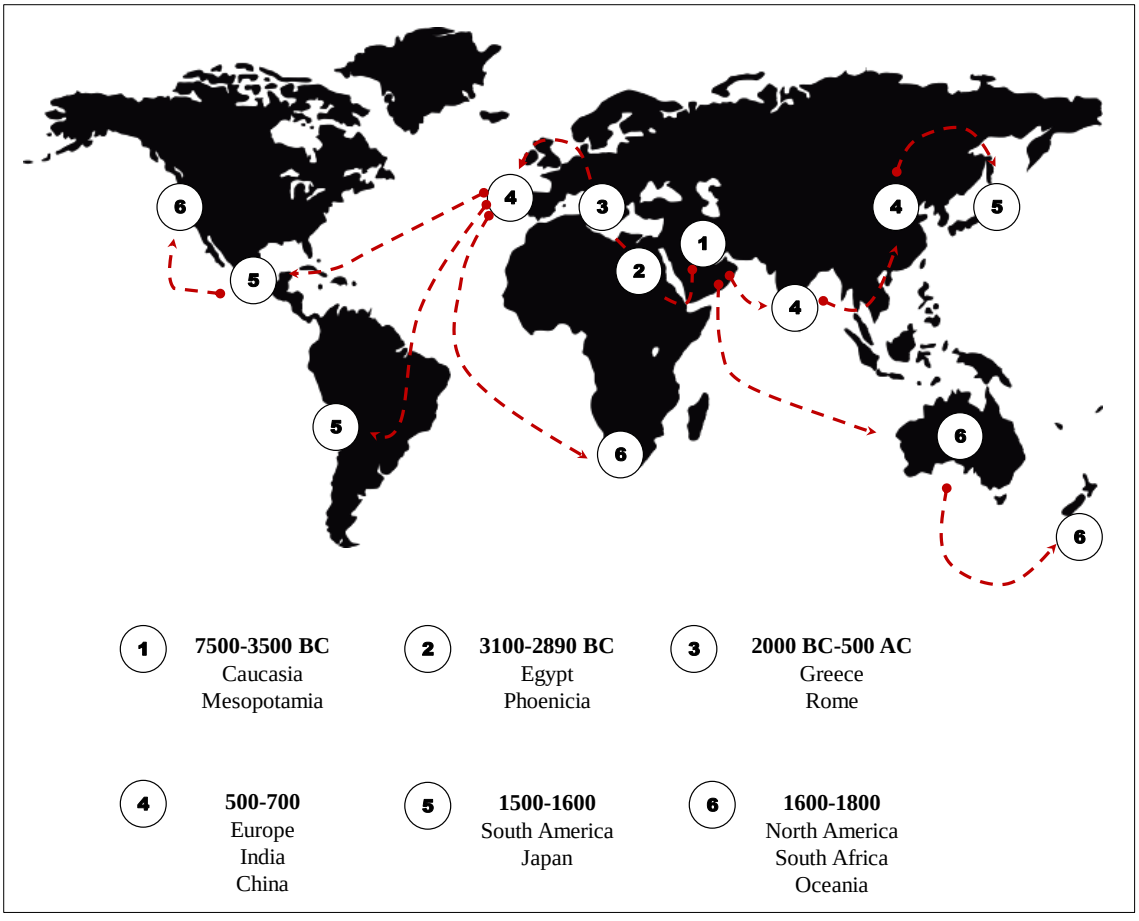


**Figure 2** Vine and wine production expansion through centuries (adapted from (9)).

## 2. Wine adulteration and frauds: historical examples

Adulteration, which was known in olden times as "sophistication", is the most employed word to refer to fraud, committed exclusively for economic gain. In 1820, Frederick Accum suggested that "it is sufficiently obvious that few of those commodities, which are objects of commerce, are adulterated to a greater extent than wine" (10) which has come a fully reinforced statement nowadays. Wine fraud may take several forms, typically chemical falsifications can be committed through the addition of water, glycerol, alcohol, dyes, sweeteners, flavour substances, non-authorised sugars, preservatives and acidity adjustments (4). Currently, determination of wine authenticity is an important issue in quality control due to the potential hazard of some substances which can negatively affect the health and safety of consumers. Apart from such adulteration forms, wine fraud can be committed by the replacement of a lesser quality wine or through misinformation about the wine (i.e. mislabelling) (11). Two glaring examples in recent years are certainly the Rodenstock affair and the case of Rudy Kurniawan, one of the world's most prodigious wine *connoisseurs*, which came to light in 2015 and perpetrated one of the most accomplished wine frauds in history.

However, fraudulent practices relating to wine go far back in history. Already at the Roman Empire, it was popular among winemakers to boil the grape juice in a lead vessel and reduce its volume to one-third. This syrup, called *sapa*, kept wine from spoiling and made its taste sweeter. This practise was widely spread until the 17$^{th}$ century, causing severe lead poisoning among wine drinkers known as the colic of Poitou (12). Watering down and chaptalization – sugar addition - were also commonly used for wine adulteration. As a curiosity, the chaptalization takes its name from Jean-Antoine Chaptal, Count of Chanteloup, Napoleon's Minister of Agriculture. He added cane or beet sugar to wine during the fermentation process to increase its alcoholic grade, reduce the astringency and improve the aroma (13). In the 19$^{th}$ century, aluminium salts were added to enhance the brightness of the wine colour, elderberry extracts to improve its purple colour and barrel aging was simulated using oak wood sawdust, a predecessor of today's legalized technique of oak chips addition while ageing is carried out in stainless steel tanks (14).

The most well-known wine fraud in recent times is the so-called glycol-scandal from Austria in 1985 when around 70 wine producers added diethylene glycol to increase sweetness. However, this substance is not a sweetener itself but it masks the addition of sugar to the wine, making its detection tricky. Traces of diethylene glycol were detected in some German wines which pointed out that these had been illegally blended with Austrian wine. Although diethylene glycol is not a hazardous substance, the scandal had severe consequences on the reputation of Austrian wine industry. A much more serious case is the Italian wine adulterated with methanol in 1986 which

caused several death among consumers due to its high toxicity (11, 14). Between November 2015 and February 2016, in Greece, three illicit factories producing counterfeit alcohol were discovered and the equipment used in the manufacturing process, including labels, caps, empty bottles and more than 7.400 bottles of fake alcohol, was seized. Moreover, in the United Kingdom, authorities recovered nearly 10.000 litres of fake or adulterated alcohol including wine, whisky and vodka (15). It is estimated that approximately 10% of the European wine is of lesser quality in comparison with what is specified in the label but most consumers are not able to detect the fraud as the products cannot be organoleptically differentiated, even by wine experts (11).

In view of the above, it could be concluded that among centuries fraud has always existed and forgers are constantly in search of new ways of counterfeiting wine. There is no doubt that counterfeited wine will continue to haunt the market and consequently, winemakers and wineries will must adapt to the various forms of fraud, mainly by resorting to modern technology (16). The wine industry provides relatively little information about the effects of counterfeiting on their firm to avoid scaring customers and losing their investment. In consequence, they invest considerable sums of money to counter the threat from piracy. In fact, several wineries are already laser-engraving their bottles with unique serial number, adding tracer elements on their tagged inks, using tamperproof capsule seals or experimenting with hologrammed or bar-coded stickers placed half on the bottle-half on the capsule, that serve as identification tag and will shred if removed. There are several enterprises dedicated to the security of industries and markets such as Tesa Scribos®, SICPA and ATT Advance Track & Trace. All of them provide item-specific product markings and systems to ensure individual bottle traceability and counterfeit protection, even refilling of original bottles. These visible or invisible markings, which can be incorporated whatever the part of the wine bottle packaging, cannot be easily reproduced and at the same time could act as a powerful marketing tool.

## 3. Wine fraud financial impact on figures and actions taken

Wine is a beverage which value is influenced by many factors among which the origin, vintage, grape variety and growing conditions play the major role (17) .The European Union leads the world wine market, accounting for 55% of wine growing areas, 60% of production and 70% of exports in global terms, making a considerable contribution of the value of final agricultural output (4). The main EU producers of wine are France (€9 billion), Italy (€8 billion) and Spain (€6 billion) which represent 80% of total EU production of wine in 2013.

The wine industry, therefore, forms an extremely important part of the European Union's economy. Concretely, the EU wine manufacturing industry contains 10.900 enterprises, of which 3.700 are located in Spain, 1.800 in Italy and less than 1.500 in France. Overall, total employment in the EU in the wine manufacturing industry is more than 120 thousand workers (18). Vineyards outside Europe appeared to grow slightly. Particularly, the total vineyard surface area continued to grow in China being the second largest vineyard surface area worldwide with wine production of 11,6 mhl (2014) which placed it in the 9$^{th}$ position of the world ranking. Similarly, China had a very significant rise in its imports (+44%/2014) being the domestic demand the biggest contributory factor (19) (Figure 3).

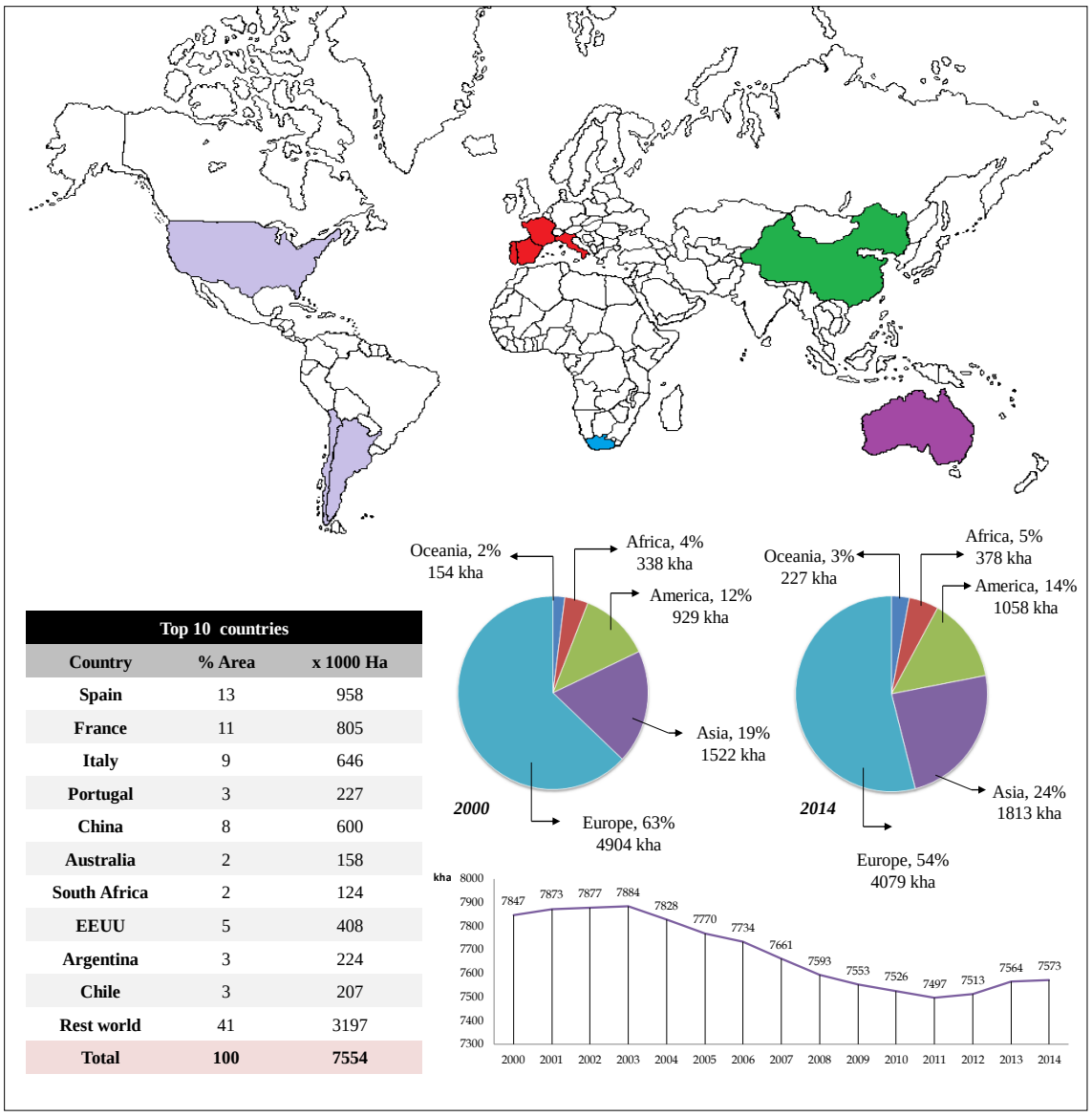


| Top 10 countries | | |
|---|---|---|
| **Country** | **% Area** | **x 1000 Ha** |
| **Spain** | 13 | 958 |
| **France** | 11 | 805 |
| **Italy** | 9 | 646 |
| **Portugal** | 3 | 227 |
| **China** | 8 | 600 |
| **Australia** | 2 | 158 |
| **South Africa** | 2 | 124 |
| **EEUU** | 5 | 408 |
| **Argentina** | 3 | 224 |
| **Chile** | 3 | 207 |
| **Rest world** | 41 | 3197 |
| **Total** | **100** | **7554** |

**Figure 3** Area under vines according to continent/country and year (Source: OIV, 2017).

***Current situation of Spanish wine sector***

According to the Ministry of Agriculture, Fisheries, Foodstuffs and Environment, there are 957.573 ha dedicated to the cultivation of vineyard, being the country with greater extension of vineyard of the EU (25% of EU's total area) which represents the 13.4% worldwide total, followed closely by France and Italy (20).

Spain has a total of 90 production areas of quality wines with Protected Designations of Origin (*Denominaciones de Origen Protegida*, DOP) of which: i) 67 are considered Designation of Origin (*Denominación de Origen*, DO), ii) 2 are considered Designation of Qualified Origin (*Denominación de Origen Calificada*, DOCa), Rioja and Priorato respectively, iii) 7 are Quality Wines with Geographical Indication and iv) 14 are Table Wines. Absolutely all of them follow the European model for production which ensures a strict control over the quantity of produced wine, the good oenological practices and the quality of the wines of each sector. All mentioned concepts are thoroughly detailed in the law 24/2003 about the Vine and Wine published in BOE 11-07-2003) (21).

The cultivation of the grapevine is spread over several Communities among which Castilla La Mancha stands out as it owns the 48.8% of the surface of national vineyard. It is followed far behind by Extremadura (8.6%), Valencia and Castilla y León (7%), Catalonia (5.7%) and La Rioja (5.1%). In this last region, the vineyard represents the 30.6% of the community's farmland (Figure 4).

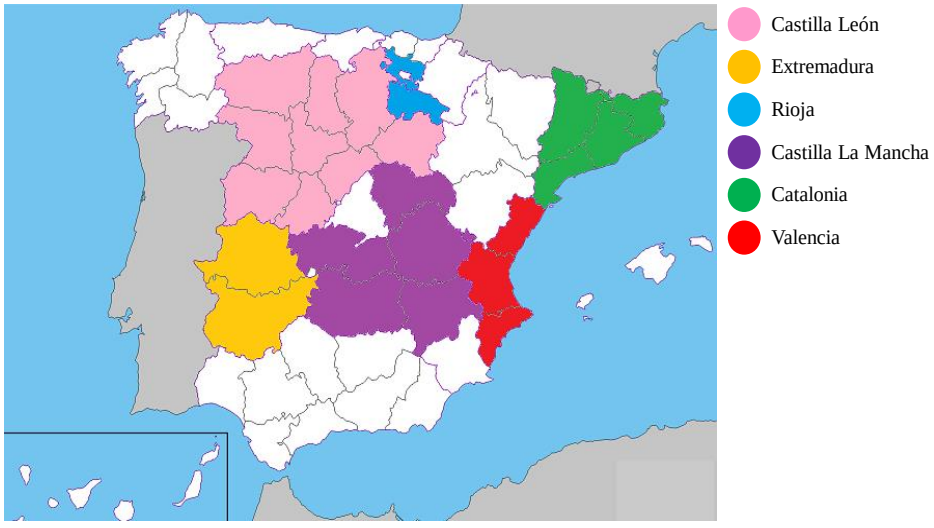


**Figure 4** Area under vines in Spain.

In the last decade, in the Basque Autonomous Community, the wine sector of the region of Rioja Alavesa has experienced a spectacular qualitative leap, standing at the forefront of the European zones that produce quality wines. The exports of wine from the Basque Country, particularly those with a designation of origin, have grown considerably in terms of volume and improved their value and price stability, unlike the trend followed by the Spanish wines. High quality bottled wines are the engine of Basque wine exports being almost the 84% of the revenues. In 2015, historical highs were recorded which exceed 203 million euro. The Basque Country accounted for 14.2% of the total value of bottled wine with denomination of origin exported by Spain in 2015. Rioja Alavesa wine largely marks the evolution of the Basque wine export trade, accounting for more than 90% of the total value. According to the data obtained, the wine sector, with a total of 378 wineries, comprises 15% of the gross domestic product (GDP) of the sub-area, reaching 50% if the auxiliary industry is included.

***Current situation of French wine sector***

Based on FranceAgriMer (*Etablissement National des Produits de l'Agriculture et de la Mer*), France had 755.200 ha of vineyards for wine production in 2013 and the 62% of them were devoted to wines produced in denominated regions or areas (*Vins de Qualité Produits dans des Regions Determinés*, VQPRD). These wines include Appellation of Origin wines (*Appellation d'Origine Controllée*, AOC) and Superior Quality Wines (*Appellation d'Origine-vin de qualité supérieure*, AO-VDQS). These wines are controlled and officially agreed to the French Institute for Appellation of Origin (INAO) (22). AOC wines, which nearly reach the 45% of French wines and spirits, have a label which certifies the wine characteristics, including region of origin, manufacturing process, character and alcohol content. AO-VDQS wines, instead, are also provided with a label which certifies the origin but is less restrictive in testing. Figure 5 shows the wine production in France during the last decade.

Among Table Wines, *Vin de Pays* Wines, which are named IGP (*Indication Géographique Protegée*), should originate exclusively from the region specified on the label and has different status from the AOP (*Appellation d'Origine Protegée*). 2016 European Union vinified production is likely to reach 162 mhl from which 43.5 mhl were produced in France, a non-negligible decrease (-7%) compared to 2015. Figure 5 shows the French wine production tendency in the last decade according to the data extracted from the OIV (updated data in 15/03/2016).

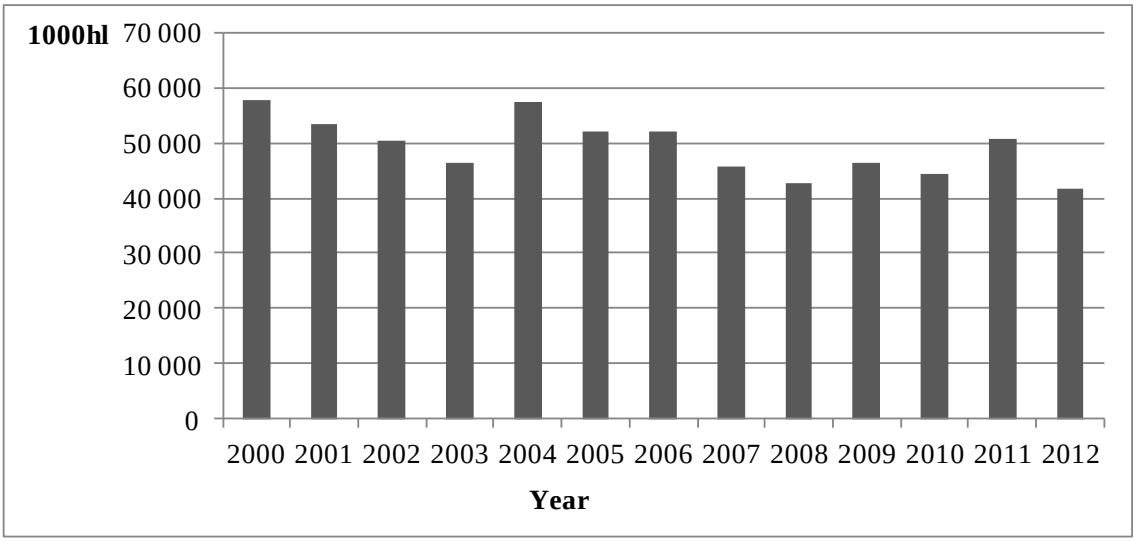


**Figure 5** French wine production from 2000-2012 (Source: OIV, 2016).

The main grape growing and wine production regions of France are the following (Figure 6): Alsace (15300 ha), North-East region (4460 ha), Champagne (34300 ha), Bourgogne (28000 ha), Beaujolais (17000 ha), Val-de-Loire (65000 ha), Bordeaux (113000 ha), South-West region

(65000 ha) and South-East (95000 ha), Vallée du Rhône (70000 ha), Languedoc (232000 ha) and Roussillon (33000 ha) (23).

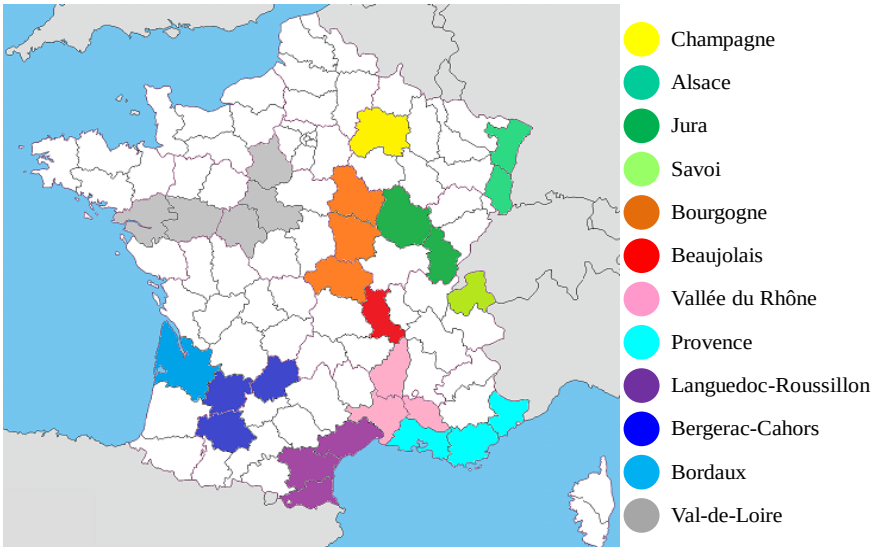


**Figure 6** Area under vines in France.

Counterfeiting and piracy are terms to describe a range of illicit activities linked to intellectual property rights (IPR) infringements. This issue is especially sensitive in the food and drink sector because of the possibility of contamination or the use of poor-quality ingredients in products intended to be for human consumption that could lead in health related problems. Alcohol products are prime targets for counterfeiters in the drinks sector, being the wine and spirits the most affected items due to their brand value and excise duty of the final price (24).

The great wines are particularly exposed to counterfeiting, mainly coming from the Asian market. China has surpassed France as the largest consumer of red wine in the world. This booming consumption has made wine counterfeits grow at the same pace as their sales. The National Committee of Foreign Trade Advisers of France (*Comité National des Conseillers du Commerce Extérieur de la France*, CNCCEF) published in May 2015 a report stating that wine fraud is not just a matter of a few bottles but also includes an entire clandestine industry. According to the Wine and Spirits Commission of the CNCCEF, there is at least one bottle of forged wine for each bottle of original French wine in China (Figure 7). Although China is not the only supplier of counterfeited wines, the rapid growth of the wine market in this country and the absence of laws protecting intellectual property have triggered the counterfeit market.

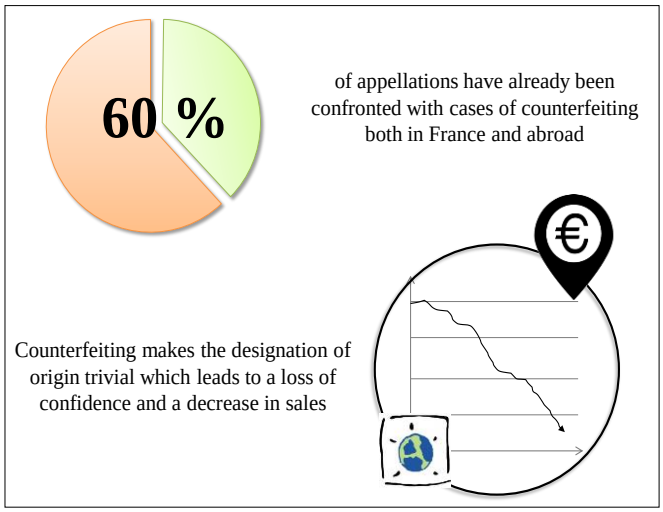


**Figure 7** Scope of counterfeiting (Source: CNAOC).

The geographical indication (GI) is an intellectual property right expressly recognized in the 22 article of the World Trade Organization (WTO) agreements: *"Geographical indications are, for the purposes of this Agreement, indications which identify a good as originating in the territory of a Member, or a region or locality in that territory, where a given quality, reputation or other characteristic of the good is essentially attributable to its geographical origin"*. The scope of this definition also includes the notion of appellation of origin which was defined in the Lisbon Agreement (1958): *"An appellation of origin is the geographical name of a country, region or locality, which serves to designate a product originating therein, the quality and characteristics of which are due exclusively or essentially to the geographic environment, including natural and human factors" (25).*

According to the European Union Intellectual Property Office (EUIPO), the major problem related with the Intellectual Property Rights (IPR) in the EU is the lack of knowledge in relation to the precise scope, scale and impact of IPR infringements. The challenge remains on the absence of a consensual and consistent methodology for collecting and analyzing data on counterfeiting and piracy. Different approaches have been used, such as surveys, mystery shopping and monitoring of online activities. However, the collection of data for hidden and unregulated shadow secret activities is an extremely challenging issue. In summary, it is estimated that the legitimate industries lose approximately €1.3 billion of revenue annually due to the presence of counterfeit spirits and wine in the EU marketplace, corresponding to 3.3% of the sector. These lost sales translate into direct employment losses of approximately 4,800 jobs (18, 26).In the context of this globalization of trade, the International Organization of Vine and Wine (OIV, *L'Organisation International de la Vigne et du Vin*) was created in 2001 and replaced the International Vine and Wine Office established by the Agreement of 29 November 1924, becoming the scientific and technical reference organization for the entire viticultural field, with recognized competence for its work concerning vines, wine, wine-based beverages, grapes, raisins and other vine products. Its 46 Member States account for more than 85% of global wine production and nearly 80% of world consumption. There are also 10 non-governmental international organizations that participate as observers. Among its duties, the OIV defines the characteristics of vitivinicultural products and their specifications, and contributes to the promotion of good regulatory practices in order to ensure fair trading, as well as the integrity and sustainability of different viticultural products on the global market. The OIV contributes to the harmonization and definition of new international standards in order to improve conditions for producing and marketing vitivinicultural products (27).

Meanwhile, the EFOW (European Federation of Origin Wines) was firstly funded in 2003 when the French *Confédération Nationale des producteurs de vins et eaux de vie de vin à Appellations d'Origine Contrôlées* (CNAOC) and the Italian *Confederazione Nazionale di Consorzi Volontari per la Tutela delle Denominazioni Italiane di Origine* (FEDERDOC) decided to work jointly on promoting their views towards EU decision-makers. Further to the 2006, European Commission proposals for a wine reform, organizations in charge of the appellation of origin wines from other EU Member States decided to join the non-profit platform: the Spanish *Conferencia Española de Consejos Reguladores Vitivinícolas* (CECRV) , the Portuguese *Instituto dos Vinhos do Douro e Porto* (IVDP) and finally, the Hungarian *Hegyközségek Nemzeti Tanácsa* (HNT). Together the five associations lobbied the European Commission, the European Parliament and the Council of Ministers to secure the enhancement of origin wines' protection and promotion. Indeed, EFOW

is the voice of European origin wines, its mission is to promote the interests of European wines with an appellation of origin and/or a protected geographical indication towards EU and international institutions and facilitate the exchange of ideas and the adoption of common positions between organizations in charge of origin wines. At European level, the Regulation (EC) nº479/2008, which has been recently integrated into the Single Common Market Organization (CMO) Reg. (EC) nº1234/2009, is one of the largest and more complex CMO in the Common Agricultural Policy (CAP). Further action at international level, the most important legal framework for the protection of origin wines is the WTO Agreement on Trade-Related Aspects of International Property Rights (TRIPs) which has a specific section dedicated to geographical indications (GIs) (28).

## 4. Wine authentication methods

Wine has an economic value associated with luxury products and the global wine market needs objective analysis tools for authentication, making international trade more transparent. The globalization of food markets and the relative ease with which raw materials are transported through and between countries and continents present an unequalled chance to misdescribe the origin of foodstuff. In addition, the interest of consumers in high quality foods with an unequivocal geographical identity has grown considerably. Therefore, there is a growing requirement to have access to reliable analytical methods that can verify origin and composition labels on foodstuffs (29). A greater number of studies have been performed on the provenance and composition of wine due to the relatively high value of wine in comparison with other agricultural products and the fact that high quality wines producing in particular regions have been long recognized through European legislation (30). Single values or parameters are often not enough on their own to detect fraudulent wine or to determine product identity with respect of the labelling. Two important concepts in this area are traceability and authenticity. Traceability means to individuate chemical markers to find a link among the geographical zone where a wine is made and the final product of the winemaking process, while authenticity refers to the possibility to identify and discriminate true samples from false samples by the verification of the features declared in the label and can be defined as classification issue (31).

This chapter section concerns a brief research of the current analytical techniques that are being used for the determination of geographical origin, real composition according to the labelling and vintage of wine. In fact, the information given on the wine label is directly related to consumer's expectations concerning the sensory and quality criteria. The principles of the analytical techniques together with their advantages and drawbacks will be briefly discussed as well. The

analytical approaches have been subdivided in two groups; invasive verification methods for which it is necessary to open the bottle for wine sampling and non-invasive verification methods in which wine is directly analyzed through the packaging. Then, chemometric analysis of the data is an indispensable tool to detect subtle differences among samples. If the measured components are highly discriminatory, they will form a characteristic "fingerprint" that could be related to the geographical origin of the sample. Thus, chemometrics provides the ability to clarify these patterns and offers an inestimable help when the number of components necessary to differentiate samples from different geographical origins increase (32). The statistical data analysis involves methods of univariate descriptive and exploratory data analysis as well as multivariate methods (33-35). Statistical data analysis techniques have been widely increased for the classification of wine in recent years and a number of examples have been reported in the literature, which will be cited when different analysis techniques for wine analysis are discussed (36).

Several analytical methods have been developed and reported for physical, chemical and microbiological analyses of wine, during all stages of its production. The Compendium of International Methods of Analysis of Wines and Musts was firstly published by The International Organisation of Vine and Wine (OIV) in 1962. It proposes a list of analytical methods and procedures aiming its standardisation for scientific, legal and practical interest to facilitate international trade (37). Although recognized by the international community as robust and precise, some of these reported methodologies are slow, expensive, time-consuming, laborious, destructive and toxic waste generators, limiting their application to a restricted number of parameters and making them inappropriate to fulfill all the winemaking industry demands (38).

An overview of several characteristics of the analytical techniques used for the determination of the geographical origin and composition of wine is given in Table 1.

**Table 1** Analytical techniques used for wine verification. Adapted table from (32).
Favorable (+), moderate (+/-) and unfavorable (-).

| | Analytical technique | Sensitivity | Simplicity | Time analysis | Cost | Analytes |
|---|---|---|---|---|---|---|
| Invasive analytical techniques | ***Mass spectrometry*** | | | | | |
| | ICPMS | + | +/- | + | - | Elements |
| | IRMS | + | +/- | +/- | - | Isotopes |
| | GC-MS | + | + | +/- | - | Volatile molecules |
| | HPLC-MS | + | + | +/- | - | Non-volatiles molecules |
| | ***Spectroscopy*** | | | | | |
| | NMR | - | +/- | +/- | - | Molecules |
| | Molecular spectroscopic techniques | +/- | + | + | + | Molecules |
| | ***Other*** | | | | | |
| | DNA analysis (PCR) | + | +/- | +/- | + | Molecules |
| | Sensory | +/- | +/- | - | - | Mouthfeel sensation |
| | Sensor | - | + | + | +/- | Volatile |
| Non-invasive analytical techniques | ***Radioactivity*** | + | +/- | +/- | - | Isotopes |
| | ***Molecular spectroscopic techniques*** | +/- | + | + | + | Molecules |
| | ***NMR*** | - | +/- | +/- | - | Molecules |
| | ***Other*** | - | +/- | + | - | Dielectric/ diamagnetic properties |

### 4.1 Invasive verification methods: direct wine analysis

Conventional invasive techniques are commonly used for wine verification purposes, which are mainly based on liquid sampling and consequently require opening the bottle. The chemical composition of wine includes several type of molecules derived from three different sources: the grape berry, the yeast strain used in fermentation and the containers used for winemaking and storage (39). The combined sum of these molecules present in the wine describe all wine-specific features such as cultivar, vintage and origin (40).

#### 4.1.1 Mass spectrometry for elemental analysis

Wine reflects the composition of the soil, atmosphere and the climate where the grapes have been grown. Thus, using mineral determinations and their isotopic ratios is a must for determining their geographical origin and obtaining fingerprints of the elemental pattern. In general, mass spectrometry is applied to elucidate the composition of a sample by generating a mass spectrum representing the masses of the sample components. Several atomic spectrometry methods have

been developed and successfully employed for wine trace and ultra-trace mineral analysis as this powerful analytical tool gives access to the majority of elements of the periodic table and their isotopes. Trace and ultratrace elements act as markers, providing information on the origin of raw materials with which a wine was prepared (41, 42) .

Inductively coupled plasma mass spectrometry (ICPMS) has shown to be a valuable tool for multi-elemental analysis and discrimination of wines from different geographical origin (43). In fact, due to high sensitivity, ability to measure isotopes and multi-elemental feature is one of the most appropriate techniques for the determination of trace elements in wine (44). Elemental composition has to mainly sources: i) natural or endogenous sources, that represents the uptake of minerals from soil which are after transported through the roots and plant to the grapes and does not change during winemaking process, ii) winemakers interventions in the vineyard (fertilizers, pesticides/herbicides) and technological processes applied during manufacturing and iii) environmental pollution (45-47). ICPMS has been widely used to screen the geographical origin of wine by the analysis of numerous inorganic elements and obtaining fingerprints of the elemental pattern (48-54). Figure 8 shows the ICP ionization source coupled to different mass analyzers which have been used for wine elemental analysis.

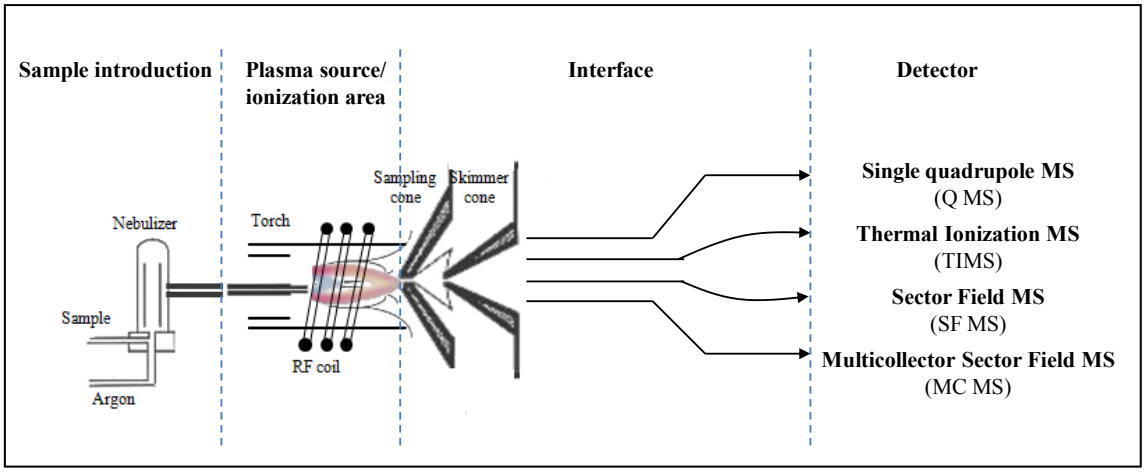


**Figure 8** Inductively Coupled Plasma based mass spectrometry technique for trace element and isotope analysis in wine**.** The sample is atomised in a high-temperature argon plasma and the elemental ions are detected based on their mass-to-charge ratios (m/z). This analytical technique can be coupled to chromatographic separation techniques depending on the nature of the analyte and the target of the analysis.

Isotope Ratio Mass Spectrometry (IRMS) is a useful technique to differentiate chemically identical compounds based on their isotope content which could be indicative of the geographical origin and production or manipulation methods (30, 55). The implementation of stable isotope applications in official food analyses began in 1990 (56). Stable light isotope ratio determination

such as carbon ($^{13}C/^{12}C$), nitrogen ($^{15}N/^{14}N$), oxygen ($^{18}O/^{16}O$, $^{18}O/^{17}O$, $^{17}O/^{16}O$), hydrogen ($^{2}H/^{1}H$) and sulphur ($^{34}S/^{32}S$, $^{34}S/^{33}S$, $^{36}S/^{34}S$) are of major interest in biosynthetic and biochemical processes. They are employed for identifying the origin of alcohol based on the botanical origin or verifying compliance with specific regulations which include chaptalization and watering down (31, 57).

Additionally, there are several studies in which the determination of lead ($^{206}Pb/^{207}Pb$) and strontium ($^{87}Sr/^{86}Sr$) isotope ratios in wine have been used for origin traceability (58-63). Lead in wines results almost exclusively from anthropogenic air pollution and strontium isotope ratios are a characteristic of the soil. Therefore, the only determination of lead and strontium allows a simple and full characterization of wine, the first giving information about the air and the second about the soil. Furthermore, the study of other elements (Nd, Sm and U) allows other geochemical information, such as the age of a soil and a probable location where the vine was grown (64).

### 4.1.2 Mass spectrometry for molecular analysis

In order to assure the quality control in the viticulture and oenology fields, mass spectrometry seems to have a very important role (65, 66). The metabolomics approaches offer the opportunity to study as many metabolites as possible in order to discriminate or classify wine according to variety, origin, vintage and quality. It also enables to check all time-related metabolic changes of wine throughout its elaboration process to assure wine authentication and to prevent adulteration (67, 68).

Gas chromatography-mass spectrometry (GC-MS) and liquid chromatography-mass spectrometry (LC-MS) techniques, which can be performed in multiple mass spectrometry (MS/MS and $MS^n$) modes according to the detector (Figure 9), are nowadays the more effective, powerful and robust analytical approaches for the structural characterization of low molecular weight compounds such as the aroma compounds (69, 70), polyphenols (71), pesticides and compounds from the yeast and bacterial metabolism (72, 73) in grapes and wine.

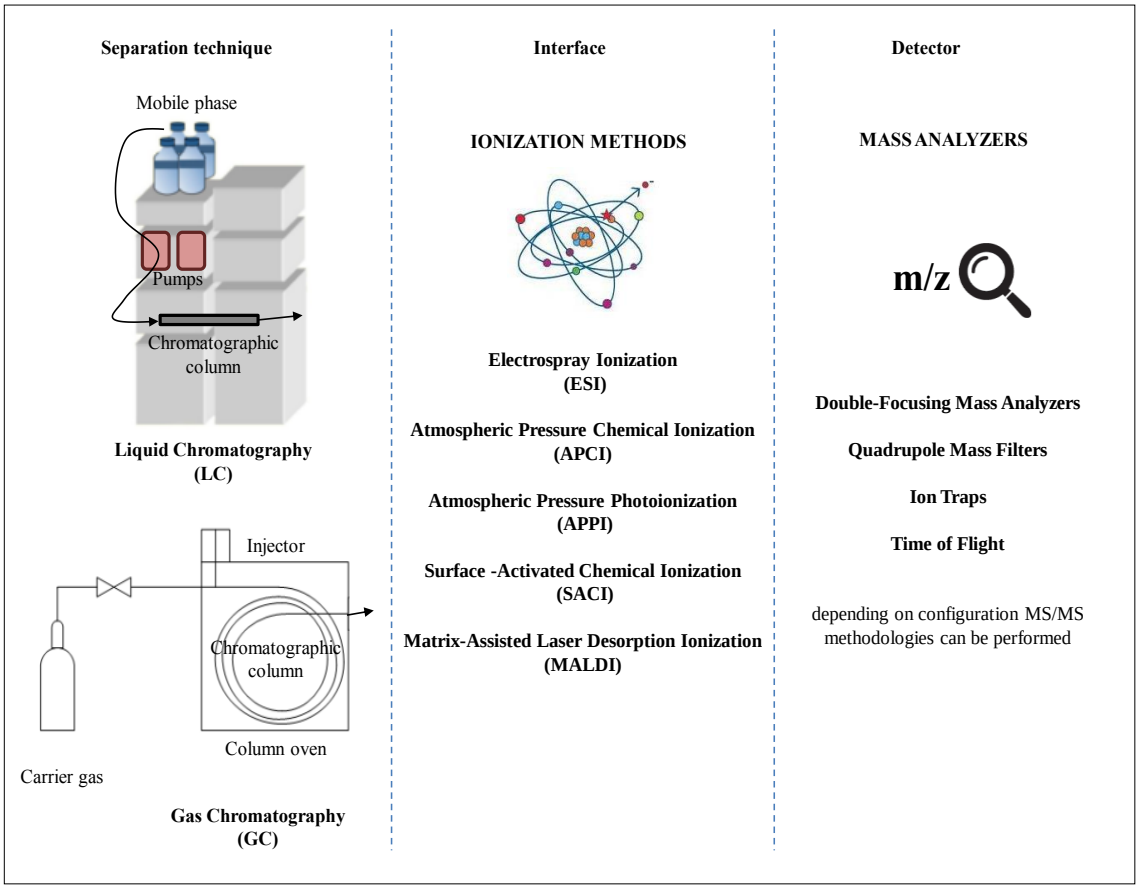


**Figure 9** Chromatography coupled to mass spectrometry techniques for molecular analysis in wine. Firstly, analytes are separated in the chromatographic column. After, they are ionized in the interface and finally, detected according to m/z ratio.

### 4.1.3 Spectroscopy

#### *4.1.3.1 Nuclear Magnetic Resonance (NMR)*

Nuclear Magnetic Resonance (NMR) is based on the measurement of absorption of radiofrequency radiation by atomic nuclei with non-zero spins in a strong magnetic field. The absorption of the atomic nuclei is affected by surrounding atoms, which cause local modifications to the external magnetic field. Among nuclei with non-zero spin, the isotopes of hydrogen-1 and carbon-13 are the most used but other isotopes such as nitrogen-15, oxygen-17, fluorine-119 or phosphorous-31 are also widely employed. The official European method for detecting illegal chaptalization of wine was developed in the early 90s and is based on measuring the 2H/1H ratio at the methyl and methylene positions of ethanol by Deuterium –Nuclear Magnetic Resonance spectroscopy ($^2$H-NMR) (Commission Regulation No 2348/91). This method is based on the SNIF-NMR® method, pioneered by Professor G.J. Martin of the University of Nantes., which offers a means of verifying botanical, synthetic and geographical origin of a product (56). Later on, Eurofins Analytics purchased the rights to SNIF-NMR® and provided a comprehensive

authenticity and quality control screening test by the way of the Proton Nuclear Magnetic Resonance Profiling ($^1$H-NMR) Wine Screener. Using a unique fingerprint to analyze against a catalogue of authentic samples, this test can confirm grape variety and origin, detect if there has been any adulteration and with certain white wines even confirm the year of vintage. In addition, the combination of 1H NMR and 13C NMR with chemometric data analysis is a powerful tool for obtaining the fingerprinting according to the wine geographical origin (30).

*4.1.3.2 Molecular spectroscopic techniques*

Vibrational spectroscopy comprises a number of techniques including, Fourier transform infrared spectroscopy (FTIR) (74, 75), UV-Vis-NIR spectroscopy (76-80) and Raman spectroscopy (81, 82). Both techniques are considered to be complementary as weak bands in IR spectrum are among the strongest bands in the Raman spectrum. Moreover, they do not require sample preparation and they are non-invasive and non-destructive. These techniques are based on the interaction of an incident excitation laser light with the electrons of atoms and molecules. Each functional group of a molecule has unique vibrational frequency and when the effects of all different functional groups are taken into account together, the result is a unique molecular fingerprint of the identity of the sample (83, 84).

### 4.1.4 Other

*4.1.4.1 Sensory analysis*

Sensory analysis is considered as an important technique to determine a product quality and the simplest wine verification method which has been in use since man first fermented grapes (85) with the aim of comparison, setting price, the determination of provenance or the detection of defects. Grape and wine flavour is complex and many different sensory modalities (i.e. taste, smell, chemesthesis, tactile and vision) and several chemical compounds have influence on its perception. Specifically, ethanol, glycerol, residual sugars, polysaccharides, carbon dioxide and polyphenols are the most cited wine components for providing a sensorial response. Moreover, interactions and synergies between compounds have a stronger influence on the organoleptic characteristic than individual components (86). Thus, the mouthfeel is defined as the group of sensations characterised by a given response in the mouth (87). Even following the appropriate quality assurance/quality control procedure (ISO 17025) is mandatory in ensuring confidence in results; sensory evaluation comprises a set of techniques for accurate measurements of human responses to food (88). Nevertheless, the evaluation of wine quality by a sensory panel made up of trained experts may come to be subjective, expensive and time consuming. Over the last few decades, electronic noses (e-noses) and electronic tongues have been developed for quality assurance. On the one hand, multisensory systems used in electronic noses are based on an array

of electronic semi-selective gas sensors of the volatile compounds present in the headspace of a wine sample capable of recognizing simple or complex odours (89). They have been successfully applied to the quality control, aging control and detection of fraudulence of wine (90). On the other hand, electronic tongues are a multisensory system in which electrochemical sensors (potenciometric, amperometric, voltametric or impedimetric) are the most widely used (91).

#### *4.1.4.2 DNA analysis*

A wide diversity of *Vitis Vinifera* L. varieties can be used in the production of wine even though few of them are of commercial importance. Since it was found that wines have small amount of DNA from grapes, their analysis is done in order to identify the variety of the wine. In fact, the recognition of varietals and elucidation of blends is performed according to European Regulation (RCE 491/2009 and 207/2009) which specifies that varietal wine must consist of at least 85% of the variety mentioned (92). Several methods have been used for varietal elucidation purposes with varying degrees of success but microsatellite markers (Simple Sequence Repeat, SSR) are universally used for the identification of the grape varieties (93, 94). However, the difficulties like low content of DNA in wine and the degradation of residual DNA, contamination, modification during processing and the presence of inhibitors for the PCR reaction are the most limiting factors in this field (95). Thus, modification in DNA extraction methods (96), the use of markers targeting mitochondrial or chloroplast genomes (97, 98) or the development of new set of PCR primers (99) could become an alternative to deal with the mentioned drawbacks.

### 4.2 Quasi non-invasive verification methods

Unfortunately, the analytical techniques described in the previous section generally violate the wine bottle cork and seal for sampling. Consequently, they devaluate the wine making it less attractive to investors prepared to spend huge amounts of money for a single bottle. For that reason, wine direct analysis through packaging or the analysis of the packaging itself for verification and traceability purposes represent a big challenge from the analytical point of view and it is a great step forward against counterfeiting. However, some sampling techniques using needles punching the capsule and the cork with limited damages have been reported (100). In addition, a new system for extracting wine directly from the bottle has been recently commercialized. Coravin ® has been designed by Greg Lambrecht from the Technological Institute of Massachusetts. With this system, there is no need to remove the cork or the capsule, simply it must be placed on the capsule and the cork stopper, attached to the neck of the bottle, and proceed to operate the hydraulic system that inserts a needle inside the bottle. Interior atmosphere is pressurized with argon. After the pressurization, the wine will flow through the inserted needle filling the cup. When the accessory is removed, the cork will re-seal, avoiding

wine leaking and maintaining its initial properties as the oxygen could not come into contact with the wine and start the degradation process.

### 4.2.1 Wine analysis through the packaging

*4.2.1.1 Radioactivity*

The radioactivity process is based on the spontaneous transformation of a nucleus into a daughter nucleus with emission of a beta or alpha particle. These decays are followed by several gamma rays whose energies are typical of the decaying nucleus. The detection of these rays with a high energy resolution gamma spectrometer indicates the presence of these radioactive nuclei in the sample. In addition, the intensities of these lines are directly related to the amount of radioactive nuclei ($Bq \cdot kg^{-1}$) (101). Since the first nuclear tests of the 1950s and 1960s and the Chernobyl accident (1986), large quantities of artificial radionuclides were released into the atmosphere and nowadays those having a long radioactive period such as Cs137 still remain diluted in the upper atmosphere. Then, Cs137 nuclei falls to the earth and is deposited on plants and animals on the soil surface because of rain, aerosols and dust. As a consequence of this deposition on vines and grapes, the radioactivity is locked in the wine bottle during the winemaking process and storage. However, the radioactivity level is extremely low ($< 1\ Bq \cdot L^{-1}$) and it was not until the late 1990s and the development of low background germanium (Ge) semiconductor detectors when such low levels of radioactivity could be measured to highlight the presence of Cs137 and variation in its activity as a function of years (102). Fahrni et al. (100) developed a novel non-invasive procedure which relies on radiocarbon dating of the trace amounts of ethanol and other gases that diffuse into and through the cork as bottled wine ages and matures.

*4.2.1.2 Molecular spectroscopic techniques*

The possibility of determining wine chemical composition directly from the bottle represents an ideal methodology for the wine industry. Vibrational spectroscopy could provide fast, nondestructive and non-invasive measurements to detect unwanted problems in bottled wine prior to retail sale (38). Nowadays, low cost and miniaturized portable spectrometers are increasingly available, opening a wide range of applications for these techniques. Visible and short wavelength near-infrared (Vis-NIR, $\lambda$ 600-1100 nm) and Raman spectroscopy have been successfully employed for screening purposes for the estimation of alcohol content, total sulfur, free sulfur and pH in intact bottles. However, the non-invasive approach is only possible with optical techniques if the vessel is made of a transparent material or has a suitable window (103, 104). Spatially Offset Raman Spectroscopy (SORS) is based on the collection of Raman scattered light from surface regions that are laterally offset away from the excitation laser spot on the sample. When compared with conventional Raman, a substantially enhanced sensitivity is achieved by the

technique's inherent ability to effectively suppress fluorescence and Raman contributions originating from the wall of the container. This technique has been applied to investigate liquid explosive precursor mixtures in containers, mainly focused on challenging mixtures of hydrogen peroxide solution, a critical component of a number of liquid explosives (105-107). Despite their potential and complementarity, few studies are published in the literature on the use of IR and Raman spectroscopy for the analysis of organic compounds of bottled wine (83, 108).

*4.2.1.3 Nuclear Magnetic Resonance (NMR)*

Nuclear Magnetic Resonance is one of the most powerful analytical tool to study the structure of molecules in solids, liquids and gases with high resolution. The NMR study of wine is well documented and it has been also applied for the analysis of wine through the glass with the aim of determining wine devaluation due to pollutants, vinegarization/maceration and oxidation of ethyl alcohol into acetic acid and acetaldehyde mediated by leaky corks (109-111).

*4.2.1.4 Other*

Harley et al. employed a low frequency spectrometer capable of non-invasively and non-destructively screening the dielectric or diamagnetic properties of full intact bottles of wine by the use of low frequency radio waves. In the first one, the pass of the electricity through the wine is monitored on applying an electric field. In the second one, the frequency dependent magnetic properties of wine in sealed intact bottles are probed by monitoring the effect of the frequency dependent magnetic susceptibility on the amplitude and phase of an applied oscillating magnetic field. Component analysis was used to compare and contrast sealed bottles of wine and reduce the collected data (112, 113).

### 4.2.2 Packaging analysis

Among the elemental analytical techniques used for the elemental analysis of glass, proton induced X-ray emission (PIXE) and X-ray fluorescence (XRF) are multi-elemental, fast and non-destructive techniques for the determination of elemental concentrations. In addition, PIXE can be also applied to the label pigments with great precision (114). However, due to the need of a complex installation and a high running cost, they are not the first choice for the direct analysis of glass. Nonetheless, it may be noted that handheld portable XRF analyzers have been recently developed for rapid *in situ* measurements. They are small, lightweight and easy-to-use and provide exceptional measurement speed and sensitivity, enabling low detection limits for optimum screening accuracy. Vibrational spectroscopy based methodologies, in which Raman spectroscopy is included, enable the estimation of several properties from a single measurement in a short period of time (≈ 2 min per spectrum). Raman spectroscopy can be also employed as an

efficient and complementary analysis tool allowing chemical identification of pigments present in the composition of the labels' inks and capsules (115). In addition, it does not require sample preparation, is non-invasive and non-destructive due to the coupling of a Raman spectrometer with other technologies such as low cost lasers and optical fibers aiming to develop miniaturized portable instruments with increased sensitivity and robustness, therefore opening a wide range of applications. However, the fluorescence obscuring the Raman spectrum, produced by the sample itself, is one of the main limitations of Raman spectroscopy (38). Vis-NIR infrared spectroscopy combined with multivariate statistical analysis has been also applied for identifying the geographical origin of cork from the most representative cork-producing areas in the world, with at least 90% of the samples being correctly classified (116). Therefore, it is possible to identify fraud by comparison of a suspicious bottle with an original. In case of not having a reference bottle it is possible the identification of different pigments, dyes and printing methods to go back to their time of creation.

However, taking into account the characteristic of each constituent and the advantages and main drawbacks of previous analytical techniques for packaging analysis, laser ablation sampling coupled to inductively coupled plasma mass spectrometry (LA-ICPMS) seems to be an alternative to be considered. When laser pulses interact with the sample, tiny particles are formed and transported to the argon inductively coupled plasma (ICP) where they are atomised and atom ions are detected according to their mass to charge ratio by the mass spectrometer (MS). This tool of characterization at the micro and macro-scale shows advantages in terms of sample integrity preservation, sensitivity (the limits of detection can be as low as tens attograms, $10^{-18}$ g in some conditions), spatial resolution (from 5µm to several mm), versatility (every type of solid sample can be analysed) and fast sample throughput (the analysis takes few minutes since no sample preparation is needed) which makes this technology a tool of choice for quasi non-destructive analysis particularly suitable for precious samples and which has not equivalent in terms of performance to date (117). Therefore, it is not surprising that this analytical technique has been increasingly used and accepted in forensic science. Broken glass is often found as physical evidence in different scenarios surrounding a crime or delict and its varying composition allows it to be discriminated by physical, optical and elemental characteristics. Numerous studies documented the accuracy, precision, selectivity, detection limits and discrimination potential of glass (118, 119). Moreover, glass is considered as a model matrix for LA-ICPMS due to its homogeneity, rigidity and chemical composition, which makes it easy to ablate and fractionation can be controlled with appropriate instrumental parameters.

A brief description of each packaging constituent is given in the sub-sections below.

*4.2.2.1 How the glass could help in wine authentication?*

Glass is known to have been employed for wine storage since the Roman era and its production processes have evolved from the craftsmanship techniques of the 18th century to the computer controlled industrial process of the 21st century. In fact, glass is the best material to preserve foodstuff as it is chemically inert and does not require protective layer between content and container. Container glass is made of sand (silicon), lime, soda, alumina and other fining agents (called *batch*) melted together at a fusion temperature around 1500ºC (120). In addition, metal oxides are added to modify colour (iron, chromium, selenium, manganese, etc.) or mechanical/thermal properties (titanium, boron) (121). Recycled glass (called *cullet*) is increasing being added to the batch to reduce melting point temperature and save cost in pure raw materials, leading to the addition of traceable minerals. Each wine bottle thus has a characteristic signature according to the factory it came from and can reveal a period of time when it was produced (122, 123). Glass packaging production is a widespread industry in Europe, with manufacturing operations occurring in 21 EU Member States. There are more than 60 corporate members belonging to approximately 20 independent corporate groups according to European Container Glass Federation (FEVE).

*4.2.2.2 How the paper and the ink could help in wine authentication?*

The first contact that consumers have with a wine bottle is visual. The primary function of the label is therefore to inform the consumer about the wine. It covers part of the surface of the bottles, showing information required by the regulation. Wine labelling often indicates the year of production, grape variety and production site *"mise en bouteille au château"*- often an indicator of a high quality product (23). Counterfeit relabelling, repackaging of products and the abuse of certification labels with false designation thus induce misleading in the consumer which could affect its health and safety due to the possibility of contamination or the use of poor-quality ingredients (124).

Papermaking is considered to have originated in China and for many centuries it has been the main material for recording cultural achievements all over the world. Papermaking technology and manufacturing has undergone significant advances in the last two centuries in response to economic and environmental reasons. These innovations and modifications can establish the earliest date or period when a particular sheet of paper was manufactured. Paper is mostly made from cellulose with small amounts of organic and inorganic additives, which allows its identification and characterization (125). If a label can be analyzed and compared to an original, both the determination of the percentage of fibres and the determination of the paper composition could be used as comparators and be employed for anti-counterfeiting purposes.

The ink was first manufactured in both ancient Egypt and China in about 2500BC with the aim to produce a permanent colour image on paper or other material. These inks were made of soot bound together with gums. This paste was formed into rods and dried, then mixed with water immediately before use. Modern ink formulations are rather more complex homogeneous mediums. In addition to the colouring agent, it is composed of solvents, resins, lubricants, solubilizers, surfactants, particulate matter, fluorescers and other materials. This mixture of components, usually under patent, is useful for giving colour, controlling density or flow, modifying the drying kinetic and providing the final appearance (126).

There are also analytical methods for analyzing and dating modern writing instrument inks on paper (127). The challenge remains on the analysis of paper and ink without causing visible damages. The most promising methods in the 1980s involved the analysis of sequential extraction of dyes using thin layer chromatography (TLC) whereas during the last decades interest has shifted to methods based on sequential extraction and analysis of ink volatile components by gas chromatography (GC) coupled with mass spectrometry (MS) (128). The purpose of the methodology is to be applied to printed paper label comparison. Therefore ideally is not only discrimination between manufactures according to their origin but also discrimination between different bottles from same manufacturer according to production year.

*4.2.2.3 How the capsule could help in wine authentication?*

Lead contamination of wine is a problem dating back to ancient time. It was widely used in cellars for wine storage due to its malleability and resistance to corrosion (129). In addition, lead was first used on the cap covering the cork back in the 18$^{th}$ century, when it was useful to cover the cork to protect it from vermin and insects. However, the migration of lead in wine through old or defective corks (130) and thus potential environmental and health related problems, lead capsules were phased out in 1990 (131). Nowadays, the use of aluminium is widespread and tin capsules have replaced lead capsules for expensive wines. In some cases, polyethylene (PE) and polyethlyne terephthalate (PET) can be added between two-layer aluminium foil that are stuck together through adhesive. These capsules are a two-piece construction. The “skirt” is made from a multi-layer lamination of aluminium-polyethylene-aluminium and the top disk is made from a single layer of aluminium. Other plastics, such as polyvinyl chloride (PVC), can be used for entire manufacturing. Therefore, the composition of the alloy is specific and cannot easily be imitated as well as the inks employed to color the capsules, which could be useful for counterfeiting detection (122).

## 5. Chemometrics in analytical chemistry

Studies in the field of analytical chemistry involve several steps. An appropriate experimental planning is crucial for ensuring that the obtained data is relevant for further interpretation. Figure 10 shows a typical workflow in analytical chemistry.

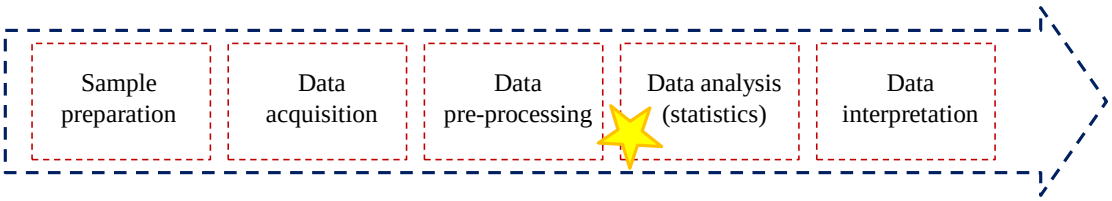


**Figure 10** Common workflow in analytical chemistry studies.

Briefly, 1) *sample storage and preparation* are the most compromising, the most error prone and the most time/resources-consuming steps of most chemical analyses, which have a direct influence on the sample stabilization and integrity. Thus, short term storage and minimal sample preparation are usually preferred. Otherwise, selective sample preparation protocols could be used based on preliminary data or knowledge (132). Furthermore, 2) no single technique is suitable for the *analysis* of certain analytes and matrices and a mixture of complementary techniques has to be used. The selection of the most suitable analytical technique is generally a compromise between quickness, selectivity and sensitivity. Finally, 3) *data pre-processing* transforms the raw data extracted from the instrument into a format that is easy to handle within the data analysis steps. Indeed, raw data files are transformed into a representation that enables easy access to measured variables. In general, this step includes i) filtering the raw signal to remove noise and ii) normalization of systematic variation between samples.

Chemometrics was launched 30 years ago to cope with the rapidly increasing volumes of data produced in laboratories, being Svante Wold and Bruce Kowalski two pioneers in the field (133). However, it is generally accepted that the revolution in the use of multivariate methods took place in psychometrics in the 1930s and 1940s. In this work, multivariate statistical data evaluation was done with software packages XLSTAT® (2016) and The Unscrambler (version 9.1, CAMO, Canada) in which Principal Component Analysis (PCA), Agglomerative Hierarchical Clustering (AHC) and Soft Independent Modelling of Class Analogy (SIMCA) were employed.

The best way to get useful information from a high amount of data is to process it by multivariate pattern recognition methods, which facilitate consideration of intercorrelations between measured variables, providing what is called an analytical fingerprint (134). There are several groups of methods for chemical pattern recognition.

On the one hand, exploratory data analysis (EDA), mainly consisting of the unsupervised pattern recognition as principal component analysis (PCA), is an approach to summarize the main characteristic of data in easy-to-understand form, often with visual graphs, without using a statistical model or having formulated a hypothesis (Tukey, 1977). Principal component analysis (PCA) is a dimension reduction/data compression tool that is used to reduce a large set of variables to a small set that still contains most of the information in the large set. The data is organized in a matrix were the rows are samples and columns are variables. Then, each sample is represented as a point in the variable space (Figure 11). It uses a mathematical procedure which transforms a number of (possibly) correlated variables into a smaller number of uncorrelated variables called principal components.

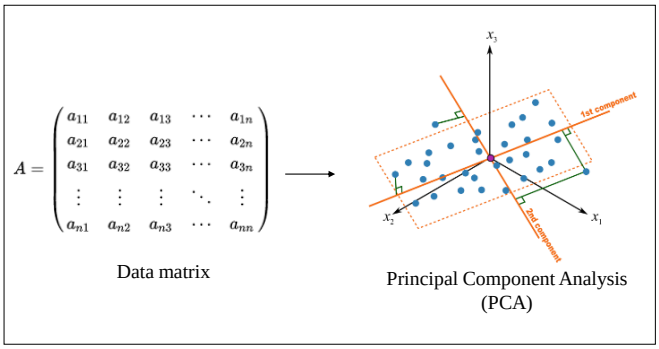


**Figure 11** PCA compresses the information given in a data matrix into uncorrelated PC and projects it down on different dimensions.

On the other hand, a more formal way of treating samples by unsupervised pattern recognition consists of cluster analysis which is able to identify groupings among samples by means of a similarity measurement. The result of this kind of analysis is a picture of these similarities, called dendrogram, in which more closely related samples are closer to each other. The main branches of the dendrogram represent bigger divisions. Cluster analysis differs from principal component analysis in its aim to detect similarities, whereas using PCA there is no particular prejudice to how many groups will be found (135).

Finally, in the Soft Independent Modeling of Class Analogy (SIMCA) approach a Partial Least Squares (PLS) classification is performed in order to identify local models for possible groups and to predict a probable class membership for new observations. Multivariate calibration has developed to become a standard tool in chemometrics for relating two data matrices by a linear multivariate model. PLS is one of the most publicized as the major regression technique for multivariate data. Its goal is to classify samples using a training test for which the desired target value of each sample is known and specified. However, it cannot compensate for poorly designed experiments or inadequate experimental data (136, 137).

In conclusion, the use of PCA provides an informative overlook at the dataset and establishes relationships between variables. Ideally, the results obtained by PCA analyses would be used to

formulate initial hypotheses which PLS could verify and test in more detail. Therefore, PLS classification guided by well-separated PCA scores has a greater likelihood of producing relevant results.

## 6. Conclusions and future trends

Wine, which is the beverage most extensively consumed by humans for pleasure, is one of the foundations of Western civilization, being the grapevine the oldest cultivated plant. The evidence shows that about ten thousand years the story of wine is that of discovery, religion and medicine. In the recent times, due to the technological development and industry, wine making is a kind of art and science. Indeed, scientific research is greatly supporting the search for quality wine in wine production.

However, wine counterfeiting methods have evolved at the same time as wine industry, from the simplest wine sophistication tricks to the most complex ones. In the ongoing fight, counterfeiters seem to be always one step ahead when it comes to evade law enforcement or be able to exploit perceived loopholes in the regulations, which leads on: 1) general socioeconomic effects (on innovation and growth, criminal activities, environment, employment, foreign direct investment and trade), 2) effects on right holders (on sales volume and prices, brand value and firm reputation, royalties, firm-level investment, cost and the scope of operations), 3) effects on consumers (health and safety risk) and 4) effects on government (tax revenues, expenditures and corruption). Priority has therefore been given to enhancing international co-operation to reduce commerce in counterfeit products and authentication and traceability are becoming more demanded. Thus, tracing geographical origin and authenticity of food is now a social demand and a scientific challenge.

The authentication of wine involves several aspects, like geographical origin, year of vintage and grape cultivar. More and more sophisticated and powerful analytical techniques are available but most of them require opening the bottle for liquid sampling which can be fateful when it comes to great value wines. However, new innovative techniques are being developed for ensuring the integrity of the packaging and providing means to authenticate the product for both the producer and the consumer. Nevertheless, a bottle can still be uncorked or refilled through meticulously done small holes and ultimately the wine has to be analyzed as final proof. In addition, the main problem lies in the absence of data banks which are very necessary for all of these techniques. Thus, it can be concluded that the authentication of wine is slightly simple but sometimes puzzling.

## 7. Bibliography


1. Jackson RS. Introduction. In: Wine Science. 3th ed. San Diego: Academic Press; 2008. p. 1-14.
2. Unwin T. Terroir: At the Heart of Geography. In: The Geography of Wine: Regions, Terroir and Techniques. Dordrecht: Springer Netherlands; 2012. p. 37-48.
3. Jackson RS. Wine Laws, Authentication, and Geography. In: Wine Science (3th ed). San Diego: Academic Press; 2008. p. 577-640.
4. Schlesier K, Fauhl-Hassek C, Forina M, Cotea V, Kocsi E, Schoula R, et al. Characterisation and determination of the geographical origin of wines. Part I: overview. European Food Research and Technology. 2009;230(1):1-13.
5. Dodds ER. The origins of viticulture: symbols and mysteries. In: Wine and the Vine: An Historical Geography of Viticulture and the Wine Trade. London: Taylor and Francis; 2005. p. 47-77.
6. Intangible Heritage. United Nations Educational, Scientific and Cultural organization (UNESCO); 2017 [cited 23 June 2017]. Available from: http://www.unesco.org/archives/multimedia/?pg=33&s=films_details&id=3515.
7. Estreicher S. Wine: from Neolithic Times to the 21st Century. New York: Algora Publishing; 2006.
8. Dougherty P. Introduction to the Geographical Study of Viticulture and Wine Production. In: The Geographyof Wine: Regions, Terroir and Techniques. Dordrecht: Springer Netherlands;2012. p. 3-36.
9. Martin C. La spectroscopie Raman pour la lutte contre la contrefaçon et pour la sécurisation de la filière vin. Université de Bordeaux; 2015.
10. Accum F. A treatise on adulterations of food and culinary poisons: exhibiting the fraudulent sophistications of Bread, Beer, Wine, Spirituous Liquors, Tee, Coffee, Cream, Confectionery, Vinegar, Mustard, Pepper, Cheese, Olive Oil, Pickles and other articles employed in domestic economy, and methods of detecting them. London; 1820.
11. Holmberg L. Wine fraud. International Journal of Wine Research. 2010;10:105-13.
12. Eisinger J. Lead and wine. Eberhard Gockel and the colica Pictonum. Medical History. 1982;26(3):279-302.
13. Hornsey I. Winemaking Processes. In: The Chemistry and Biology of Winemaking. The Royal Society of Chemistry; 2007. p. 161-202.

14. Lachenmeier DW. Advances in the Detection of the Adulteration of Alcoholic Beverages Including Unrecorded Alcohol. In: Advances in Food Authenticity Testing. Woodhead Publishing; 2016. p. 565-584.
15. Largest-ever seizures fake food and drink Interpol-Europol operation. The European Union Agency for Law Enforcement Cooperation (EUROPOL). 2016 [cited 19 March 2017]. Available from: https://www.europol.europa.eu/newsroom/news/largest-ever-seizures-of-fake-food-and-drink-in-interpol-europol-operation.
16. Lecat B, Brouard J, Chapuis C. Fraud and counterfeit wines in France: an overview and perspectives. British Food Journal. 2016;119(1):84-104.
17. Lecocq S, Visser M. What Determines Wine Prices: Objective vs. Sensory Characteristics. Journal of Wine Economics. 2006;1(1):42-56.
18. The economic cost of IPR infringement in spirits and wine. Quantification of infringement in distilling, rectifying and blending of spirits (NACE 11.01) and manufacture of wine from grape (NACE 11.02). European Union of Intellectual Property Office (EUIPO). 2016 [cited 13 February 2017]. Available from: http://www.sacg.org/wp-content/uploads/2016/07/wines_and_spirits_en.pdf.
19. State of the Viticulture World Market. Organisation International de la Vigne et du Vin (OIV). 2016 [cited 18 March 2017]. Available from: http://www.oiv.int/public/medias/4710/oiv-noteconjmars2016-en.pdf.
20. Vitivinicultura. Ministerio de Agricultura y Pesca, Alimentación y Medioambiente. [cited 28 March 2017]. Available from: http://www.mapama.gob.es/es/agricultura/temas/producciones-agricolas/vitivinicultura/.
21. Ley 24/2003, de 10 de Julio, de la Viña y el Vino. Sistema de protección del origen y la calidad de los vinos. Boletín Oficial del Estado (BOE). [cited 28 March 2017]. Available from: https://www.boe.es/buscar/pdf/2003/BOE-A-2003-13864-consolidado.pdf.
22. Wine Annual Report and Statistics Foreign Agricultural Service (United States Department of Agriculture, USDA) 2015 [cited 28 March 2017] Available from: https://gainfasusdagov/Recent%20GAIN%20Publications/Wine%20Annual%20Report%20and%20Statistics_Paris_France_7-7-2015pdf.
23. Labruyere A, Schirmer R and Spurr M. Les vins de France et du monde. Nathan; 2015.
24. The Economic Impact of Counterfeiting and Piracy. Organisation for Economic , Co-operation and Development (OECD). 2008 [cited 19 March 2017]. Available from: http://apps.who.int/medicinedocs/documents/s19845en/s19845en.pdf.
25. Giovanucci D, Josling T, Kerr W, O'Connor B, Yeung M. Guide to Geographical Indications: linking products to their origin. Geneva: International Trace Center; 2009 [cited 31 March

2017]. Available from: http://www.origin-gi.com/images/stories/PDFs/English/E-Library/geographical_indications.pdf.

26. Fink C, Maskus K, Qian Yi. The Economic Effects of Counterfeiting and Piracy: A Review and Implications for Developing Countries. World Bank Policy Research Working Paper No. 7586. Available from: https://ssrn.com/abstract=2740120.
27. Establising the International Organization of Vine and Wine. Organisation International de la Vigne et du Vin (OIV). 2001 [cited 19 March 2017]. Available from: http://www.oiv.int/public/medias/2197/en-oiv-accord-20010403.pdf.
28. Por qué cuestiones de Origen. European Federation of Origin Wine (EFOW). [cited 19 March 2017]. Available from: http://www.eumedia.es/portales/files/documentos/EFOW-es.pdf.
29. Vergara C, von Baer D, Mardones C, Gutiérrez L. Overview of Chemical Markers for Varietal Authentication of Red Wines. Progress in Authentication of Food and Wine. ACS Symposium Series. 1081: American Chemical Society; 2011. p. 101-11.
30. Kelly S, Heaton K, Hoogewerff J. Tracing the geographical origin of food: The application of multi-element and multi-isotope analysis. Trends in Food Science & Technology. 2005;16(12):555-67.
31. Aceto M, Baldizzone M, Oddone M. Keeping the track of quality: authentication and traceability studies on wine. Nova Science Publishers, Inc.; 2009. p. 429-466.
32. Luykx D, van Ruth S. An overview of analytical methods for determining the geographical origin of food products. Food Chemistry. 2008;107(2):897-911.
33. Smeyers-Verbeke J, Jäger H, Lanteri S, Brereton P, Jamin E, Fauhl-Hassek C, et al. Characterization and determination of the geographical origin of wines. Part II: descriptive and inductive univariate statistics. European Food Research and Technology. 2009;230(1):15.
34. Römisch U, Jäger H, Capron X, Lanteri S, Forina M, Smeyers-Verbeke J. Characterization and determination of the geographical origin of wines. Part III: multivariate discrimination and classification methods. European Food Research and Technology. 2009;230(1):31.
35. Arvanitoyannis IS, Katsota MN, Psarra EP, Soufleros EH, Kallithraka S. Application of quality control methods for assessing wine authenticity: Use of multivariate analysis (chemometrics). Trends in Food Science & Technology. 1999;10(10):321-36.
36. Kwan WO, Kowalski BR. Classification of wines by applying pattern recognition to chemical compostion data. Journal of Food Science. 1978;43(4):1320-3.
37. Compendium of International Methods of Wine and Must Analysis. International Organisation of Vine and Wine (OIV). 2016 [cited 14 March 2017]. Available

from: http://www.oiv.int/en/technical-standards-and-documents/methods-of-analysis/compendium-of-international-methods-of-analysis-of-wines-and-musts-2-vol.

38. dos Santos C, Páscoa R, Lopes J. A review on the application of vibrational spectroscopy in the wine industry: From soil to bottle. TrAC Trends in Analytical Chemistry. 2017;88:100-18.
39. Gago P, Iland P. Australian wine : styles and tastes. Campbelltown: Patrick Iland Wine Promotions; 2002.
40. Cozzolino D, Smyth H. Analytical and Chemometric-Based Methods to Monitor and Evaluate Wine Protected Designation. Comprehensive Analytical Chemistry. 2013;60:385-408.
41. Rodrigues SM, Otero M, Alves AA, Coimbra J, Coimbra MA, Pereira E, et al. Elemental analysis for categorization of wines and authentication of their certified brand of origin. Journal of Food Composition and Analysis. 2011;24(4–5):548-62.
42. Grindlay G, Mora J, Gras L, de Loos-Vollebregt M. Atomic spectrometry methods for wine analysis: A critical evaluation and discussion of recent applications. Analytica Chimica Acta. 2011;691(1–2):18-32.
43. Šelih VS, Šala M, Drgan V. Multi-element analysis of wines by ICP-MS and ICP-OES and their classification according to geographical origin in Slovenia. Food Chemistry. 2014;153:414-23.
44. Gonzálvez A, Llorens A, Cervera ML, Armenta S, de la Guardia M. Elemental fingerprint of wines from the protected designation of origin Valencia. Food Chemistry. 2009;112(1):26-34.
45. Aceto M, Robotti E, Oddone M, Baldizzone M, Bonifacino G, Bezzo G, et al. A traceability study on the Moscato wine chain. Food Chemistry. 2013;138(2):1914-22.
46. Rusjan D, Strlič M, Pucko D, Šelih VS, Korošec-Koruza Z. Vineyard soil characteristics related to content of transition metals in a sub-Mediterranean winegrowing region of Slovenia. Geoderma. 2006;136(3):930-6.
47. Almeida M, Vasconcelos T. Multielement Composition of Wines and Their Precursors Including Provenance Soil and Their Potentialities As Fingerprints of Wine Origin. Journal of Agricultural and Food Chemistry. 2003;51(16):4788-98.
48. Coetzee PP, Steffens FE, Eiselen RJ, Augustyn OP, Balcaen L, Vanhaecke F. Multi-element Analysis of South African Wines by ICP−MS and Their Classification According to Geographical Origin. Journal of Agricultural and Food Chemistry. 2005;53(13):5060-6.
49. Coetzee PP, van Jaarsveld FP, Vanhaecke F. Intraregional classification of wine via ICP-MS elemental fingerprinting. Food Chemistry. 2014;164:485-92.

50. Bentlin FRS, Pulgati FH, Dressler VL, Pozebon D. Elemental analysis of wines from South America and their classification according to country. Journal of the Brazilian Chemical Society. 2011;22:327-36.
51. Geana I, Iordache A, Ionete R, Marinescu A, Ranca A, Culea M. Geographical origin identification of Romanian wines by ICP-MS elemental analysis. Food Chemistry. 2013;138(2):1125-34.
52. J. Baxter M, M. Crews H, John Dennis M, Goodall I, Anderson D. The determination of the authenticity of wine from its trace element composition. Food Chemistry. 1997;60(3):443-50.
53. Szentmihályi K, Csiktusnádi-Kiss GA, Keszler Á, Kótai L, Candeaias M, Bronze MR, et al. Method development for measurement of elements in Hungarian red wines by inductivelvy coupled plasma optival emission spectrometry (ICP-OES). Acta Alimentaria. 2000;29(2):105-22.
54. Dutra SV, Adami L, Marcon AR, Carnieli GJ, Roani CA, Spinelli FR, et al. Determination of the geographical origin of Brazilian wines by isotope and mineral analysis. Analytical and Bioanalytical Chemistry. 2011;401(5):1571.
55. Kaya AD, Bruno de Sousa R, Curvelo-Garcia AS, Ricardo-da-Silva JM, Catarino S. Effect of Wood Aging on Wine Mineral Composition and 87Sr/86Sr Isotopic Ratio. Journal of Agricultural and Food Chemistry. 2017.
56. Christoph N, Hermann A, Wachter H. 25 Years authentication of wine with stable isotope analysis in the European Union – Review and outlook. BIO Web of Conferences. 2015;5.
57. Dutra SV, Adami L, Marcon AR, Carnieli GJ, Roani CA, Spinelli FR, et al. Characterization of wines according the geographical origin by analysis of isotopes and minerals and the influence of harvest on the isotope values. Food Chemistry. 2013;141(3):2148-53.
58. Victor V, Ross S, Karine P, André P, Jean-François H, David W. Strontium Isotope Characterization of Wines from the Quebec (Canada) Terroir. Procedia Earth and Planetary Science. 2015;13:252-5.
59. Saurina J. Characterization of wines using compositional profiles and chemometrics. TrAC Trends in Analytical Chemistry. 2010;29(3):234-45.
60. Suhaj M, Korenovská M. Application of elemental analysis for identification of wine origin. Acta Alimentaria. 2005;34(4):393-401.
61. Augagneur S, Medina B, Grousset F. Measurement of lead isotope ratios in wine by ICP-MS and its applications to the determination of lead concentration by isotope dilution. Fresenius' Journal of Analytical Chemistry. 1997;357(8):1149-52.

62. Horn P, Holzl S, Todt W, Matthies D. Isotope abundance ratios of sr in wine provenance determinations, in a tree-root activity study, and of pb in a pollution study on tree-rings. Isotopes in Environmental and Health Studies. 1997;33(1-2):31-42.
63. Barbaste M, Robinson K, Guilfoyle S, Medina B, Lobinski R. Precise determination of the strontium isotope ratios in wine by inductively coupled plasma sector field multicollector mass spectrometry (ICP-SF-MC-MS). Journal of Analytical Atomic Spectrometry. 2002;17(2):135-7.
64. Costinel D, Tudorache A, Ionete RE, Vremera R. The Impact of Grape Varieties to Wine Isotopic Characterization. Analytical Letters. 2011;44(18):2856-64.
65. Rubert J, Lacina O, Fauhl-Hassek C, Hajslova J. Metabolic fingerprinting based on high-resolution tandem mass spectrometry: a reliable tool for wine authentication? Analytical and Bioanalytical Chemistry. 2014;406(27):6791-803.
66. Flamini R, De Rosso M. Mass spectrometry in the analysis of grape and wine proteins. Expert Review of Proteomics. 2006;3(3):321-31.
67. Alañón ME, Pérez-Coello MS, Marina ML. Wine science in the metabolomics era. TrAC Trends in Analytical Chemistry. 2015;74:1-20.
68. Ebeler, S. Analysis of Grapes and Wines: An Overview of New Approaches and Analytical Tools. In: Advance in Wine Research. American Chemical Society; 2015. p. 3-12.
69. Panighel A, Flamini R. Applications of solid-phase microextraction and gas chromatography/mass spectrometry (SPME-GC/MS) in the study of grape and wine volatile compounds. Molecules. 2014;19(12):21291-309.
70. Cynkar W, Dambergs R, Smith P, Cozzolino D. Classification of Tempranillo wines according to geographic origin: combination of mass spectrometry based electronic nose and chemometrics. Anal Chim Acta. 2010;660(1-2):227-31.
71. Flamini R. Mass spectrometry in grape and wine chemistry. Part I: polyphenols. Mass Spectrometry Reviews. 2003;22(4):218-50.
72. Čuš F, Česnik HB, Bolta ŠV, Gregorčič A. Pesticide residues and microbiological quality of bottled wines. Food Control. 2010;21(2):150-4.
73. Reagan F. Determination of pesticides in water using ATR-FTIR spectroscopy on PVC/chloroparaffin coatings. Analytica Chimica Acta. 1996;334:85–92.
74. Basalekou M, Pappas C, Tarantilis P, Kotseridis Y, Kallithraka S. Wine authentication with Fourier Transform Infrared Spectroscopy: a feasibility study on variety, type of barrel wood and ageing time classification. International Journal of Food Science & Technology. 2017;52(6):1307-13.

75. Fragoso S, Aceña L, Guasch J, Mestres M, Busto O. Quantification of Phenolic Compounds during Red Winemaking Using FT-MIR Spectroscopy and PLS-Regression. Journal of Agricultural and Food Chemistry. 2011;59(20):10795-802.
76. Canal C, Ozen B. Monitoring of Wine Process and Prediction of Its Parameters with Mid-Infrared Spectroscopy. Journal of Food Process Engineering. 2017;40(1):e12280-n/a.
77. Cayuela JA, Puertas B, Cantos-Villar E. Assessing wine sensory attributes using Vis/NIR. European Food Research and Technology. 2017;243(6):941-53.
78. Sen I, Ozturk B, Tokatli F, Ozen B. Combination of visible and mid-infrared spectra for the prediction of chemical parameters of wines. Talanta. 2016;161:130-7.
79. Urickova V, Sadecka J. Determination of geographical origin of alcoholic beverages using ultraviolet, visible and infrared spectroscopy: A review. Spectrochim Acta A: Molecular and Biomolecular Spectroscopy. 2015;148:131-7.
80. Cozzolino D. The role of visible and infrared spectroscopy combined with chemometrics to measure phenolic compounds in grape and wine samples. Molecules. 2015;20(1):726-37.
81. Gallego ÁL, Guesalaga AR, Bordeu E, Gonzalez ÁS. Rapid Measurement of Phenolics Compounds in Red Wine Using Raman Spectroscopy. IEEE Transactions on Instrumentation and Measurement. 2011;60(2):507-12.
82. Rodriguez SB, Thornton MA, Thornton RJ. Raman Spectroscopy and Chemometrics for Identification and Strain Discrimination of the Wine Spoilage Yeasts Saccharomyces cerevisiae, Zygosaccharomyces bailii, and Brettanomyces bruxellensis. Applied and Environmental Microbiology. 2013;79(20):6264-70.
83. Cozzolino D. Sample presentation, sources of error and future perspectives on the application of vibrational spectroscopy in the wine industry. Journal of the Science of Food and Agriculture. 2015;95(5):861-8.
84. Gishen M, Dambergs RG, Cozzolino D. Grape and wine analysis - enhancing the power of spectroscopy with chemometrics. Australian Journal of Grape and Wine Research. 2005;11(3):296-305.
85. McGovern PE, Glusker DL, Exner LJ, Voigt MM. Neolithic resinated wine. Nature. 1996;381(6582):480-1.
86. Jackson RS. Sensory Perception and Wine Assesesment. In: Wine Science. 3th ed. SanDiego: Academic Press; 2008. p. 641-685.
87. Laguna L, Bartolomé B, Moreno-Arribas MV. Mouthfeel perception of wine: Oral physiology, components and instrumental characterization. Trends in Food Science & Technology. 2017;59:49-59.

88. Elortondo FJP, Ojeda M, Albisu M, Salmerón J, Etayo I, Molina M. Food quality certification: An approach for the development of accredited sensory evaluation methods. Food Quality and Preference. 2007;18(2):425-39.
89. Strike DJ, Meijerink MGH, Koudelka-Hep M. Electronic noses – A mini-review. Fresenius' Journal of Analytical Chemistry. 1999;364(6):499-505.
90. Persaud, K. Electronic Noses and Tongues in the Food Industry. In: Electronic Noses and Tongues in Food Science. San Diego: Academic Press; 2016. p. 1-12.
91. Rodríguez-Méndez ML, De Saja JA, González-Antón R, García-Hernández C, Medina-Plaza C, García-Cabezón C, et al. Electronic Noses and Tongues in Wine Industry. Frontiers in Bioengineering and Biotechnology. 2016;4:81.
92. SalagoiTy H, Guyon F, Chauvet S, Viateau M, Morere M, Chabreyrie D, et al. Contribution à l'identification des cépages dans les vins blancs et les vins rouges. Bulletin de l'OIV. 2006;79(904-906):271-6.
93. This P, Jung A, Boccacci P, Borrego J, Botta R, Costantini L, et al. Development of a standard set of microsatellite reference alleles for identification of grape cultivars. Theoretical and Applied Genetics. 2004;109(7):1448-58.
94. Stefano M, Luigi B, Antonio C, Angelo C. Stefano M, Bavaresco L, Caló, A, Costacurta, A. Inter- and Intra-Varietal Genetic Variability in Vitis vinifera L. In: The Mediterranean Genetic Code - Grapevine and Olive. InTech; 2013. p. 73-95.
95. Siret R, Gigaud O, Rosec JP, This P. Analysis of Grape Vitis vinifera L. DNA in Must Mixtures and Experimental Mixed Wines Using Microsatellite Markers. Journal of Agricultural and Food Chemistry. 2002;50(13):3822-7.
96. Savazzini F, Martinelli L. DNA analysis in wines: Development of methods for enhanced extraction and real-time polymerase chain reaction quantification. Analytica Chimica Acta. 2006;563(1–2):274-82.
97. Arroyo-Garcia R, Lefort F, de Andres MT, Ibanaez J, Borrego J, Jouve N, et al. Chloroplast microsatellite polymorphisms in Vitis species. Genome. 2002;45(6):1142-9.
98. Baleiras-Couto MM, Eiras-Dias JE. Detection and identification of grape varieties in must and wine using nuclear and chloroplast microsatellite markers. Analytica Chimica Acta. 2006;563(1–2):283-91.
99. Weising K, Gardner RC. A set of conserved PCR primers for the analysis of simple sequence repeat polymorphisms in chloroplast genomes of dicotyledonous angiosperms. Genome. 1999;42(1):9-19.
100. Fahrni SM, Fuller BT, Southon JR. Angel's Share Combats Wine Fraud: 14C Dating of Wine without Opening the Bottle. Analytical Chemistry. 2015;87(17):8646-50.

101. Hubert P, Perrot F, Gaye J, Médina B, Pravikoff MS. Radioactivity measurements applied to the dating and authentication of old wines. Comptes Rendus Physique. 2009;10(7):622-9.
102. Hubert P. From the mass of the neutrino to the dating of wine. Nuclear Instruments and Methods in Physics Research Section A: Accelerators, Spectrometers, Detectors and Associated Equipment. 2007;580(1):751-5.
103. Cozzolino D, Kwiatkowski MJ, Waters EJ, Gishen M. A feasibility study on the use of visible and short wavelengths in the near-infrared region for the non-destructive measurement of wine composition. Analytical and Bioanalytical Chemistry. 2007;387(6):2289-95.
104. Nordon A, Mills A, Burn RT, Cusick FM, Littlejohn D. Comparison of non-invasive NIR and Raman spectrometries for determination of alcohol content of spirits. Analytica Chimica Acta. 2005;548(1–2):148-58.
105. Hargreaves MD, Matousek P. Threat detection of liquid explosive precursor mixtures by Spatially Offset Raman Spectroscopy (SORS), Proc. SPIE 7486, Optics and Photonics for Counterterrorism and Crime Fighting V, 74860B. 2009.
106. Matousek P, Clark IP, Draper ERC, Morris MD, Goodship AE, Everall N, et al. Subsurface Probing in Diffusely Scattering Media Using Spatially Offset Raman Spectroscopy. Applied Spectroscopy. 2005;59(4):393-400.
107. Ellis DI, Eccles R, Xu Y, Griffen J, Muhamadali H, Matousek P, et al. Through-container, extremely low concentration detection of multiple chemical markers of counterfeit alcohol using a handheld SORS device. Nature Scientific Reports. 2017;7(1):12082.
108. Martin C, Bruneel J-L, Guyon F, Médina B, Jourdes M, Teissedre P-L, et al. Raman spectroscopy of white wines. Food Chemistry. 2015;181:235-40.
109. Weekley AJ, Bruins P, Sisto M, Augustine MP. Using NMR to study full intact wine bottles. Journal of Magnetic Resonance. 2003;161(1):91-8.
110. Sobieski DN, Mulvihill G, Broz JS, Augustine MP. Towards rapid throughput NMR studies of full wine bottles. Solid State Nuclear Magnetic Resonance. 2006;29(1–3):191-8.
111. Weekley AJ, Bruins P, Augustine MP. Nondestructive Method of Determining Acetic Acid Spoilage in an Unopened Bottle of Wine. American Journal of Enology and Viticulture. 2002;53(4):318.
112. Harley SJ, Lim V, Augustine MP. Using low frequency dielectric absorption to screen full intact wine bottles. Analytica Chimica Acta. 2011;702(2):188-94.
113. Harley SJ, Lim V, Stucky PA, Augustine MP. Using low frequency full bottle diamagnetic screening to study collectible wine. Talanta. 2011;85(5):2437-44.

114. DeYoung PA, Hall CC, Mears PJ, Padilla DJ, Sampson R, Peaslee GF. Comparison of Glass Fragments Using Particle-Induced X-Ray Emission (PIXE) Spectrometry. Journal of Forensic Sciences. 2011;56(2):366-71.
115. Baert K, Meulebroeck W, Wouters H, Cosyns P, Nys K, Thienpont H, et al. Using Raman spectroscopy as a tool for the detection of iron in glass. Journal of Raman Spectroscopy. 2011;42(9):1789-95.
116. Prades C, Gómez-Sánchez I, García-Olmo J, González-Adrados JR. Discriminant analysis of geographical origin of cork planks and stoppers by near infrared spectroscopy. Journal of Wood Chemistry and Technology. 2012;32(1):54-70.
117. Fernández B, Claverie F, Pécheyran C, Donard OFX. Direct analysis of solid samples by fs-LA-ICP-MS. TrAC Trends in Analytical Chemistry. 2007;26(10):951-66.
118. Trejos T, Montero S, Almirall JR. Analysis and comparison of glass fragments by laser ablation inductively coupled plasma mass spectrometry (LA-ICP-MS) and ICP-MS. Analytical and Bioanalytical Chemistry. 2003;376(8):1255-64.
119. Schenk ER, Almirall JR. Elemental analysis of glass by laser ablation inductively coupled plasma optical emission spectrometry (LA-ICP-OES). Forensic Science International. 2012;217(1–3):222-8.
120. Vignes JL, Beurroies I, Guignard D. Un vie de verre: expériences sur l'elaboration et les propiétés d'un matériau. Bulletin de l'union des physiciens. 1997;91(790).
121. Ott JG. Quelle peut être l'influence de la teinte du verre sur l'evolution du vin en bouteille. Revue française d'oenologie 1977.
122. Médina B, Salagoïty M, Guyon F, Gaye J, Hubert P, Guillaume F, Using new analytical approaches to verify the origin of wine. In: New Analytical Approaches for Verifying the Origin of Food. Woodhead Publishing: Paul Brereton; 2013. p. 149-188.
123. Médina B, Sudraud P. Teneur des vins en chrome et en nickel. Causes d'enrichissement. Journal international des sciences de la vigne et du vin. 1980;14.
124. Situation Report on Counterfeiting in the European Union. Europol and the Office of Harmonization in the Internal Market. 2015 [cited 13 February 2017]. Available from: file:///C:/Users/ngrijalba001/Downloads/en_executive-summary.pdf.
125. Manso M, Carvalho ML. Application of spectroscopic techniques for the study of paper documents: A survey. Spectrochimica Acta Part B: Atomic Spectroscopy. 2009;64(6):482-90.
126. Calcerrada M, García-Ruiz C. Analysis of questioned documents: A review. Analytica Chimica Acta. 2015;853(0):143-66.
127. Ezcurra M, Góngora JMG, Maguregui I, Alonso R. Analytical methods for dating modern writing instrument inks on paper. Forensic Science International. 2010;197(1–3):1-20.

128. Weyermann C, Almog J, Bügler J, Cantu AA. Minimum requirements for application of ink dating methods based on solvent analysis in casework. Forensic Science International. 2011;210(1):52-62.
129. Kaufmann A. Lead in wine. Food Additives and Contaminants. 1998;15(4):437-45.
130. Médina B, Guimberteau G, Sudraud P. Dosage du plomb dans les vins, une cause d'enrichissement : les capsules de surbouchage. Journal international des sciences de la vigne et du vin. 1977;11.
131. Gulson BL, Lee TH, Mizon KJ, Korsch MJ, Eschnauer HR. The Application of Lead Isotope Ratios to the Determine the Contribution of the Tin-Lead to the Lead Content of Wine. American Journal of Enology and Viticulture. 1992;43(2):180.
132. Ramos L. Critical overview of selected contemporary sample preparation techniques. Journal of Chromatography A. 2012;1221:84-98.
133. Wold, S. Chemometrics and Bruce: Some Fond Memories. In: 40 Years of Chemometrics – From Bruce Kowalski to the Future. American Chemical Society; 2015. p, 1-13.
134. Oliveri P, Simonetti R. Oliveri P, Simonetti R. Chemometrics for Food Authenticity Applications. In: Advancesin Food Authenticity Testing. Woodhead Publishing; 2016. p. 701-728.
135. Brereton RG. Pattern Recognition. In: Chemometrics. John Wiley and Sons, Ltd; 2003. p. 183-269.
136. Brereton RG. Introduction to multivariate calibration in analytical chemistry. Analyst. 2000;125(11):2125-54.
137. Wold S, Sjöström M, Eriksson L. PLS-regression: a basic tool of chemometrics. Chemometrics and Intelligent Laboratory Systems. 2001;58(2):109-30.

# CHAPTER 2:

# Objectives

The main purpose of the present work is the development **of an unambiguous diagnostic tool based ultratrace analysis of packaging (glass, paper, ink and capsule) by fast and non-invasive multifactorial analysis of bottled wine by femtosecond laser ablation ICPMS, Raman spectroscopy and Infrared spectroscopy, which induces no visible degradation of the bottle that could affect its value.**

Thus, this work has been structured around **i) the design and the development of a new ablation cell adjustable to different bottle shapes and its application to the analysis of wine packaging by fsLA-ICPMS and ii) application of Raman and Infrared spectroscopies for the qualitative analysis of wine packaging**, each of them constituting the main objectives of this work.

The first step to accomplish the first objective is **the development of an ablation cell capable of adapting to the different shapes of the bottles**. This first step is crucial as the ablation chamber plays a very important role in laser ablation allowing quantitative and rapid transport of the laser-induced aerosol to the ICP plasma source. To achieve this first objective, the following methodological objectives are established:

- ✓ *Design of an initial ablation cell* based on designs previously described in the literature capable of adapting to different bottle curvatures.

- ✓ *Ablation cell manufacturing by 3D printer* due to its characteristics that are not achievable by conventional high precision micromachining.

- ✓ *Verification of the suitability* in terms of quantitative and rapid transport of the aerosol to the ICP plasma source. Sensitivity ($^{115}$In) and elemental fractionation ($^{238}$U/$^{232}$Th) are evaluated in NIST 612. In addition, the transfer line (≈ 1,5 m) must guarantee an optimal/fast transport of laser-induced aerosol (wash-out time < 5s).

- ✓ *Design and manufacturing of a bottle holder* that matches with the XY stage and allows the inclusion of the new ablation cell into the laser ablation system.

The second step to fulfil the first objective is focused on **the development of a fast (≈ 5 min) and non-invasive approach for ultratrace (below ng·g$^{-1}$) analysis of wine packaging (glass, paper, ink and capsule) inducing no visible degradation of the bottles**, which has not equivalent in terms of performance to date. For this aim, a series of methodological objectives are fixed:

- ✓ *Optimization of laser ablation parameters for each matrix*. The ALFAMET (KGW-Yb, 1030 nm) femtosecond laser used in this project operates at high repetition rates (1-100000 Hz) and allows virtual beam shaping, which represents a new approach in analytical laser ablation. This optimization of laser ablation parameters includes:
  - Selection of an appropriate carrier gas (He or Ar) and its flow optimization.
  - Optimization of laser fluence (J/cm$^2$), pulse frequency (Hz) and spot diameter (µm).
  - Selection of the ablation pattern that best matches matrix characteristics.

- ✓ *Optimization of ICPMS parameters for each matrix*. The laser ablation system is coupled to an ELAN DRC II ICPMS (Perkin Elmer) whose working parameters must be optimized for each matrix:
  - Selection of the elements and isotopes to be monitored according to the nature of the matrix and optimization of the integration time for the best signal resolution.
  - Selection of working plasma conditions (wet plasma or dry plasma).

- ✓ *Analysis of glass on bottle samples:*
  - Selection of the calibration strategy.
  - Analytical assessment of the developed method in terms of reproducibility, repeatability, homogeneity, linearity, limits of detection and spectral interferences.
  - Analysis of bottle samples according to: i) genuine and counterfeited bottles, ii) origin (country and/or continent) and iii) vintage.

- ✓ *Analysis of paper and ink on bottle samples*. This methodological objective will be carried out similarly to what is described in the previous section. However, special attention will be paid here to the development of relevant calibration strategy with the development of homemade standards.

- ✓ *Analysis of capsules on bottle samples*. For the analysis of capsules a development of a new ablation cell is considered, which will be able to adapt to the high curvature of the bottleneck. However, a preliminary test will be done using a conventional laser ablation cell in order

evaluate the suitability of capsule analysis for the differentiation of genuine and counterfeited bottles and discrimination according to origin and vintage.

- ✓ *Statistical data analysis for the establishment of discrimination parameters*:
  - Statistical data processing based on multivariate analysis (PCA, PLS, ascendant hierarchical classification) will be applied for draw distinction between genuine and counterfeited bottles by isolating and prioritizing the most important trace elements and distinguish the chemical signature of bottles according to their origin country and vintage.
  - The development of a database will be considered for quantitative data collection obtained by the elementary analysis of packaging.

The second objective of the present work is to **develop a novel method for the qualitative molecular analysis packaging by Raman spectroscopy and Diffuse Reflectance Infrared Fourier Transform (DRIFT) spectroscopy, what would provide complementary information to elementary analysis carried out by fsLA-ICPMS**. For this purpose, a series of methodological objectives are established:

- ✓ Raman spectroscopy:
  - *Selection of the best radiation source* (red laser, 785 nm or green laser, 532 nm) according to the nature of the matrix (ink and paper).
  - *Optimization of Raman spectrometer parameters* (accumulations per measurement, acquisition time and number of spectrum per sample).
  - *Application of Raman spectroscopy* for the identification of genuine and counterfeited bottles as well as vintage classification.
  - *Evaluation of the obtained spectral information and statistical data analysis of the spectra* for qualitative discrimination of genuine/counterfeited bottles and vintage.
  - *Evaluate if the information provided by the Raman spectroscopy improves the capacity of discrimination* of the data obtained by the elemental analysis of the bottles.

- ✓ Diffuse Reflectance Infrared Fourier Transform (DRIFT) spectroscopy:
  - *Optimization of DRIFT spectrometer parameters* (accumulations per measurement, acquisition time and number of spectrum per sample).
  - *Application of DRIFT spectroscopy* for the identification of genuine and counterfeited bottles as complementary technique to Raman spectroscopy for the identification of the major component of the label.

- *Evaluate if the information provided by DRIFT spectroscopy improves the capacity of discrimination* of the data obtained by Raman spectroscopy.

L'objectif principal du travail présenté ici est **le développement d'un nouvel outil de diagnostic non ambigu basé sur l'analyse ultra-trace des matériaux constituant l'emballage (verre, papier et encres, capsule) par une analyse multifactorielle rapide et non invasive en utilisant l'ablation laser femtoseconde ICPMS et l'spectroscopie Raman et Infrarouge**, qui n'induisent aucune dégradation visible de la bouteille qui pourrait affecter à sa valeur.

Ainsi, ce travail a été structuré autour de i**) la conception et le développement d'une nouvelle cellule d'ablation réglable à différentes formes de bouteilles et son application à l'analyse des bouteilles de vin par fsLA-ICPMS et ii) l'application de la spectroscopie Raman et Infrarouge pour l'analyse qualitative de l'emballage de vin**, chacun d'eux constituant les principaux objectifs de ce travail.

Le premier pas pour réussir le premier objectif est le développement d'une cellule d'ablation capable de s'adapter aux différentes formes des bouteilles. Cette première étape est cruciale car la chambre d'ablation joue un rôle très important dans l'ablation laser permettant un transport quantitatif et rapide de l'aérosol induit par laser à la source de plasma de l'ICP. Pour atteindre ce premier objectif, les objectifs méthodologiques suivants ont été établis:

- ✓ *Conception d'une cellule d'ablation initiale* basée sur des modèles décrits précédemment dans la littérature capable de s'adapter à différentes courbures des bouteilles.

- ✓ *Fabrication de la nouvelle cellule d'ablation par impression 3D* en raison de ses caractéristiques qui ne sont pas réalisables par le *micro-machining* conventionnel de haute précision.

- ✓ *Vérification de l'adéquation en termes de transport quantitatif et rapide de l'aérosol à la source de plasma ICP*. La sensibilité ($^{115}$In) et le fractionnement élémentaire ($^{238}$U / $^{232}$Th) sont évalués dans le NIST 612. En outre, la ligne de transfert (≈ 1.5 m) doit garantir un transport optimal / rapide de l'aérosol induit par laser (temps de lavage <5s).

- ✓ *Conception et fabrication d'un porte-bouteille* amoldable à la platine XY de la machine laser et qui permet au même temp l'inclusion de la nouvelle cellule d'ablation dans le système d'ablation laser.

La deuxième pas pour réussir le premier objectif est le développement d'une approche rapide (≈ 5 min) et non invasive pour l'analyse ultratrace de l'emballage du vin (verre, papier, encre et capsule) induisant aucune dégradation visible des bouteilles, ce qui n'a pas équivalent en termes de performances à ce jour. Pour ce but, une série d'objectifs méthodologiques ont été fixés:

- ✓ *Optimisation des paramètres d'ablation laser pour chaque type d'échantillon*. Le laser ALFAMET (KGW-Yb, 1030 nm) utilisé dans ce projet travaille à hautes taux de répétition (1-100000 Hz. La combinaison d'une haute cadence de tir et d'un dispositif de scanner galvanometrique 2D permet de créer des trajectoires variées, ce qui représente une nouvelle approche dans l'ablation laser analytique.

  Cette optimisation des paramètres d'ablation laser comprend:
  - Sélection d'un gaz porteur approprié (He ou Ar) et l'optimisation de son flux.
  - Optimisation de l'énergie laser (J/cm2), la fréquence d'impulsion (Hz) et le diamètre du spot (μm).
  - Sélection d'une stratégie d'ablation qui s'adapte le mieux aux caractéristiques de l'échantillon.

- ✓ *Optimisation des paramètres ICPMS pour chaque type de matrice*. Le système d'ablation laser est couplé à un instrument ICPMS ELAN DRC II (Perkin Elmer) dont les paramètres de travail doivent être optimisés pour chaque type d'échantillon :
  - Sélection des éléments et des isotopes à suivre en fonction de la nature de la matrice et optimisation du temps d'intégration pour la meilleure résolution du signal.
  - Sélection des conditions du plasma (plasma humide ou plasma sec).

- ✓ *Analyse du verre*
  - Sélection de la stratégie d'étalonnage
  - Évaluation analytique de la méthode développée en termes de réproducibilité, répétabilité, homogeneité, linéarité, limites de détection et interférences spectrales.
  - Analyse du verre selon: i) les bouteilles authentiques et contrefaites, ii) origine (pays et / ou continent) et iii) millésime.

- ✓ *Analyse du papier et de l'encre sur les etiquettes des bouteilles.* Cet objectif méthodologique sera réalisé de manière similaire à ce qui est décrit dans la section précédente. L'analyse du papier et des encres, en raison du manque de matériaux de référence certifiés, représente un véritable challenge analytique. Une nouveau approche

quantitative será mis au point en développant nos propres standards par impression jet d'encre de papier à partir de solutions dopées.

- ✓ *Analyse des capsules sur les échantillons de bouteilles.* Pour l'analyse des capsules, on envisage le développement d'une nouvelle cellule d'ablation, qui pourra s'adapter à la courbure du goulot. Cependant, un test préliminaire sera effectué en utilisant une cellule d'ablation classique afin d'évaluer l'adéquation de l'analyse des capsules pour la différenciation des bouteilles authentiques et contrefaites et la discrimination selon l'origine et le millésime.

- ✓ *Analyse statistique des données pour l'établissement de paramètres de discrimination :*
  - Le traitement statistique des données basé sur l'analyse multivariée (PCA, PLS, classification hiérarchique ascendante) sera appliqué pour la distinction entre les bouteilles authentiques et les contrefaites en isolant les éléments les plus importants et en distinguant la signature chimique des bouteilles selon leur pays d'origine et millésime.
  - Le développement d'une base de données sera pris en considération pour la collecte de données quantitatives obtenues par l'analyse élémentaire de l'emballage.

Le deuxième objectif de ce travail est le développement d'une nouvelle méthode pour l'analyse moléculaire qualitative par la spectroscopie Raman et Infrarouge, ces qui fournirait des informations complémentaires à l'analyse élémentaire réalisée par fsLA-ICPMS. À cette fin, une série d'objectifs méthodologiques ont été établis:

- ✓ Spectroscopie Raman :
  - *Sélection de la meilleure source de rayonnement (laser rouge, 785 nm ou laser vert, 532 nm)* selon la nature de l'échantillon (papier et encre).
  - *Optimisation des paramètres du spectromètre Raman* (nombre de spectre par échantillon, accumulation par mesure et temps d'acquisition).
  - *Application de la spectroscopie Raman* pour l'identification de bouteilles authentiques et contrefaites ainsi que la classification par vintage.
  - *Évaluation de l'information spectrale obtenue et analyse statistique des spectres* pour la discrimination qualitative des bouteilles authentiques/contrefaites et vintage.
  - *Évaluer si l'information fournie par la spectroscopie Raman améliore la capacité de discrimination* des données obtenues par l'analyse élémentaire des bouteilles.

- ✓ Spectroscopie infrarouge à transformée de Fourier et réflexion diffuse (DRIFT) :
  - *Optimisation des paramètres du spectromètre DRIFT* (nombre de spectres par échantillon accumulations par mesure et temps d'acquisition).
  - *Application de la spectroscopie DRIFT* pour l'identification de bouteilles authentiques et contrefaites en tant que technique complémentaire à la spectroscopie Raman pour l'identification du composant principal de l'étiquette.
  - *Évaluer si l'information fournie par la spectroscopie DRIFT améliore la capacité de discrimination* des données obtenues par spectroscopie Raman.

El objetivo principal del presente trabajo es el desarrollo **de una herramienta de diagnóstico irrefutable basada en el análisis a nivel ultra-traza del envase del vino (vidrio, papel, tinta y cápsula) mediante la ablación láser femtosegundo acoplado a ICPMS y las espectroscopias Raman e Infrarroja, lo cual permite realizar un análisis rápido, no-destructivo y multifactorial de la botella sin inducir en ella una degradación visible que pudiera afectar su valor.**

Por ello, este trabajo se ha estructurado entorno a **i) el diseño y desarrollo de una nueva cámara de ablación capaz de adaptarse a las diferentes formas de las botellas y su aplicación al análisis de las botellas de vino por fsLA-ICPMS y ii) la aplicación de las espectroscopias Raman e Infrarroja para el análisis cualitativo de las botellas**, siendo cada uno de los puntos anteriores los objetivos principales del mismo.

El primer paso para la consecución del primer objetivo es el **desarrollo de una cámara de ablación que se adapte a las diferentes formas de las botellas.** Este primer paso resulta de vital importancia debido a que la cámara de ablación juega un papel crucial en la ablación láser, la cual debe permitir un transporte rápido y cuantitativo del aerosol inducido por el láser a la fuente de plasma del ICP. En consecuencia, se establecen los siguientes objetivos metodológicos para el alcance de este primer objetivo:

- ✓ *Diseño inicial de la nueva cámara* en base a los diseños previamente descritos en la literatura.

- ✓ *Fabricación de la cámara de ablación mediante impresión 3D* ya que sus características no son alcanzables mediante técnicas de micro-mecanizado convencional de alta precisión.

- ✓ *Verificación de la idoneidad* en cuanto a un transporte rápido y cualitativo del aerosol inducido por el láser a la fuente de plasma del ICP. La sensibilidad ($^{115}$In) y el fraccionamiento elemental ($^{238}$U/$^{232}$Th) serán evaluados con el material de referencia NIST612. Además, la línea de transferencia (≈ 1,5 m) debe garantizar el transporte óptimo del aerosol (tiempo de lavado de la cámara de ablación < 5s).

- ✓ *Diseño y fabricación de un soporte para las botellas* adaptado a la plataforma XY del instrumento y que permita a su vez la inclusión de la nueva cámara de ablación en el sistema de ablación láser.

El segundo paso para lograr el primer objetivo se centra en el desarrollo de una metodología rápida (≈ 5 min) y no invasiva para el análisis a nivel ultra traza de las botellas de vino (vidrio, papel, tinta y cápsula) sin inducir ninguna degradación visible en ellas, debido a que no existe otra técnica equivalente en términos de rendimiento hasta la fecha. Para ello se establecen los siguientes objetivos metodológicos:

- ✓ *Optimización de los parámetros de operación del láser para cada tipo de matriz.* El instrumento de ablación láser de femtosegundo ALFAMET (KGW-Yb, 1030 nm) utilizado en este trabajo opera a altas tasas de repetición (1-100000 Hz) y permite la modificación virtual del haz del láser, lo que representa un adelanto de la ablación láser en el campo analítico.
  La optimización de estos parámetros de ablación incluye:
  - Selección del gas portador (He o Ar) y optimización del flujo del gas portador.
  - Optimización de la fluencia o energía del láser ($J/cm^2$), la frecuencia del pulso (Hz) y el diámetro del haz del láser (µm).
  - Selección del patrón de ablación que mejor se adapte a las características de cada matriz.

- ✓ *Optimización de los parámetros de operación del ICPMS para cada tipo de matriz.* El sistema de ablación láser está acoplado a un ICPMS modelo ELAN DRC II (Perkin Elmer), cuyas condiciones de operación también deben ser optimizadas para cada matriz:
  - Selección de los elementos e isótopos a monitorizar en función de la naturaleza de cada matriz. El elevado número de elementos que se pretende monitorizar puede condicionar la resolución de las señales detectadas y podrá requerir del ajuste del tiempo de integración.
  - Selección de las condiciones de plasma (plasma húmedo o plasma seco)

- ✓ *Análisis del vidrio:*
  - Selección de la estrategia de calibración.
  - Validación del método en términos de reproducibilidad, repetitividad, homogeneidad, linealidad, límites de detección e interferencias espectrales.
  - Análisis de botellas de acuerdo a: i) botellas originales y sus falsificaciones, ii) origen (país y/o continente) y iii) cosecha.

- ✓ *Análisis del papel y de la tinta.* Este objetivo metodológico se llevará a cabo de manera similar a lo descrito en la sección anterior. Sin embargo, se debe prestar una mayor atención al desarrollo de una nueva estrategia de calibración, la cual incluye la síntesis de estándares de papel y tinta propios.

- ✓ *Análisis de las cápsulas.* Para el análisis de las cápsulas es necesario considerar el diseño y desarrollo de una segunda cámara de ablación que se adapte a la curvatura del cuello de la botella. En tal caso, sería necesario evaluar su idoneidad, la optimización de las condiciones de operación fsLA-ICPMS y el análisis de las botellas de vino. Sin embargo, se realizará un breve test preliminar mediante el uso de una cámara de ablación convencional, cuyo objetivo es evaluar la capacidad del análisis de las cápsulas para la diferenciación de las botellas originales de las falsas y establecer su origen y cosecha.

- ✓ *Análisis estadístico y establecimiento de los parámetros de discriminación:*
  - Se realizará el análisis multivariante de los datos mediante el análisis de componentes principales (PCA) y/o análisis discriminante por mínimos cuadrados parciales (PLS-DA) y clasificación jerárquica ascendente con el fin de: 1. distinguir botellas originales de sus falsificaciones; 2. establecer los parámetros de discriminación a considerar para establecer su origen y cosecha.
  - Se considerará la creación de una base de datos en la que se recopilen los resultados obtenidos del análisis elemental cuantitativo de vidrio.

El segundo objetivo del este trabajo es **el desarrollo de una nueva metodología para el análisis molecular cualitativo de las botellas de vino mediante la espectroscopia Raman y espectroscopia Infrarroja de reflectancia difusa por transformada Fourier (DRIFT), las cuales aportarán información complementaria al análisis elemental llevado a cabo por fsLA-ICPMS**. En consecuencia, se establecen los siguientes objetivos metodológicos:

- ✓ Espectroscopia Raman:
  - *Selección de la fuente de radiación más apropiada* (láser rojo, 785 nm o láser verde, 532 nm) en función del tipo de matriz (papel o tinta).
  - *Optimización de los parámetros de operación del espectrómetro* Raman (número de acumulaciones por medida, tiempo de adquisición y número de espectros por muestra).
  - *Aplicación de la espectroscopia Raman* para la identificación de botellas originales y falsificadas, así como para su clasificación en función de la cosecha.
  - *Evaluación de la información espectral obtenida y tratamiento estadístico de los espectros* para la discriminación cualitativa de botellas originales y falsas y cosecha.
  - *Evaluar si la información obtenida por espectroscopia Raman mejora la capacidad de discriminación* de los datos obtenidos mediante el análisis elemental de las botellas.

- ✓ Espectroscopia Infrarroja de reflectancia difusa por transformada Fourier (DRIFT):
  - *Optimización de los parámetros de operación del espectrómetro DRIFT* (número de acumulaciones por medida, tiempo de adquisición y número de espectros por muestra).
  - *Aplicación de la espectroscopia DRIFT como técnica complementaria a la espectroscopia Raman* para la identificación de las botellas originales y falsas a través de la identificación del material principal de la etiqueta.
  - *Evaluar si la información obtenida por la espectroscopia DRIFT mejora la capacidad de discriminación* de los datos obtenidos por la espectroscopia Raman.

# CHAPTER 3:

# Instrumentation

# 1. Laser ablation coupled to inductively coupled plasma mass spectrometry (LA-ICPMS) for the analysis of trace elements in solid samples

## 1.1 INDUCTIVELY COUPLED PLASMA MASS SPECTROMETRY (ICPMS)

### 1.1.1 Basic concepts of Inductively Coupled Plasma Mass Spectrometry (ICPMS)

Since Houk et al. introduced the inductively coupled plasma mass spectrometry (ICPMS) in 1980 (1), it is accepted as the most powerful analytical technique capable of multi-elemental detection over a wide linear dynamic range with very low detection limits, while also providing isotopic ratio measurement capability (2). These features make the ICPMS an invaluable tool in a wide range of research disciplines which include health, environment, forensic, material and nuclear sciences, amongst others (3).

But it was not until 1983 when the first commercially available instrument was introduced. Since then, although the basic principle remains constant, the instrument has continuously improved. In fact, more reliable and robust instruments with very low detection limits (ppt) and high spectral resolution are every so often developed (4).

The basic principle of ICPMS is elemental differentiation on the basis of atomic mass but it cannot differentiate between neutral atoms. Therefore, the ICP serves as a separate excitation source, a highly ionized phase at a very high temperature, where atoms are first ionized to form positively charged ions by removal of an electron (5). Subsequently, ions are extracted by the vacuum interface and guided into the mass analyzer, separated by mass to charge ratio and finally detected (6). Figure 1 shows the elements traditionally measured by ICPMS and their approximate detection limit (LD) range.

It should be pointed out that some elements including B, Si, P, Br, I, K, Ca and Se have higher detection limits via ICPMS. On the one hand, elements whose ionization potentials exceed that of Ar, such as the lighter noble gases, fluorine and chlorine are not efficiently ionized. On the other hand, for elements as K, Ca, P, S and Se isobaric and molecular interferences coming from either the sample matrix or plasma species stand in the way of detection of the primary isotope. Consequently, less interfered isotope must be used for the determination of these elements which could degrade its detection and quantitation capabilities (7). Figure 1 shows the approximate detection limits of elements by ICPMS.

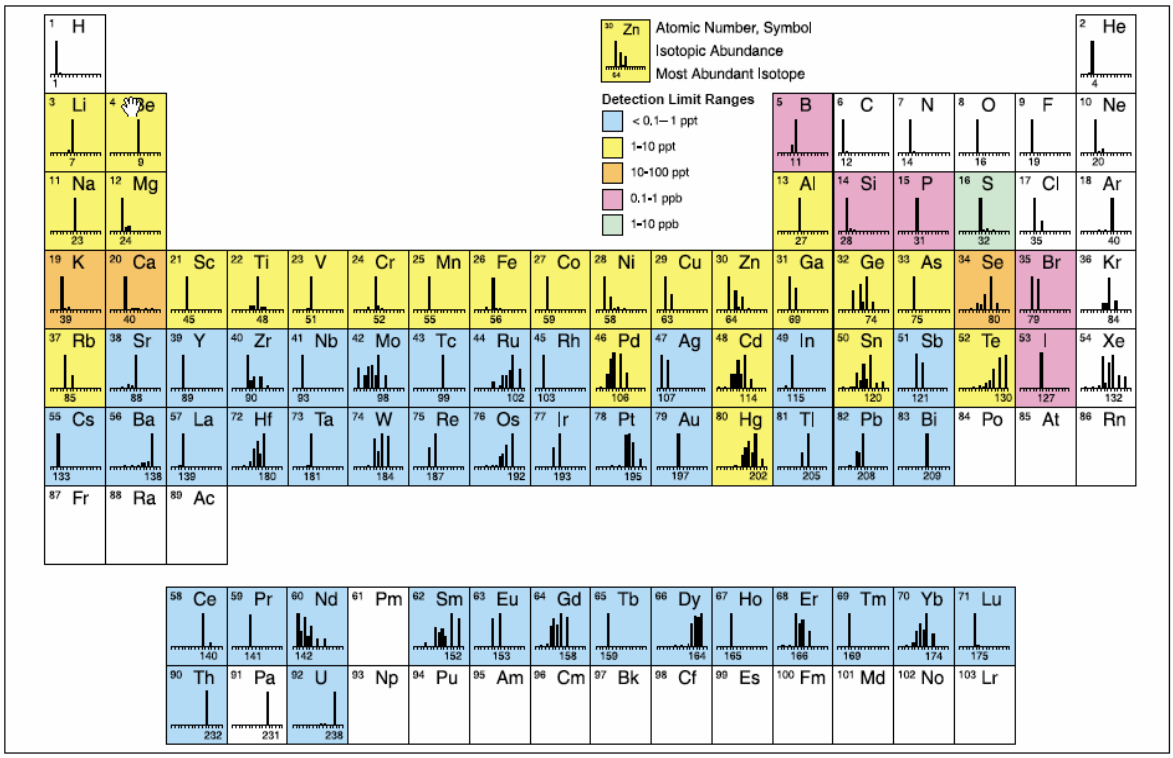


**Figure 1** Approximate detection capabilities of the ICPMS (Source: PerkinElmer, Inc. (8)).

### 1.1.2 ICPMS process description

The ICPMS instrument consists of 5 main components (Figure 2): sample introduction system, ionization source, interface, mass analyzer and detector.

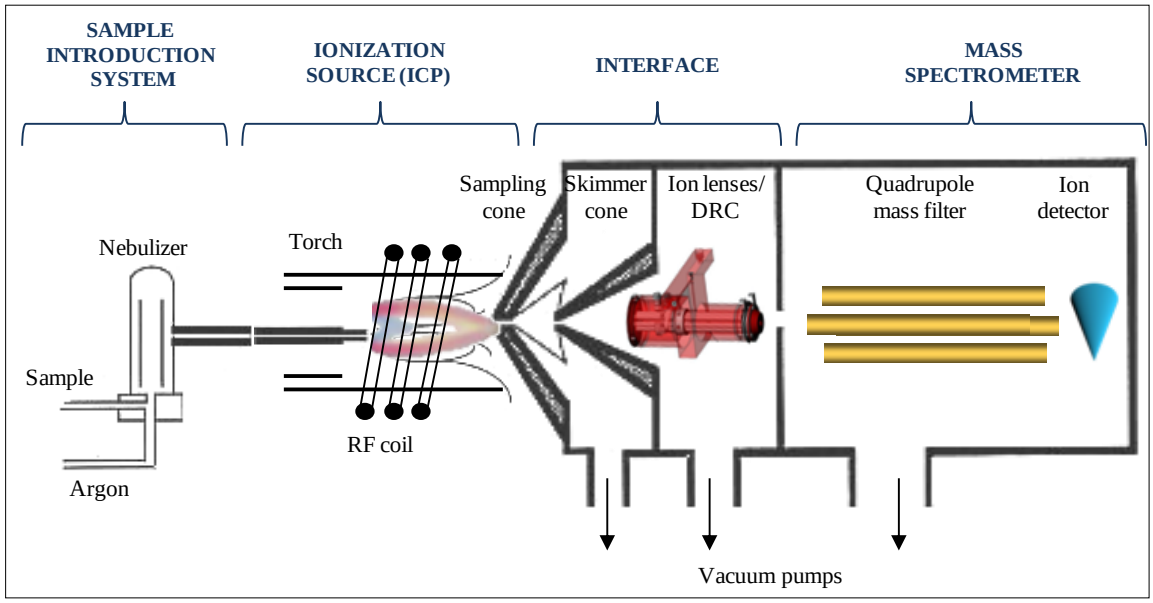


**Figure 2** Inductively Coupled Plasma Mass Spectrometer diagram.

*1.1.2.1 Sample introduction system*

The main goal of a sample introduction system is to introduce the maximum amount of analyte into the plasma in the most suitable form. However, it is considered to be *the Achilles' hell* of ICPMS as the generated aerosol must be stoichiometrically equivalent to the sample. Even though a several techniques have been developed for the introduction of solids, gases and liquids (Figure 3) into ICPMS instrumentation (5), the wet way remains being the most used procedure via a nebulizer (9) due to homogeneity, easy of handling and the possibility of preparing calibration standards (10).

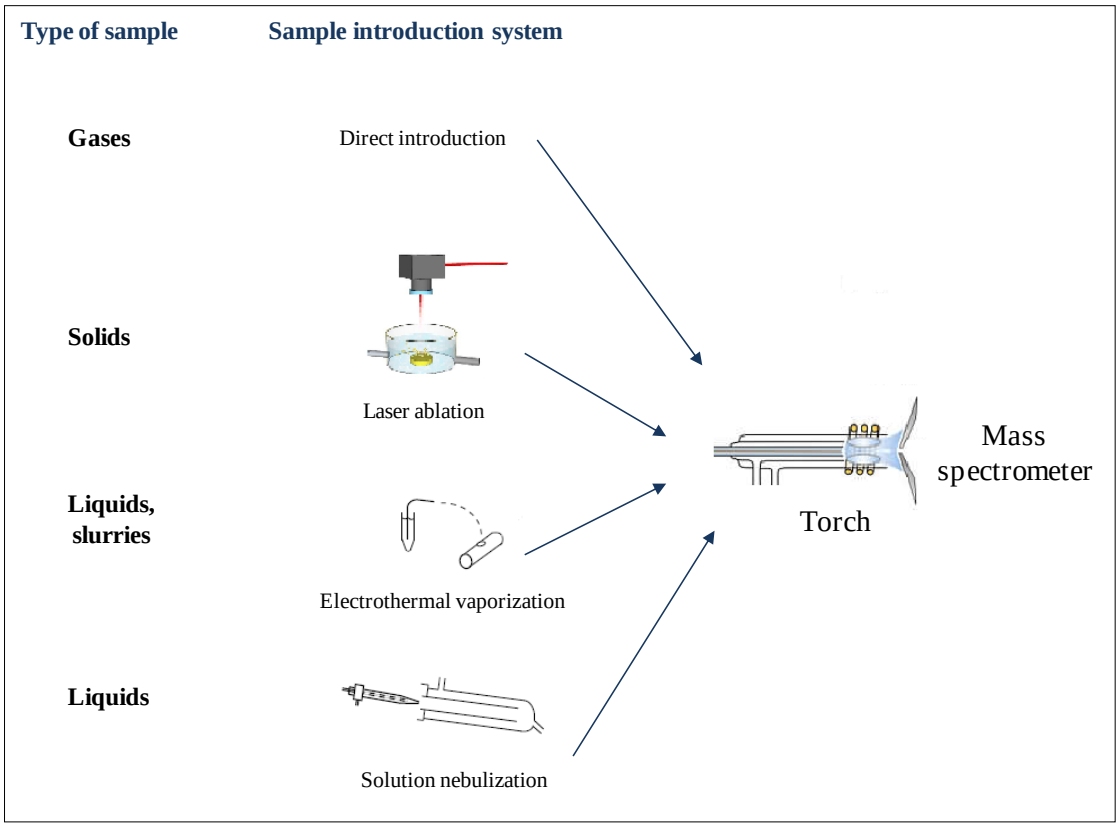


**Figure 3** Principles of sample introduction in ICPMS(3).

In general terms, nebulizer disperses the solution into a fine, gas-borne aerosol and a spray chamber is used to remove larger droplets (> 10 µm) from the aerosol through gravity or inertia (10). Typically, pneumatic nebulizer is employed which convert a liquid into a fine spray using a gas (argon) as the driving force (Figure 4) (11, 12).

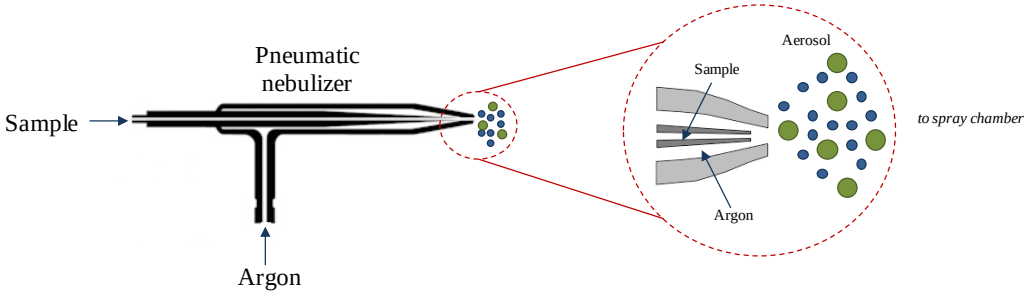


**Figure 4** Nebulization process scheme (pneumatic concentric nebulizer).

*1.1.2.2 Ionization source and sample ionization*

The plasma is generated by passing an argon flow through the torch which is wrapped by a radio frequency (RF) coil. The energy (1000 – 1500 W) supplied to the coil induces an oscillating electric and magnetic field- (27 or 40 MHz) inside the torch and a high- voltage spark is applied to the argon flow to snatch electrons from the argon atoms, forming argon ions. These ions are caught in the oscillating fields and come into collision with each other, forming coupled plasma at atmospheric pressure. The temperature reached inside plasma is around 7000 K which makes it an excellent ion source. Therefore, sample is introduced into the plasma where it will be desolvated, vaporized, atomized and finally, ionized (Figure 5) (5, 8) .

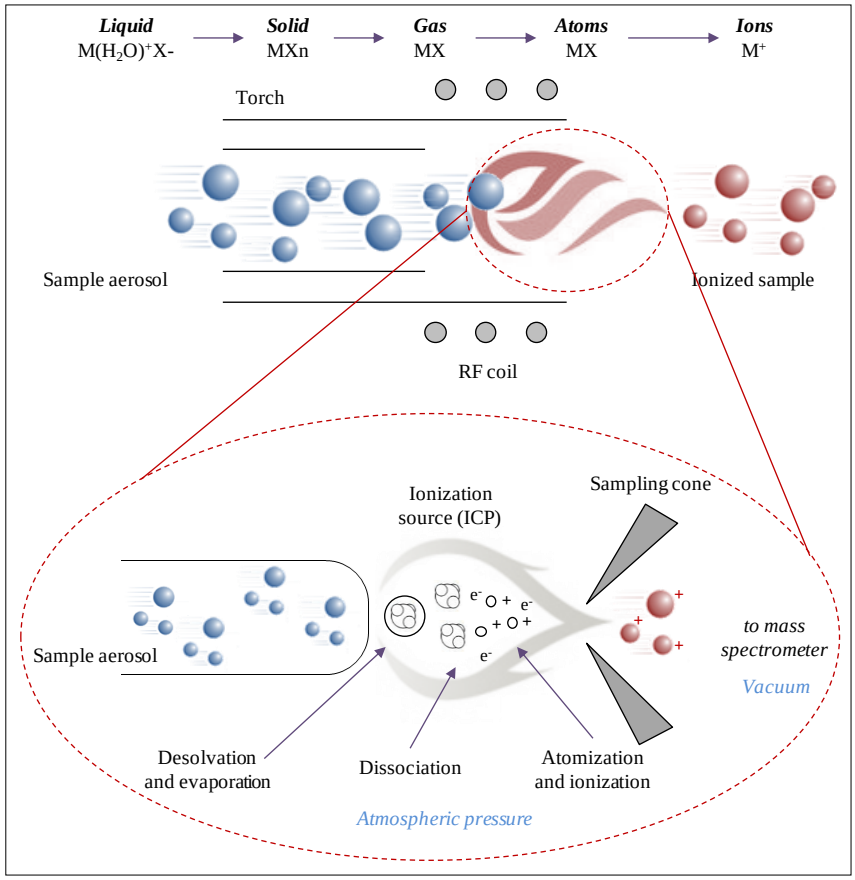


**Figure 5** Sample ionization process.

*1.1.2.3 Interface*

The interface, consisting of an intermediate vacuum region created by two cones, allows the ions travelling from the plasma at atmospheric pressure (1 – 2 torr) to the low pressure region of the mass spectrometer (<1 x $10^{-5}$ torr). The sampler (Ø orifice ≈ 1 mm) and skimmer (Ø orifice ≈ 0.4 – 0.9 mm) cones, typically made of nickel or platinum, sample the ions coming from the centre portion of the ion beam and accelerate them thanks to vacuum made by the rotary pump (≈ $10^2$ Pa). The ions are after rapidly introduced into an electrostatic lenses system which collimates the ion beam and focuses it into the entrance of the mass spectrometer (8).

*1.1.2.4 Quadrupole mass filter*

Due to the mass-discriminating properties based on mass-to-charge ratio (m/z), the ions can be separated from the ion beam and counted. Although different mass analyzer could be used coupled with the ICP ion source (time-of-flight mass spectrometer or magnetic sector mass spectrometer), the quadrupole mass filter is the most common analyzer used in ICPMS. It consists of four parallel metal rods. The opposite rods are electrically connected and a combination of a time-independent and a time-dependent potential is applied to them. The applied potential makes the ions entering the quadrupole to oscillate according to its m/z ratio. Extreme oscillations cause the ions to be defocused from the stable region and launched against the rods to be ejected (Figure 6) (5, 13). In other words, only ions having a stable trajectory along the quadrupole will be counted by the electron multiplier. Then, only a proper combination of the rod potentials allows counting ions of a given m/z ratio. By rapidly adjusting these potentials (in the ms range), the quadrupole can scan the full elemental ions mass spectrum (6-238 amu).

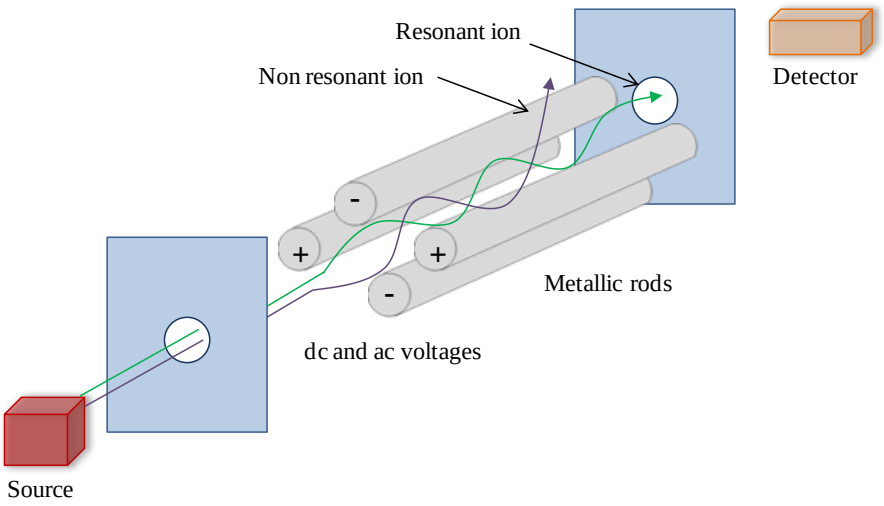


**Figure 6** Quadrupole mass filter scheme.

*1.1.2.5 Ion detector*

The task of the detector is to detect the ion signals emerging from the mass analyzer of a mass spectrometer and transform them into a measurable electronic signal. The ions exiting the mass filter strike the detector where they are converted into an electrical pulse. Once the ions hit the active surface of the detector, known as dynode, a number of electrons is released which will strike the next active surface, amplifying the signal. This cascade of electrons continues until a measurable pulse is created (Figure 7).

Over the years, the channel electron multiplier (CEM) detector, used in the earliest ICPMS instruments, has been replaced by the discrete dynode type detectors. Last ones can run in two

modes, pulse counting and analogue, which further extent the instrument's linear dynamic range to protect the detector from excessively high signals (8).

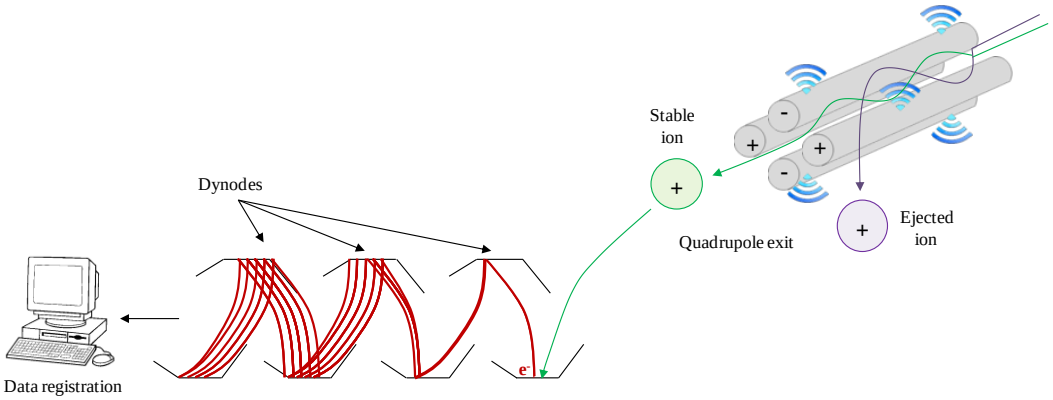


**Figure 7** Discrete dynode detector operating scheme.

### 1.1.3 Advantages and limitations of ICPMS

Since the introduction of inductively coupled plasma mass spectrometry (ICPMS), significant improvements have been observed for most parts of the instrument which have made to be launched to the forefront of "hot" fields like metallomics (14) and nanoparticles analysis(15). The main advances are focused on 1) more stable and compact high frequency (hf) generators, 2) optimized torch design for sample introduction and plasma gas consumption, 3) interface efficiency and ion optics, 4) collision reaction cells for the removal of spectral interferences, 5) new mass analyzers and detectors and 6) sophisticated software to make easier driving the instrument, data acquisition and processing (16, 17). Therefore, ICP mass spectrometry is nowadays a mature analytical technique in terms of figures of merit which are summarized in Table 1 (18, 19).

**Table 1** Figure of merits for ICPMS.

| | |
|---|---|
| ***Number of elements*** | Li (6) up to U (238) in 0.1s |
| ***Sensitivity*** | LOD - ng $L^{-1}$<br>(linear dynamic range of 8 to 9 orders of magnitude) |
| ***Background signal*** | 1 – 10 counts $s^{-1}$<br>(for quadrupole-based instruments) |
| ***Selectivity*** | Low resolution (from 0.3 to 0.8u)<br>*Susceptibility to spectral interferences* |
| ***Precision*** | RSDs ≤ 2% |
| ***Accuracy*** | CRM - validated quantification |
| ***Robustness*** | Content of dissolved solids ≤ 1 - 2 g $L^{-1}$<br>*Susceptibility to non-spectral interferences* |
| ***Long term stability*** | RSD % ≤ 1%<br>(warming-up time ≤ 15 min) |

Due to these features, inductively coupled plasma mass spectrometry (ICPMS) is considered to be a versatile, robust and high sensitive (ppt) analytical technique which is also capable of providing accurate and reliable information about concentrations and species identity required both in research and industry.

### 1.1.4 Spectral and non-spectral interferences in ICPMS

Since its introduction as primary and immensely powerful technique for trace and ultra-trace elemental analysis in many routine laboratories, its performance has been often hampered by spectral and non-spectral interferences.

- *Spectral interferences: inability to resolve same nominal masses*

Spectroscopic interferences arise when different ions with the same m/z are counted together owing to the limited resolution capability of the quadrupole mass spectrometer when ion masses differ by less than 0.5 mass units from the analyte ion. Thereby, analysis is interfered by an erroneous large signal at the m/z of interest (20, 21).

Such interferences can be divided into two categories depending on their origin: *isobaric interferences* and *polyatomic interferences (20-22).*

*Isobaric interferences* are caused by the overlap of isotopes of different elements. These interferences are easy to predict as they are well known and documented, so they can be overcome by use of alternative non-interfered isotopes or mathematical correction equations for analysis.

Example: Cr ($Cr^{54}$ = 53.938882) and Fe ($Fe^{54}$ = 53.939612) both have an isotope of 54 amu. However, the exact masses differ in 0.00073 amu which cannot be resolved by quadrupole the mass analyzer (5). Even high resolution ICPMS capable to achieve spectral resolution of 10000 will not succeed here since a resolution of 74000 is required. However, recent developments in triple quadrupole ICPMS technology, based on the selection and the chemical reaction of the analytes and the interfering species in a series of three quadrupoles, now allow to unravel this interference.

*Polyatomic interferences* are caused by the polyatomic ions (also called adduct ions) originating from the plasma gas (Ar), entrained atmospheric gases (C, N and O), sample matrix (O, H, C, N, Cl, S and P) and water and/or acids used for dissolution. These interferences are more prone to be significant under m/z = 80 (Table 2).

**Table 2** Some common Plasma/Matrix/Solvent-Related polyatomic spectral interferences in ICPMS (22).

| ***Element of interest*** | ***Interference*** |
|---|---|
| $^{24}Mg^+$ | $^{12}C^{12}C^+$ |
| $^{27}Al^+$ | $^{13}C^{14}N^+$ |
| $^{39}K^+$ | $^{38}ArH^+$ |
| $^{40}Ca^+$ | $^{40}Ar^+$ |
| $^{44}Ca^+$ | $^{14}N^{14}N1^6O^+$ |
| $^{51}V^+$ | $^{16}O^{35}Cl^+$ |
| $^{52}Cr^+$ | $^{40}Ar^{12}C^+$, $^{16}O^{35}ClH^+$ |
| $^{55}Mn^+$ | $^{40}Ar^{15}N^+$ |
| $^{56}Fe^+$ | $^{40}Ar^{16}O^+$ |
| $^{58}Ni^+$ | $^{58}Fe^+$, $^{42}Ca^{16}O^+$ |
| $^{63}Cu^+$ | $^{40}Ar^{23}Na^+$ |
| $^{64}Zn^+$ | $^{32}S^{16}O^{16}O^+$ |
| $^{75}As^+$ | $^{40}Ar^{35}Cl^+$, $^{40}Ca^{35}Cl^+$ |
| $^{80}Se^+$ | $^{40}Ar^{2+}$, $^{40}Ca^{2+}$, $^{40}Ca^{40}Ar^+$ |

Some approach can be carried out to solve polyatomic spectral interferences which include alternative sample preparation methods, the use of cool plasma technology, collision/reaction cell including triple quadrupole systems or high-resolution mass analyzers.

- *Non-spectral interferences: result from sample matrix*

Non-spectral interferences are characterized by suppression/enhancement effects and signal drifts which cannot be considered as a recognizable overlapping. In fact, this type of interference is often referred to as matrix-effects which exert an influence on sample transport, ionization on the plasma, ion extraction and transmission of the ion beam.

The elimination of matrix-effects requires the reduction of the amount of matrix which reaches the sample introduction and ion extraction systems and the use of the appropriate calibration method (internal standardization, standard additions and isotope dilution).

## 1.2 LASER ABLATION

### 1.2.1 Basic concepts of laser ablation

Since the early 80s (Alan Gray, University of Surrey, 1985) (23), laser-ablation inductively-coupled plasma mass spectrometry (LA-ICPMS) has been widely explored and nowadays is considered to be one of the most versatile analytical techniques for the direct trace elemental and isotopic analysis of solid samples. The most remarkable features are ease of use, fast sample throughput, limited sample damages, high sensitivity and wide dynamic range which allows the simultaneous acquisition of major and trace elements, as well as the measurement of isotope ratios.

However, problems related to matrix-dependent ablation requirements, elemental fractionation and sensitivity issues have limited its use for routine analysis(24). Therefore, in recent years a permanent optimization of the instrumentation and analytical procedures as well as the development of strategies to limit elemental fractionations have been performed for a more accurate and precise analysis(25).

The basic layout of LA-ICPMS system (Figure 8) is simple and has not changed significantly in the last decades, although significant improvements in ICPMS and laser technologies have been noted. The sample is placed into a hermetic ablation cell flushed with a carrier gas (Ar or He) and a laser beam (Ø = 1 – 200 µm generally) is focused onto the sample surface through a cell window transparent to the laser wavelength. If the provided irradiance ($W/m^2$) is high enough, the material will be extracted from the sample surface in the form of an aerosol (generating vapor, particles and agglomerates), which will be subsequently transported to the ICPMS via a tube connecting the ablation cell to the torch of the ICPMS. Once in the ICPMS, the laser-generated particles are vaporized, atomized and atomic ions are formed in the inductively coupled plasma. Then, ions are extracted by the vacuum interface and guided into the mass analyzer (quadrupole, magnetic sector field, multi-collector or time-of-flight) by a series of lenses where they will be separated according to their mass to charge ratio and finally detected.

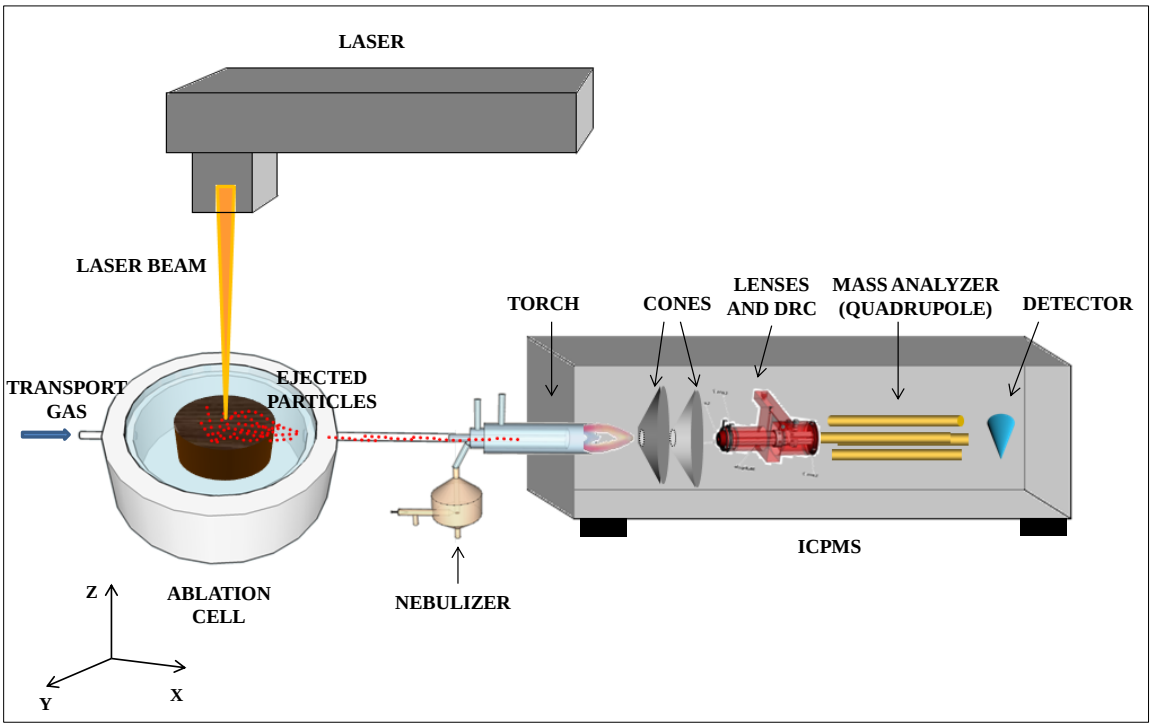


**Figure 8** Laser ablation (LA) sample introduction system coupled to ICPMS.

### 1.2.2 Laser ablation: an alternative to liquid sample introduction and microchemistry

Conventional analysis of solid samples by ICPMS is generally done by the previous mineralization of the whole sample (*bulk analysis method*), which involves its destruction and solubilization. In order to perform the digestion of the sample, mixtures of acids ($HNO_3$, HCl, HF) and oxidizing agents ($H_2O_2$) are commonly used with the aid of a heating plate or microwave reaction system which significantly improve its performance. This is a tedious time-consuming step, complex and often half-finished (26, 27).

Contrary to this sample preparation procedure, laser ablation has become an effective and attractive sample introduction system for solids (28) as well as refractory materials (aluminosilicates, ceramics or quartz, for instance) which are difficult to digest (29). On the one hand, sample preparation is small or non-existent and so contamination risk, and required time and resources are remarkably limited. On the other hand, the amount of sample used for each analysis is small (from fg to µg) compared to the large amount of sample employed in liquid-ICPMS (from mg to µg). Moreover, the use of a laser beam allows the micro-sampling of sample's inclusions, imperfections or heterogeneities as it can be focused on the sample surface (topochemical microscopic information) with a high spatial resolution and sensitivity. In Table 3 the performances of ICPMS and LA-ICPMS are shown.

**Table 3** Performance comparison of ICPMS and LA-ICPMS

Adapted from Becker et al. (30).

| *Evaluable feature* | *ICPMS* | *LA-ICPMS* |
|---|---|---|
| *Sample preparation* | Simple (often expensive because of matrix removal) | Small or non-existent |
| *Quantification* | Excellent | Difficult, CRM required |
| *Detection limits* | 0.001-0.1 ppt (solution) | 0.00001 -0.1 ppm |
| *Amount of sample used* | From mg to µg | From µg to fg |
| *Precision* | ± 1 - 5% | ± 1 – 10% |
| *Spatial resolution* | No | > 5 µm |
| *Depth profiling resolution* | No | 0.01 – 9 µm |
| *Time-consuming step* | Sample preparation | Quantification |
| *Contamination risk* | High | Low |
| *Limitations* | Interferences | Heterogeneity, interferences |

However, the possibility to perform analyses at a micron and different spatial scales plays a key role in developing new analytical applications. In fact, global sample surface analysis (elemental or isotopic composition) is easily achievable by the ablation of a determined area ($mm^2$) and it has been successfully applied as a powerful imaging (mapping) technique to produce quantitative images of detailed regionally specific element distributions (31) in different kind of matrices (32-34). Owing to the advantages shown, LA-ICPMS has turned into a reference analytical technique for the microscopic and non-destructive analysis of complex matrices with very low detection limits (geochemical and biological samples, multiple layer samples, artwork, pieces of archaeology and gemstones, for example) (33, 35, 36). Applications of LA-ICPMS are more extensively described hereinafter.

### 1.2.3 Laser technology and laser ablation systems

LASER is the acronym that stands for **L**igth **A**mplification by the **S**timulated **E**mission of **R**adiation, coined in 1957 by the laser pioneer Gordon Gould. Generally, a laser is a device which creates monochromatic and unidirectional beam of light within all the photons are in a coherent state, usually with the same frequency and phase. Laser technology properties are: i) laser beam can propagate over long lengths with moderate divergence and can be focused to very small spots, ii) laser beam has a very narrow optical bandwidth and iii) it can be emitted continuously or alternatively in the form of short or ultra- short pulses, with durations from microseconds down to a few femtoseconds (and even few attoseconds in some very specific conditions).

A laser oscillator comprises a laser cavity (laser resonator) in which the laser radiation circulates between two mirrors and passes a gain medium which serves to amplify the light for compensating the optical losses. The gain medium requires some external energy supply by light (optical pumping) or electric current (electrical pumping). The principle of laser amplification is stimulated emission, in which the photon emission is stimulated by incoming photons (Figure 9). In that case, a photon is emitted into the mode of the incoming photon. In effect, the power of the incoming radiation is amplified (37).

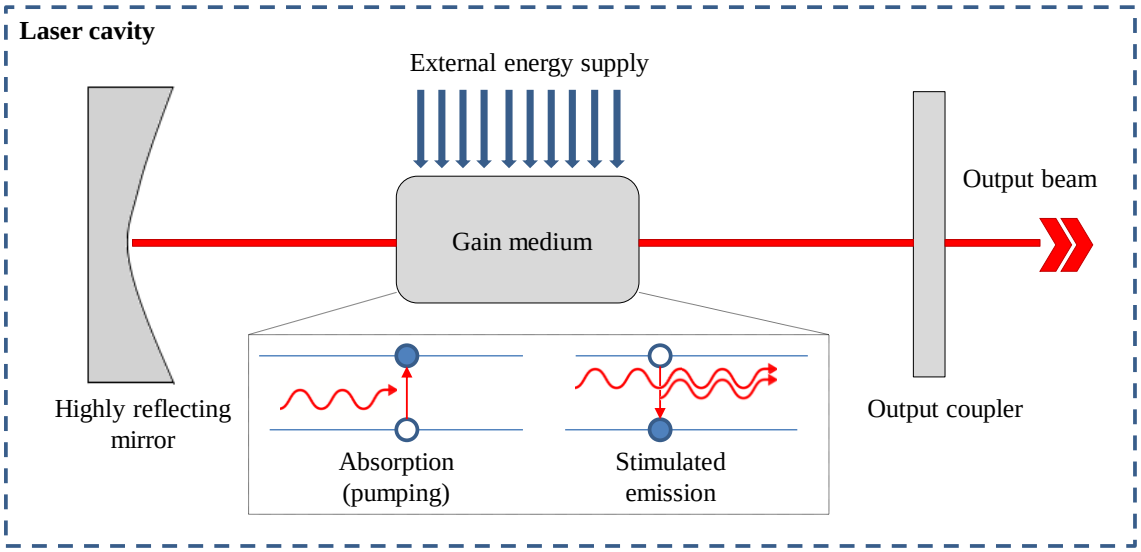


**Figure 9** Setup of a simple laser cavity composed by highly reflecting curve mirror, the gain medium and a partially transmissive flat mirror.

Common type of lasers are: 1) **semiconductor lasers** which are usually electrically pumped efficiently generating very high output powers with poor beam quality or low powers with good spatial properties (e.g. application in CD and DVD players) and 2) **solid-state lasers based on ion-doped crystals** which are pumped by discharge lamps or laser diodes and generate a very high quality and stability beam and ultra-short pulse durations (picoseconds and femtosecond pulse durations). Therefore, these lasers are preferred for analytical purposes. For laser ablation analysis purposes, most employed gain media are Nd:YAG, Yb-KGW and Ti:sapphire. A special type of ion-doped glass lasers are excimer lasers based on gases which are typically excited with electrical discharges. Common excimers are ArF, KrF, XeF and $F_2$ (38).

An ideal laser ablation system for LA-ICPMS would have the following key abilities: i) laser-matter interaction must be similar regardless of the matrix of the sample, ii) representative aerosol composition (39), iii) high transport efficiency (40) and iv) complete atomization and ionization of laser-induced particles in the plasma source (41, 42). Even the operating principle of this technique has practically not changed since its introduction, some notable developments have been done in order to improve the capabilities of laser ablation systems (Table 4) to achieve previously described ideal conditions. The intrinsic developments which are related to laser technology (pulses duration and stability (43, 44), wavelength (45) and optics) and the extrinsic developments concerning aerosol transport (the nature of transport gas and flux, the geometry of the ablation cell and its volume) (46) play an important role in the amelioration of the LA-ICPMS analytical performance.

**Table 4** Key developments in the history of laser ablation systems for LA-ICPMS
Adapted from Sylvester et al.(47).

| *Development* | *Advantages* | *Reference* |
|---|---|---|
| *Reduction of laser wavelength* | Higher absorption and improved ablation of transparent materials<br>Reduction of large particle, improving ionization | (48) |
| *Use of helium as carrier gas* | Improved analyte signal intensity, faster cell washout | (49) |
| *New ablation cell designs* | Better access to large samples analysis<br>Quantitative and qualitative particle transport<br>Improved cell washout | Chapter 4 |
| *Ultra-short pulse lasers* | Reduction of target heating minimizing sample damage and fractionation and improving accuracy/precision | (50) |

However, among all the new instrumental improvements, two developments –shorter pulses and shorter wavelengths– are the most significant and they are discussed in more detail in the following paragraphs. Both aimed at unifying the idea of better localization of LA event and a more efficient energy delivery.

Femtosecond laser systems are based on chirped pulse amplification (CPA) in order to obtain short and energetic pulses. This process was firstly investigated by Strickland et al. (51) and it is divided in 3 steps (Figure 10): i) the pulse is stretched with the aim of reducing its peak power, ii) the stretched pulse is safely amplified and iii) it is finally recompressed to its initial duration. However, the major drawback of CPA is the difficulty to recover the initial pulse duration and pulse quality.

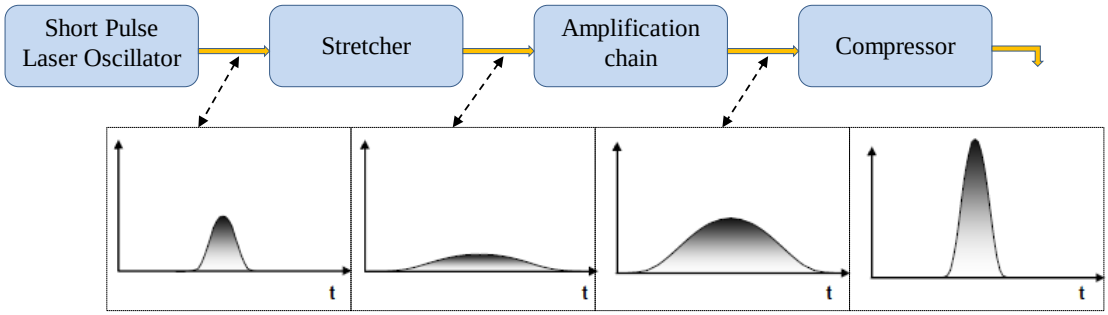


**Figure 10** CPA process in ultra-short laser systems.

Since 2000, femtosecond lasers could be regarded as a valid alternative to nanosecond lasers to reduce the sample damage at the ablation site. The ultra-short pulse duration does not provide sufficient time for energy to dissipate into the target lattice to heat and to induce melting prior to the explosive release of sample material (Figure 11) (50).

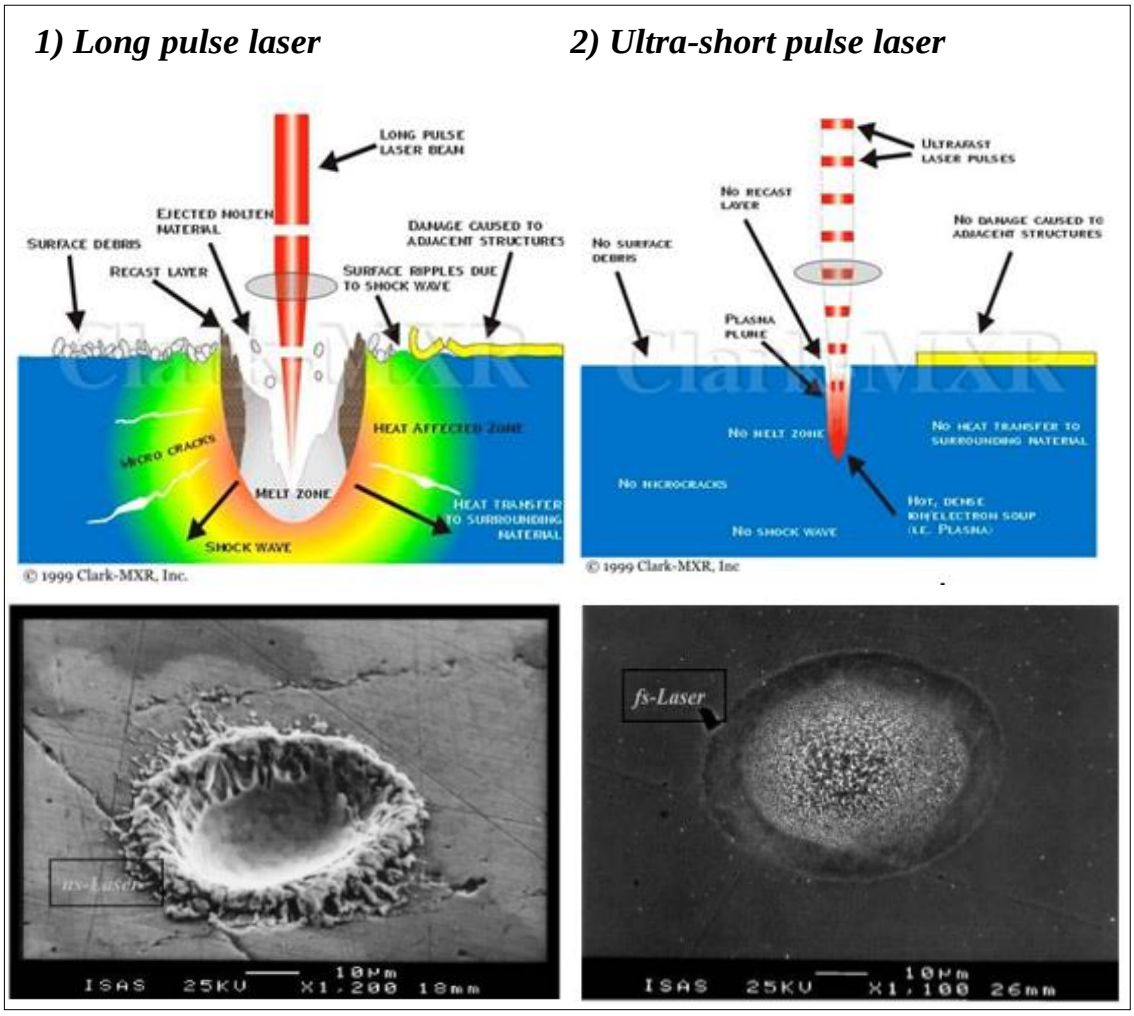


**Figure 11** Laser-matter interactions in both long and ultra-short pulse lasers (Clark-MXR, Inc.). Images show fs- and ns- ablation of polished brass. The ablation crater produced by the nanosecond laser shows a clear melting ring whereas femtosecond laser produced crater is neat and clean.

The most fundamental feature of laser-matter interaction in the long pulse regime (nanosecond lasers) is that the heat deposited by the laser in the material diffuses away into the surrounding area. This happens when the pulse duration is longer than the heat diffusion time and it is a detrimental process especially in regard to micro-analysis. Heat diffusion reduces the efficiency of the ablation process as it sucks energy from the working spot, reducing the amount of material removed from the sample. In addition, energy diffusion leads to melting, evaporation and condensation of the material producing cracks to adjacent structures and large-particles agglomerates which can obstruct its transportation, evaporation, atomization and ionization in the plasma source leading to fractionation and loss of measurement accuracy (52).

Conversely, the most fundamental feature of laser-matter interaction in the ultra-short pulse regime (femtosecond lasers) is that the heat has not time enough to spread to surrounding area during the time the laser is interacting with the sample. Because the energy does not have enough time to diffuse, the efficiency of the ablation process is quite higher. Femtosecond lasers deliver a great amount of peak power in a small spot and the pressure created by the force within the sample surface allows the material to expand outward in a highly energetic gas, causing no shock-waves around. This gas plume is formed by electrons and ionized atoms. Because the electrons are lighter and more energetic, they come off the material first and the remaining ions repel each other during expansion. The melting layer is extremely small under these conditions, and melted particles ejected from there due to hydrodynamic sputtering are almost inexistent compared to nanosecond laser ablation. Thermal effects are then very limited then improving drastically the ablation quality (less damages around the ablation spot) with no preferential evaporation of siderophile elements and formation of small particles (essentially by gas phase condensation) (Figure 12); these points are of great importance for sensitive accurate and precise analysis of trace element by laser ablation.

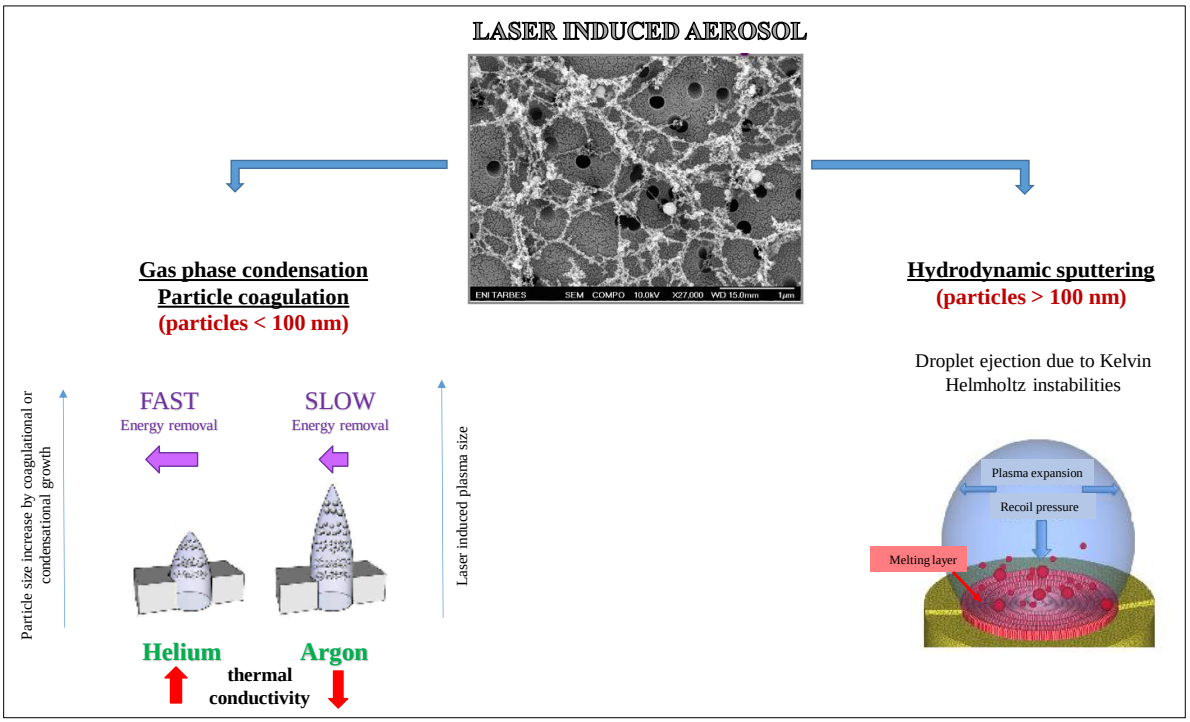


**Figure 12** Laser induced aerosol behavior according to particle size. Adapted from Horn et al (49).

The following table (Table 5) provides an overview of the most significant characteristic of ns-LA and fs-LA systems for LA-ICPMS analysis. It must be highlighted that the main difference between two ablation modes can be found at the IR wavelengths, since the negative effects of ns-LA are reduced at the UV range. In summary, the improved analytical performance of fs-LA process lies in the higher irradiance which leads to higher signal intensity for similar fluence, reduced matrix effects, better particle-size distribution and reduced elemental fractionation (53).

**Table 5** Comparison of analytical performances of ns-LA and fs-LA systems for LA-ICPMS measurements.

| *Feature* | *ns-LA* | *fs-LA* |
|---|---|---|
| *Thermal effects* | ↑ high thermal diffusion | ↓ low thermal diffusion |
| *Influence of laser wavelength* | ↑ shorter wavelengths are preferred | ↓ little effects |
| *Laser ablation efficiency* | ↓ decrease in the laser energy | ↑ better usage of laser energy |
| *Fractionation effects* | ↑ material redistribution | ↓ production of ultra-fine aerosol |
| *Matrix effects* | ↑ high matrix dependence | ↓ low matrix dependence |
| *Precision* | ↓ limited, less reproducible ablation process | ↑ reproducible ablation process |
| *Accuracy* | ↓matrix dependent behaviour | ↑low matrix dependence |
| *Repeatability* | ↓limited | ↑improved |
| *Sensitivity* | ↓moderate | ↑enhancement of signal intensity |
| *Spatial resolution* | ↓sample layers mixture due to thermal effects | ↑better lateral/depth resolution |

Figure 13 shows the progression of laser types used for LA-ICPMS over the past 30 years. The ruby (693 nm) laser was the first dedicated to analytical applications of solid samples followed by long wavelength (1064 nm Nd: YAG) lasers which were not well absorbed by transparent materials, leading into physical fragmentation of the ablation site. Later on, shorter wavelengths (266 nm and 213 nm Nd: YAG, 193nm ArF) were employed which produced aerosols containing only a little fraction of large particles difficult to be vaporized in the plasma source. Nanosecond lasers have been more widely used, both in the infra-red (IR) and the ultraviolet (Vis-UV). Because they have demonstrated better performance in analytical chemistry, nanosecond UV lasers are now the most common in this field. The easiest way to produce UV pulses is to start with a near-IR (NIR) laser source and select second, third or fourth -harmonic generation. However, there are still troubles to overcome concerning sample heating and melting at the ablation site. Many parameters can influence the capabilities of a laser and even if shorter wavelength can minimize many of the problems encountered in laser ablation analytical performance, it can be also improved by reducing the pulse duration below the material-specific thermal relaxation time.

Up to day, taking into account the studies published about the performance of femtosecond lasers emitting at infrared and ultraviolet wavelengths there is not a consensus about the most appropriate choice in terms of data quality (inaccurate quantification due to mass-load-induced matrix effects and elemental fractionation) (25). In order to get further information about the coupling of infrared and ultraviolet femtosecond laser ablation to ICPMS and not extend the state-of-the-art much longer, the works carried out by Fanny Claverie and Ariane Donard show deep studies and knowledge in this domain (54, 55).

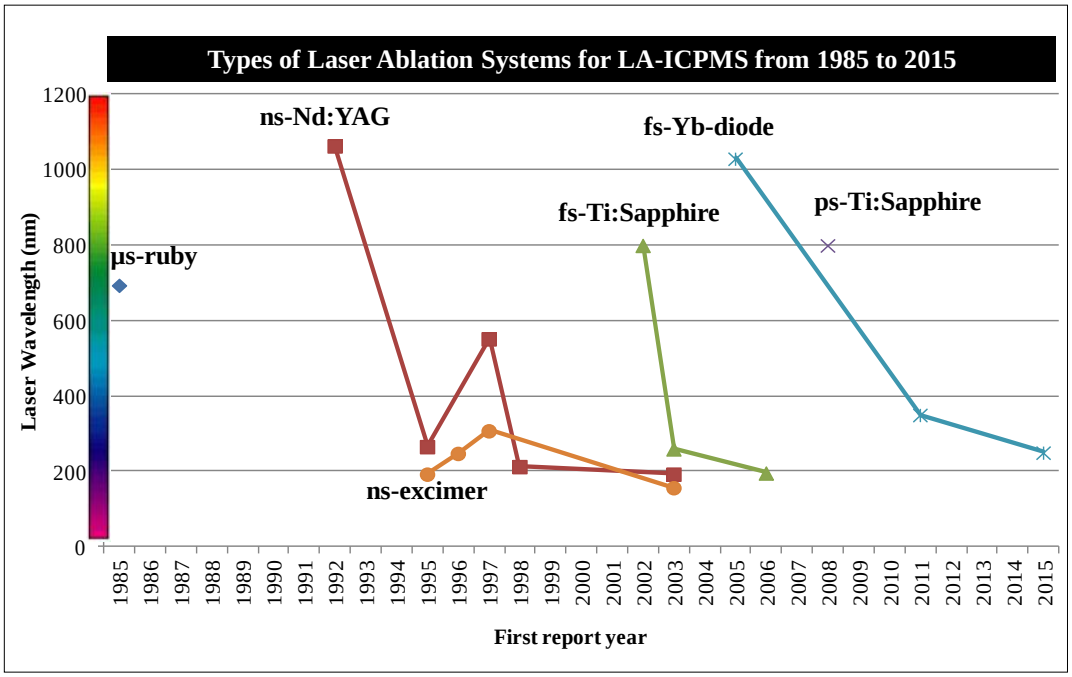


**Figure 13** Evolution of tested laser ablation systems for LA-ICPMS between 1985 and 2015. Adapted from (47) and (56).

### 1.2.4 Limitations and drawbacks of LA-ICPMS

Despite all the advantages cited above, the main limitations of LA-ICPMS, which negatively affect the accuracy of measurements, are the following: 1) matrix effects, non-linear calibrations and the lack of certified reference materials for the majority of the samples of interest and 2) the occurrence of non-stoichiometric effects in the transient signals, defined as elemental fractionation, which means that the ion signals recorded by the ICPMS often do not represent the sample composition. Fractionation occurs during ablation, aerosol transportation or the atomization and ionization processes within the ICP.

For a given sample, the amount of ablated material depends on its physical properties (optical, mechanical, thermal) and established laser operating conditions (wavelength, pulse duration, energy, repetition rate, focalization of laser beam, etc.). Assuming that laser parameters are constant over time, the performance of ablation varies from sample to sample if the nature of the matrix or the laser focusing change. Theoretically, it is possible to correct these effects using an internal standard or normalizing element to compensate for differences in ablation yields. The internal standard is generally an element that is spiked at a known concentration into the matrix or a major element that is already present in the matrix, whose concentration has been previously quantified by other analytical methods. It must be noted that if the concentration of the internal standard is not known, it would not be possible to determine the concentration of the analytes with accuracy and precision and simply establish "analyte/internal standard" ratio. The behavior of the element of interest is supposed to be the same during the analysis of the sample and the certified standard. However, standardization may not be successful depending on the sample or standard matrix and the selected analytes which lead to analytical bias.

This lack of accuracy was barely identified in the 90s and it is known as elemental fractionation in which the chemical composition of the aerosol produced during ablation, and after transported and detected, differs from that of the sample (57). Three main sources of fractionation have been identified (Figure 14) (58): 1) preferential evaporation of volatile elements during sample ablation process and formation of large particles (39), 2) large particle loss during transportation to plasma source (40) and 3), unequal and incomplete atomization and ionization of particles and preferential evaporation of light isotopes within plasma source (41, 42).

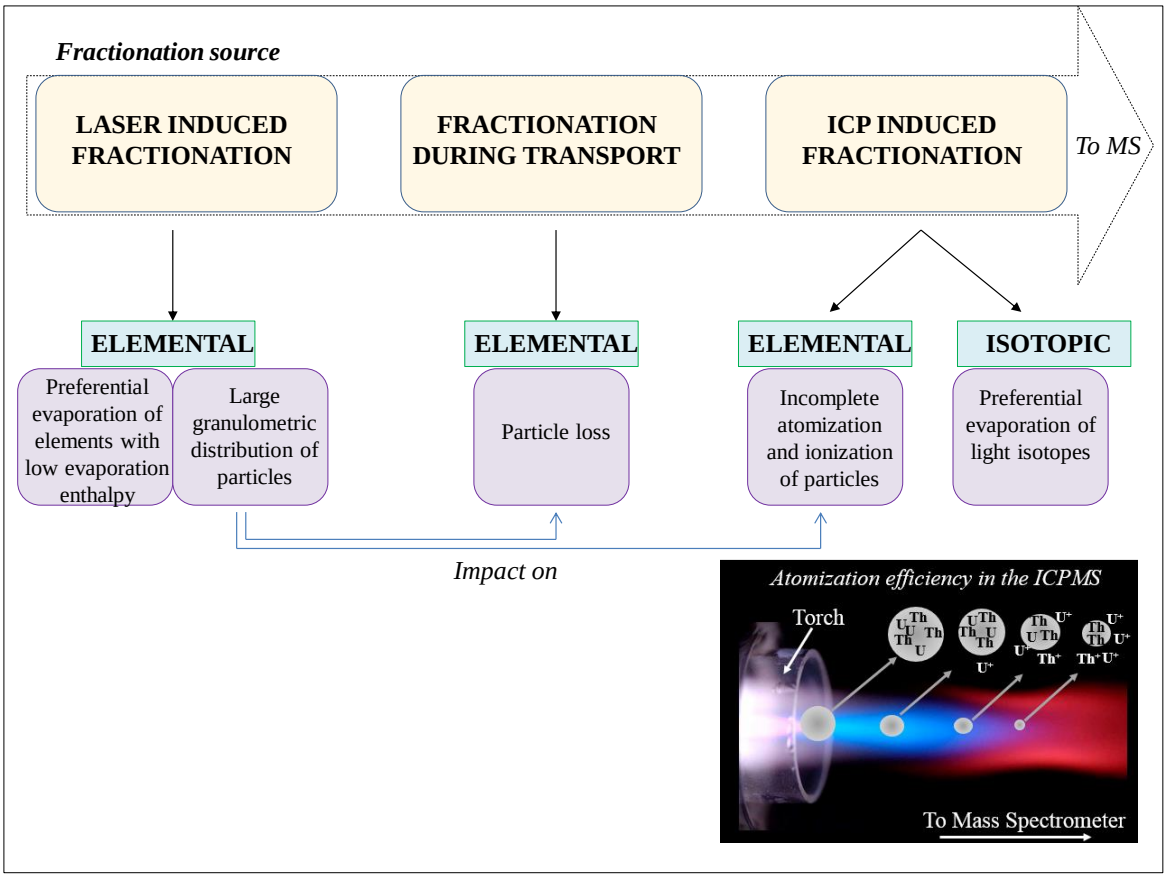


**Figure 14** Elemental and isotopic fractionation sources during LA-ICPMS measurements.

The use of certified reference materials (CRM) whose matrix is equal to sample allows offsetting the fractionation effect and narrowly correcting the problem. Nevertheless, this correction method has a limited capacity as the fractionation effect could occur similarly both in the sample and reference material. In addition, there is a lack of certified reference materials for certain scientific fields (environmental, biomedical) that makes the quantification task even more difficult. Therefore, the "home-made" synthesis of doped materials is a feasible way to compensate this absence of CRM. In this case, a known concentration of elements is added to a matrix similar to the sample. For the synthesis, the matrix is crushed until getting a fine powder, doped and compacted in a pellet. However, the homogeneity of analytes and the consistence and the crumbliness of the pellet, which cannot be monitored during fabrication process, are the mayor drawbacks. The second alternative, developed in 1989 by Thompson et al (59), is based on the double introduction of a dry aerosol originating from the laser and a liquid aerosol. It consist in the ablation of the sample and the simultaneous nebulization of certified solution. Nonetheless, it is necessary to correct the detection difference between both aerosols and the advantages of laser ablation in terms of oxides reduction are lost due to the introduction of a liquid aerosol (60). Finally, isotopic dilution coupled to mass spectrometry is regarded as reference calibration method which has been largely applied in several fields. Contrary to the previous analytical strategies, if there is

an homogeneous distribution of the solid sample and the added enriched isotope, the analytical performance will not be affected neither by the matrix effects, signal drifts or analyte loses (61-63). In addition, deep nanosecond UV lasers (≤193 nm) or even better femtosecond lasers (that might also be used in the UV range) have demonstrated to limit significantly elemental fractionation due to the laser-matrix interactions previously mentioned (64). Femtosecond laser ablation systems provide elemental ratio measurements that remain more stable with respect to time, which allows a greater degree of confidence in LA results (65), and then somehow limiting the need of perfect matrix matching to obtain accurate results or even allowing non-matrix-matched calibration on brass, aluminum and glass (66, 67).

### 1.2.5 Femtosecond laser ablation system used in this work (ALFAMET, Novalase, France)

#### *1.2.5.1 Industrial design and creation*

The ALFAMET (*Ablation Laser Femtoseconde pour l'Analyse de Métaux Traces*) laser ablation system is a laser prototype constructed in 2003 which was carried out thanks to the collaboration between the *Laboratoire de Chimie Analytique Bio-Inorganique* (LCBIE, Pau, France), Novalase (Canéjan, France) which is specialized in the integration of optics and laser systems and Amplitude Systèmes (Pessac, France) which is skilled in the development of laser sources. It was constructed according to the specifications given by the chemistry laboratory who was in charge of testing and demonstrate the potential of the equipment by developing analytical techniques and methods for the analysis of different types of matrices, ablation cells, etc. Figure 15 shows the laser ablation station. In the front side of the machine (a), the main controller computer, the screen and the ablation chamber equipped with an X-Y slide are located for their easy access. In the back side (b), laser source and cooling system are placed.

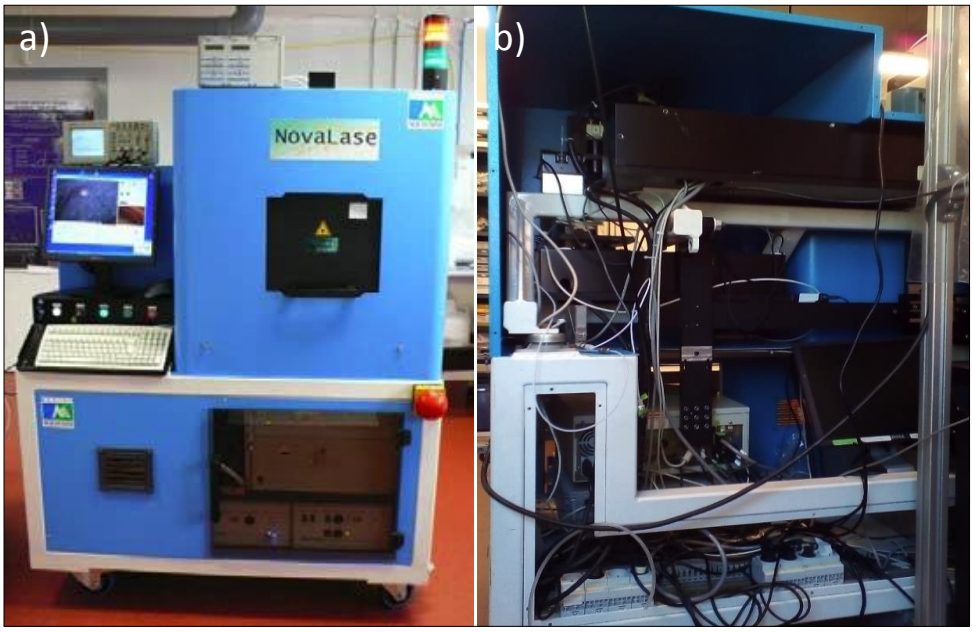


**Figure 15** Front and back views of ALFAMET laser ablation device.

*1.2.5.2 Technical characteristics*

Due to its ***1)*** compact dimension (1.4 x 0.9 x 1.7 m), ***2)*** all-in-one integration which allows a complete management from the computer (energy, frequency, design of complex trajectories, sample location and focalization) and ***3)*** the fact that the frame is mounted on wheels for an easy displacement of the machine, it is possible to modify its location to facilitate the access to ICPMS instruments distributed across the laboratory without the need of optic realignment.

The femtosecond laser source used by the system is fitted with a diode-pump KGW-Yb crystal delivering 360 femtosecond pulses at 1030 nm. The initial laser source operated at low energy (< 200 µJ/pulse) and high repetition rate (1-100000 Hz). This made a huge forward leap in analytical laser ablation as to date, high energy (> 1 mJ/pulse) and low repetition rates (< 20 Hz) were commonly used. A new femtosecond laser source (HP1, Amplitude Systèmes), much more robust and delivering 1 mJ/pulse @ 1kHz and allowing repetition rate from 1Hz to 100000 Hz is now fitted into ALFAMET. The ablation cell is mounted on a motorized XY stage for sample positioning (± 1 µm) or for slow sample displacement during laser firing. Principal technical characteristics are summarized in the following table (Table 6):

**Table 6** Technical characteristic of ALFAMET ablation system.

| | |
|---|---|
| *Laser source* | KGW-Yb pumped by diode laser |
| *Pulse width* | 360 fs |
| *Wavelength* | 1030 nm |
| *Repetition rate* | 1 Hz – 10 kHz |
| *Spot size* | 20 µm |
| *Laser beam movement* | Galvanometric mirrors |
| *Energy* | E = 0.1 – 100 µJ/pulse ± 0.1% |
| *Inter-pulse stability* | < 0.5% |
| *Sample positioning* | ± 0.1 µm |

Additionally, the system is equipped with both macroscopic (x 10) and microscopic (x 110) CCD cameras. Full-color macroscopic camera allows visualizing the sample on a large scale and having pictures of areas of interest. However, black and white microscopic camera allows focalizing the laser beam onto the sample at a micrometric scale.

*1.2.5.3 System components*

a) Optics

Several optical units are situated on the laser beam path to modify its size and energy (Figure 16): a half waveplate, a cubic wave splitter, a beam enlarger and a diaphragm.

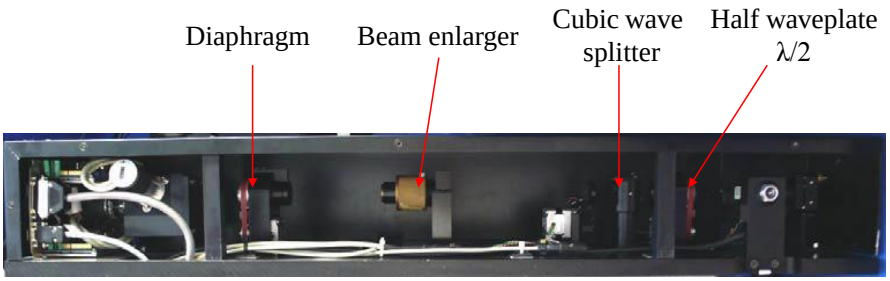


**Figure 16** ALFAMET laser optics.

The ***half waveplate*** (λ/2) linked to the cubic wave splitter allows to adjust precisely the laser beam energy from 0.1% to 100% (0.1 – 100 µJ/pulse) with a better precision than 0.1%. The plate is an optical tool used to modify the light polarization without distorting its wavelength. In fact, it is birefringent and anisotropic crystal which has an optical axis. Consequently, whatever it is the polarization of the light, it will be converted into a symmetric polarization due to optical axis of the waveplate. So, the polarization of the resulting light beam will be determined by the polarization of the entering light beam and the orientation of its polarization in relation to optical axis of the plate. The rotation of the half plate, and then of the optical axis, is controlled by a step motor. Later on, the ***cubic wave splitter*** will select a determined polarization and will induce a diminution of the

laser intensity. Thus, the combination of these two optical elements allows controlling the energy of the laser.

A ***beam expander*** **(x3)**, which involves two convergent lenses, is just placed after the cubic wave splitter in order to enlarge the size of the laser beam from 3,5 to ≈11 mm diameter. By expanding the laser beam, the fluence of the laser beam at the surface of the next optical components (galvanometric mirrors, dichroic mirror, objective, etc…) is reduced then preventing damages. In addition, it allows obtaining small spot diameters at the focal point on the sample (typically 20 um or less). Finally, a ***diaphragm*** is situated at the end of the light path to select the amount of light transmitted through the overture.

b) Galvanometric scanner: the key for new ablation strategies

High repetition rate (1-100000 Hz) coupled to a 2D galvanometric scanner (Figure 17) allows to create complex ablation trajectories.

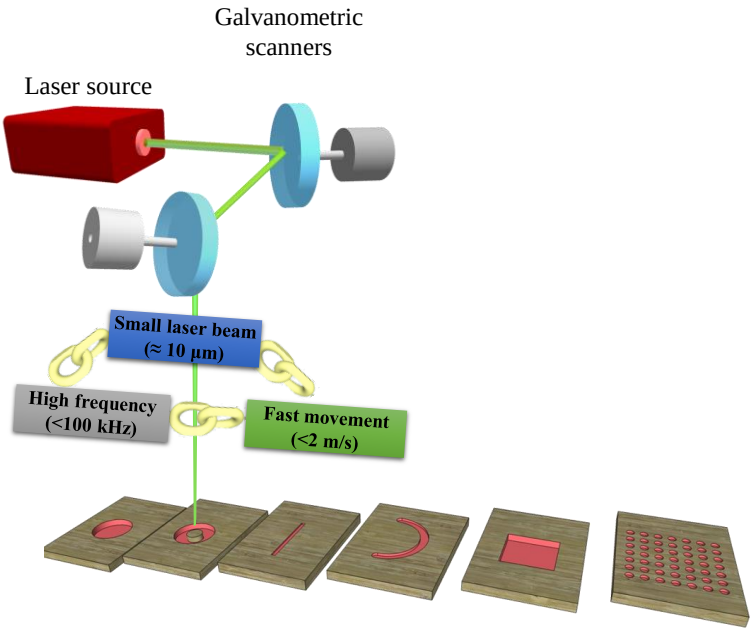


**Figure 17** Schematic representation of the galvanometric scanner. Courtesy of C. Pécheyran.

The 2D scanner is an optical arrangement consisting of two galvanometric mirrors. The rotation of these mirrors makes possible to move the laser beam extremely fast (< 2m/s) in the horizontal plane of the sample, both X and Y directions, with a high positioning precision. This, combined with the simultaneous movement of the sample, enables to produce complex trajectories in order to virtually enlarge or change the laser beam shape and adapt it to sample morphology (68, 69). This is a virtual beam shaping. Table 7 summarizes the ablation strategies that could be carried out with ALFAMET.

**Table 7** Schematic representation of the galvanometric scanner.

| *Characteristic* / *Type of analysis* | **Ablation strategy** | **Schematic representation** | **Description** | **Applications** |
|---|---|---|---|---|
| **Micro analysis** | ***Single pulse*** | | Ablation is made in one fixed point: 20 µm or less Ø | Inclusions analysis, micro particles |
| | ***Scan 1D*** | | Ablation is made in line due to the movement of the sample or the laser beam | Rasters for 1D profile or imaging. (the scan 1D is repeated N times).<br>Otoliths, jewellery, nanoparticles |
| **Macro analysis** | ***Circular ablation or square ablation*** | 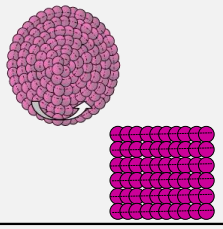 | Ablation of a large Ø crater carrying out circular trajectories overlapping laser impulsions | Bulk analysis |
| | ***Scan 2 D*** | 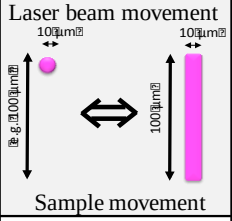 | Simulation of elongated laser beam. Signal enhancement while keeping spatial resolution in the advancement axis. | Rasters for 1D profile or imaging. (the scan 1D is repeated N times). |
| **Complex trajectories** | ***Simultaneous ablation of two samples*** | 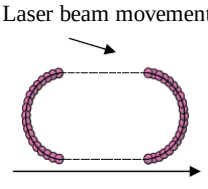 | Formation of an homogeneous mixture of both aerosols coming from different samples | Isotopic dilution analysis |
| | ***Branding*** | 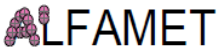 | Fast writing of logos | Branding and simultaneous analysis |

### 1.2.6 Applications of LA-ICPMS

The selection of the laser and the mass spectrometer to be coupled to the laser ablation system and their both operating parameters must be thoroughly selected according to the sample characteristics and the specific analytic purpose. In general terms, ablation strategy depends on the size, shape and heterogeneity of the sample. Other parameters to be optimized includes the size of the laser beam, pre-ablation conditions to remove any surface contamination, laser energy and repetition rate and the carrier gas and its flow. Similarly, it must be cleared up what the final aim of the analysis is, whether if it is conducted as a full quantitative, semi-quantitative or qualitative (70). Laser ablation coupled to ICPMS is nowadays a well-established analytical technique for the direct analysis of solid samples in a wide range of fields which are briefly described in the following paragraphs.

#### *1.2.6.1 Biology and environment*

The study of the impact of pollution in the ecosystems is of great importance. Several chemical pollutants (heavy metals, pesticides, hydrocarbons, etc.) might pose a physiological hazard to organisms. Thus, it is an indispensable issue to know about their presence and the disruptions that they might cause to environment. For this purpose, organisms and tissues which have a kind of tendency to accumulate environmental xenobiotics are preferable (71). The laser ablation ICPMS analysis of major, minor and trace elements in tree-rings seems to be a reliable record of the pollution within the area (72-74). Similarly, leaves, mosses and lichens can be employed for the study of water, air and soil pollution (75-77). For the study of aquatic environment contamination and its impact, biominerals such as corals and seashells are employed (78, 79). Birds' feathers, fish's otoliths, spines and scales and human bones and teeth have been also widely studied in order to reconstruct migrations (80-84).

#### *1.2.6.2 Health and medicine*

The visualization of the spatial element distribution of essential and beneficial metals (Cu, Fe, Zn, Mn, Co, Ti, Al, Ca, K, NA, Cr), toxic metals (Cd, Pb, Hg, U), metalloids (As, Se, Sb) and non-metals (C, P, S, Cl, I) in biological tissues is a challenging task for life science studies and nanotechnologies which would have a great impact in the areas of physiology, physiopathology, pharmacology and toxicology (85, 86). On the one side, the nervous system is the main target of several metals. In fact, the presence and accumulation can strongly affect the normal functioning of biological processes and potentially be lethal, being children and elderly people the most vulnerable. Aluminium has been associated with dementia, arsenic causes peripheral neuropathy and thallium induces nervous collapse (87).

On the other side, some transition metals are mandatory for the basic physiological functions (Mn, Zn and Cu, for example) as they are usually part of receptors and enzymes. So mayor or minor modifications on their concentrations have been related to neurological disorders (88), Parkinson (89-92) and Alzheimer (93-96). In addition, it is of a great usefulness in the area of oncology to measure element distribution and expansion in small-size tumours (97).

*1.2.6.3 Geochemistry*

Elemental and isotopic composition of geological material are a kind of fingerprint that has been use in geochemistry to identify various sources of rocks and processes that have shaped our Earth. Most geological materials are heterogeneous in both occurrence and composition and laser ablation-ICPMS allows its sampling and analysis on the sub-micron scale at high spatial resolution as well as depth-profiling analysis. Several studies have been carried out to clarify mineral formation processes, soil (98, 99), provenance and dating and environmental conditions in which a mineral was formed (100).

*1.2.6.4 Forensic science*

Due to unique capabilities of laser ablation-ICPMS for qualitative and quantitative elemental and isotopic analysis of solid samples without minimal sample preparation and destruction, it has been increasingly used and accepted in forensic science (101). Therefore, this technique has been widely use for the forensic analysis of glass (102, 103), paint (104), ink and paper (105, 106), bone and other biological materials, gunshot residues (107, 108), drugs (109), jewellery (110, 111), food and nuclear materials (112, 113).

*1.2.6.5 Archaeology*

Laser ablation-ICPMS is highly sensitive microprobe technique which makes possible to characterize individual components of heterogeneous matrices or to characterize surface materials, such as pigments, slips and glazes on ceramics (114) and metallic objects (115), coins (116) and sculptures with the aim of a better comprehension of human evolution, creation techniques and provenance (114).

*1.2.6.6 Material sciences*

Laser ablation-ICPMS has been widely employed for the chemical characterization of high purity materials such as metals, alloys and semiconductors and insulating materials. In fact, this technique is particularly useful in metallurgical and electronic industry for the identification of metallic compounds, cartography and quality control of their final products. In addition, deep profiling capability is an asset for multi-layer materials (117, 118).

## 2. Optical spectroscopy

The term "spectroscopy" was first used in 1666 when Isaac Newton demonstrated the dispersal of white light through a prism into different colors. This term has its origin in the Latin word *spectrum* (=ghost) and Greek word *scopos* (=watcher). Optical spectroscopy encompasses a wide variety of techniques which use nonionizing radiation (UV to IR region) to study how matter interacts with light, the four main methods of optical spectroscopy are absorption, emission, luminescence and scattering concretely (Figure 18). This interaction involves specific transitions between energy states. This means that optical spectroscopy is actually the measure of the interaction of photons with matter as function of the photon energy. There also other types of radiation/matter interaction, such as diffraction, refraction, reflection and some types of scattering that do not involve the transition between energy levels. These interactions generally cause changes in the optical properties of the radiation, such as direction and polarization, and they are often a result of the bulk sample properties rather than a specific chemical properties. Advantages of the optical spectroscopy methods are their non-destructive nature and the possibility to monitor the studied object without physical contact, making it popular in a wide range of applications (119, 120).

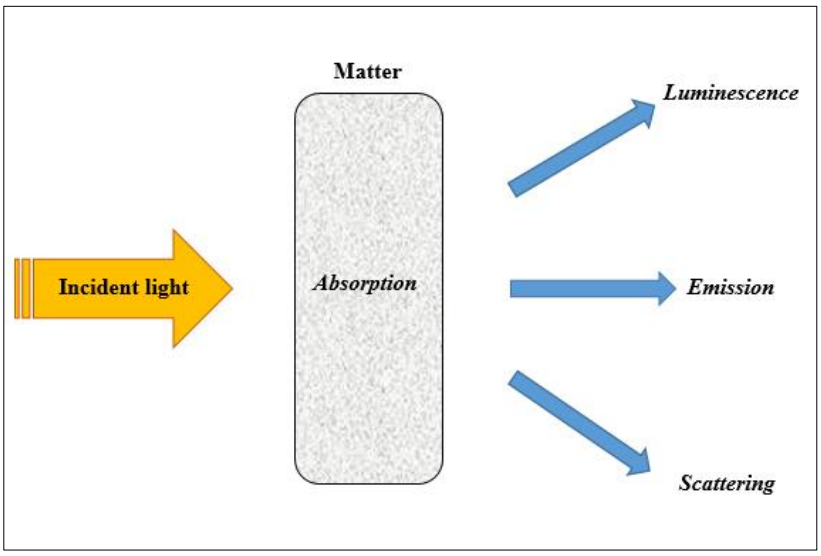


**Figure 18** Light-matter interaction types in Optical Spectroscopy.

## 2.1 Scattering spectroscopy: Raman spectroscopy

### 2.1.1 Basic concepts of Raman spectroscopy

When light interacts with matter, the photons which make up the light may be absorbed or scattered, or may not interact with the material and may pass straight through it (121).

Raman spectroscopy is based on the irradiation of the sample with a visible or infrared monochromatic light source ($v_0$ frequency) photons from the laser beam produce an oscillating polarization in the molecules, exciting them to a virtual energy state. The polarizability is the deformation of the electron cloud about the molecule by an external electric field (122).

Most of the radiation is scattered by the sample at the same wavelength of the incoming laser radiation in a process known as elastic Rayleigh scattering. Nonetheless, a small percentage of the inbound light is scattered at a wavelength that is shift from the original laser wavelength (123). Inelastic scattering of monochromatic light, which means that the frequency of photons in the light changes upon interaction with a sample, provides key information for the elucidation of molecular structure of analytes (124). In this case, two different situations could happen (Figure 19):

1) If a photon with $v_0$ frequency is absorbed by Raman-active molecule which at the time of interaction is in the basic vibrational state, part of the photon's energy is transferred to the molecule with $v_m$ frequency. As a result, the frequency of the scattered light is reduced to $v_0 - v_m$. This Raman frequency is called Stokes frequency.

2) If a photon with $v_0$ frequency is absorbed by Raman-active molecule which at the time of interaction is already in the excited vibrational state, molecule returns to the basic vibrational state and the resulting frequency of scattered light goes up to $v_0 + v_m$. This Raman frequency is called Anti-Stokes frequency (125).

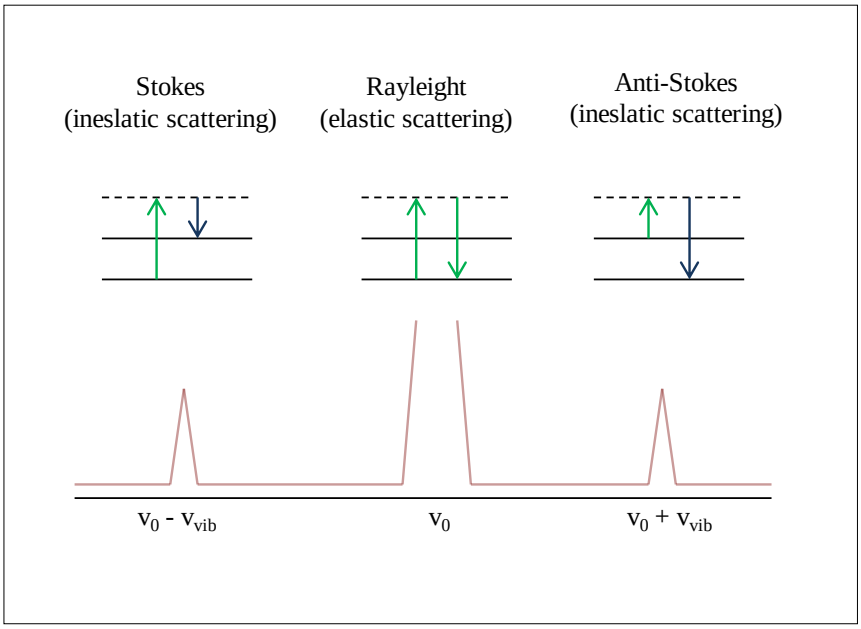


**Figure 19** The different possibilities of light scattering in Raman spectroscopy: Rayleigh scattering (no exchange of energy: incident and scattered photons have the same energy), Stokes Raman scattering (atom or molecule absorbs energy: scattered photon has less energy than the incident photon) and anti-Stokes Raman scattering (atom or molecule loses energy: scattered photon has more energy than the incident photon).

Raman spectra can provide multitude of information. First of all, every molecule or chemical species has its own unique Raman spectrum which can be interpreted as molecular fingerprint. This allows developing databases of known standards that can be later use for identification or verification of unknowns (126).

Since measured Raman signals are characteristic for analyzed compounds, Raman spectroscopy allows for the analysis of very complex samples and the intensity of scattered light is proportional to the amount of material present. Therefore, Raman spectroscopy provides both qualitative and quantitative information about the sample. All this permits spectral interpretation, library searching, data manipulation and the application of chemometric methods.

In addition to providing unique information about a sample Raman technique offers several additional benefits as narrow bandwidths, minimal or no sample preparation, non-destructive/non-intrusive analysis, no interference from atmospheric $CO_2$ or $H_2O$ and it is easily interfaced to fiber-optics for remote analysis.

### 2.1.2 Raman Spectroscopy technology

In recent years, Raman Spectroscopy has emerged as an important analytical tool both in academia and particularly in industry due to its outstanding technological progress through the development of new detectors and the advent of fiber optics which have renewed interest in the technique (127).

In 1928, the Indian physicist Sir Chandrasekhar Venkata Raman discovered the phenomenon that bears his name. The visible wavelength of a small fraction of the radiation scattered by certain molecules differs from the incident beam and the displacements depended on the chemical structure of the molecules (128).

In the original experiment sunlight was focused by a telescope onto a sample which was either a purified liquid or a dust-free vapor. A second lens was placed by the sample to collect the scattered radiation and a system of optical filters was used to show the existence of scattered radiation with an altered frequency from the incident light (129). Because of this discovery and the systematic study of the phenomenon, Raman was awarded the Nobel Prize in Physics in 1931 (128).

However, challenges were also exposed. These included the lack of a good Raman source, lack of a good detector and well-known today interference from fluorescence, which in some cases could mask the Raman signal. Until approximately 1986, the Raman literature was dominated by physical and structural investigations, with relatively few reports of Raman spectroscopy applied to "real-world" chemical analysis (130).

Gradually, improvements in the various components of Raman instrumentation took place to overcome fundamental and technical issues. Since the early 1980s and up to today, research has been focused on the development of better excitation sources, optical trains and detection systems which has helped to enhance the fundamental problems of a weak Raman signal and interference from fluorescent to a great extent.

The two main technical innovations used to collect the Raman spectra, charge-couple device (CCD)-based dispersive Raman and Fourier transform (FT)-Raman, were responsible for the progress of Raman Spectroscopy (131).

The major restriction on the routine application of Raman spectroscopy is the interference caused by the fluorescence, either of impurities or of the sample itself and thus, obtaining a weak Raman signal. In order to completely limit the absorption process which gives rise to fluorescence, several

methods have been developed. Although none of them offer a universal approach to the problem, *FT-Raman* is an effective optical filtering of the intense Rayleigh scattered radiation.

Moreover, by choosing an excitation wavelength away from any electronic transition fluorescence stimulation is avoided. For this purpose, the use of a long-wavelength near-infrared laser is preferable, for example, a solid state Nd:YAG laser working at 1064 nm. However, this result in a strong decrease of the Raman effect which could be compensated by using spectrometers equipped with an interferometer enabling a higher throughput of the instrument by collecting the entire Raman spectrum simultaneously (*NIR FT-Raman*) (132).

Resonance Raman spectroscopy (RRS) and Surface Enhanced Raman spectroscopy (SERS) are another strategies to avoid fluorescence and amplify the weak Raman signal, which can enhance the Raman scattering intensities significantly by several orders of magnitude.

In *Resonance Raman spectroscopy (RRS),* the wavelength of the excitation laser is coincident with the wavelength of an electronic transition of the analyte and it results in a $10^2$ - $10^6$ increase in the Raman signal compared with dispersive Raman spectroscopy (130). In terms of sensitivity, this means that compared to the non-resonant Raman spectroscopy, components at low concentrations can be detected and analyzed. As far as specificity is concerned different resonance Raman spectra of the same molecule can be obtained by varying the excitation wavelength. So, if the excitation wavelength harmonized the absorption of a specific part of the molecule, then the Raman spectrum associated with this part of the molecule is selectively enhanced and separated from the rest of the molecule (131).

In comparison to "normal" Raman scattering, *Surface enhanced Raman spectroscopy (SERS)* requires the presence of metal nanostructures as an integral component since the signal amplification comes through the electromagnetic interaction of light with metals, extending the range of Raman applications to diluted samples and trace analysis. To this end, the analyte is adsorbed onto or in close proximity to a prepared metal surface which produces large amplifications of the laser field through excitations generally known as plasmon resonances (coherent electron oscillations). These surface plasmons interact with the analyte to greatly enhance the Raman emission (133, 134).

Apart from the variations of ordinary Raman spectroscopy described above, some other modifications must be mentioned: *Confocal Raman microscopy* for dealing with microscopic samples and *Nonlinear (coherent) Raman techniques (Coherent anti-Stokes Raman scattering – CARS)* which is an excellent tool for non-invasive diagnostic in reacting systems (131).
Parallel developments in the instrumentation were the introduction of charge-coupled devices (CCDs) and the liquid nitrogen-cooled germanium (Ge) and indium gallium arsenide (InGaAs) detectors. On the one hand, CCDs devices for dispersive Raman permit multiwavelength detection and show a better signal to noise ratio (SNR) for a given measurement time while on the other hand the Germanium (Ge) and Indium Gallium Arsenide (InGaAs) detectors are suitable for *NIR FT-Raman* owing to its higher sensitivity in this spectral range (130).

All these post-1980 technological upgrades that carried out the Raman spectroscopy resurgence have made it to become a much viable technique for a variety of fields and applications, reaching well the present state of the art (127).

### 2.1.2 Raman spectroscopy system

As a general rule, the sample is illuminated with a monochromatic laser and the scattered light is after collected with collecting optics and sent through the spectrophotometer to obtain the Raman spectrum (125). However, the different parts of the equipment as well as its operation will be explained briefly in the following lines.

A Raman system typically consists of four major components:

#### *2.1.3.1 Excitation source*

The sources used in modern Raman spectrometry are nearly always lasers because their high intensity is necessary to produce Raman scattering of sufficient intensity to be measured with a reasonable signal-to-noise ratio. Because the intensity of Raman scattering varies as the fourth power of the frequency, argon and krypton ion sources that emit in the blue and green region of the spectrum have an advantage over the other sources. Different types of lasers can be used (gas lasers, diode lasers and neodymium-YAG (Nd:YAG) solid-state lasers) to irradiate the sample with a laser beam in the ultraviolet (UV), visible (Vis) or near infrared (NIR) range (127) (Table 8).

**Table 8** Common laser sources in Raman spectroscopy.

| *Laser type* | *Wavelength, nm* |
|---|---|
| ***Argon*** | 488.0 or 514.5 |
| ***Krypton*** | 530.9 or 647.1 |
| ***Helium-neon*** | 632.8 |
| ***Diode laser*** | 785 or 830 |
| ***Nd:YAG*** | 1064 |

Lasers are ideal excitation sources for Raman spectroscopy due to the following characteristics of the laser beam:

a) Laser beams have high output energy, produce huge peak powers between 10-100 mW and are almost completely linearly polarized.

b) Laser beams are highly monochromatic and odd lines are much weaker. Moreover, those weird lines can be easily eliminated by using notch filters or pre-monochromators.

c) Laser beams have small diameters (1-2 mm) which can be reduced to 0.1 mm by using lens systems. Consequently, all the radiant flux can be focused to a small spot of the sample, enabling profitable studies of microliquids and crystals.

*2.1.3.2 Sample illumination system and light collection optics*

Since the Raman scattering is considerably weak, the laser beam has to be focused properly onto the sample and the scattered radiation must also be efficiently collected. Because of the small diameter of the laser beam (≈ 1 mm) the focusing of it onto the sample surface can be easily achieved and the incoming radiation is after collected by the collection optics which consists of an achromatic lenses system with a collecting lens and a focusing lens.

*2.1.3.3 Wavelength selector*

Because of the weakness of the Raman signal the main difficulty of Raman spectroscopy is separating it from the intense Rayleigh scattering (125). Therefore, the collected Raman scattered light needs to be separated into its composite wavelengths. This is accomplished by a diffraction grafting which is an array of finely spaced lines on a reflective surface that splits the beam into wavelengths (135).

Gratings have many grooves blazed into the surface, which disperse the incoming light. The higher the number of grating lines per unit length, the broader the dispersion angle and the higher the spectral resolution obtained (136) .

*2.1.3.4 Detection and computer control/processing system*

As mentioned above, Raman signals are inherently feeble so the problems involved with detection and amplification are severe. Therefore, selecting the appropriate detector is critical depending on the excitation laser employed (126).

Initially, detectors such as photon-counting Photomultiplier Tubes (PMT) were used (126) . The PM tube consists of a photocathode that emits electrons when photons strike it; a series of dynodes, each of which emits a number of secondary electrons when struck by an electron; and an anode that collects these electrons as an output signal. However, obtaining a single Raman spectrum with this kind of detector takes substantial period of time which makes Raman spectroscopy unfit as a routine technique (127).

Consequently, multi-channel detectors like Photodiode Arrays (PDA) and Charge-Coupled Devices (CCDs) were rapidly developed.

Multi-channel photon detectors (PDA) consist of an array of small photosensitive devices that can convert an optical image into a charge pattern that can be read as a Raman spectrum. Unfortunately, these array-type detectors are not sensitive enough for detecting Raman signals.

Hence, the use of the Charge-Coupled Devices (CCDs) was rapidly increased due to the sensitivity and performance of these detectors which have led them to be the first choice for Raman spectroscopy (125). Regarding the operation of these detectors, they are a silicon-based semiconductor arranged as a two-dimensional array of photosensitive elements called pixels, each one of which generates photoelectrons and stores them as a small charge. Charges are stored on each individual pixel as a function of the number of photons striking that pixel which are after converted to digital values (127).

### 2.1.4 Applications

Due to its sensitivity, high information content, and non-destructive nature, Raman is now used in applications involved across the following fields:

#### *2.1.4.1 Pharmaceutical industry*

Raman spectroscopy seems to be a promising analytical tool for on-line process monitoring and analysis in the pharmaceutical industry. By building databases for the identification of unknowns, the previous identification of incoming raw material (active ingredients, additives and with excipients) regard to purity and quality is possible which is of great importance as it affects the rest of the production processes such as drying, coating and blending (137). In addition, Raman spectroscopy can also be employed for the analysis of the manufactured drugs due to its non-destructive nature which does not required previous sample preparation and allows the direct analysis even through the blister packs (126).

#### *2.1.4.2 Bioscience and medical diagnosis*

The capability of Raman spectroscopy to detect small chemical and structural changes as well as molecular interactions has enhanced the development of methods to mark out healthy tissues from unhealthy ones, or to determine the degree of progress of a certain disease, predominantly focused on *ex vivo* samples such as biofluids or biopsied tissues. Two of the areas that have drawn considerable interest in the last years are the application of Raman spectroscopy in dermatological research and for the early identification of cancer and precursor lesions (138).

The great advance of Raman spectroscopy lies in its potential for *in vivo* applications and consequently, its ability for direct real-time therapeutic intervention. An example is the use of an intravascular fiber optic Raman probe which reported *in vivo* information about an atherosclerotic plaque (139). These kind of diagnosis tools are totally needed in many fields of medicine to replace current invasive methods by less or non-invasive techniques and avoid delays caused by *ex vivo* evaluation of patients biopsies (138).

#### *2.1.4.3 Food and agriculture industries*

Raman spectroscopy has also been used in food safety and quality inspection areas since recent food related illness, caused by contaminants, went public (e.g., *E. coli* O157:H7 in fresh spinach in 2006, melamine in infant formula in 2008 and *Salmonella spp.* in peanut butter in 2009). These events have brought new challenges for monitoring food ingredients and products during processing operations (140).

Early detection of food adulteration is also important for the food industry because it also interferes in health. Owing to Raman spectroscopy advantages (high sensitivity to C=C, C≡C and C≡N bonds, low sensitivity to water and high selectivity to inorganic salts) and its feasible combination with chemometric analysis, Raman technique has a potential use in food and agriculture industries. An example is the detection of adulteration of olive oil samples with hazelnut oil (141) or the detection of beet and cane syrups in honey samples (142). So, this sensing technology can be effectively and efficiently applied for food safety and quality which would reduce the risk of unsafe food for consumers and enhance the competitiveness and profitability of the food industry (140).

*2.1.4.4 Environmental applications*

Typically, environmental analysis is categorized according to the media in which the analysis is performed and it is especially focused in the remote analysis of pollutants (143). There is a large variety of particles in suspension in the atmosphere which are commonly known as aerosols that differ in chemical composition and size distribution depending on the region of the atmosphere, the meteorological conditions and the anthropogenic activity. Furthermore, their atmospheric lifespan can be as long as several days up to some weeks so they can affect the global as well as regional climates. Therefore, the knowledge of the chemical composition of these aerosols is of great importance due to their potential adverse effects on the environment and human health as they can be deposited in crop fields and water reservoirs for human consumption (144).

One of the applications of Raman spectroscopy for the environment and human health is the identification of the species of airborne pollen. The prevalence of allergies has increased drastically during the past 15-20 years. The impact of this respiratory disease reaches up to 15-25% of people in western countries, especially during the blooming season. It is noteworthy that the allergenicity of pollen depends on the species so it is important to identify, characterize and quantify the airborne pollen to have a clear scheme of the allergen exposure (145).

*2.1.4.5 Forensic science*

There are many forensic challenges in which the instantaneous and non-invasive measurements of chemical and biological hazards is fundamentally important since these challenges can encompass the detection and identification of explosives in emergency alerts, illegal drug trafficking or body fluids in the crime scene. In these cases Raman spectroscopy offers an accurate, non-invasive and non-destructive alternative over other previously used methods (127) as it allows the measurement of chemicals and their mixtures in different environments without any sample preparation.

Techniques for detecting explosives are extremely important in areas susceptible to terrorist activity (public transports, aviation transport, etc.) as well as for cleaning decommissioned military bases and detecting unexploded ordinance (146). Several studies have appeared in the literature addressing the application of Raman spectroscopy to the detection and identification of explosives (147) since it is a suitable analytical technique for a rapid, remote and in real-time detection of explosive materials.

Raman spectroscopy is a very sensitive technique that is often used in forensic laboratories, mostly to analyze textile fibers and paints (148). However, and thanks to its portable version, another forensic application field of Raman spectrometry is the *on-site* unambiguous characterization of body fluids commonly found at crime scenes while not destroying the sample in the process. The results obtained by Virkler et. al (149, 150) showed that the five fluids (semen, vaginal fluid, saliva, sweat and blood) can be differentiated from one another by visual comparison of their Raman spectra.

Finally, unequivocal Raman data have contributed to the outcome of high profile fraud cases. The Raman effect is highly sensitive to slight differences in chemical composition and crystallographic structure. These features are very useful for the investigation of illegal drugs as it permits the detection of very small composition alterations and therefore it provides valuable information regarding the origin of the synthesis method of the drugs (151). Raman spectroscopy has been also applied for the structural analysis of degraded or questioned paper documents and can be also used for studying the paper ageing process and products added during manufacturing (152). Moreover, it has rapidly gained interest for ink analysis because it also provides relevant chemical information about the ink composition with little or no contributions from the paper (153). A more detailed insight about the use of Raman spectroscopy for paper and ink analysis will done in Chapter 7.

## 2.2 Absorption spectroscopy: Infrared spectroscopy

### 2.2.1 Basic concepts of Infrared spectroscopy

Infrared spectroscopy is a specialized analytical technique of molecular spectroscopy whose theory relies on the principle that molecular rotations and vibrations of chemical compounds absorb specific frequencies of electromagnetic waves. The Infrared, a particular portion of the electromagnetic spectrum, is especially suitable for the detection of molecular vibrations of the atoms of a molecule (154).

In Infrared spectroscopy infrared radiation is passed through a sample and then which fraction of the incident radiation is absorbed at a particular energy is determined. The energy at which any peak in an absorption spectrum appears corresponds to the frequency of a vibration of a part of a molecule of the sample. To show infrared absorptions a molecule must have a specific feature: an electric dipole moment of the molecule must change during the vibration. This is the *selection rule* for infrared spectroscopy (155).

The Infrared spectrum refers to electromagnetic waves whose wavelengths range from 0.78 μm to 1000 μm. However, for more comprehensible numbers, the wavenumber unit ($cm^{-1}$) is generally used instead of microns so the total IR spectrum goes from 14000 $cm^{-1}$ to 10 $cm^{-1}$. Both for instrumentation and applications, the IR spectrum is divided in three sections. Table 9 below displays the ranges of the IR spectrum.

**Table 9** Infrared Spectral Ranges (128).

| Infrared Section | Wavelength Range (μm) | Wavenumber Range ($cm^{-1}$) |
|---|---|---|
| *Near Infrared (NIR)* | 0.78 – 2.5 | 12800 – 4000 |
| *Mid Infrared (MIR)* | 2.5 – 50 | 4000 – 200 |
| *Far Infrared (FIR)* | 50 - 1000 | 200 - 10 |
| *The most used IR range* | 2.5-15 | 4000-650 |

The absorptions observed in the near infrared region (12800-4000 $cm^{-1}$) are overtones or combinations of the fundamental stretching bands which occur in the 3000-1700 $cm^{-1}$ region. The bands involved are usually due to C-H, N-H or O-H stretching but they are weak in intensity (155).

The fundamental vibrations take place in the mid infrared region (4000-200 $cm^{-1}$) which can be divided into four regions. The nature of a group is generally determined by the region in which is located and they are generalized as follows: the X-H stretching region (4000-2500 $cm^{-1}$), the triple-

bond region (2500-2000 $cm^{-1}$), the double-bond region (2000-1500 $cm^{-1}$) and the fingerprint region (1500-600 $cm^{-1}$) (155).

The far infrared region goes from 400 to 100 $cm^{-1}$ and it is more limited for spectra-structure correlations. But it provides information regarding the vibrations of molecules containing heavy atoms, molecular skeleton vibrations, molecular torsions and crystal lattice vibrations (155).

Vibration modes of a molecule depend on its spatial structure and number of atoms. In general, they can be classified in two types (Figure 20) (156):

- ***Stretching vibrations*** which produce a variation in the interatomic distance along the axis of the bond between two atoms. They may be symmetric or asymmetric.

- ***Bending vibrations*** which produce a change in the angle between two bonds. They may occur in the plane (rocking and scissoring) or out of the plane (wagging and twisting).

As stated previously, the interactions of infrared radiation with matter is understood in terms of changes in molecular dipole moment. The larger is this change, then the more intense will be the absorption band. In order to make it as understandable as possible a basic model is shown in Figure 21 where a molecule represented as a system of masses joined by bonds with spring-like properties (155).

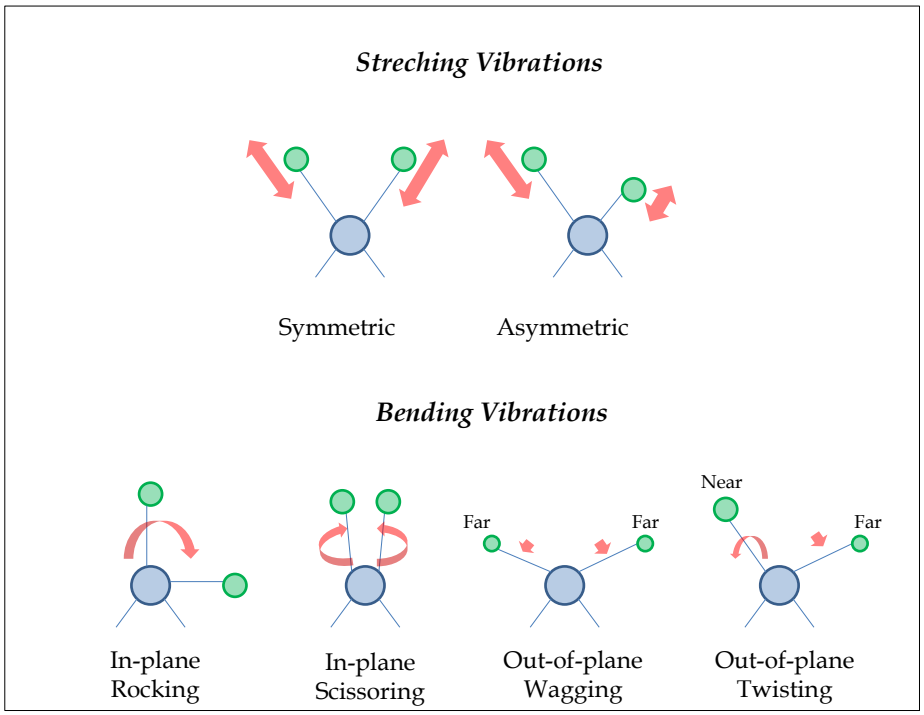


**Figure 20** Types of Molecular Vibration.

Once Infrared spectrum and molecular vibrations have been described it must be pointed out that in Infrared spectroscopy there are two different methods to work: transmission and reflectance methods. Transmission spectroscopy is the oldest and most straightforward infrared method which is based upon the absorption of infrared radiation at specific wavelengths as it passes through a sample. It is possible to analyze sample in any physic state (liquid, solid or gas) when using this approach (155). Aside from the conventional IR spectroscopy of measuring light transmitted from the sample, the reflection IR spectroscopy was developed, in which the absorption properties of a sample can be extracted from the reflected light. These reflectance methods are commonly used with samples that are difficult to analyze by conventional transmittance methods. In all, reflectance techniques can be divided into two categories (Figure 21) (157-159):

- ***Internal reflection methods***: interaction between the electromagnetic radiation and the sample is studied through an interface crystal with higher refraction index.

Internal reflection spectroscopy, often termed as Attenuated Total Reflectance (ATR), was first reported in 1959. The infrared light is introduced into a prism at an angle exceeding the critical angle for internal reflection. This produces an evanescent wave at the reflecting surface (a surface which is transparent to infrared such as thallium bromide) on which the sample is supported, and the distortion of the evanescent wave by the sample is measured.

A property of the evanescent wave which makes ATR a powerful technique is that the intensity of the wave decays exponentially with the distance from the surface of the ATR crystal which makes ATR generally insensitive to sample thickness, allowing the analysis of thick or strongly absorbing samples.

So, Attenuated Total Reflectance (ATR) is today the most versatile and powerful FT-IR sampling tool used. Minimal or no sample preparation is usually required which greatly speeds sample analysis. Nevertheless, the main advantage of ATR sampling comes from the very thin sampling pathlength and depth of penetration of the IR beam into the sample. This is in contrast to traditional FT-IR sampling by transmission where the sample must be diluted with IR transparent salt and pressed into a pellet or thin film to prevent totally absorbing the infrared spectrum (157-159).

- ***External reflection methods***: the radiation reflected from the sample surface is directly analyzed. External reflection covers two different types of reflection: ***specular or regular*** reflection usually associated with smooth and polished surfaces and ***diffuse reflection*** associated with the reflection from rough surfaces, causing the infrared energy to reflect at angles other than the incident energy and from different locations within the sample. The accessories can be used for sample that are large enough and, thus, there is no need to focalize small areas. They give us information on a large area of the surface (about 2 mm).

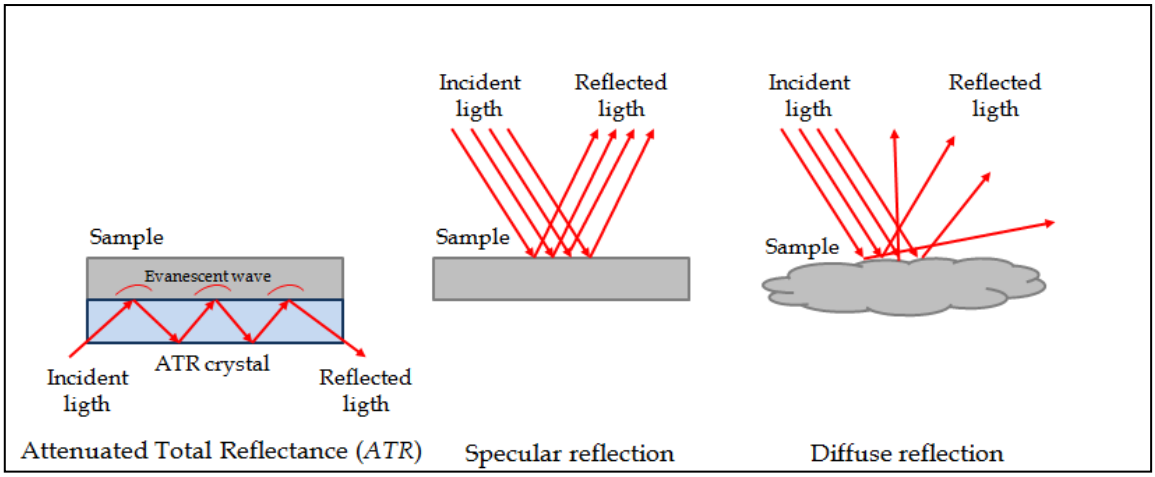


**Figure 21** Infrared Spectroscopy reflection methods.

### 2.2.2 Infrared Spectroscopy technology

Infrared spectroscopy provides characteristic fundamental vibrations that are employed for the elucidation of molecular structure which is used for compound identification. Samples can be examined either in bulk or in microscopic amounts over a wide range of temperatures and physical states (e.g., gases, liquids, powders, fibers or embedded layers) (155). Moreover, Infrared spectroscopy is an easy-to-use and reliable analytical technique that has a very broad range of applications and provides solutions to a host of important and challenging analytical problems (122).

In 1800, Sir Friedrich Wilhelm Herschel (1738-1822) published a series of papers describing experiments which led him to discover infrared radiation, a form of radiation beyond the red end of the spectrum of visible light. Herschel passed sunlight through a prism which divided the light into a rainbow of colors called spectrum and he measured the temperature of each color. He noticed that the temperature increased from the blue to the red part of the spectrum and that it was even higher if he placed the thermometer just past the red part of the spectrum, in a region where there was no visible light. He named this invisible heat source infrared light.

However, William Weber Coblentz (1873-1962) laid the real background work for Infrared spectroscopy as he investigated the spectra of hundreds of substances, both organic and inorganic, which it still usable due to its thoroughness and accuracy. The final result of this work was the recognition that each compound had a unique IR spectra and that certain groups, even when they were in different molecules, gave absorption bands that were found at approximately the same wavelength.

Over the years, and as consequence of the improved instrumentation, a wide variety of new sensitive techniques have been developed in order to analyze formerly intractable samples. Infrared spectrometers are commercially available since the 1940s. During this decade, the instruments relied on prisms to act as dispersive elements until the mid-1950s when diffraction gratings were introduced into the dispersive equipments (160) .

Nevertheless, the most outstanding advance concerning Infrared spectroscopy has been the introduction of Fourier-Transform spectrometers which has improved the quality of infrared spectra. Compare to traditional dispersive IR spectrometers, FT-IR spectrometers have tree main advantages: quicker data collection, higher IR throughput and greater precision due to a reliable internal calibration source. These advantages are a result of the implementation of a laser-referenced interferometer instead of a monochromator (155).

Another advance in recent years is the development of reflectance techniques which are used for samples that are difficult to analyze by the conventional transmittance methods. Among these methods, Attenuated Total Reflectance Spectroscopy (ATR) must be stand out as it was used in the present work and whose theoretical basis will be explained in the following paragraphs (155).

### 2.2.3 Infrared spectroscopy system

Historically, dispersive instruments have been available since the 1940s. However, a very different method of obtaining an infrared spectrum has superseded the dispersive instrument. Nowadays, Fourier-transform infrared spectrometers are predominantly used which have improved the acquisition of infrared spectra. Both spectrometers use similar components, but the method in which spectral data is captured is inherently different. Dispersive spectrometers utilize a monochromator, which is a device that filters incoming IR frequencies of radiation to output a specific frequency. The main problem of the dispersive instruments lies with its monochromator as it contains narrow slits at the entrance and exit which limit the wavenumber range of the radiation reaching the detector (155, 160).

Fourier-transform infrared spectrometers contain a laser-reference interferometer instead of a monochromator. This interferometer allows all desired frequencies to be recorded by the detector at each data sampling point allowing faster data collection. Moreover, it also allows greater IR radiation intensity through the detector and it is also a reliable calibration source because of its consistent wavelength (160).

All FT-IR equipments are basically composed of the following components (Figure 22):

*2.2.3.1 Source of Infrared emission*

Infrared emission source must be intense enough over the wavenumber range and transmittance range. For the mid-infrared region, sources of infrared emission have included the Globar, which is made of silicon carbide. There are also other heat radiation sources such as the Nernst filament, which is a mixture of the oxides of zirconium, yttrium and erbium but it only conducts electricity at elevate temperatures (155).

However, it must be mentioned that there are other emission sources depending on the working infrared region (Table 10):

**Table 10** FT-IR sources (160).

| Source | Material | Spectral Range |
|---|---|---|
| *Mercury Arc Lamp* | Mercury Gas | FIR |
| *Globar* | Silicon Carbide | FIR/MIR |
| *Nernst Filaments* | Oxides of Zr, Y and Er | MIR |
| *Tungsten Lamp* | Tungsten | MIR/NIR |
| *Xenon Arc Lamp* | Xenon Gas | VIS/UV |

*2.2.3.2 Interferometer*

The most common interferometer used in FT-IR spectrometry is a Michelson interferometer which was developed by Albert Michelson in 1887, which can be decomposed into a beam splitter, a moving mirror and a stationary mirror (Figure 22).

Instrument's principle of function is the following: IR radiation from the source hits the beam splitter and it is splitted into two perpendicular beams of equal energy, one of which impinges on the movable mirror and the other on the stationary mirror. A Helium Neon laser is commonly used for controlling the interferometer's moving mirror and data sampling points because of its availability and cost.

Then, both beams are reflected by the mirrors and recombine to reach beam splitter. This gives rise to interference, which can be constructive or destructive depending on the relative position of the movable mirror about the fixed mirror. The result will be an interferogram. After the combined beam has passed through the sample, wherein a selective absorption occurs, the detector will record the Fourier transform of the IR spectrum of the sample. After the amplification of the signal, in which the high frequency contributions are removed by a filter, the data obtained is the digitalized by a computer system that performs an additional Fourier transform to back-transform the interferogram into an IR spectrum (155, 161, 162).

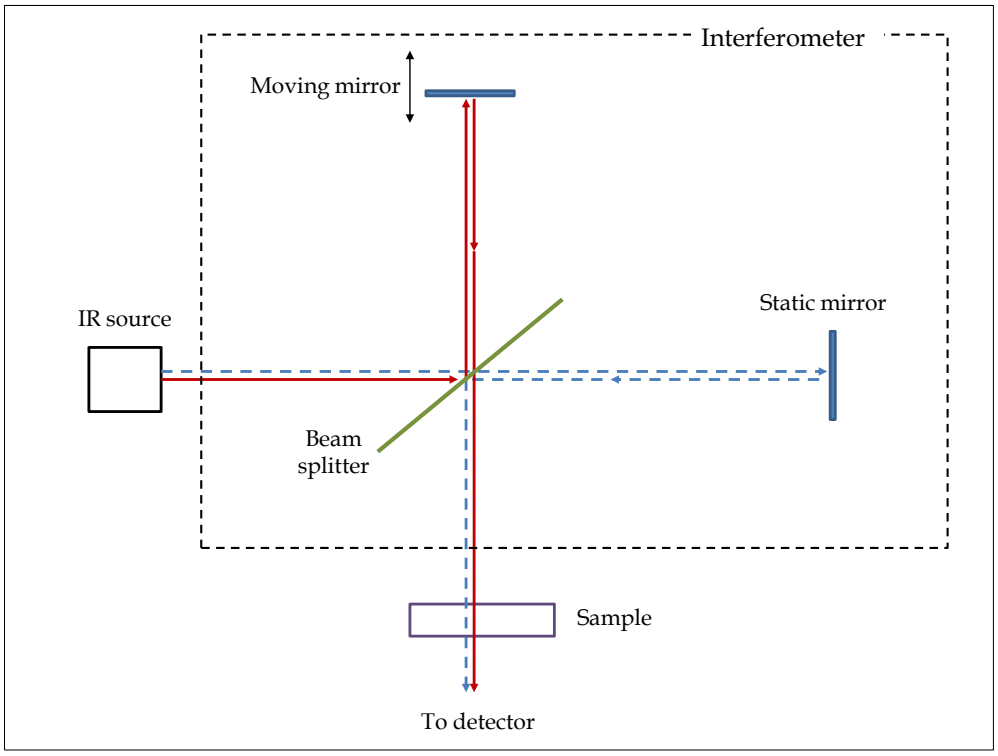


**Figure 22** A schematic representation of an interferometer used in FT-IR spectrometers.

*2.2.3.3 Detector and signal processor*

Detectors are divided into two categories depending on the detection methodology: thermal and quantum.

Thermal detectors use a conductor or semiconductor whose resistance changes depending on temperature changes. These detectors have been widely used but they have a significant drawback with the response time. Thus, for faster sampling requirements, a second category of detectors, the quantum type, is used.

Quantum detectors basis rely on the principle that radiation causes the excitation of the electrons in a material to a higher, quantized energy state. The energy of the incident radiation is proportional to the wavelength and by measuring the voltage of the detector, the wavelength of the incident radiation can be determined. These types of detectors are more sensitive and have shorter response times but they require cooling to eliminate background noise in the detection material (160).
In any case, the most common detectors used in FT-IR spectrometers are deuterated tryglicine sulfate (DTGS) which are thermal detectors, and mercury cadmium telluride (MCT) which is a quantum detector but this has to be cooled to liquid nitrogen temperatures. However, MCT and DTGS detectors were not widely used until the 1970's and 1980's respectively. Prior to 1970's, triglycine sulfate (TGS) detectors, the precursors of DTGS, were used (163).

### 2.2.4 Applications

*2.2.4.1 Biological applications*

The basis for these applications is that Infrared spectroscopy is a vibrational spectroscopic technique capable of providing details of the chemical composition and molecular structures in cells and tissues. Diseases and pathological anomalies lead to chemical and structural changes at molecular level which modify the vibrational spectra that can be used as sensitive markers of the disease (164).

*2.2.4.2 Disease diagnosis*

Infrared spectroscopy is an emerging biophotonic tool to assess soft tissues, hard tissues and body fluids and hence recognize diseases (165). The ability to detect the early onset of a disease, rapidly, non-invasively and unequivocally has multiple advantages including early intervention of therapeutic strategies leading to a reduction in morbidity and mortality and the releasing of economic resources within health care systems (166).

Infrared absorption spectrum can be used as an infrared "fingerprint" characteristic of any biochemical specie. For most disease diagnose, the mid-IR part of the spectrum is used as it contains many sharp peaks and is very information rich (166). Vibrations in the wavenumber region 2800-3050 $cm^{-1}$ can be described to $CH_2$ and $CH_3$ stretching vibrations from fatty acids, while those in the wavenumber region 1500-1700 $cm^{-1}$ are described to C=O, NH and C-N from proteins and peptides (167).

Infrared spectroscopy was used to estimate diagnostic accuracy in differentiating patients with Alzheimer disease from control subjects by analyzing protein level in cerebrospinal fluid (CSF) and lipid and nucleic acid structures involved in oxidative stress dependent processes in blood (168, 169).

*2.2.4.3 Clinical chemistry*

The infrared spectrum of mixture as blood, urine, saliva or amniotic fluid serves as the basis to quantitate its constituents and a number of common clinical chemistry test have been proved to be feasible using this approach (170).

The analysis for glucose is surely the most common blood/serum test due to the frequent self-testing in the diabetic population. Thus, the majority of attempts to quantify glucose using IR spectroscopy have been motivated by the prospect of a non-invasive *in vivo* test. Due to the fact that NIR radiation penetrates depths of millimeters into tissues and measurements can be carried out by using fiber optics, a NIR method has been held out to quantitate blood glucose *in vivo (171, 172).*

*2.2.4.4 Pharmaceutical industry*

Infrared spectroscopy has been extensively used in both qualitative and quantitative pharmaceutical analysis (173). For better understanding of the manufacturing processes used for pharmaceutical formulations and for the ability to solve issues if they arise, Infrared spectroscopy is important for the evaluation of the raw materials used in production, the active ingredients and the excipients as it can provide valuable additional structural information. Another important aspect of pharmaceutical analysis is the characterization of different crystalline forms, usually knows as polymorphs, of pharmaceutical solids (174).

*2.2.4.5 Food and agricultural industries*

Foods are complex matrices with the main components being water, proteins, fats and carbohydrates and NIR technique allows several constituents to be measured simultaneously. NIR spectra of foods comprises broad bands corresponding to vibrational modes involving C-H, O-H

and N-H chemical bonds (175) which makes this analytical technique very feasible for measurements to be made in organic and biological systems. Therefore, it has been successfully employed for the in-/online monitoring of meat , fruit and vegetables, grain and grain products, dairy products, oils, fish and fish products and beverages (176).

*2.2.4.6 Environmental applications*

Infrared spectroscopy has been applied to a broad range of environmental samples including air, water and soils being a powerful tool for both qualitative and quantitative studies (177). The development of remote sensing infrared equipments has been advantageous in these fields. Simple and easy-to-use methods have been set up for measuring trace gases in atmosphere (industrial gas emissions, biomass burning, emissions from fires, etc.) and pollutants and pesticides in soils and human consumable water tanks (178, 179).

Identification and quantification of atmospheric gases is important for a better understanding of global climate changes and Infrared spectroscopy can be used for measuring the most abundant and important greenhouse gases as $CO_2$, $CH_4$, $N_2O$ and CO (180). Attenuated total reflectance/Fourier transform infrared spectroscopy (ATR/FT-IR) is a valuable and well-established surface spectroscopic technique for on field multi-measurements of hazardous substances (179).

*2.2.4.7 Forensic science*

Spectrometric non-destructive techniques give information on the main components of the examined samples. The new generation of compact and portable spectrometers which have good signal-to-noise ratio as well as short time of measurement and low-power laser, makes this technique appropriate for the forensic investigation of paints (181, 182), bones (183), latent fingerprint within a crime scene (184) and body fluids (185). In addition, unequivocal Infrared data have contributed to the outcome of high profile fraud cases of document paper and inks by assigning chemical groups to the peaks in a spectrum or inferring the chemical formula of the sample, or by comparing the spectrum to those of known compounds and making the identification the best match (186). A more detailed insight about the use of Infrared spectroscopy for paper and ink analysis will done in Chapter 7.

## 3. Bibliography


1. Houk RS, Fassel VA, Flesch GD, Svec HJ, Gray AL, Taylor CE. Inductively coupled argon plasma as an ion source for mass spectrometric determination of trace elements. Analytical Chemistry. 1980;52(14):2283-9.
2. Beauchemin D. Inductively Coupled Plasma Mass Spectrometry. Analytical Chemistry. 2010;82(12):4786-810.
3. Ammann AA. Inductively coupled plasma mass spectrometry (ICP MS): a versatile tool. Journal of Mass Spectrometry. 2007;42(4):419-27.
4. Hieftje GM. Introduction – A Forward-Looking Perspective. In: Inductively Coupled Plasma Spectrometry and its Applications. Blackwell Publishing Ltd.;2006. p. 1-26.
5. Linge KL, Jarvis KE. Quadrupole ICP-MS: Introduction to Instrumentation, Measurement Techniques and Analytical Capabilities. Geostandards and Geoanalytical Research. 2009;33(4):445-67.
6. Günther D, Hattendorf B. Solid sample analysis using laser ablation inductively coupled plasma mass spectrometry. TrAC Trends in Analytical Chemistry. 2005;24(3):255-65.
7. Falkner KK, Klinkhammer GP, Ungerer CA, Christie DM. Inductively Coupled Plasma Mass Spectrometry in Geochemistry. Annual Review of Earth and Planetary Sciences. 1995;23(1):409-49.
8. Mass Spectrometry, The 30-Minute Guide to ICPMS. Perkin Elmer, Inc. 2001 [cited 20 April 2016]. Available from: https://www.perkinelmer.com/CMSResources/Images/44-74849tch_icpmsthirtyminuteguide.pdf.
9. Todolí JL, Mermet JM. Sample introduction systems for the analysis of liquid microsamples by ICP-AES and ICP-MS. Spectrochimica Acta Part B: Atomic Spectroscopy. 2006;61(3):239-83.
10. Mora J, Maestre S, Hernandis V, Todolí JL. Liquid-sample introduction in plasma spectrometry. TrAC Trends in Analytical Chemistry. 2003;22(3):123-32.
11. Gaines, P. Sample Introduction for ICP-MS and ICP-OES. Spectroscopy, Solutions for Material Analysis. 2005 [cited 21 April 2016]. Available from: https://www.inorganicventures.com/sites/default/files/sample-introdruction-for-icp-ms-and-icp-oes.pdf.
12. Todoli JL, Mermet JM. Pneumatic Nebulizer Design. In: Liquid Sample Introduction in ICP Spectroscopy. Amsterdam:Elsevier; 2008. p. 17-76.
13. Miller PE, Denton MB. The quadrupole mass filter: Basic operating concepts. Journal of Chemical Education. 1986;63(7):617.
14. Mounicou S, Szpunar J, Lobinski R. Metallomics: the concept and methodology. Chemical Society Reviews. 2009;38(4):1119-38.

15. Laborda F, Bolea E, Jiménez-Lamana J. Single Particle Inductively Coupled Plasma Mass Spectrometry: A Powerful Tool for Nanoanalysis. Analytical Chemistry. 2014;86(5):2270-8.
16. Bush L. Analysis of the State of the Art: ICP-MS .Spectroscopy, Solutions for Material Analysis. 2015 [cited 26 April 2016].Available from: http://www.spectroscopyonline.com/analysis-state-art-icp-ms.
17. Todoli JL, Mermet JM. Introduction. In: Liquid Sample Introduction in ICP Spectroscopy. Amsterdam:Elsevier; 2008. p. 1-2.
18. Zhang X, Zhang C, Tyson JF, Vanhaecke F, Köllensperger G,Leach AM, et al. Detection. In: Handbook of Elemental Speciation: Techniques and Methodology. John Wilely and Sons, Ltd.;2003. p. 241-504.
19. Montaser, A. An introduction to ICP spectrometries for elemental analysis. In: Inductively Coupled Plasma Mass Spectrometry. New York:John Wiley and Sons Ltd.; 1998. p. 2-28.
20. Dams RFJ, Goossens J, Moens L. Spectral and non-spectral interferences in inductively coupled plasma mass-spectrometry. Microchimica Acta. 1995;119(3):277-86.
21. Evans EH, Giglio JJ. Interferences in inductively coupled plasma mass spectrometry. A review. Journal of Analytical Atomic Spectrometry. 1993;8(1):1-18.
22. Thomas R. A beginner's guide to ICP-MS part XII - a review of interferences. Spectroscopy, Solutions for Material Analysis. 2002 [cited 27 April 2016]. Available from: https://www.uam.es/personal_pas/txrf/imagenes/tutorial12.pdf.
23. Gray AL. Solid sample introduction by laser ablation for inductively coupled plasma source mass spectrometry. Analyst. 1985;110(5):551-6.
24. Pécheyran C, Cany S, Chabassier P, Mottay E, Donard O. High repetition rate and low energy femtosecond laser ablation coupled to ICPMS detection: a new analytical approach for trace element determination in solid samples. Journal of Physics: Conference Series. 2007;59(1):112.
25. Koch J, Gunther D. Femtosecond laser ablation inductively coupled plasma mass spectrometry: achievements and remaining problems. Analytical and Bionalytical Chemistry. 2007;387(1):149-53.
26. Russo RE, Mao X, Liu H, Gonzalez J, Mao SS. Laser ablation in analytical chemistry—a review. Talanta. 2002;57(3):425-51.
27. Voellkopf U, Paul M, Denoyer ER. Analysis of solid samples by ICP-mass spectrometry. Fresenius' Journal of Analytical Chemistry.342(12):917-23.
28. Gunther D, Horn I, Hattendorf B. Recent trends and developments in laser ablation-ICP-mass spectrometry. Fresenius J Anal Chem. 2000;368(1):4-14.

29. Kosler J, Wiedenbeck M, Wirth R, Hovorka J, Sylvester P, Mikova J. Chemical and phase composition of particles produced by laser ablation of silicate glass and zircon-implications for elemental fractionation during ICP-MS analysis. Journal of Analytical Atomic Spectrometry. 2005;20(5):402-9.
30. Becker JS. Applications of inductively coupled plasma mass spectrometry and laser ablation inductively coupled plasma mass spectrometry in materials science. Spectrochimica Acta Part B: Atomic Spectroscopy. 2002;57(12):1805-20.
31. Becker JS, Zoriy M, Matusch A, Wu B, Salber D, Palm C. Bioimaging of metals by laser ablation inductively coupled plasma mass spectrometry (LA-ICP-MS). Mass Spectrometry Reviews. 2010;29(1):156-75.
32. Becker JS, Zoriy MV, Dobrowolska J, Matucsh A. Imaging mass spectrometry in biological tissues by laser ablation inductively coupled plasma mass spectrometry. European Journal of Mass Spectrometry. 2007;13(1):1-6.
33. Liu Y, Hu Z, Li M, Gao S. Applications of LA-ICP-MS in the elemental analyses of geological samples. Chinese Science Bulletin. 2013;58(32):3863-78.
34. da Silva M, Arruda M. Laser ablation (imaging) for mapping and determining Se and S in sunflower leaves. Metallomics. 2013;5(1):62-7.
35. Durrant SF, Ward NI. Recent biological and environmental applications of laser ablation inductively coupled plasma mass spectrometry (LA-ICP-MS). Journal of Analytical Atomic Spectrometry. 2005;20(9):821-9.
36. Neff H. Laser Ablation ICP-MS in Archaeology. In: Mass Spectrometry Handbook. John Wiley and Sons, Inc.;2012. p. 829-843.
37. Stimulated Emission. RP Photonics Encyclopedia. [cited 28 Juin 2017]. Available from: https://www.rp-photonics.com/stimulated_emission.html.
38. Lasers. RP Photonics Encyclopedia. [cited 19 April 2017]. Available from: https://www.rp-photonics.com/lasers.html.
39. Figg D, Kahr MS. Elemental Fractionation of Glass Using Laser Ablation Inductively Coupled Plasma Mass Spectrometry. Applied Spectroscopy. 1997;51(8):1185-92.
40. Figg DJ, Cross JB, Brink C. More investigations into elemental fractionation resulting from laser ablation–inductively coupled plasma–mass spectrometry on glass samples. Applied Surface Science. 1998;127–129:287-91.
41. Hattendorf B, Latkoczy C, Günther D. Peer Reviewed: Laser Ablation-ICPMS. Analytical Chemistry. 2003;75(15):341 A-7 A.
42. Kuhn HR, Gunther D. Elemental fractionation studies in laser ablation inductively coupled plasma mass spectrometry on laser-induced brass aerosols. Analytical Chemistry. 2003;75(4):747-53.

43. Margetic V, Pakulev A, Stockhaus A, Bolshov M, Niemax K, Hergenröder R. A comparison of nanosecond and femtosecond laser-induced plasma spectroscopy of brass samples. Spectrochimica Acta Part B: Atomic Spectroscopy. 2000;55(11):1771-85.
44. Mozna V, Pisonero J, Hola M, Kanicky V, Gunther D. Quantitative analysis of Fe-based samples using ultraviolet nanosecond and femtosecond laser ablation-ICP-MS. Journal of Analytical Atomic Spectrometry. 2006;21(11):1194-201.
45. Koch J, von Bohlen A, Hergenroder R, Niemax K. Particle size distributions and compositions of aerosols produced by near-IR femto- and nanosecond laser ablation of brass. Journal of Analytical Atomic Spectrometry. 2004;19(2):267-72.
46. Wang Z, Hattendorf B, Günther D. Analyte Response in Laser Ablation Inductively Coupled Plasma Mass Spectrometry. Journal of the American Society for Mass Spectrometry. 2006;17(5):641-51.
47. Sylvester P, Jackson S. A brief history of Laser Ablation Inductively Coupled Plasma Mass Spectrometry (LA-ICP-MS). Elements. 2016(12):307-10.
48. Guillong M, Gunther D. Effect of particle size distribution on ICP-induced elemental fractionation in laser ablation-inductively coupled plasma-mass spectrometry. Journal of Analytical Atomic Spectrometry. 2002;17(8):831-7.
49. Horn I, Günther D. The influence of ablation carrier gasses Ar, He and Ne on the particle size distribution and transport efficiencies of laser ablation-induced aerosols: implications for LA–ICP–MS. Applied Surface Science. 2003;207(1–4):144-57.
50. Russo RE, Mao X, Gonzalez JJ, Mao SS. Femtosecond laser ablation ICP-MS. Journal of Analytical Atomic Spectrometry. 2002;17(9):1072-5.
51. Strickland D, Mourou G. Compression of amplified chirped optical pulses. Optics Communications. 1985;56(3):219-21.
52. Clark-MXR I. Micromachining handbook: Machining with Long Pulses Lasers. Clark-MRX, Inc. [cited 20 April 2017]. Available from: http://www.cmxr.com/Education/Long.html.
53. Fernández B, Claverie F, Pécheyran C, Donard OFX. Direct analysis of solid samples by fs-LA-ICP-MS. TrAC Trends in Analytical Chemistry. 2007;26(10):951-66.
54. Donard A. Développements méthodologiques pour l'analyse élémentaire et isotopique de particules nano et micrométriques par couplage ablation laser femtoseconde-ICPMS à secteur magnétique: conception et validation de signaux transitoires brefs en vue de leur application dans le contexte de la lutte contre la prolifération nucléaire. Université de Pau et des Pays de l'Adour; 2015.
55. Claverie F. Developpement et applications d'un systeme laer femtoseconde infrarouge basse energie et haute cadence de tir pour l'analyse d'elements trace dans les solides par couplage ablation laser/ICPMS. Université de Pau et des Pays de l'Adour; 2009.

56. Ugarte A. Development of new applications of inductively coupled plasma mass spectrometry (ICP-MS) hyphenated with different sample introduction systems. Universidad del País Vasco/Euskal Herriko Unibertsitatea (UPV/EHU); 2011.
57. Hager JW. Relative elemental responses for laser ablation-inductively coupled plasma mass spectrometry. Analytical Chemistry. 1989;61(11):1243-8.
58. Horn I, von Blanckenburg F. Investigation on elemental and isotopic fractionation during 196 nm femtosecond laser ablation multiple collector inductively coupled plasma mass spectrometry. Spectrochimica Acta Part B: Atomic Spectroscopy. 2007;62(4):410-22.
59. Thompson M, Chenery S, Brett L. Calibration studies in laser ablation microprobe-inductively coupled plasma atomic emission spectrometry. Journal of Analytical Atomic Spectrometry. 1989;4(1):11-6.
60. Koch J, Feldmann I, Jakubowski N, Niemax K. Elemental composition of laser ablation aerosol particles deposited in the transport tube to an ICP. Spectrochimica Acta Part B: Atomic Spectroscopy. 2002;57(5):975-85.
61. Heumann KG. Isotope-dilution ICP-MS for trace element determination and speciation: from a reference method to a routine method? Analytical and Bionalytical Chemistry. 2004;378(2):318-29.
62. Rodríguez-González P, Marchante-Gayón JM, García Alonso JI, Sanz-Medel A. Isotope dilution analysis for elemental speciation: a tutorial review. Spectrochimica Acta Part B: Atomic Spectroscopy. 2005;60(2):151-207.
63. Rodriguez-Gonzalez P, Garcia Alonso JI. Recent advances in isotope dilution analysis for elemental speciation. Journal of Analytical Atomic Spectrometry. 2010;25(3):239-59.
64. Garcia CC, Lindner H, von Bohlen A, Vadla C, Niemax K. Elemental fractionation and stoichiometric sampling in femtosecond laser ablation. Journal of Analytical Atomic Spectrometry. 2008;23(4):470-8.
65. Saetveit NJ, Bajic SJ, Baldwin DP, Houk RS. Influence of particle size on fractionation with nanosecond and femtosecond laser ablation in brass by online differential mobility analysis and inductively coupled plasma mass spectrometry. Journal of Analytical Atomic Spectrometry. 2008;23(1):54-61.
66. Bian Q, Koch J, Lindner H, Berndt H, Hergenroder R, Niemax K. Non-matrix matched calibration using near-IR femtosecond laser ablation inductively coupled plasma optical emission spectrometry. Journal of Analytical Atomic Spectrometry. 2005;20(8):736-40.
67. Bian Q, Garcia CC, Koch J, Niemax K. Non-matrix matched calibration of major and minor concentrations of Zn and Cu in brass, aluminium and silicate glass using NIR femtosecond laser ablation inductively coupled plasma mass spectrometry. Journal of Analytical Atomic Spectrometry. 2006;21(2):187-91.

68. Ricard E, Pecheyran C, Sanabria Ortega G, Prinzhofer A, Donard OF. Direct analysis of trace elements in crude oils by high-repetition-rate femtosecond laser ablation coupled to ICPMS detection. Analytical and Bioanalytical Chemistry. 2011;399(6):2153-65.
69. Ballihaut G, Claverie F, Pécheyran C, Mounicou S, Grimaud R, Lobinski R. Sensitive Detection of Selenoproteins in Gel Electrophoresis by High Repetition Rate Femtosecond Laser Ablation-Inductively Coupled Plasma Mass Spectrometry. Analytical Chemistry. 2007;79(17):6874-80.
70. Russo RE, Suen TW, Bol'shakov AA, Yoo J, Sorkhabi O, Mao X, et al. Laser plasma spectrochemistry. Journal of Analytical Atomic Spectrometry. 2011;26(8):1596-603.
71. Pozebon D, Scheffler GL, Dressler VL, Nunes MAG. Review of the applications of laser ablation inductively coupled plasma mass spectrometry (LA-ICP-MS) to the analysis of biological samples. Journal of Analytical Atomic Spectrometry. 2014;29(12):2204-28.
72. Hoffmann E, Lüdke C, Scholze H, Stephanowitz H. Analytical investigations of tree rings by laser ablation ICP-MS. Fresenius' Journal of Analytical Chemistry. 1994;350(4):253-9.
73. Garbe-Schönberg CD, Reimann C, Pavlov VA. Laser ablation ICP-MS analyses of tree-ring profiles in pine and birch from N Norway and NW Russia – a reliable record of the pollution history of the area? Environmental Geology. 1997;32(1):9-16.
74. Narewski U, Werner G, Schulz H, Vogt C. Application of laser ablation inductively coupled mass spectrometry (LA-ICP-MS) for the determination of major, minor, and trace elements in bark samples. Fresenius' Journal of Analytical Chemistry. 2000;366(2):167-70.
75. Guerra M, Amarasiriwardena D, Schaefer C, Pereira C, Spielmann A, Nobrega J, et al. Biomonitoring of lead in Antarctic lichens using laser ablation inductively coupled plasma mass spectrometry. Journal of Analytical Atomic Spectrometry. 2011;26(11):2238-46.
76. Bi M, Austin E, Smith BW, Winefordner JD. Elemental analysis of Spanish moss using laser ablation inductively coupled plasma mass spectrometry. Analytica Chimica Acta. 2001;435(2):309-18.
77. da Silva M, Arruda M. Laser ablation (imaging) for mapping and determining Se and S in sunflower leaves. Metallomics. 2013;5(1):62-7.
78. Barats A, Pécheyran C, Amouroux D, Dubascoux S, Chauvaud L, Donard OFX. Matrix-matched quantitative analysis of trace-elements in calcium carbonate shells by laser-ablation ICP–MS: application to the determination of daily scale profiles in scallop shell (Pecten maximus). Analytical and Bioanalytical Chemistry. 2007;387(3):1131-40.
79. Sinclair DJ, Kinsley LPJ, McCulloch MT. High resolution analysis of trace elements in corals by laser ablation ICP-MS. Geochimica et Cosmochimica Acta. 1998;62(11):1889-901.
80. Tabouret H, Bareille G, Claverie F, Pecheyran C, Prouzet P, Donard OF. Simultaneous use of strontium:calcium and barium:calcium ratios in otoliths as markers of habitat: application to

the European eel (Anguilla anguilla) in the Adour basin, South West France. Marine Environmental Research. 2010;70(1):35-45.

81. Ek K, Morrison G, Lindberg P, Rauch S. Comparative Tissue Distribution of Metals in Birds in Sweden Using ICP-MS and Laser Ablation ICP-MS. Archives of Environmental Contamination and Toxicology. 2004;47(2):259-69.
82. Borcherding J, Pickhardt C, Winter HV, Becker JS. Migration history of North Sea houting (Coregonus oxyrinchus L.) caught in Lake IJsselmeer (The Netherlands) inferred from scale transects of 88Sr:44Ca ratios. Aquatic Sciences. 2008;70(1):47-56.
83. Ugarte A, Unceta N, Pecheyran C, Goicolea MA, Barrio RJ. Development of matrix-matching hydroxyapatite calibration standards for quantitative multi-element LA-ICP-MS analysis: application to the dorsal spine of fish. Journal of Analytical Atomic Spectrometry. 2011;26(7):1421-7.
84. Prohaska T, Latkoczy C, Schultheis G, Teschler-Nicola M, Stingeder G. Investigation of Sr isotope ratios in prehistoric human bones and teeth using laser ablation ICP-MS and ICP-MS after Rb/Sr separation. Journal of Analytical Atomic Spectrometry. 2002;17(8):887-91.
85. Becker JS. Imaging of metals, metalloids, and non-metals by laser ablation inductively coupled plasma mass spectrometry (LA-ICP-MS) in biological tissues. Methods in Molecular Biology. 2010;656:51-82.
86. Becker JS, Zoriy M, Becker JS, Dobrowolska J, Dehnhardt M, Matusch A. Elemental imaging mass spectrometry of thin sections of tissues and analysis of brain proteins in gels by laser ablation inductively coupled plasma mass spectrometry. physica status solidi (c). 2007;4(6):1775-84.
87. Clarkson TW. Metal toxicity in the central nervous system. Environmental Health Perspectives. 1987;75:59-64.
88. Gaeta A, Hider RC. The crucial role of metal ions in neurodegeneration: the basis for a promising therapeutic strategy. British Journal of Pharmacology. 2005;146(8):1041-59.
89. Guilarte TR. Manganese and Parkinson's disease: a critical review and new findings. Environmenatal Health Perspectives. 2010;118(8):1071-80.
90. Aschner M, Erikson KM, Herrero Hernandez E, Tjalkens R. Manganese and its role in Parkinson's disease: from transport to neuropathology. Neuromolecular Medicine. 2009;11(4):252-66.
91. Olanow CW. Manganese-induced parkinsonism and Parkinson's disease. Annals of the New York Academy of Science. 2004;1012:209-23.
92. Matusch A, Depboylu C, Palm C, Wu B, Höglinger GU, Schäfer MKH, et al. Cerebral Bioimaging of Cu, Fe, Zn, and Mn in the MPTP Mouse Model of Parkinson's Disease Using

Laser Ablation Inductively Coupled Plasma Mass Spectrometry (LA-ICP-MS). Journal of the American Society for Mass Spectrometry. 2010;21(1):161-71.

93. Bush A. The metal theory of Alzheimer's disease. Journal of Alzheimers Disease. 2013;33(1):S277-81.
94. Schrag M, Mueller C, Oyoyo U, Smith MA, Kirsch WM. Iron, zinc and copper in the Alzheimer's disease brain: a quantitative meta-analysis. Some insight on the influence of citation bias on scientific opinion. Progress in Neurobiology. 2011;94(3):296-306.
95. Hare DJ, Raven EP, Roberts BR, Bogeski M, Portbury SD, McLean CA, et al. Laser ablation-inductively coupled plasma-mass spectrometry imaging of white and gray matter iron distribution in Alzheimer's disease frontal cortex. Neuroimage. 2016;137:124-31.
96. Hutchinson RW, Cox AG, McLeod CW, Marshall PS, Harper A, Dawson EL, et al. Imaging and spatial distribution of beta-amyloid peptide and metal ions in Alzheimer's plaques by laser ablation-inductively coupled plasma-mass spectrometry. Analytical Biochemistry. 2005;346(2):225-33.
97. Becker JS, Zoriy MV, Dehnhardt M, Pickhardt C, Zilles K. Copper, zinc, phosphorus and sulfur distribution in thin section of rat brain tissues measured by laser ablation inductively coupled plasma mass spectrometry: possibility for small-size tumor analysis. Journal of Analytical Atomic Spectrometry. 2005;20(9):912-7.
98. Jantzi SC, Almirall JR. Elemental analysis of soils using laser ablation inductively coupled plasma mass spectrometry (LA-ICP-MS) and laser-induced breakdown spectroscopy (LIBS) with multivariate discrimination: tape mounting as an alternative to pellets for small forensic transfer specimens. Applied Spectroscopy. 2014;68(9):963-74.
99. Arroyo L, Trejos T, Hosick T, Machemer S, Almirall JR, Gardinali PR. Analysis of Soils and Sediments by Laser Ablation Inductively Coupled Plasma Mass Spectrometry (LA-ICP-MS): An Innovative Tool for Environmental Forensics. Environmental Forensics. 2010;11(4):315-27.
100. Ridley WI, Koenig AE, Pribil MJ. Laser Ablation ICP-MS in Geochemistry and Biogeochemistry: A Progress Report. Microscopy and Microanalysis. 2008;14(S2):534-5.
101. Trejos T, Almirall JR. Laser Ablation Inductively Coupled Plasma Mass Spectrometry in Forensic Science. In: Encyclopedia of Analytical Chemistry. John Wiley and Sons, Ltd.;2006.
102. Trejos T, Montero S, Almirall JR. Analysis and comparison of glass fragments by laser ablation inductively coupled plasma mass spectrometry (LA-ICP-MS) and ICP-MS. Analytical and Bioanalytical Chemistry. 2003;376(8):1255-64.
103. Schenk ER, Almirall JR. Elemental analysis of glass by laser ablation inductively coupled plasma optical emission spectrometry (LA-ICP-OES). Forensic Science International. 2012;217(1–3):222-8.

104. Hobbs AL, Almirall JR. Trace elemental analysis of automotive paints by laser ablation–inductively coupled plasma–mass spectrometry (LA–ICP–MS). Analytical and Bioanalytical Chemistry. 2003;376(8):1265-71.
105. Trejos T, Flores A, Almirall JR. Micro-spectrochemical analysis of document paper and gel inks by laser ablation inductively coupled plasma mass spectrometry and laser induced breakdown spectroscopy. Spectrochimica Acta Part B: Atomic Spectroscopy. 2010;65(11):884-95.
106. Trejos T, Corzo R, Subedi K, Almirall J. Characterization of toners and inkjets by laser ablation spectrochemical methods and Scanning Electron Microscopy-Energy Dispersive X-ray Spectroscopy. Spectrochimica Acta Part B: Atomic Spectroscopy. 2014;92(0):9-22.
107. Abrego Z, Ugarte A, Unceta N, Fernandez-Isla A, Goicolea MA, Barrio RJ. Unambiguous characterization of gunshot residue particles using scanning laser ablation and inductively coupled plasma-mass spectrometry. Analytical Chemistry. 2012;84(5):2402-9.
108. Abrego Z, Grijalba N, Unceta N, Maguregui M, Sanchez A, Fernandez-Isla A, et al. A novel method for the identification of inorganic and organic gunshot residue particles of lead-free ammunitions from the hands of shooters using scanning laser ablation-ICPMS and Raman micro-spectroscopy. Analyst. 2014;139(23):6232-41.
109. Deimler RE, Razunguzwa TT, Reschke BR, Walsh CM, Powell MJ, Jackson GP. Direct analysis of drugs in forensic applications using laser ablation electrospray ionization-tandem mass spectrometry (LAESI-MS/MS). Analytical Methods. 2014;6(13):4810-7.
110. Rege S, Jackson S, Griffin WL, Davies RM, Pearson NJ, O'Reilly SY. Quantitative trace-element analysis of diamond by laser ablation inductively coupled plasma mass spectrometry. Journal of Analytical Atomic Spectrometry. 2005;20(7):601-11.
111. Dalpe C, Hudon P, Ballantyne DJ, Williams D, Marcotte D. Trace element analysis of rough diamond by LA-ICP-MS: a case of source discrimination? Journal of Forensic Science. 2010;55(6):1443-56.
112. Donard A, Pottin AC, Pointurier F, Pecheyran C. Determination of relative rare earth element distributions in very small quantities of uranium ore concentrates using femtosecond UV laser ablation - SF-ICP-MS coupling. Journal of Analytical Atomic Spectrometry. 2015;30(12):2420-8.
113. Mayer K, Wallenius M, Varga Z. Nuclear Forensic Science: Correlating Measurable Material Parameters to the History of Nuclear Material. Chemical Reviews. 2013;113(2):884-900.
114. Neff H. Analysis of Mesoamerican Plumbate Pottery Surfaces by Laser Ablation-Inductively Coupled Plasma-Mass Spectrometry (LA-ICP-MS). Journal of Archaeological Science. 2003;30(1):21-35.

115. Walaszek D, Senn M, Faller M, Philippe L, Wagner B, Bulska E, et al. Metallurgical and chemical characterization of copper alloy reference materials within laser ablation inductively coupled plasma mass spectrometry: Method development for minimally-invasive analysis of ancient bronze objects. Spectrochimica Acta Part B: Atomic Spectroscopy. 2012;79–80:17-30.
116. Pańczyk E, Sartowska B, Waliś L, Dudek J, Weker W, Widawski M. The origin and chronology of medieval silver coins based on the analysis of chemical composition. Nukleonika. 2015;60(3):657.
117. Koch KH. Process analysis in the metallurgical industry. TrAC Trends in Analytical Chemistry. 1993;12(8):333-9.
118. Pisonero J, Kroslakova I, Gunther D, Latkoczy C. Laser ablation inductively coupled plasma mass spectrometry for direct analysis of the spatial distribution of trace elements in metallurgical-grade silicon. Analytical and Bionalytical Chemistry. 2006;386(1):12-20.
119. Hof M, Machán R. Basics of Optical Spectroscopy. In: Handbook of Spectroscopy. Wiley-VCH Verlag GmbH; 2014. p. 31-38.
120. Tkachenko N. Introduction. In: Optical Spectroscopy. Amsterdam : Elservier Science;2006. p. 1-14. 2006.
121. Plekhanov V. Isotopes in Condensed Matter. Springer; 2013.
122. Larkin P. Infrared and Raman Spectroscopy : Principles and spectral interpretation. San Diego (California): Elsevier; 2011.
123. Introduction to Raman Spectroscopy. Thermo Scientific. 2008 [cited 7 April 2016]. Available from: http://www.biotechprofiles.com/companyfiles/madisonnetwork/5bdd0a9f37694d6c9fb6e62db5049477.pdf.
124. Larkin P. Infrared and Raman Spectroscopy : Principles and spectral interpretation. San Diego: Elsevier; 2011.
125. Raman Spectroscopy Basics. Princenton Instruments. [cited 7 April 2016]. Available from: http://web.pdx.edu/~larosaa/Applied_Optics_464564/Projects_Optics/Raman_Spectroscopy/Raman_Spectroscopy_Basics_PRINCETON-INSTRUMENTS.pdf.
126. Fundamentals of Raman spectroscopy. B&W Tek - Laser Focus World. [cited 14 January 2015]. Available from: http://faculty.kfupm.edu.sa/PHYS/zhyamani/teaching/Coupled_Oscillations/lectures/lecture_8/Raman%20study%20material/fundamentals-of-raman-spectroscopy.whitepaperpdf.render.pdf.
127. Ferraro JR, Nakamoto K, Brown CW. Introductory Raman Spectroscopy. Elsevier; 2003.
128. Skoog DA. Principios de Análisis Instrumental. Madrid:Ediciones Paraninfo; 2009.

129. Smith E, Dent G. Modern Raman Spectroscopy - A Practical Approach. Chichester:John Wiley and Sons; 2005.
130. McCreery RL. Raman Spectroscopy for Chemical Analysis. John Wiley and Sons; 2005.
131. Baena JR, Lendl B. Raman spectroscopy in chemical bioanalysis. Current Opinion in Chemical Biology. 2004;8(5):534-9.
132. Chase B. Fourier transform Raman spectroscopy. Journal of the American Chemical Society. 1986;108(24):7485-8.
133. Le Ru EC, Etchegoin PG. Principles of Surface-Enhanced Raman Spectroscopy. Elsevier; 2009.
134. Schlucker S. Surface-Enhanced Raman Spectroscopy: Concepts and Chemical Applications. Angew. Chem. Int;2014.
135. Considerations of Grating Selection in Optimizing a Raman Spectrograph. Spectroscopy Solutions for Material Analysis. 2013 [cited 14 January 2015]. Available from: http://www.horiba.com/fileadmin/uploads/Scientific/Documents/Raman/Spec_Workbench_Considerations_of_Grating_Selection-_Oct2013.pdf.
136. Introduction to Raman Spectroscopy. Thermo Scientific. 2008 [cited 7 April 2016]. Availablefrom: http://www.biotechprofiles.com/companyfiles/madisonnetwork/5bdd0a9f37694d6c9fb6e62db5049477.pdf.
137. Vankeirsbilck T. Applications of Raman spectroscopy in pharmaceutical analysis. TrAC Trends in Analytical Chemistry. 2002;21(12):869–77.
138. Choo-Smith LP, Edwards HG, Endtz HP, Kros JM, Heule F, Barr H, et al. Medical applications of Raman spectroscopy: from proof of principle to clinical implementation. Biopolymers. 2002;67(1):1-9.
139. Buschman HP, Marple ET, Wach ML, Bennett B, Schut TCB, Bruining HA, et al. In Vivo Determination of the Molecular Composition of Artery Wall by Intravascular Raman Spectroscopy. Analytical Chemistry. 2000;15(72):3771-5.
140. Qin J, Chao K, Kim MS. Raman Chemical Imaging system for food safety and quality inspection. American Society of Agricultural and Biological Engineers. 2010;53(6):1873-82.
141. Lopez C, Bianchi G, Goodacre R. Rapid Quantitative Assesment of the Adulteration of Virgin Olive Oils with Hazelnut Oils Using Raman Spectroscopy and Chemometrics. Journal of Agricultural and Food Chemistry. 2003;51:6145-50.
142. Paradkar M, Irudayaraj J. Discrimination and classification of beet and cane inverts in honey by FT-Raman spectroscopy. Food Chemistry. 2002;76(2):231–9.
143. Williams TL, Collette TW. Environmental Applications of Raman Spectroscopy to Aqueous Systems. In: Handbook of Raman Spectroscopy: From the Research Laboratory to the Process Line. New York: Marcel Dekker Incorporated; 2001.

144. Sobanska S. Confocal Raman microspectrometry imaging combined with chemometric methods for environmental applications. Application Note. Horiba Scientific. 2011 [cited 22 January 2015]. Available from: http://www.horiba.com/fileadmin/uploads/Scientific/Documents/Raman/RA48.pdf.
145. Larat V. Identification of airborne pollen by Raman spectroscopy. Application Note. Horiba Scientific. 2014 [cited 22 January 2015]. Available from: http://www.horiba.com/fileadmin/uploads/Scientific/Documents/Raman/RA56.pdf.
146. Gupta N, Dahmani R. AOTF Raman spectrometer for remote detection of explosives. Spectrochimica Acta Part A: Molecular and Biomolecular Spectroscopy. 2000;56(8):1453–6.
147. Esam MA. Raman spectroscopy and security applications: the detection of explosives and precursors on clothing. Journal of Raman Spectroscopy. 2009;40(12):2009-14.
148. Boyd S, Bertino MF, Seashols SJ. Raman spectroscopy of blood samples for forensic applications. Forensic Science International. 2011;208(1-3):124-8.
149. Virkler K, Lednev IK. Raman spectroscopy offers great potential for the nondestructive confirmatory identification of body fluids. Forensic Science International. 2008;181(1-3):e1-5.
150. Sikirzhytski V, Virkler K, Lednev IK. Discriminant Analysis of Raman Spectra for Body Fluid Identification for Forensic Purposes. Sensors. 2010;10(4):2869-84.
151. The non-destructive and in-situ identification of controlled drugs and narcotics. Application Note. Horiba Scientific. 2013 [cited 23 January 2015]. Available from: http://www.horiba.com/fileadmin/uploads/Scientific/Documents/Raman/RA19.pdf.
152. Zięba-Palus J, Wesełucha-Birczyńska A, Trzcińska B, Kowalski R, Moskal P. Analysis of degraded papers by infrared and Raman spectroscopy for forensic purposes. Journal of Molecular Structure. 2017;1140:154-62.
153. Braz A, López-López M, García-Ruiz C. Raman spectroscopy for forensic analysis of inks in questioned documents. Forensic Science International. 2013;232(1):206-12.
154. Osborne BG, Fearn T, Hindle PH. Practical NIR spectroscopy with applications in food and beverage analysis. Longman Scientific and Technical; 1993.
155. Stuart B. Infrared Spectroscopy: Fundamentals and Applications. United Kingdom:John Wiley and Sons; 2005.
156. Silverstein RM, Webster FX. Spectrometric identification of organic compounds. New York:Willey; 1998.
157. ATR Theory and Applications. Application Note 0402. Pike Technologies. 2015 [cited 4 February 2015]. Available from: http://www.piketech.com/skin/fashion_mosaic_blue/application-pdfs/Diamond-Crystal-Plates.pdf.

158. FT-IR spectroscopy Attenuated Total Internal Reflectance (ATR). Perkin Elmer Technical Note. [cited 4 February 2015]. Available from: http://www.utsc.utoronto.ca/~traceslab/ATR_FTIR.pdf.
159. Monsef Z. Infrared Spectroscopy - Materials Science, Engineering and Technology. InTech;2012.
160. Higdon T. FT-IR spectroscopy technology, market evolution and future strategies of Bruker Optics Inc. Massachusetts Institute of Technology. 2010.
161. Smith BC. Fundamentals of Fourier Transform Infrared Spectroscopy (2nd Ed). Boca Raton:CRC Press; 2011.
162. Simonescu C. Applictaion of FTIR Spectroscopy in Environmental Studies. In: Advance Aspects of Spectroscopy. InTech; 2012. p. 49-84.
163. Griffiths P, Haseth J. Fourier Transform Infrared Spectrometry (2nd Edition). Wiley; 2007.
164. Krafft C, Sergo V. Biomedical applications of Raman and Infrared spectroscopy to diagnose tissues. Spectroscopy. 2006;20:195-218.
165. Krafft C, Steiner G, Beleites C, Salzer R. Disease recognition by infrared and Raman spectroscopy. Journal of Biophotonics. 2009;2(1-2):13-28.
166. Ellis DI, Goodacre R. Metabolic fingerprinting in disease diagnosis: biomedical applications of infrared and Raman spectroscopy. Analyst. 2006;131(8):875-85.
167. Ellis DI, Harrigan GG, Goodacre R. Metabolic Profiling: Its Role in Biomarker Discovery and Gene Function Analysis. Boston:Kluwer Academic; 2003.
168. Griebe M, Daffertshofer M, Stroick M, Syren M, Ahmad-Nejad P, Neumaier M, et al. Infrared spectroscopy: a new diagnostic tool in Alzheimer disease. Neuroscience Letters. 2007;420(1):29-33.
169. Peuchant E, Richard-Harston S, Bourdel-Marchasson I, Dartigues JF, Letenneur L, Barberger-Gateau P, et al. Infrared spectroscopy: a reagent-free method to distinguish Alzheimer's disease patients from normal-aging subjects. Translational Research. 2008;152(3):103-12.
170. Shaw RA, Mantsch HH. Infrared Spectroscopy in Clinical and Diagnostic Analysis. In: Encyclopedia of Analytical Chemistry. Chichester:Wiley; 2006.
171. Arnold MA. Non-invasive glucose monitoring. Current Opinion in Biotechnology. 1996;7(1):46–9.
172. Khalil OS. Spectroscopic and clinical aspects of noninvasive glucose measurements. Clinical Chemistry. 1999;45(2):165-77.
173. Clark D. The Analysis of Pharmaceutical Substances and Formulated Products by Vibrational Spectroscopy. In: Handbook of Vibrational Spectroscopy. Chichester:Wiley; 2002. p. 3574-3589.

174. Rustichelli C, Gamberini G, Ferioli V, Gamberini MC, Ficarra R, Tommasini S. Solid-state study of polymorphic drugs: carbamazepine. Journal of Pharmaceutical and Biomedical Analysis. 2000;23(1):41-54.
175. Osborne BG. Near Infrared Spectroscopy in food analysis. In: Encyclopedia of Analytical Chemistry. Chichester:Wiley; 2006. p. 1-14.
176. Huang H, Yu H, Xu H, Ying Y. Near infrared spectroscopy for on/in-line monitoring of quality in foods and beverages: A review. Journal of Food Engineering. 2008;87(3):303-13.
177. Visser T. Infrared Spectroscopy in Environmental Analysis. In: Encyclopedia of Analytical Chemistry. Chichester:Wiley; 2000. p. 1-21.
178. Mattson J, Mark H. Application of internal reflectance spectroscopy to water pollution analyses. Environmental Science and Technology. 1969.
179. Reagan F. Determination of pesticides in water using ATR-FTIR spectroscopy on PVC/chloroparaffin coatings. Analytica Chimica Acta. 1996;334:85–92.
180. Griffith D, Jamie I. Fourier-Transform Infrared Spectrometry in Atmospheric and Trace Gas Analysis. In: Encyclopedia of Analytical Chemistry. Chichester:Wiley; 2000. p. 1979-2007.
181. Zięba-Palus J. Application of micro-Fourier transform infrared spectroscopy to the examination of paint samples. Journal of Molecular Structure. 1999;511:327-35.
182. Flynn K, O'Leary R, Lennard C, Roux C, Reedy BJ. Forensic applications of infrared chemical imaging: multi-layered paint chips. Journal of Forensic Science. 2005;50(4):832-41.
183. Thompson TJU, Gauthier M, Islam M. The application of a new method of Fourier Transform Infrared Spectroscopy to the analysis of burned bone. Journal of Archaeological Science. 2009;36(3):910-4.
184. Crane NJ, Bartick EG, Perlman RS, Huffman S. Infrared Spectroscopic Imaging for Noninvasive Detection of Latent Fingerprints. Journal of Forensic Sciences. 2007;52(1):48-53.
185. Orphanou CM, Walton-Williams L, Mountain H, Cassella J. The detection and discrimination of human body fluids using ATR FT-IR spectroscopy. Forensic Science International. 2015;252:e10-6.
186. Causin V, Marega C, Marigo A, Casamassima R, Peluso G, Ripani L. Forensic differentiation of paper by X-ray diffraction and infrared spectroscopy. Forensic Science International. 2010;197(1-3):70-4.

REVIEW

# Laser bidezko ablazioaren egungo egoera eta aplikazioak

## (State-of-the-Art of laser ablation and its applications)

*Nagore Grijalba*[1,2]*, *Fanny Claverie*[2], *Ariane Donard*[2], *Hélène Tabouret*[2], *Christophe Pecheyran*[2], *Nora Unceta*[1], *M.ª Aránzazu Goicolea*[1], *Ramón J. Barrio*[1]

[1] Kimika Analitikoa Saila, Farmazia Fakultatea (UPV/EHU)

[2] Laboratoire de Chimie Analytique Bio-inorganique et Environnement (IPREM-UMR UPPA/CNRS 5254)

* nagore.grijalba@ehu.eus

DOI: 10.1387/ekaia.16332

Jasoa: 2016-05-13 Onartua: 2016-07-27

**Laburpena:** 80ko hamarkadaz geroztik, laser bidezko ablazioa eta akoplamendu induktibozko plasma-masa espektrometria (LA-ICPMS) konbinatzen dituen teknika analitikoa sakonki ikertu eta garatu da, eta, gaur egun, lagin solidoen analisi elemental zein isotopiko zuzena egiteko erreferentziazko teknika bilakatu da. Ezaugarri bereizgarrienak hauexek dira: erabilpen erraza, analisi-denbora laburra, laginari eragindako kalte urriak, sentsibilitate handia eta elementu nagusi zein minoritarioen eta ratio isotopikoen aldibereko neurketa ahalbidetzen duen tarte dinamiko zabala. Lan honetan, LA-ICPMS teknikaren oinarriak eta konfigurazio orokorra azaldu eta femtosegundo/nanosegundo laser bidezko ablazioaren erabileraren arteko desberdintasun nagusiak nabarmentzen dira. Azkenik, teknika honen egungo egoeraz jabetzeko, jatorri askotariko laginen analisi elementala laburbildu eta berrikusten da biologian eta ingurumenean, osasunean, geokimikan zein auzitegi zientzien alorretan.

**Hitz gakoak:** Laser bidezko ablazioa (LA), akoplamendu induktibozko plasma-masa espektrometria (ICPMS), femtosegundo, nanosegundo, lagin solidoen analisi zuzena.

**Abstract:** Since the early 80s, laser-ablation inductively-coupled-plasma mass spectrometry (LA-ICPMS) has been widely explored and nowadays is considered to be one of the most versatile analytical techniques for the direct trace elemental and isotopic analyses of solid samples. The most remarkable features are ease of use, fast sample throughput, limited sample damages, high sensitivity and wide dynamic range which allows the simultaneous acquisition of major and trace elements, as well as the meas-

*N. Grijalba, F. Claverie, A. Donard , H. Tabouret, C. Pecheyran, N. Unceta, M.ªA. Goicolea, R.J. Barrio*

urement of isotope ratios. Throughout this manuscript, the principles and general set-up of LA-ICPMS will be extensively explained and the performance of femtosecond-LA in comparison to nanosecond-LA discussed. In order to show the state of the art in this field a variety of examples for elemental analysis of solid samples in biological/environmental science, geochemistry and forensic science applications will be presented.

**Keywords:** laser ablation (LA), inductively-coupled-plasma mass spectrometry (ICPMS), femtosecond, nanosecond, solid sample direct analysis.

## 1. SARRERA

Azken urtcotan, laser bidezko ablazioa eta akoplamendu induktibozko plasma-masa espektrometria (LA-ICPMS) konbinatzen dituen teknikak interes bizia piztu du komunitate zientifikoan. Laser bidezko ablazioa masa-espektrometroan lagina sartzeko teknika erabat desberdina da ohiko soluzioen lainoztapen teknikekin alderatuz. Hori dela eta, ikerketa ugari egin dira teknikaren oinarriak hobeto ulertzeko (laser-materia elkarrekintza, aerosolen sorrera eta kuantifikazio metodoak, besteak beste) eta lagin solidoen mikrolaginketa ahalbidetzeko asmoz.

Laser-iturria edozein izanda, laser bidezko ablazioaren eta masa-espektrometroaren arteko lotura erabat erraza da (1. irudia). Lagina hermetikoki itxita dagoen gelaxka batean kokatzen da. Pultsu laburreko eta energia han-

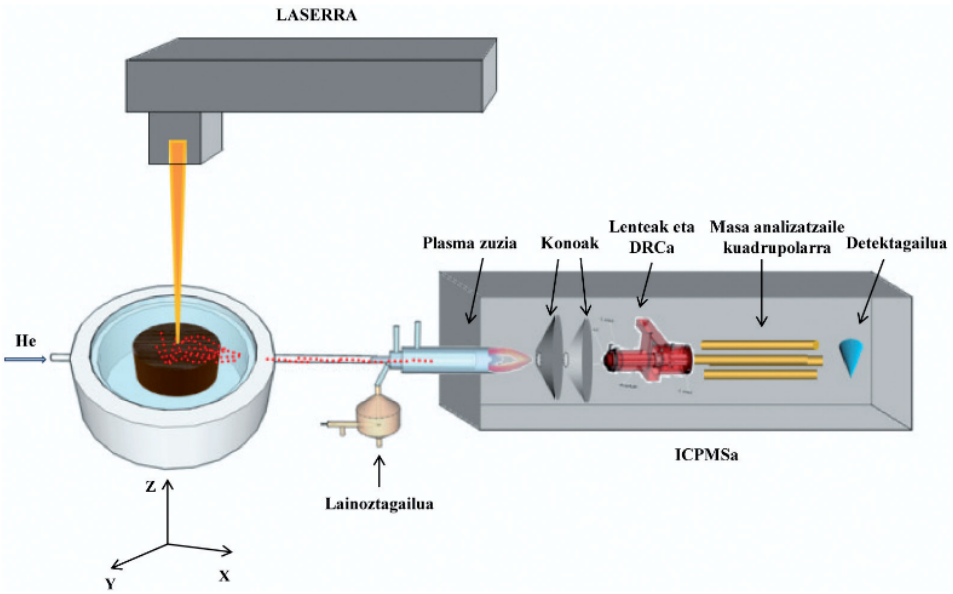


**1. irudia.** Akoplamendu induktibozko plasma-masa espektrometroari loturiko laser bidezko ablazioaren (LA-ICPMS) eskema.

diko laser-izpi bat laginaren gainazalean fokatu eta partikulak, atomoak, ioiak eta elektroiak erauzten ditu. Gas inerte batek (He edo Ar) gelaxka zeharkatu eta ICPMSra garraiatzen ditu. Bertan, aerosola lurrundu, atomizatu eta ionizatu ondoren sortzen diren ioi positiboak masa-espektrometroan analizatzen dira [1]. Hortaz, laserrak lagin solidoaren analisi zuzena ahalbidetzen du, aurretratamendurik gabe eta analisi-denbora nabarmen murrizten da. Gainera, ICPMS teknikak analisi multielemental eta isotopiko azkarra, selektiboa eta sentikorra egiteko aukera eskaintzen du eta parametro horiek masa-espektrometroan hainbat analizatzaile erabiliz hobetu daitezke (kuadrupolo hirukoizdun masa-espektrometroa, masa-espektrometro multikolektorea edo hegaldi-denbora masa-espektrometroa, besteak beste) [2].

Lagin solidoen analisi elementala ICPMS teknikaren bidez egin ohi da lagina bere osotasunean analizatuz (*bulk analysis method*). Aldez aurretik laginaren mineralizazioa egiten da, non materia suntsitu eta laginaren disoluzioa gertatzen den. Horretarako, ohikoena da azidoen ($HNO_3$, HCl, HF) edota agente oxidatzaileen ($H_2O_2$) nahasketak erabiltzea, prozesua bizkortzen duten plaka-berogailuen edo mikrouhinen laguntzaz. Mineralizazio etapa hori luzea eta neketsua da, konplexua eta, askotan, amaigabea [3, 4]. Izan ere, 80ko hamarkadaz geroztik laser bidezko ablazioa lagin-sartze sistema eraginkor eta erakargarria bilakatu da, nekez mineralizatzen diren zenbait material erregogorren (aluminosilikatoak, zeramikak eta kuartzoa, kasu) [5] eta gainerako material solidoen analisi zuzena egiteko [6].

Hori dela eta, gaur egun, laser bidezko ablazioa lehen aukerako teknika analitikoa da material solidoen analisi zuzena egiteko. Alde batetik, ez da beharrezkoa laginaren aurretratamendua egitea eta horrek dakarren denbora luzea eta zeharkako kutsadura saihesten da. Bestalde, analisia aurrera eramateko beharrezkoa den lagin kantitatea txikia da eta, gainera, teknikaren ezaugarri espezifikoen abantailak kontuan izanik, analisiak eskala mikroskopikoan (5-200 $\mu$m) egin daitezke. Hala ere, laginak oso homogeneoak ez badira, analisiaren adierazgarritasuna bermatzeko sakonera edota gainazal handiagoak analiza daitezke laserraren diametroa, energia eta abiadura areagotuz [7]. Horrela, laser-izpi baten erabilerak mikrolaginketa egitean informazio zehatza eskaintzen du (inklusioak, akatsak, heterogeneotasunak), laginaren gainazalean bereizmen espazial handiarekin fokatu baitaiteke [8, 9]. 1. taulan ICPMS eta LA-ICPMS tekniken ezaugarriak konparatu dira .

Erakutsitako abantailei esker laser bidezko ablazioa erreferentziazko teknika bilakatu da kimika analitikoaren esparruan lagin konplexuen (material geokimikoak, geruza anizkoitzeko laginak, ingurune-laginak eta lagin biologikoak, artelanak, arkeologia-piezak eta harribitxiak, esaterako) analisi mikroskopikoa egiteko [10-12].

**1. taula.** ICPMS eta LA-ICPMS tekniken konparazioa [16].

| | ICPMS | LA-ICPMS |
|---|---|---|
| Laginaren aurretratamendua | Mineralizazioa | Gutxi edo bat ere |
| Kuantifikazioa | Bikaina | Zaila, erreferentziazko material solidoen beharra |
| Detekzio-limitea | 0,001-0,1 pg/g | 0,0001-0,1 $\mu$g/g |
| Zehaztasuna | % ±1-5 | % ±1-10 |
| Bereizmen espaziala | Ez du horrelakorik | >5 $\mu$m |
| Sakoneko bereizmena | Ez du horrelakorik | 0,01-9 $\mu$m |
| Kutsadura arriskua | Altua | Txikia |
| Desabantailak | Interferentziak | Interferentziak, heterogeneotasuna |

Hala ere, teknika honek badu zehaztasunean eragiten duen desabantaila. Zatikatze elementala (edo *elemental fractionation*) laginaren matrizearen izaeraren arabera (matrize efektua, hain zuzen) gertatu eta kuantifikazioan eragina duen prozesua da [13, 14]. Fenomeno hau honela defini daiteke: laserrak eragindako ablazio ez-estekiometrikoa, hau da, erlazio elementalaren eraldaketa ablazioa gertatzen ari den bitartean. Hori dela eta, laser-laginaren elkarrekintzaren ondorioz sortutako aerosola ez da laginaren adierazgarria eta kuantifikazioa eragozten da [15]. Horregatik, laginak berak kuantifikazioan eragin ditzakeen desbiderapenak zuzentzeko laginaren antzeko konposizioa duten erreferentziazko materialak erabiltzen dira (*matrix-matching*).

Gaur egun, LA-ICPMS teknikaz gain, material solidoen analisi zuzena egiteko beste teknika batzuk daude eskuragarri, esate baterako, laser bidez induzitutako plasma-emisio optikoko espektroskopia (*Laser Induced Breakdown Spectroscopy*, LIBS), deskarga luminiszente bidezko emisio optikoko espektroskopia (*Glow Discharge Optical Emission Spectroscopy*, GD-OES), X izpien bidezko espektroskopia fotoelektronikoa (*X-Ray Photoelectron Spectroscopy*, XPS) eta bigarren mailako ionizazio bidezko masa-espektrometria (*Secondary Ion Mass Spectrometry*, SIMS) [17] (2. taula). Teknika horiek aurretratamendurik gabeko lagin solidoen analisirako erabiltzen dira. Hala ere, LA-ICPMSaren abantailak nabarmenak dira. Alde batetik, bestelako izaerako eta formako laginei moldatzeko gaitasuna dauka, eta bestetik, zehaztasun eta sentikortasun handiko neurketak azkar egiteko ahalmena eskaintzen du.

**2. taula.** Lagin solidoen analisirako teknika desberdinen konparaketa.

| | LA-ICPMS | LIBS | SDL edo GD | XPS/ESCA | XRF | SIMS | Nano-SIMS |
|---|---|---|---|---|---|---|---|
| Oinarri teorikoa | Laser-izpiak materiarekin elkarreragin ondoren sortzen den aerosolaren atomizazio/ionizazio/detekzioa | Laser bidez lainaren gainazalean sortutako plasmaren emisio-espektroaren analisia | Argon plasma batek higatutako gainazalaren argi-emisio (OES) edo ioien analisia (MS) | Laginaren gainazala X izpiekin irradiatu ondoren askatutako fotoelektroien analisia | Laginaren gainazala X izpiekin irradiatu ondoren askatutako X izpien analisia | Laginaren gainazala ioi sorta batekin eraso eta sortutako ioi sekundarioen detekzioa | |
| Eskainitako informazioa | Konposizio elementala eta isotopikoa. Irudia eta sakoneko analisia | Konposizio elementala | Konposizio elemental eta isotopikoa. Sakoneko analisia | Konposizio elementala, espezia-zioa. Sakoneko analisia | Konposizio elementala eta irudia | Konposizio elementala, isotopikoa eta molekularra. Sakontasun-analisia | |
| Detekzio muga | $10^{-4}$-$10^{-1}$ mg kg$^{-1}$ | $10^{-1}$-5,$10^{2}$ mg kg$^{-1}$ | $10^{-3}$-1 mg kg$^{-1}$ | $10^{3}$ mg kg$^{-1}$ | 1-$10^{3}$ mg kg$^{-1}$ | $10^{-3}$-1 mg kg$^{-1}$ | $\approx$ mg kg$^{-1}$ |
| Zehaztasuna | % 1-10 | % 1-10 | $\% \approx 5$ | % 0,1 | % 1-10 | % 10-20 | % 5-10 |
| Sakoneko bereizmena | 20-9000 nm | 100-500 nm | <5 nm | 0,5-2,5 nm | 10-100 $\mu$m | 0,5-1,5 nm | 10-20 nm |
| Bereizmen espaziala | > 5 $\mu$m | 1-100 $\mu$m | 2,4 edo7 mm | 100 nm | 30 nm-100 $\mu$m | 1 $\mu$m | 0,05-0,15 $\mu$m |
| Analisi denbora | Azkarra | Azkarra | Azkarra | Luzea | Azkarra | Bitartekoa | |
| Desabantailak | Matrize efektua, erreferentzia materialik ez | Interferentziak, erreferentzia materialik ez | Bereizmen espaziala, lagin zapala | Emaitzen interpretazio zaila | Matrize efektua, erreferentzia materialik ez | Lagin zapala, matrize efektua | |
| Erref. | [2-4,7,8] | [18-20] | [21,22] | [23,24] | [25,26] | [17,27] | [28] |

*N. Grijalba, F. Claverie, A. Donard , H. Tabouret, C. Pecheyran, N. Unceta, M.ªA. Goicolea, R.J. Barrio*

## 2. LASER BIDEZKO ABLAZIOAREN BILAKAERA

LA-ICPMS teknikaren bidez analisiak modu ezin hobean egiteko lau baldintza bete behar dira: i) laser-lagin elkarrekintza egonkor eta iraunkor mantendu behar da, ii) laginetik askatutako partikulen konposizioa laginaren adierazgarri izan behar du [29], iii) partikulen aerosola modu errazean garraiatu behar da masa-espektrometrora [30] eta iv) akoplamendu induktibozko plasman erabat atomizatu eta ionizatu behar dira aerosolaren osagaiak [7, 13].

Alan Gray-k, 1985. urtean [31], laser bidezko ablazioa garatu zuenetik teknikaren oinarriak ez dira asko aldatu. Hala ere, hobekuntza nabariak egin dira laser-pultsuen iraupenean eta egonkortasunean [32, 33], uhin-luzeran (UV-Vis, IR) [34, 35], laser-izpiaren bide optikoaren hobekuntzan eta aerosolaren garraioan (gas garraiatzailearen natura eta fluxua, ablazio-gelaxkaren geometria eta bolumena) [36]. Hobekuntza guztien helburua etapa kritikoetan gerta daitezkeen arazoak saihestea da: i) laginak berotzen eta hondatzen direla laserraren eta laginaren arteko elkarrekintzaren ondorioz, ii) aerosola eratzea, iii) aerosolaren garraio desegokia, eta iv) aerosolaren atomizazio/ionizazio/detekzio ez-eraginkorra masa-espektrometroan.

Laser-iturrien azken belaunaldiak, femtosegundo laserrak hain zuzen, $10^{-15}$ segundotan askatzen dute energia. Femtosegundo laserrak nanosegundo laserrak ($10^{-9}$ s) baino milioi bat aldiz azkarragoak dira. Ondorioz, laser-materia elkarrekintza eta ablazio mekanismoak erabat desberdinak dira (2. irudia). Nanosegundo laserrak eragindako efektu termikoek laginaren gainazala kaltetzen dute, laser-izpiak eragin duen gunearen inguruan

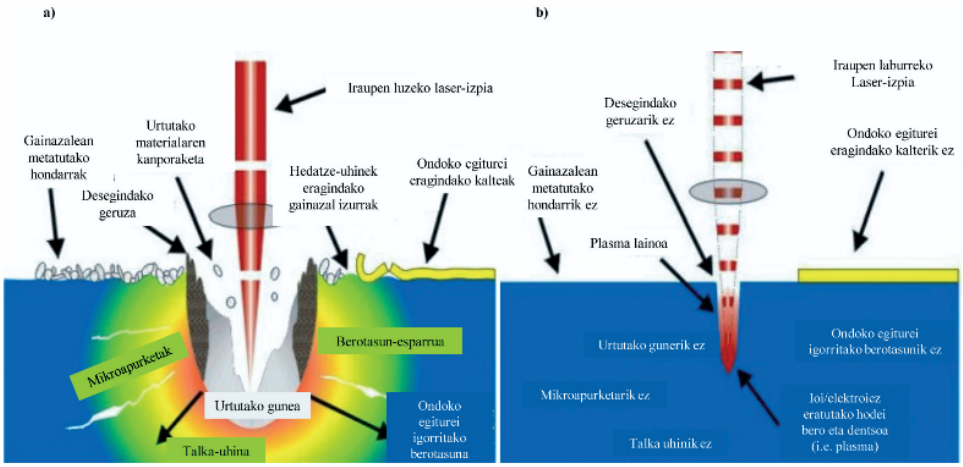


**2. irudia.** Laser-materia interakzioa a) nanosegundo laser bidezko ablazioan eta b) femtosegundo laser bidezko ablazioan (Clark-MXR, Inc.en baimenarekin erabilitako irudiak).

hondarrak metatu eta izurrak azaltzen baitira. Gainera, laser-materia elkarrekintza bortitzak tamaina handiko partikulak erauzten ditu, eta horrek aerosolaren garraioan eta atomizazio/ionizazio/detekzio prozesuetan eragina du. Femtosegundo laserrak, alabaina, efektu termiko mugatuak ditu, eta horrek ia kalterik ez egotea eta neurketaren doitasuna hobea izatea eragiten du [37-39].

Uhin-luzerak zeregin garrantzitsua jokatzen du ablazio prozesuan, laser-materia elkarrekintzan laser-izpiak laginean barneratzeko ahalmena baldintzatzen baitu. Nanosegundo ablazio sistemetan uhin-luzeraren murrizketak, infragorritik (1.064 nm) argi ultramore ikusgarrira (157-532 nm), neurketaren zehaztasuna eta errepikakortasuna hobetzen ditu. Uhin-luzeraren eragina femtosegundoko ablazio sistemetan gutxi ikertu da eta ez dago oraindik adostasunik gai honetan [40].

Masa-espektrometroan jasotako seinalea aerosolaren konposizioaren eta banaketa granulometrikoaren naturaren araberakoa da. Horregatik, arreta handia jarri behar zaio partikulen eratze prozesuari, tamainaren araberako banaketari eta konposizioari eta, azkenik, garraioaren eraginkortasunari. Ablazio-gelaxka zeharkatzen duen gas garraiatzailea oinarrizko faktorea da, ablazio prozesuan sortutako beroa disipatu eta aerosolaren homogeneotasunean eragina baitu. Askotan, helioa eta argona erabiltzen dira, baina helioa erabiltzean garraioaren eraginkortasuna hobea da, berezko propietate fisikoak (ionizazio potentziala, masa atomikoa, eroankortasun termikoa, dentsitatea) direla eta [41]. Azkenik, ablazio-gelaxkak bi baldintza bete behar ditu: batetik, aerosol osoaren garraioa ziurtatu behar du seinale/zarata ratio handia eta detekzio-muga baxuak bermatzeko; bestetik, garraioak ahalik eta azkarrena izan behar du (*wash-out time* balio txikiak) seinaleak bereizmen ona izan dezan [42].

## 3. LASER BIDEZKO ABLAZIOAREN APLIKAZIOAK

Hurrengo orrialdeetan LA-ICPMS teknikaren zenbait aplikazio laburbiltzen dira.

### 3.1. Biologia eta ingurumen-zientziak

Gizakiak planetan utzi dituen aztarnek ekosistema akuatikoen kutsadura ekarri dute. Poluitzaile kimiko ugarik (metal astunak, pestizidak, hidrokarburoak, etab.) arazo fisiologikoak eragin ditzakete organismoetan eta bere onera etortzeko mekanismoak ahuldu. Beraz, ezinbesteko lana da kutsatzaile horien presentzia ezagutzea eta naturan eragin ditzaketen desorekak ikertzea. Hortaz, organismoek ingurumen-faktoreei emandako berehalako erantzunen azterketak (egokitzapen fisiologiko eta jokaera-aldaketak) eta esposizio-markatzaileen bilaketak (ehunetan metatutako poluitzaileen

kontzentrazioa, haziera-tasa, aktibitate entzimatikoaren neurketa, etab.) berebiziko garrantzia du. Horretarako, nolanahiko izaera duten xenobiotikoak metatu eta horiei aurre egiteko gaitasuna duten organismoak dira aztergai. Europako aingira (*Anguilla anguilla, L.*) aurretik aipatutako ezaugarriak biltzen dituen kate trofikoaren goi mailako harrapakaria da, baina desagertzeko arriskuan dago (3. irudia) [43].

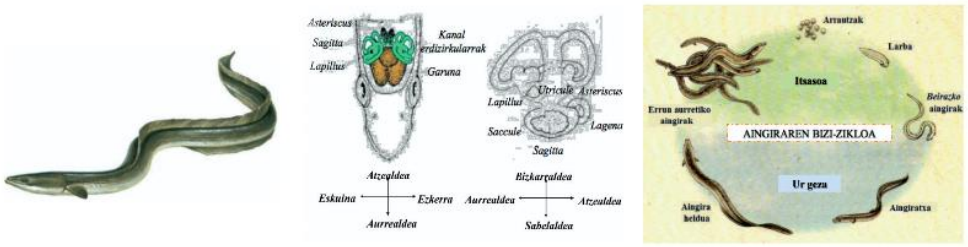


**3. irudia.** Aingira (*Anguilla anguilla, L.*) otolitoen kokalekua eta bizi-zikloa.

Izan ere, giza faktore eta baldintza natural ugarik eragin negatiboa dute aingiren populazioan. Horregatik, beharrezkoa da aingiren habitatak identifikatzea migrazio-fenomenoak hobeto ulertzeko eta aingiren populazioaren erreserbak kontrolpean izateko [44,45]. Arlo horretan, otolitoen mikrokimikaren azterketa erabilgarritasun handikoa da. Otolitoak arrain teleosteoen barne-belarrian aurki daitezkeen kaltzifikazio txikiak eta metabolikoki inerteak dira, hazierarekin batera sortzen diren eraztunez osatuak. Izan ere, eraztunak nukleotik (N) ertzera eratzen dira eta hazieraren etapa bakoitzari dagozkion markak ageri dira, itxuraldaketaren markak (MC), hain zuzen (4. irudia) [46,47]. Eraztun horiek poluitzaileak harrapatzeko eta me-

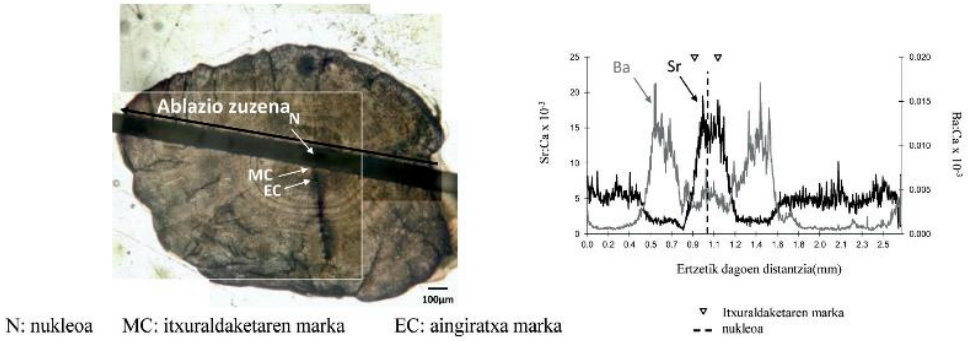


N: nukleoa MC: itxuraldaketaren marka EC: aingiratxa marka

**4. irudia.** Aingira (*Anguilla anguilla, L.*, Adour ibaia, Frantzia) otolito baten gainazalean egindako ablazio zuzena fsLA-ICPMS bidez eta lortutako seinaleak: Sr:Ca (marra beltza, ur gazian igarotako aldia) eta Ba:Ca (marra grisa, ur gezan igarotako aldia) ratioen eboluzio jarraituak aingira nomada batek izandako migrazioa erakusten du.

tatzeko ahalmena dute; hortaz, eraztunen konposizio elementala (Sr:Ca eta Ba:Ca ratioak) arrainek egin duten migrazio-bidea berregiteko baliagarria da [48,49].

Otolitoak ez ezik beste ehun batzuk erabili dira ingurumen-kutsadura aztertzeko (arrain-ezkatak [50], koralak [51] eta oskolak [52]). Ugarte eta lankideek [53], aldiz, atungorrien (*Thunnus thynnus*) eta atunzurien (*Thunnus alalunga*) bizkarraldeko hegatseko hezurrak ingurumeneko poluitzaileen bioadierazle gisa erabiltzeko prozedura analitikoa garatu dute. Bizkarraldeko hezurren konposatu nagusia hidroxiapatita ($Ca_{10}(PO_4)_6(OH)_2$) da, eta arrainaren haziera erakusten duten eraztunak dituzte. Eraztun horiek urtaroko maiztasuna dute. Udazkenean eta neguan haziera-tasa motelagoa da eta, ondorioz, eraztunak estuak eta zeharrargiak dira. Udaberrian eta udan, aldiz, baldintzak onuragarriak dira hazierarako, eta eraztunak zabalagoak eta opakoagoak dira. Haziera-banda horien eraketa eta biomineralizazioa faktore metaboliko eta ingurumen-faktoreen (klima, migrazioak, elikadura, etab.) menpe dago (5. irudia).

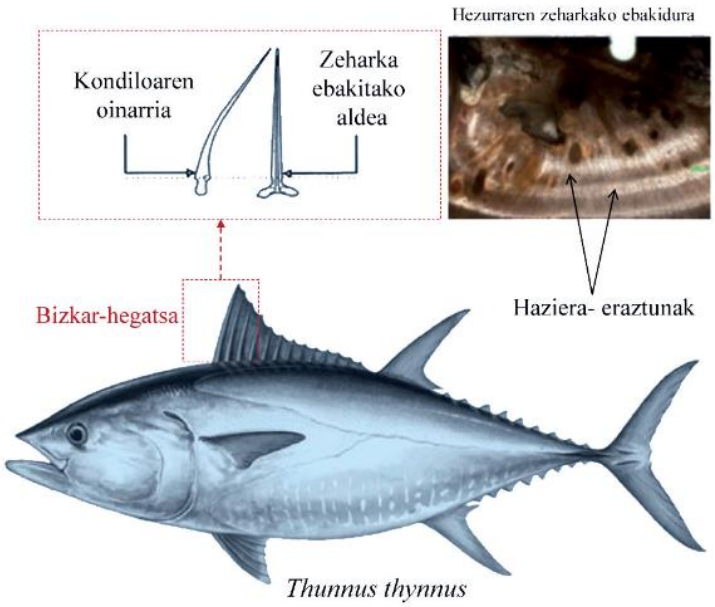


**5. irudia.** Bizkar-hegatsaren lehenengo hezurraren kokalekua eta zeharkako ebakiduraren argazkia.

Otolitoen laginen prestaketarekin konparatuz, hezurren aurretratamendua errazagoa da, arraina ez baita disekzionatu behar. Prozedura ondorengoa da [54]: aurreko bi hezurren arteko mintza ebaki egiten da eta, ondoren, lehenengo hezurra aurrera eraman eta alde batera eta bestera biratu egiten da. Behin aterata, urarekin garbitu eta lehortzen uzten da. Azkenik,

1,3 mm-ko zehar-ebakidura egiten da kondiloaren oinarritik gertu eta beirazko porta batean finkatzen da analizatzeko.

## 3.2. Osasun-zientziak

Metalek ehun biologikoen sekzio finetan duten banaketa irudikatzea edo *mapping*-a (*bioimaging*) interes biologikoa duten elementuei buruzko informazio fisiopatologikoa, farmakologikoa eta toxikologikoa eskaintzen duen erronka analitiko berria da [55,56].

Alde batetik, nerbio-sistema metal ugariren itua da. Izan ere, elementu toxikoen presentziak eta metaketak (Al, Cd, As, Cr, Pb, Tl, Hg) prozesu biologikoak kaltetu ditzakete eta heriotza eragin. Aluminioa zahartzaroko dementziaren garapenarekin erlazionatzen da, artsenikoak neuropatia periferikoak eragiten ditu eta talioak potasioa ordezkatzen du eta nerbio-sistema kolapsatzen du, besteak beste. Hori dela eta, metalek garunean duten banaketa-patroia interes handikoa da medikuntzan [57].

Bestalde, zenbait trantsizio-metal (Mn, Zn eta Cu, esaterako) ezinbestekoak dira oinarrizko funtzio fisiologikoak betetzeko. Errezeptoreen eta entzimen parte dira, eta gehienezko edo gutxienezko kontzentrazioa zenbait gaixotasun neurologikorekin erlazionatu da [58], Parkinsonekin [59-61] eta Alzheimerrarekin [62,63], adibidez. Behar-beharrezko elementu horien kantitate txikiak nahikoak dira gorputzaren nutrizio-eskakizunak asetzeko.

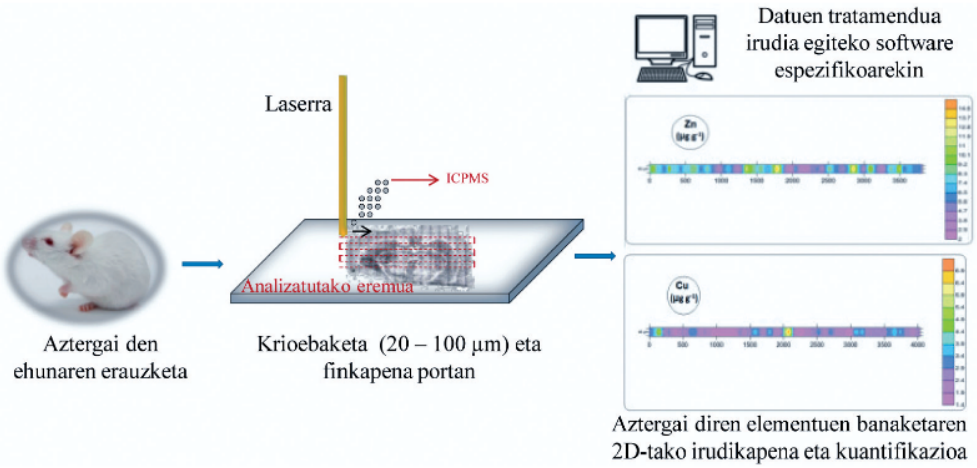


**6. irudia.** LA-ICPMS bidez mapping-a egiteko jarraitu beharreko prozedura.

Endekapenezko gaixotasunen eta gaixotasun psikiatrikoei buruzko ikerketa egiteko ez ezik, laser bidezko *mapping*-a onkologian ere erabilgarria den teknika analitikoa da. Kasu honetan, fosforoak berebiziko garrantzia du glikolisia eta azido nukleikoen sintesia bezalako prozesu biologikoetan.

Izan ere, adenosin trifosfatoaren (ATP) sintesirako eta arnasketa-katean gertatzen den fosforilazio oxidatiborako ezinbestekoa da. Tumoreek energia-eskakizun eta glikolisi-tasa handia dute [64]. Hortaz, elementu ez-metaliko horren banaketa irudikatzea lagungarria izan daiteke tamaina txikiko tumoreen diagnostiko-erreminta gisa.

Halere, metalek ehun biologikoetan duten banaketa irudikatzearen arrazoia edozein izanda, jarraitu beharreko urratsak parekoak dira kasu guztietan [65] (6. irudia). Lehendabizi, 20 eta 100 $\mu$m tarteko lodiera duten ehun sekzio finak kriotomoarekin (–20 °C) moztu eta portan finkatzen dira. Zenbait ikerlarik lagin biologikoen analisia egiteko ablazio-gelaxka kriogenikoak [66] garatu dituzte ablazio prozesua hobetzeko asmoz. Behin lagina gelaxkan dagoela, laser-izpia laginaren gainean fokatzen da eta interesekoa den eremua ablazionatu egiten da. Azkenik, *bioimaging* egiteko programen laguntzaz, datuak tratatzen dira, elementuen banaketa erakusten duten irudiak eraikitzeko.

## 3.3. **Geokimika**

Aztarna elementuen eta isotopoen determinazioek garrantzizko zeregina betetzen dute petrolio-industrian. Izan ere, agente trazatzaile gisa erabil daitezke petrolio-petrolio edo petrolio-iturburu korrelazioa ezartzeko. Nikela eta banadioa, elementu metaliko arruntenak petrolio gordinean, zabalki erabili dira petrolioaren eta petrolio-hobiaren arteko erlazioa aztertzeko eta biodegradazio maila ezagutzeko. Gainera, berunaren analisi isotopikoak petrolioaren jatorriari buruzko informazioa eskaintzen du (mantu, lurrazal edo giza jatorria) eta Renio-Osmio erlazioa geokronometro gisa erabil daiteke petrolio gordinaren kanporatze-data kalkulatzeko. Petrolioaren miaketatik aparte, metalak interes handiko aztergaiak dira petrolioaren produkzio eta fintasun prozesuan korrosioari, katalizatzaile kimikoen kutsadurari eta poluzioaren kontrolari dagokienez [67].

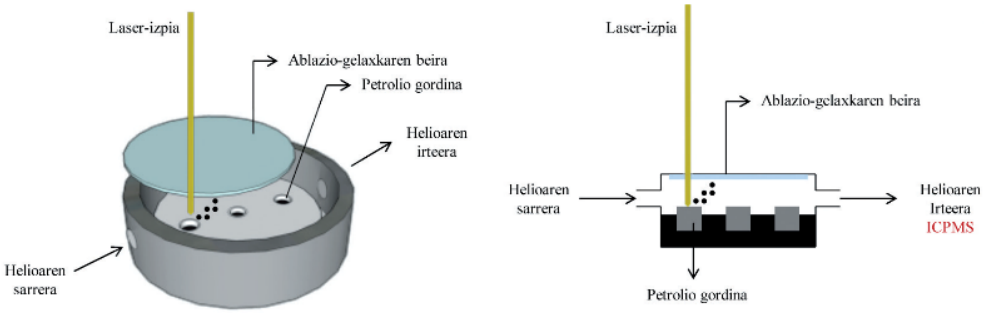


**7. irudia.** Petrolioaren ablazioaren eskema Ricard eta lankideek diseinatutako ablazio-gelaxka [65].

ICPMSa petrolioaren analisirako asko erabili den teknika da, baina, lagin organikoa izanik, analisia arretaz egitea ezinbestekoa da: alde batetik, laginaren mineralizazioa luzea, neketsua eta askotan amaigabea da; bestalde, lagina zuzenean ICPMSan sartzean plasma ezegonkortu eta itzali dezake. Gainera, plasman laginaren errekuntza egokia ez bada, karbonozko metakinak sor daitezke kono eta lenteetan eta ioien erauzketaren eraginkortasuna eta seinalearen intentsitatea murriztu [68,69].

Laser bidezko ablazioa lagin likido organikoen analisirako berriki erabilitako etorkizun handiko teknika da (7. irudia). Halere, teknika honek zenbait eragozpen baditu, besteak beste, petrolio-zipriztinek ablazio-kamera zikindu dezakete eta petrolio-metakinek LA-ICPMS transferentzia sistema blokea dezakete. Arazo horiei irtenbidea emateko ablazio-angelua aldatu edo zelulosa ehun batean absorbatutako lagina ablaziona daiteke [70].

## 3.4. **Auzitegiko ikerketa**

### 3.4.1. *Tiro-aztarnen identifikazioa*

Su-armen erabilpena modu kezkagarrian igo da gure gizartean eta horrek tiro egin ondoren sortutako partikulen analisirako metodologia analitiko berriak garatzea ekarri du. Tiro-aztarnak (*gunshot residue, GSR*) arma kliskatu bezain azkar eta munizioaren errekuntza prozesuaren ondorioz sortutako partikula sorta da [71,72]. Krimen agertokian tiro-aztarnak osatzen dituzten konposatuen detekzioak eta identifikazioak su-armen erabileraren ebidentzia fidagarria eskaintzen du. Hala ere, auzitegi-analisiaren ikuspuntutik, su-arma bat ustez kliskatu duen pertsona baten identifikazioa argitzeko, ezinbestekoa da bere gorputzean aurki daitezkeen tiro-aztarnak ziurtasun osoz identifikatzea [73].

Gaur egun, auzitegiaren ikuspuntutik baliagarria den teknika analitiko bakarra da X izpien energia dispertsiboaren espektroskopiari akoplatutako ekorketa bidezko mikroskopia elektronikoa (SEM-EDX). Teknika horrek partikulen morfologia eta konposizio ez-organikoari buruzko aldibereko informazioa eskaintzen du. Hala ere, teknika horrek baditu zenbait desabantaila: analisi-denbora luzea (8 eta 10 ordu artean) eta laginketa-dispositiboan itsatsita gera daitezkeen azal, ile eta besteek partikulen bana-banako identifikazioa oztopa dezakete [74,75].

Hori dela eta, Abrego eta lankideek [76,77] tiro-partikulen zalantzarik gabeko identifikazioa egiteko LA-ICPMS teknikan oinarritutako metodoa garatu dute, laginaren aurretratamendurik behar ez duena eta analisi-denbora nabarmenki murrizten duena (66 min), eta horrela, SEM-EDX teknikak dituen desabantailak gainditu. Metodo horretan, tiro-aztarnen laginketarako karbonozko zinta itsaskorra erabiltzen da eta laserra gainazaletik

abiadura jakin batekin desplazatzen da, sigi-saga erako patroi bat jarraituz. ICPMSan analizatzean denborarekiko aldakorra den seinalearen erregistro bat lortzen da. Tiro-aztarnen partikula bereizgarriak (Pb-Sb-Ba) baldin badaude, hiru elementu horien seinaleak aldi berean agertu behar dira (8. irudia).

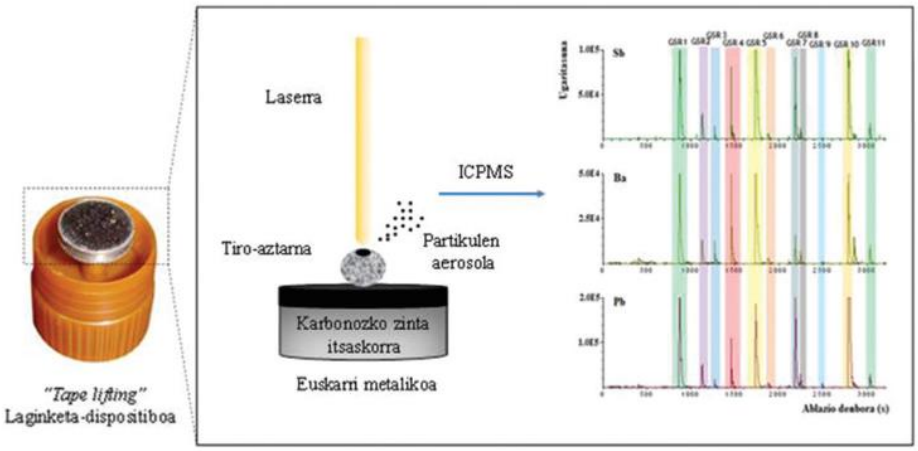


**8. irudia.** Laser-izpiak tiro-aztarnaren gain eragin eta materia erauzten du. Ondoren, ICPMS detektagailuan denborarekin aldakorra den seinalearen erregistroa lortzen da. Sb, Ba eta Pb elementuen seinaleen aldibereko erregistroak partikula tiro-aztarna bati dagokiola egiaztatzen du.

### 3.4.2. *Material nuklearraren trafikoaren aurkako borroka*

1990. urteaz geroztik material nuklearraren legez kanpoko trafikoa areagotu egin da eta *auzitegi-zientzia nuklearra* deritzon zientzia analitikoaren sorreran lagundu du. Auzitegi-zientzia nuklearrak konfiskatutako material nuklear ez-legalari buruzko informazioa (jatorria eta erabilera-asmoa) eskaintzea du helburu. Informazio horrek berebiziko garrantzia du segurtasun nuklearra sustatzeko eta galerak edo lapurretak saihesteko [78,79]. Uranio-mea kontzentratua meategian bertan egindako aurrearazketa prozesuaren ondoren lortzen da eta, ondoren, instalazio nuklearretara garraiatzen da kontzentrazio prozesuarekin jarraitzeko. Uranioaren konposizio isotopikoa desberdina da ondoren izango duen erabileraren arabera (9. irudia). Ondorioz, markatzaileen identifikazioa beharrezkoa da material nuklearraren trazabilitatearen jarraipena egiteko [80]. Hori dela eta, gaiari buruz adituak direnek (*JRC Institute for Transuranium Elements*, JRC-ITU) funtsezkoak diren parametroen identifikazioaren eta ezarpenaren garrantzia azpimarratzen dute behin eta berriz [81].

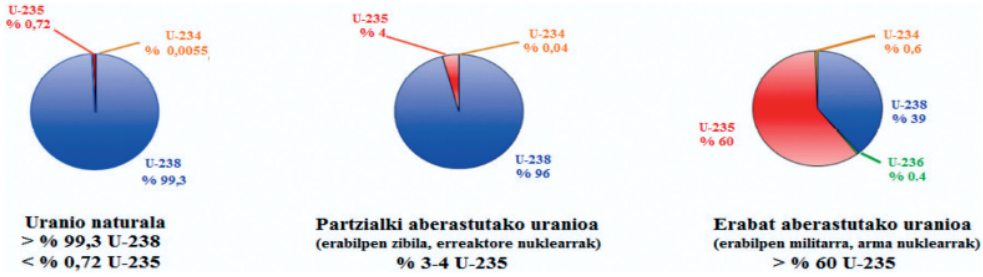


**9. irudia.** Uranioaren konposizio isotopikoa erabileraren arabera.

Konfiskatutako material nuklearraren karakterizazio kimikoa egiteko giza aktibitateen aztarnak (fisiko zein kimikoak) edo erradiazio parametroak ikertzen dira. Adierazle guztien artean, lur arraroek (eskandioa (Sc), itrioa (Y), lantanidoak eta aktinidoak) oreetan duten banaketa aukera interesgarria da iturburua zehazteko, banaketa-patroiak mineralizazio prozesuarekin eta baldintza geologikoekin erlazio zuzena baitu. Elementu horiek mineralaren formazio prozesuan eransten dira eta banaketak egonkor irauten du mearen kontzentrazio-urratsean [82].

Auzitegiko zientzia nuklearraren eremuan eskuragai dagoen lagin-kantitatea arazoa da maiz. Gainera, azpilaginketak egitea beharrezkoa da analisi mota desberdinak egiteko eta, zoritxarrez, lagina berreskuratzea ahalbidetzen ez duten teknika analitiko suntsikorrak erabili ohi dira (laginaren mineralizazioa eta diluzioa, prezipitazio eta erauzketa, etab) [83]. LA-ICPMSaren erabilpenak, alabaina, nabarmen murrizten du analisian erabili beharreko lagin-kantitatea.

Beraz, LA-ICPMS teknikarekin egindako analisiak azkarrak eta errazak dira eta, gainera, analitoek laginean duten banaketari buruzko informazio espaziala ere eskaintzen du. Hau da, ore-nahasketa batean, analisia tamaina txikiko ($\mu$m) partikula mailan egiteak iturburu desberdinak bereiztea ahalbidetzen du. Hori ezinezkoa izango litzateke ohizko analisi-teknikekin, zeinetan lagina bere osotasunean analizatzen den.

## 4. ONDORIO OROKORRAK

Laser bidezko ablazioa (LA) bi aplikazio alorretan erabiltzen da bereziki. Alde batetik, lagina osotasunean analizatu eta bereizmen espazial txikiko beharra duten (80-150 $\mu$m-ko zulotxo diametroa) aplikazioetan eta bestetik, bereizmen espazial handia behar dutenetan. Laginetik erauzitako materia-kantitate txikia dela eta, sentikortasun handiko masa-espektrometroak behar dira. Laser bidezko ablazioa eta akoplamendu induktibozko plasma-masa espektrometriaren konbinazioa erakargarria da, sentikorta-

sun handia eta abian jartzeko erraztasuna direla eta. Hortaz, laser bidezko ablazioa solidoen analisi zuzena egiteko, azken urteotan sakonki ikertu eta hobetu den laginketa-teknika da eta, gaur egun, erreferentziazko teknika gisa erabiltzen da laborategietan eguneroko lagin solidoen analisia egiteko.

## 5. ESKER ONAK

Egileek Eusko Jaurlaritzako Hezkuntza, Hizkuntza Politika eta Kultura Sailari Euskal Unibertsitate Sistemako ikerketa-taldeen jarduera bultzatzeko diru-laguntza eskertzen diote (METABOLOMIPs taldea GIC10/25). Nagore Grijalbak Université de Pau et Des Pays de L'Adourri (UPPA) eta Euskal Herriko Unibertsitateari (UPV/EHU) tutorekidetza erregimenean doktorego-tesia egiteko diru-laguntza eskertzen die.

## 6. BIBLIOGRAFIA

[1] FERNÁNDEZ, B.; CLAVERIE, F.; PÉCHEYRAN, C. eta DONARD, O.F.X. 2007. «Direct analysis of solid samples by fs-LA-ICP-MS». TrAC Trends in Analytical Chemistry, 26, 951-966.

[2] KOCH, J. eta GUNTHER, D. 2011. «Review of the state-of-the-art of laser ablation inductively coupled plasma mass spectrometry». Applied Spectroscopy, 65, 155-62.

[3] RUSSO, R.E.; MAO, X.; LIU, H.; GONZALEZ, J. eta MAO, S.S. 2002. «Laser ablation in analytical chemistry—a review». Talanta, 57, 425-451.

[4] VOELLKOPF, U.; PAUL, M. eta DENOYER, E.R. 1992. «Analysis of solid samples by ICP-mass spectrometry». Fresenius' Journal of Analytical Chemistry, 342, 917-923.

[5] KOSLER, J.; WIEDENBECK, M.; WIRTH, R.; HOVORKA, J.; SYLVESTER, P. eta MIKOVA, J. 2005. «Chemical and phase composition of particles produced by laser ablation of silicate glass and zircon-implications for elemental fractionation during ICP-MS analysis». Journal of Analytical Atomic Spectrometry, 20, 402-409.

[6] GUNTHER, D.; HORN, I. eta HATTENDORF, B. 2000. «Recent trends and developments in laser ablation-ICP-mass spectrometry». Fresenius J Anal Chem, 368, 4-14.

[7] HATTENDORF, B.; LATKOCZY, C. eta GÜNTHER, D. 2003. «Peer Reviewed: Laser Ablation-ICPMS». Analytical Chemistry, 75, 341 A-347 A.

[8] WATLING, R.J.; F. LYNCH, B. eta HERRING, D. 1997. «Use of Laser Ablation Inductively Coupled Plasma Mass Spectrometry for Fingerprinting Scene of Crime Evidence». Journal of Analytical Atomic Spectrometry, 12, 195-203.

[9] TREJOS, T.; MONTERO, S. eta ALMIRALL, J.R. 2003. «Analysis and comparison of glass fragments by laser ablation inductively coupled plasma mass spectrometry (LA-ICP-MS) and ICP-MS». Anal Bioanal Chem, 376, 1255-64.

[10] DURRANT, S.F. eta WARD, N.I. 2005. «Recent biological and environmental applications of laser ablation inductively coupled plasma mass spectrometry (LA-ICP-MS)». Journal of Analytical Atomic Spectrometry, 20, 821-829.

[11] LIU, Y.; HU, Z.; LI, M. eta GAO, S. 2013. «Applications of LA-ICP-MS in the elemental analyses of geological samples». Chinese Science Bulletin, 58, 3863-3878.

[12] NEFF, H. 2012. «Laser Ablation ICP-MS in Archaeology». Mass Spectrometry Handbook. John Wiley & Sons, Inc.

[13] KUHN, H.R. eta GUNTHER, D. 2003. «Elemental fractionation studies in laser ablation inductively coupled plasma mass spectrometry on laser-induced brass aerosols». Analytical Chemistry, 75, 747-53.

[14] LOEWEN, M.W. eta KENT, A.J.R. 2012. «Sources of elemental fractionation and uncertainty during the analysis of semi-volatile metals in silicate glasses using LA-ICP-MS». Journal of Analytical Atomic Spectrometry, 27, 1502-1508.

[15] RUSSO, R.E.; MAO, X.L.; LIU, C. eta GONZALEZ, J. 2004. «Laser assisted plasma spectrochemistry: laser ablation». Journal of Analytical Atomic Spectrometry, 19, 1084-1089.

[16] BECKER, J.S. 2002. «Applications of inductively coupled plasma mass spectrometry and laser ablation inductively coupled plasma mass spectrometry in materials science». Spectrochimica Acta Part B: Atomic Spectroscopy, 57, 1805-1820.

[17] BECKER, J.S. eta DIETZE, H.J. 2000. «Inorganic mass spectrometric methods for trace, ultratrace, isotope, and surface analysis1». International Journal of Mass Spectrometry, 197, 1-35.

[18] HAHN, D.W. eta OMENETTO, N. 2010. «Laser-induced breakdown spectroscopy (LIBS), part I: review of basic diagnostics and plasma-particle interactions: still-challenging issues within the analytical plasma community». Appl Spectrosc, 64, 335-66.

[19] HAHN, D.W. eta OMENETTO, N. 2012. «Laser-induced breakdown spectroscopy (LIBS), part II: review of instrumental and methodological approaches to material analysis and applications to different fields». Appl Spectrosc, 66, 347-419.

[20] PAPAZOGLOU, D.G.; PAPADAKIS, V. eta ANGLOS, D. 2004. «In situ interferometric depth and topography monitoring in LIBS elemental profiling of multi-layer structures». Journal of Analytical Atomic Spectrometry, 19, 483-488.

[21] PISONERO, J.; FERNÁNDEZ, B.; PEREIRO, R.; BORDEL, N. eta SANZ-MEDEL, A. 2006. «Glow-discharge spectrometry for direct analysis of thin and ultra-thin solid films». TrAC Trends in Analytical Chemistry, 25, 11-18.

[22] SANDERSON, N.E.; HALL, E.; CLARK, J.; CHARALAMBOUS, P. eta HALL, D. «Glow discharge mass spectrometry-a powerful technique for the elemental analysis of solids». Microchimica Acta, 91, 275-290.

[23] RENIERS, F. eta TEWELL, C. 2005. «New improvements in energy and spatial (x, y, z) resolution in AES and XPS applications». Journal of Electron Spectroscopy and Related Phenomena, 142, 1-25.

[24] WATTS, J.F. eta WOLSTENHOLME, J. 2003. «Electron Spectroscopy: Some Basic Concepts». An Introduction to Surface Analysis by XPS and AES. John Wiley & Sons, Ltd,

[25] TSUJI, K.; NAKANO, K.; TAKAHASHI, Y.; HAYASHI, K. eta RO, C.-U. 2012. «X-ray Spectrometry». Analytical Chemistry, 84, 636-668.

[26] WEST, M.; ELLIS, A.T.; POTTS, P.J.; STRELI, C.; VANHOOF, C. eta WOBRAUSCHEK, P. 2014. «Atomic Spectrometry Update - a review of advances in X-ray fluorescence spectrometry». Journal of Analytical Atomic Spectrometry, 29, 1516-1563.

[27] WILLIAMS, P. 1985. «Secondary Ion Mass Spectrometry». Annual Review of Materials Science, 15, 517-548.

[28] HERRMANN, A.M.; RITZ, K.; NUNAN, N.; CLODE, P.L.; PETT-RIDGE, J.; KILBURN, M.R.; MURPHY, D.V.; O'DONNELL, A.G. eta STOCKDALE, E.A. 2007. «Nano-scale secondary ion mass spectrometry — A new analytical tool in biogeochemistry and soil ecology: A review article». Soil Biology and Biochemistry, 39, 1835-1850.

[29] FIGG, D. eta KAHR, M.S. 1997. «Elemental Fractionation of Glass Using Laser Ablation Inductively Coupled Plasma Mass Spectrometry». Applied Spectroscopy, 51, 1185-1192.

[30] FIGG, D.J.; CROSS, J.B. eta BRINK, C. 1998. «More investigations into elemental fractionation resulting from laser ablation–inductively coupled plasma–mass spectrometry on glass samples». Applied Surface Science, 127-129, 287-291.

[31] GRAY, A.L. 1985. «Solid sample introduction by laser ablation for inductively coupled plasma source mass spectrometry». Analyst, 110, 551-556.

[32] MARGETIC, V.; PAKULEV, A.; STOCKHAUS, A.; BOLSHOV, M.; NIEMAX, K. eta HERGENRÖDER, R. 2000. «A comparison of nanosecond and femtosecond laser-induced plasma spectroscopy of brass samples». Spectrochimica Acta Part B: Atomic Spectroscopy, 55, 1771-1785.

[33] MOZNA, V.; PISONERO, J.; HOLA, M.; KANICKY, V. eta GUNTHER, D. 2006. «Quantitative analysis of Fe-based samples using ultraviolet nanosecond and femtosecond laser ablation-ICP-MS». Journal of Analytical Atomic Spectrometry, 21, 1194-1201.

[34] GÜNTHER, D. eta HATTENDORF, B. 2005. «Solid sample analysis using laser ablation inductively coupled plasma mass spectrometry». TrAC Trends in Analytical Chemistry, 24, 255-265.

[35] KOCH, J.; VON BOHLEN, A.; HERGENRODER, R. eta NIEMAX, K. 2004. «Particle size distributions and compositions of aerosols produced by

near-IR femto- and nanosecond laser ablation of brass». Journal of Analytical Atomic Spectrometry, 19, 267-272.

[36] WANG, Z.; HATTENDORF, B. eta GÜNTHER, D. 2006. «Analyte Response in Laser Ablation Inductively Coupled Plasma Mass Spectrometry». Journal of the American Society for Mass Spectrometry, 17, 641-651.

[37] HERGENRODER, R.; SAMEK, O. eta HOMMES, V. 2006. «Femtosecond laser ablation elemental mass spectrometry». Mass Spectrometry Reviews, 25, 551-72.

[38] DONARD, C.P.A.S.C.A.P.C.A.E.M.A.O.F.X. 2007. «High repetition rate and low energy femtosecond laser ablation coupled to ICPMS detection: a new analytical approach for trace element determination in solid samples». Journal of Physics: Conference Series, 59, 112.

[39] GONZALEZ, J.J.; OROPEZA, D.; MAO, X. eta RUSSO, R.E. 2008. «Assessment of the precision and accuracy of thorium (232Th) and uranium (238U) measured by quadrupole based inductively coupled plasma-mass spectrometry using liquid nebulization, nanosecond and femtosecond laser ablation». Journal of Analytical Atomic Spectrometry, 23, 229-234.

[40] KOCH, J. eta GUNTHER, D. 2007. «Femtosecond laser ablation inductively coupled plasma mass spectrometry: achievements and remaining problems». Analytical and Bioanalytical Chemistry, 387, 149-53.

[41] HORN, I. eta GÜNTHER, D. 2003. «The influence of ablation carrier gasses Ar, He and Ne on the particle size distribution and transport efficiencies of laser ablation-induced aerosols: implications for LA-ICP-MS». Applied Surface Science, 207, 144-157.

[42] ARROWSMITH, P. eta HUGHES, S.K. 1988. «Entrainment and Transport of Laser Ablated Plumes for Subsequent Elemental Analysis». Applied Spectroscopy, 42, 1231-1239.

[43] TESCH, F.W. eta THORPE, J.E. 2003. «Harvest and Environmental Relationships». The Eel. Blackwell Science Ltd., New Jersey.

[44] ARAI, T. eta HIRATA, T. 2006. «Differences in the Trace Element Deposition in Otoliths Between Marine- and Freshwater-resident Japanese Eels, Anguilla japonica, as Determined by Laser Ablation ICPMS». Environmental Biology of Fishes, 75, 173-182.

[45] TESCH, F.W. eta THORPE, J.E. 2003. «Post-Larval Ecology and Behaviour». The Eel. Blackwell Science Ltd., New Jersey.

[46] CAMPANA, S.E. eta THORROLD, S.R. 2001. «Otoliths, increments, and elements: keys to a comprehensive understanding of fish populations?» Canadian Journal of Fisheries and Aquatic Sciences, 58, 30-38.

[47] TESCH, F.W. eta THORPE, J.E. 2003. «Developmental Stages and Distribution of the Eel Species». The Eel. Blackwell Science Ltd., New Jersey.

[48] KENNEDY, B.P.; KLAUE, A.; BLUM, J.D.; FOLT, C.L. eta NISLOW, K.H. 2002. «Reconstructing the lives of fish using Sr isotopes in otoliths». Canadian Journal of Fisheries and Aquatic Sciences, 59, 925-929.

[49] TABOURET, H.; BAREILLE, G.; CLAVERIE, F.; PECHEYRAN, C.; PROUZET, P. eta DONARD, O.F. 2010. «Simultaneous use of strontium:calcium and barium:calcium ratios in otoliths as markers of habitat: application to the European eel (Anguilla anguilla) in the Adour basin, South West France». Marine Environmental Research, 70, 35-45.

[50] HOLÁ, M.; KALVODA, J.; BÁBEK, O.; BRZOBOHATÝ, R.; HOLOUBEK, I.; KANICKÝ, V. eta SKODA, R. 2008. «LA-ICP-MS heavy metal analyses of fish scales from sediments of the Oxbow Lake Certak of the Morava River (Czech Republic)». Environmental Geology, 58, 141-151.

[51] MCCULLOCH, M.; FALLON, S.; WYNDHAM, T.; HENDY, E.; LOUGH, J. eta BARNES, D. 2003. «Coral record of increased sediment flux to the inner Great Barrier Reef since European settlement». Nature, 421, 727.

[52] BARATS, A.; PÉCHEYRAN, C.; AMOUROUX, D.; DUBASCOUX, S.; CHAUVAUD, L. eta DONARD, O.F.X. 2007. «Matrix-matched quantitative analysis of trace-elements in calcium carbonate shells by laser-ablation ICP-MS: application to the determination of daily scale profiles in scallop shell (Pecten maximus)». Analytical and Bioanalytical Chemistry, 387, 1131-1140.

[53] UGARTE, A.; UNCETA, N.; PECHEYRAN, C.; GOICOLEA, M.A. eta BARRIO, R.J. 2011. «Development of matrix-matching hydroxyapatite calibration standards for quantitative multi-element LA-ICP-MS analysis: application to the dorsal spine of fish». Journal of Analytical Atomic Spectrometry, 26, 1421-1427.

[54] RUIZ, M.; RODRÍGUEZ-MARÍN, E. eta LANDA, J. Protocol for sampling of hard parts for bluefin tuna (Thunnus tuna) growth studies. Spain, Instituto Español de Oceanografía. Centro Oceanográfico de Santander.

[55] BECKER, J.S. 2010. «Imaging of metals, metalloids, and non-metals by laser ablation inductively coupled plasma mass spectrometry (LA-ICP-MS) in biological tissues». Methods in Molecular Biology, 656, 51-82.

[56] BECKER, J.S.; ZORIY, M.; BECKER, J.S.; DOBROWOLSKA, J.; DEHNHARDT, M. eta MATUSCH, A. 2007. «Elemental imaging mass spectrometry of thin sections of tissues and analysis of brain proteins in gels by laser ablation inductively coupled plasma mass spectrometry». Physica Status Solidi (c), 4, 1775-1784.

[57] CLARKSON, T.W. 1987. «Metal toxicity in the central nervous system». Environmental Health Perspectives, 75, 59-64.

[58] GAETA, A. eta HIDER, R.C. 2005. «The crucial role of metal ions in neurodegeneration: the basis for a promising therapeutic strategy». British Journal of Pharmacology, 146, 1041-59.

[59] ASCHNER, M.; ERIKSON, K.M.; HERRERO HERNANDEZ, E. eta TJALKENS, R. 2009. «Manganese and its role in Parkinson's disease: from transport to neuropathology». Neuromolecular Medicine, 11, 252-66.

[60] GUILARTE, T.R. 2010. «Manganese and Parkinson's disease: a critical review and new findings». Environmental Health Perspectives, 118, 1071-80.

[61] OLANOW, C.W. 2004. «Manganese-induced parkinsonism and Parkinson's disease». Annals of the New York Academy of Science, 1012, 209-23.

[62] BUSH, A.I. 2013. «The metal theory of Alzheimer's disease». Journal of Alzheimer's Disease, 33 Suppl 1, S277-81.

[63] SCHRAG, M.; MUELLER, C.; OYOYO, U.; SMITH, M.A. eta KIRSCH, W.M. 2011. «Iron, zinc and copper in the Alzheimer's disease brain: a quantitative meta-analysis. Some insight on the influence of citation bias on scientific opinion». Progress in Neurobiology, 94, 296-306.

[64] BECKER, J.S.; ZORIY, M.V.; DEHNHARDT, M.; PICKHARDT, C. eta ZILLES, K. 2005. «Copper, zinc, phosphorus and sulfur distribution in thin section of rat brain tissues measured by laser ablation inductively coupled plasma mass spectrometry: possibility for small-size tumor analysis». Journal of Analytical Atomic Spectrometry, 20, 912-917.

[65] BECKER, J.S.; ZORIY, M.; BECKER, J.S.; DOBROWOLSKA, J. eta MATUSCH, A. 2007. «Laser ablation inductively coupled plasma mass spectrometry (LA-ICP-MS) in elemental imaging of biological tissues and in proteomics». Journal of Analytical Atomic Spectrometry, 22, 736-744.

[66] FELDMANN, J.; KINDNESS, A. eta EK, P. 2002. «Laser ablation of soft tissue using a cryogenically cooled ablation cell». Journal of Analytical Atomic Spectrometry, 17, 813-818.

[67] RICARD, E.; PECHEYRAN, C.; SANABRIA ORTEGA, G.; PRINZHOFER, A. eta DONARD, O.F. 2011. « Direct analysis of trace elements in crude oils by high-repetition-rate femtosecond laser ablation coupled to ICPMS detection «. Analytical and Bioanalytical Chemistry, 399, 2153-2165.

[68] HAUSLER, D. 1987. «Trace element analysis of organic solutions using inductively coupled plasma-mass spectrometry». Spectrochimica Acta Part B: Atomic Spectroscopy, 42, 63-73.

[69] HUTTON, R.C. 1986. «Application of inductively coupled plasma source mass spectrometry (ICP-MS) to the determination of trace metals in organics». Journal of Analytical Atomic Spectrometry, 1, 259-263.

[70] FICHET, P.; MAUCHIEN, P.; WAGNER, J.-F. eta MOULIN, C. 2001. «Quantitative elemental determination in water and oil by laser induced breakdown spectroscopy». Analytica Chimica Acta, 429, 269-278.

[71] DALBY, O.; BUTLER, D. eta BIRKETT, J.W. 2010. «Analysis of gunshot residue and associated materials--a review». Journal of Forensic Science, 55, 924-43.

[72] SAVERIO ROMOLO, F. eta MARGOT, P. 2001. «Identification of gunshot residue: a critical review». Forensic Science International, 119, 195-211.

[73] CHANG, K.H.; JAYAPRAKASH, P.T.; YEW, C.H. eta ABDULLAH, A.F.L. 2013. «Gunshot residue analysis and its evidential values: a review». Australian Journal of Forensic Sciences, 45, 3-23.

[74] ZEICHNER, A. 2001. «Is there a real danger of concealing gunshot residue (GSR) particles by skin debris using the tape-lift method for sampling GSR from hands?» Journal of Forensic Science, 46, 1447-55.

[75] ZEICHNER, A. 2003. «Recent developments in methods of chemical analysis in investigations of firearm-related events». Analytical and Bioanalytical Chemistry, 376, 1178-1191.

[76] ABREGO, Z.; GRIJALBA, N.; UNCETA, N.; MAGUREGUI, M.; SANCHEZ, A.; FERNANDEZ-ISLA, A.; GOICOLEA, M.A. eta BARRIO, R.J. 2014. «A novel method for the identification of inorganic and organic gunshot residue particles of lead-free ammunitions from the hands of shooters using scanning laser ablation-ICPMS and Raman micro-spectroscopy». Analyst, 139, 6232-41.

[77] ABREGO, Z.; UGARTE, A.; UNCETA, N.; FERNANDEZ-ISLA, A.; GOICOLEA, M.A. eta BARRIO, R.J. 2012. «Unambiguous characterization of gunshot residue particles using scanning laser ablation and inductively coupled plasma-mass spectrometry». Analytical Chemistry, 84, 2402-9.

[78] MAYER, K.; WALLENIUS, M. eta FANGHÄNEL, T. 2007. «Nuclear forensic science—From cradle to maturity». Journal of Alloys and Compounds, 444-445, 50-56.

[79] MAYER, K.; WALLENIUS, M. eta RAY, I. 2005. «Nuclear forensics-a methodology providing clues on the origin of illicitly trafficked nuclear materials». Analyst, 130, 433-441.

[80] DONARD, A.; POTTIN, A.C.; POINTURIER, F. eta PECHEYRAN, C. 2015. «Determination of relative rare earth element distributions in very small quantities of uranium ore concentrates using femtosecond UV laser ablation - SF-ICP-MS coupling». Journal of Analytical Atomic Spectrometry, 30, 2420-2428.

[81] MAYER, K.; WALLENIUS, M. eta VARGA, Z. 2013. «Nuclear Forensic Science: Correlating Measurable Material Parameters to the History of Nuclear Material». Chemical Reviews, 113, 884-900.

[82] VARGA, Z.; WALLENIUS, M. eta MAYER, K. 2010. «Origin assessment of uranium ore concentrates based on their rare-earth elemental impurity pattern». Radiochimica Acta, 98, 771-778.

[83] KRAJKO, J.; VARGA, Z.; WALLENIUS, M. eta MAYER, K. 2015. «Development of a versatile sample preparation method and its application for rare-earth pattern and Nd isotope ratio analysis in nuclear forensics». Journal of Radioanalytical and Nuclear Chemistry, 304, 177-181.

# CHAPTER 4:

# Development of a new ablation cell adjustable to different bottle shapes

## 1. Ablation cells for laser ablation-inductively coupled plasma-mass spectrometry

Nowadays, laser ablation inductively coupled plasma-mass spectrometry (LA-ICPMS) is a widely used analytical tool for the analysis of solid samples. Direct solid micro-analysis has been successfully employed in several areas and a wide range of applications have been developed, e.g. forensic, art and cultural heritage, biology, geochemistry and material science. Laser ablation allows quick and easy sampling without much sample preparation. However, it is currently limited by the size of the samples that could be analyzed as the sample is usually placed in an airtight ablation cell. This cell is flushed with a carrier gas (He or Ar) to avoid the intrusion of atmospheric gases into the central plasma channel, especially oxygen and nitrogen that can make an ICP unstable, leading to the extinction of the plasma and enhancing the abundance of unwanted molecular ions (1). Additionally, due to relatively low thermal conductivity of the air, larger particles can be formed in the ablated aerosol through condensation/agglomeration processes which can result in both inefficient particle processing within the plasma (lower sensitivity) and elemental fractionation (2). Nonetheless, the need to find viable alternatives for the direct ablation of any sample, regardless of its size, made popular the idea of developing new ablation cell designs.

By the middle of the 80s, there was an increased interest in direct solid sampling and the design of ablation cells was widely studied. The optimum construction of ablation cells should allow its use irrespective of the particular size or the shape of the samples and be insensitive to sample surface irregularity (3). Therefore, it can be stated that during laser ablation coupled to ICPMS, the ablation cell plays a crucial role because i) it has to guarantee a *quantitative transport* of the laser-induced aerosol and ii) lead to a *rapid transport* from the ablation site to the plasma source (Figure 1). Quantitative transport means that the ablation cell must assure mass conservation and minimize aerosol loss as it is important for obtaining high signal-to-noise ratios, low detection limits as well as for avoiding biased particle transport, which would lead to elemental fractionation (4).

The potential source responsible for mass losses during the aerosol transport is the particle size distribution, which is mainly related with the laser-matter interaction previously described in Chapter 3. The biggest particles are subjected to inertia loss whereas the thinner particles are subjected to diffusion losses. Inertia loss means that particles whose diameter is bigger than few microns can be deposited on the surface of the sample, and in a lesser extent on the walls of the ablation chamber and in the transfer line carrying the aerosol until the ICP source (5).

Meanwhile, rapid aerosol transport has strong influence in the minimization of signal dispersion signal, particle residence time in the ablation cell and particle-particle or particle-wall reaction (6). The main strategy to minimize sample dispersion is the confinement of the particles (through gas flows, pressure or cell walls) forming a controlled environment less than few $cm^3$ in volume and preventing further expansion of the ablation plume inside the cavity of the chamber (7). Therefore, the cell design, including the cell volume and shape, places great importance to avoid difficulties with sample transport and excessive long wash-out and wash-out times. The air flow topology will determine, in fact, the wash-out time and the peak width of the detected signals. While the laminar gas flow moves particle directly to the outlet, the turbulent flow spread them over the chamber volume (4). In general terms, small ablation cells are preferred as large volume cells could have a negative influence in the recorded signal due to a non-straightforward and turbulent gas circulation. In addition, increased volumes induce aerosol loss by gravitation in regions of low flush efficiency. However, in very small ablation cells, reactions between the aerosol and the wall may limit the transportation efficiency (8). Regarding the shape of ablation cells, the suppression of vertexes minimizes the wash-out times considerably due to a reduction of the turbulent gas flow and consequently particles will not flow chaotically following the flow-lines of the vortexes. The transfer line length and diameter have been also widely investigated for their role in the transportation of particles and specific signal structures. Transfer tube volume had been showed to have a modest but linear influence on the signal dispersion. The major loss mechanism appears to be gravitational deposition of relatively large particles formed during ablation and possibly by coalescence within the transfer tube (9).

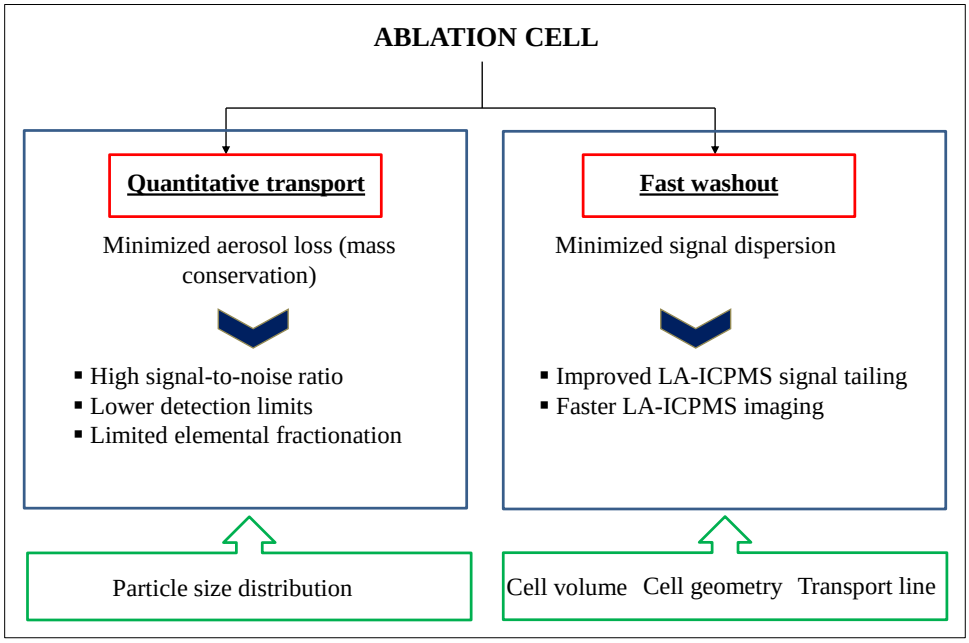


**Figure 1** Design of an ablation cell: factors to take into account.

The different ablation cells can be schematically divided into two groups: *closed design* and *open design* ablation cells (10).

**Closed designs cells** are the most conventional "box-like" cells which enclose the entire sample in an inert environment. This is the most widely used ablation cell type. In fact, Alan Gray (11) employed a 130 $cm^3$ cylindrical closed sample cell with inlet and outlet at different levels and movable sample stage to match the sample surface position with the gas inlet level. The advantage of these cells is that the sample does not need to be previously polished and also reduce the risk of gas leaks. However, these ablation cells have disadvantages such as specific size restrictions, less reproducible sampling positions and increased cell volume, which enhances sample dilution and the possibility of aerosol loss by gravitation in regions of low flush efficiency. Several designs have been developed as concern on the carrier gas flow dynamics became an important issue, beyond mere sample holding requirements. Table 1 shows a list of closed laser ablation cells in the literature and their most remarkable characteristics.

**Table 1.** Closed laser ablation cells and aerosol transport characteristic simulations in the literature.

| Characteristic | Author and year | Ref |
|---|---|---|
| Cylindrical closed cell with different in-/outlet levels | Gray, 1985 | (11) |
| Bottled-shaped design with ablation direction parallel to gas flow | Arrowstmith, 1987 | (12) |
| Model calculation of entrainment and transport of ablated material | Arrowsmith and Hughes, 1988 | (9) |
| Study of factors that affect aerosol transport processes | Bleiner and Gunther, 2001 | (10) |
| Soft tissue analysis by cryogenically cooled ablation cell | Feldmann et al., 2002 | (13) |
| A novel gas inlet system for improved aerosol entrainment | Bleiner and Altorfer, 2005 | (8) |
| Optimisation of a laser ablation cell for detection of hetero-elements in proteins blotted onto membranes | Feldmand et al., 2006 | (14) |
| High efficiency aerosol dispersion (HEAD) closed ablation cell | Pisonero et al., 2006 | (15, 16) |
| Transport efficiency of ablation cells with short and long wash-out times | Garcia et al., 2007 | (5) |
| Volume optional and low memory (VOLM) chamber for laser ablation | Liu et el.,2007 | (17) |
| Computer simulations of ablation chambers | Bleiner and Bogaerts, 2007 | (4) |

| | | |
|---|---|---|
| A simple closed ablation cell with wash-out time less than 100 ms | Gurevich Hergenroder, 2007 | (18) |
| Design analysis of a new closed ablation cell by computational fluid dynamics techniques | Autrique et al.,2008 | (19) |
| Two-volume closed laser ablation cell | Müller et al., 2009 | (20) |
| Design and performance of a cyclonic flux cell | Monticelli et al., 2009 | (21) |
| Assessment of a commercially available large ablation cell | Carugati et al., 2010 | (22) |
| A close ablation cell capable to host large or several samples | Fricker et al., 2011 | (23) |
| Modification of conventional cell for oil analysis | Ricard et al., 2011 | (24) |
| Low dispersion tube cell for fast chemical imaging | Wang et al., 2013 | (25) |
| Peltier cooled with on sample temperature control | Konz et al, 2014 | (26) |
| High-speed integrated ablation cell | Douglas et al., 2015 | (27) |
| Low dispersion cell for sub-µm scanning of layered materials | Van Malderen et al., 2015 | (28) |

It must be pointed out that two volume closed cells are now fitting most of the new laser ablation devices as they combine the advantages of low volume cell with the ability to install large volume samples (limited to 10 cm) and wash-out times below less than one second (Figure2).

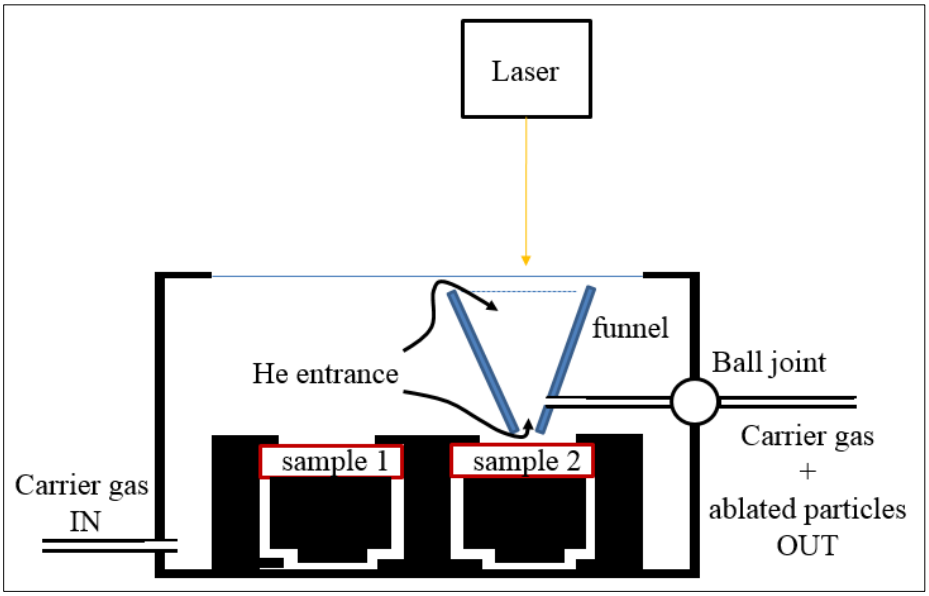


**Figure 2** Schema of two volume closed cell. Adapted from Müller et al. (20). The carrier gas enters the cell body at its bottom, and flows from both bottom and top through the funnel, where the carrier gas flow entrains the aerosol that condensed out from the laser-induced plasma. Funnel-shaped upper cell (effective volume 1–2 $cm^3$) allows rapid signal wash-out and invariant gas flow around the ablation site to ensure

reproducible elemental and/or isotopic fractionation, irrespective of sample position relative to gas in/outlets. Sample aerosol and carrier gas leave the LA cell for the ICPMS via an exit tube connected to the cell body via a ball joint, and Ar and $N_2$ (optional) are admixed downstream.

**Open design cells** are independent of the sample size and are placed onto the sample surface as a seal, minimizing the dead volume. Nevertheless, they demand polish and smooth sample surfaces prior to the analysis to provide optimal sealing. The open cells offer advantages in terms of shortened washout times and increased flexibility in sample size. Table 2 shows a list of open laser ablation cells in the literature and their remarkable characteristics.

**Table 2** Open laser ablation cells in the literature and their main characteristics.

| Characteristic | Author and year | Ref |
|---|---|---|
| Designed to fit the ICP torch tail | Carr and Horlick, 1982 | (29) |
| Cap cell for polished surfaces | Ishizuka and Uwamino, 1982 | (30) |
| Design of an open ablation cell for the study of large silver objects | Devos et al., 1999 | (31) |
| Open ablation cell for the study of historic objects | Wagner and Jedral, 2011 | (3) |
| Gas flow optimization for brass sample analysis | Kántor et al., 2012 | (32) |

Unfortunately, the key feature of all the previously described cells is that the sample is either contained in a box or contacts the sample for final seal. Thus, the sample size is a constraining factor and makes complicate multisampling or high throughput analysis. In order to overcome this drawback they have been developed **open and non-contact design cells** that do not physically touch the sample and use a gas curtain for sealing.

**Table 3** Open and non-contact ablation cells in the literature and their main characteristics.

| Characteristic | Author and year | Ref |
|---|---|---|
| An open and non-contact cell for laser ablation | Asogan et al., 2009 | (33) |
| Numerical simulations of an open and non-contact cell | Asogan et al., 2011 | (34) |

In this case, the first and foremost criteria for the design of the ablation cell are the following: i) no contact with the sample surface, ii) full exclusion of atmospheric gases, iii) capacity to accept samples of indeterminate size, iv) low gas consumption, v) rapid wash-out time and vi) good

reproducibility and sensitivity. They have been initially optimized for planar samples or samples with little curvature and they work effectively over sampling distances of 50-200 µm.

Several authors also reported the development of a novel online laser atmospheric sampling approach using ambient air as ablation environment and omitting the need of an ablation cell. The laser-induced aerosol containing air is directly sucked into a transport tube and transported towards the ICPMS by a diaphragm pump. The gas exchange is accomplished in a gas exchange device, which was originally designed for direct multi-elemental analysis of airborne particulate matter by ICPMS (35, 36), located just before the plasma source (Figure 3). The new gas converter apparatus consists of a porous inner silica tube and an outer borosilicate tube. Gas exchange process is based on diffusion because of the difference in the partial pressures of the gas molecules when the aerosol passes through the apparatus. After exchanging air into argon, oxide formation, count rates of the gas blank and spectral interferences are found to be similar or lower in comparison to conventional setup in which helium is exchanged by argon, which indicates a complete exchange of air by argon (1). However, the atmospheric sampling showed lower intensities, by up to a factor of 5. Indeed, the visualization of the aerosol extraction indicates that some particles are lost prior to gas exchange (37). Later on, Tabersky et al. (38) developed a large-capacity gas exchange device (Q-GED) that allows a carrier gas flow of 0.8 L $min^{-1}$ atmospheric air to be exchanged with Ar combined with an aerosol plume entrainment device to improve particle transport efficiency. No significant differences in sensitivity were noticed comparing Ar and air. Consequently, since this novel laser ablation sampling approach has no previous requirements of the sample geometry, it can be useful for the direct analysis of large and valuable samples.

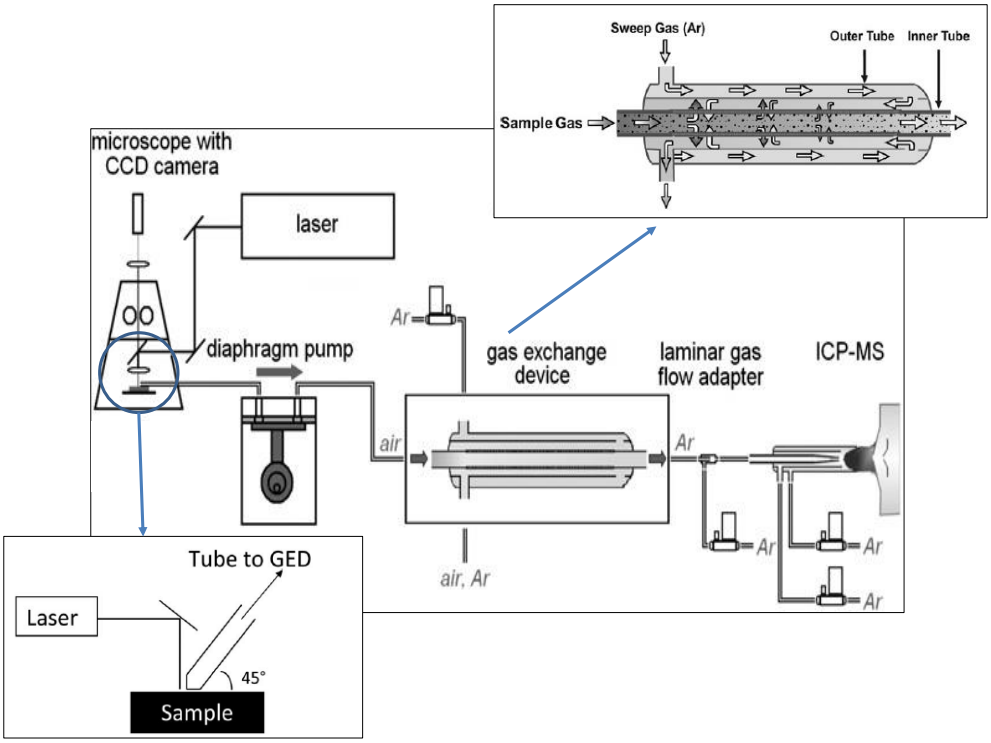


**Figure 3** Sketch of the experimental setup for the direct atmospheric sampling for LA-ICPMS *(4)*. The sample is place in a holder under ambient conditions. A transport tube, which is directly placed as close as possible to the sample surface, is connected to the diaphragm pump. During laser ablation, the laser-induced aerosol is sucked into the system and carried to the gas exchange device and further to the ICPMS by the pump.

Finally, a laser-based in situ sampling strategy for the elemental analysis of paintings was reported by Smith et al. (39), but a detailed description of the sampling prototype was not given. In the proposed procedure, the ablated materials were sampled on membrane filters and were analyzed subsequently in the laboratory by LA-ICPMS in a qualitative manner. Later, Glaus et al. (40) developed a portable laser ablation sampling device in order to extend the field of application to arbitrary sized objects outside laboratory. The element analytical capabilities of the approach were demonstrated on glass, gold and ceramic samples. It was shown to be suitable for the sampling of metals and opaque nonmetallic samples. Drilling of well-defined craters removes a minimal amount of sample material required for the subsequent quantification and preserves the integrity of the objects on a macroscopic scale. It consists of a pulsed laser, an optical fiber attached to a hand-held LA module, a sampling filter mounting, and a membrane pump. Picture and schematic of the system are shown in Figure 4 extracted from Glaus et al. (40).

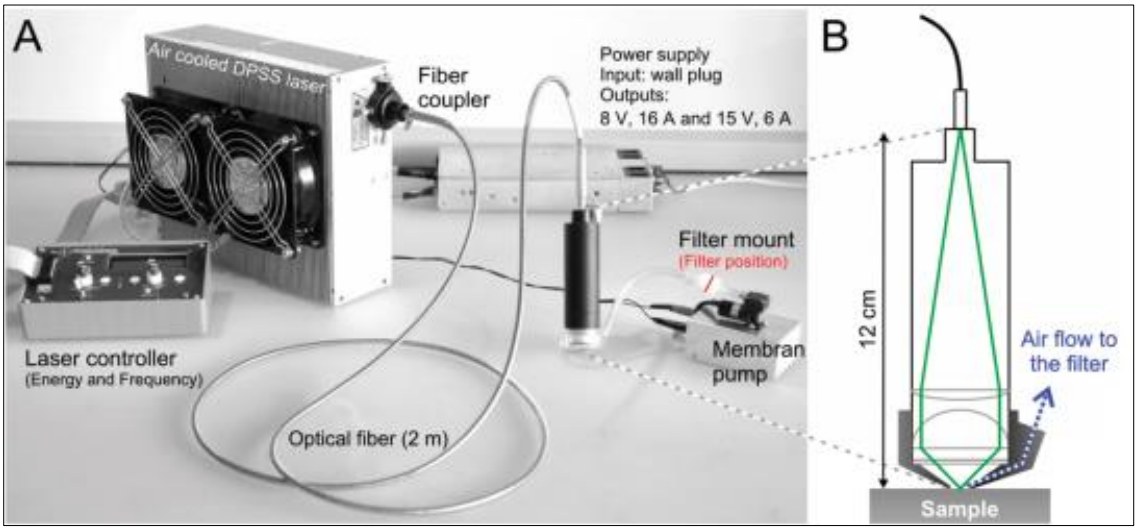


**Figure 4** Assembled portable laser ablation sample device (A) and details of the LA module (B).

## 2. Design and development of a new ablation cell adjustable to different bottle shapes

Any sampling on unique and valuable object is only acceptable after careful consideration of the preservation state and the influence of the sampling procedure; therefore the priority is given to all non-destructive over micro-destructive methods of analysis. Some valuable wine bottles are considered masterpieces, antiques or art treasures. In 1985, the publisher Malcolm Forbes paid the astronomical figure of $156,000 for a bottle of 1787 Château Lafite allegedly belonging to the third President of the United States of America Thomas Jefferson's cellar with the initials ThJ etched in the glass. However, its authenticity has been a subject of speculation (41). In such cases, the common ground of wine as an alimentary product is put aside and it is in the packaging itself where the importance lies for authentication and traceability purposes, taking into account that both packaging and content must keep intact. With the aim of a direct analysis of wine bottles, we have designed and constructed a new ablation cell adjustable to different bottle shapes. Its development is based on simplicity, cost-efficiency, ease of manufacturing, allowing fast sample throughput and efficient transport of laser-induced particles to ICP plasma source. It consists of an open ablation cell whose geometry ensures a complete assembly between cell and the bottle assuring no gas leaks and a maximum laser induced aerosol transportation to ICP plasma source. The first prototype of the model (Figure 5) was designed with Google SketchUp (2015). The size of the cell was adapted to cover homogeneously the bottle body, adapting its shape to the curvature.

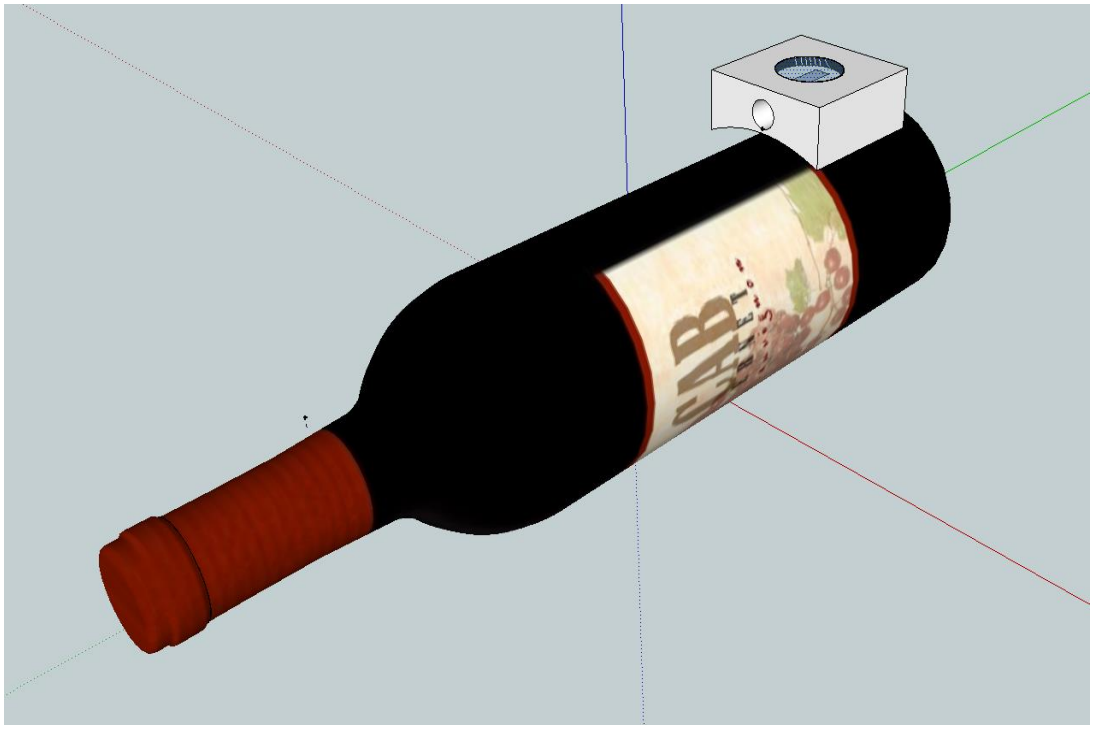

**Figure 5** Prototype of the ablation cell adjustable to bottle shape.

Several approaches were carried out before finally leading to a fully optimized ablation cell in terms of cell dimensions, assembling, tightness and surface treatment by removing the detected drawbacks. An exhaustive explanation of the actions taken for the development of the new ablation cell is featured below.

## 2.1 1st design

The construction of the new cell was developed in collaboration with the atelier of physics of the Université de Pau et des Pays de l'Adour who was in charge to implement the prototype. The LA cell design had to meet all of the following requirements: 1) open cell adapted to the bottles (*Bordelaise* bottle shape or equivalent) to guarantee full flexibility in sample size, 2) tightness as regards with carrier gas, 3) small internal volume, 4) shape must favour particle transportation (avoid edges) and 5) the distance between the laser window and the focal point must be lower than 18 mm which is the theoretical back-focus distance of ALFAMET laser lens (2/3" 50 mm f1.8 w/locking Iris&Focus, Computar). Figure 6 shows the upper, bottom, lateral and cross sections of the new ablation cell designed by the atelier of physics of the University.

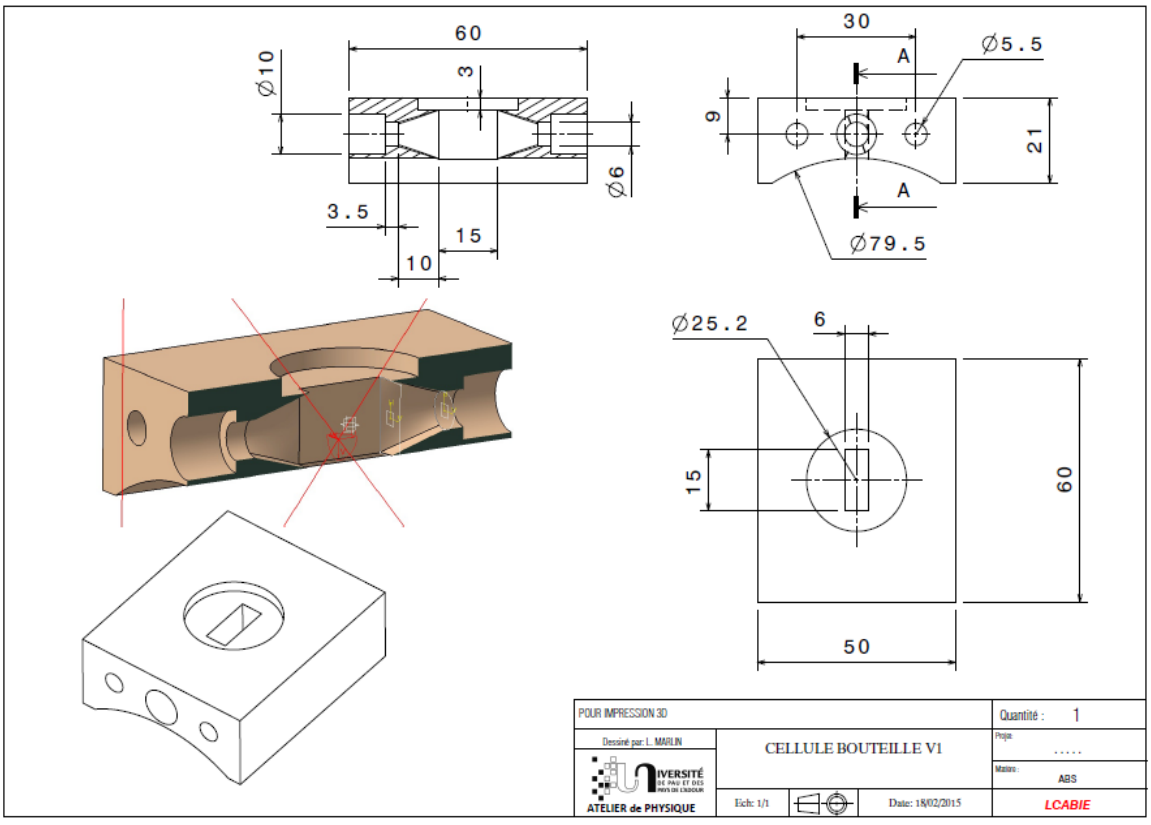


**Figure 6** Upper, bottom, lateral and cross sections of the new ablation cell.

The first prototype has relatively small dimensions (5 x 6 x 2.1 cm) with an internal volume of approximately 5.3 $cm^3$. It must be pointed out that we designed the inner cavity in funnel shape then avoiding sharp corners to favour laminar gas flow for a better transport efficiency.

The cell was built using a commercially available 3D printer (Ultimaker 2 Extended+, Ultimaker B.V., Geldermalsen, The Netherlands). This Fused Deposition Modelling (FDM) 3D printer was used as an alternative to conventional machining techniques that cannot machine such small funnel shape and rounded corners inside a single piece due to the size of the cutting tool. The printer has a theoretical precision of 20 µm and printing speed of 300 mm/s, and allows printing details of about 100 to 200 microns. The cell was printed in poly (lactic acid) (PLA) which belongs to the family of aliphatic polyesters commonly made from α-hydroxy acids and is considered biodegradable and compostable (Figure 7). It is degraded by simple hydrolysis of the ester bond and does not require the presence of enzymes to be catalyzed. It has a degradation time in the environment on the order of six months to two years, in comparison with 500 to 1000 years for conventional plastics such as polystyrene (PS) and polyethylene (PE). PLA is a thermoplastic, high-strength, high malleable polymer that can be made from renewable resources. Due to its properties, it is widely used on large-scale production lines in applications such as injection molding, blow molding, thermoforming and extrusion for which it must possess adequate thermal stability to prevent degradation and maintain molecular weight and properties (42). Figure 8 shows the first design of the ablation cell in which upper, bottom and lateral views are presented.

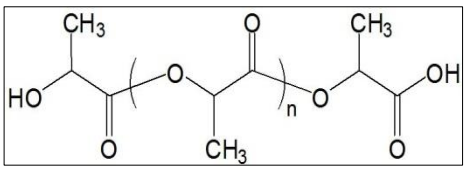


**Figure 7** Poly (lactic acid) polymer chain.

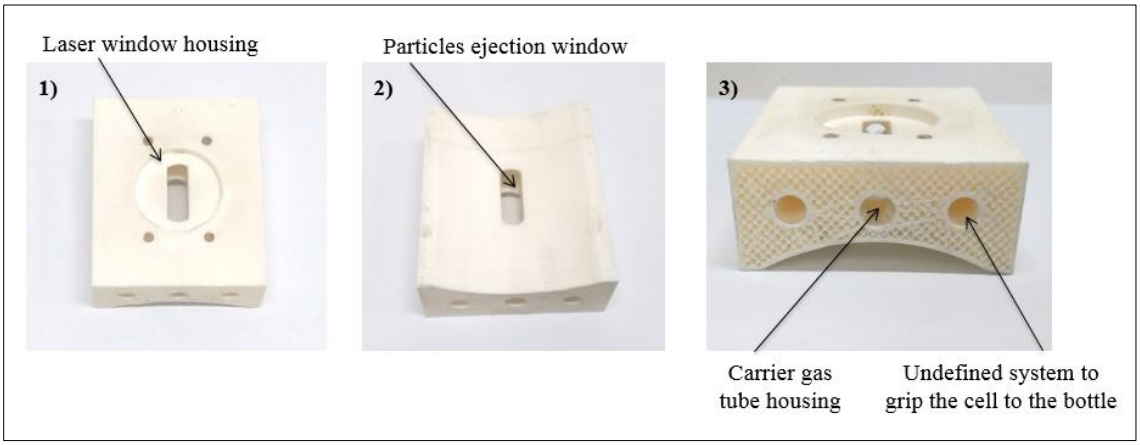


**Figure 8** 1st design of the ablation cell: 1) upper, 2) bottom and 3) lateral views.

Note that in the upper part there is a circle (Ø 25.2 mm and 3 mm depth) to house the laser window and an internal aperture (15 x 6 mm) for laser focusing and particle ejection. The four holes in the upper part have an unspecific task and they will be removed in the later designs. On the side view there are three round openings (Ø 5.5 mm). The both in the sides are intended for anchoring the cell to the bottle and the one in the middle aims to host the transport gas tubing through the cell.

However, this first design turned out to have an excessive height as no laser beam focusing could be achieved. In fact the specifications of the lens manufacturer there is a back focal of 18 mm; however after measuring it, we realised that this distance takes into account the backside of the lens, the real distance between the lens and the sample being then reduced by the lens thickness. A working distance of 13 mm was then evaluated in the focus conditions by measuring the distance between the lens and the micro laser induced plasma formed in the air (Figure 9); a cell thickness of 10 mm (previously 15 mm) was considered to be satisfactory as it leaves now 3 mm between the lens and the laser window of the cell. This distance will be reduced since a layer of elastomer is planned to be added at the bottom of the cell to insure leak tightness in the following designs.

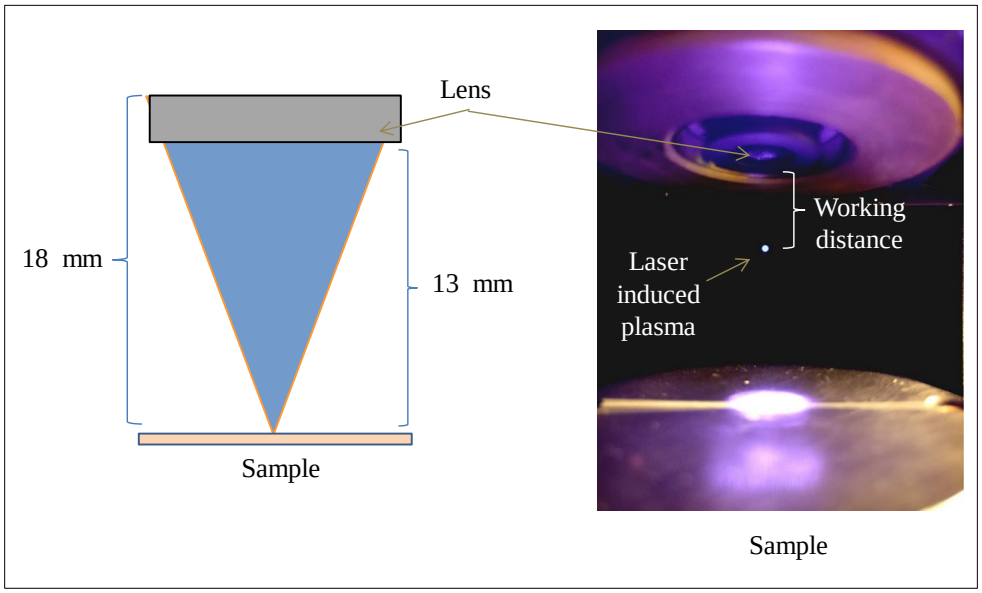


**Figure 9** Laser beam focusing and effective working distance in air.

A metallic holder, which totally fitted the laser 2D stage, was constructed (Figure 10). It consists of a screwed metal plate (19.5 x 11 cm) with two sidebars to avoid bottle slipping. The particular advantages of this holder are: i) its fixing clamps can be clipped at any desired location and 2) its rotation movement that allows rotating the sample according to the sampling position.

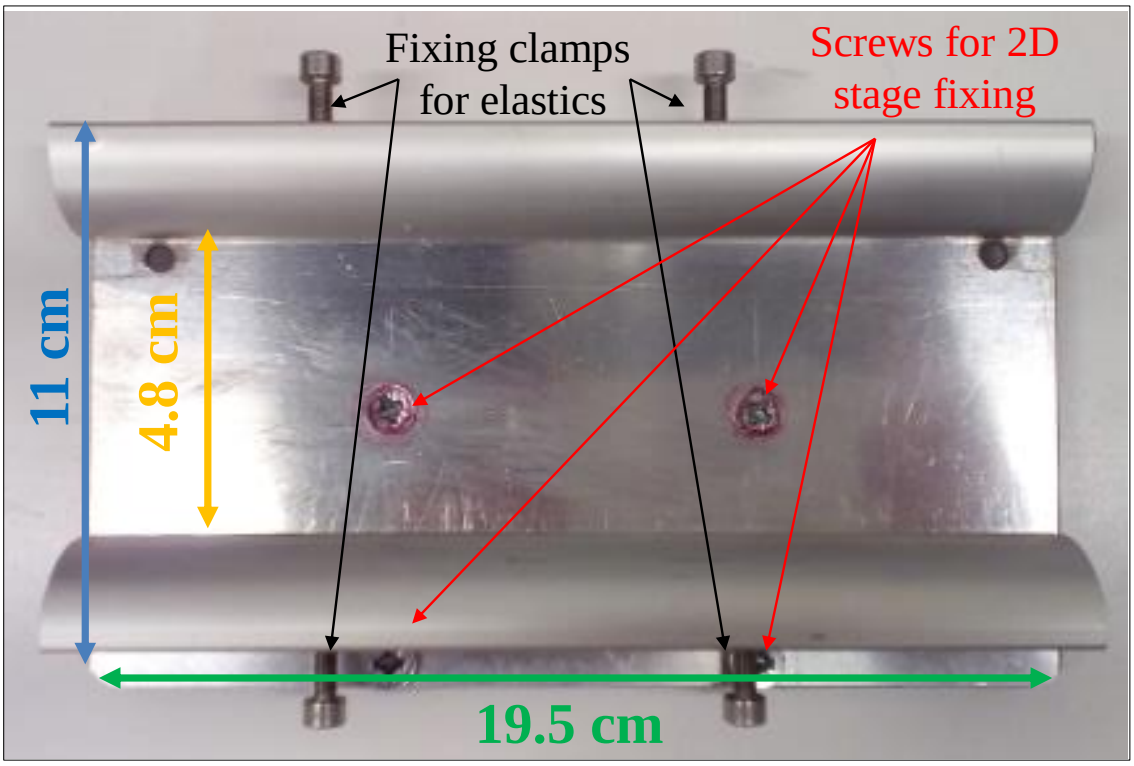


**Figure 10** Metallic holder for bottles.

## 2.2 2nd design

When previously described modifications were done, a new design was performed (Figure 11):

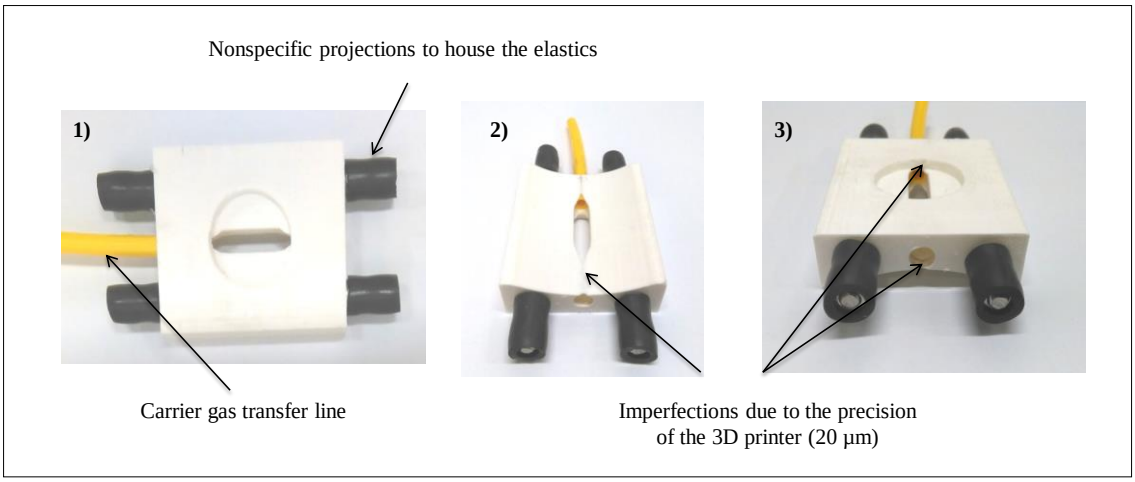


**Figure 11** 2nd design of the ablation cell: 1) upper, 2) bottom and 3) lateral views.

This new design, whose height is 10 mm, includes longitudinal nonspecific projections to house the elastics which will help to fix the cell to the bottle surface. However, there are transport gas leaks due to the imperfections caused by low printing precision. In this case, carrier gas transfer line is directly inserted into the ablation cell which causes a high pressure in the thin and faulty cell wall. In consequence, small connection pipes are incorporated to the final design which allow direct tubing.

### 2.3 3th design: final design

The final ablation cell design includes small pipes (Ø 5 mm) where transport gas tubes can be directly placed, allowing a better manipulation of the cell. In addition, two channels were added for a more effective positioning of the elastic to balance the forces equally on the bottle (Figure 12). A neoprene foam layer (2.5 x 4x 0.25 cm) was fixed to the bottom of the ablation cell with the aim of improving the contact area between the cell and the bottle as it could adapt to slight irregularities that could happen on the bottle surface, ensuring leak tightness. Neoprene foam was preferred over silicon as the hardness of the later was found to be high to compensate of surface irregularities. Nevertheless, the cell showed gas leaks across its structure when it was immersed in a water bath and flushed with He. These leaks are caused by the minor flaws on printing procedure. In order to solve this problem the ablation cell was firstly exposed to chloroform vapours as PLA is soluble in most organic solvents such as tetrahydrofuran (THF), chlorinated solvents, benzene acetonitrile and dioxane (43). However, this approach proved not to be adequate to close the small gaps between polymer strands because it causes deformation and structural failure leading to an inefficient transport of laser-induced aerosol. Therefore, as an alternative, the cell was firstly polished with a very finely grained sandpaper, coated with a thin layer of epoxy based resin (Araldite 20:20, Basel, Switzerland) and allowed to dry overnight at room temperature.

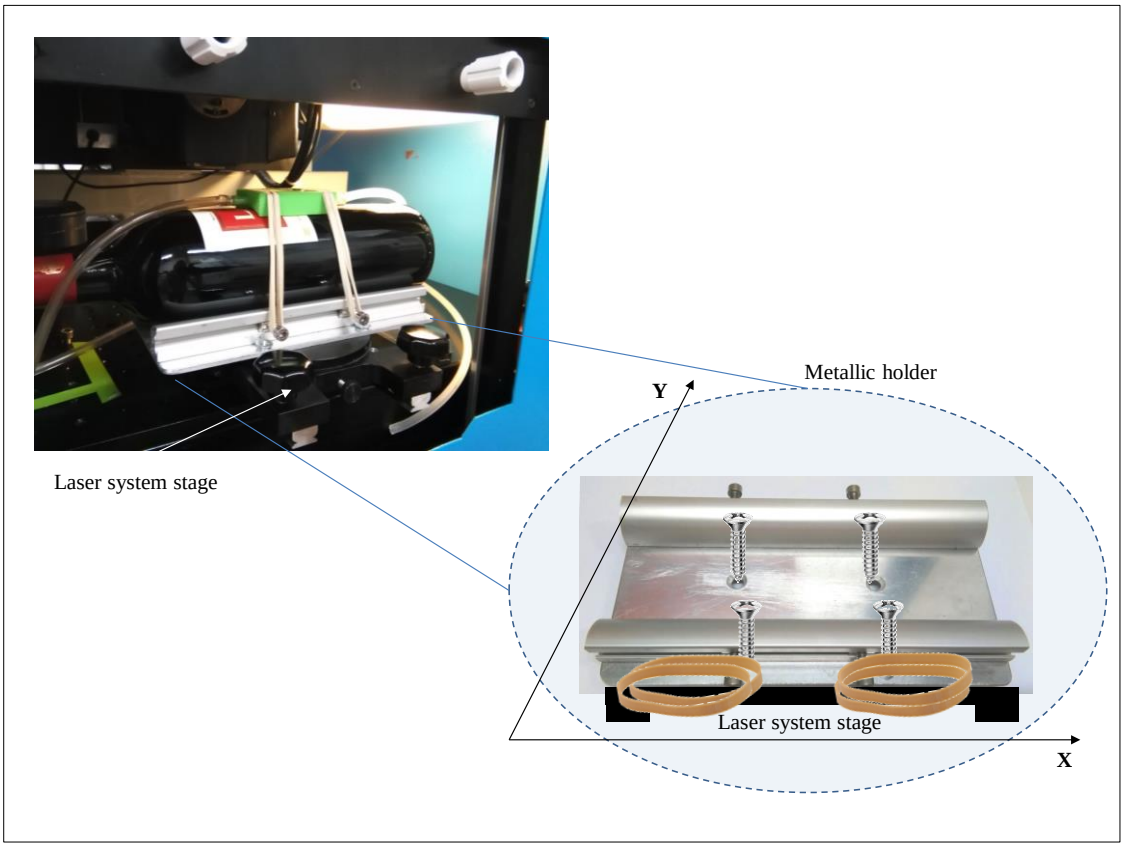


**Figure 12** Final design of the ablation cell and its inclusion on the laser ablation system.

The amount of particles reaching the ICPMS has several implications for the elemental analysis. Firstly, sensitivity. The higher the transported number of particles, the more intense is the analytical signal. Secondly, elemental fractionation. The ablation cell could operate as a particle size filter which induces the formation of a compositionally heterogeneous aerosol. Finally, cross contamination. The particles that remain in the ablation cell could cause interference with the subsequent determinations (4). Therefore, in order to test the performance of the new ablation cell, transport efficiency and wash-out time were evaluated. The evaluation was performed by ablating a 100 µm wide line in a SRM NIST612 glass in wet plasma conditions (1 $\mu g \cdot l^{-1}$ Rh, 4 rpm). Each isotope was acquired with a dwell time of 20 ms. Helium was flushed through the cell at a flow rate of 290 ml/min. Table 4 shows ion-signal intensities measured in CRM NIST612 using *home-made* ablation cell. Indium was measured as indicator of sensitivity, reaching to obtain about 250000 counts per second. Uranium and thorium ratio was measured to evaluate the elemental fractionation. The resulting fractionation ratio values indicate values were low, ranging between 0.95 and 1.05. In addition, oxide formation which measured for the cell tightness evaluation and count rates of the gas blank were satisfactory. Therefore, it can be concluded that the accuracy of the obtained results were similar to those obtained with closed transport systems.

**Table 4** Comparison of the performance of conventional and laboratory designed cells.

| Element | Closed minicell | *Home-made* cell |
|---|---|---|
| *In (sensitivity)* | 250000 cps | 290000 cps |
| *U/Th (robustness)* | 1 ± 0.05% RSD | 1 ± 0.05% RSD |
| *Oxides (UO/<U)* | <3% | <3% |

The wash-out time was calculated considering the interval between the peak top and the peak end. The acquired signals are washed out in less than 5s for the 99.9% and the integrated peak area of the intensity measurement is constant at different locations, except for positions close to the gas inlet/outlet. However, further investigations are required for a better comprehension of gas flow topology through the ablation chamber, depending mostly on the chamber size and geometry. Computational Fluid Dynamics (CFD) simulations of ablation chambers have been shown in previous works to offer a good understanding of gas flows around the ablation site, and to estimate particle transport dynamics through the chamber (4, 34).

## 3. Bibliography


1. Kovacs R, Nishiguchi K, Utani K, Gunther D. Development of direct atmospheric sampling for laser ablation-inductively coupled plasma-mass spectrometry. Journal of Analytical Atomic Spectrometry. 2010;25(2):142-7.
2. Horn I, Günther D. The influence of ablation carrier gasses Ar, He and Ne on the particle size distribution and transport efficiencies of laser ablation-induced aerosols: implications for LA–ICP–MS. Applied Surface Science. 2003;207(1):144-57.
3. Wagner B, Jedral W. Open ablation cell for LA-ICP-MS investigations of historic objects. Journal of Analytical Atomic Spectrometry. 2011;26(10):2058-63.
4. Bleiner D, Bogaerts A. Computer simulations of sample chambers for laser ablation–inductively coupled plasma spectrometry. Spectrochimica Acta Part B: Atomic Spectroscopy. 2007;62(2):155-68.
5. Garcia CC, Lindner H, Niemax K. Transport efficiency in femtosecond laser ablation inductively coupled plasma mass spectrometry applying ablation cells with short and long washout times. Spectrochimica Acta Part B: Atomic Spectroscopy. 2007;62(1):13-9.
6. Bleiner D, Belloni F, Doria D, Lorusso A, Nassisi V. Overcoming pulse mixing and signal tailing in laser ablation inductively coupled plasma mass spectrometry depth profiling. Journal of Analytical Atomic Spectrometry. 2005;20(12):1337-43.
7. Van Malderen SJM, Managh AJ, Sharp BL, Vanhaecke F. Recent developments in the design of rapid response cells for laser ablation-inductively coupled plasma-mass spectrometry and their impact on bioimaging applications. Journal of Analytical Atomic Spectrometry. 2016;31(2):423-39.
8. Bleiner D, Altorfer H. A novel gas inlet system for improved aerosol entrainment in laser ablation inductively coupled plasma mass spectrometry. Journal of Analytical Atomic Spectrometry. 2005;20(8):754-6.
9. Arrowsmith P, Hughes SK. Entrainment and Transport of Laser Ablated Plumes for Subsequent Elemental Analysis. Applied Spectroscopy. 1988;42(7):1231-9.
10. Bleiner D, Gunther D. Theoretical description and experimental observation of aerosol transport processes in laser ablation inductively coupled plasma mass spectrometry. Journal of Analytical Atomic Spectrometry. 2001;16(5):449-56.
11. Gray AL. Solid sample introduction by laser ablation for inductively coupled plasma source mass spectrometry. Analyst. 1985;110(5):551-6.
12. Arrowsmith P. Laser ablation of solids for elemental analysis by inductively coupled plasma mass spectrometry. Analytical Chemistry. 1987;59(10):1437-44.
13. Feldmann J, Kindness A, Ek P. Laser ablation of soft tissue using a cryogenically cooled ablation cell. Journal of Analytical Atomic Spectrometry. 2002;17(8):813-8.

14. Feldmann I, Koehler CU, Roos PH, Jakubowski N. Optimization of a laser ablation cell for detection of hetero-elements in proteins blotted onto membranes by use of inductively coupled plasma mass spectrometry. Journal of Analytical Atomic Spectrometry. 2006;21(10):1006-15.
15. Pisonero J, Fliegel D, Gunther D. High efficiency aerosol dispersion cell for laser ablation-ICP-MS. Journal of Analytical Atomic Spectrometry. 2006;21(9):922-31.
16. Lindner H, Autrique D, Pisonero J, Gunther D, Bogaerts A. Numerical simulation analysis of flow patterns and particle transport in the HEAD laser ablation cell with respect to inductively coupled plasma spectrometry. Journal of Analytical Atomic Spectrometry. 2010;25(3):295-304.
17. Liu Y, Hu Z, Yuan H, Hu S, Cheng H. Volume-optional and low-memory (VOLM) chamber for laser ablation-ICP-MS: application to fiber analyses. Journal of Analytical Atomic Spectrometry. 2007;22(5):582-5.
18. Gurevich EL, Hergenroder R. A simple laser ICP-MS ablation cell with wash-out time less than 100 ms. Journal of Analytical Atomic Spectrometry. 2007;22(9):1043-50.
19. Autrique D, Bogaerts A, Lindner H, Garcia CC, Niemax K. Design analysis of a laser ablation cell for inductively coupled plasma mass spectrometry by numerical simulation. Spectrochimica Acta Part B: Atomic Spectroscopy. 2008;63(2):257-70.
20. Muller W, Shelley M, Miller P, Broude S. Initial performance metrics of a new custom-designed ArF excimer LA-ICPMS system coupled to a two-volume laser-ablation cell. Journal of Analytical Atomic Spectrometry. 2009;24(2):209-14.
21. Monticelli D, Gurevich EL, Hergenroder R. Design and performances of a cyclonic flux cell for laser ablation. Journal of Analytical Atomic Spectrometry. 2009;24(3):328-35.
22. Carugati G, Rauch S, Kylander ME. Experimental assessment of a large sample cell for laser ablation-ICP-MS, and its application to sediment core micro-analysis. Microchimica Acta. 2010;170(1):39-45.
23. Fricker MB, Kutscher D, Aeschlimann B, Frommer J, Dietiker R, Bettmer J, et al. High spatial resolution trace element analysis by LA-ICP-MS using a novel ablation cell for multiple or large samples. International Journal of Mass Spectrometry. 2011;307(1–3):39-45.
24. Ricard E, Pecheyran C, Sanabria Ortega G, Prinzhofer A, Donard OF. Direct analysis of trace elements in crude oils by high-repetition-rate femtosecond laser ablation coupled to ICPMS detection. Analytical and Bioanalytical Chemistry. 2011;399(6):2153-65.
25. Wang HAO, Grolimund D, Giesen C, Borca CN, Shaw-Stewart JRH, Bodenmiller B, et al. Fast Chemical Imaging at High Spatial Resolution by Laser Ablation Inductively Coupled Plasma Mass Spectrometry. Analytical Chemistry. 2013;85(21):10107-16.

26. Konz I, Fernández B, Fernández ML, Pereiro R, Sanz-Medel A. Design and evaluation of a new Peltier-cooled laser ablation cell with on-sample temperature control. Analytica Chimica Acta. 2014;809:88-96.
27. Douglas DN, Managh AJ, Reid HJ, Sharp BL. High-Speed, Integrated Ablation Cell and Dual Concentric Injector Plasma Torch for Laser Ablation-Inductively Coupled Plasma Mass Spectrometry. Analytical Chemistry. 2015;87(22):11285-94.
28. Van Malderen SJM, van Elteren JT, Vanhaecke F. Development of a fast laser ablation-inductively coupled plasma-mass spectrometry cell for sub-micron scanning of layered materials. Journal of Analytical Atomic Spectrometry. 2015;30(1):119-25.
29. Carr JW, Horlick G. Laser vaporization of solid metal samples into an inductively coupled plasma. Spectrochimica Acta Part B: Atomic Spectroscopy. 1982;37(1):1-15.
30. Ishizuka T, Uwamino Y. Inductively coupled plasma emission spectrometry of solid samples by laser ablation. Spectrochimica Acta Part B: Atomic Spectroscopy. 1983;38(3):519-27.
31. Devos W, Moor C, Lienemann P. Determination of impurities in antique silver objects for authentication by laser ablation inductively coupled plasma mass spectrometry (LA-ICP-MS). Journal of Analytical Atomic Spectrometry. 1999;14(4):621-6.
32. Kántor T, Király E, Bertalan É, Bartha A. Gas-flow optimization studies on brass samples using closed and open types of laser ablation cells in inductively coupled plasma mass spectrometry. Spectrochimica Acta Part B: Atomic Spectroscopy. 2012;68:46-57.
33. Asogan D, Sharp BL, O' Connor CJP, Green DA, Hutchinson RW. An open, non-contact cell for laser ablation-inductively coupled plasma-mass spectrometry. Journal of Analytical Atomic Spectrometry. 2009;24(7):917-23.
34. Asogan D, Sharp BL, O'Connor CJP, Green DA, Wilkins J. Numerical simulations of gas flows through an open, non-contact cell for LA-ICP-MS. Journal of Analytical Atomic Spectrometry. 2011;26(3):631-4.
35. Nishiguchi K, Utani K, Fujimori E. Real-time multielement monitoring of airborne particulate matter using ICP-MS instrument equipped with gas converter apparatus. Journal of Analytical Atomic Spectrometry. 2008;23(8):1125-9.
36. Nishiguchi K, Utani K, Gunther D, Ohata M. Gas to Particle Conversion-Gas Exchange Technique for Direct Analysis of Metal Carbonyl Gas by Inductively Coupled Plasma Mass Spectrometry. Analytical Chemistry. 2014;86(20):10025-9.
37. Dorta L, Kovacs R, Koch J, Nishiguchi K, Utani K, Gunther D. Determining isotope ratios using laser ablation sampling in air with MC-ICPMS. Journal of Analytical Atomic Spectrometry. 2013;28(9):1513-21.
38. Tabersky D, Nishiguchi K, Utani K, Ohata M, Dietiker R, Fricker MB, et al. Aerosol entrainment and a large-capacity gas exchange device (Q-GED) for laser ablation inductively

coupled plasma mass spectrometry in atmospheric pressure air. Journal of Analytical Atomic Spectrometry. 2013;28(6):831-42.

39. Smith K, Horton K, Watling RJ, Scoullar N. Detecting art forgeries using LA-ICP-MS incorporating the in situ application of laser-based collection technology. Talanta. 2005;67(2):402-13.
40. Glaus R, Koch J, Günther D. Portable Laser Ablation Sampling Device for Elemental Fingerprinting of Objects Outside the Laboratory with Laser Ablation Inductively Coupled Plasma Mass Spectrometry. Analytical Chemistry. 2012;84(12):5358-64.
41. Wallace, B. The billionaire's vinegar: the mystery of the world's most expensive bottle of wine. Crown Books; 2008.
42. Hartmann MH. High Molecular Weight Polylactic Acid Polymers. In: Biopolymers from Renewable Resources. Berlin: Springer Berlin Heidelberg; 1998. p. 367-411.
43. Garlotta D. A Literature Review of Poly(Lactic Acid). Journal of Polymers and the Environment. 2001;9(2):63-84.

# CHAPTER 5:

# Analysis of packaging for wine authentication:

## Part 1: Elemental analysis of glass by femtosecond laser ablation coupled to ICPMS

## General introduction: what is glass?

The first items objects used by man probably originated from naturally occurring sources such as obsidian (a form of naturally occurring volcanic glass), from which sharp tools may be chipped. However, it was not until 3500 ago when rudimentary manmade glass originated in the regions now knows as Egypt and Iraq mainly in the manufacture of vessels and jewelry (1). Two thousand years ago, the Roman historian Pliny, recounted a story whereby shipwreck Phoenician sailors accidentally discovered crude glass while they were lighting a bonfire for cooking. They noticed that the sand beneath the fire had melted and assumed the properties of a liquid until it hardened into the material now known as glass. The quality of glass manufacturing was improved by the Romans due to their contributions in oven technology. Since then, glass manufacturing has evolved towards a better quality products and automated and cost-efficient processes (2).

Glass is defined as an inorganic product of fusion that has cooled to a rigid condition without crystallization (ASTM, 2000). In contrast to crystalline solids, which have an ordered internal arrangement of atoms, the internal structure of glass consists of a network of atoms lacking long-range symmetry. Most of the container glass manufactured around the world is soda-lime glass and consists mainly of geologically derived raw materials – sand (63-74%),  (12-16%) and limestone (4-17%) – and recycled broken glass, or *cullet*, which is added to the batch to decrease the melting temperature, reducing the cost of manufacturing process. The components of glass can be classified according to their function as (Table 1): formers, fluxes, modifiers /stabilizers, refining agents and colorants/decolorants/opacifiers (metal oxides).

**Table 1.** Main components of glass according to their principal manufacturing function.

| Glass components | Function | Common components |
|---|---|---|
| ***Formers*** | Main component | $SiO_2$* |
| ***Fluxes*** | Lower melting temperature | $Na_2CO_3$, $K_2CO_3$ |
| ***Modifiers/stabilizers*** | Improve chemical resistance | CaO, $Na_2O$, MgO, $Li_2O$, BaO, SrO |
| ***Refining agents*** | Remove bubbles from molten glass | $As_2O_3$, $CaSO_4$ |
| ***Colorants/decolorants/opacifiers*** | Appearance modifiers | Metal oxides** |

*Intermediate formers are also added to the batch ($Al_2O_3$, $ZrO_2$, $V_2O_5$, $Sb_2O_5$, PbO, ZnO)

** The particular colour is a function of the specific additive while the intensity is a function of its concentration in the glass matrix. For example, manganese and selenium (decolorants) are added to counterbalance the green or yellow colour caused by iron. Common colorants are chromium (emerald green), cobalt (dark blue), copper (light blue), sulphur (amber), titanium (purple, opacifier), cerium (yellow) and gold (red). Additional components can be added as

physical properties modifiers, for example: lead (brightness and weight), boron (thermal resistance) and silver or strontium (protection against radiation).

Each of these raw materials contains impurities that cannot be easily controlled by manufacturers and consequently can produce measurable variations either in the chemical, optical and physical properties of the final glass product.

Until the second half of the 19th century bottles were made by hand gathering, blowing and manually finishing the neck. Even traditional glass-blowing and blow-molding methods are still used by artists and for custom applications, handcrafted bottle making has been replaced by the fully automatic process which was developed after 1850. Glass bottle manufacturing comprises multiple steps. First of all, the raw materials are mixed together to form a batch and it is feeded and melted into the furnace (> 1500ºC). During this process, a refining and homogenizing process takes place to eliminate bubbles from the molten glass and get a uniform composition of the final product. This process is followed by the forming procedure in which molten glass is mould into the final shape of the product. Usually, the blow and blow process is used for the manufacturing of glass bottles (Figure 1).

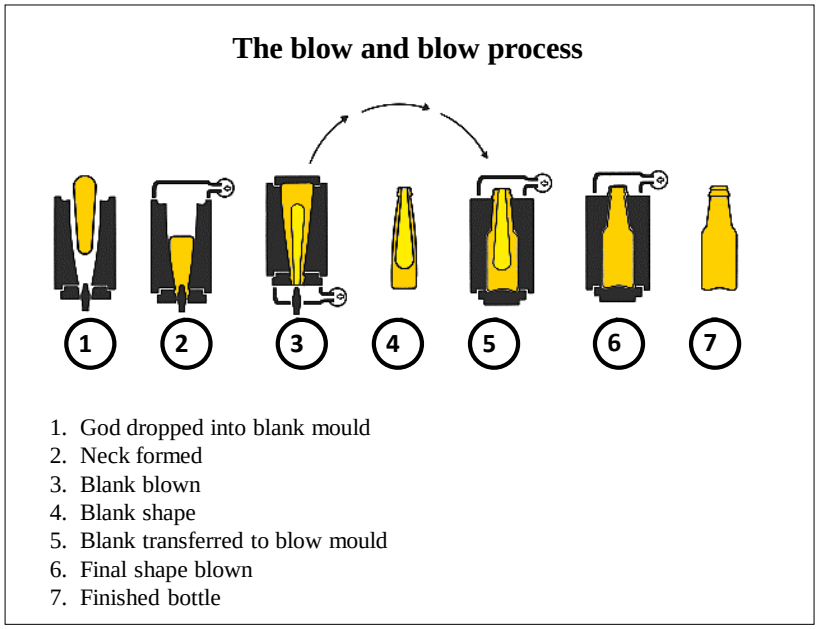


**Figure 1** The blow and blow process employed in the manufacturing process of glass bottles. Molten 'gobs' of glass are delivered into a blank mould. A puff of compressed air blows the glass down into the base of the mould to form the neck of the bottle. This is after transferred to a second mould in which the bottle is blown to its final form.

The time required to completely flush a particular glass from the tank during continuous production can be days to weeks, and the glass that is produced in the transition will have an intermediate composition. The bottle is then removed and transferred to an annealing oven where it is reheated to remove the stresses produced during forming and then cooled under carefully controlled conditions to avoid crystallization. A secondary processing, such as coating and coloring/decolorizing, can be applied depending on the final intention of the product for decoration, protection or strengthen purposes.

In recent years, due to an increase in the means of technological advances, the subject of glass analysis and its use in investigating the circumstances surrounding a delict have seen giant leaps. A forensic glass analysis is typically a comparison of two or more glass fragments in an attempt to determine if they originated from different sources or its provenance (3). Numerous studies have been conducted in order to investigate these aspects, mainly focused in automobile crashes, hit-and-run accidents, burglaries and vandalism. However, the most common type of glass encountered in these forensic caseworks is flat glass, which is widely used in automotive industry and architecture (4-8) comparing to blow glass used for containers (9).

Forensic discrimination of glass has been traditionally carried out by physical examination and comparison of color and thickness, measurement of physical properties (10, 11), such as refractive index (RI) and density and observation of surface under interference microscopy (12). These tests are rapid and non-destructive. In fact, refractive index is considered as the primary tool for the analysis of glass fragments. The RI of a glass is the ratio of speed of light in vacuum to that of speed of light in glass, measured using the immersion method detailed by ASTM E1967-98 (13). Although these techniques have been highly discriminative with traditional glass, modern glass has a greater degree of chemical and physical similarity. In fact, due to the advances in glass manufacturing, it has been noted that the range of the RI values, beginning roughly 1960s is narrowing in the last decades (14). Figure 2 show IR values for flat glass extracted from FBI database for the periods of 1964-1979 and 1980-1997 (15). Nevertheless, refractive index measurements are limited in their ability to distinguish between many different types of glass (16) and it is influenced not only by chemical components but also by the cooling process when it was produced. For this reasons, it is possible that glass fragments taken from the same bottle might show different RI values between surface and inner part due to different cooling rates (17). Scanning electron microscopy coupled with an energy dispersive x-ray spectrometer (SEM EDX) has been also routinely used for the forensic investigation of glass but it has the drawback that it can only provide information about major and minor elements as trace elements exist in concentrations below the detection limits of this method (18).

Therefore, for discrimination purposes, the elements of interest in glass are not the major components but rather the trace and ultra-trace, frequently unintended components, which inherently make glass sources distinguishable.

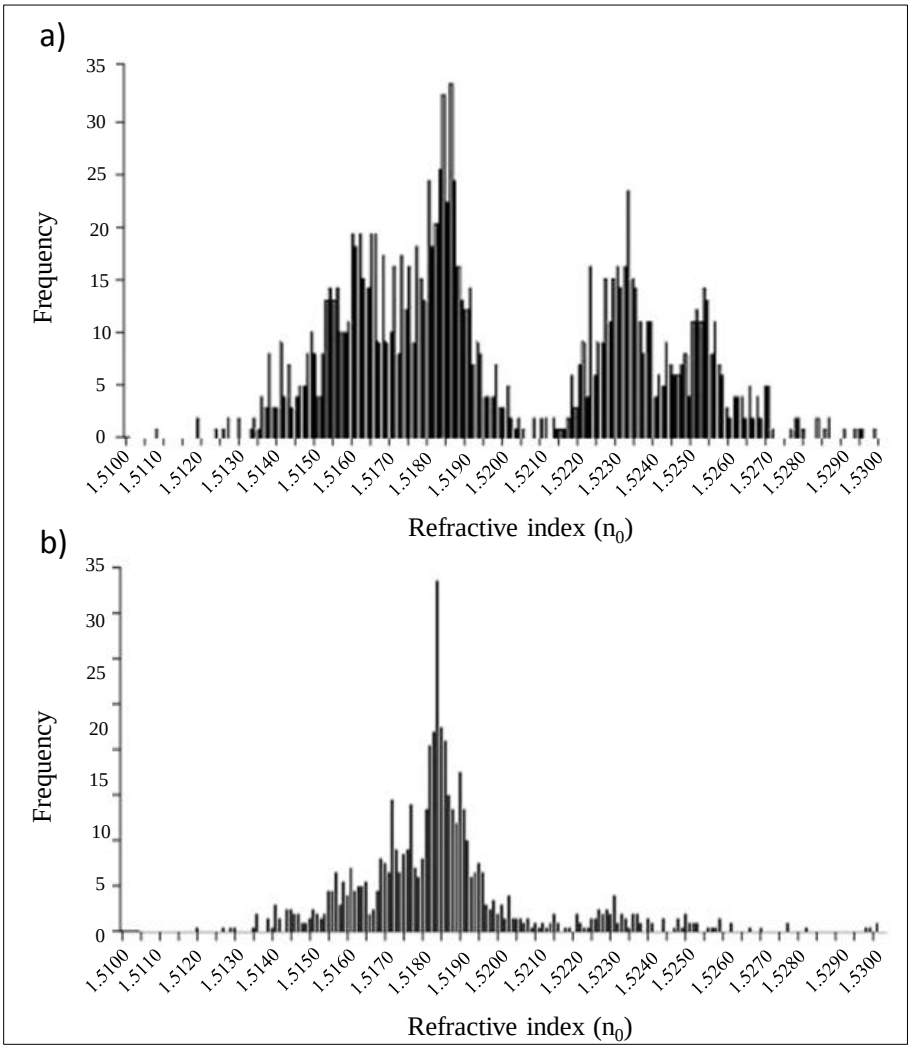


**Figure 2** Histograms showing the distribution of refractive index values for flat glasses from FBI for the periods of a) 1964 to 1979 and b) 1980 to 1997 (15).

As a consequence, the elemental analysis can provide additional information for discrimination. Instrumental analysis, which includes Particle Induced X-ray Emission Spectroscopy (PIXE) (19), X-ray Fluorescence (XRF) (20), Neutron Activation Analysis (NAA) (21), Flame Atomic Absorption Spectroscopy (22), Laser Induced Breakdown Spectroscopy (LIBS) (23, 24) and Inductively Coupled Plasma (ICP) techniques (25), have been applied to enhance the informing power of the comparison between fragments. The practical application and success of one or more of these techniques depends on the sample size requirements, whether or not the technique is destructive, sensitivity, precision, multi-elemental capability and the analysis time (26, 27).

Although each technique has its own advantages and limitations, ICPMS has been shown to be the most effective analytical method for the comparison of trace elements in small glass fragments due to its multi-elemental capability, excellent sensitivity, high sample throughput and the capability to provide isotopic information (28-30). Nevertheless, conventional ICPMS requires the dissolution of the sample, thereby destroying the sample prior to introduction into the mass spectrometer (31). A protocol was developed and published by the American Society of Testing and Materials (ASTM) for the forensic analysis of glass by dissolution by ICPMS (ASTM E-2330-2004) (32).

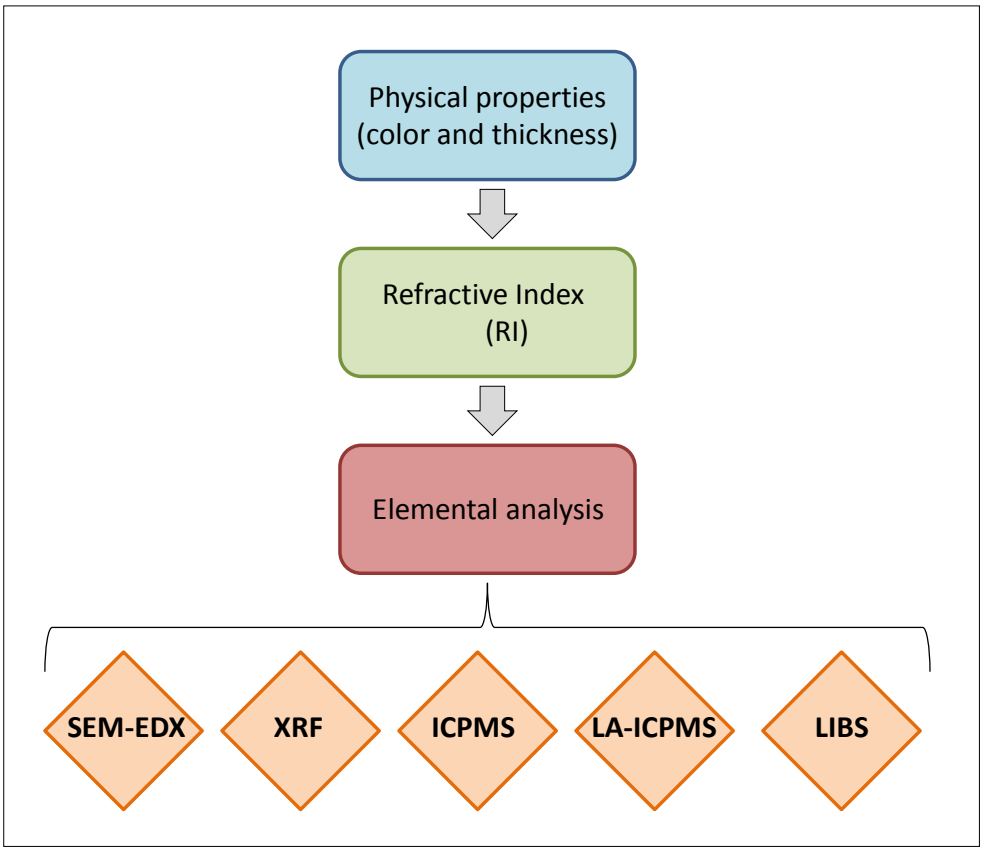


**Figure 3** Scheme for the forensic analysis of glass and current main analytical techniques for its elemental analysis.

This limitation can be overcome by using alternative sample introduction techniques. LA-ICPMS has proved to be a very useful analytical tool for the direct, faster and non-destructive analysis of forensic glass samples, overcoming the limitations associated with very small sample types or samples composed of chemically inert material and elemental fractionation (33, 34). In recent years, several studies have focused on the use of LA-ICPMS to evaluate the capabilities of this technique to discriminate glass produced by different manufacturers or in the same manufacturing plant at different time intervals and to associate samples that originated for a singles source (35-37).

## 1. Introduction

Despite the existing anti-counterfeiting measures, which have shown to be ineffective, wine counterfeiting has a great impact on the European economy (38). In consequence, current wine verification methods are based on wine direct analysis, which implies opening the bottle. When olfactory and taste senses fall short, latest technologies come into play to elucidate the key questions. The International Organisation of Vine and Wine (OIV) proposes a list of analytical methods and procedures aiming its standardisation for scientific, legal and practical interest (39). The new innovative methods used to face the toughest problems are based on mass spectrometry techniques (IRMS, ICP-MS, PTR-MS and GC-MS), spectroscopic techniques (NMR, IR, fluorescence spectroscopy and atomic spectroscopy) and separation techniques (HPLC, GC) (40).

With the aim of authenticating the wine without opening the bottle, the research work described in this manuscript aims to develop a new irrefutable diagnostic tool based on ultratrace analysis of glass packaging by minimally-invasive femtosecond laser ablation ICPMS, which induces no visible degradation of the bottle that could affect its value. The production of glass bottles for wine storage goes back very far into antiquity, imposed in response to the practical difficulties of handling, storing, transporting, trading and keeping wooden barrels. It did not take so long for users to notice the improvement of bottle wine. Indeed, glass isolates wine from oxygen and allows the biochemical reactions to take place spontaneously, boosting and stabilizing its color, bouquet and taste. The bottle thus participates in the development of the wines (41). Some are considered as antiques or artworks. Consequently, analysis of all of the items that constitute the packaging is important avenue.

Forensic discrimination of glass has been traditionally carried out by physical examination and comparison of color and thickness, measurement of physical properties. Refractive index (RI) is considered as the primary tool for the analysis of glass fragments but technological improvements in the glassmaking process have resulted in less variability in physical and optical properties among manufacturers, reducing the discriminatory power of these techniques (14). Consequently, the analysis of impurities present at trace level in raw materials emerges as a useful alternative for discrimination purposes. ICP-based methods provide the most information of all the elemental analysis methods and are being rapidly adopted in forensic laboratories. Zurhaar and Mullings reported an early work in ICPMS in forensic glass analysis for the discrimination among glasses of different origins (42). However, multi-elemental analysis by ICPMS requires careful attention to preparative chemistry. Laser-ablation inductively-coupled plasma mass spectrometry (LA-ICPMS) is considered to be one of the most versatile analytical techniques for the direct trace elemental and isotopic analysis of solid samples. The most remarkable features are ease of use, fast sample throughput, limited sample damages, high sensitivity and wide dynamic range that

allows the simultaneous acquisition of major and trace elements, as well as the measurement of isotope ratios. In addition, laser ablation sampling has a unique advantages over digestion-based methods, such as reducing the sample consumption from milligrams to just few a hundred nanograms, reducing the time of analysis and eliminating the used of hazardous digestion reagents (43).

The goal of this work was to investigate the glass composition of three different caseworks which comprises a total of 268 wine bottles, and discriminate them according to original/falsification, origin and vintage. The following procedure was used for this purpose: i) qualitative determination of the elemental menu which could be determined in bottle samples with line ablation strategy, ii) determination of the minimum quantity of ablated sample for the consistent determination of the elemental ratios of the major, minor and trace elements, iii) evaluation of the reproducibility of the elemental ratios and iv) implementation of an appropriate statistical method which is able to discriminate the samples and determine which elements are useful and necessary for the discrimination of the sample groups. In the field of forensic analysis of glass the aim in most cases is to prove or disprove the common origin of two or more sources of glass. Several strategies for the interpretation of the results of comparative elemental analysis of glass have been generally applied (44-46).The best way to get useful information from a high amount of data is to process it by multivariate pattern recognition methods, which facilitate consideration of intercorrelations between measured variables, providing what is called an analytical fingerprint. In this case, the interpretation of the obtained results is based on comparison of elemental ratios within a spectral profile and it has been carried out by data processing methods, including Principal Components Analysis (PCA), Soft Independent Modelling of Class Analogies (SIMCA) and Hierarchical Ascendant Classification (HAC).

## 2. Material and methods

### 2.1 Description of the sample set

A total of 237 wine bottle samples were collected in a period of 3 years, originating from different countries, wineries and vintages. The collection of wine bottles has been divided into 3 different batches for a better comprehension of the current work (Table 2). Minimal sample preparation is required for the direct analysis of bottle sample by fsLA-ICPMS. Thus, each bottle was carefully cleaned with a wet cloth in acetone in order to remove surface wine, fat and contaminant traces coming from manipulation.

**Table 2.** Batches of bottles analyzed in this work.

| | 1st batch | 2nd batch | 3rd batch |
|---|---|---|---|
| ***Source*** | Private collection | Private collection | Individual's donations |
| ***Number of bottles*** | 8 | 34 | 195 |
| ***Origin*** | France and China | France | Worldwide |

**Table 3.** Distribution of 3rd batch of bottles according to their origin (continent) and color.

| **Worldwide total bottles: 195** | | | |
|---|---|---|---|
| **Continent** | **Country** | **Green bottles: 160** | **Transparent bottles: 35** |
| ***Europe*** | France | 65 | 24 |
| | Spain | 32 | 6 |
| | Italy | 6 | 0 |
| | Czech Republic | 2 | 0 |
| | Slovenia | 1 | 0 |
| | Portugal | 0 | 3 |
| ***Asia*** | China | 33 | 1 |
| | Japan | 1 | 0 |
| | Korea | 1 | 0 |
| | Lebanon | 1 | 1 |
| ***America*** | USA | 13 | 0 |
| | Chile | 2 | 0 |
| ***Oceania*** | Australia | 1 | 0 |
| | New Zealand | 1 | 0 |
| ***Africa*** | Tunisia | 1 | 0 |

On one hand, 1st batch includes 8 green bottles among which 5 are original French bottles and 3 counterfeited Chinese bottles. On the other hand, 2nd batch is a series of 34 green bottles belonging to the same winery which comprises the vintages from 1969 to 2010. Finally, 3rd batch consists of actual 195 wine bottles coming from all over the world, being more abundant European and Asiatic bottles. It must be highlight that a wine bottle is commonly assigned to a given country based on the indication specified in the label, which certainly means that the wine has been produced in this country. However, it is not possible to assume that the packaging is originating from the same country/continent. Table 3 shows the distribution of the bottles according to their origin and color. It must be noted that these bottles were voluntarily donated by anonymous persons during the research period. Therefore, there is not an equitable distribution between origins and it will be taken into account in the following sections for statistical data treatment.

### 2.2 Instrumentation

A high repetition rate femtosecond laser ablation device (ALFAMET, Novalase & Amplitude Systèmes, France) has been use in this work. The femtosecond laser source used in this instrument is fitted with a diode-pumped KGW-Yb crystal delivering 360 femtosecond pulses at an IR wavelength of 1030 nm. The laser source operates at high repetition rate (1 – 100000 Hz) and a 2D galvanometric scanning module is fitted to the optical line for rapid displacement (up to 280 $mm \cdot s^{-1}$) of the laser beam (typically 20 µm) at the sample surface with high repositioning precision (< 1µm, 280 $mm \cdot s^{-1}$) in order to design complex trajectories in 2D. The main features of this instrument are unusual compared to more conventional lower repetition rate lasers commonly used for chemical analysis by commercially available nanosecond or femtosecond laser ablation set up. The challenge of this study is to discriminate and classify the bottles of wine based on the elemental composition of glass matrix while causing no visible damage that could affect their value. Therefore, a new ablation cell, which was designed and constructed in our laboratory, consisting of an open ablation cell was used for the direct analysis of bottle samples (See Chapter 4).

The ICPMS used in this study was an ELAN DRC II (Perkin Elmer, USA) in wet plasma conditions using a two inlet nebulization chamber that mixed the dry aerosol together with a nebulized aerosol (Rh 1 $\mu g \cdot L^{-1}$, $HNO_3$ 2% in MilliQ water) via the pneumatic nebulizer. Ablation of transect in glass standard CRM NIST 612 was used on a daily basis to optimize the parameters of the ICPMS to ensure high sensitivity, robustness, reliability and stability (RSD < 3%). Laser ablation of solids can be accompanied by undesirable processes such as fractionation or non-stoichiometric generation of vapor species. Although the study of this phenomenon is out of the scope of the current work, to ensure complete atomization and ionization efficiency of the plasma,

parameters were adjusted to keep the $^{238}U/^{232}Th$ ratio as close as possible to 1 ± 0.05, concluding that the effect of fractionation does not represents a major problem in the proposed methodology.

### 2.3 Ablation parameters and data acquisition

Laser ablation of the glass was performed using ALFAMET laser ablation device (KGW-Yb, 1030 nm) working at 1000 Hz, pulse duration of 360 fs and with an energy of 8.5 J/cm$^2$. The laser beam was operated with a scan speed of 2 mm·s$^{-1}$ and a 50 mm focal length objective was used for laser beam focusing, producing a spot size diameter of 30 µm at the sample surface. The laser beam movement was synchronized with the displacement of the sample (5 µm·s$^{-1}$), via two motorized XY stage, in order to perform more complex trajectories. In this case, a line template (500 x 100 µm) on the glass surface of the bottle was used as ablation pattern. Analyses were made in triplicate. The ablated material was transported through a 1 m-long polyurethane tube (i.d. 4 mm) by an argon gas stream (500 ml·min$^{-1}$) to the ICPMS. Even He is the most employed carrier gas due to its advantages (47), Ar was found to increase the sensitivity significantly (factor 1.5) while keeping U/Th ratio around 1 and then, was preferred. However, the wash-out time (at 99%) was found to be larger (5s) comparing to He (2s), but this criterion was not found to be critical for the study. During the laser ablation analyses, the stability of the plasma was monitored by continuously nebulizing a 1 µg·L$^{-1}$ rhodium standard solution. A 1.8 mL·min$^{-1}$ $H_2$ gas flow (Hydrogen generator, Parker Balston) was introduced in the dynamic reaction cell to prevent polyatomic interferences which could affect the accuracy of the measurements (48, 49). The DRC is a high precision quadrupole that is enclosed and uses a reaction gas to overcome these interferences. The principle of operation is that ions from plasma enter the cell and interact with the gas within the cell. Reactions of charge exchange, atom transfer, adduct formation, condensation and analyte association/condensation are the main mechanisms (50). As shown in Table 4, multiple isotopes of a wide number of elements were analyzed. Potential polyatomic interferences were investigated (51) by comparing the results obtained on different isotopes for given elements (isotopic ratios) to those publish in the literature (52). Where a discrepancy was found, the difference in the calculated ratio was compared against the ratio of major and other abundant element to identify the interference and select a reliable isotope for analysis.

70 isotopes corresponding to 64 analytes, including $^{29}Si$ and $^{103}Rh$, were monitored. CRM NIST 612 and 610 were used as a means of calibration and were also measured in triplicate at the beginning, middle and end of the analytical sequence. Table 4 summarizes the operating conditions used for the laser ablation and ICPMS system.

**Table 4** Operating conditions of fsLA-ICPMS system for glass analysis.

| Laser ablation system: ALFAMET | |
|---|---|
| Wavelength (crystal KGW-Yb) | 1030 |
| Pulse width | 360 fs |
| Spot size | 30 |
| Scan speed | 2 $mm \cdot s^{-1}$ |
| Stage movement | 5 $\mu m \cdot s^{-1}$ |
| Fluence | 8.5 $J \cdot cm^{2}$ |
| Carrier gas (Ar) | 0,5 $L \cdot min^{-1}$ |
| Virtual beam shaping | Line 500x100 µm |
| Wet plasma conditions | Rh 1 ppb, 0.4 rpm |
| Calibrators | CRM NIST 612 and 610 |
| **Mass spectrometer: ELAN DRC II** | |
| RF power | 1100 |
| Nebulizer gas (Ar) | 0.30 $L \cdot min^{-1}$ |
| Plasma gas (Ar) | 17 $L \cdot min^{-1}$ |
| Auxiliary gas (Ar) | 0.85 $L \cdot min^{-1}$ |
| DRC mode ($H_2$) | 1.8 $L \cdot min^{-1}$ |
| Detector | Dual mode |
| Dwell time | 5 ms |
| Signal acquisition | Time Resolved Analysis (TRA) |
| Isotopes | $^{7}Li$, $^{9}Be$, $^{11}B$, $^{23}Na$, $^{24}Mg$, $^{27}Al$, $^{28}Si$, $^{39}K$, $^{43}Ca$, $^{45}Sc$, $^{47}Ti$, $^{51}V$, $^{52}Cr$, $^{53}Cr$, $^{55}Mn$, $^{56}Fe$, $^{59}Co$, $^{60}Ni$, $^{63}Cu$, $^{66}Zn$, $^{71}Ga$, $^{74}Ge$, $^{75}As$, $^{82}Se$, $^{85}Rb$, $^{88}Sr$, $^{89}Y$, $^{90}Zr$, $^{93}Nb$, $^{98}Mb$, $^{103}Rh$, $^{104}Pd$, $^{105}Pd$, $^{107}Ag$, $^{111}Cd$, $^{115}In$, $^{118}Sn$, $^{121}Sb$, $^{133}Cs$, $^{137}Ba$, $^{138}Ba$, $^{139}La$, $^{140}Ce$, $^{141}Pr$, $^{142}Nd$, $^{152}Sm$, $^{15}3Eu$, $^{157}Gd$, $^{158}Gd$, $^{159}Tb$, $^{163}Dy$, $^{164}Dy$, $^{165}Ho$, $^{166}Er$, $^{169}Tm$, $^{174}Yb$, $^{175}Lu$, $^{178}Hf$, $^{180}Hf$, $^{181}Ta$, $^{182}W$, $^{184}W$, $^{187}Re$, $^{189}Os$, $^{195}Pt$, $^{197}Au$, $^{205}Tl$, $^{208}Pb$, $^{209}Bi$ and $^{232}Th$ |

Data was recorded for 20 seconds before the laser was fired to establish a background level. The laser was fired for 90 s and the signal for the three replicates was acquired, although the first and last 10 seconds were not used due to the inherent instability which results when the laser starts and finishes interacting with the sample. After the laser was turned off, the signal was recorded for an additional 20 seconds to confirm that values returned to its blank values (Figure 3). The data was imported into Focal Flash data reduction software (laboratory internal tool for data analysis) for an easier handle of data for the purposed stated.

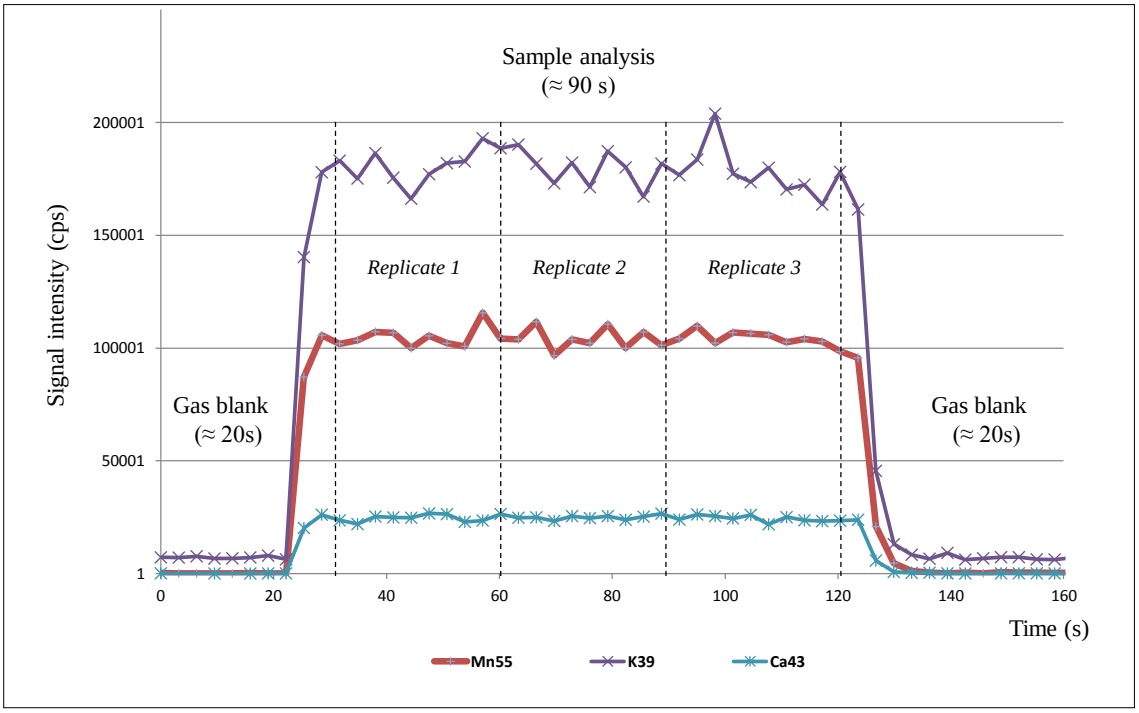


**Figure 4** A typical laser ablation signal for selected isotopes for a bottle glass analysis.

## 2.4 Minimally invasive analysis

Depending on the information required, one might use a combination of truly non-invasive techniques (do not require a sample to be removed from the object), micro-destructive techniques (consume or damage a few amount of material and which may require the removal of a sample) and non-destructive techniques (i.e. a sample or complete object can be re-analyzed for further examination). The development of new analytical methods for quasi-non destructive trace element and isotopic analysis has become increasingly essential in forensic field. Either because the amount of sample is very limited or the samples are precious, non-destructive in situ analysis which not obviously impact the object's visible shape is certainly preferred (53). Chemical analysis using laser ablation requires a small amount of sample (< micrograms). In fact, depending on the analytical measurement system, picogram to femtogram sample quantities may be sufficient for laser ablation analysis (54) . The micro-destructiveness of

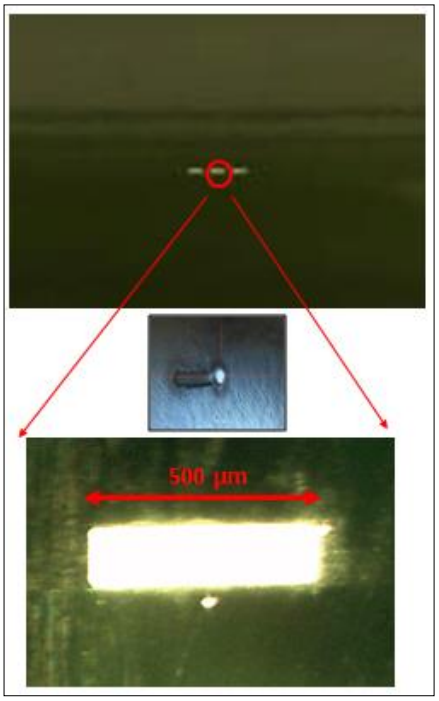


**Figure 5** Line ablation strategy on glass surface (500 x 100 µm) which is almost invisible to naked eye.

ablation processes remains usually within the scale acceptable for environmental, geological, archaeological and forensic applications and, therefore the capability to perform multi-elemental, ultra-trace and isotopic analysis (55). The laser parameters described in the precedent sections result in ablation line 500 x 100 µm (Figure 5). The ablated area is small enough to be almost invisible to naked eye and analysis is thus virtually non-destructive. Although the ablated area dimensions could be reduced, this might affect representativeness of the sampling.

### 2.5 Data pre-processing

Data preprocessing consisted of peak-area integration, background subtraction, and arranging the data in a form suitable for multivariate analysis. The baseline estimated by the average signal measured during the 20 s prior to the ablation was subtracted point by point from the signals measured for each isotope in the ablation peak. The intensity was after normalized relative to the intensity of the internal standard. Normalization in LA-ICPMS allows compensating potential variations in the ablation yield (caused by laser energy drift or sample density), as well as sample transport efficiency and ICPMS detection. A general rule for selecting an internal standard is to use one of the lowest abundant isotopes of the most abundant element supposed to be homogenously distributed in the material to be analyzed. Since glass has a high concentration of silicon (>70%), the intensities of the isotopes were systematically normalized against the Si signal. $^{30}Si$ has the lowest relative abundance (3.09%) but $NO^+$ produces a high background signal at m/z 30. That is why $^{29}Si$ (4.7%) was the best choice to use as internal standard. In order to avoid saturation of the detector, Rpq and Rpa values from the quadrupole of the reaction cell were adjusted to attenuate the number of ions transmitted into the second quadrupole mass filter. Since the concentration of the internal standard (Si) might vary from sample to sample, accurate determination of the 64 analytes concentration would require a precise determination of Si in each sample using an external technique (XRF for instance). Therefore, in this study, interpretation is based on the comparison of the calibrated concentration ratios [M]/[Si] within a spectral profile called M/Si. The calibration curve was obtained by ablating CRM NIST 612 and 610, according to the procedure shown in Figure 6.

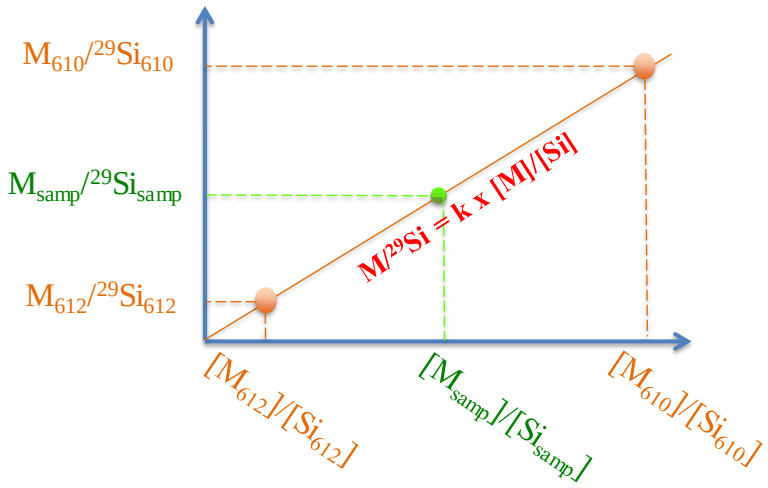


**Figure 6** Construction of calibration curves by ablating CRM NIST 612 and 610.

Where,

$\mathbf{M_{612,\ 610}}$ : NET (blank corrected) signal intensity of the analyte M measured in NIST612 or NIST610

$\mathbf{^{29}Si_{612,\ 610}}$: NET (blank corrected) signal intensity of $^{29}$Si (internal standard) measured in NIST612 or NIST610

$\mathbf{M_{Samp}}$ : NET (blank corrected) signal intensity of the analyte measured in the sample

$\mathbf{^{29}Si_{samp}}$: NET (blank corrected) signal intensity of $^{29}$Si (internal standard) measured in the sample

**[ ]:** Concentration

**k**: slope of the calibration curve

Then, the calculation of the concentration ratios is done according to equation 1.

$$\frac{[M]}{[Si]} = \frac{1}{k} \times \frac{M}{^{29}Si}$$

**Eq. 1**

## 3. Results and discussion

### 3.1 Optimization of the ablation strategy

Compared to static ablation, scanning pattern across a surface produces a constant supply of large and small particles and might lead to more matrix effects and elemental fractionation. The particles that are formed within a single spot ablation are larger when the laser first interacts with the sample and decrease in size with time (56). In addition, single spot ablation generally allows sampling lower amount of material than scanning patterns. This can result in a less representative sampling compared to scan ablation and less reproducible signals if inclusions are ablated. Moreover, depending on the laser operating conditions (e.g. spot size, repetition rate, depth of field, energy), the signal duration within a single spot might not be large enough to perform trustworthy chemometric data analysis. If longer ablation times are desired with a single spot ablation, shorter repetition rates have to be used which would considerably reduce the signal to noise ratios leading to higher detection limits. In the work presented here, the ablation strategy consists of a line of 500 µm large and 100 µm wide (≈ 100 s of ablation). The signal drifts derived from the formation of larger particles that could affect the analytical performance of the method have been compensated by: 1) SRM NIST 612 and 610 matrix-matching calibration standard and 2) the use of a femtosecond pulses resulting in the generation of ultra-fine (Ø <≈ 0,10 nm) which in total better reflects the composition of the bulk material, assuming that losses due to diffusion, gravitational settling and inertial deposition are negligible. As a result, such aerosols should be (i) transportable without significant losses and (ii) sufficiently fine to be atomized within the ICP (57).

### 3.2 Analytical performance of the fsLA-ICPMS method

Analytical performance of the fsLA-ICPMS method was evaluated in terms of long-term reproducibility, in-day repeatability, homogeneity, linearity, method limits of detection and polyatomic interferences.

#### 3.2.1 Long-term reproducibility

In order to know the variability of the developed fsLA-ICPMS based analytical method for the analysis of the glass of the wine packaging, the reproducibility of the obtained results was studied. A randomly selected reference bottle was analyzed in each analysis session (n = 9 sessions) during 3 years for testing the reproducibility of the entire method for long-term method performance validation. A final list of isotopes was selected utilizing approximately 47 isotopes from the 70 analytes originally determined. The selection was based the on analytes giving count rates that were consistently above the limit of quantification (10 σ above the background) during the full

research period. Table 5 shows the final elemental menu and reproducibility of the elemental ratios over 3 years.

**Table 5** Final isotopes list and reproducibility of the Element/Si ratio in a reference bottle (n = 9 sessions) during 3 years.

| Isotope | Average measured elemental ratio (M/Si) | RSD (%) | Isotope | Average measured elemental ratio (M/Si) | RSD (%) |
|---|---|---|---|---|---|
| **Li7** | 3,39E-05 | 11,2 | **Cs133** | 4,57E-06 | 14,3 |
| **Na23** | 2,75E-01 | 2,6 | **Ba138** | 8,02E-04 | 11,0 |
| **Mg24** | 6,00E-03 | 15,3 | **La139** | 1,64E-05 | 12,0 |
| **Al27** | 3,23E-02 | 2,8 | **Ce140** | 4,36E-05 | 10,7 |
| **Ca43** | 2,27E-01 | 5,2 | **Pr141** | 3,60E-06 | 11,0 |
| **Ti47** | 1,42E-03 | 10,0 | **Nd142** | 2,20E-05 | 8,9 |
| **V51** | 2,47E-05 | 4,6 | **Sm152** | 2,97E-06 | 12,6 |
| **Cr52** | 2,15E-03 | 6,2 | **Eu153** | 8,57E-07 | 11,9 |
| **Mn55** | 2,21E-04 | 4,2 | **Gd158** | 2,87E-06 | 7,8 |
| **Fe56** | 9,48E-03 | 8,2 | **Tb159** | 4,02E-07 | 12,2 |
| **Co59** | 8,17E-06 | 6,3 | **Dy164** | 2,00E-06 | 6,1 |
| **Ni60** | 3,40E-05 | 7,5 | **Ho165** | 4,01E-07 | 10,0 |
| **Cu63** | 3,69E-05 | 8,4 | **Er166** | 2,38E-06 | 7,1 |
| **Zn66** | 6,78E-05 | 14,4 | **Tm169** | 1,80E-07 | 7,52 |
| **Ge74** | 2,72E-06 | 13,4 | **Yb174** | 1,22E-06 | 8,4 |
| **As75** | 9,24E-06 | 13,0 | **Lu175** | 1,97E-07 | 11,6 |
| **Rb85** | 1,30E-04 | 12,3 | **Hf180** | 6,07E-06 | 4,2 |
| **Sr88** | 2,92E-04 | 11,4 | **Ta181** | 7,25E-07 | 5,8 |
| **Y89** | 1,27E-05 | 8,7 | **W184** | 1,06E-06 | 8,4 |
| **Zr90** | 2,41E-04 | 6,0 | **Tl205** | 5,17E-07 | 15,0 |
| **Nb93** | 6,18E-06 | 9,4 | **Pb208** | 1,64E-04 | 14,4 |
| **Mo98** | 3,80E-06 | 12,1 | **Bi209** | 9,39E-07 | 13,8 |
| **Ag107** | 1,55E-06 | 12,3 | **Th232** | 5,97E-06 | 13,7 |
| **Sb121** | 1,29E-05 | 10,0 | | | |

### 3.2.2 In-day repeatability

Repeatability is defined as the dispersion of the obtained results, using the same analytical method, the same type of matrix and done it in the same laboratory, by the same operator and using the same equipment. According to European Legislation, repeatability should be expressed as relative standard deviation (RSD, %) indicating the number of replicates (n). In general, RSD values must be equal to or less than 20%. The repeatability of the method was also studied by analyzing the selected reference bottle three times within a same day. The intra-day variation was lower than 10% for most of the elements.

### 3.2.3 Homogeneity

For data quality control purposes, it is very important to provide a good sampling in order to arrive to accurate conclusions. Therefore, it is recommended to sample the known material from different areas to account for natural heterogeneity and to conduct at least three replicates per test sample (58). In this case, it was desirable to know if the non-destructive microanalysis of wine bottles with the proposed method is representative from the full sample. With this aim, a homogeneity study was conducted within given entire bottles (n = 3 bottles, 30 replicates per bottle) and within a given batch of bottles (n= 20 bottles, 3 replicates per bottle) belonging to the same winery and vintage (Chateau Haut Nivelle 2014). Intra-bottle homogeneity and inter-bottle homogeneity were found to be generally consistent, most of them being less than 10% RSD. Zn, Ag, Sb showed higher RSD values, between 12 and 15%. However, some elements (Cr, Mn, Fe, Co, Ni) exhibited excellent intra bottle homogeneity (from 0,6% to 2,3% RSD) while the inter-bottle homogeneity was significantly higher (from 8 to 14% RSD). This might be related to the industrial process, as the melted glass in the oven might be homogenously distributed at a local scale (one bottle is about 450g), but not at the global scale then producing some variations from bottle to bottle. However, the reproducibility was found to be adequate for the purpose of the method in terms of relative standard deviation (RSD < 15%) (Table 6).

**Table 6** Reproducibility of selected isotopes within a single bottle (n = 3 bottles, 30 replicates per bottle) and within a lot of bottles belonging to a same winery and vintage (n = 20 bottles, 3 replicates per bottle).

| | **Homogeneity within a bottle (M/Si)** | | **Homogeneity within a batch (M/Si)** | |
|---|---|---|---|---|
| | **Average elemental ratio (M/Si)** | **RSD (%)** | **Average elemental ratio ( M/Si)** | **RSD (%)** |
| **Li7** | 4,27E-05 | **7,5** | 4,28E-05 | **9,8** |
| **Na23** | 2,65E-01 | **1,1** | 2,67E-01 | **2,6** |
| **Mg24** | 1,25E-02 | **2,2** | 1,38E-02 | **7,3** |
| **Al27** | 2,78E-02 | **0,8** | 2,90E-02 | **6,2** |
| **Ca43** | 2,29E-01 | **0,5** | 2,38E-01 | **3,1** |
| **Ti47** | 8,92E-04 | **2,1** | 1,03E-03 | **5,4** |
| **V51** | 2,40E-05 | **1,8** | 2,40E-05 | **6,4** |
| **Cr52** | 1,94E-03 | **2,2** | 1,86E-03 | **9,2** |
| **Mn55** | 7,12E-04 | **0,6** | 6,73E-04 | **13,8** |
| **Fe56** | 9,39E-03 | **1,0** | 9,20E-03 | **9,5** |
| **Co59** | 2,45E-05 | **2,3** | 2,31E-05 | **10,8** |
| **Ni60** | 3,86E-05 | **1,9** | 3,59E-05 | **8,2** |
| **Cu63** | 5,19E-05 | **6,1** | 4,93E-05 | **11,4** |
| **Zn66** | 2,31E-04 | **13,9** | 2,34E-04 | **11,6** |
| **Ge74** | 2,33E-06 | **8,4** | 2,27E-06 | **10,8** |
| **As75** | 2,94E-05 | **10,8** | 2,65E-05 | **5,8** |
| **Rb85** | 7,97E-05 | **6,8** | 7,19E-05 | **8,3** |
| **Sr88** | 6,40E-04 | **7,3** | 5,72E-04 | **7,0** |
| **Y89** | 1,27E-05 | **7,0** | 1,21E-05 | **4,2** |

| | | | | |
|---|---|---|---|---|
| **Zr90** | 4,42E-04 | **5,3** | 4,31E-04 | **10,3** |
| **Nb93** | 1,52E-05 | **7,3** | 1,34E-05 | **12,0** |
| **Mo98** | 4,85E-06 | **8, 8** | 4,36E-06 | **15,0** |
| **Ag107** | 3,28E-06 | **13,8** | 3,80E-06 | **15,0** |
| **Sb121** | 4,16E-05 | **13,1** | 3,85E-05 | **13,9** |
| **Cs133** | 4,83E-06 | **10,0** | 4,14E-06 | **7,2** |
| **Ba138** | 2,23E-03 | **10,2** | 1,99E-03 | **3,9** |
| **La139** | 2,11E-05 | **9,5** | 1,88E-05 | **4,7** |
| **Ce140** | 8,37E-05 | **9,2** | 7,26E-05 | **8,2** |
| **Pr141** | 3,82E-06 | **9,2** | 3,42E-06 | **3,8** |
| **Nd142** | 3,62E-05 | **6,7** | 3,28E-05 | **6,8** |
| **Sm152** | 3,38E-06 | **10,0** | 3,89E-06 | **8,0** |
| **Eu153** | 1,20E-06 | **10,1** | 1,50E-06 | **10,2** |
| **Gd158** | 3,11E-06 | **10,2** | 2,95E-06 | **5,9** |
| **Tb159** | 3,76E-07 | **8,7** | 3,86E-07 | **7,9** |
| **Dy164** | 2,25E-06 | **6,5** | 2,25E-06 | **6,4** |
| **Ho165** | 3,70E-07 | **6,2** | 3,57E-07 | **8,0** |
| **Er166** | 9,87E-06 | **5,5** | 9,24E-06 | **11,6** |
| **Tm169** | 1,71E-07 | **7,7** | 1,66E-07 | **10,3** |
| **Yb174** | 1,29E-06 | **5,6** | 1,30E-06 | **7,8** |
| **Lu175** | 1,95E-07 | **6,3** | 1,90E-07 | **8,6** |
| **Hf180** | 1,05E-05 | **2,3** | 1,08E-05 | **9,9** |
| **Ta181** | 9,11E-07 | **5,8** | 8,86E-07 | **8,4** |
| **W184** | 2,15E-06 | **4,3** | 2,07E-06 | **9,8** |
| **Tl205** | 1,44E-07 | **8,4** | 1,58E-07 | **13,5** |
| **Pb208** | 6,58E-04 | **12,0** | 6,35E-04 | **8,4** |
| **Bi209** | 2,42E-06 | **11,8** | 2,35E-06 | **7,8** |
| **Th232** | 5,20E-06 | **9,4** | 4,77E-06 | **4,3** |

### 3.2.4 Linearity

There are few number of glass standards that are certified for the elements of interest at trace levels. SRM NIST 612 (about 50 $\mu g \cdot g^{-1}$) and 610 (about 500 $\mu g \cdot g^{-1}$) synthetic glasses were employed for matrix-matching external calibration. Whenever the concentrations are not certified, the values used were obtained from concentrations reported in the literature (GEOREM) (59). For all elements, linear regression correlation coefficients, $r^2$, were better than 0.9999.

### 3.2.5 Limits of detection

Detection limits in LA-ICPMS depend on the volume of ablated material, the analyte mass, the ionization energy of the analyte, its isotopic abundance and the ion transmission efficiency. In addition, the actual detection limits of a method depend also on the operational conditions of the instrument. The values presented are calculated for SRM NIST 612 and were used as reference values since they were obtained as the average of several sets of conditions used in different days during the full research period (Table 7). The values were calculated using the 3σ criterion, which is three times the standard deviation of the noise (gas blank) divided by the slope without internal

standard normalization. Under our conditions, detection limits range between 2 ppm (Fe) and 6 ppb (Ce).

**Table 7** Limits of Detections for the selected isotopes calculated by the 3σ criterion.

| Isotope | LD (ppm) | Isotope | LD (ppm) | Isotope | LD (ppm) |
|---|---|---|---|---|---|
| **Li7** | 0,514 | **Rb85** | 0,323 | **Gd158** | 0,112 |
| **Na23** | 4,057 | **Sr88** | 0,089 | **Tb159** | 0,012 |
| **Mg24** | 0,404 | **Y89** | 0,009 | **Dy164** | 0,040 |
| **Al27** | 1,218 | **Zr90** | 0,012 | **Ho165** | 0,008 |
| **Ca43** | 509,031 | **Nb93** | 0,018 | **Er166** | 0,017 |
| **Ti47** | 20,491 | **Mo98** | 0,072 | **Tm169** | 0,022 |
| **V51** | 0,322 | **Ag107** | 0,013 | **Yb174** | 0,023 |
| **Cr52** | 0,251 | **Sb121** | 0,086 | **Lu175** | 0,008 |
| **Mn55** | 0,237 | **Cs133** | 0,013 | **Hf180** | 0,020 |
| **Fe56** | 2,005 | **Ba138** | 0,042 | **Ta181** | 0,013 |
| **Co59** | 0,124 | **La139** | 0,006 | **W184** | 0,016 |
| **Ni60** | 0,539 | **Ce140** | 0,006 | **Tl205** | 0,005 |
| **Cu63** | 0,134 | **Pr141** | 0,027 | **Pb208** | 0,025 |
| **Zn66** | 1,124 | **Nd142** | 0,131 | **Bi209** | 0,028 |
| **Ge74** | 0,288 | **Sm152** | 0,022 | **Th232** | 0,016 |
| **As75** | 0,333 | **Eu153** | 0,025 | | |

### 3.3 Casework glass sample set

It is generally accepted the revolution in the use of multivariate methods took place in psychometrics in the 1930s and 1940s. In this research, multivariate statistical data evaluation was done with software package XLSTAT® (2016) and The Unscrambler from CAMO version 9.1 (Computer Aided Modelling, Trondheim, Canada) in which different classification or pattern recognition techniques such as Principal Component Analysis (PCA), Agglomerative Hierarchical Clustering (AHC) and Soft Independent Modelling of Class Analogy (SIMCA) have been employed. A matrix was constructed with rows representing wine bottle samples and columns representing the M/Si elemental ratios from fsLA-ICPMS.

For an initial classification, the principal component analysis (PCA) is commonly used as an exploratory data analysis (EDA) technique to detect groups in the measured data set. PCA attempts to identify underlying variables or factors that better explain the pattern of correlations within a set of variables without having previously formulated a hypothesis. The first principal component represents the maximum variation of the data set and corresponds to the direction explaining the maximum variance; the second PC corresponds to the direction, orthogonal to the first PC, explaining the maximum variance not explained by the first PC, and so on. It is therefore

a data reduction tool which allows identifying a small number of factors that explain most of the variance observed in a much larger number of manifest variables as well as outlier samples (60).

In addition, agglomerative hierarchical classification (AHC) was also employed for unsupervised pattern recognition, mainly consisting of cluster analysis which is able to identify groupings among samples by means of a similarity measurement. The results of a hierarchical clustering study are usually displayed as a dendrogram, which is a tree shaped map of the inters ample distances in the data set. The dendrogram shows the merging of samples into clusters at various stages of the analysis and the similarities at which the clusters merge, with the clustering displayed hierarchically. The main branches of the dendrogram represent bigger divisions. There is no cluster validity measure that can serve as an indicator of the quality. Hence, clusters are defined intuitively, depending on the context of the problem, not mathematically, which limits the utility of this technique. Clearly, prior knowledge about the problem is essential when using these methods (61). In this work, specifically, there was previous information about the original and counterfeited origin of the bottle samples.

Finally, as a second classification step, supervised classification tool as the soft independent modelling of class analogy (SIMCA) approach was employed in which a partial least squares (PLS) classification is performed in order to identify local models for possible groups and to predict a probable class membership for new observations. At first, this statistical approach runs a global principal component analysis on the whole dataset in order to identify groups of observations. Local models are then estimated for each class. Finally, new observations are classified to one of the established class models on the basis of their best fit to the respective model. Full cross-validation (leaving some of the known samples out) ensures that the model size can be determined directly from the data. While other supervised classification tools require large sample sizes and low within-class variability for good classification results, SIMCA is an established method for multivariate classification especially for high within-class variability, which result to be valuable for the objectives of this work in which high sample variability is expected (62, 63).

As a pre-treatment before statistical analysis, all data was centered-normalized with logarithm and mean normalization provided by both XLSTAT and The Unscrambler softwares. Mean normalization is the most classical case of normalization. It consists of dividing each row of a data matrix by its average, thus neutralizing the influence of the hidden factors such as noise or drift between analyses. Only the relative values of the variables are used to describe the sample (64).

### 3.3.1 Casework 1: genuine vs. counterfeited bottles

The first sample set analyzed in this work consists of 8 green bottles supposed to originate from the French region of Pauillac, divided into genuine (5 samples) and counterfeited (3 samples coming from China). The high quality of the counterfeited bottle makes impossible to discriminate them from the genuine bottles with the naked eye.

A PCA model with two PCs explains 99% of the variation in the data for the genuine and counterfeited wine bottles, being the residuals < 1 for all the scores, was developed. The biplot (Figure 7) reveals that separation along PC1 accounts for the 88% of the variation in the sample set, while separation along PC2 accounts for the 11%. Two groups FRANCE and CHINA are clearly distinguished. Among the forty seven monitored isotopes, four of them ($Al^{27}$, $Eu^{153}$, $Ba^{138}$ and $W^{184}$, respectively) were found to be the responsible for such discrimination. Chinese bottles are characterized by the selected descriptors while French bottles shown lack of them. For this variable reduction, an initial PCA was run taking into account all the analyzed variables. After, the most significant (contribution of the observations, %) variables were selected from PC1, PC2 and PC3 and their correlations were studied within the correlation matrix (Pearson (n)). To select correlation threshold value from which two variables are significantly correlated, the statistical significance of the Coefficient of Correlation (r) values were studied by transforming them into t experimental values according to the equation 2 for a *p value < 0.005* and n-2 grades of freedom.

$$t_{exp} = \frac{r}{\sqrt{\frac{1 - r^2}{n - 2}}}$$

**r** = Coefficient of correlation
**n** = number of samples

$\mathbf{t_{exp}} < \mathbf{t_{crit}}$ → there is no correlation between the studied variables
$\mathbf{t_{exp}} > \mathbf{t_{crit}}$ → there is high correlation between the studied variables

**Eq. 2**

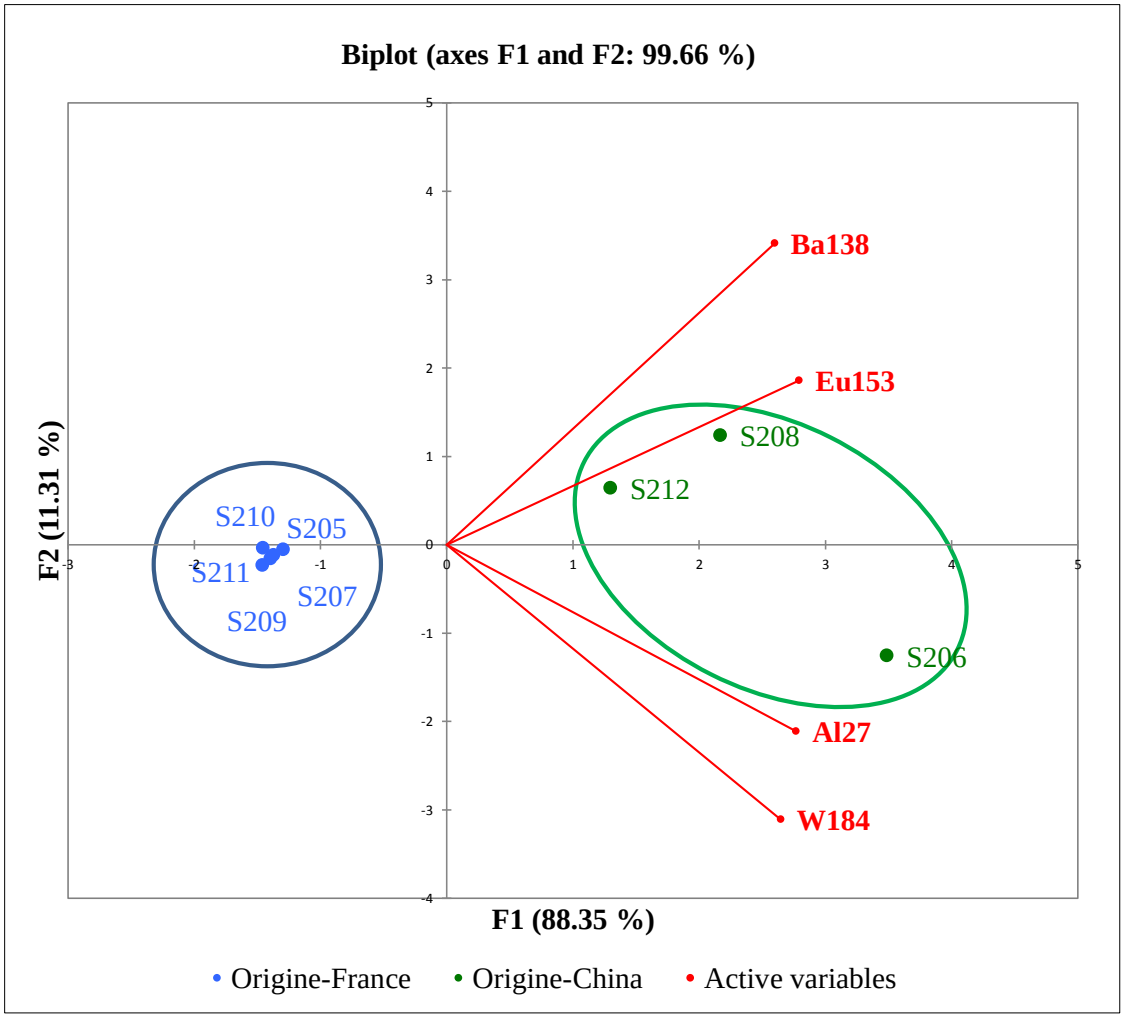


**Figure 7** Biplot (PC1 vs PC2) representing French original bottles (in blue) and Chinese counterfeited bottles (in green) with the loadings (variables) responsible of such discrimination.

On the second attempt for classifying the original and counterfeited bottles a cluster analysis has been carried out to discover sample grouping within a data. Clustering methods attempt to find clusters of patterns in the measurement space. Although several clustering algorithms exist, hierarchical clustering is by far the most widely used clustering method. The starting point for a hierarchical clustering experiment is the similarity matrix which is formed by first computing the distances between all pairs of points in the data set.

To perform the cluster analysis the factor scores (F1, F2, F3 and F4) from the previous PCA were used. In fact, a factor analysis reduces the dimensions and therefore the number of variables makes it easier to run the cluster analysis. The classification was run by applying straight-line distance and Ward's agglomeration method. This type of distance is also referred to as Euclidean distance and is the most commonly used type when it comes to analyzing ratio data. In agglomerative clustering, clusters are consecutively formed from objects. Initially, this type of procedure starts with each object representing an individual cluster. These clusters are then

sequentially merged according to their similarity. It appears, from the dendrogram in Figure 8, that the data can be represented by 3 classes. Class 1 corresponds exclusively to the original French bottles while counterfeited Chinese bottles are divided into Class 2 and Class 3.

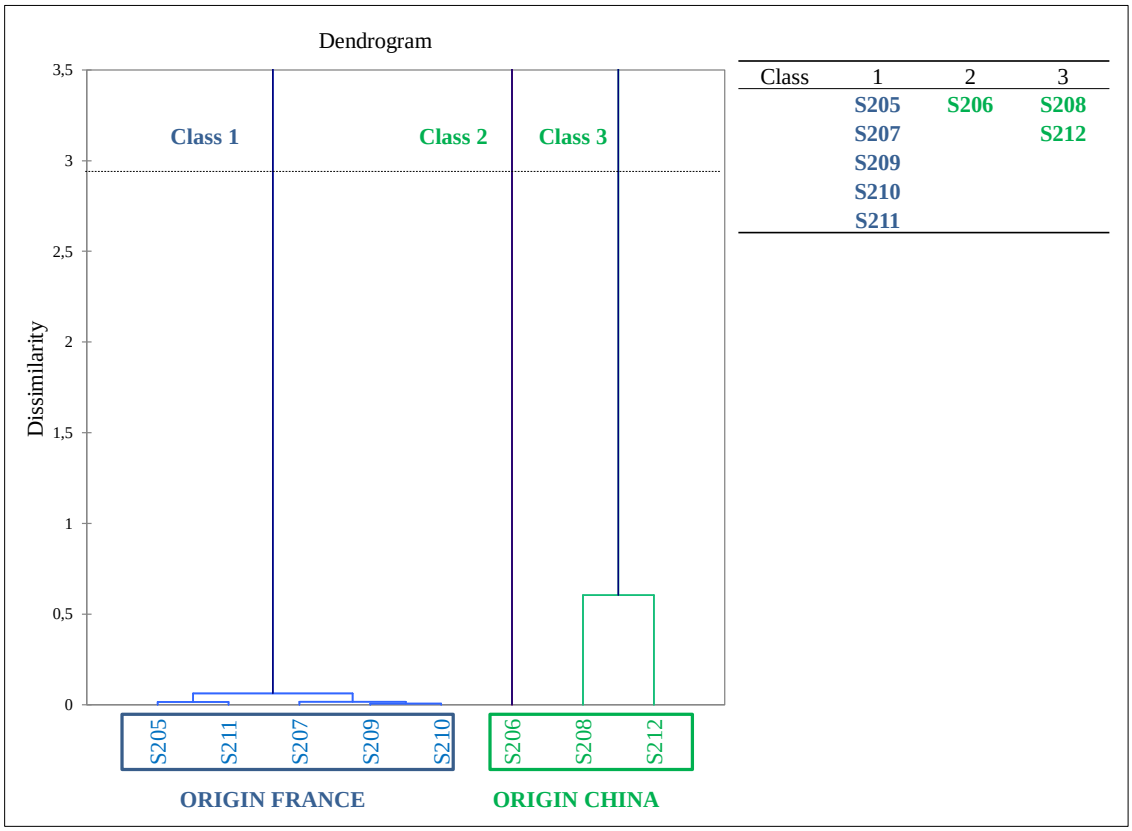


**Figure 8** Clustering of original French bottles (in blue) and counterfeited Chinese bottles (in green). Dendrogram showing dissimilarity (Euclidian distance) and Ward agglomeration method.

The distances between samples are usually expressed by means of a distance matrix, which provides information on the objects being combined at each stage of the clustering process (Table 8). Objects with smaller distances between one another are more similar, whereas objects with larger distances are more dissimilar.

**Table 8** Proximity matrix (Euclidian distance) of the original French bottles (in blue) and counterfeited Chinese bottles (in green).

| | S205 | S206 | S207 | S208 | S209 | S210 | S211 | S212 |
|---|---|---|---|---|---|---|---|---|
| S205 | 0 | 5,093 | 0,345 | 3,848 | 0,248 | 0,217 | 0,176 | 2,842 |
| S206 | 5,093 | 0 | 5,051 | 2,825 | 5,005 | 4,988 | 4,928 | 2,904 |
| S207 | 0,345 | 5,051 | 0 | 3,912 | 0,124 | 0,204 | 0,331 | 2,902 |
| S208 | 3,848 | 2,825 | 3,912 | 0 | 3,828 | 3,787 | 3,698 | 1,099 |
| S209 | 0,248 | 5,005 | 0,124 | 3,828 | 0 | 0,115 | 0,212 | 2,817 |
| S210 | 0,217 | 4,988 | 0,204 | 3,787 | 0,115 | 0 | 0,154 | 2,785 |
| S211 | 0,176 | 4,928 | 0,331 | 3,698 | 0,212 | 0,154 | 0 | 2,689 |
| S212 | 2,842 | 2,904 | 2,902 | 1,099 | 2,817 | 2,785 | 2,689 | 0 |

### 3.3.2 Casework 2: collection of a bottle series from the same wine cellar

The second sample set comprises 34 *bordelaise* bottles belonging to a famous French Château and which are classified according to their vintage:

*60s*: 1969

*70s*: 1973, 1974, 1978, 1979

*80s*: 1981, 1982, 1983, 1984, 1985, 1986, 1987, 1988, 1989

*90s*: 1990, 1992, 1993, 1994, 1995, 1996, 1997, 1998, 1999

*00s*: 2000, 2001, 2002, 2003, 2004, 2005, 2006, 2007, 2008, 2009

*10s*: 2010

A PCA (PC1 vs. PC2) explaining the 70% of the variation in the dataset, the residuals < 1 for all the scores, is shown in Figure 9. It reveals that separation along PC1 accounts for the 52% of the variation in the sample set, while separation along PC2 accounts for the 18%. Five groups chronologically arranged are distinguishable. Among the forty-seven monitored isotopes, thirty-five of them ($^{7}$Li, $^{23}$Na, $^{24}$Mg, $^{27}$Al, $^{43}$Ca, $^{51}$V, $^{52}$Cr, $^{55}$Mn, $^{60}$Ni, $^{63}$Cu, $^{66}$Zn, $^{75}$As, $^{85}$Rb, $^{89}$Y, $^{93}$Nb, $^{121}$Sb, $^{133}$Cs, $^{138}$Ba, $^{139}$La, $^{140}$Ce, $^{141}$Pr, $^{142}$Nd, $^{152}$Sm, $^{153}$Eu, $^{158}$Gd, $^{159}$Tb, $^{164}$Dy, $^{165}$Ho, $^{166}$Er, $^{169}$Tm, $^{174}$Yb, $^{175}$Lu, $^{181}$Ta, $^{184}$W and $^{208}$Pb, respectively) were found to be the responsible for such group discrimination. For this variable reduction and finding which ones were the most discriminant, an initial PCA was run taking into account all the analyzed variables. After, the most significant (contribution of the observations, %) variables were selected from PC1, PC2 and PC3 and their correlations were studied within the correlation matrix (Pearson (n)). To select correlation threshold value from which two variables are significantly correlated, the statistical significance of the Coefficient of Correlation (r) values were studied by transforming them into t experimental values according to the equation 1 for a $p\ value < 0.005$ and n-2 grades of freedom.

Having a look to Figure 10, which shows the distribution of the selected variables in PC1 and PC2, it is observable how they are almost symmetrically divided among the negative and positive sides of the PC1 axis. In general, it is possible to observe how major elements as sodium, magnesium and aluminium together with rare earths are located in the right side of the axis, being responsible for the discrimination of the ancient bottles (60s, 70s and mid-80s). On the contrary, the left side of the axis is represented by fewer amounts of major elements (absence of sodium, magnesium and aluminium) and trace elements, being responsible for the discrimination of the recent bottles (90s, 00s and 10s).

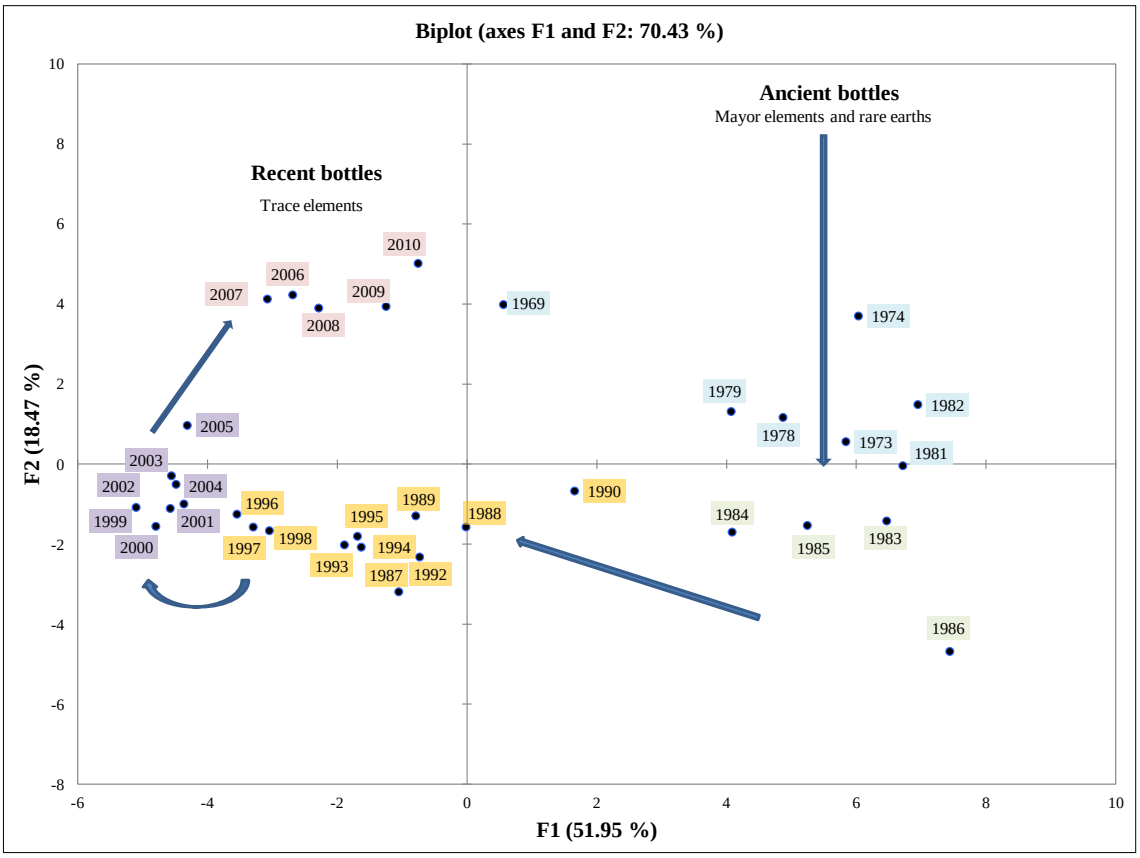


**Figure 9** PCA (PC1 vs. PC2) for the 34 samples coming from the same winery but different vintage.

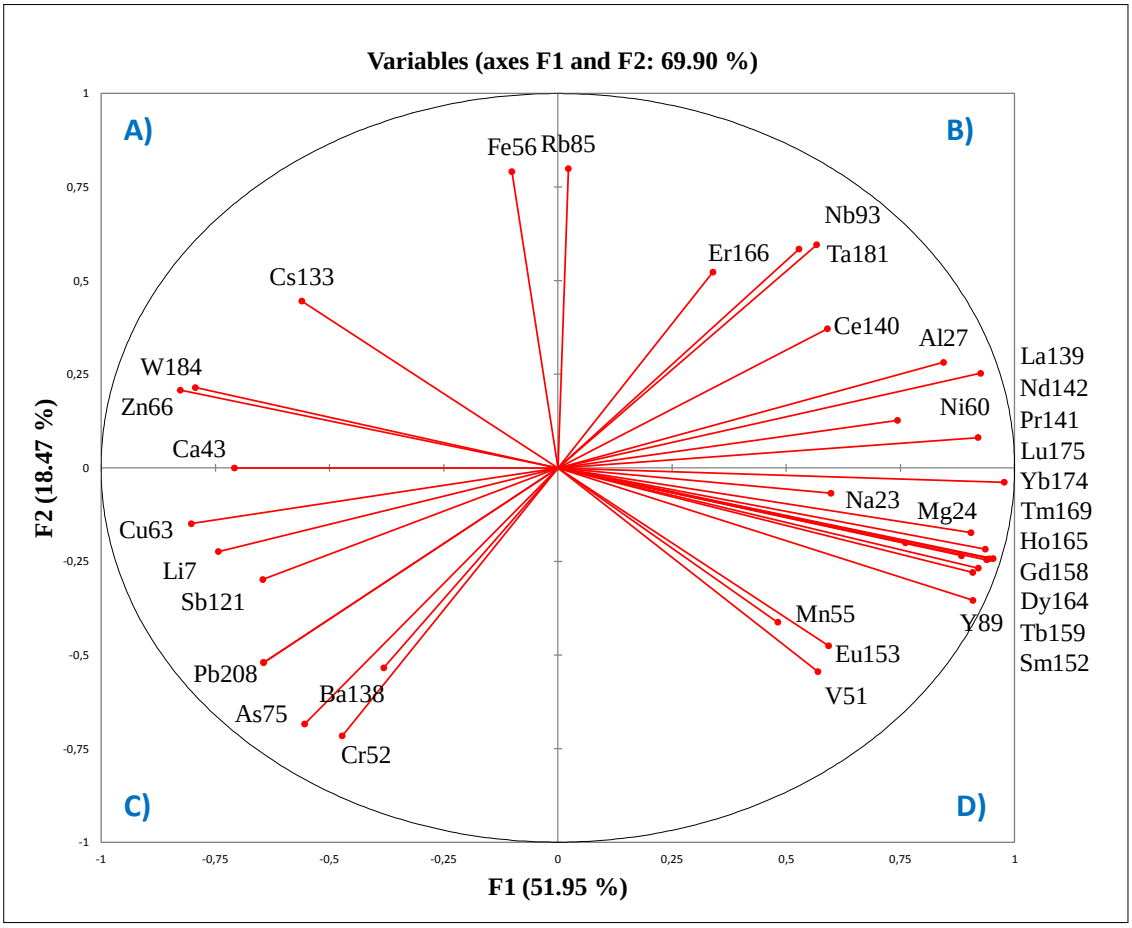


**Figure 10** Distribution of the selected variables in PC1 and PC2. A, B, C and D (in blue) indicate the quadrants for a better comprehension of the variables having influence in each sample group.

For a deeper insight into the variables having influence in each group, one's must pay attention to the variables located in each quadrant (A, B, C, and D) in Figure 10 and the individual charts for each isotope/vintage in Figure 11.

On the one hand, the isotopes having more influence in the classification of the bottles from the 60s, 70s and early 80s (▭) are those located in the upper-right quadrant (B). Special attention must to be paid to Rb and Fe that makes the difference for the 1969 bottle. In this case, Rb has great influence in the 00s and 10s bottles as well. In addition, $^{27}$Al, $^{60}$Ni, $^{93}$Nb, $^{140}$Ce, $^{166}$Er and $^{181}$Ta are the most remarkable isotopes for the 60s, 70s and early 80s (1981 and 1982).

On the other hand, for the bottles situated in the lower-right quadrant (D) corresponding to the mid- 80s (1983, 1984, 1955 and 1986) ( ▭), the most remarkable elements are V, Mn, and Eu. A special mention must to be done to the manganese and chromium (isotope corresponding to C quadrant). According to the literature, green color was firstly given by iron or chromium oxide, and manganese was added to achieve a more stable and lighter color (65). However, from the year

1986 the elemental ratio of manganese decrease considerably while chromium elemental ratio increase. Furthermore, the chromium level decreases from the year 2000, being this drop more noticeable from 2006-2010. In fact, these bottles have a high elemental ratio of iron which is added to protect wine from UV radiation during storage and they have a noticeable darker green color (Figure 12) (66).

**Figure 12** Change of the intensity of green color from the ancient bottles (light green) to newest bottles (dark green)

Apart from the specific elements that have influence in the bottles of 60s, 70s and mid-80s in the upper-lower right quadrants (B and D), rare earths and major elements are the responsible variables for the discrimination of these ancient bottles from the newest bottles. Authors' hypothesis for explaining such change concerning the major elements, which mainly arise from raw material, could possibly be the recycling. In the 70s, recycling started becoming more popular which reduced the need for raw materials to be quarried thus saving precious resources. In addition, less energy is needed to melt recycled glass than to melt down raw materials, thus saving energy too (67). Consequently, as the recycling practice has been gradually implemented in the last years, which reduces the use of raw materials and leads to the homogenization of the impurities.

The bottles situated in the lower-left quadrant (C) correspond to last-80s (1987, 1988 and 1989), 90s and mid-00s (2000, 2001, 2002, 2003, 2004 and 2005). However, a distinction can be observed between last-80s and 90s (▭) bottles from mid-00s bottles (▭). For the last-80s and 90s bottles, $As^{75}$, $Cr^{52}$, $Ba^{138}$ and $Pb^{208}$ seems to be the most influent isotopes. The addition of lead to glassmaking is characterized by more brighter and more refractive glass. For the mid-00s, $Li^{7}$, $Cu^{63}$ and $Sb^{121}$ are the most remarkable isotopes.

Finally, the late-00s and 2010 bottles ( ) are characterized by the $Ca^{43}$, $Zn^{66}$, $Cs^{133}$ and $W^{184}$. But above all, the most representative isotope of this group is $Fe^{56}$, as it has been mentioned above, is the responsible of the darker green color. It's also worth noticing that some vintages could be identified with only one M/Si ratio, these remarkable M/Si ratios exhibiting "abnormal" values are: 2010 (Fe/Si), 1990 (Zn/Si, Mo/Si, Ag/Si), 1987 (Sr/Si, Sb/Si, Pb/Si), 1986 (V/Si, Eu/Si), 1982 (Cr/Si, Co/Si), 1981 (Co/Si), 1979 (Mn/Si), 1974(Cu/Si, Nb/Si) and 1973 (Cu/Si).

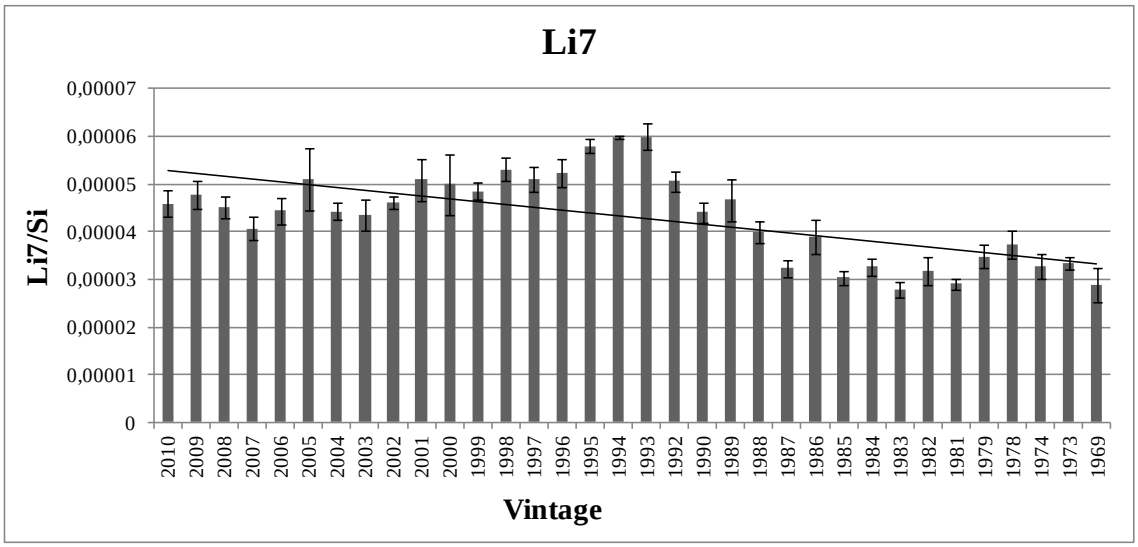
Li7
Li7/Si
0,00007
0,00006
0,00005
0,00004
0,00003
0,00002
0,00001
0
2010 2009 2008 2007 2006 2005 2004 2003 2002 2001 2000 1999 1998 1997 1996 1995 1994 1993 1992 1990 1989 1988 1987 1986 1985 1984 1983 1982 1981 1979 1978 1974 1973 1969
Vintage

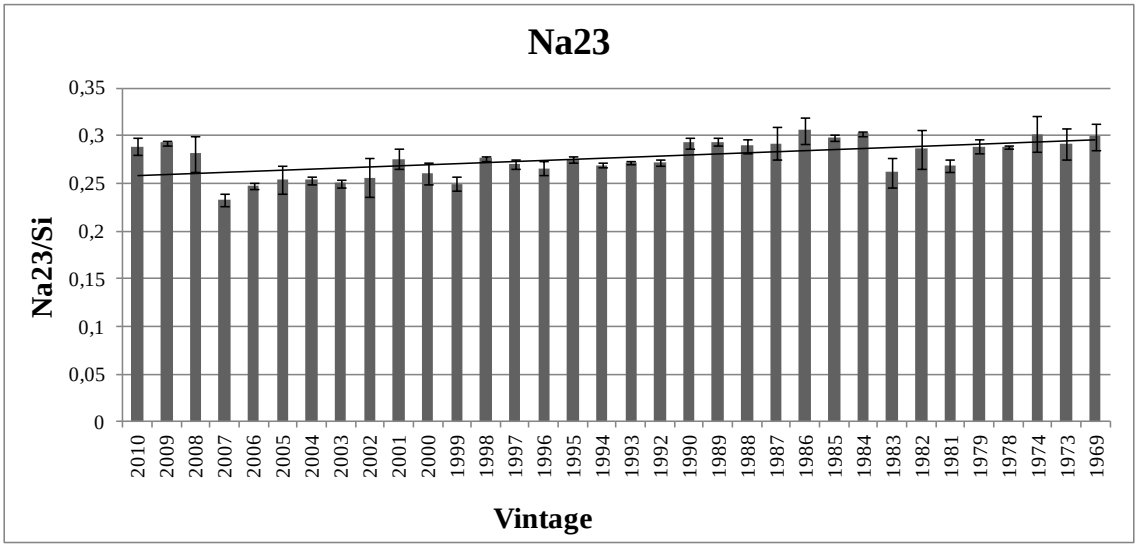
Na23
Na23/Si
0,35
0,3
0,25
0,2
0,15
0,1
0,05
0
2010 2009 2008 2007 2006 2005 2004 2003 2002 2001 2000 1999 1998 1997 1996 1995 1994 1993 1992 1990 1989 1988 1987 1986 1985 1984 1983 1982 1981 1979 1978 1974 1973 1969
Vintage

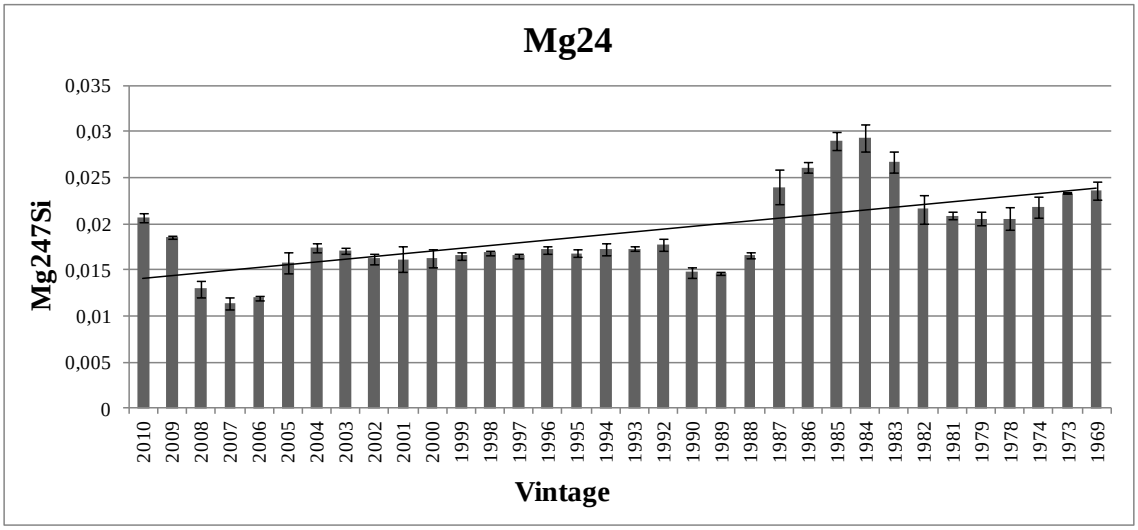
Mg24
Mg247Si
0,035
0,03
0,025
0,02
0,015
0,01
0,005
0
2010 2009 2008 2007 2006 2005 2004 2003 2002 2001 2000 1999 1998 1997 1996 1995 1994 1993 1992 1990 1989 1988 1987 1986 1985 1984 1983 1982 1981 1979 1978 1974 1973 1969
Vintage

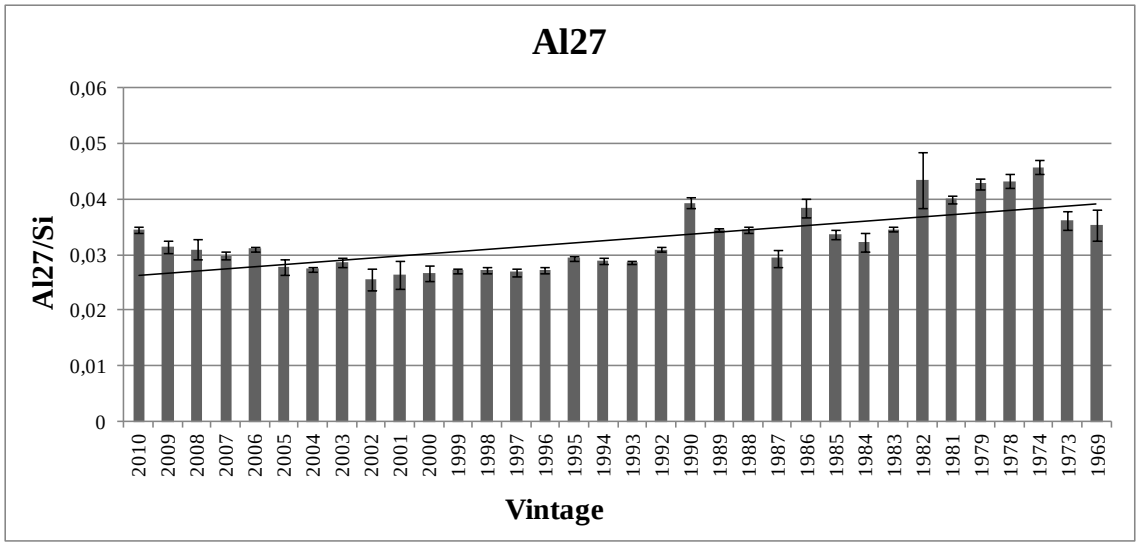
Al27
Al27/Si
0,06
0,05
0,04
0,03
0,02
0,01
0
2010 2009 2008 2007 2006 2005 2004 2003 2002 2001 2000 1999 1998 1997 1996 1995 1994 1993 1992 1990 1989 1988 1987 1986 1985 1984 1983 1982 1981 1979 1978 1974 1973 1969
Vintage

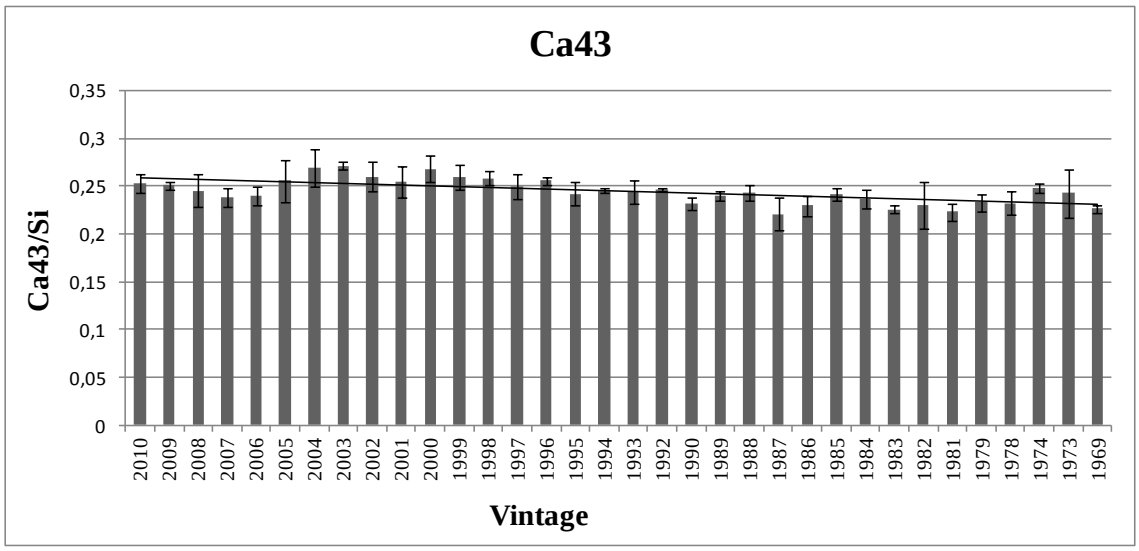
Ca43
Ca43/Si
0,35
0,3
0,25
0,2
0,15
0,1
0,05
0
2010 2009 2008 2007 2006 2005 2004 2003 2002 2001 2000 1999 1998 1997 1996 1995 1994 1993 1992 1990 1989 1988 1987 1986 1985 1984 1983 1982 1981 1979 1978 1974 1973 1969
Vintage

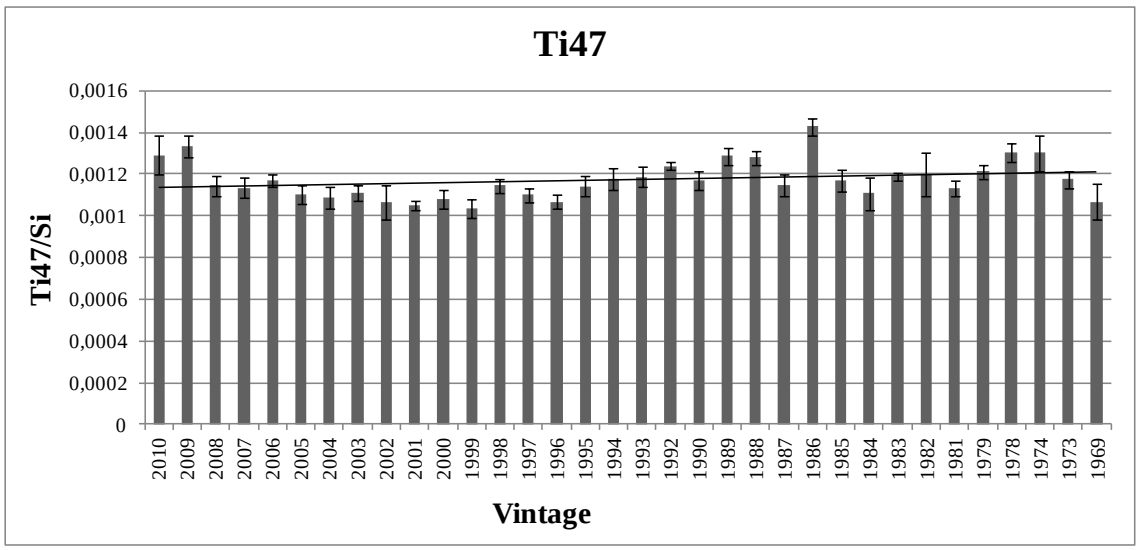
Ti47
Ti47/Si
0,0016
0,0014
0,0012
0,001
0,0008
0,0006
0,0004
0,0002
0
2010 2009 2008 2007 2006 2005 2004 2003 2002 2001 2000 1999 1998 1997 1996 1995 1994 1993 1992 1990 1989 1988 1987 1986 1985 1984 1983 1982 1981 1979 1978 1974 1973 1969
Vintage

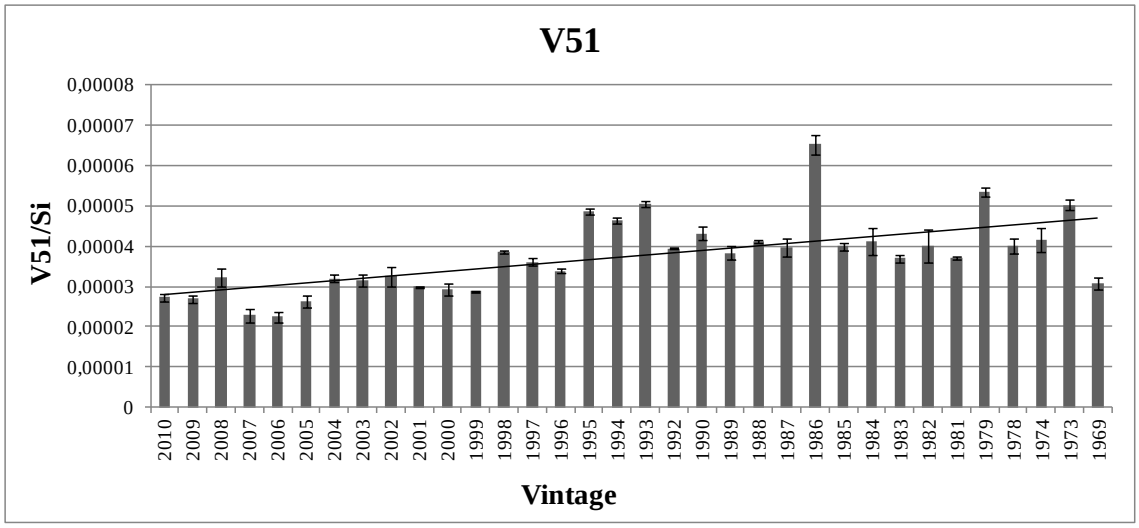
V51
V51/Si
0,00008
0,00007
0,00006
0,00005
0,00004
0,00003
0,00002
0,00001
0
2010 2009 2008 2007 2006 2005 2004 2003 2002 2001 2000 1999 1998 1997 1996 1995 1994 1993 1992 1990 1989 1988 1987 1986 1985 1984 1983 1982 1981 1979 1978 1974 1973 1969
Vintage

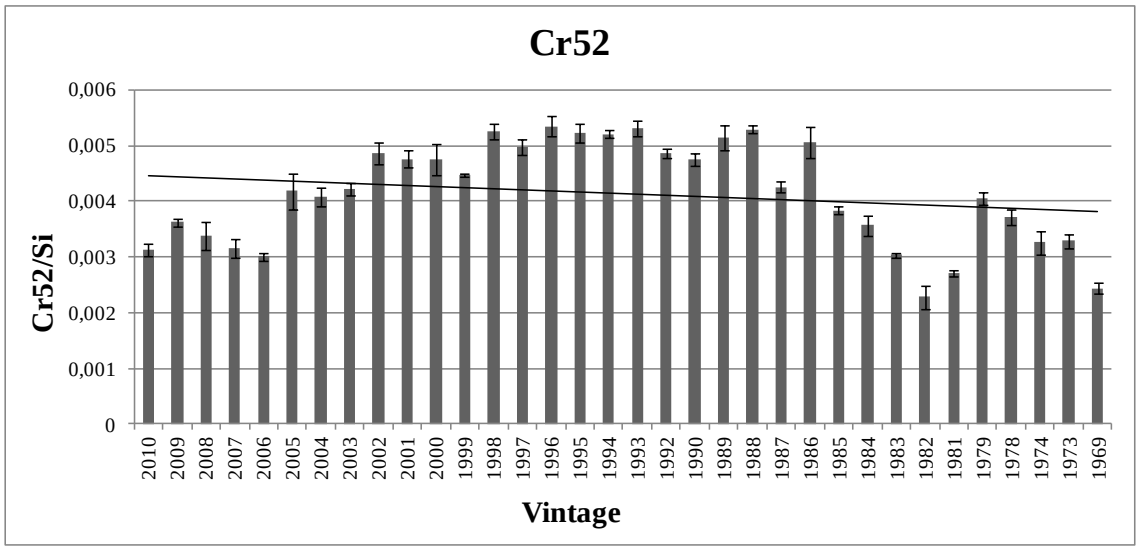
Cr52
Cr52/Si
0,006
0,005
0,004
0,003
0,002
0,001
0
2010 2009 2008 2007 2006 2005 2004 2003 2002 2001 2000 1999 1998 1997 1996 1995 1994 1993 1992 1990 1989 1988 1987 1986 1985 1984 1983 1982 1981 1979 1978 1974 1973 1969
Vintage

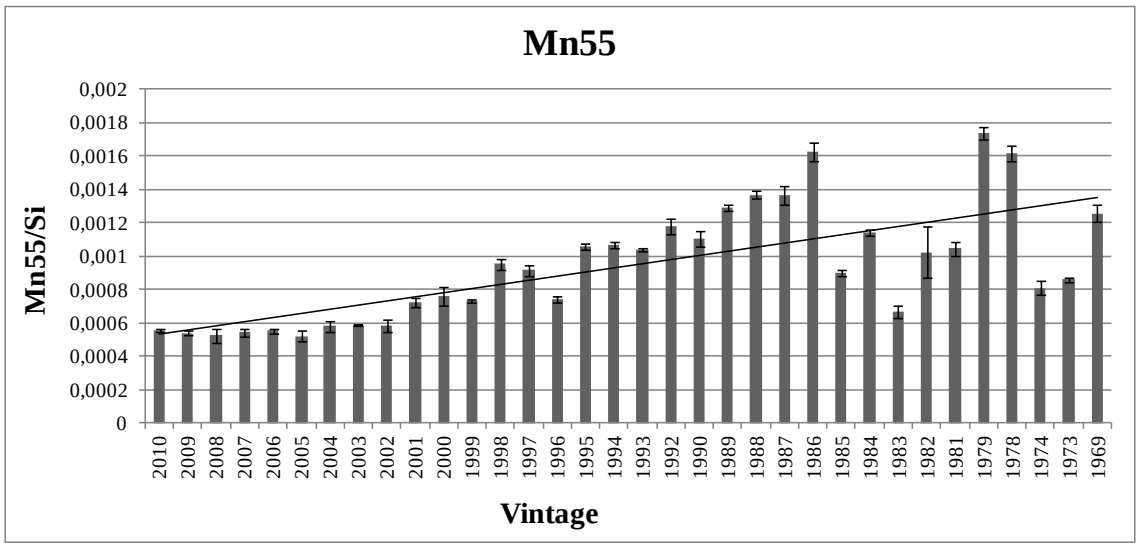
Mn55
Mn55/Si
0,002
0,0018
0,0016
0,0014
0,0012
0,001
0,0008
0,0006
0,0004
0,0002
0
2010 2009 2008 2007 2006 2005 2004 2003 2002 2001 2000 1999 1998 1997 1996 1995 1994 1993 1992 1990 1989 1988 1987 1986 1985 1984 1983 1982 1981 1979 1978 1974 1973 1969
Vintage

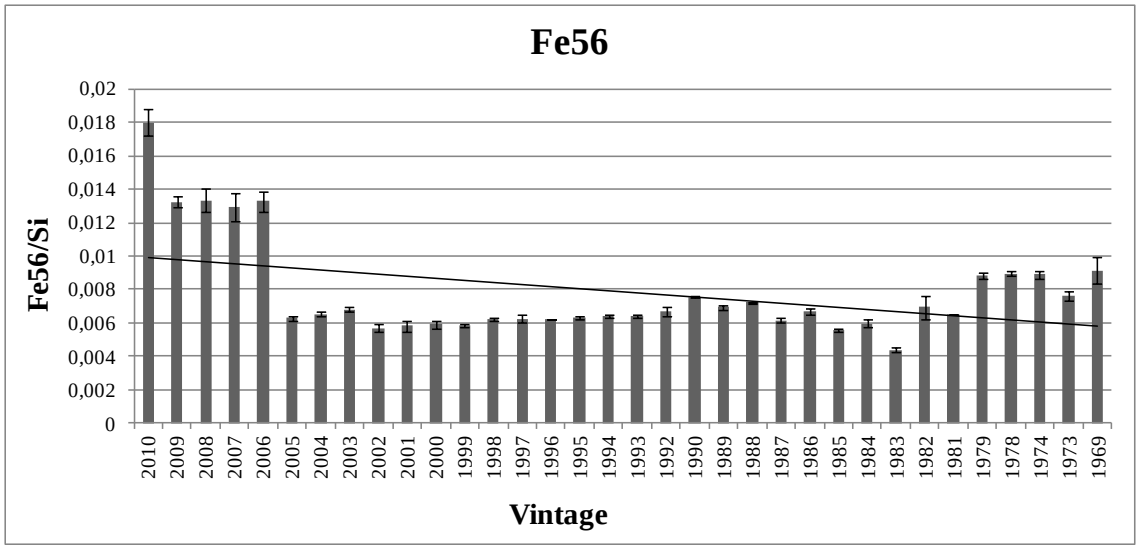
Fe56
Fe56/Si
0,02
0,018
0,016
0,014
0,012
0,01
0,008
0,006
0,004
0,002
0
2010 2009 2008 2007 2006 2005 2004 2003 2002 2001 2000 1999 1998 1997 1996 1995 1994 1993 1992 1990 1989 1988 1987 1986 1985 1984 1983 1982 1981 1979 1978 1974 1973 1969
Vintage

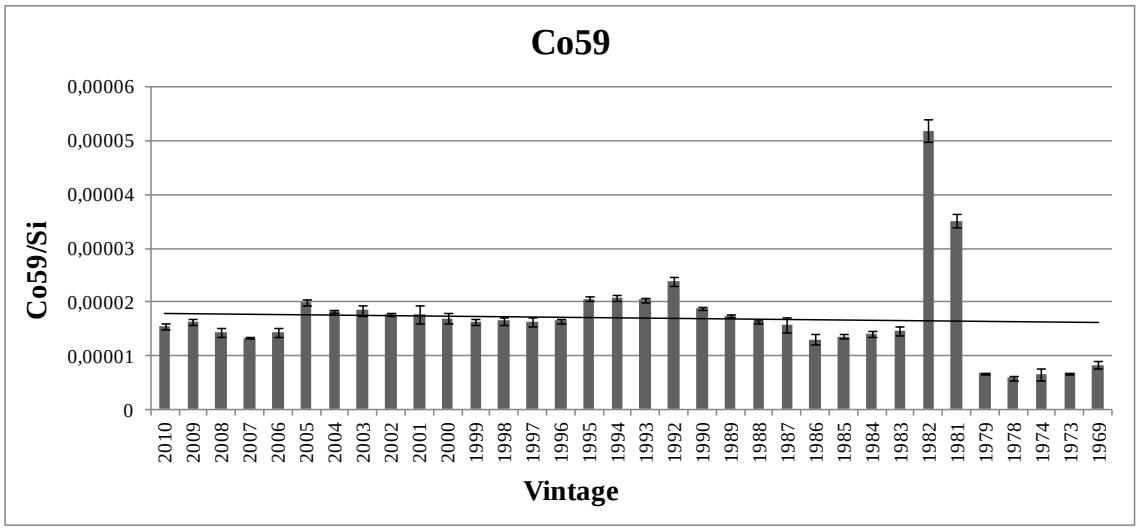
Co59
Co59/Si
0,00006
0,00005
0,00004
0,00003
0,00002
0,00001
0
2010 2009 2008 2007 2006 2005 2004 2003 2002 2001 2000 1999 1998 1997 1996 1995 1994 1993 1992 1990 1989 1988 1987 1986 1985 1984 1983 1982 1981 1979 1978 1974 1973 1969
Vintage

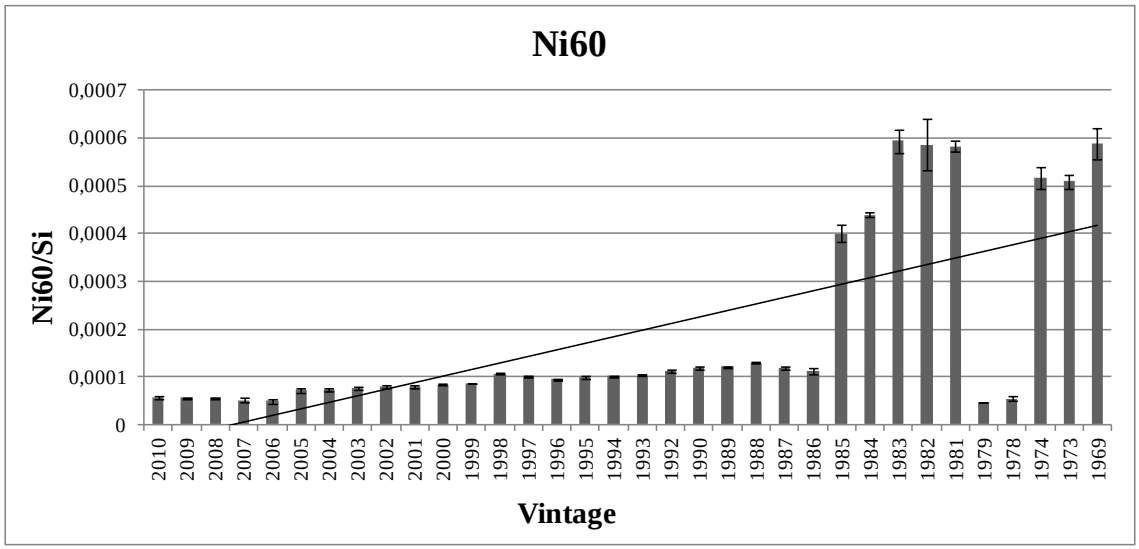
Ni60
Ni60/Si
0,0007
0,0006
0,0005
0,0004
0,0003
0,0002
0,0001
0
2010 2009 2008 2007 2006 2005 2004 2003 2002 2001 2000 1999 1998 1997 1996 1995 1994 1993 1992 1990 1989 1988 1987 1986 1985 1984 1983 1982 1981 1979 1978 1974 1973 1969
Vintage

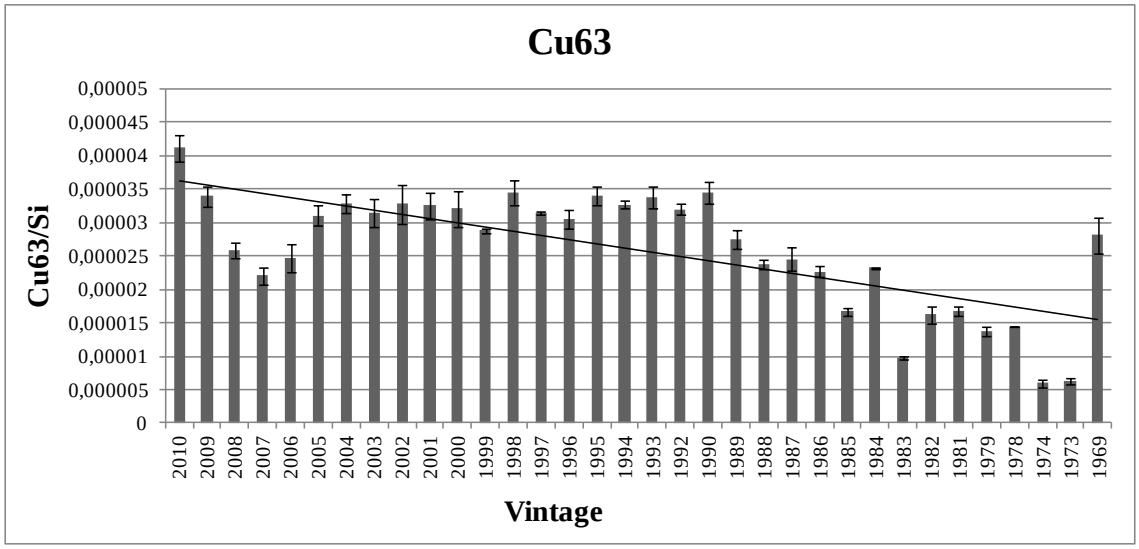
Cu63
Cu63/Si
0,00005
0,000045
0,00004
0,000035
0,00003
0,000025
0,00002
0,000015
0,00001
0,000005
0
2010 2009 2008 2007 2006 2005 2004 2003 2002 2001 2000 1999 1998 1997 1996 1995 1994 1993 1992 1990 1989 1988 1987 1986 1985 1984 1983 1982 1981 1979 1978 1974 1973 1969
Vintage

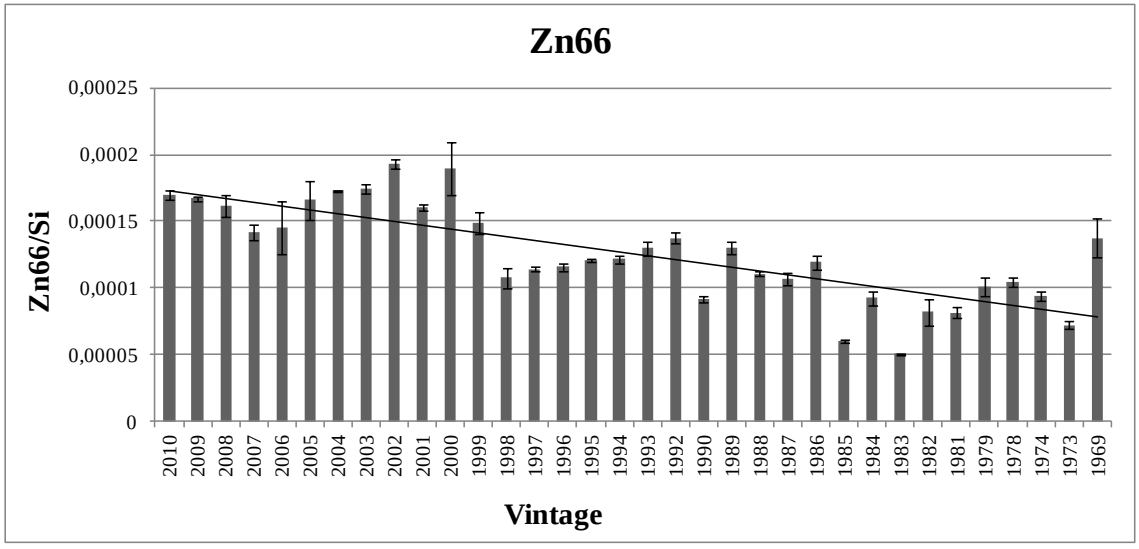
Zn66
Zn66/Si
0,00025
0,0002
0,00015
0,0001
0,00005
0
2010 2009 2008 2007 2006 2005 2004 2003 2002 2001 2000 1999 1998 1997 1996 1995 1994 1993 1992 1990 1989 1988 1987 1986 1985 1984 1983 1982 1981 1979 1978 1974 1973 1969
Vintage

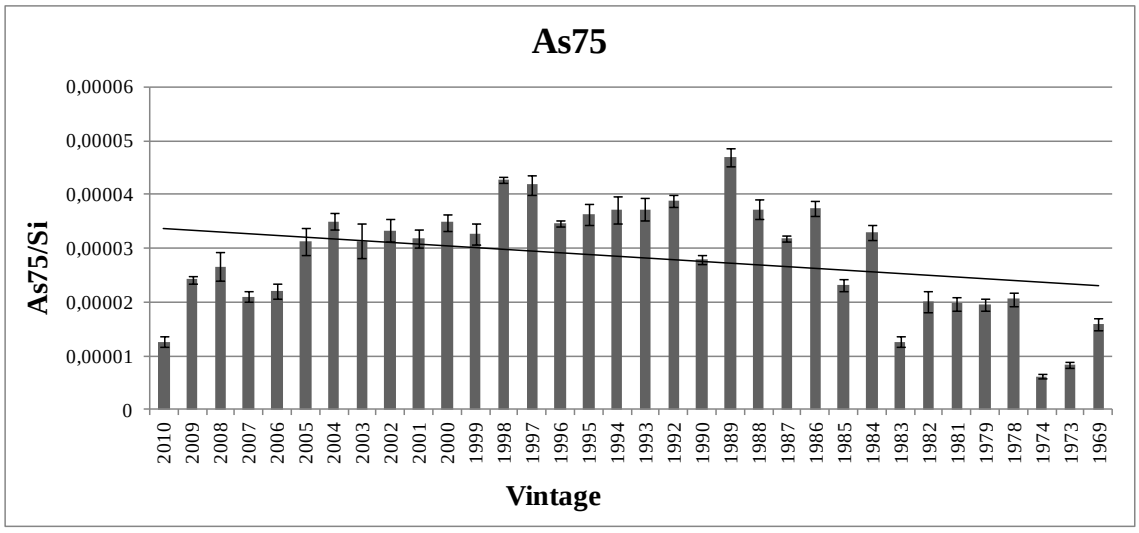
As75
As75/Si
0,00006
0,00005
0,00004
0,00003
0,00002
0,00001
0
2010 2009 2008 2007 2006 2005 2004 2003 2002 2001 2000 1999 1998 1997 1996 1995 1994 1993 1992 1990 1989 1988 1987 1986 1985 1984 1983 1982 1981 1979 1978 1974 1973 1969
Vintage

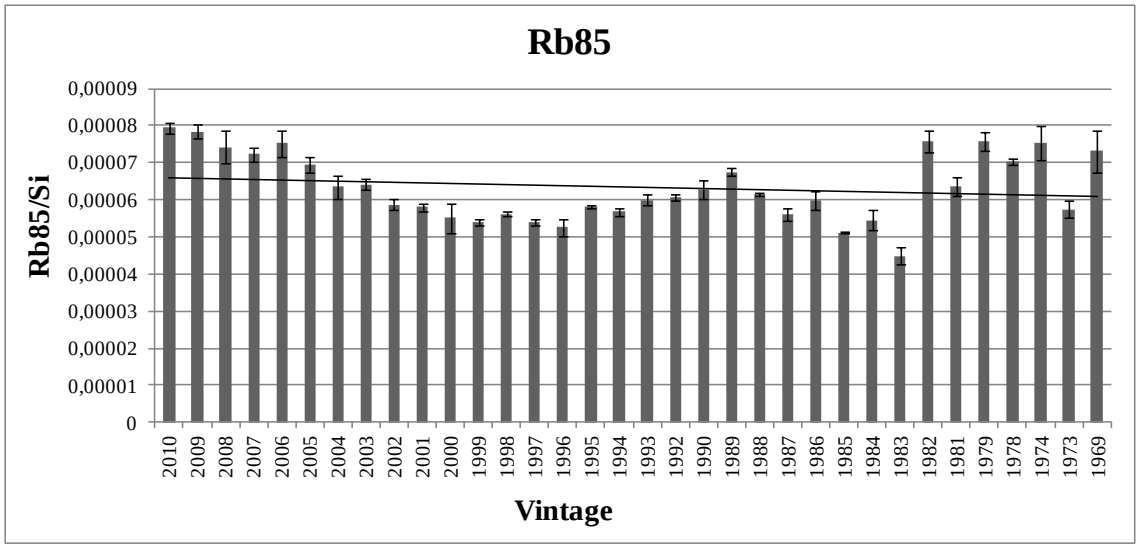
Rb85
Rb85/Si
0,00009
0,00008
0,00007
0,00006
0,00005
0,00004
0,00003
0,00002
0,00001
0
2010 2009 2008 2007 2006 2005 2004 2003 2002 2001 2000 1999 1998 1997 1996 1995 1994 1993 1992 1990 1989 1988 1987 1986 1985 1984 1983 1982 1981 1979 1978 1974 1973 1969
Vintage

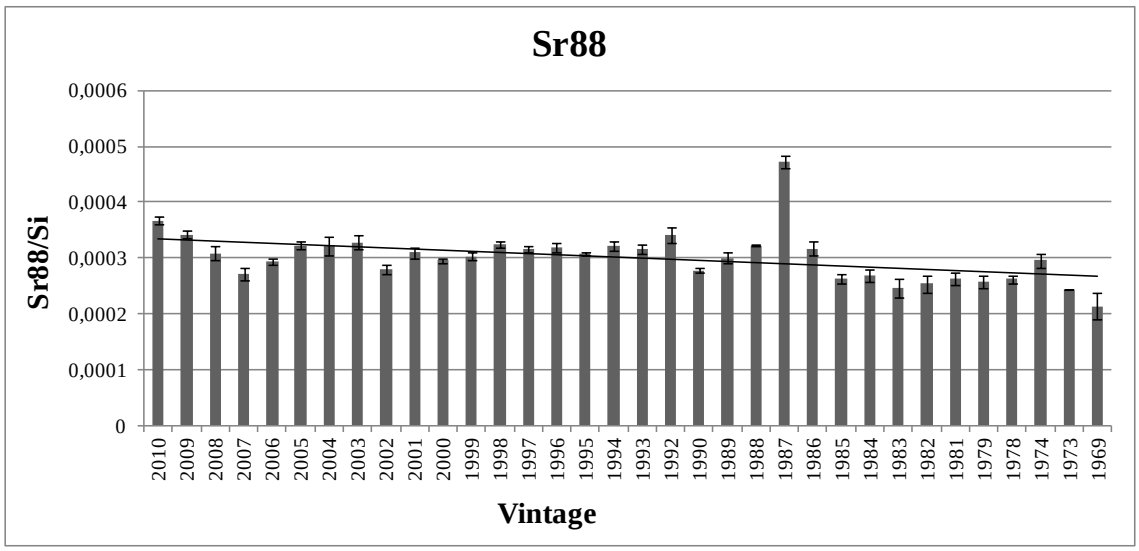
Sr88
Sr88/Si
0,0006
0,0005
0,0004
0,0003
0,0002
0,0001
0
2010 2009 2008 2007 2006 2005 2004 2003 2002 2001 2000 1999 1998 1997 1996 1995 1994 1993 1992 1990 1989 1988 1987 1986 1985 1984 1983 1982 1981 1979 1978 1974 1973 1969
Vintage

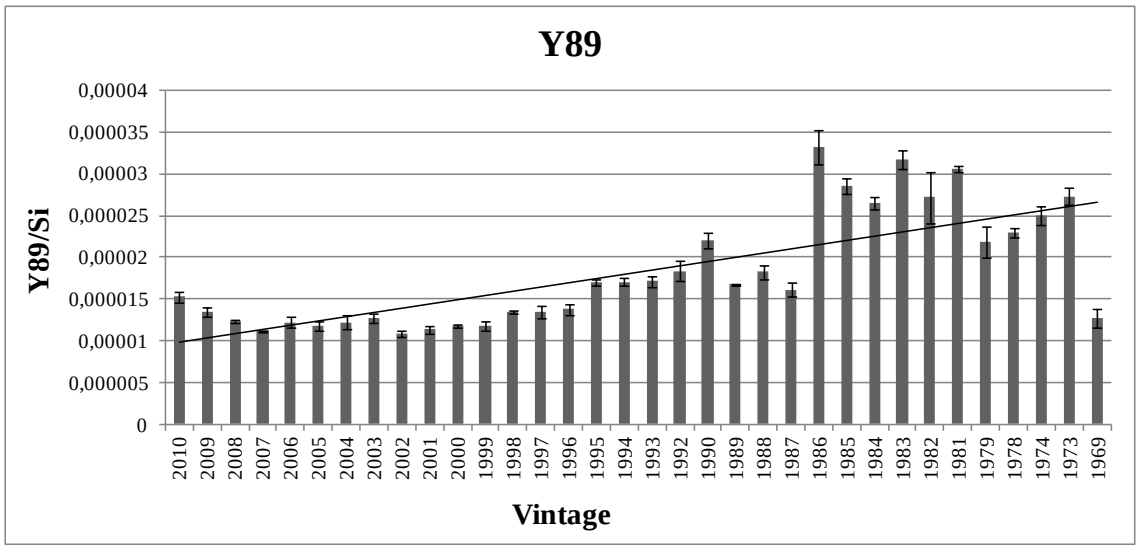
Y89
Y89/Si
0,00004
0,000035
0,00003
0,000025
0,00002
0,000015
0,00001
0,000005
0
2010 2009 2008 2007 2006 2005 2004 2003 2002 2001 2000 1999 1998 1997 1996 1995 1994 1993 1992 1990 1989 1988 1987 1986 1985 1984 1983 1982 1981 1979 1978 1974 1973 1969
Vintage

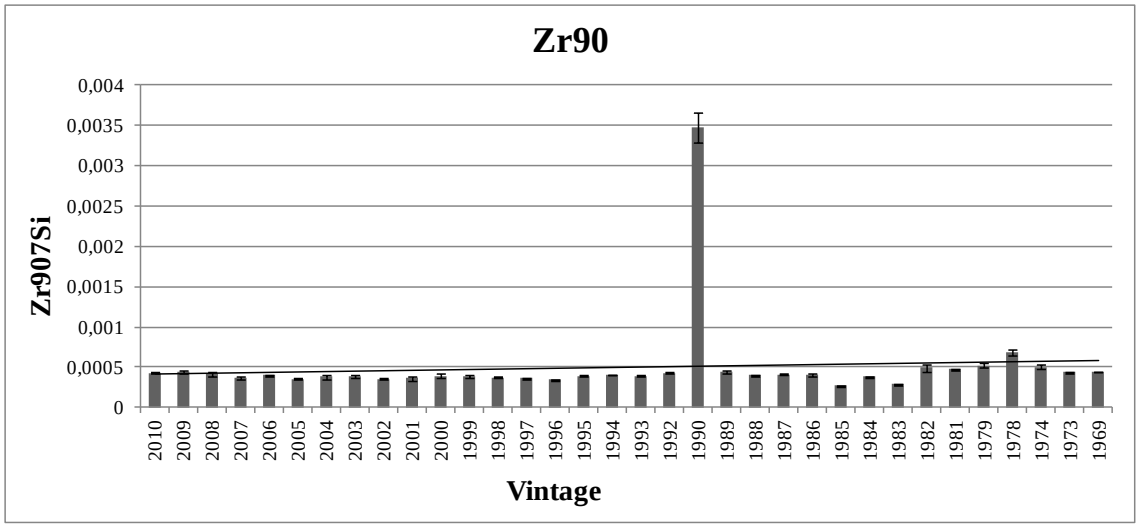
Zr90
Zr907Si
0,004
0,0035
0,003
0,0025
0,002
0,0015
0,001
0,0005
0
2010 2009 2008 2007 2006 2005 2004 2003 2002 2001 2000 1999 1998 1997 1996 1995 1994 1993 1992 1990 1989 1988 1987 1986 1985 1984 1983 1982 1981 1979 1978 1974 1973 1969
Vintage

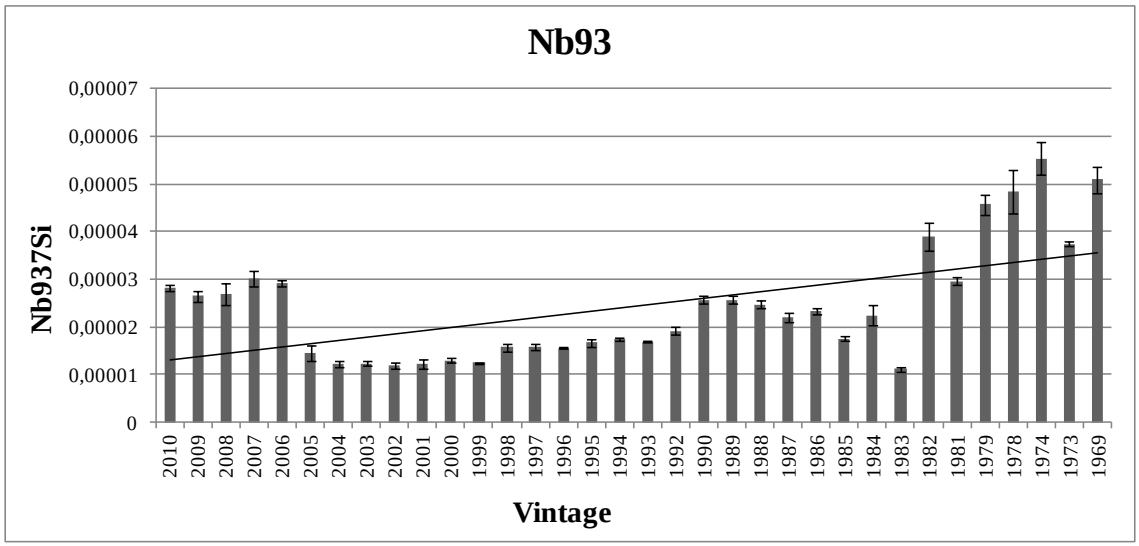
Nb93
Nb937Si
0,00007
0,00006
0,00005
0,00004
0,00003
0,00002
0,00001
0
2010 2009 2008 2007 2006 2005 2004 2003 2002 2001 2000 1999 1998 1997 1996 1995 1994 1993 1992 1990 1989 1988 1987 1986 1985 1984 1983 1982 1981 1979 1978 1974 1973 1969
Vintage

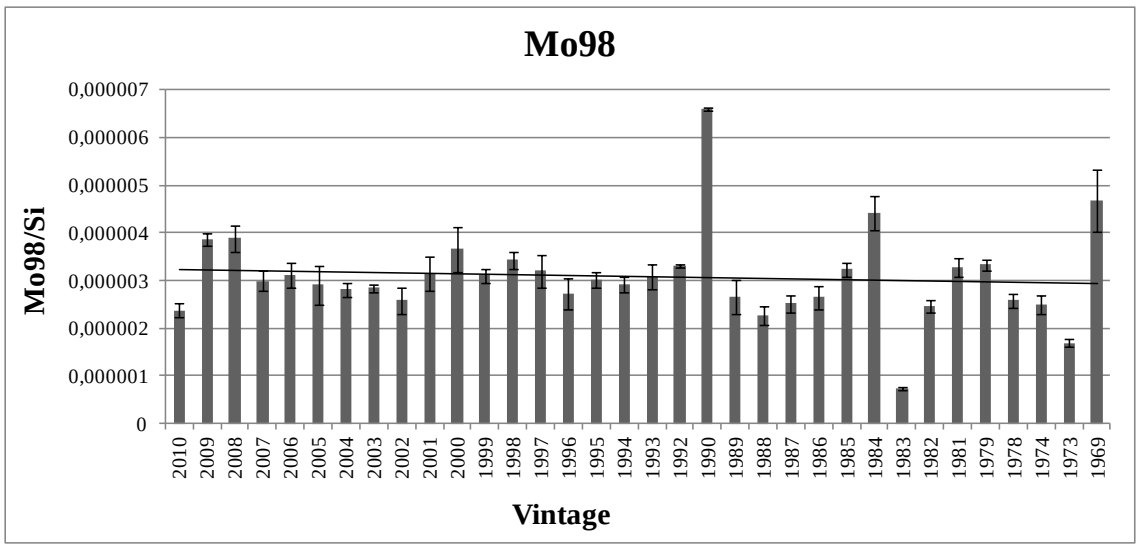
Mo98
Mo98/Si
0,000007
0,000006
0,000005
0,000004
0,000003
0,000002
0,000001
0
2010 2009 2008 2007 2006 2005 2004 2003 2002 2001 2000 1999 1998 1997 1996 1995 1994 1993 1992 1990 1989 1988 1987 1986 1985 1984 1983 1982 1981 1979 1978 1974 1973 1969
Vintage

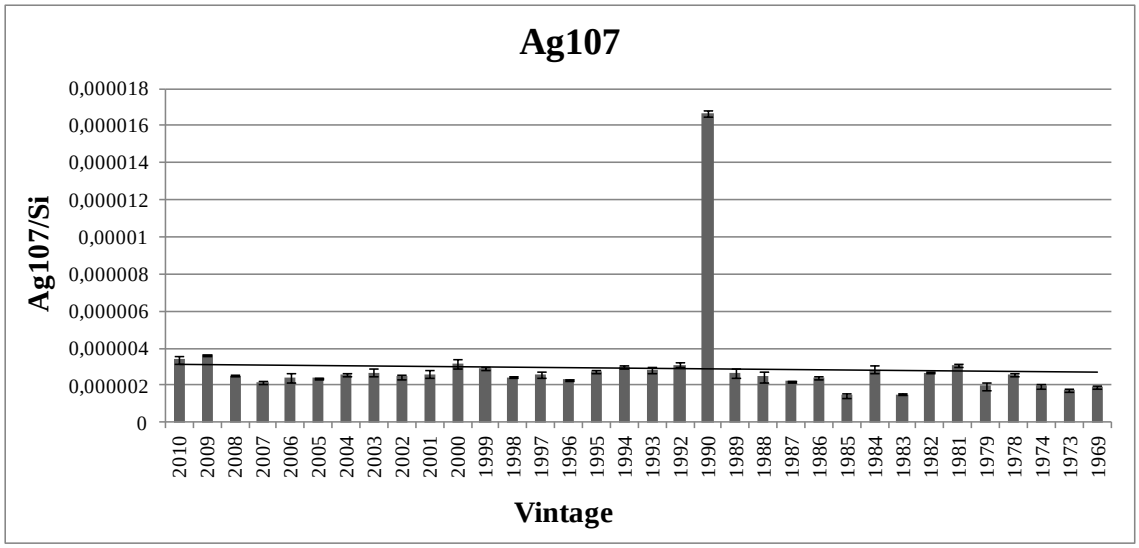
Ag107
Ag107/Si
0,000018
0,000016
0,000014
0,000012
0,00001
0,000008
0,000006
0,000004
0,000002
0
2010 2009 2008 2007 2006 2005 2004 2003 2002 2001 2000 1999 1998 1997 1996 1995 1994 1993 1992 1990 1989 1988 1987 1986 1985 1984 1983 1982 1981 1979 1978 1974 1973 1969
Vintage

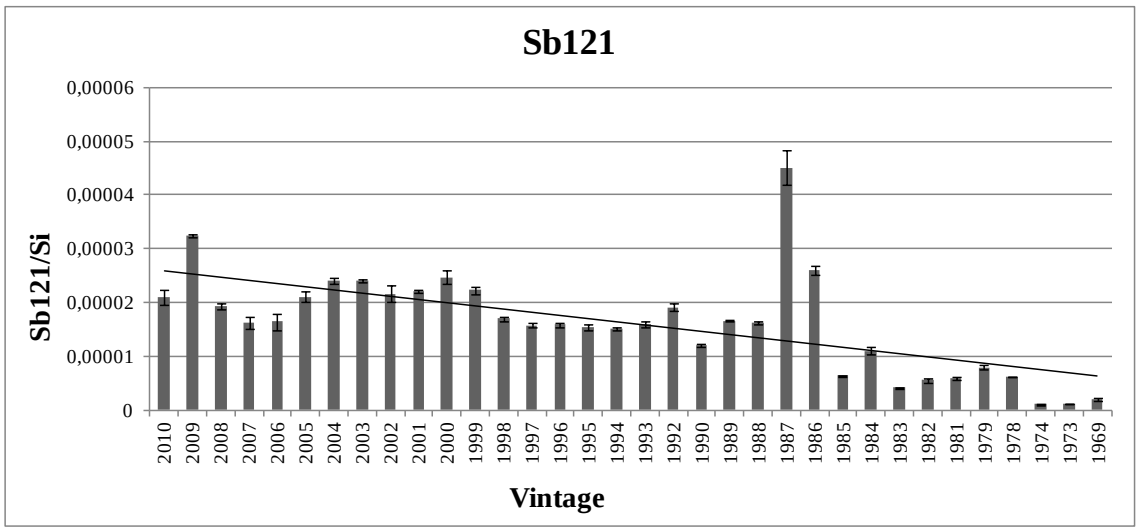
Sb121
Sb121/Si
0,00006
0,00005
0,00004
0,00003
0,00002
0,00001
0
2010 2009 2008 2007 2006 2005 2004 2003 2002 2001 2000 1999 1998 1997 1996 1995 1994 1993 1992 1990 1989 1988 1987 1986 1985 1984 1983 1982 1981 1979 1978 1974 1973 1969
Vintage

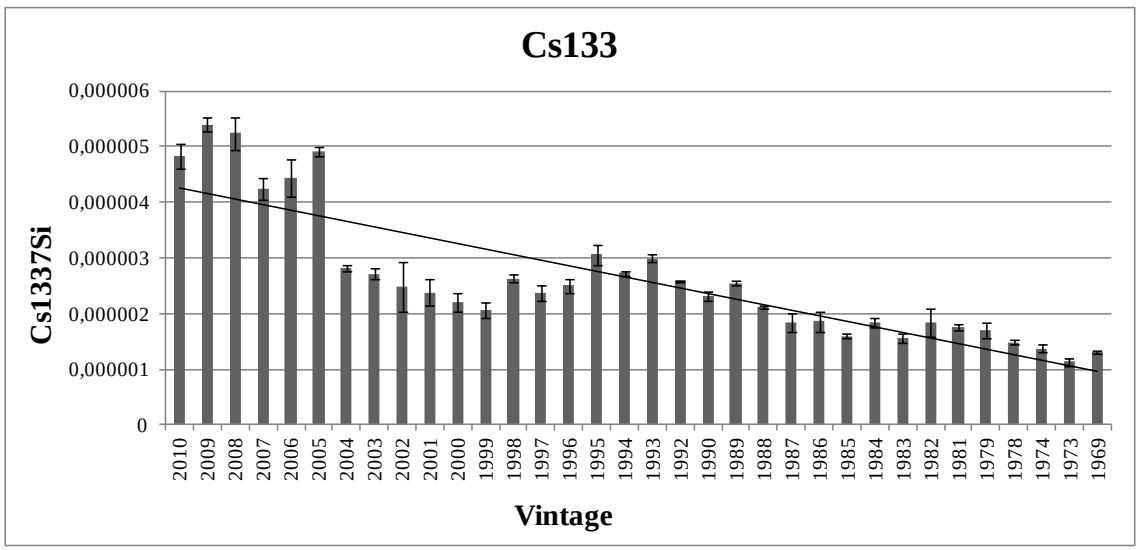
Cs133
Cs1337Si
0,000006
0,000005
0,000004
0,000003
0,000002
0,000001
0
2010 2009 2008 2007 2006 2005 2004 2003 2002 2001 2000 1999 1998 1997 1996 1995 1994 1993 1992 1990 1989 1988 1987 1986 1985 1984 1983 1982 1981 1979 1978 1974 1973 1969
Vintage

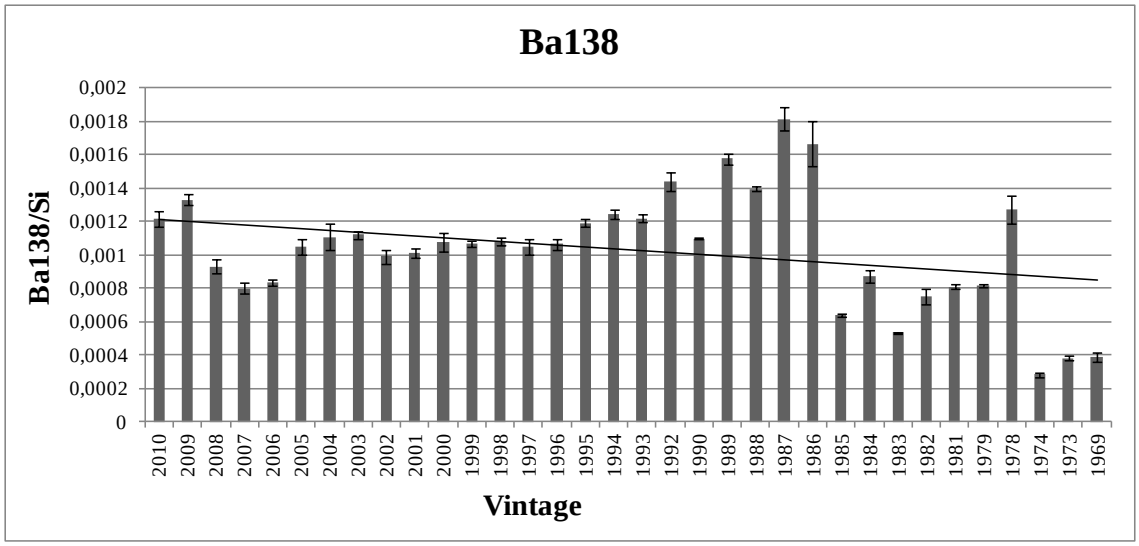
Ba138
Ba138/Si
0,002
0,0018
0,0016
0,0014
0,0012
0,001
0,0008
0,0006
0,0004
0,0002
0
2010 2009 2008 2007 2006 2005 2004 2003 2002 2001 2000 1999 1998 1997 1996 1995 1994 1993 1992 1990 1989 1988 1987 1986 1985 1984 1983 1982 1981 1979 1978 1974 1973 1969
Vintage

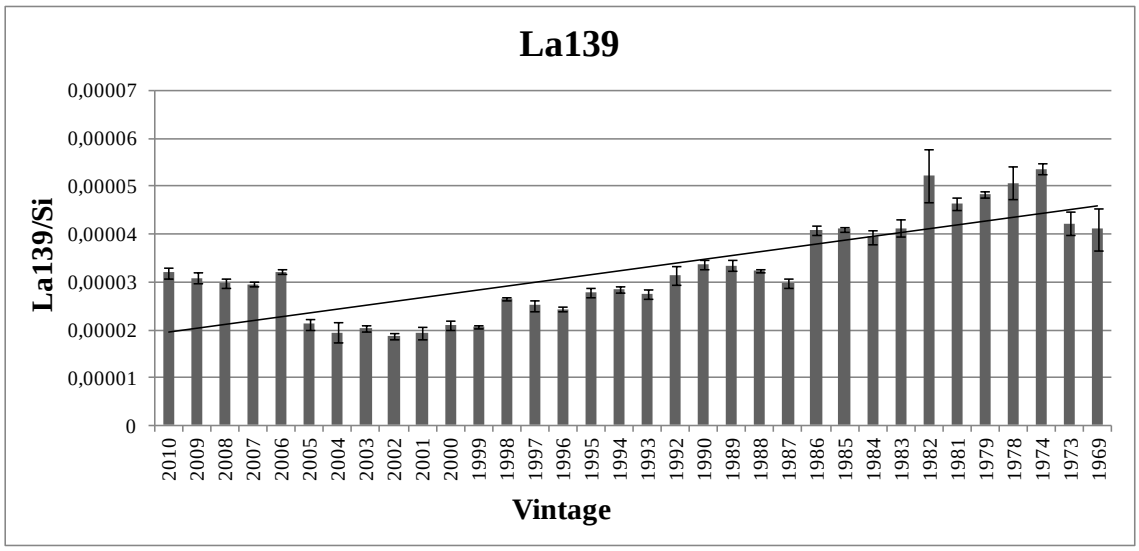
La139
La139/Si
0,00007
0,00006
0,00005
0,00004
0,00003
0,00002
0,00001
0
2010 2009 2008 2007 2006 2005 2004 2003 2002 2001 2000 1999 1998 1997 1996 1995 1994 1993 1992 1990 1989 1988 1987 1986 1985 1984 1983 1982 1981 1979 1978 1974 1973 1969
Vintage

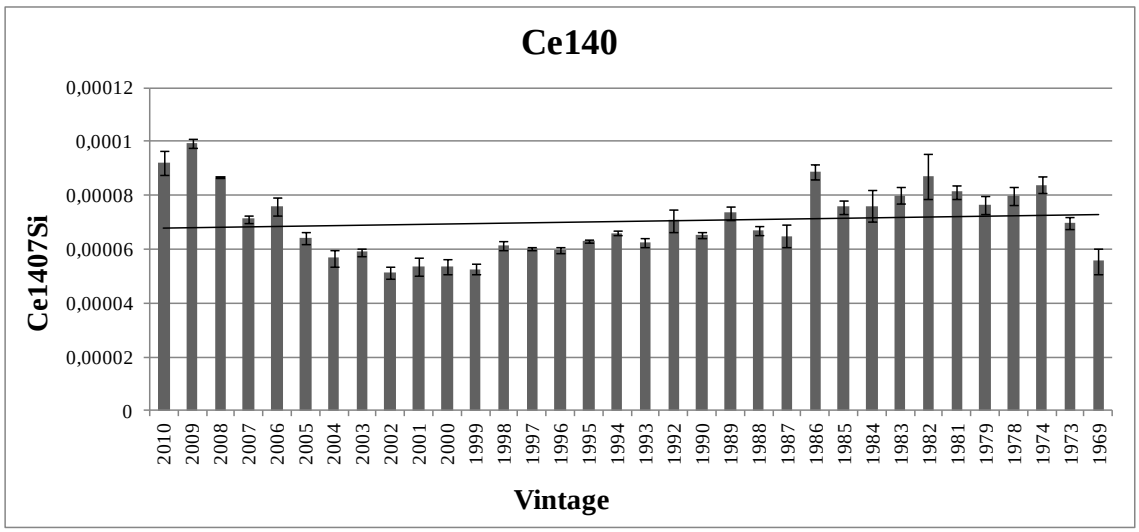
Ce140
Ce1407Si
0,00012
0,0001
0,00008
0,00006
0,00004
0,00002
0
2010 2009 2008 2007 2006 2005 2004 2003 2002 2001 2000 1999 1998 1997 1996 1995 1994 1993 1992 1990 1989 1988 1987 1986 1985 1984 1983 1982 1981 1979 1978 1974 1973 1969
Vintage

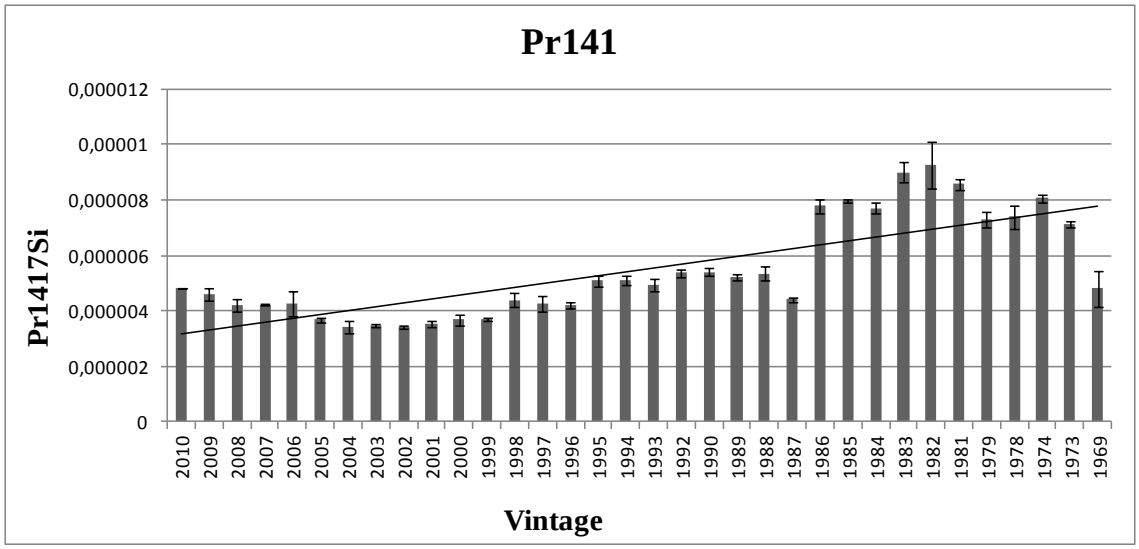
Pr141
Pr1417Si
0,000012
0,00001
0,000008
0,000006
0,000004
0,000002
0
2010 2009 2008 2007 2006 2005 2004 2003 2002 2001 2000 1999 1998 1997 1996 1995 1994 1993 1992 1990 1989 1988 1987 1986 1985 1984 1983 1982 1981 1979 1978 1974 1973 1969
Vintage

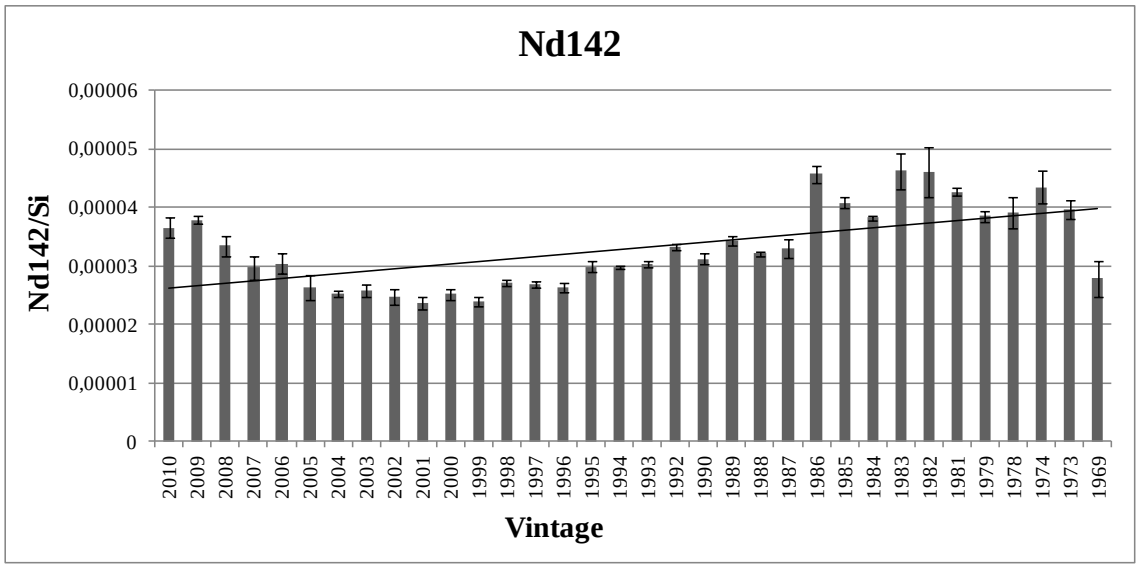
Nd142
Nd142/Si
0,00006
0,00005
0,00004
0,00003
0,00002
0,00001
0
2010 2009 2008 2007 2006 2005 2004 2003 2002 2001 2000 1999 1998 1997 1996 1995 1994 1993 1992 1990 1989 1988 1987 1986 1985 1984 1983 1982 1981 1979 1978 1974 1973 1969
Vintage

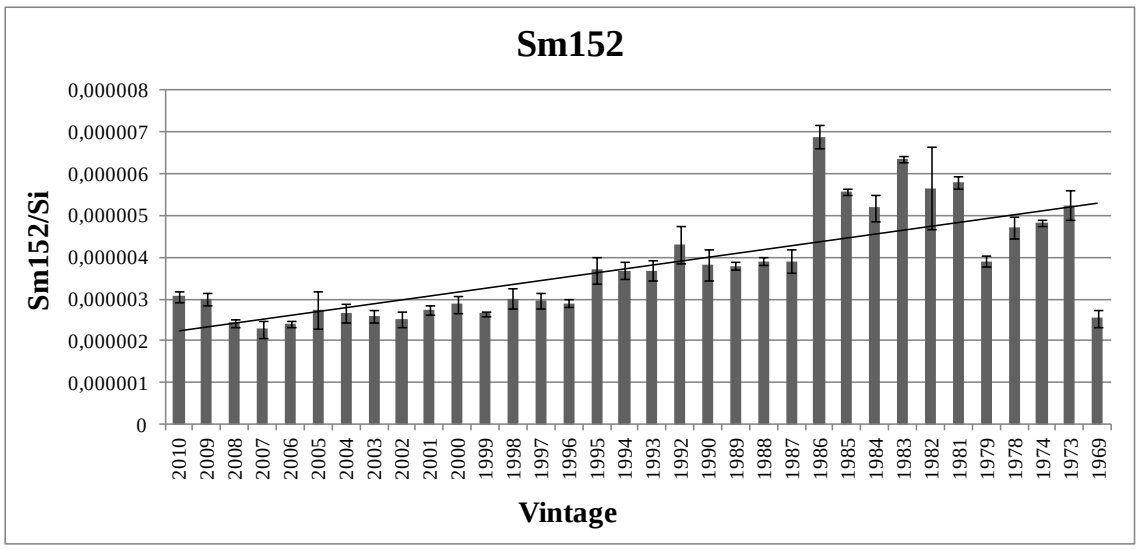
Sm152
Sm152/Si
0,000008
0,000007
0,000006
0,000005
0,000004
0,000003
0,000002
0,000001
0
2010 2009 2008 2007 2006 2005 2004 2003 2002 2001 2000 1999 1998 1997 1996 1995 1994 1993 1992 1990 1989 1988 1987 1986 1985 1984 1983 1982 1981 1979 1978 1974 1973 1969
Vintage

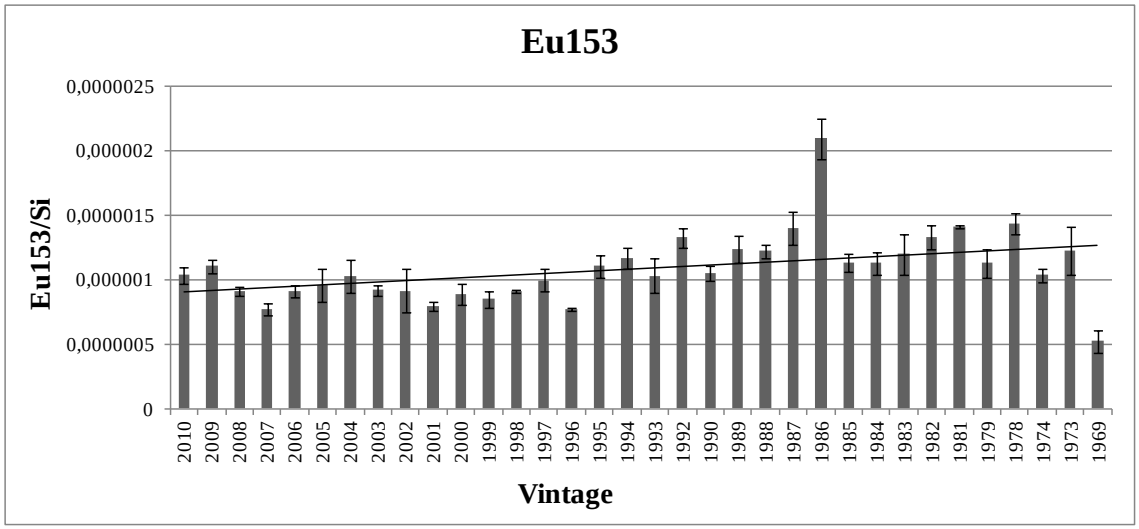
Eu153
Eu153/Si
0,0000025
0,000002
0,0000015
0,000001
0,0000005
0
2010 2009 2008 2007 2006 2005 2004 2003 2002 2001 2000 1999 1998 1997 1996 1995 1994 1993 1992 1990 1989 1988 1987 1986 1985 1984 1983 1982 1981 1979 1978 1974 1973 1969
Vintage

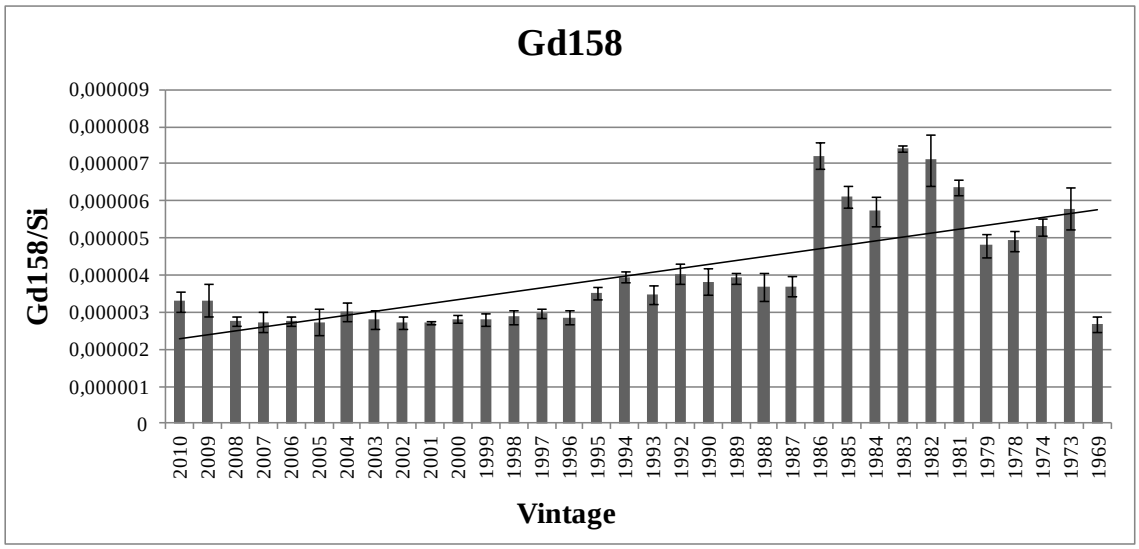
Gd158
Gd158/Si
0,000009
0,000008
0,000007
0,000006
0,000005
0,000004
0,000003
0,000002
0,000001
0
2010 2009 2008 2007 2006 2005 2004 2003 2002 2001 2000 1999 1998 1997 1996 1995 1994 1993 1992 1990 1989 1988 1987 1986 1985 1984 1983 1982 1981 1979 1978 1974 1973 1969
Vintage

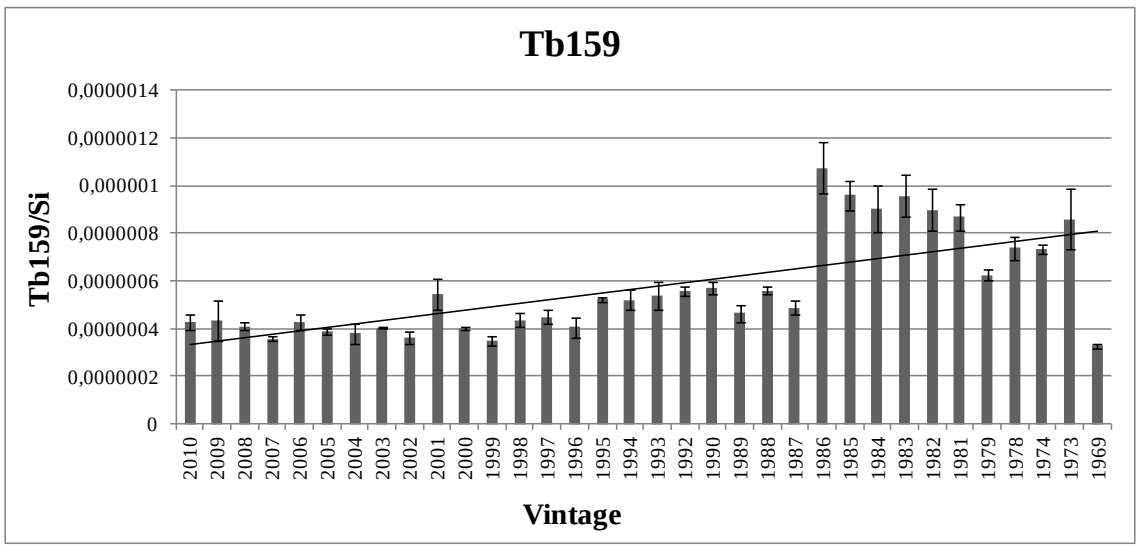
Tb159
Tb159/Si
0,0000014
0,0000012
0,000001
0,0000008
0,0000006
0,0000004
0,0000002
0
2010 2009 2008 2007 2006 2005 2004 2003 2002 2001 2000 1999 1998 1997 1996 1995 1994 1993 1992 1990 1989 1988 1987 1986 1985 1984 1983 1982 1981 1979 1978 1974 1973 1969
Vintage

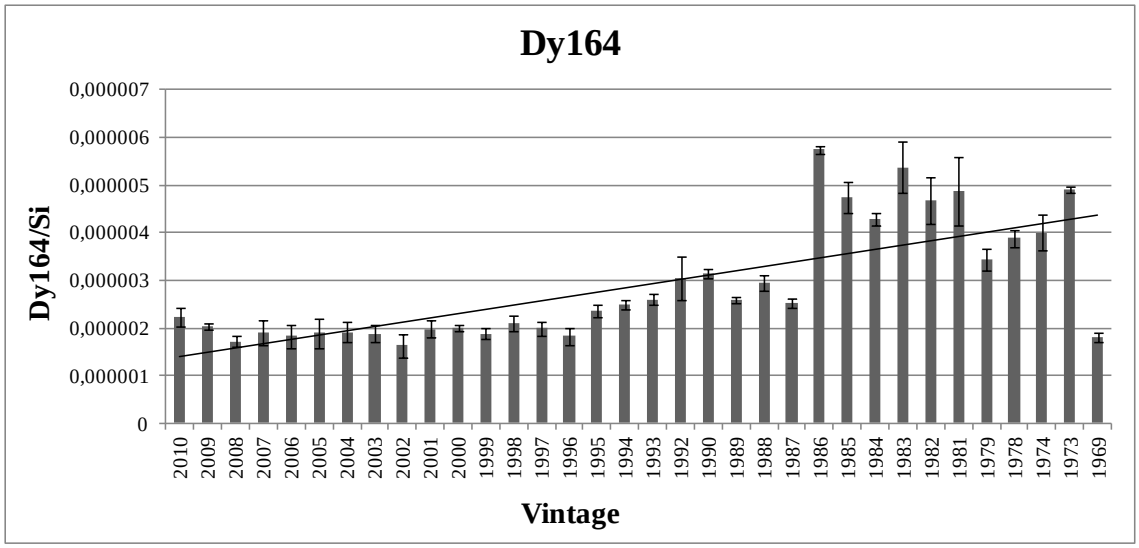
Dy164
Dy164/Si
0,000007
0,000006
0,000005
0,000004
0,000003
0,000002
0,000001
0
2010 2009 2008 2007 2006 2005 2004 2003 2002 2001 2000 1999 1998 1997 1996 1995 1994 1993 1992 1990 1989 1988 1987 1986 1985 1984 1983 1982 1981 1979 1978 1974 1973 1969
Vintage

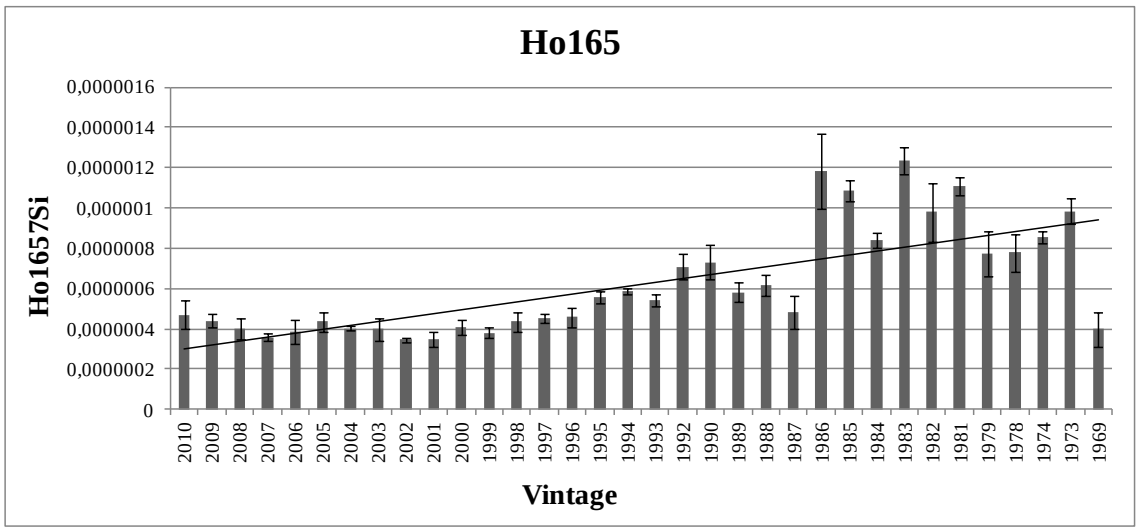
Ho165
Ho1657Si
0,0000016
0,0000014
0,0000012
0,000001
0,0000008
0,0000006
0,0000004
0,0000002
0
2010 2009 2008 2007 2006 2005 2004 2003 2002 2001 2000 1999 1998 1997 1996 1995 1994 1993 1992 1990 1989 1988 1987 1986 1985 1984 1983 1982 1981 1979 1978 1974 1973 1969
Vintage

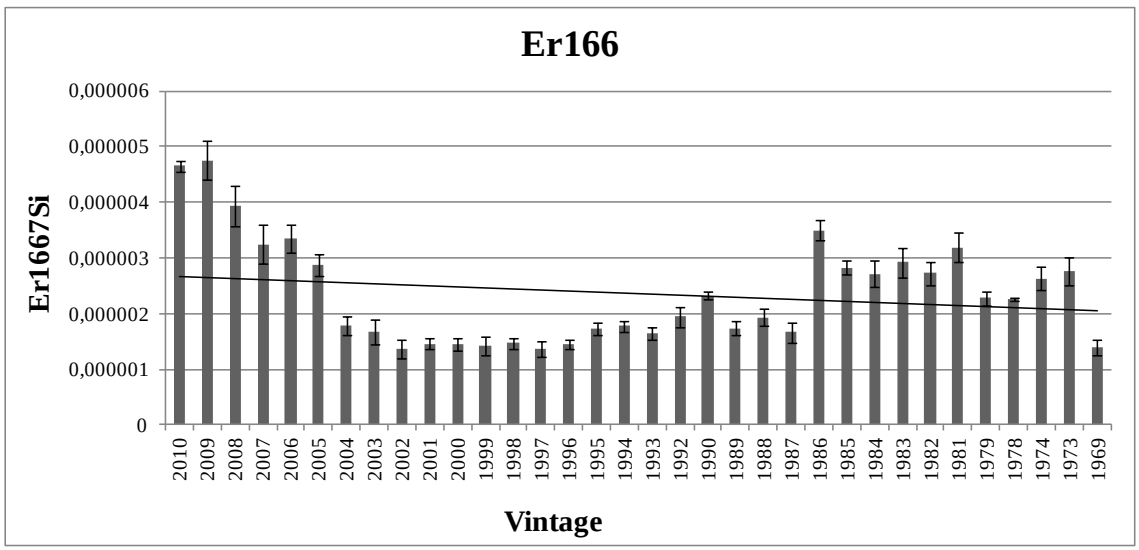
Er166
Er1667Si
0,000006
0,000005
0,000004
0,000003
0,000002
0,000001
0
2010 2009 2008 2007 2006 2005 2004 2003 2002 2001 2000 1999 1998 1997 1996 1995 1994 1993 1992 1990 1989 1988 1987 1986 1985 1984 1983 1982 1981 1979 1978 1974 1973 1969
Vintage

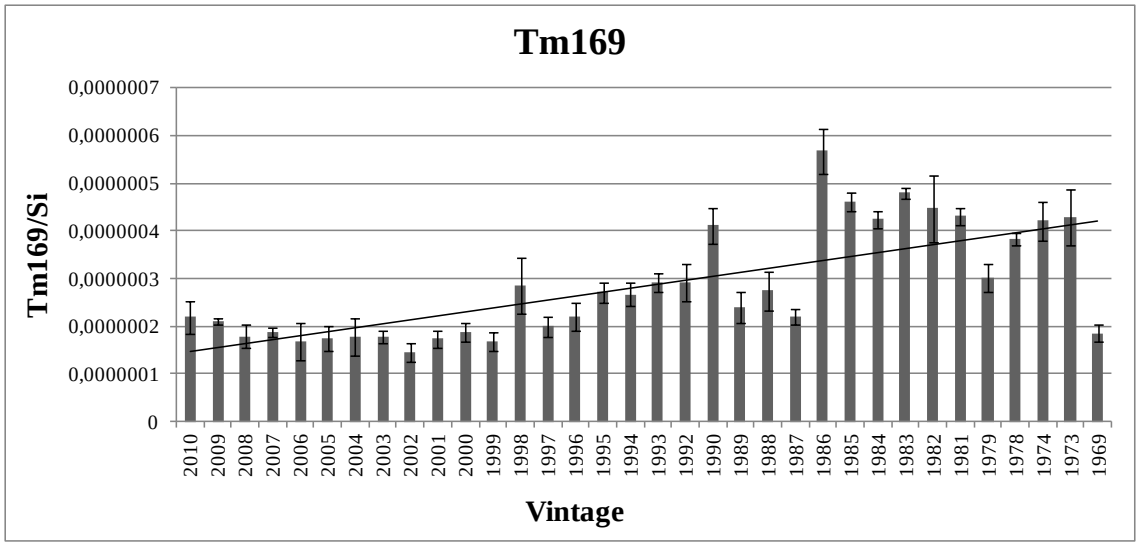
Tm169
Tm169/Si
0,0000007
0,0000006
0,0000005
0,0000004
0,0000003
0,0000002
0,0000001
0
2010 2009 2008 2007 2006 2005 2004 2003 2002 2001 2000 1999 1998 1997 1996 1995 1994 1993 1992 1990 1989 1988 1987 1986 1985 1984 1983 1982 1981 1979 1978 1974 1973 1969
Vintage

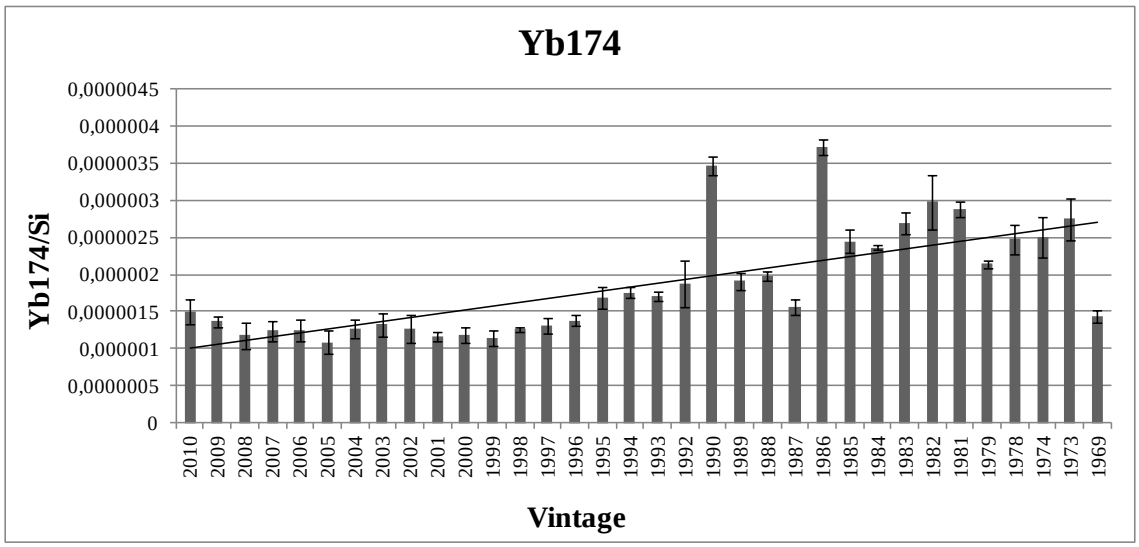
Yb174
Yb174/Si
0,0000045
0,000004
0,0000035
0,000003
0,0000025
0,000002
0,0000015
0,000001
0,0000005
0
2010 2009 2008 2007 2006 2005 2004 2003 2002 2001 2000 1999 1998 1997 1996 1995 1994 1993 1992 1990 1989 1988 1987 1986 1985 1984 1983 1982 1981 1979 1978 1974 1973 1969
Vintage

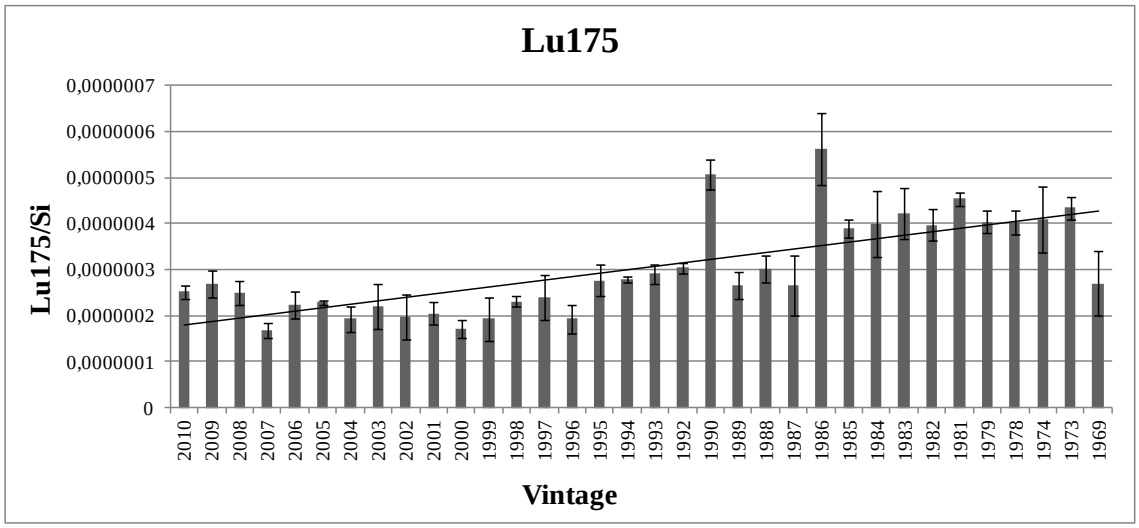
Lu175
Lu175/Si
0,0000007
0,0000006
0,0000005
0,0000004
0,0000003
0,0000002
0,0000001
0
2010 2009 2008 2007 2006 2005 2004 2003 2002 2001 2000 1999 1998 1997 1996 1995 1994 1993 1992 1990 1989 1988 1987 1986 1985 1984 1983 1982 1981 1979 1978 1974 1973 1969
Vintage

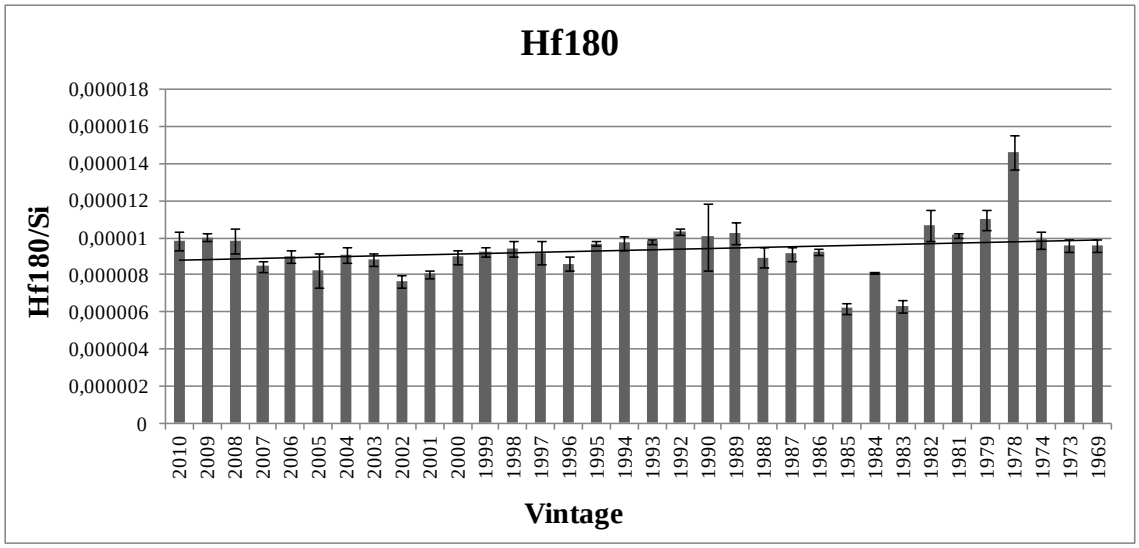
Hf180
Hf180/Si
0,000018
0,000016
0,000014
0,000012
0,00001
0,000008
0,000006
0,000004
0,000002
0
2010 2009 2008 2007 2006 2005 2004 2003 2002 2001 2000 1999 1998 1997 1996 1995 1994 1993 1992 1990 1989 1988 1987 1986 1985 1984 1983 1982 1981 1979 1978 1974 1973 1969
Vintage

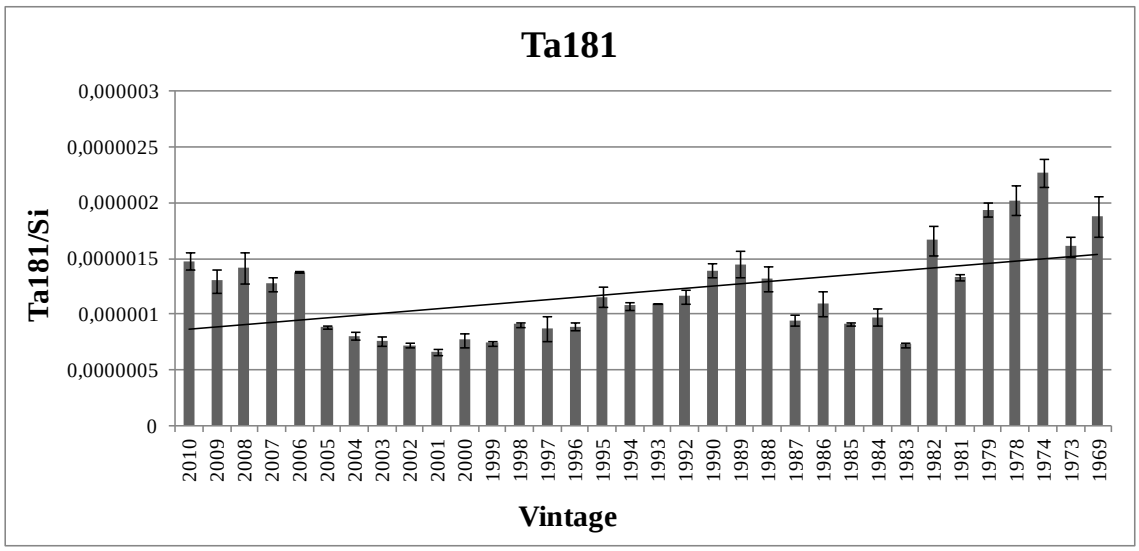
Ta181
Ta181/Si
0,000003
0,0000025
0,000002
0,0000015
0,000001
0,0000005
0
2010 2009 2008 2007 2006 2005 2004 2003 2002 2001 2000 1999 1998 1997 1996 1995 1994 1993 1992 1990 1989 1988 1987 1986 1985 1984 1983 1982 1981 1979 1978 1974 1973 1969
Vintage

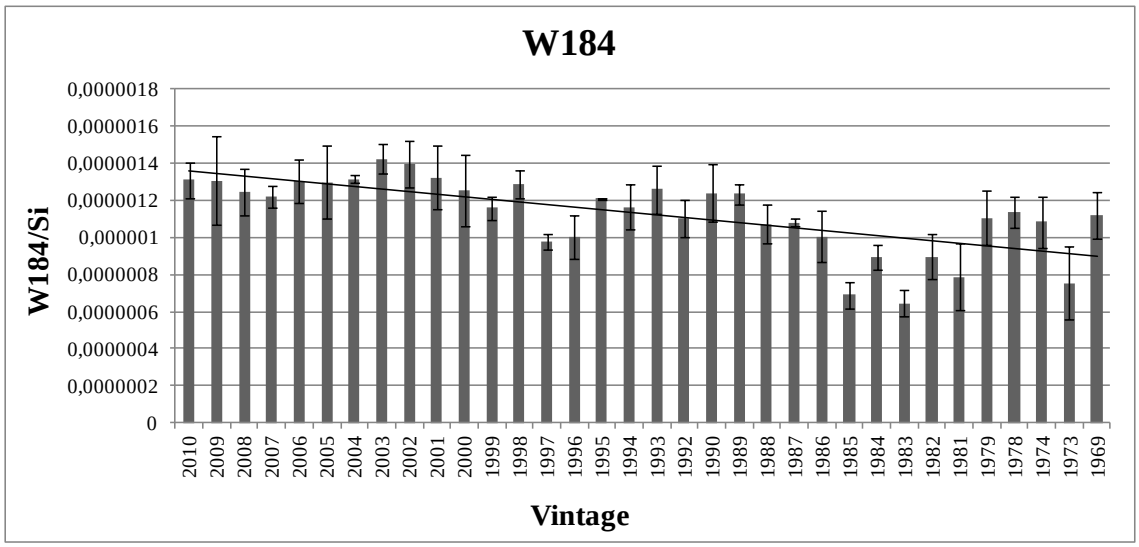
W184
W184/Si
0,0000018
0,0000016
0,0000014
0,0000012
0,000001
0,0000008
0,0000006
0,0000004
0,0000002
0
2010 2009 2008 2007 2006 2005 2004 2003 2002 2001 2000 1999 1998 1997 1996 1995 1994 1993 1992 1990 1989 1988 1987 1986 1985 1984 1983 1982 1981 1979 1978 1974 1973 1969
Vintage

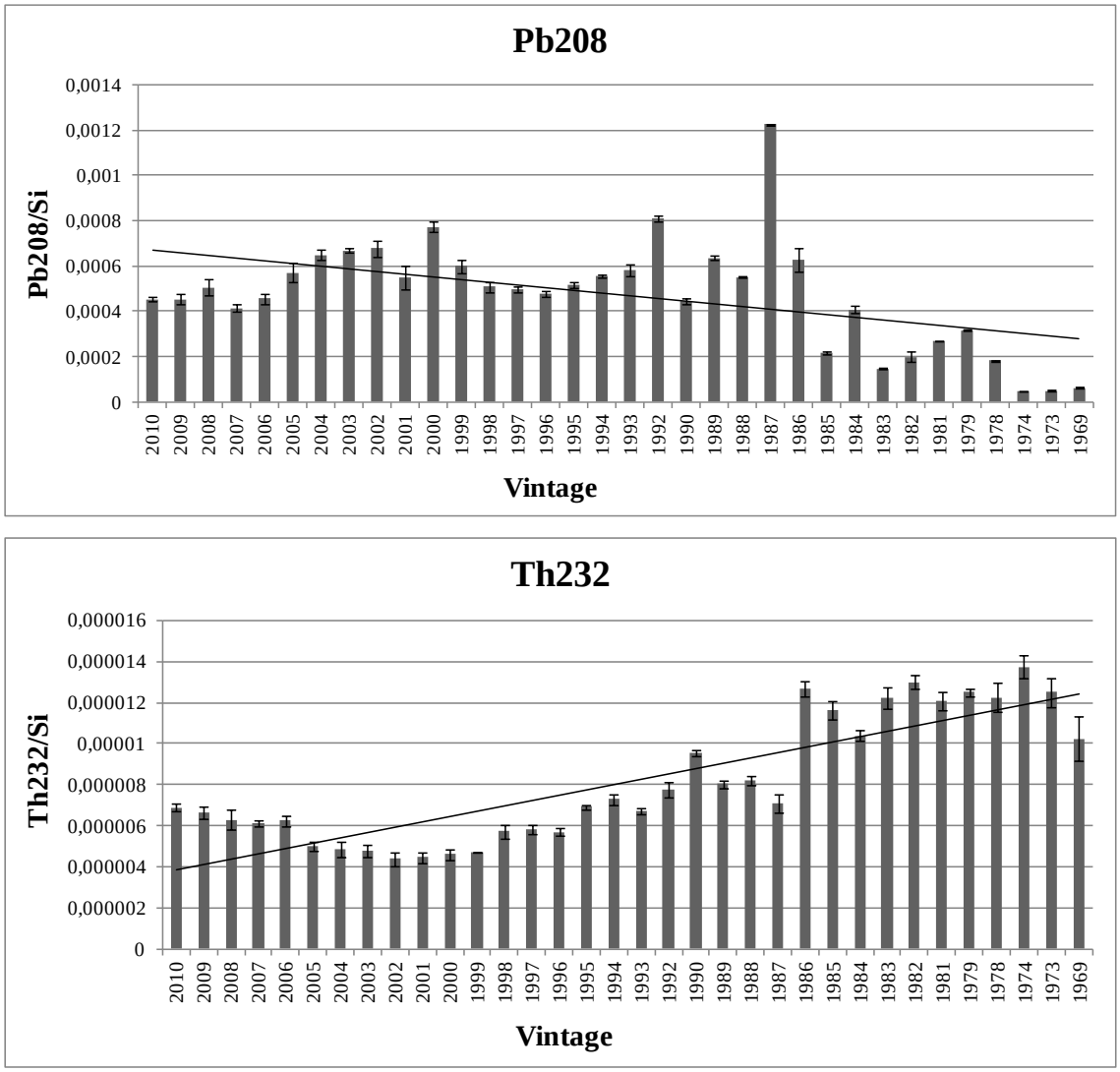


**Figure 11 Individual** charts for each isotope and vintage. Lineal tendency line shows how elemental ratios change in function of production time.

### 3.3.3 Casework 3: collection of worldwide bottles

A total of 195 bottles coming from all continents were analyzed from which 160 were green bottles and 35 transparent bottles. For classification purposes, green and transparent bottles were studied separately. Ordinary soda-lime glass appears colorless to the naked eye but the addition of metal oxides during its manufacture can change its color for enhancing its aesthetic appeal or modify its physical properties. The particular colour is a function of the specific additive while the intensity is a function of its concentration in the glass matrix.

In Figure 13 it can be easily observed how green and transparent bottles are clearly differentiated from each other. A PCA model with two PCs (PC1 vs. PC2) explains 68% of the variation in the data for the transparent and green wine bottles coming from all around the world, being the residuals < 1 for all the scores. The PCA reveals that separation along PC1 accounts for the 56% of the variation in the sample set, while separation along PC2 accounts for the 12%. For the computing of this study, all variables have been taken into account and they are represented in the x-loadings chart. Note that all loadings are found in the positive part of the PC1 axis where are, concretely, located the green bottles.

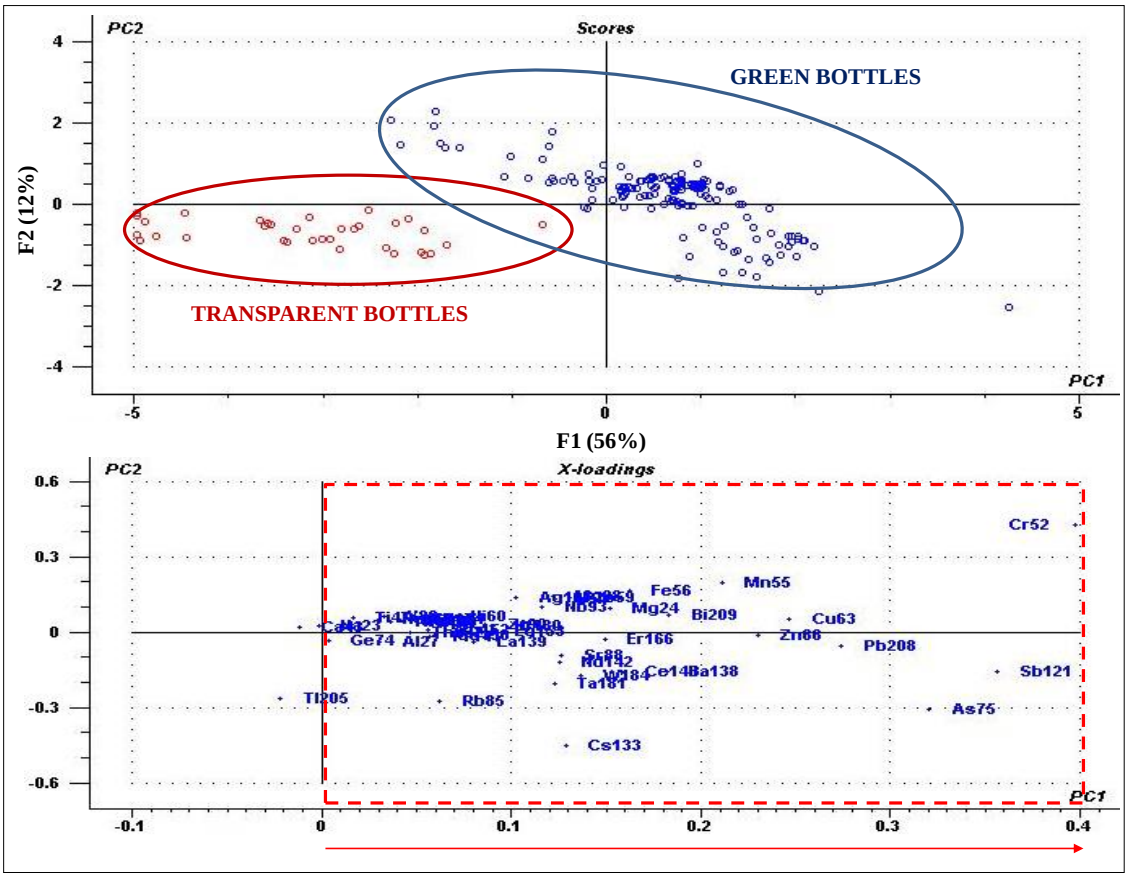


**Figure 13** PCA (PC1 vs PC2) and loadings of the transparent and green bottles.

The conclusions extracted from the PCA about the green and transparent glasses have a remarkable consistency about literature and data, which stands out the absence of specific additives in transparent glass. Therefore, from now on, green bottles and transparent bottles will be studied separately for more accurate conclusions.

#### 3.3.3.1 Classification of green wine bottles

***Worldwide green bottles***

For the classification study of green wine bottles 160 samples were analyzed. However, and due to the poor information that these bottles could add to the model, the bottles coming from Oceania (2 samples) and Africa (1 sample) were removed for statistical data analysis.

A PCA model with two PCs explains 78% of the variation in the data for the green wine bottles being the residuals < 1 for all the scores was developed. The biplot (Figure 14) reveals that separation along PC1 accounts for the 58% of the variation in the sample set, while separation along PC2 accounts for the 20%. Three groups corresponding to EUROPE, AMERICA and ASIA are distinguishable. However, the groups are not completely separated from each other. In fact, European and American bottles, which are gathered together in tight groups, are quite close to each other while Asiatic bottles are separated from them, but showing a more expanded shape. Among the forty-seven monitored isotopes, ten of them ($^{75}As$, $^{85}Rb$, $^{121}Sb$, $^{133}Cs$, $^{138}Ba$, $^{140}Ce$, $^{142}Nd$, $^{181}Ta$, $^{184}W$ and $^{208}Pb$ respectively) were found to be the responsible for such discrimination. Asiatic bottles are characterized by the selected descriptors while European and American bottles shown lack of them. For this variable reduction, an initial PCA was run taking into account all the analyzed variables. After, the most significant (contribution of the observations, %) variables were selected from PC1, PC2 and PC3 and their correlations were studied within the correlation matrix (Pearson (n)). To select correlation threshold value from which two variables are significantly correlated, the statistical significance of the Coefficient of Correlation (r) values were studied by transforming them into t experimental values according to the equation 1 for a $p\ value < 0.005$ and n-2 grades of freedom.

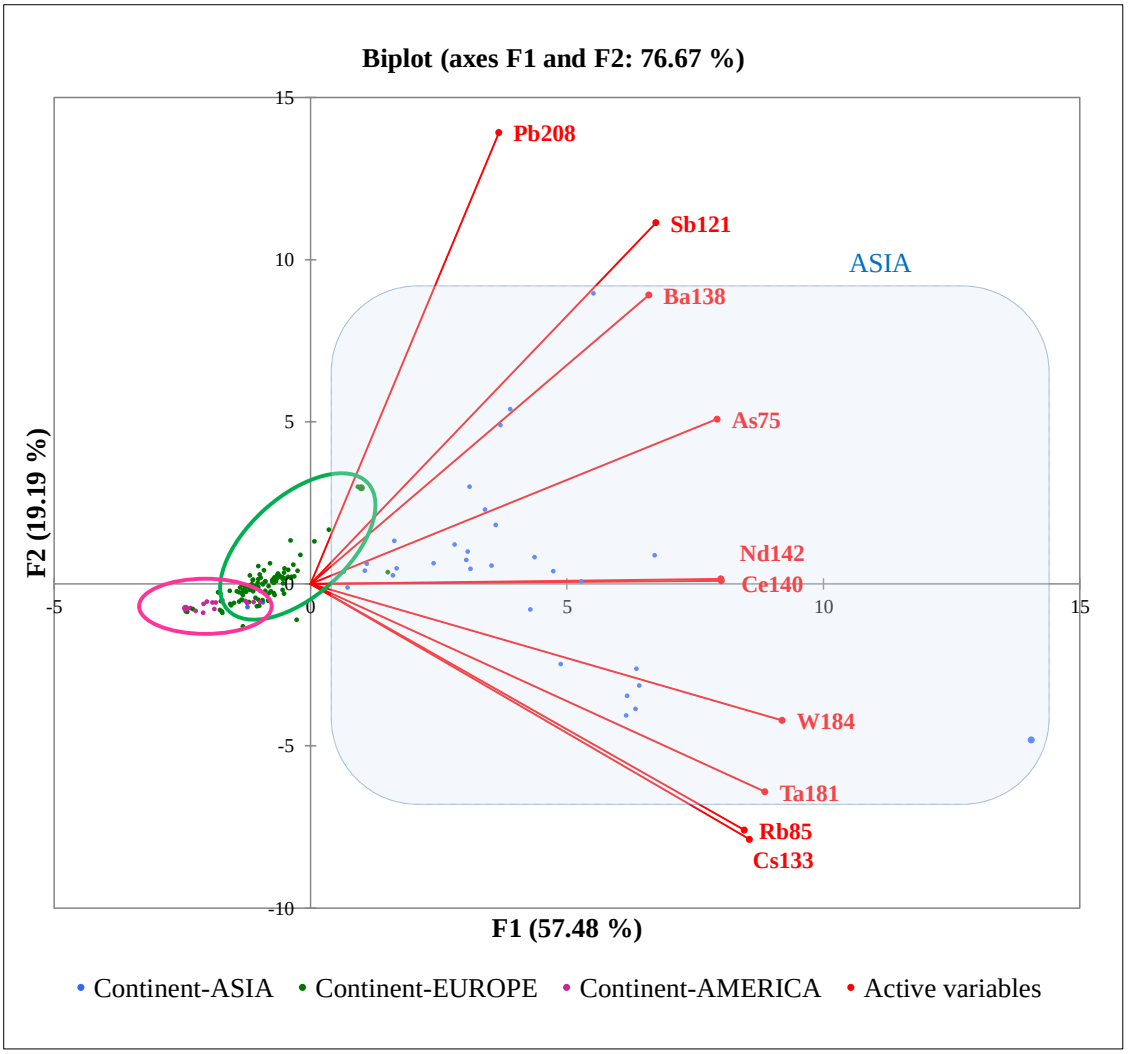


**Figure 14** Biplot (PC1 vs. PC2) representing Asian (in blue), European (in green) and American (in pink) bottles with the loadings (variables) responsible of such discrimination.

Due to the fact that American/European bottles are quite distinguished from Asian bottles, which is a prerequisite for a possible classification via SIMCA modelling, an attempt to develop a classification model was done. Soft Independent Modelling of Class Analogies (SIMCA) is a classification procedure that makes separate PCA models for each group in the training set. Unknown samples are then compared with the class models and assigned to classes according to their analogy and distance from the category model.

In this casework, previously centered and scaled data was employed to construct a global PCA excluding seven test samples (3 Asian, 2 European and 2 American) of each class in the training set was done. This means that individual PCA were done for American/European bottles and Asian bottles using the ten variables previously selected and randomly chosen seven test samples were extracted from the models. The Cooman's plot (Figure 15) indicated a half-baked separation. The test samples are distributed according to the distance (similarity) to the model. In this case,

AMERICA/EUROPE model is in the X axis while ASIA model is represented in the Y axis. The models were not sufficiently different for classification and discrimination of samples. In fact, using a significance level of 5%, the 57% of the samples contained in the test set (4 out of 7) were recognized by the correct class model according to the classification table. Figure 16 shows the discrimination power of each variable used in the model, being the $^{133}Cs$ the most discriminant.

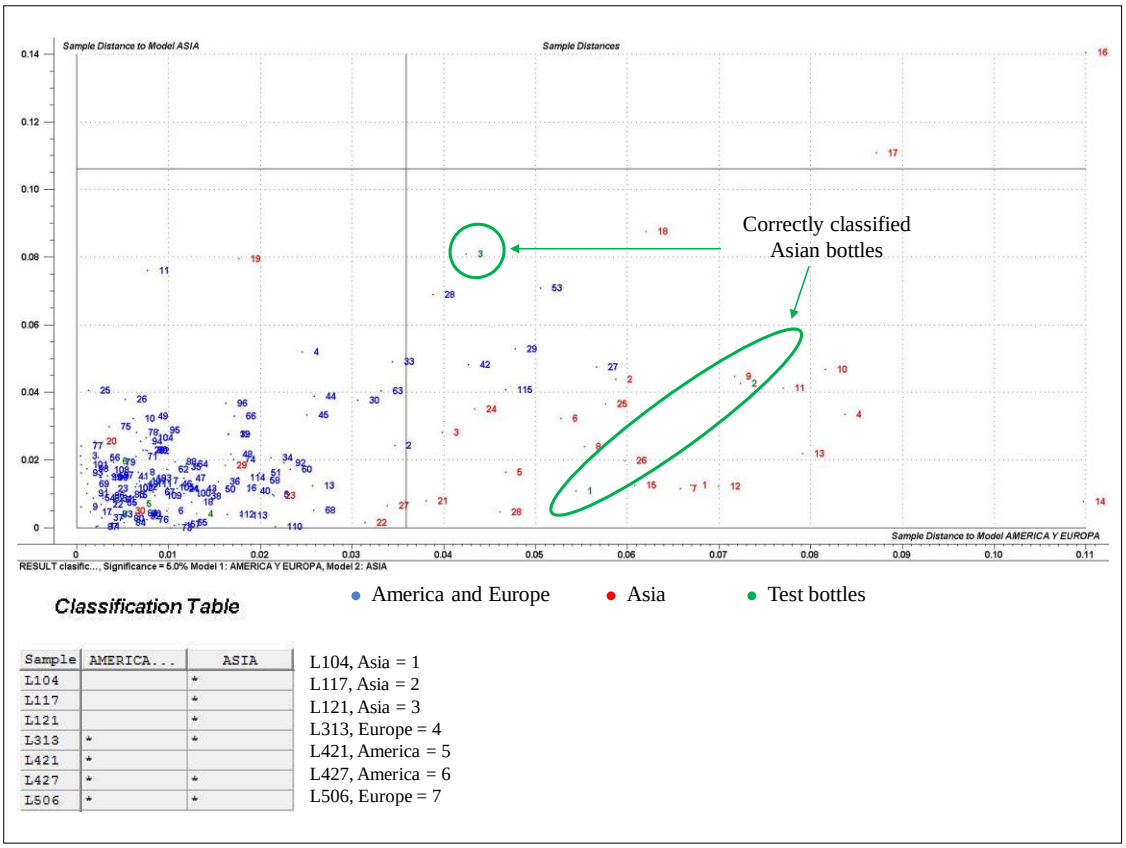


| Sample | AMERICA... | ASIA |
|---|---|---|
| L104 | | * |
| L117 | | * |
| L121 | | * |
| L313 | * | * |
| L421 | * | |
| L427 | * | * |
| L506 | * | * |

**Figure 15** Cooman's plot obtained from SIMCA modelling with its corresponding classification table.

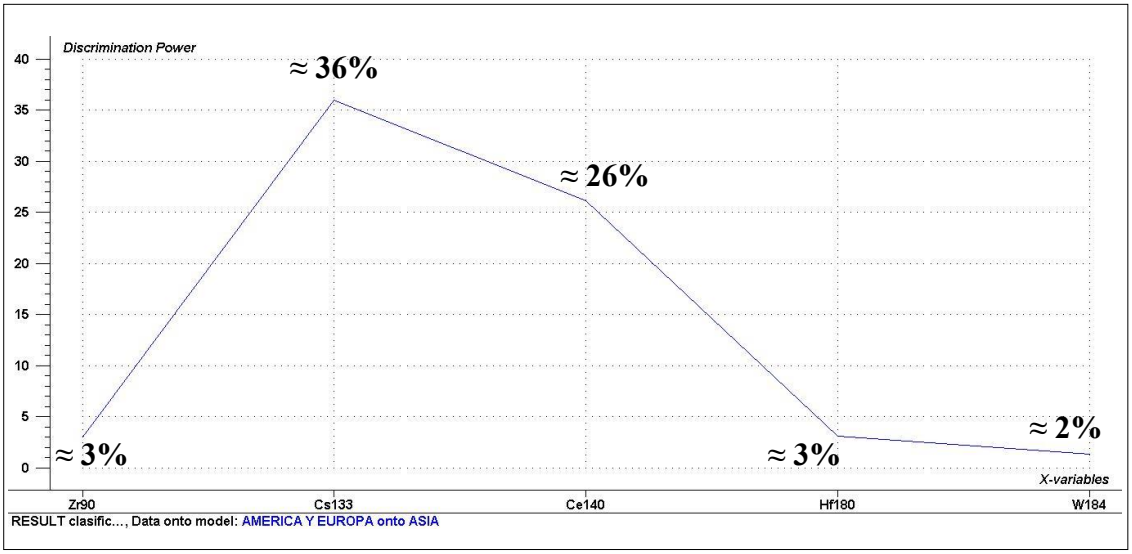


**Figure 16** Discrimination power of each variable used in the SIMCA modelling.

Although SIMCA classification proved to be a suitable classification tool, the small number of samples per continent and even more the absence of two continents (Oceania and Africa), prevented the development of a definitive prediction model for SIMCA, but was still sufficient to enable a preliminary assessment of the potential of this technique to classify bottles of wine according to their continent of origin.

***European green bottles***

In order to take a step forward in the discrimination of the green bottles according to their origin, it has been tried to classify the European green bottles. For this purpose, a PCA model (PC1 vs. PC2) which explains 88% of the variation in the data for the European green wine bottles, being the residuals < 1 for all the scores, was developed. The biplot (Figure 17) reveals that separation along PC1 accounts for the 73% of the variation in the sample set, while separation along PC2 accounts for the 14%. In this case, there is not a clear distinction between the origin of these bottles even reducing the initial isotopes only to five ($^{66}$Zn, $^{121}$Sb, $^{133}$Cs, $^{138}$Ba and $^{208}$Pb).

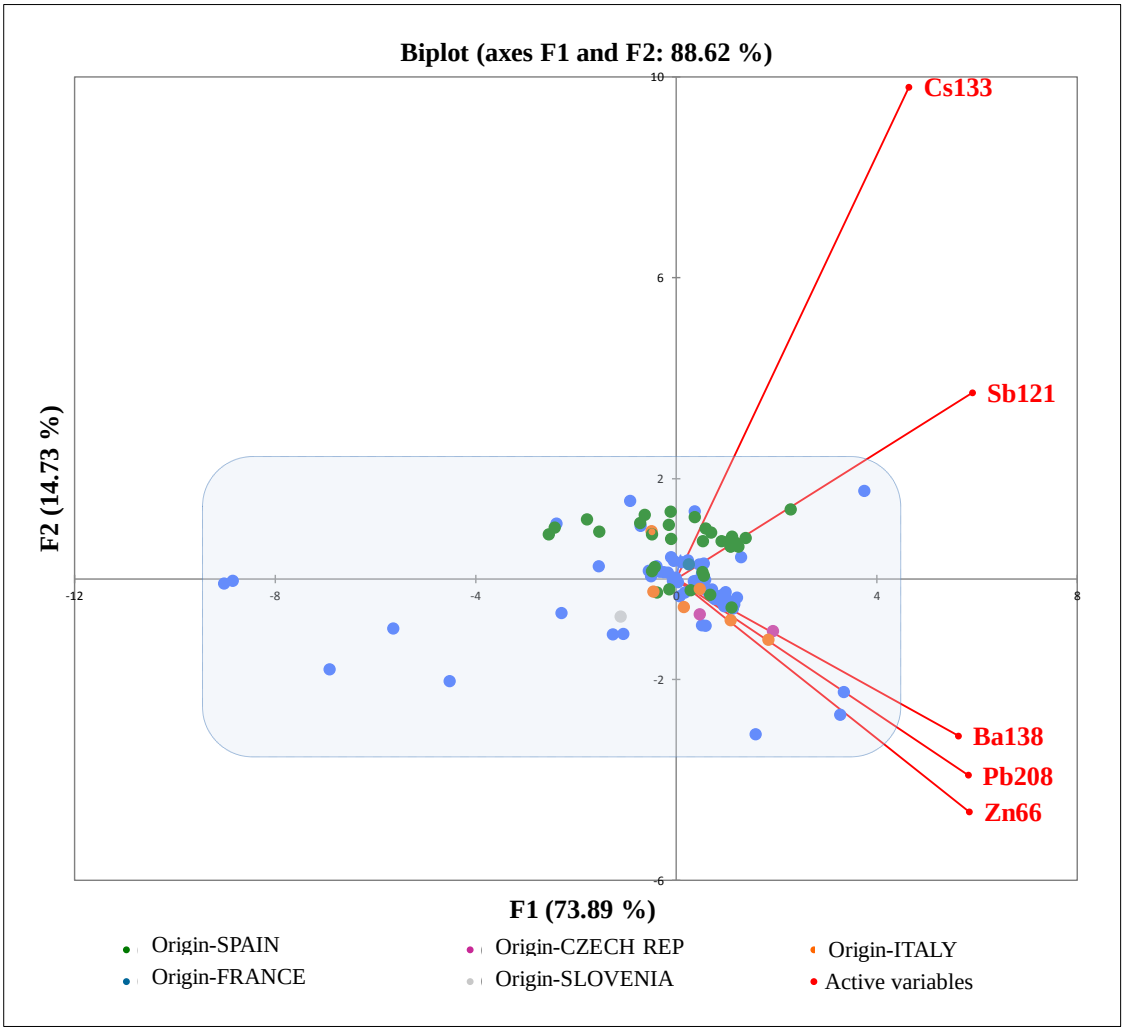


**Figure 17** Biplot (PC1 vs. PC2) representing European green bottles and the corresponding loadings.

These results can be derived from the situation of the glass industry in the EU. On the one hand, according to the Glass Alliance Europe, the European Alliance of Glass Industries, the production level maintains the EU as the largest glass producer in the world with a market share of around one-third of the total world market. Germany remains the EU's biggest producer with about one fifth of the volume, closely followed by France, Spain, Italy, and the UK. It must be noted that due to the strongly rising production costs and the growing legislative burden, investments are still increasingly made outside the EU. In fact, foreign trade from third countries does not play a dominant role in the EU glass market, although imports from Asian countries, and particularly China, are steadily increasing regarding in some glass applications (tableware, special glass and reinforcement glass fibres, concretely).

On the other hand, FEVE is the Federation of European manufacturers of glass containers and machine-made glass tableware. The association has some 60 corporate members belonging to approximately 20 independent corporate groups, who have 162 manufacturing plants distributed all over Europe. Manufacturing plants are located across 23 European States and include global major companies working for the world's biggest consumer brands. Therefore, taking into account that EU is the world's biggest producer of glass and that it counts with only 20 independent corporate groups located all along Europe, it is hardly surprising to achieve a strong differentiation among bottles coming from Europe.

#### 3.3.3.2 Classification of transparent wine bottles

Finally, transparent bottles were classified according to their origin. In this case, the sample set includes 35 bottles, but due to the low representativeness of Asian samples (2 bottles), it was chosen to remove them from the model.

A PCA (PC1 vs. PC2) explains 78% of the variation in the data for the green wine bottles being the residuals < 1 for all the scores was computed. The Figure 18 reveals that separation along PC1, which accounted for the 59% of the variation in the sample set, while separation along PC2 accounted for the 19% of the variation of in the sample set. Two groups corresponding to PORTUGAL/SPAIN and FRANCE are distinguishable. However, the groups are not completely separated from each other. In fact, three French bottles are included in the Portuguese/Spanish group. In this case, it is also a difficult task to discriminate among bottles coming from Europe for the same reason that has been previously described above. Among the forty seven monitored isotopes, ten of them ($^{24}$Mg, $^{51}$V, $^{52}$Cr, $^{55}$Mn, $^{63}$Cu, $^{66}$Zn, $^{107}$Ag, $^{138}$Ba, $^{166}$Er and $^{180}$Hf, respectively) were found to be the most discriminant variables. For this variable reduction, an initial PCA was run taking into account all the analyzed variables (Figure 16.B). After, the most significant (contribution of the observations, %) variables were selected from PC1, PC2 and PC3 and their

correlations were studied within the correlation matrix (Pearson (n)). To select correlation threshold value from which two variables are significantly correlated, the statistical significance of the Coefficient of Correlation (r) values were studied by transforming them into t experimental values according to the equation 1 for a p *value* < *0.005* and n-2 grades of freedom. It should be underlined that these loadings are slightly offset to the right positive side of the PC1 axis where the French bottles are located whereas none of them are found in the negative side. Indeed, Mg/Si is the most influent elemental ratio.

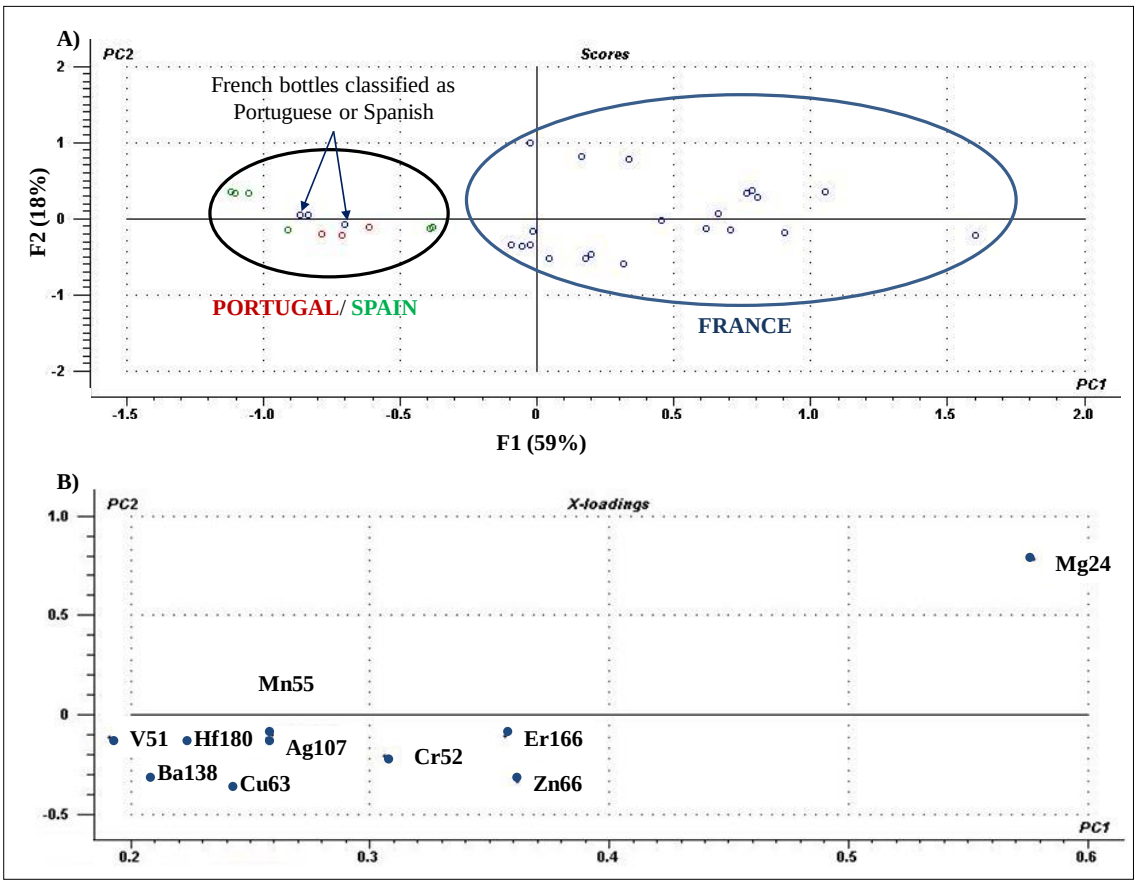


**Figure 18** A) PCA (PC1 vs. PC2) of the European transparent bottles and B) corresponding loadings for distinguishable each group (Portugal/Spain vs. France)

## 4. Conclusions

The aim of this work was to develop a fast unambiguous characterization method based on the ultra-trace analysis of glass packaging by minimally-invasive femtosecond laser ablation ICPMS, which induces no visible degradation of the bottle which could affect its value. It is mainly motivated by the increased number of wine fraud cases reported annually and the need to protect consumers and intellectual assets. Up to day, the capability to detect fraudulent wine or to check for spoilage markers has typically required opening the bottle to sample the liquid, a destructive process that can render the wine no longer storable and thus worthless for future resale.

In this framework, taking into account the previously stated objectives and based on the results derived from this study, the following conclusions can be drawn:

1. A minimally-invasive ablation strategy (< 0.5 mm) have been optimized which cause non-visible damage to the bottle, allowing the analysis of a single bottle in a very competitive time (90 seconds).

2. The method has demonstrated good reproducibility and homogeneity as well as good linearity and low limits of detection.

3. Developed methodology has been successfully applied for the analysis of glass of 237 bottles which have divided into 3 different batches: i) original vs. counterfeited bottles, ii) a series of 34 bottles from the same winery and which comprises the vintages from 1969 to 2010 and iii) 190 bottles coming from all around the world and which have been divided into green and transparent bottles for a better comprehension of the obtained results.

4. Statistical data analysis based on multivariate analysis including Principal Component Analysis (PCA), Hierarchical Ascendant Classification (HAC) and Soft Independent Modelling of Class Analogy (SIMCA) have allowed:

   4.1 Discrimination between original and counterfeited bottles pointing out the main trace elements involved in this discrimination which are $^{27}Al$, $^{153}Eu$, $^{138}Ba$ and $^{184}W$, respectively.

   4.2 Distinction of the chemical profile of each bottle according to their vintage and origin.

4.2.1 The series comprising 34 bottles was classified in 4 different groups according to their vintage. In general terms, it could be concluded that ancient bottles are mainly characterized by rare earths and slightly higher amount of major elements whereas recent bottles are characterized for having higher amount of trace elements. This is attributed to a recycling process. Special mention has to be done to the great addition of iron in the last group belonging to the most recent samples, which has been added with the purpose to enhance the UV protection to preserve wine during storage and has a visual influence on their darker green color. Some specific vintages can be identified with only one v M/Si ratio, without the use of sophisticated statistic data processing.

4.2.2 An attempt to classify wine bottles coming from all around the world was done. Firstly, green and transparent bottles were separated for statistical data analysis. It was observed from derived PCA that green bottles are characterized for having much more impurities than transparent bottles, fact that supports literature findings.

Secondly, the computed PCA for European, American and Asian green bottles shows two major groups, Europe/America and Asia, respectively. For this purpose, 10 isotopes among the 47 isotopes monitored were used: $^{75}$As, $^{85}$Rb, $^{121}$Sb, $^{133}$Cs, $^{138}$Ba, $^{140}$Ce, $^{142}$Nd, $^{181}$Ta, $^{184}$W and $^{208}$Pb, concretely. Due to the fact that American/European bottles are quite distinguished from Asian bottles, a classification attempt was carried out using SIMCA statistical tool. Unfortunately, the models were not sufficiently different for classification and discrimination of the samples. In fact, using a significance level of 5%, the 57% of the samples contained in the test set (4 out of 7) were recognized by the correct class model according to the classification table, being the $Cs^{133}$ the most discriminant isotope of the model. Although SIMCA classification proved to be a suitable classification tool, the small number of samples representing each continent prevented the development of a more accurate prediction model for SIMCA but was still sufficient to enable a preliminary assessment of the potential of this technique to classify bottles of wine according to their continent of origin.

In order to take a step forward in the discrimination of the green bottles according to their origin, a PCA was run with European green bottles, not having a good classification. In fact, being the EU the world's biggest producer of glass, there are only few independent corporate groups dedicated to glass containers manufacturing.

Finally, European transparent bottles were classified according to their country of origin. In this case, French bottles are quite separate from Portuguese and Spanish bottles, although 3 French bottles remains in the Portuguese/Spanish group. Similarly to what happens with green bottles, there are few glass container manufacturers who share the trade monopoly reducing the possibility of finding heterogeneities and making difficult the task of glass bottle classification according to the origin. In addition, once again, the small number of samples representing each country prevented the development of a more accurate classification and prediction model.

Therefore, taking into account the drawn conclusion and the fact that there are not bibliographical precedents on this topic, this work shows a valuable new alternative way to perform authentication and traceability analysis on wine, based on the direct analysis of the glass packaging by the minimally-destructive technique of femtosecond laser ablation coupled to ICPMS. This quasi non invasive approach is fast and allows to detect trace concentrations below $ng \cdot g^{-1}$, which has not equivalent in terms of performance to date.

## 5. Bibliography


1. Zerwick C. A Short History of Glass. New York: Harry N Adams Publishers; 1990.
2. Examination of glass. Forensic Interpretation of Glass Evidence: CRC Press; 2000.
3. Hickman DA. Glass types identified by chemical analysis. Forensic Science International. 1987;33(1):23-46.
4. Hickman DA. A classification scheme for glass. Forensic Science International. 1981;17(3):265-81.
5. Locke J, Unikowski JA. Breaking of flat glass — Part 1: Size and distribution of particles from plain glass windows. Forensic Science International. 1991;51(2):251-62.
6. Locke J, Unikowski JA. Breaking of flat glass—part 2: Effect of pane parameters on particle distribution. Forensic Science International. 1992;56(1):95-106.
7. Locke J, Scranage JK. Breaking of flat glass — Part 3: Surface particles from windows. Forensic Science International. 1992;57(1):73-80.
8. Allen TJ, Locke J, Scranage JK. Breaking of flat glass—part 4: Size and distribution of fragments from vehicle windscreens. Forensic Science International. 1998;93(2–3):209-18.
9. Koons R, Fiedler C, Rawalt R. Classification and Discrimination of Sheet and Container Glasses by Inductively Coupled Plasma-Atomic Emission Spectrometry and Pattern Recognition. 1988.
10. Locke J, Underhill M. Automatic Refractive Index Measurement of Glass particles. Forensic Science International. 1985;27(4):247-60.
11. Stoney DA, Thornton JI. The forensic significance of the correlation of density and refractive index in glass evidence. Forensic Science International. 1985;29(3–4):147-57.
12. Locke J, Zoro JA. The examination of glass particles using the interference objective: Part 1. Methods for rapid sample handling. Forensic Science International. 1983;22(2–3):221-30.
13. Standard test method for the automated determination of refractive index of glass samples using the oil immersion method and a phase contrast microscope, E1967-98 (2003).
14. Buscaglia JA. Elemental analysis of small glass fragments in forensic science. Analytica Chimica Acta. 1994;288(1–2):17-24.
15. Koons R, Buscaglia J. Distribution of Refractive Index Values in Sheet Glasses. Forensic Science Communications. 2001.
16. Umpierrez S, Trejos T, Neubauer K, Almirall J. Determination of Iron in Glass by Solution and Laser Ablation DRC-ICP-MS. Atomic Spectroscopy. 2006;27(3):76-9.
17. Suzuki Y, Sugita R, Suzuki S, Marumo Y. Forensic Discrimination of Bottle Glass by Refractive Index Measurement and Analysis of Trace Elements with ICP-MS. Analytical Sciences. 2000;16(11):1195-8.

18. Zadora G. Classification of glass fragments based on elemental composition and refractive index. J Forensic Sci. 2009;54(1):49-59.
19. Calligaro T. PIXE in the study of archaeological and historical glass. X-Ray Spectrometry. 2008;37(2):169-77.
20. Revenko AG. Estimation and account for matrix effects in studying glass materials of cultural heritage by X-ray spectral analysis. X-Ray Spectrometry. 2010;39(1):63-9.
21. Coleman RF, Goode GC. Comparison of glass fragments by neutron activation analysis. Journal of Radioanalytical Chemistry. 1973;15(1):367-88.
22. Catterick T, Wall CD. Rapid analysis of small glass fragments by atomic-absorption spectroscopy. Talanta. 1978;25(10):573-7.
23. Bridge CM, Powell J, Steele KL, Sigman ME. Forensic comparative glass analysis by laser-induced breakdown spectroscopy. Spectrochimica Acta Part B: Atomic Spectroscopy. 2007;62(12):1419-25.
24. Bridge CM, Powell J, Steele KL, Williams M, Macinnis JM, Sigman ME. Characterization of automobile float glass with laser-induced breakdown spectroscopy and laser ablation inductively coupled plasma mass spectrometry. Appl Spectrosc. 2006;60(10):1181-7.
25. Catterick T, Hickman DA. The quantitative analysis of glass by inductively coupled plasma-atomic-emission spectrometry: A five-element survey. Forensic Science International. 1981;17(3):253-63.
26. Meinttjes-Van Der Walt L. Shattering the silence: how glass analysis speaks. South African Journal of Criminal Justice. 2005;18(1):56-65.
27. Koons RD, Peters CA, Rebbert PS. Comparison of refractive index, energy dispersive X-ray fluorescence and inductively coupled plasma atomic emission spectrometry for forensic characterization of sheet glass fragments. Journal of Analytical Atomic Spectrometry. 1991;6(6):451-6.
28. Duckworth DC, Bayne CK, Morton SJ, Almirall J. Analysis of variance in forensic glass analysis by ICP-MS: variance within the method. Journal of Analytical Atomic Spectrometry. 2000;15(7):821-8.
29. Montero S, Hobbs AL, French TA, Almirall JR. Elemental analysis of glass fragments by ICP-MS as evidence of association: analysis of a case. J Forensic Sci. 2003;48(5):1101-7.
30. Duckworth DC, Morton SJ, Bayne CK, Koons RD, Montero S, Almirall JR. Forensic glass analysis by ICP-MS: a multi-element assessment of discriminating power via analysis of variance and pairwise comparisons. Journal of Analytical Atomic Spectrometry. 2002;17(7):662-8.

31. Trejos T, Montero S, Almirall JR. Analysis and comparison of glass fragments by laser ablation inductively coupled plasma mass spectrometry (LA-ICP-MS) and ICP-MS. Anal Bioanal Chem. 2003;376(8):1255-64.
32. Standard Test Method for Determination of Trace Elements in Glass Samples Using Inductively Coupled Plasma Mass Spectromety (ICP-MS), ASTM E2330-04 (2004).
33. May CD, Watling RJ. A comparison of the use of refractive index (RI) and laser ablation inductively coupled plasma mass spectrometry (LA-ICP-MS) for the provenance establishment of glass bottles. Forensic Sci Med Pathol. 2009;5(2):66-76.
34. Trejos T, Almirall JR. Effect of fractionation on the forensic elemental analysis of glass using laser ablation inductively coupled plasma mass spectrometry. Anal Chem. 2004;76(5):1236-42.
35. Trejos T, Koons R, Weis P, Becker S, Berman T, Dalpe C, et al. Forensic analysis of glass by [small mu ]-XRF, SN-ICP-MS, LA-ICP-MS and LA-ICP-OES: evaluation of the performance of different criteria for comparing elemental composition. Journal of Analytical Atomic Spectrometry. 2013;28(8):1270-82.
36. Trejos T, Koons R, Becker S, Berman T, Buscaglia J, Duecking M, et al. Cross-validation and evaluation of the performance of methods for the elemental analysis of forensic glass by XRF, ICP-MS, and LA-ICP-MS. Anal Bioanal Chem. 2013;405(16):5393-409.
37. Latkoczy C, Becker S, Ducking M, Gunther D, Hoogewerff JA, Almirall JR, et al. Development and evaluation of a standard method for the quantitative determination of elements in float glass samples by LA-ICP-MS. J Forensic Sci. 2005;50(6):1327-41.
38. The economic cost of IPR infringement in spirits and wine. Quantification of infringement in distilling, rectifying and blending of spirits (NACE 11.01) and manufacture of wine from grape (NACE 11.02). European Union Intellectual Property Office (EUIPO); July 2016.
39. Compendium of International Methods of Wine and Must Analysis. International Organisation of Vine and Wine (OIV). 2016 [cited 14 March 2017]. Available from: http://www.oiv.int/en/technical-standards-and-documents/methods-of-analysis/compendium-of-international-methods-of-analysis-of-wines-and-musts-2-vol.
40. Médina B, Salagoïty MH, Guyon F, Gaye J, Hubert P, Guillaume F. 8 - Using new analytical approaches to verify the origin of wine A2 - Brereton, Paul. New Analytical Approaches for Verifying the Origin of Food: Woodhead Publishing; 2013. p. 149-88.
41. A. Labruyere RSaMS. Les vins de France et du monde: Nathan; 2015.
42. Zurhaar A, Mullings L. Characterisation of forensic glass samples using inductively coupled plasma mass spectrometry. Journal of Analytical Atomic Spectrometry. 1990;5(7):611-7.

43. Watling RJ, F. Lynch B, Herring D. Use of Laser Ablation Inductively Coupled Plasma Mass Spectrometry for Fingerprinting Scene of Crime Evidence. Journal of Analytical Atomic Spectrometry. 1997;12(2):195-203.
44. Weis P, Ducking M, Watzke P, Menges S, Becker S. Establishing a match criterion in forensic comparison analysis of float glass using laser ablation inductively coupled plasma mass spectrometry. Journal of Analytical Atomic Spectrometry. 2011;26(6):1273-84.
45. Aeschliman DB, Bajic SJ, Baldwin DP, Houk RS. Multivariate Pattern Matching of Trace Elements in Solids by Laser Ablation Inductively Coupled Plasma-Mass Spectrometry: Source Attribution and Preliminary Diagnosis of Fractionation. Analytical Chemistry. 2004;76(11):3119-25.
46. Schmidt T, Vogt T, Surmann JP, Kossler W. Glass classification by linear discriminant analysis of LA-ICP-MS data. Pharmazie. 2002;57(6):396-8.
47. Gunther D, A. Heinrich C. Enhanced sensitivity in laser ablation-ICP mass spectrometry using helium-argon mixtures as aerosol carrier. Journal of Analytical Atomic Spectrometry. 1999;14(9):1363-8.
48. van der Velde-Koerts T, de Boer JLM. Minimization of spectral interferences in inductively coupled plasma mass spectrometry by simplex optimization and nitrogen addition to the aerosol carrier gas for multi-element environmental analysis. Journal of Analytical Atomic Spectrometry. 1994;9(10):1093-8.
49. Tan SH, Horlick G. Background Spectral Features in Inductively Coupled Plasma/Mass Spectrometry. Applied Spectroscopy. 1986;40(4):445-60.
50. D'Ilio S, Violante N, Majorani C, Petrucci F. Dynamic reaction cell ICP-MS for determination of total As, Cr, Se and V in complex matrices: Still a challenge? A review. Analytica Chimica Acta. 2011;698(1):6-13.
51. May TW, Wiedmeyer RH. A table of polyatomic interferences in ICP-MS. Atomic Spectroscopy. 1998;19(5):150-5.
52. Henderson W, McIndoe JS. Appendix 1: Naturally Occurring Isotopes. Mass Spectrometry of Inorganic, Coordination and Organometallic Compounds: John Wiley & Sons, Ltd; 2005. p. 235-46.
53. Adriaens A. Non-destructive analysis and testing of museum objects: An overview of 5 years of research. Spectrochimica Acta Part B: Atomic Spectroscopy. 2005;60(12):1503-16.
54. Donard A, Pottin AC, Pointurier F, Pecheyran C. Determination of relative rare earth element distributions in very small quantities of uranium ore concentrates using femtosecond UV laser ablation - SF-ICP-MS coupling. Journal of Analytical Atomic Spectrometry. 2015;30(12):2420-8.

55. Guillong M, Günther D. Quasi 'non-destructive' laser ablation-inductively coupled plasma-mass spectrometry fingerprinting of sapphires. Spectrochimica Acta Part B: Atomic Spectroscopy. 2001;56(7):1219-31.
56. Kuhn H-R, Gunther D. Laser ablation-ICP-MS: particle size dependent elemental composition studies on filter-collected and online measured aerosols from glass. Journal of Analytical Atomic Spectrometry. 2004;19(9):1158-64.
57. Koch J, von Bohlen A, Hergenroder R, Niemax K. Particle size distributions and compositions of aerosols produced by near-IR femto- and nanosecond laser ablation of brass. Journal of Analytical Atomic Spectrometry. 2004;19(2):267-72.
58. Guideline on bioanalytical method validation. European Medicines Agency (EMA). 2011 (cited 22 September 2017). Available from: http://www.ema.europa.eu/docs/en_GB/document_library/Scientific_guideline/2011/08/WC500109686.pdf.
59. Jochum KP, Weis U, Stoll B, Kuzmin D, Yang Q, Raczek I, et al. Determination of Reference Values for NIST SRM 610–617 Glasses Following ISO Guidelines. Geostandards and Geoanalytical Research. 2011;35(4):397-429.
60. Lavine BK. Clustering and Classification of Analytical Data. Encyclopedia of Analytical Chemistry: John Wiley & Sons, Ltd; 2006.
61. Mooi E, Sarstedt M. Cluster Analysis. In: Mooi E, Sarstedt M, editors. A Concise Guide to Market Research: The Process, Data, and Methods Using IBM SPSS Statistics. Berlin, Heidelberg: Springer Berlin Heidelberg; 2011. p. 237-84.
62. Fdez-Ortiz de Vallejuelo S, Arana G, de Diego A, Madariaga JM. Pattern recognition and classification of sediments according to their metal content using chemometric tools. A case study: The estuary of Nerbioi-Ibaizabal River (Bilbao, Basque Country). Chemosphere. 2011;85(8):1347-52.
63. Stumpe B, Engel T, Steinweg B, Marschner B. Application of PCA and SIMCA Statistical Analysis of FT-IR Spectra for the Classification and Identification of Different Slag Types with Environmental Origin. Environmental Science & Technology. 2012;46(7):3964-72.
64. Cozzolino D, Smyth HE, Cynkar W, Dambergs RG, Gishen M. Usefulness of chemometrics and mass spectrometry-based electronic nose to classify Australian white wines by their varietal origin. Talanta. 2005;68(2):382-7.
65. Médina B, Sudraud P. Teneur des vins en chrome et en nickel. Causes d'enrichissement. OENO One; Vol 14, No 2 (1980): Journal international des sciences de la vigne et du vin. 1980.
66. Donald SB, Swink AM, Schreiber HD. High-iron ferric glass. Journal of Non-Crystalline Solids. 2006;352(6):539-43.

67. The truth about recycling2007 22 June 2017. Available from: http://www.economist.com/node/9249262.

# CHAPTER 6:

# Analysis of packaging for wine authentication:

## Part 2.1: Elemental analysis of label matrix and ink by femtosecond laser ablation coupled to ICPMS

## General introduction: what are paper and ink?

Any written document paper whose source or authenticity is doubtful could be considered as a *questioned* document. In general terms, questioned documents consist of handwritten, typed or printed information on paper. Therefore, both the paper and the ink are often the subject of forensic analysis as part of the overall examination carried out in order to make a decision about a questioned document's authenticity (1, 2). The questions to answer may be quite different, depending on the information required: i) to determine the authenticity of these documents, ii) to identify the source of questionable ink or paper, iii) to compare the ink and paper of different documents, iv) to stablish a common origin of different documents or inks, v) to discriminate between different paper and ink manufacturers, vi) to determine the printer used to print the document and vii) to date documents (3).

Paper making is considered to have originated in China for writing and record keeping purposes in AD 105 by Ts'ai Lun, an official of the Chinese Imperial Court. Since that time, paper has been playing a major role in the development of cultures over the world (4). Although the modern product differs considerably from its ancestral materials, papermaking retains distinct similarities to the processes developed by Ts'ai Lun.

The paper is basically made from cellulose and hemicellulose from wood or by the re-pulping of paper for recycling. Figure 1 schematically shows the papermaking process. In the first step of the paper making process, the wood is debarked and chipped. The woodchips are then pulped to remove lignin which is the compound that cements the wood fibers together and the main responsible for the yellowing of paper over time. There are two main pulping processes: mechanical and chemical pulping. In general terms, mechanical pulping involves grinding the wood chips between stone plates in water to break the bonds between the fibers and increasing the temperature to soften the lignin. Meanwhile, chemical pulping involves the use of aqueous chemical solutions and elevated temperature and pressure to extract pulp fibers. Chemical pulping is made by using the Kraft (sulphate) and sulphite processes. This last method uses sodium dioxide and lime to remove lignin. Kraf method, instead, uses sodium hydroxide and sodium sulfate to remove lignin from the fiber. The Kraf process is the more commonly used chemical pulping method because it produces a better quality paper with improved smoothness and printability. The next stage of the process is washing to obtain pulp that is free of unwanted solubles and in which several chemical additives are added to the pulp to improve the quality of the final paper, such as bleaching agents (improved brightness), fillers (improved optical qualities), sizing agents (water repellents and improve printing properties) and coatings (improved

gloss, brightness and opacity). Then, the pulp solution is drained into a fourdrinier to create a continuous paper web and subsequently moved to dandy rolls to further remove water and air by compression and smooth the paper surface. Finally, the paper passes between through calenders which consist of rolls of cast iron, chilled on the surface to make it hard, and ground and polished to a very smooth surface (5).

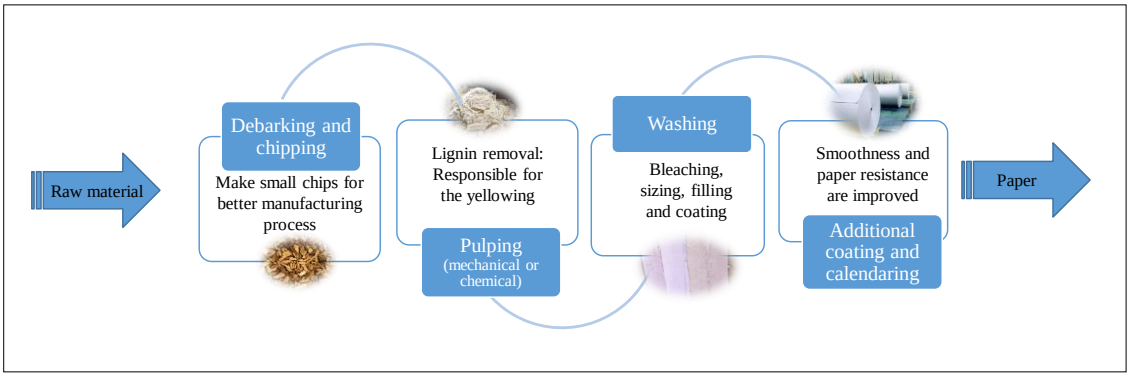


**Figure 1** Overview of the papermaking process.

The evolution of papermaking from the 12$^{th}$ century, in Europe, was characterized by continuous changes of fibrous and non-fibrous materials as cellulose, wood pulp, sizing agents, fillers and coatings. Some changes in the manufacturing process occurred for economic or environmental reasons (6). The most significant change occurred during the late 1980s and early 1990s when manufacturers stopped producing acidic paper in favor of alkaline or neutral process paper. Therefore, these innovations and modifications can stablish the earliest date or period a particular sheet of paper was manufactured (7).This finding can be corroborated if certain chemicals that were introduced after the date on the document are present in the paper. Then the product has, besides cellulose, certain compounds characteristic of each production. The variability in paper manufacture makes it possible to identify a great variety of subtle distinctions that give each batch of paper or each sheet of paper a unique chemical fingerprint. Consequently, paper is capable of yielding clues about the production of manuscripts, labels, books and any other document that are unavailable from other kind of evidence (4).

Meanwhile, writing inks were first manufactured in both ancient Egypt and China in about 2500BC. These inks were made of soot bound together with gums. This paste was formed into rods and dried, then mixed with water immediately before use. Contrary, today's printing inks are an extremely complex homogeneous mediums, composed of coloring agents (dyes and pigments), vehicles (solvents and resins) and additives, which are added in smaller proportion to modify the rheological properties of inks (lubricants, solubilizers, plasticizers, waxes, chelating agents, antioxidants surfactants and fluorescers, for example). In addition, ink manufacturing is carried

out in two stages. First, a mixture of solvent, resins and additives called varnish is done and then coloring agents are mixed into it. The mixture of components, usually kept secret by the manufacturing industry, is useful for giving the color, controlling the density of flow, modifying the drying kinetic and providing the final appearance. In addition to this basic composition, a chemical marker can be included as tag and tracer (chemical marker as rare earth organometallic compounds and traces of optical whiteners) which does not vary over time. The identification of these markers can lead forensic scientists to define the earliest possible date of the studied document or to compare with certainty a suspect counterfeit item with its original. However, this labeling system would undoubtedly imply the need for knowing which manufacturer used which chemical marker. Regarding the employed technology, the following classification must be considered: pen inks and printer inks. Printer inks which form the subject matter of this work, can be divided into toner based printers and liquid inkjet printers. The new printer technologies provide copies very similar to the original documents, increasing the problem of forgery (8-10).

The analysis of questioned documents therefore involves different types of analyses including comparisons of the ink and printing procedure as well as physical and chemical characterization of the paper itself. Forensic examiners are hence faced with the extreme diversity of combinations between ink formulations and writing instrument and paper brands/models when attempting to identify the source of questioned evidences (11). In routine examination, non-destructive analytical methods such as microscopic and optical testing methods are applied first. They are simpler to perform, involve little or no manipulation of the document and can provide sufficient information without loss of the documents evidential value. Nevertheless, such techniques do not provide a complete set of information, especially about their chemical composition. Consequently, developing more informative and effective tools for question documents examinations become necessary and simultaneously a challenge as the methods for falsification and document alteration grow more sophisticated (12). In any case, fraud detection involves a static approach, which searches for inconsistencies in the compositional profile of the object, and a dynamic approach, which examines the aging process (13).

Counterfeiting often occurs after a genuine item is made and its detection is based on finding a component in suspect item that did not exist when genuine one was made, which is called anachronism. The compositional profile or chemical fingerprint of an item consists of its major, minor and trace organic and inorganic components. Thus, the specificity or discriminating power of an analytical technique depends on the amount of the information included in the compositional profile (13). In the following paragraphs a brief revision of the literature will be done for the both elemental and molecular analysis of paper and ink (Figure 2).

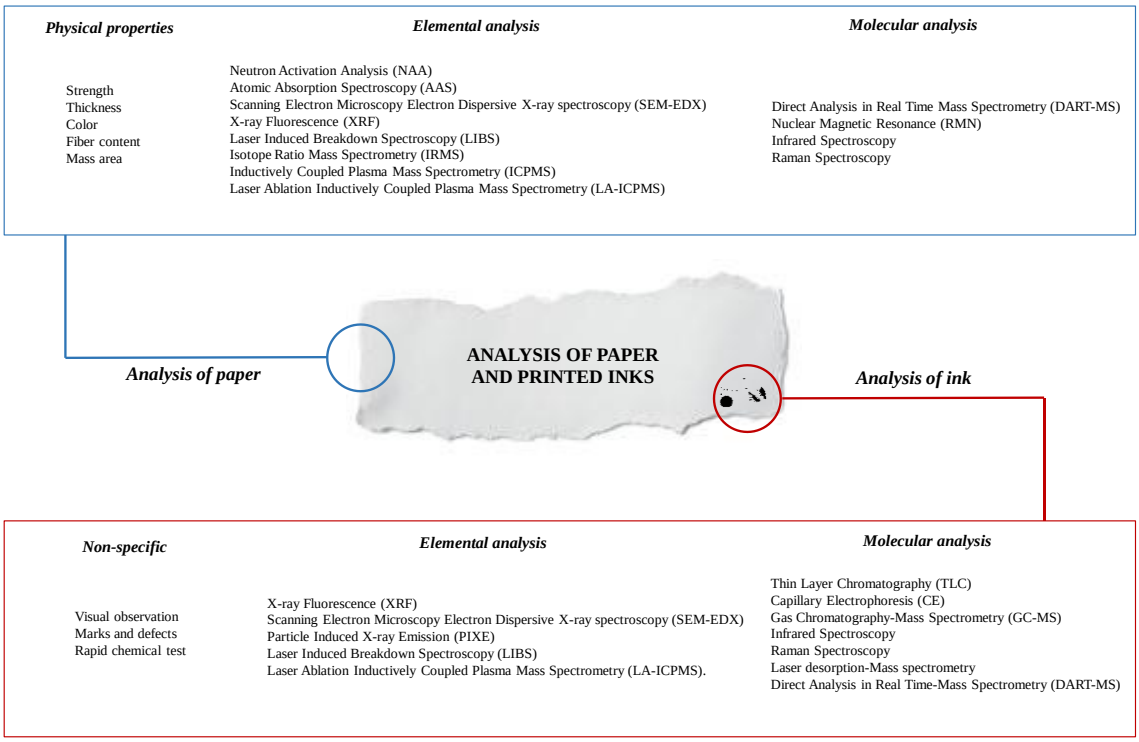


**Figure 2** Analysis methods for paper and printed ink.

*Elemental and molecular analysis of paper*

The forensic document examination usually first involves the study of gross physical properties like strength, thickness, color, fiber content, fluorescence or mass area which can be measured to compare different sheets of paper (3). These techniques are both inexpensive and easy to perform. However, the problem with using these methods for the characterization of paper remains the inability to match two sheets of paper with a high degree of confidence as well as the relatively large number of samples required for most of these methods (14). In addition, due to improvements in quality control during the modern manufacturing process, the final paper product is very uniform with few physical or chemical differences among paper samples of the same type, even batches from different manufacturers in different countries can be very similar physically. Nonetheless, even if the main components of the paper are similar, there can still be variation in the trace elemental composition. Interestingly, the forensic utility of elemental analysis of paper has been documented since the 1970s and relies upon the premise that, as paper is produced from natural materials and recycled consumer waste, it is possible to characterize them through their trace elements, which can be different from one manufacturer to another (9).

Elemental analysis of paper has been reported in the literature, using a wide variety of analytical techniques. These techniques include Neutron Activation Analysis (NAA) (15-17), Atomic Absorption Spectroscopy (AAS) (18-20), Scanning Electron Microscopy Electron Dispersive X-ray spectroscopy (SEM-EDX) (21), X-ray Fluorescence (XRF) (22-26), Laser Induced Breakdown Spectroscopy (LIBS) (27, 28), Isotope Ratio Mass Spectrometry (IRMS) (26), and Inductively Coupled Plasma Mass Spectrometry (ICPMS) (29-32).

Each of these techniques has their own advantages and limitations, ICP-MS providing significant advantages over the other methods. On the one hand, ICP-MS allows rapid quantitative multi-elemental analysis of elements with superior detection limits. The potential of detecting more elements also provides improved discrimination capabilities. On the other hand, ICP-MS methods also offer excellent precision, reproducibility and selectivity. However, the main disadvantages of the conventional digestion technique rely on the fact that the sample is destructed, and some time consuming and complex digestion protocols are required. Consequently, laser based methods provide some advantages over solution-ICP methods since there is no need to digest the paper and the sample consumption is substantially reduced. The laser-based methods reported here remove only ~9–15 μg of paper from microscopic areas, leaving the paper almost intact after the analysis (27). Despite the inherent advantages of LA-ICP-MS, to date there are few studies reporting the use of this technique for the analysis of paper. Table 1 summarizes the research done for the analysis of paper using LA-ICPMS.

**Table 1** Experimental conditions of main applications of LA-ICPMS to the analysis of paper.

| Sample | Analytes | Laser | ICPMS | CRM | Ref |
|---|---|---|---|---|---|
| **Document papers** | **Fe and Cu** | **Nd:YAG (266 nm)** | **VG Elemental PlasmaQuad3** | **Liquid standard solutions** | **(20)** |
| **Document papers** | **Fe, Cu and Mn** | **CETAC LSX-200 (266 nm)** | **Perkin Elmer ELAN 9000** | **NIST 612** | **(33)** |
| **Document papers** | **Ca, Na, K, Al and Fe** | **QUANTEL Nd:YAG (266, 355, 532 and 1064 nm)** | **Laser ablation is applied for surface cleaning. The spectra of ablated products are obtained by LIBS** | **No specified** | **(34)** |
| **Document papers** | **Mg** | **CETAC LSX-200 (266 nm)** | **Perkin Elmer ELAN 9000** | **No specified** | **(35)** |
| **Document papers** | **Li, B, Na, Mg, Al, Si, K, Ca, Ti, V, Cr, Mn, Fe, Ni, Co, Cu, Zn, Ga, As, Rb, Sr, Zr, Nb, Mo, Sn, Sb, Cs, Ba, LA, Ce, Nd, Sm, Eu, Tb, Ho, Tm, Lu, Hf, Ta, W, Pt, Au, Pb, Bi, Th, U** | **New Wave UP-213 Nd:YAG (213 nm)** | **Perkin Elmer ELAN DRC plus** | **No specified** | **(26)** |

The detection of the molecular constituents of document papers with minimal destructive sampling can significantly enhance the capacity to study their manufacturing process in terms of their pulp composition and pitch contaminants. Direct Analysis in Real Time Mass Spectrometry (DART-MS) (36) has been successfully applied to obtain unique mass spectra bleached Kraft, chemithermomechanical, and stone groundwood pulp papers in real time without extractions, derivatizations, chromatographic separations, and other time- and chemical-consuming sample preparations. Nuclear Magnetic Resonance (NMR) is particularly useful for the characterization of paper internal structure, water transport properties and for evaluating the general state of conservation, thus NMR spectroscopy has proved to be valuable in assessing paper quality (37-39). However, both Infrared spectroscopy and Raman spectrometry are the most important methods for the identification and characterization of paper chemical structures. Both are essential analytical tools for the structural analysis of paper and pulp chemistry. The studies of cellulose, hemicellulose, lignin, thermal- and photo-induced oxidation; cross-linking; and various chemical treatments of pulp and paper products are all made possible using these forms of molecular spectroscopy (6).

On the one hand, Infrared spectroscopy is of major importance in paper characterization as it allows the identification of chemical functional groups from vibrational spectra. Mainly it permits the identification of the provenance of fibers and the determination of the chemical composition of additives used in papermaking and identification of impurities distributed on the surface of the paper (40). It plays an important role in the study of paper deterioration processes as well (41, 42). In fact, the ageing process of paper, related to different factor such as oxidative agents, light, moisture, pollution and acidity, is characterized by oxidized groups (carbonyl and carboxyl groups) on the cellulose chain (4). Paper degradation is manifested by changes in the mechanical and physical properties of paper. On the other hand, Raman spectroscopy was proven to show some important advantages in the study of materials that strongly scatter light, such as cellulose. With the excitation frequency well removed from any absorption band, the refractive index variations of the sample normally observed in the infrared spectra are not observed as an interference in Raman spectroscopy. In addition, the water bands are very weak and thus do not overlap with the hydroxy bands of cellulose. Therefore, Raman spectroscopy has proved to be a valuable tool for getting information about the presence of fillers in the cellulose and the degradation mechanism (1, 40, 43).

*Elemental and molecular analysis of ink*

Methods for the detection of fraudulent components in ink were slowly developed up to 1950. Before then, inks on questioned documents were primarily observed and examined by photography, using filters to enhance different contrast between different inks. The documents were also examined by observing the colors under various wavelengths of light ranging from the ultraviolet to infrared. Occasionally, chemical test were also employed to detect metals such as copper, vanadium and chromium in pen inks. These procedures showed sometimes a kind of usefulness to distinguish among different types of inks. But they did not provide individualization information to characterize the various formulations. Nowadays, in routine examinations of inks non-destructive analytical methods are applied first, which have not significantly varied over the years. Using these methods, selected parameters of the ink, such as its color, luminescence and absorption or radiation can be determined. They do not provide information on all components of the ink and they do not allow to identify the kind of ink on the basis of its chemical composition. In fact, they take into account only those components, which strongly interact with a given region of electromagnetic radiation and therefore they show merely differences between compared samples (44). It must be pointed out that the amount of research is much more extended for pen inks than for printer inks (9). However, due to the subject of this work in which printed wine labels have been analyzed, the revision of the analytical techniques for the elemental and molecular analysis of inks will be exclusively focused on printing inks.

The improvements in high quality commercial printers have promoted the counterfeiting of documents. Thus, it has pushed the development of more sensitive and robust techniques for the detection of fraudulent activities related to printing inks. Non-analytical technique, such as the analysis of marks or defects produced by printer have been also investigated (45, 46). The chemical characterization of printing inks can aid forensic document examiners to both discriminate between different sources of printers and, equally important to associate documents that have originated from the same printing source. The inorganic portion of the ink can be a valuable tool for the characterization and discrimination of printing inks. It has been reported that a variety of elements are used in driers, charge control agents, additives, pigments, and dyes, during the manufacturing process to provide specific properties to the ink pertaining to dryness, flexibility, gloss, and color. Printing inks may contain a variety of inorganic components in their formulation that are used as extenders (Al, Mg, Ca, Si, Ti), pigments/dyes (Cu, Fe, Cr, Ba), driers (Co, Ce, W, Zr, Pb), and/or other additives (Li, Si, Zn, Mg) that modify a particular characteristic of the ink (47). Ink manufacturers use a distinctive combination of the inorganic components or add specific markers, which can make it possible to distinguish formulations among manufacturing sources and even between batches of the same manufacturer over different manufacturing dates (48).

Differences in the elemental content of printing inks may therefore be useful for discrimination between sources. The analytical techniques traditionally employed for the elemental analysis of printing inks includes X-ray Fluorescence (XRF) (49-51), Scanning Electron Microscopy coupled to Electron Dispersive X-ray spectroscopy (SEM-EDX) (52-54), Particle Induced X-ray Emission (PIXE) (55), Laser Induced Breakdown Spectroscopy (LIBS) (53) and Laser Ablation Inductively Coupled Plasma Mass Spectrometry (LA-ICPMS). Table 2 summarizes the research done for the analysis of printing ink using LA-ICPMS.

**Table 2** Experimental conditions of main applications of LA-ICPMS to the analysis of ink.

| Sample | Analytes | Laser | ICPMS | CRM | Ref |
|---|---|---|---|---|---|
| **Printing ink** | **Al, Si, Ti, V, Cr, Cu, Mn, Zn, Sr, Ta, W, Th, U** | **CETAC LSX-500 (266 nm)** | **OptiMass 8000 ICP-TOF-MS** | **No specified** | **(56)** |
| **Printing ink** | **Li, Mg, S, K, Cu, Ni, Zr, Sn** | **CETAC LSX-500 (266 nm)** | **Perkin Elmer ELAN DRC II** | **No specified** | **(53)** |
| **Printing ink** | **No specified** | **New Wave UP-266 nm** | **Perkin Elmer ELAN DRC II** | **No specified** | **(54)** |

The analysis of organic components of inks, such us colorants, volatile compounds, resins and other additives, has been typically performed by Thin Layer Chromatography (TLC) (57-59) and Capillary Electrophoresis (CE) (60-64). Other important techniques used in forensic analysis of inks are Gas Chromatography-Mass Spectrometry (GC-MS) (65, 66) and Infrared Spectroscopy (49, 66-69). However, more recently, additional techniques such as Raman (70-73), Laser desorption-Mass spectrometry (70, 74), Direct Analysis in Real Time-Mass Spectrometry (DART-MS) (75, 76) have also been employed. Each method applied in the ink examination has its advantages and limitations. In practice, several methods are required for characterization and identification of inks.

## 1. Introduction

The wine label takes few seconds to make an impact on the potential customer. Labels have a fundamental role to launch a wine into the market. For the average consumer, the wine label is one of the most important things taken into account while on the hunt for a bottle of wine to purchase. In fact, the first contact that consumers have with a wine bottle is visual and the information on the label acts as an aid to decisions. Beyond the fact than the quality of the label design is important for creating shelf appeal and brand recognition, wine label information reveals the special qualities of a bottle's content as they provide vital product information. The story behind the wine has become just as important as the visual appeal of the wine's label and packaging. In wine marketing, the wine's label is key for delivering information, such as: i) attributes (describes the character of the wine in terms of how it appears, smells or tastes), ii) uniqueness (reflection of quality in that the product is without equal), iii) parentage (reflection of the history), iv) manufacture (winemaking process description), v) target-end user (addressed consumer, a person type), vi) target-end use (addressed consumption situation) and vii) endorsements (experts opinion and/or recognition of awards and medals) (79).

Wine fraud may come in several forms, committed exclusively for economic gain. Even the most prevalent type of fraud is one were wines are adulterated, the relabeling of inferior and cheaper wines to more expensive brands is another common type of wine fraud. Concretely, rare, expensive and cult wine characterize this type of fraud. The availability of affordable, high-quality printing technology has made it easier for the general public, as well as skilled counterfeiters, to create more sophisticated counterfeit labels that closely resemble the authentic. In general, older vintages are easier to fake as they are more likely to remain in cellars unopened, as collectors' items. In this case, even if they were drunk, the wine inside may have been transformed over time and the sensorial analysis would not be a reliable indicator of authenticity. An example of relabeling counterfeiting occurred in 2002 when bottles of the weaker 1991 vintage of Château Lafite Rothschild were relabeled and sold as the acclaimed 1982 vintage in China. Hong Kong police uncovered 30 bottles of the mentioned winery, today worth about $800 per bottle at auction. The counterfeiters had simply bought bottles of Lafite 1991, then worth only $100 a bottle, and relabeled them (80).

With the aim of authenticating the wine without opening the bottle, the research work described in this manuscript aims to develop a new irrefutable diagnostic tool based on the direct ultratrace analysis of paper and printed ink on the label by minimally-invasive femtosecond laser ablation ICPMS, which induces no visible degradation of the bottle that could affect its value and its posterior resale.

On the one hand, although the main components of the paper are similar, there can still be variation in the trace elemental composition. As paper is produced from natural materials and recycled consumer waste, it is possible to characterize them through their trace elements, which can be different from one manufacturer to another (9). Therefore, the variability in paper manufacture makes it possible to identify a great variety of subtle distinctions that give each batch of paper or each sheet of paper a unique chemical fingerprint (4). On the other hand, the improvements in high quality commercial printers favorizes the counterfeiting of labels. The inorganic portion of the ink can be a valuable tool for the characterization and discrimination of printing inks (47). As such, advanced analytical techniques may be necessary in order to better characterize inks for forensic comparisons.

ICP-based methods provide the most information of all the elemental analysis methods. Concretely, ICP-MS allows rapid quantitative multi-elemental analysis of elements with superior detection limits and excellent precision, reproducibility and selectivity. Thus, the potential of detecting more elements also provides improved discrimination capabilities. However, the main disadvantages of the conventional digestion technique rely on the fact that it is destructive of the sample, time consuming and complex digestion protocols are required. Consequently, laser based methods provide some advantages over solution-ICP methods since there is no need to digest the paper and the amount of sample consumption is substantially reduced, leaving the paper almost intact after the analysis, which is crucial for this work (27). Additionally, owing to the lack of certified reference materials, in-house matrix-matched standards have been synthesized as external calibrators by using commercially available inkjet printer to perform quantitative determinations. These homemade matrix-matched standards were used in order to compensate for matrix effects as well as variations in ablated and transported mass and instrumental drift. Calibration and standardization procedures for LA-ICPMS using a conventional ink jet printer have been already developed mainly for the quantification of proteins in electro-and Western-blot assays (81, 82), mapping of elemental distribution on biological samples (2, 83-85) and molecular mass spectral imaging (86).

To the authors' knowledge, there are nowadays only few studies reporting the use of LA-ICPMS for the analysis of paper and ink despite the advantages of this technique (see Table 1 and Table 2). The significance of the present work is to offer practical and robust LA-ICPMS method for the elemental analysis of paper and ink and its application to wine counterfeiting as a means to improve the discrimination between wine bottles. Figures of merit such as precision, homogeneity, reproducibility and linearity have been investigated. Three different caseworks have been studied based on the elemental composition of label paper and printed ink, black and red inks concretely. They comprises 90 wine bottles of controlled origin and bottles originating

from other countries and millesime. Interpretation of the obtained results is, in this case, based on comparison of elemental ratios within a spectral profile, has been carried out by data processing methods, including Principal Components Analysis (PCA), Soft Independent Modelling Class Analogy (SIMCA) and Hierarchical Ascendant Classification (HAC) using the XLSTAT ® (2016) software for Microsoft Excel application and Unscramble from CAMO version 9.1 (Computer Aided Modelling, Trondheim, Canada).

## 2. Materials and methods

### 2.1 Description of the sample set

A total of 91 wine bottle samples were collected in a period of 3 years, originating from different countries, wineries and vintages. The collection of wine bottles has been divided into 3 different batches for a better comprehension of the current work (Table 3). No sample preparation is required for the direct analysis of label paper and ink sample by fsLA-ICPMS.

**Table 3** Batches of bottles analyzed in this work.

| | 1st batch | 2nd batch | 3rd batch |
|---|---|---|---|
| ***Source*** | Private collection | Private collection | Individual's donations |
| ***Number of bottles*** | 8 | 34 | 49 |
| ***Origin*** | France and China | France | Worldwide |

On one hand, 1st batch includes 8 bottles among which 5 are original French bottles and 3 counterfeited Chinese bottles. On the other hand, 2nd batch is a series of 34 bottles belonging to the same winery which comprises the vintages from 1969 to 2010. Finally, 3rd batch consists of actual 49 wine bottles coming from all over the world, being more abundant European bottles. Table 4 shows the distribution of the bottles according to their continent of origin.

**Table 4** Distribution of 3rd batch of bottles according to their origin (continent/country).

| | | |
|---|---|---|
| ***Europe*** | Spain | 7 |
| | France | 5 |
| | Italy | 4 |
| | Slovenia | 1 |
| | Czech Rep | 2 |
| | Portugal | 2 |
| ***Asia*** | China | 7 |
| | Lebanon | 2 |
| | Japan | 1 |
| | Korea | 1 |
| ***America*** | USA | 12 |
| | Chile | 2 |
| ***Oceania*** | Australia | 1 |
| | New Zealand | 1 |
| ***Africa*** | Tunisia | 1 |

## 2.2 Instrumentation

The ALFAMET (Novalase & Amplitude Systèmes, France) compact and integrated femtosecond laser ablation device has been use in this work in which the laser source is fitted with a diode-pumped KGW-Yb crystal delivering 360 femtosecond pulses at an IR wavelength of 1030 nm. This laser source can operate at high repetition rate (from 1 to to 100000Hz). A galvanometric scanning module is fitted to the optical line for rapid displacement of the beam at the sample surface with high repositioning precision (< 1µm, 280 $mm \cdot s^{-1}$) which allows to design complex trajectories in 2D. The challenge of this study is to discriminate and classify the bottles of wine based on the elemental composition of label paper and printed inks causing no visible damage which could affect their value. A new ablation cell, which was designed and constructed in our laboratory, consisting of an open ablation cell was used for the direct analysis of label samples (See Chapter 4).

The ICPMS used in this study was an ELAN DRC II (Perkin Elmer, Wellesley, MA, USA) in wet plasma conditions using a two inlet nebulization chamber that mixed the dry aerosol together with a nebulized aerosol (Rh 1 $\mu g \cdot L^{-1}$, $HNO_3$ 2% in MilliQ water) via the pneumatic nebulizer. Ablation of transect in glass standard CRM NIST 612 was used on a daily basis to optimize the parameters of the ICPMS to ensure high sensitivity ($^{115}In$ > 200.000 cps) and good stability (RSD < 3%). Laser ablation of solids can be accompanied by undesirable processes such as fractionation or non-stoichiometric generation of vapor species. Although the study of this phenomenon is out of the scope of the current work, to ensure complete atomization and ionization efficiency of the plasma, parameters were adjusted to keep the $^{238}U/^{232}Th$ ratio as close as possible to 1 ± 0.05, concluding that the effect of fractionation does not represents a major problem in the proposed methodology.

### 2.3 Ablation parameters and data acquisition

Laser ablation of the paper and the ink was performed using ALFAMET laser ablation device (KGW-Yb, 1030 nm) working at 100 Hz and with a fluence of 3.7 $J/cm^2$. The laser beam was operated with a scan speed of 30 $mm \cdot s^{-1}$ and a 50 mm focal length objective was used for laser beam focusing, producing a spot size diameter of 15 µm at the sample surface. In this case, a matrix template (500 x 500 µm, 30 spots per line and 5 pulses per spot) on the paper surface of the label was used as the ablation pattern. Analyses were made in triplicate. The ablated material was transported through a 1 m-long polyurethane tube (i.d. 4 mm) by an argon gas stream (500 $ml \cdot min^{-1}$) to the ICPMS. During the laser ablation analyses, the stability of the plasma was monitored by continuously nebulizing a 1 $\mu g \cdot L^{-1}$ rhodium standard solution. The ICPMS was used in a reaction mode and a 1.8 $mL \cdot min^{-1}$ $H_2$ (Parker Balston) gas flow was introduced in the cell reaction system to prevent polyatomic interferences which could affect the accuracy of the measurements. 68 isotopes corresponding to 64 analytes, including $^{13}C$ and $^{103}Rh$, were monitored. *Homemade* spiked matrix-matched standards were used for calibration purposes and were also measured in triplicate at the beginning, middle and end of the analytical sequence. Detailed operating conditions for the laser and ICPMS are listed in Table 5.

**Table 5** Operating conditions of fsLA-ICPMS system for paper and ink analysis.

| Laser ablation system: ALFAMET | |
|---|---|
| Wavelength (crystal KGW-Yb) | 1030 |
| Pulse width | 360 fs |
| Spot size | 15 µm |
| Scan speed | 30 $mm \cdot s^{-1}$ |
| Fluence | 3.7 $J \cdot cm^{2}$ |
| Carrier gas (Ar) | 500 $mL \cdot min^{-1}$ |
| Virtual beam shaping | Matrix 500x500 µm |
| Wet plasma conditions | Rh 1 ppb, 4 rpm |
| Standards | Homemade matrix-matched std |
| **Mass spectrometer: ELAN DRC II** | |
| RF power | 1100 W |
| Nebulizer gas (Ar) | 0.30 $L \cdot min^{-1}$ |
| Plasma gas (Ar) | 17 $L \cdot min^{-1}$ |
| Auxiliary gas (Ar) | 0.85 $L \cdot min^{-1}$ |
| DRC mode ($H_2$) | 1.8 $mL \cdot min^{-1}$ |
| Detector | Dual mode |
| Dwell time | 5 ms |
| Signal acquisition | Time Resolved Analysis (TRA) |
| Isotopes | $^{7}Li$, $^{9}Be$, $^{11}B$, $^{13}C$, $^{23}Na$, $^{24}Mg$, $^{25}Mg$, $^{27}Al$, $^{28}Si$, $^{45}Sc$, $^{47}Ti$, $^{51}V$, $^{52}Cr$, $^{53}Cr$, $^{55}Mn$, $^{56}Fe$, $^{59}Co$, $^{60}Ni$, $^{63}Cu$, $^{66}Zn$, $^{71}Ga$, $^{74}Ge$, $^{75}As$, $^{82}Se$, $^{85}Rb$, $^{88}Sr$, $^{89}Y$, $^{90}Zr$, $^{93}Nb$, $^{98}Mb$, $^{101}Ru$, $^{103}Rh$, $^{104}Pd$, $^{105}Pd$, $^{107}Ag$, $^{111}Cd$, $^{115}In$, $^{118}Sn$, $^{121}Sb$, $^{133}Cs$, $^{138}Ba$, $^{139}La$, $^{140}Ce$, $^{141}Pr$, $^{142}Nd$, $^{152}Sm$, $^{153}Eu$, $^{157}Gd$, $^{159}Tb$, $^{163}Dy$, $^{165}Ho$, $^{166}Er$, $^{169}Tm$, $^{172}Yb$, $^{175}Lu$, $^{178}Hf$, $^{180}Hf$, $^{181}Ta$, $^{182}W$, $^{187}Re$, $^{193}Ir$, $^{195}Pt$, $^{197}Au$, $^{205}Tl$, $^{208}Pb$, $^{209}Bi$, $^{232}Th$ and $^{238}U$ |

Data was acquired as raw counts per second (cps) for 240 s. First, data was recorded for 20 seconds before the laser was fired to establish a background level. Then, the laser was fired for 50 s per replicate followed by 20 s time frame without firing to confirm that values returned to its blank values. (Figure 3). The data was imported into Focal Flash data reduction software (laboratory internal tool for data analysis) for an easier handle of data for the purposed stated.

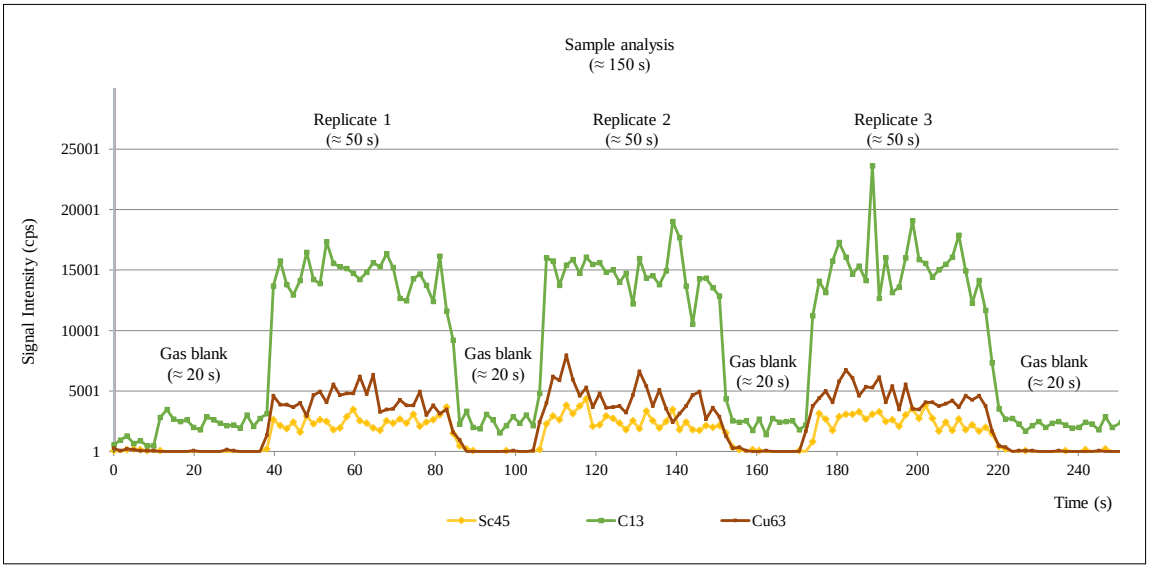


**Figure 3** A typical laser ablation signal for selected isotopes for paper and ink analysis.

## 2.4 Data preprocessing

Data preprocessing consisted of peak-area integration, background subtraction, and arranging the data in a form suitable for multivariate analysis. For each isotope, the baseline estimated by the average signal measured during the 20 s prior to the ablation was subtracted point by point to the signal measured in the ablation peak. The intensity was after normalized relative to the intensity of the internal standard. Since the major component of the document paper is cellulose (≈ 80%), a low abundance carbon isotope was selected as an internal standard ($^{13}C$, 1.1%). The use of an internal standard is a common practice in laser ablation analysis to improve the analytical performance of the method by correcting for any difference of mass ablated between replicates or ICPMS drift. In this study, interpretation is based on the comparison of the calibrated elemental ratios ([M]/[C]) within a spectral profile. However, a quantitative approach has also been done for which homemade matrix-matching standards have been synthetized.

## 2.5 Synthesis of matrix-matched standards

To obtain accurate quantitative analysis, matrix-matched standards materials with chemical and physical properties similar to the samples are preferred in laser ablation analysis. In these conditions, the ablation yield, the aerosol transport and the particle atomisation can be considered to be similar between samples and standards then insuring optimal accuracy and confidence level. For this purpose, owing to the lack of commercial reference material for printed paper, *homemade* standards were synthesized in our laboratory. For this approach, multi-elemental solutions (CCS-1, CCS-2, CCS-4, CCS-5 and CCS-6) Inorganic Ventures, Christianburg, VA, USA) were printed using a commercial printer (Canon Pixma MG5650) in office copy-/laser paper (2500xDIN A4, 210x297 mm, 109 ± 3 µm thickness, 80 g/m$^2$) from InapaTecno (Corbeil-Essonnes, France). Best quality printing was employed with spatial resolution of 1200 x 4800 dpi. For this, each 100

µg.mL$^{-1}$ stock solution was diluted to 10 µg·mL$^{-1}$ in ultrapure water (18,2 MOhm, Millipore) and poured into a new refillable cartridge (Primvert, Bérat, France). The five filled cartridges were then led to settle overnight to obtain uniform distribution of the solutions within cavities of the porous sponge in the cartridge. Standard addition calibration curves were then prepared by printing the different concentrations using the transparency (color density) tool of PowerPoint (Microsoft Office 2007) as diluter ranging target surface elemental concentrations (SEC) from 62 ng.cm$^{-2}$ to 0.125 ng·cm$^{-2}$. The printouts were carried out in an ISO7 clean room, dried with a hairdryer whenever superimposed prints were necessary (see below) and stored in a plastic bag in the clean room. Fittschen et al. (87) already developed an approach by printing picoliter droplets of few element solutions with a conventional inkjet printer. However, cartridge and printer features were modified which makes the methodology more complex and less universal than the methodology proposed here. After each printing, the solution filled cartridges were replaced by deionized water filled cartridges and several printings were done in order to clean the injectors to avoid problems concerning reproducibility due to clogging of the print head or other technical issues related to the presence of some acids (HNO3, HF, and HCl) in the diluted solutions.

Solution printed paper standards (0.08 g) were after digested with 3 mL of $HNO_3$, 1.5 mL of optima grade 30% $H_2O_2$ (Fisher Chemical) and 2 mL of $H_2O$ Milli-Q in a microwave digestion unit (Milestone, Sorisole, Italy), fitted with PTFE vessels and equipped with an internal temperature probe. The nitric acid used was purchased from Baker (INSTRA grade) and was purified by sub-boiling distillation (Savillex, PFA DST1000) in an ISO7 cleanroom. Samples were digested in triplicate and a procedural blank was prepared for each digestion run. The program used for microwave digestion is given in Table 6. The sample digest were transferred to previously cleaned 50 mL polypropylene tubes (VWR, Fontenay-sous-Bois, France) and diluted to 50 mL with ultra-pure water. In order to reduce the possibility of carryover between digestions, the vessels were soaked in 10% $HNO_3$ and then cleaned by reheating in the microwave unit with $HNO_3$-$H_2O_2$ using the program described in Table 6.

**Table 6** Operating conditions for the microwave digestor.

| Program | Step | Time (min) | Power (W) | Temperature (ºC) | Pression (Bar) |
|---|---|---|---|---|---|
| Digestion | 1 | 0-4 | 1000 | 20-200 | 40 |
| | 2 | 4-12 | 1000 | 200 | 40 |
| Cleaning | 1 | 0-20 | 1000 | 20-200 | 40 |
| | 2 | 20-40 | 1000 | 200 | 40 |

All analyses were performed using an ELAN DRC II ICPMS instrument fitted with an AS93plus autosampler (Perkin Elmer). A 1ml/min concentric nebuliser attached to a glass cyclonic spray chamber (Twister, Glass Expansion Pty. Ltd., Melbourne, Australia) was used for sample introduction. The instrumental and data acquisition parameters are given in Table 7.

**Table 7** Operating conditions for ICPMS instrument.

| RF power | 1100 |
|---|---|
| Nebulizer gas (Ar) | 0.90 $L \cdot min^{-1}$ |
| Plasma gas (Ar) | 17 $L \cdot min^{-1}$ |
| Auxiliary gas (Ar) | 0.85 $L \cdot min^{-1}$ |
| DRC mode ($H_2$) | 1.8 $mL \cdot min^{-1}$ |
| Detector | Dual mode |
| Dwell time | 5 ms |
| Signal acquisition | Spectrum |

Because the sample digest contains reasonable high matrix concentration, there is a possibility of some signal enhancement or suppression from ionization/space charge effects or nebulisation efficiency. In order to check for this type of matrix effect, standard additions and external calibration (using $^{115}In$ as internal standard) calibration methods were compared. From these results, it was concluded that matrix effects were minimal and external calibration was used for further analyses as previously described elsewhere (31, 88). The instrument response curve, across the mass range, was generated by using a daily prepared stock solution containing 64 analytes each of 1 $\mu g \cdot mL^{-1}$ concentration from CCS solutions. This standard was prepared by serial dilution in 5% v/v $HNO_3$ of a mixture of five CCS multi-elemental standards. Calibration was repeated at the beginning and the end of analysis and five blanks were analyzed.

## 3. Results and discussion

### 3.1 Optimization of the ablation strategy

A matrix template (500 x 500 µm) was found to be the best option for paper surface analysis, being the matrix small enough not to cause visual damage on the label and have representative information at the same time. Analysis were made in triplicate. For the analysis of paper and ink the spot density and the number of pulse must be optimized.

On the one hand, the spot density is the amount of spots found in the matrix to ensure the maximum ink ablation avoiding overlapping and drilling through the paper which would lead to the ablation of the glass below (Figure 4).

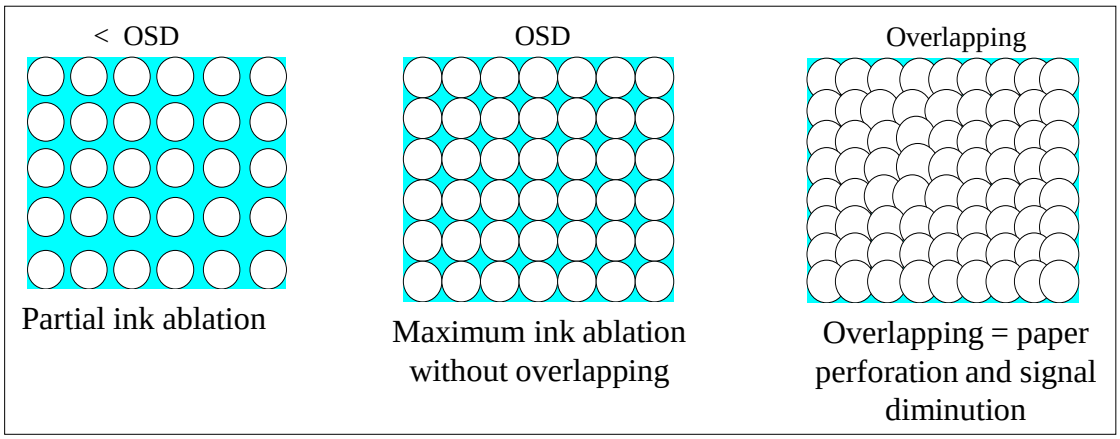


**Figure 4** Different cases of paper and ink ablation depending on the spot density.

Several spot densities ranging from 22x22 spots up to 100x100 spots were tested. For this optimization, printed paper in blue was used due to its high concentration in copper (2). A matrix of 30x30 spots, corresponding to a distance between spots of 17 µm, was found to be the optimal spot density (OSD). As it is possible to observe in Figure 5 the signal intensity in counts per seconds of copper decreases while increasing the number of spots, $^{63}$Cu showed the same trend as $^{65}$Cu. In fact, when higher spot density is applied, the spots overlapped and the amount of ablated paper increase while the amount of ink remains constant. Therefore, the copper is diluted within the plasma source and its signal decreases proportionally at the same time that total analysis time increases. The ablation of the selected OSD matrix takes 30 seconds, similar duration of each glass analysis (per replicate), which showed to be enough for trustworthy statistical data analysis.

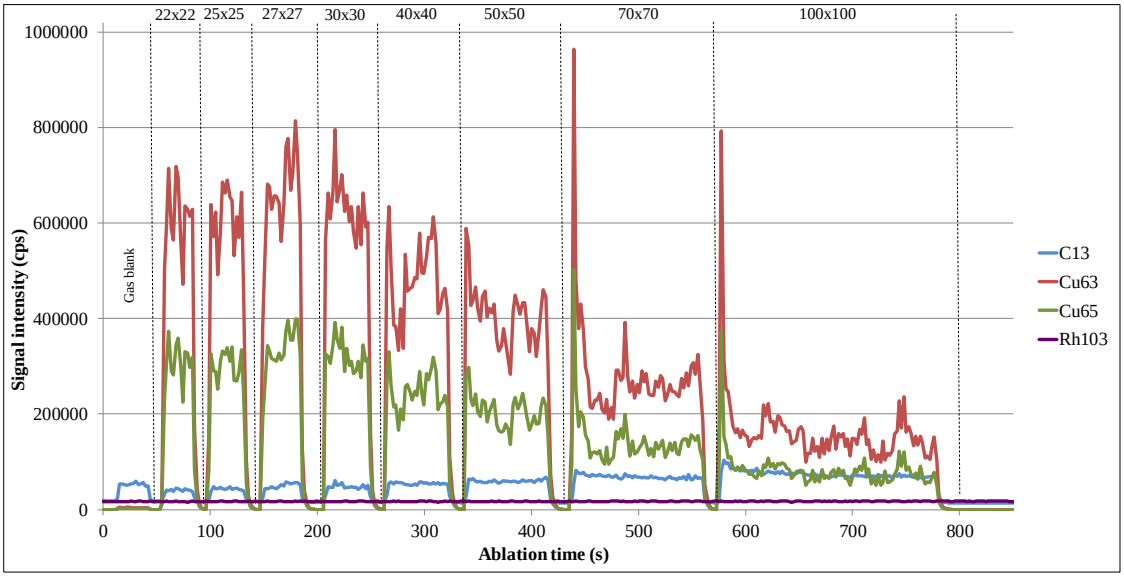


**Figure 5** Optimization of the OSD value for matrix ablation of paper and ink.

On the other hand, the number of pulses per spot is the number of times that the laser beam interacts with the sample at a given position and consequently, it must be also optimized in order not to pierce the paper. A range of pulses from 1 to 10 were tested. Figure 6 shows the different number of pulses per spot tested for the matrix ablation. For this approach, blue printed common office paper was used. As it can be observed, from 6 pulses to 10 pulses paper appears pierced as it is possible to see the sample holder through the paper, brownish areas concretely. This piercing is proportional to the number of pulses. When 6 and 7 pulses are applied little perforations occurred in some of the replicates, probably due to micro-heterogeneities of paper constitution. Therefore, in order to completely avoid paper perforation and subsequent glass ablation, 5 pulses were found to be the optimal number of pulses to ablate the maximum amount of sample avoiding its damage.

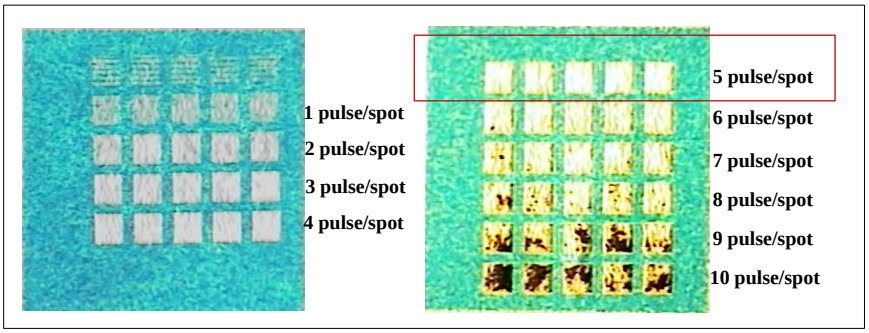


**Figure 6** Gradually increased number of pulses per spot and consequent paper piercing.

For further verification, confocal rugosimetry was used to characterize the surface aspect and roughness properties of the ablated matrix. A MICROMESURE STIL system equipped with an optical sensor of 285 µm (8 µm spot Ø, 10 nm spatial resolution) was used to evaluate the roughness by altitude measurement of each surface point on the sample without any contact. This equipment was available at École des Mines d'Alès, Pau (Hélène Garay). The instrument was set up with an intensity of 30% and a frequency of 1000 Hz. Roughness measurement were done each 2 µm. Figure 7 shows the profile of a common paper sheet in which 3 replicates of 30 OSD and 5 pulses matrix have been ablated, demonstrating that approximately the 50% of the paper depth has been ablated. It must be noted that at some points the depth surface is not totally homogeneous and flat. In fact, it is observable that the deepest ablation section is found in the middle part of the matrix while the lateral sides closer to matrix border are not so deep. This fact could be attributed to the deposition of micrometric particles during the ablation proccess which have not been effectively flushed with the carrier gas stream.

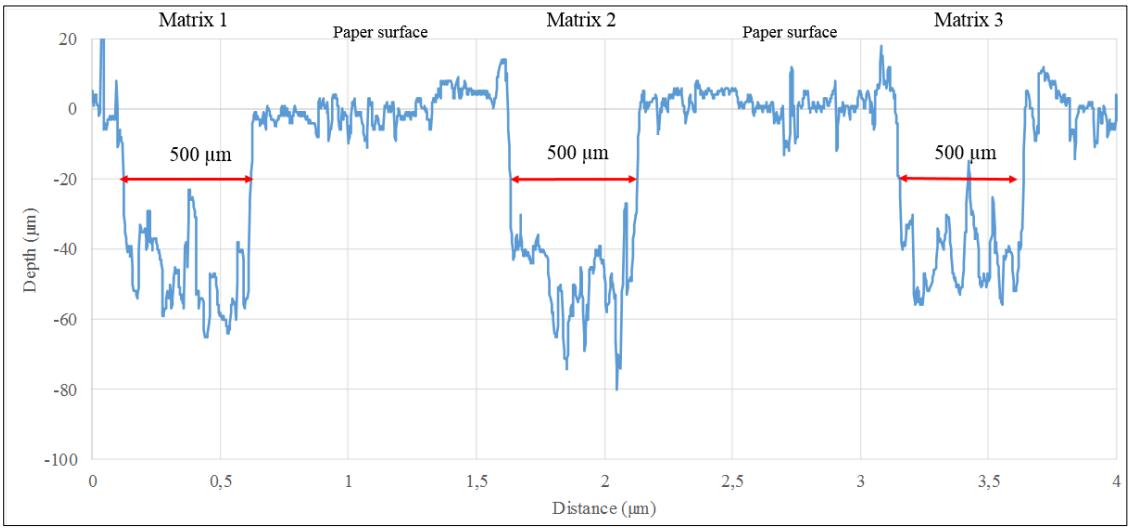


**Figure 7** Ablation profile of 30 OSD and 5 pulses per spot matrix (4 replicates).

Similarly, rugosimetry was also studied for the matrices ablated with different number of pulses per spot (at OSD = 30), from 1 pulse to 10 pulses per spot, respectively. Figure 8 shows the average ablation depth as a function of the number of pulses per spot, indicating that the amount of ablated paper is proportional to the number of pulses.

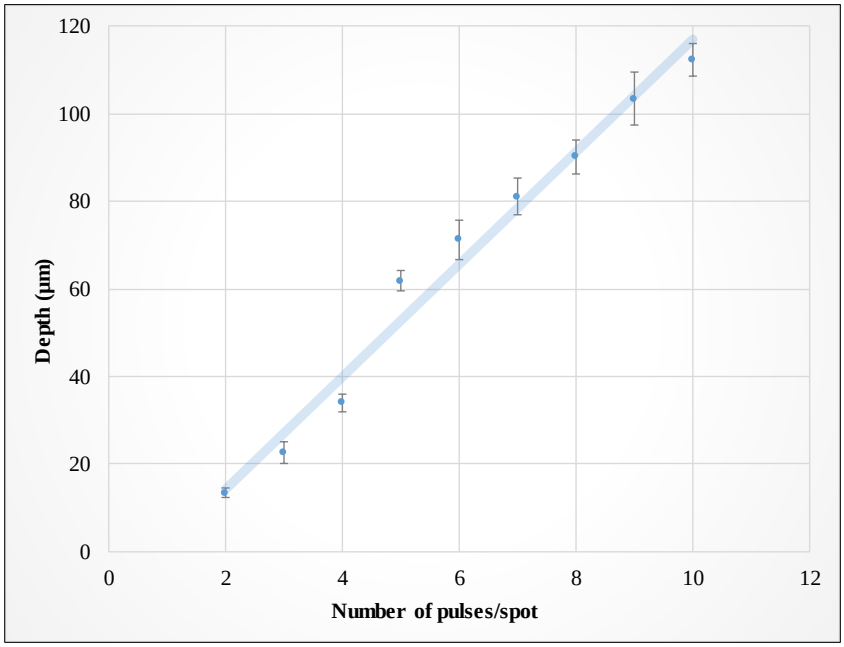


**Figure 8** Depth of ablated matrix (500 x 500 µm, 30 OSD) as a function of the number of pulses per pot.

In addition, as different types of paper can be employed for label manufacturing, five types of glossy papers were also tested. As it can be observed in Figure 9, ink deposition and absorption varies from common paper to glossy paper. In fact, ink deposition is more superficial and homogeneous when glossy paper is used due to the interactions between ink and paper internal structure which can offer resistance to ink penetration.

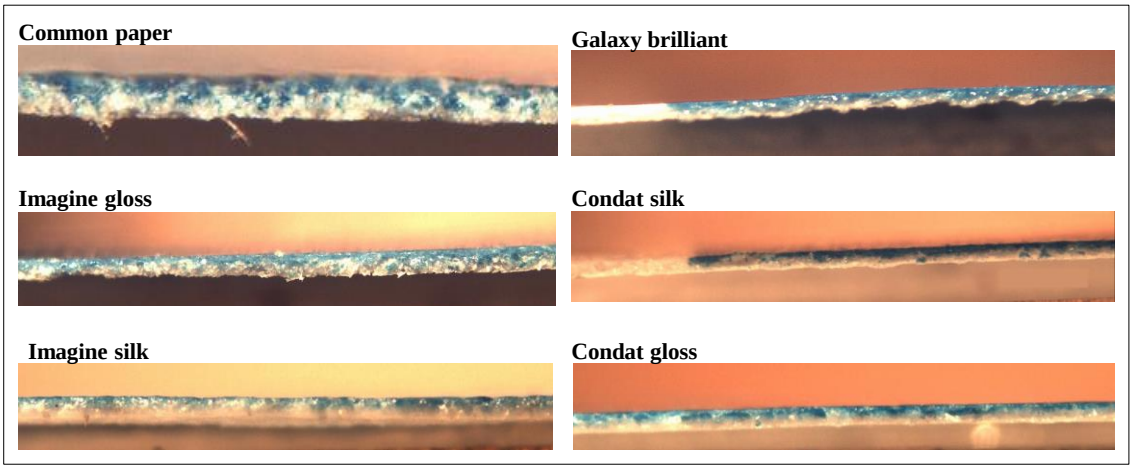


**Figure 9** Images of optical microscopy (x40) of paper edges showing the absorption of the ink when different types of glossy papers have been used.

Consequently, the ablation of the matrix (OSD = 30) was also carried out in glossy papers testing different number of pulses, ranging from 1 pulse to 10 pulses. The graphs collected in Figure 10 show that in all the cases the signal intensity in of counts per second reaches a plateau when 5 pulses are employed. Therefore, it can be concluded that 5 pulses is the most adequate amount of pulses to guarantee the maximum ink ablation without sample damage even when different types of paper are analyzed.

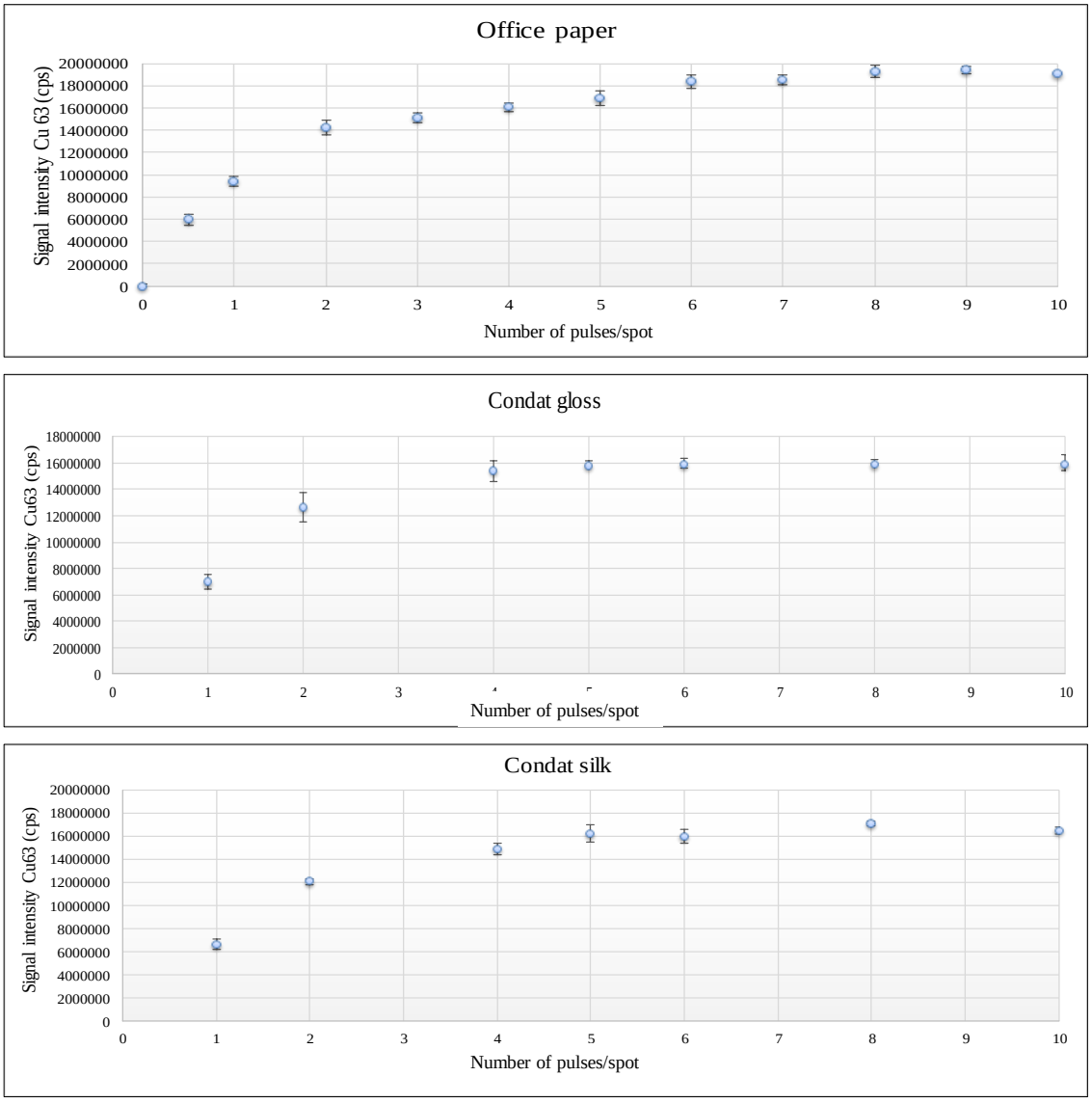


**Figure 10** Number of pulses per spots versus the signal intensity of Cu63 (cps) when different types of papers have been employed for printing (office paper and 5 glossy papers).

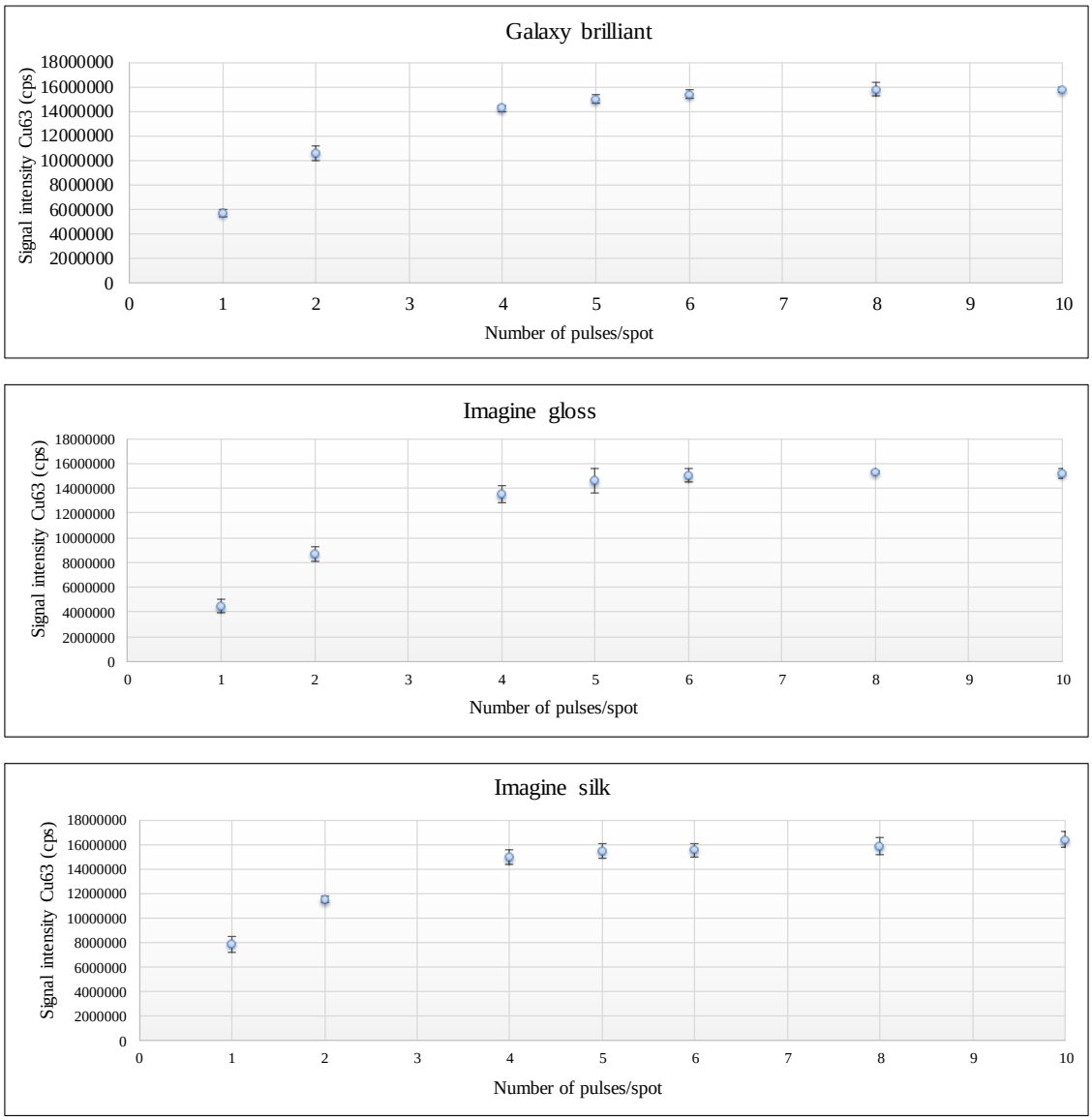


**Figure 10 Cont.** Number of pulses per spot of versus the signal Intensity of Cu63 (cps) when different types of papers haven employed for printing (office paper and 5 glossy papers).

## 3.2 Development of homemade matrix-matched standards for ink quantification

### 3.2.1 Synthesis process of homemade matrix-matched standard

The quantification is still nowadays a challenging issue in laser ablation coupled to ICPMS as it does not generally provide accurate quantification mainly due to fractionation effects and the persistent lack of reference materials (89). Matrix-matched standards used for external calibration are commonly employed for fractionation-related inaccuracies correction, as they own similar composition and morphology than the sample under investigation. Certified reference materials are commercially available for some types of solids matrices. However, available reference materials do not cover every type of sample which implies a serious restriction for LA-ICPMS accurate measurements. Many laboratories prepare matrix-matched standards, which include a

mixture of an appropriate matrix material with the analyte of interest, which is usually a difficult and time-consuming process (90). In this work, matrix-matched standards were synthetized by printing multi-elemental solutions in a common office paper using a commercial inkjet printer. By this way, there was no need for spiking ink at different concentration levels and the similarity between droplets, which were on the order of picoliter or less, was guaranteed by the printing mechanism avoiding large chromatographic effect that would happen if paper would be spiked manually (Figure 11).

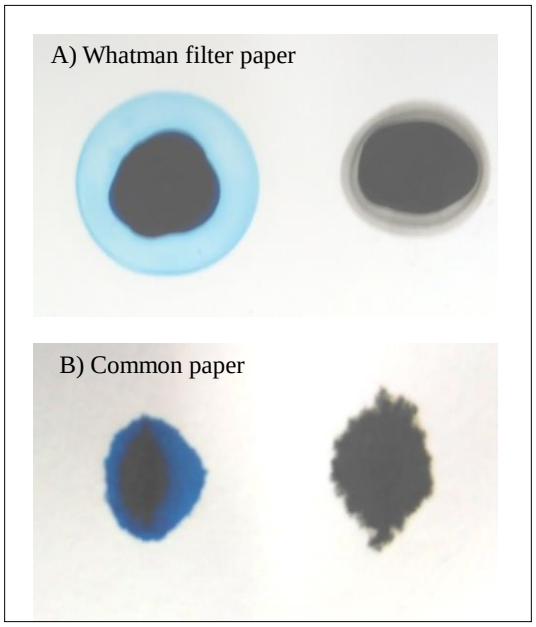


**Figure 11** Deposition of 5 µL of blue and black ink on A) Whatman filter paper (0.1 µm, 47 mm Ø) from Durapore ® and B) common office paper (2500xDIN A4, 210x297 mm, 109 ± 3 µm thickness, 80 g/m$^2$) from InapaTecno.

Calibration points were obtained by combining over printing and the transparence (color density) tool of Microsoft PowerPoint 2007 (Microsoft Corporation, Redmond, WA) software. On the one hand, a test was done using the blue ink to determine the proportionality of ink deposition. For this purpose, 3 successive printouts were done at the same area confirming that the amount of ink deposited was kept constant (Figure 12). Consequently, it can be concluded that, for example, three superimposed printouts with a 10 µg·mL$^{-1}$ solution would be equivalent to one printout with a 30 µg.mL$^{-1}$ solution.

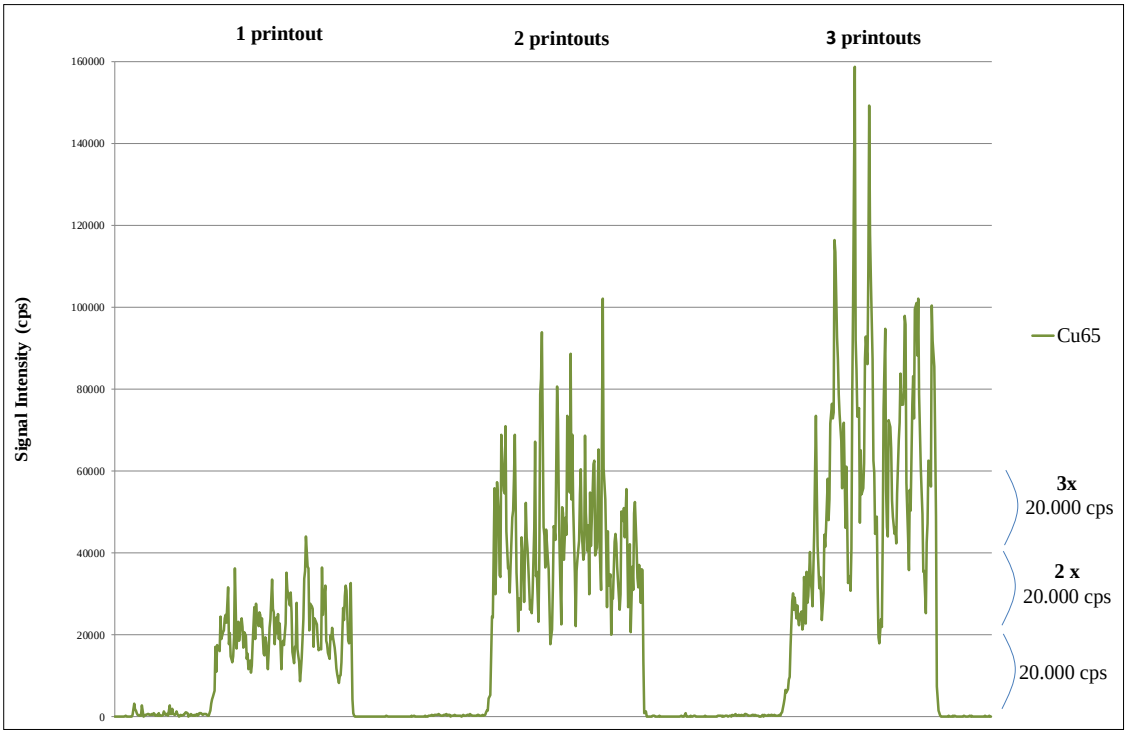


**Figure 12** Proportionality of ink deposition at each printout.

On the other hand, transparency tool of the image editor was used to modify the amount of solution deposited on the paper. For example, a printout at 50% transparency with a 10 $\mu g \cdot mL^{-1}$ solution would be equivalent to a printout at 0% transparency with a 5 $\mu g \cdot mL^{-1}$ solution. However, in order to know in which extent the transparency tool could be used, the printing homogeneity was also tested. In fact, inkjet printing does not provide a continuous region of color. Depending on the printer resolution and the paper used, either isolated spots or overlapping spots of color may compose the target of analysis, being a challenging analytical task (74). For this aim, printing homogeneity test was carried out by printing several sheets of common paper with 0%, 50%, 80%, 90%, 95% and 98% of transparency (Figure 13). As it is possible to observe, the printed spots from 0% to 80% transparency are not well distinguished and they are often overlapped, while they are quite separated for the transparencies ranging from 90 to 98%. Therefore, the spots of the 90%, 95% and 98% transparency were counted. For this approach, the printouts were observed by an optical microscope (x4) and grid of squares 500 x 500 µm was scaled, the same size of ablation pattern concretely. Figure 14 shows that distribution of the spots done with 95% and 98% transparency present a large relative dispersion and consequently, 90% was the maximum transparency applied for the synthesis of matrix-matched standards.

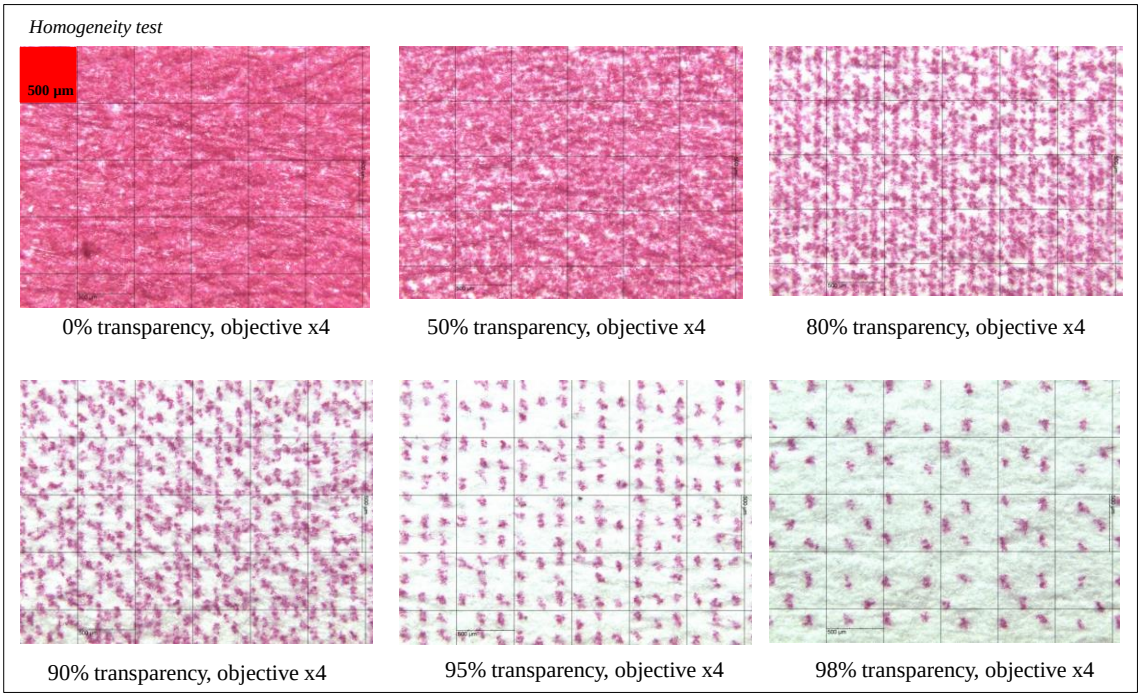


**Figure 13** Printing homogeneity test on common office paper (2500xDIN A4, 210x297 mm, 109 ± 3 µm thickness, 80 g/m$^2$) from InapaTecno with transparency of 0%, 50%, 80%, 90%, 95% and 98%. Magenta color was used for this test.

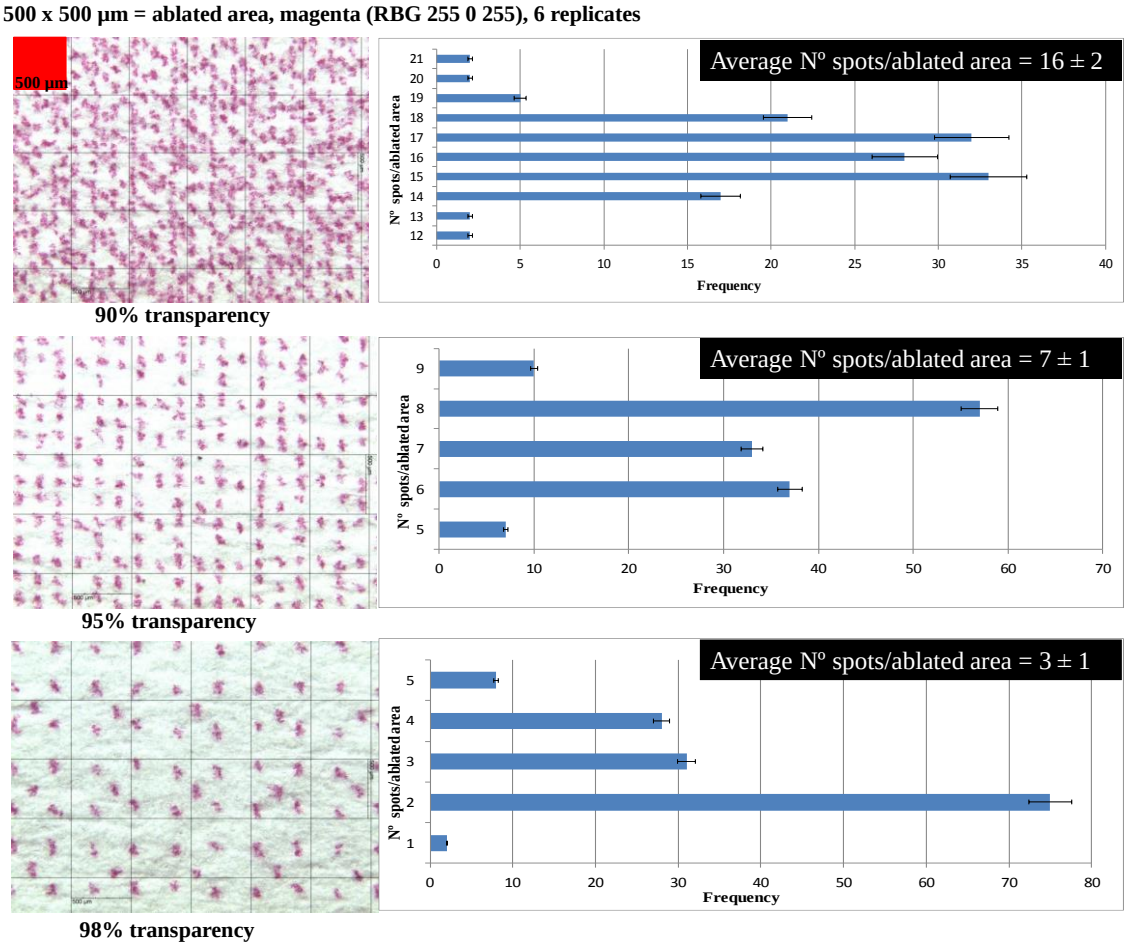


**Figure 14** Printed spot distribution and frequency for the transparencies of 90%, 95% and 98%, showing the average nº of spots per ablated and the standard deviation.

To make sure that at each printout only the selected cartridge was printing, RGB color model was used and only the corresponding filled cartridge was fitted in the printer (91), keeping the other cartridges empty (Figure 15).

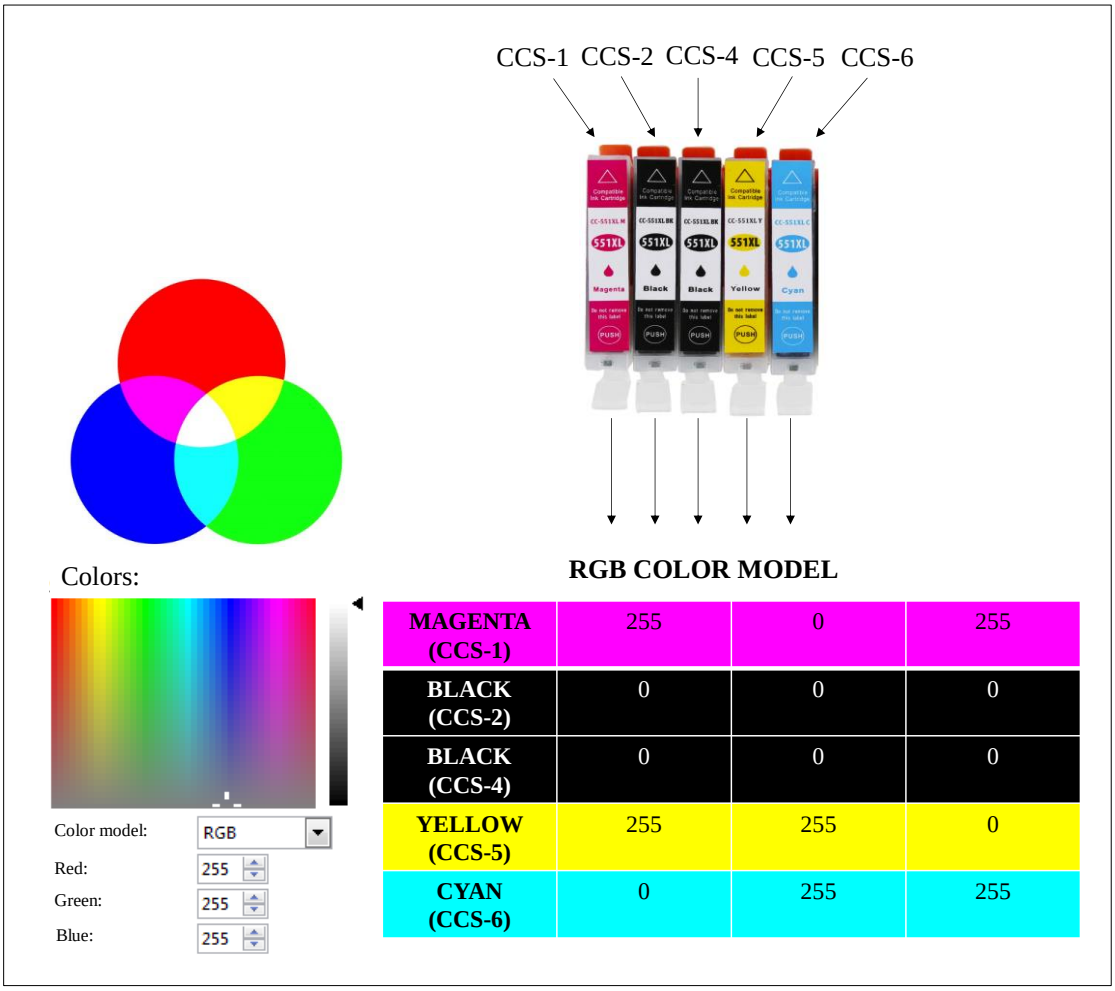


**RGB COLOR MODEL**

| | | | |
|---|---|---|---|
| **MAGENTA (CCS-1)** | 255 | 0 | 255 |
| **BLACK (CCS-2)** | 0 | 0 | 0 |
| **BLACK (CCS-4)** | 0 | 0 | 0 |
| **YELLOW (CCS-5)** | 255 | 255 | 0 |
| **CYAN (CCS-6)** | 0 | 255 | 255 |

**Figure 15** Solution printing strategy based on the RGB color model.

Using the procedure described above, six patterns of 16x20 cm were printed for a given diluted CCS solution: 1) 5 superimposed prints, 0% transparency, 2) 2 superimposed prints, 0% transparency, 3) 1 print, 0% transparency, 4) 1 print, 50% transparency, 5) 1 print, 80% transparency and 6) 1 print, 90% transparency. The amount of deposited solution was empirically calculated by printing an area equal to the printed standard pattern at 0% transparency and by weighting the cartridge before and after the printing (0.4 g  1,2% RSD, n = 5). Therefore, taking into account the printed area, the estimated amount of solution deposited at the selected transparency levels and the density of the printed solution (1 g·cm$^{-3}$), the estimated added Surface Elemental Concentrations (SEC) was 62 ng.cm$^{-2}$, 25 ng.cm$^{-2}$, 12.5 ng.cm$^{-2}$, 3.12 ng.cm$^{-2}$, 0.5 ng.cm$^{-2}$ and 0.125 ng·cm$^{-2}$ as metal, respectively.

After drying with a hairdryer, the operations described above were successively repeated for the other diluted CCS solutions, by printing exactly at the same place on the same sheets of paper, resulting in a set of 6 sheaths of paper doped with 65 elements with 6 levels of concentration. Then, the application of the printed solution approach for signal quantification requires knowledge of the exact amount of elements on these printed standards. As the exact amount of deposited ink on the printed standards is unknown the accurate elemental concentrations must be determined by acid digestion and in liquid ICPMS measurements.

Therefore, the concentrations were calculated after acid digestion and liquid ICPMS analysis as explained in section 2.5. Then Surface Elemental Concentration (SEC) was calculated and expressed as $ng \cdot cm^2$. SEC calculated at different locations of a given printout showed low relative standard deviations of less than 15% for each concentration level (n=3). Considering that this value also reflects variations from sample preparation and ICPMS measurements, the low variance of the measurement of replicates indicates a good reproducibility of the printing process and sufficient macro-homogeneity over the printed whole area.

However, although the standard solutions were printed homogenously within a given printout, it was observed that for a given cartridge, the amount of printed solution might differ significantly from one printout to the other. A cartridge was weighted before and after 16x20 cm printouts at 0% transparency 12 times and revealed that the amount of deposited solution was of 0,4 g (n=5) or 0,08 g (n=7). This erratic deposition is illustrated in Annex III, showing variation of the recoveries calculated for each element. For example, for the elements contained in solution CCS-1 (magenta cartridge) the most concentrated level have not been achievable whereas for the CCS-4 (black cartridge) and CCS-5 (yellow cartridge) lowest concentrations were not correctly printed. Additionally, the solution CCS-6 (blue cartridge), located at the blue cartridge, was not printed for none the calibration levels. This difference of the cartridge dependent printing process could be related to a physical defect in the injectors caused by the repetitive printing of acid containing solution or uncontrollable manufacturing modifications, which prevent the printing of the exact amount of solution required for each level.

### 3.2.2 Quality assessment of homemade matrix-matched standards: imaging of paper edge

In order to assess the homogeneity and reproducibility of solution printing on paper, the area of diffusion and distribution of the solutions were monitored by imaging fsLA-ICPMS of the paper edge to determine the penetration depth and area of deposition. Myllys et. al already developed a novel method for studying the toner ink-paper interface and the structural variations of a deposited layer of ink with a single printout, concluding that the toner thickness depends mainly on the local roughness variations of the substrate surface (92). Approximately 5x3 mm samples were cut and maintained in a vertical position due to labmade polycarbonate holders into a close ablation cell

with wash-out time less than 0.5 s. The operating laser conditions were as follow: spot size of 10µm, stage speed of 15 µm/s and distance between lines of 10µm. Under these conditions the ablation was complete in 20 minutes. Signal intensities were recorded in the time resolved analysis mode. XL files extensions from the fsLA-ICPMS measurements were imported into Focal Imaging data reduction software (laboratory internal tool for imaging data analysis) for an easier handle of data for the purposed stated and assembled into a matrix. The matrix was then imported to ImageJ free software and 2D color-coded image was generated for each measured isotope.

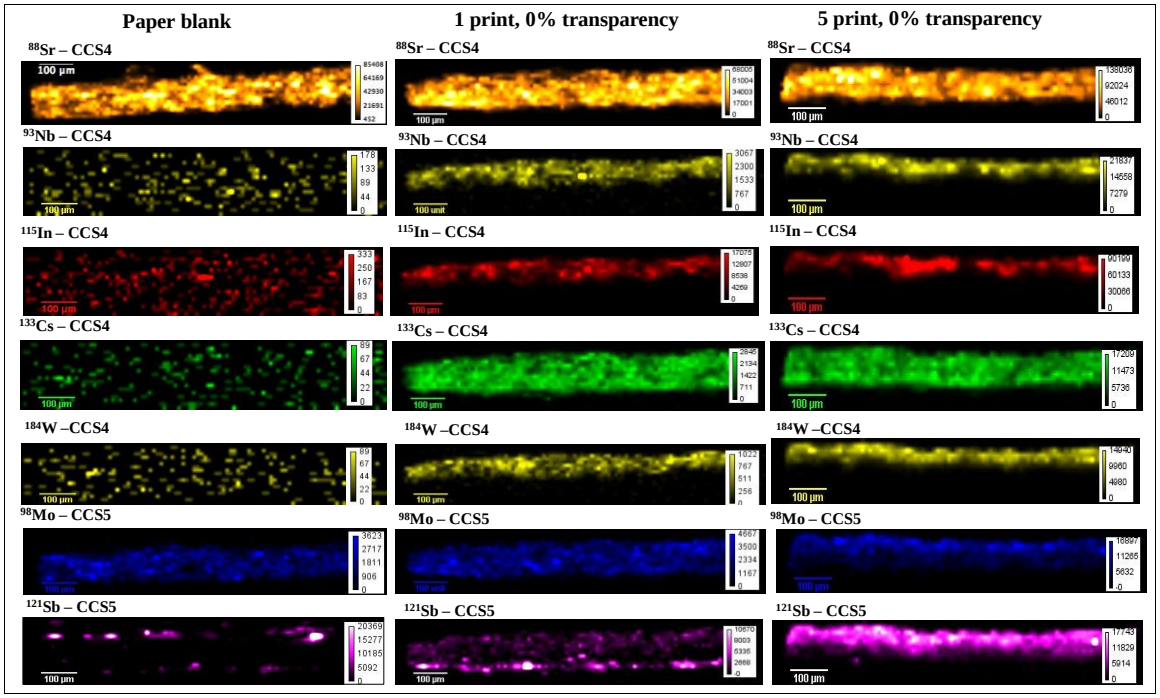


**Figure 16** Image plots of paper edge for several isotopes in standards 1 and 3 with color scale of cps.

According to Figure 16, it is possible to observe two different types of element-paper interactions. $^{88}$Sr was monitored to test its homogeneity as it is part of the paper matrix. On the one hand, elements belonging to the same printing cartridge and which were found not to be part of the paper matrix, In, Cs (CCS-4 solution) or Mo, W (CCS-5 solution), show different behavior. Molybdenum and cesium have a homogenous distribution across the paper depth while indium and tungsten are mainly retained at the surface. This different element-matrix interaction within elements belonging to the same cartridge goes well beyond the scope to the present work and no further explanation could be found. On the other hand, elements which have been printed five times at 0% of transparency have clear tendency to accumulate in the surface area. The formation of brown lines, called tidelines, at the wet-dry interface in cellulosic materials has been largely described as far back as 1930 (93). Cellulose fibers are bounded to each other by hydrogen bonds. The penetration of water molecules through the paper negatively affects its mechanical properties

by disrupting the linkage between the cellulosic chains. The diffusion of the water molecules inside the paper occurs via capillary transport mechanism through the micro-gaps between the cellulosic chains and additives, modifying the properties of the fiber network (94). Tidelines appear exclusively on the wet-dry interface where the capillary force is compensated by the water evaporation process. The area through which the water migrates show the most significant degradation. The presence of mineral and salts (silicates, calcium and sodium salts) in the tidelines added to Fenton reactions have been suggested to induce cellulose degradation and a decrease in its molar mass (95). Fenton reactions take place when the wet-dry interface is exposed to atmospheric oxygen and promote the formation of hydroperoxides species, which in the presence of trace amounts of metal ion catalyzers such as Fe, Mn or Cu can decompose to free radicals capable of increasing the rate of solubilization of cellulose (96). For the synthesis of most concentrated standard 5 prints of each cartridge were done at 0% of transparency, which means a total of 25 prints, including accelerated drying process under hot air stream between prints (97). Therefore, even if no significant degradation is observed at the wet-dry interface immediately after the formation of the tidelines, which are formed above the others, the non-intended premature paper aging could led to progress accumulation of printed solution above the formed tidelines (Figure 17). In order to limit these migration effects and to make more in-depth homogeneous standards, the printouts should have been carried out on the front and the back of the paper sheet alternatively. This couldn't not been done due to lack of time during this PhD work, but this will be considered in the next weeks.

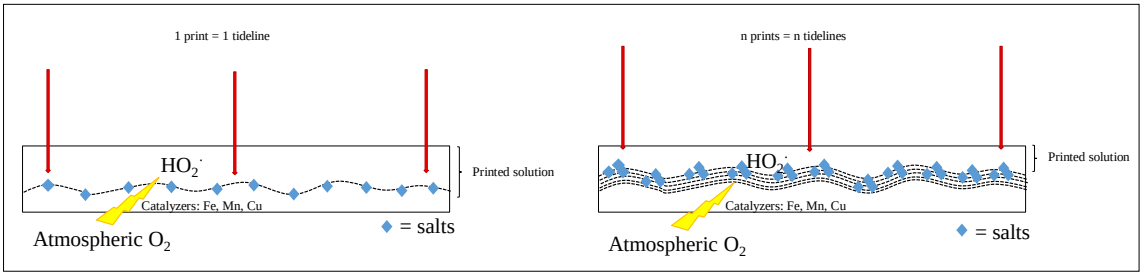


**Figure 17** Scheme of the suggested hypothesis for solution surface deposition based on subsequent tidelines formation and cellulose degradation.

### 3.2.3 Quantification of label paper and label printed ink

Although the precise composition of the paper matrix is unknown, for most papers very high count rates were observed for C and Ca. This is not surprising, since the two major components of most modern papers are cellulose (>80%) and $CaCO_3$ filler (29). Taking into account that the molecular formula of cellulose is $C_6H_{10}O_5$ (162 g · $mol^{-1}$), the carbon is the 44% of the molecular weight. Thus, if the 80% of paper is cellulose, it can be concluded that the estimated concentration of carbon in cellulose is about 355000 ppm. However, it must be consider for future work the experimental quantification of total organic carbon (TOC) for more accurate quantification of label paper and label printed ink. $^{88}Sr$ could be also employed as internal standard because it is present in all paper samples in a similar concentration and it is evenly distributed over a sheet of paper (26). Nevertheless, the distribution of strontium in ink matrix can vary from sample to sample preventing the use of a single internal standard for both matrix and making the data treatment more laborious. Therefore, despite the fact that carbon is known to be poor internal standard as it behaves more like gas than an aerosol (98), $^{13}C$ was chosen as internal standard .

According to Bonta et al. (84), the concentration of printed elements cannot be determined as a mass per mass concentration ($\mu g \cdot g^{-1}$) as they are deposited on the surface of printed patterns. They suggest an alternative notation of the element concentrations being suitable for the printed patterns which is mass per ablated area ($ng \cdot mm^{-2}$). However, this alternative does not correct for ablation drifts that could happen if different types of label are ablated, as it is not normalized against the internal standard (C). Therefore, the following calibration model for paper and ink quantification is suggested to compensate for slight differences in ablation behaviour (Figure 18):

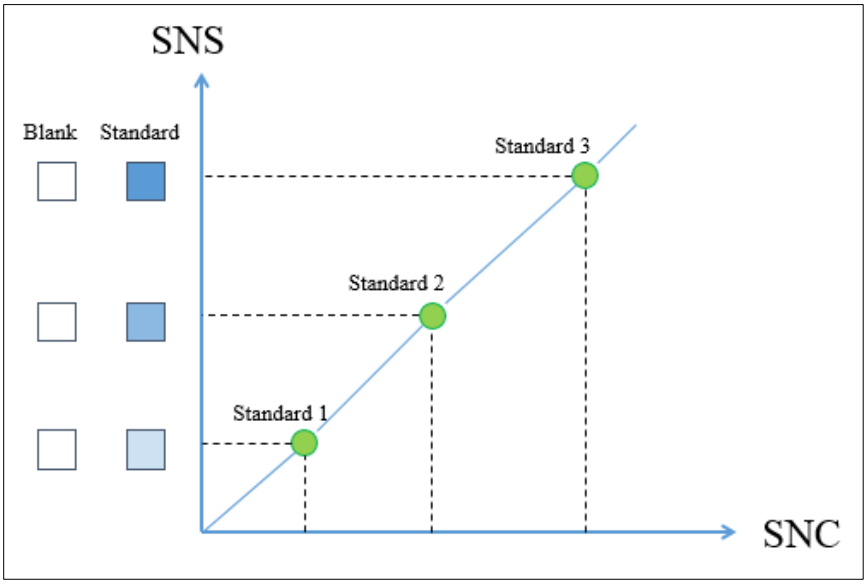


**Figure 18** Developed calibration model for ink quantification.

Where, SNC is the Surface Normalized Concentration calculated by the following equation (Eq. 1):

$$SNC = \frac{\frac{C_{element}}{C_{13C}} \times mass\ of\ printed\ area\ (g)}{Ablated\ area\ (mm^2)}$$

**Eq.1**

By this equation the concentration of an element determined in the printed standard by liquid ICPMS is normalized by the theoretically calculated internal standard concentration, multiplied by the known mass of printed area (16 x 20 cm, 80 g/m$^2$) and then, divided by the ablated surface (mm$^2$).

And, SNS is the Surface Normalized Signal calculated by the following equation (Eq. 2):

$$SNS = \frac{\frac{S_{paper+ink} - S_{Ar\ blank}}{S_{13C\ paper+ink} - S_{13C\ Ar\ blank}} - \frac{S_{paper} - S_{Ar\ blank}}{S_{13C\ paper} - S_{13C\ Ar\ blank}}}{Ablated\ area\ (mm^2)}$$

**Eq.2**

For the quantification of paper Eq.2 was simplified as it is shown in the following equation (Eq. 3):

$$SNS = \frac{\frac{S_{paper} - S_{Ar\ blank}}{S_{13Cpaper} - S_{13C\ Ar\ blank}}}{Ablated\ area\ (mm^2)}$$

**Eq.3**

The normalized signals obtained from the fsLA-ICPMS analysis of elemental solution printed patterns correlate linearly with excellent correlation coefficients of > 0.996 or better which suggest good accuracy, only limited by the quality of the standards. Furthermore, the fitted calibration lines go almost perfectly through zero, which confirms that the subtraction of the Ar gas blank together with the signal intensity of the blank paper is an adequate method for blank correction for the given experimental set-up (Figure 19).

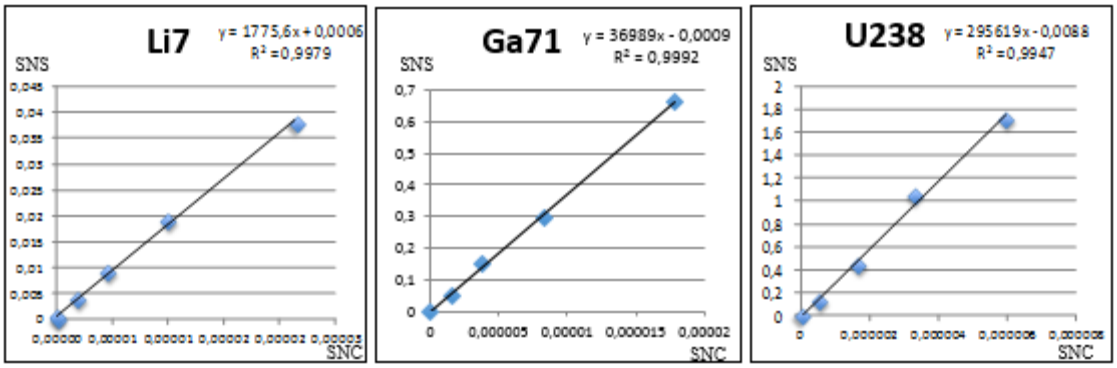


**Figure 19** Typical examples of obtained calibration curves for light, middle and heavy isotopes.

It can be concluded that the synthesis of homemade matrix-matched standards using a conventional printer, the careful control of the ablation parameters and the subsequent normalization of the concentration and signal by ablated area is a valuable approach for quantification of printed ink on label. Even if the ablation of the matrix is around 50% of the paper thickness and the distribution of the solutions within the paper depth shows variability depending on the element-matrix interactions and cellulose degradation owing to repeated prints.

### 3.3 Analytical performance of the fsLA-ICPMS method

The analytical performance of the fsLA-ICPMS method was evaluated in terms of long-term reproducibility, in-day repeatability, homogeneity, linearity and polyatomic interferences.

#### 3.3.1 Long-term reproducibility

The reproducibility of the developed fsLA-ICPMS based analytical method for the analysis of the paper and ink of the wine packaging was assessed. A randomly selected reference bottle was analyzed in each analysis session (n = 5 sessions) during 3 years for testing the reproducibility of the entire method for long-term method performance validation. A final isotope list was selected utilizing approximately 28 isotopes from the 68 analytes originally determined. The selection was based the on analytes giving count rates that were consistently above background signal (10 σ) during the full research period and were after employed for statistical data analysis. The

reproducibility was found to be in the range of 4-15%, similarly to what was obtained for glass analysis, as shown in Table 8.

**Table 8** Final elemental list and reproducibility of each isotope measured in a reference bottle (n = 9 sessions) during 3 years.

| Isotope | Average Surface Normalized Signal | RSD (%) |
|---|---|---|
| **Li7** | 9,52E-06 | 15,0 |
| **Cu63** | 1,74E-05 | 7,8 |
| **Ga71** | 5,77E-06 | 10,3 |
| **Rb85** | 3,11E-05 | 10,6 |
| **Sr88** | 6,40E-04 | 5,0 |
| **Y89** | 2,70E-06 | 9,6 |
| **Zr90** | 5,38E-05 | 12,4 |
| **Nb93** | 9,36E-07 | 9,7 |
| **Mo95** | 6,84E-07 | 7,67 |
| **In115** | 8,59E-08 | 11,3 |
| **Sn118** | 1,77E-05 | 10,8 |
| **Cs133** | 1,48E-06 | 5,5 |
| **Ba138** | 6,93E-05 | 13,1 |
| **La139** | 1,54E-05 | 10,4 |
| **Ce140** | 3,50E-05 | 11,7 |
| **Pr141** | 3,62E-06 | 13,2 |
| **Nd146** | 1,08E-05 | 11,1 |
| **Sm147** | 1,71E-06 | 9,02 |
| **Eu151** | 3,29E-07 | 4,2 |
| **Gd157** | 1,38E-06 | 7,0 |
| **Tb159** | 1,33E-07 | 13,4 |
| **Dy163** | 6,75E-07 | 14,0 |
| **Ho165** | 1,01E-07 | 3,4 |
| **Er166** | 2,92E-07 | 9,2 |
| **Yb172** | 1,90E-07 | 14,2 |
| **Lu175** | 2,57E-08 | 0,1 |
| **W182** | 2,01E-07 | 12,7 |
| **Th232** | 1,96E-06 | 12,4 |
| **U238** | 1,49E-06 | 11,0 |

### 3.3.2 In-day repeatability

Repeatability is defined as the dispersion of the obtained results, using the same analytical method, the same type of matrix and done it in the same laboratory, by the same operator and using the same equipment. According to European Legislation, repeatability should be expressed as relative standard deviation (RSD, %) indicating the number of replicates (n). In general, RSD values must be equal to or less than 20%. The repeatability of the method was also studied by analyzing the selected reference bottle three times within a same day. The intra-day variation was lower than 10% for most of the elements.

### 3.3.3 Homogeneity

For data quality control purposes, it is very important to provide a good sampling in order to arrive to accurate conclusions. Therefore, it is recommended to sample the known material from different areas to account for natural heterogeneity and to conduct at least three replicates per test sample. In this case, it was desirable to know if the minimally-invasive microanalysis of wine bottles with the proposed method is representative from the full sample. With this aim, a homogeneity study was conducted within an entire label free of ink (n = 3 bottles, 15 replicates per label) and within a set of bottles (n= 20 bottles, 3 replicates per bottle) belonging to the same winery and vintage. The homogeneity within a lot ranged from 10 to 15 % and was found to be adequate for the purpose of the method (Table 9). The homogeneity within a bottle was however found to be significantly lower, ranging from 0,3 to 5,7%. It is worth mentioning that if we know the 20 bottles analysed belonged to the same vintage and winery, we couldn’t verify that the labels originated from only one paper batch. Then these slight variations could reflect batches inhomogeneity from the paper manufacturer.

**Table 9** Reproducibility of selected isotopes within a single bottle (n = 3 bottles, 15 replicates per bottle) and within a batch of bottles belonging to the same winery and vintage (n = 20 bottles, 3 replicates per bottle).

| | Homogeneity within a bottle | | Homogeneity within a batch | |
|---|---|---|---|---|
| | **Average SNS** | **RSD (%)** | **Average SNS** | **RSD (%)** |
| **Li7** | 5,37E-04 | 1,6 | 5,73E-04 | 14,1 |
| **Cu63** | 9,13E-05 | 1,8 | 8,51E-05 | 14,2 |
| **Ga71** | 7,76E-05 | 3,2 | 7,90E-05 | 14,3 |
| **Rb85** | 1,43E-05 | 3,3 | 1,30E-05 | 14,2 |
| **Sr88** | 3,08E-04 | 2,2 | 3,35E-04 | 13,3 |
| **Y89** | 1,05E-05 | 3,3 | 9,23E-06 | 14,5 |
| **Zr90** | 7,93E-05 | 1,4 | 7,23E-05 | 12,8 |
| **Nb93** | 1,49E-05 | 0,8 | 2,10E-05 | 13,2 |
| **Mo95** | 5,64E-06 | 3,3 | 6,74E-06 | 11,8 |
| **In115** | 1,85E-07 | 1,5 | 1,90E-07 | 15,1 |
| **Sn118** | 6,64E-06 | 1,3 | 7,49E-06 | 12,7 |
| **Cs133** | 2,34E-06 | 1,7 | 2,38E-06 | 13,4 |
| **Ba138** | 1,20E-04 | 2,4 | 1,28E-04 | 14,7 |
| **La139** | 4,48E-05 | 2,0 | 4,78E-05 | 14,4 |
| **Ce140** | 7,37E-05 | 3,6 | 8,17E-05 | 14,0 |
| **Pr141** | 8,77E-06 | 3,4 | 9,39E-06 | 13,2 |
| **Nd146** | 2,73E-05 | 2,8 | 2,97E-05 | 14,4 |
| **Sm147** | 4,30E-06 | 1,4 | 5,15E-06 | 13,2 |
| **Eu151** | 1,03E-06 | 2,5 | 9,71E-07 | 14,4 |
| **Gd157** | 3,65E-06 | 2,6 | 3,45E-06 | 14,6 |
| **Tb159** | 4,76E-07 | 3,7 | 4,62E-07 | 11,6 |
| **Dy163** | 2,13E-06 | 1,7 | 2,00E-06 | 13,2 |
| **Ho165** | 3,53E-07 | 1,0 | 3,86E-07 | 13,0 |
| **Er166** | 9,47E-07 | 1,9 | 1,04E-06 | 13,5 |
| **Yb172** | 9,65E-07 | 3,8 | 1,03E-06 | 10,0 |
| **Lu175** | 1,40E-07 | 0,3 | 1,48E-07 | 13,0 |
| **W182** | 1,91E-06 | 2,2 | 2,28E-06 | 14,1 |
| **Th232** | 1,68E-05 | 5,4 | 1,47E-05 | 13,6 |
| **U238** | 4,99E-06 | 5,7 | 4,87E-06 | 11,5 |

### 3.3.4 Spectral interferences

Due to the fact that the most abundant elements found in paper matrix are Ca, Na, Mg and Al, potential interferences could arise from spectral overlap with these polyatomic ion, which are listed in Table 10. On the one hand, the measured isotopes were selected with respect to their most abundant species, absence of isobaric overlap and minimum spectral interferences. In addition, mathematical correction equations were added to the analytical method. On the other

hand, a dynamic reaction cell (DRC) flushed with $H_2$ as reaction gas was used to limit polyatomic ion interferences.

**Table 10** Potential spectral interferences due to the composition of paper matrix. Extracted from (29).

| m/z | Analyte affected (% abundance) | Potential interference |
|---|---|---|
| 39 | K (93.1) | $^{27}Al^{12}C^+$ |
| 48 | Ti (73.9) | $^{48}Ca^+$ |
| 49 | Ti (5.5) | $^{48}CaH^+$ |
| 52 | Cr (83.8) | $^{12}C^{40}Ar^+$,$^{12}C^{40}Ca^+$ |
| 53 | Cr (9.5) | $^{13}C^{40}Ar^+$,$^{13}C^{40}Ca^+$ |
| 56 | Fe (91.7) | $^{40}Ar^{16}O^+$, $^{40}Ca^{16}O^+$ |
| 57 | Fe (2.2) | $^{40}Ar^{16}OH^+$, $^{40}Ca^{16}OH^+$ |
| 58 | Ni (68.3) | $^{40}Ca^{18}O^+$ |
| 60 | Ni (26.2) | $^{44}Ca^{16}O^+$ |
| 63 | Cu (69.2) | $^{23}Na^{40}Ar^+$ |
| 65 | Cu (30.8) | $^{25}Mg^{40}Ar^+$ |

### 3.4 Minimally invasive analysis

As in the previous chapter, the quasi-non destructiveness of the analysis which irremediably would degrade the value of the bottle is desirable too. The laser parameters described in the precedent sections result in ablation matrix 500 x 500 µm (Figure 20). The matrix are small enough to be almost invisible to naked eye and thus are virtually non-destructive. Although the crater dimensions could be reduced, smaller matrix would decrease the relative sensitivity and would be less representative of the ablated matrix.

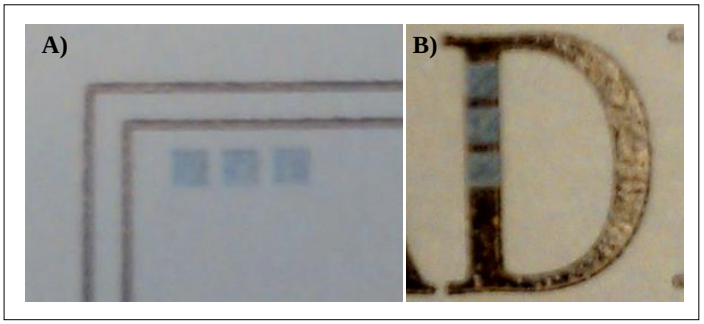


**Figure 20** Ablation matrix (500 x 500 µm) on A) label matrix and B) black ink.

### 3.5 Casework paper and ink sample set

Multivariate statistical data evaluation was done with software package XLSTAT® (2016) and The Unscrambler from CAMO version 9.1 (Computer Aided Modelling, Trondheim, Canada). This includes Principal Component Analysis (PCA), Agglomerative Hierarchical Clustering (AHC) and Soft Independent Modelling of Class Analogy (SIMCA). For each casework, a matrix was constructed with rows representing wine bottle samples and columns representing the SNC values obtained from fsLA-ICPMS measurements. For an initial classification, the principal component analysis (PCA) was used as an exploratory data analysis (EDA) technique to detect groups in the measured data set. In addition, agglomerative hierarchical classification (AHC) was also employed for unsupervised pattern recognition, mainly consisting of cluster analysis which is able to identify groupings among samples by means of a similarity measurement. Finally, as a second classification step, supervised classification tool as the soft independent modelling of class analogy (SIMCA) approach was employed in which a partial least squares (PLS) classification is performed in order to identify local models for possible groups and to predict a probable class membership for new observations. In each casework label paper and inks (black and/or red) has been analyzed according to their presence in the label.

#### 3.5.1 Casework 1: genuine vs. counterfeited bottles

***Label matrix***

The first sample set analyzed in this work consist of 8 bottles coming from the French region of Pauillac which belonging to a private enterprise, divided into genuine (5 samples) and counterfeited (3 samples). A PCA model with two PCs explains 94.08% of the variation in the data for the original and counterfeited wine bottles, being the residuals < 1 for all the scores, was developed. The biplot (Figure 21) reveals that separation along PC1 accounts for the 83.33% of the variation in the sample set, while separation along PC2 accounts for the 10.75%. Two groups FRANCE and CHINA are clearly distinguished by the element Ga, Sr, Zr, Mo, La, Ce, Nd and U. However, the French bottle 211 is noticeably differentiated from the other original bottles due to a change in label composition which will be discussed in Chapter 7. For this variable reduction, an initial PCA was run taking into account all the analyzed variables. After, the most significant (contribution of the observations, %) variables were selected from PC1, PC2 and PC3 and their correlations were studied within the correlation matrix (Pearson (n)). To select correlation threshold value from which two variables are significantly correlated, the statistical significance of the Coefficient of Correlation (r) values were studied by transforming them into t experimental values according to the equation 1, described in Chapter 5, for a $p\ value < 0.005$ and n-2 grades of freedom.

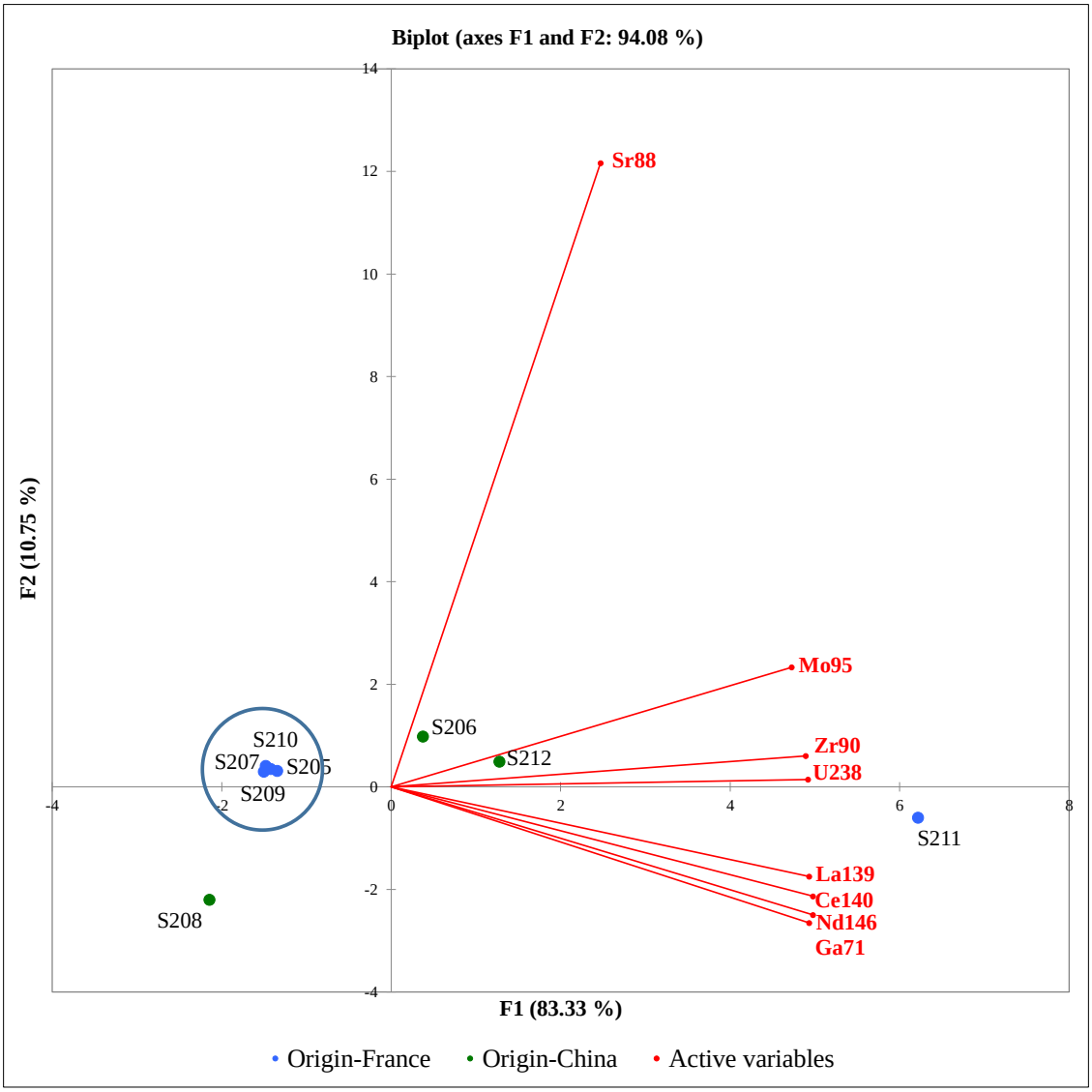


**Figure 21** Biplot (PC1 vs PC2) representing French original bottles (in blue) and Chinese counterfeited bottles (in green) with the loadings (variables) responsible of such discrimination (label paper).

On the second attempt for classifying the original and counterfeited bottles a cluster analysis was carried out to discover sample grouping within a data. For the performing of the cluster analysis the factor scores (F1, F2, F3 and F4) from the previous PCA were used. The classification was run by applying straight-line distance and Ward's agglomeration method.

It appears from the dendrogram in Figure 22 that the data can be represented by 4 classes. Class 1 corresponds exclusively to the genuine French bottles, except bottle 211, which is classified in Class 4 together with bottle 212. This fact will be later discussed in Chapter 7. The other two Chinese bottles are classified each one in different classes.

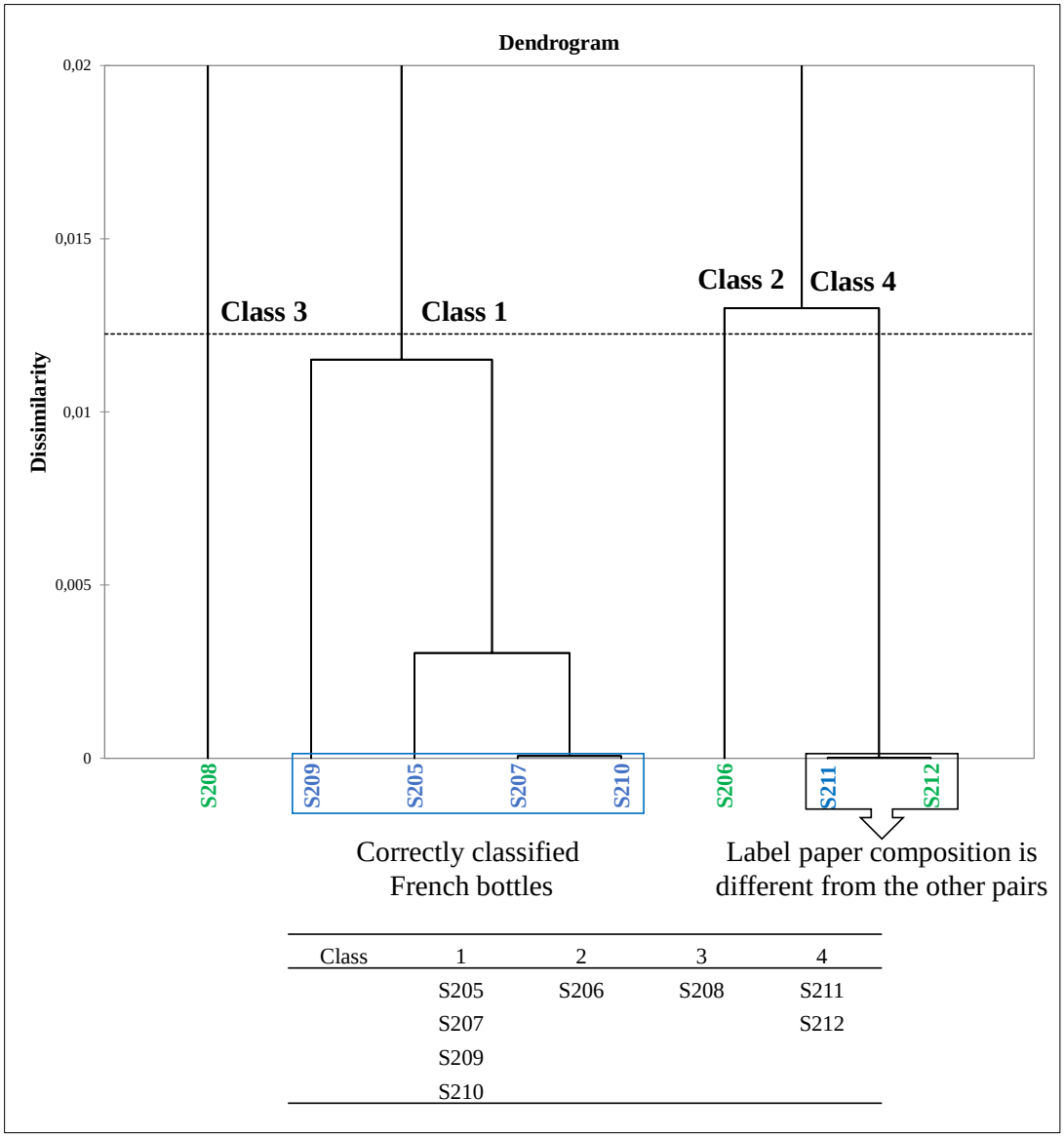


| Class | 1 | 2 | 3 | 4 |
|---|---|---|---|---|
| | S205 | S206 | S208 | S211 |
| | S207 | | | S212 |
| | S209 | | | |
| | S210 | | | |

**Figure 22** Clustering of original French bottles (in blue) and counterfeited Chinese bottles (in green). Dendrogram showing dissimilarity (Euclidian distance) and Ward agglomeration method (label paper).

***Black ink***

A PCA model with two PCs explains 94.08% of the variation in the data for the original and counterfeited wine bottles, being the residuals < 1 for all the scores, was developed. The biplot (Figure 23) reveals that separation along PC1 accounts for the 85.1% of the variation in the sample set, while separation along PC2 accounts for the 11.5%, having found the elements Ga, Zr, La, Ce and Nd the most discriminant. In this case, the French and Chinese bottles are not as clearly differentiated as with the label paper by itself. However, the pair 211 and 212 is noticeably differentiated from the other samples, indicating that the ink employed in this vintage may be different from the ink employed before. The same procedure previously described was followed for variable reduction.

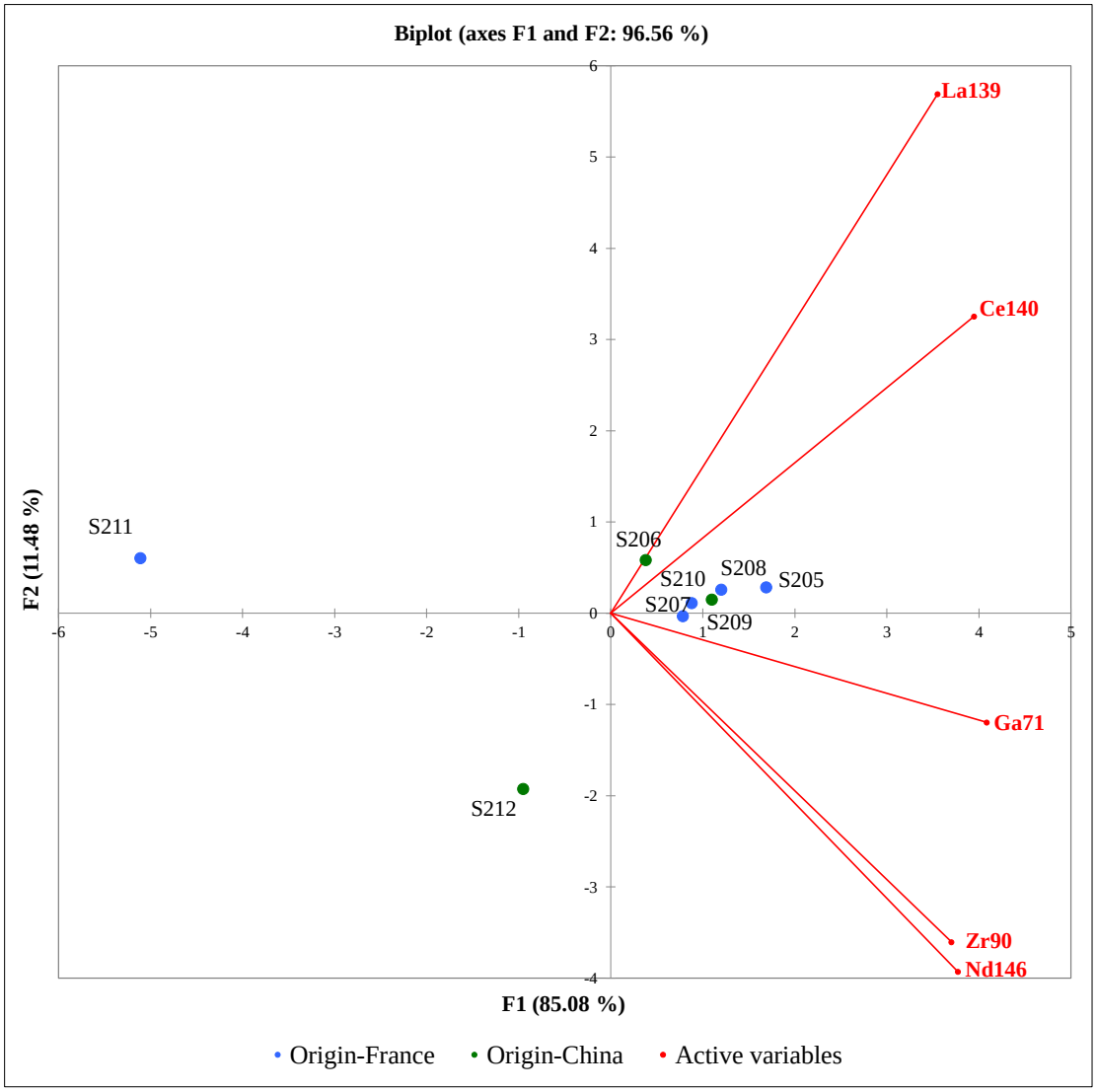


**Figure 23** Biplot (PC1 vs PC2) representing French original bottles (in blue) and Chinese counterfeited bottles (in green) with the loadings (variables) responsible of such discrimination (black ink).

For the performing of the cluster analysis the factor scores (F1, F2, F3 and F4) from the previous PCA were used. The classification was also run by applying straight-line distance and Ward's agglomeration method. Dendrogram in Figure 24 shows that the data can be represented by 3 classes. In this case, both French and Chinese bottles appears indistinguishable within classes. Class 1 gathers together all French and Chinese bottles except bottles 211 and 212 which makes by their own Class 2 and Class 3, respectively. This fact is in accordance with the state that for all vintages the same black pigment has been employed except for the pair 211-212 from 2007.

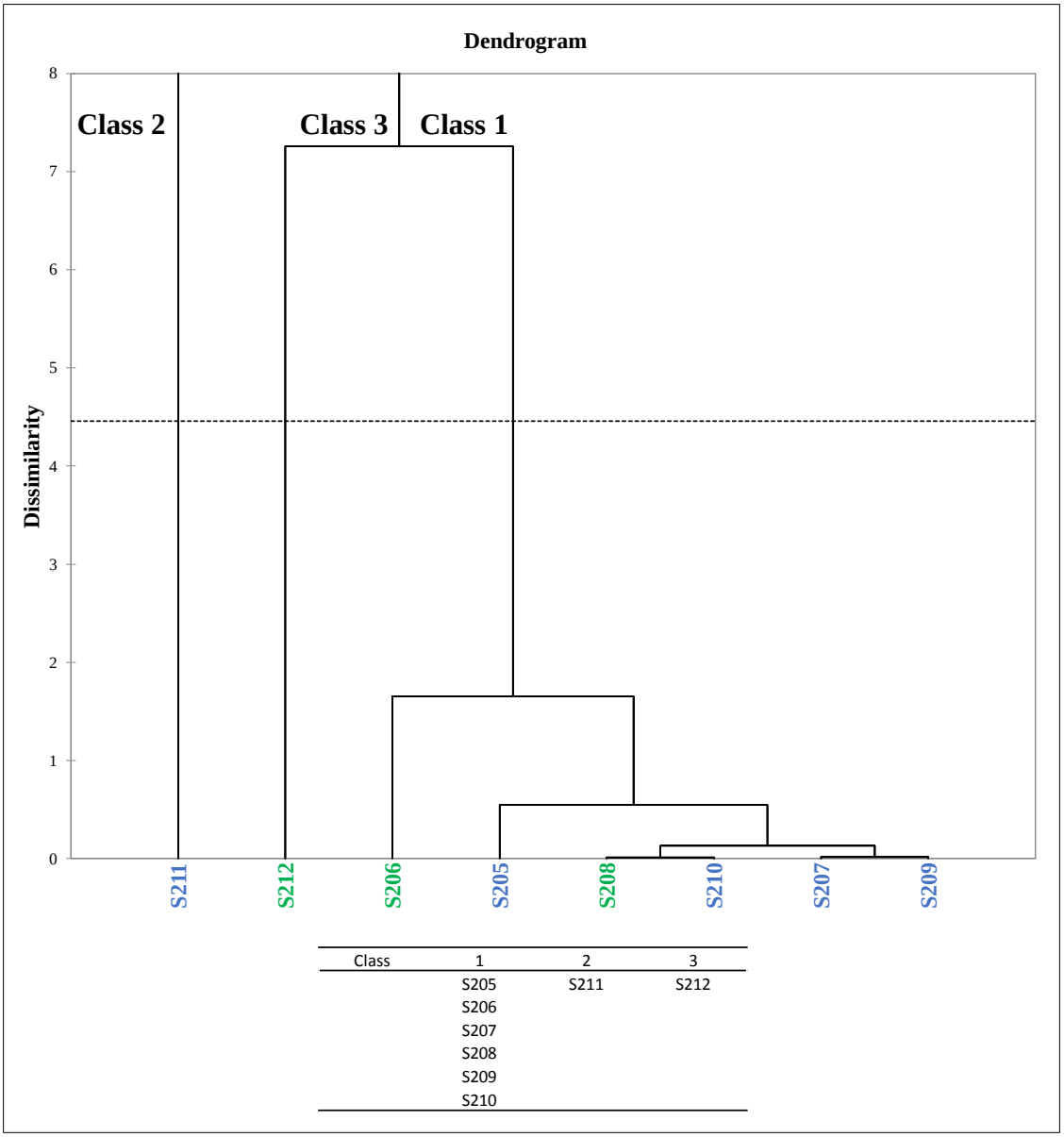


**Figure 24** Clustering of genuine French bottles (in blue) and counterfeited Chinese bottles (in green). Dendrogram showing dissimilarity (Euclidian distance) and Ward agglomeration method (black ink).

### 3.5.2 Casework 2: collection of a bottle series from the same wine cellar

The second sample set comprises 34 *bordelaise* bottles belonging to a famous French Château and which are classified according to their vintage:

*60s*: 1969
*70s*: 1973, 1974, 1978, 1979
*80s*: 1981, 1982, 1983, 1984, 1985, 1986, 1987, 1988, 1989
*90s*: 1990, 1992, 1993, 1994, 1995, 1996, 1997, 1998, 1999
*00s*: 2000, 2001, 2002, 2003, 2004, 2005, 2006, 2007, 2008, 2009
*10s*: 2010

***Label matrix***

A PCA model with two PCs explains 90.55% of the variation in the data for the original and counterfeited wine bottles, being the residuals < 1 for all the scores, was developed. The PCA (PCA1 vs. PCA2) (Figure 25) reveals that separation along PC1 accounts for the 83.75% of the variation in the sample set, while separation along PC2 accounts for the 6.80%. Among the monitored elements, eleven of them (Rb, Sr, Ba, La, Ce, Nd, Sm, Gd, Er, W and U, respectively) were found to be the responsible for such group discrimination. The same procedure previously described was followed for variable reduction.

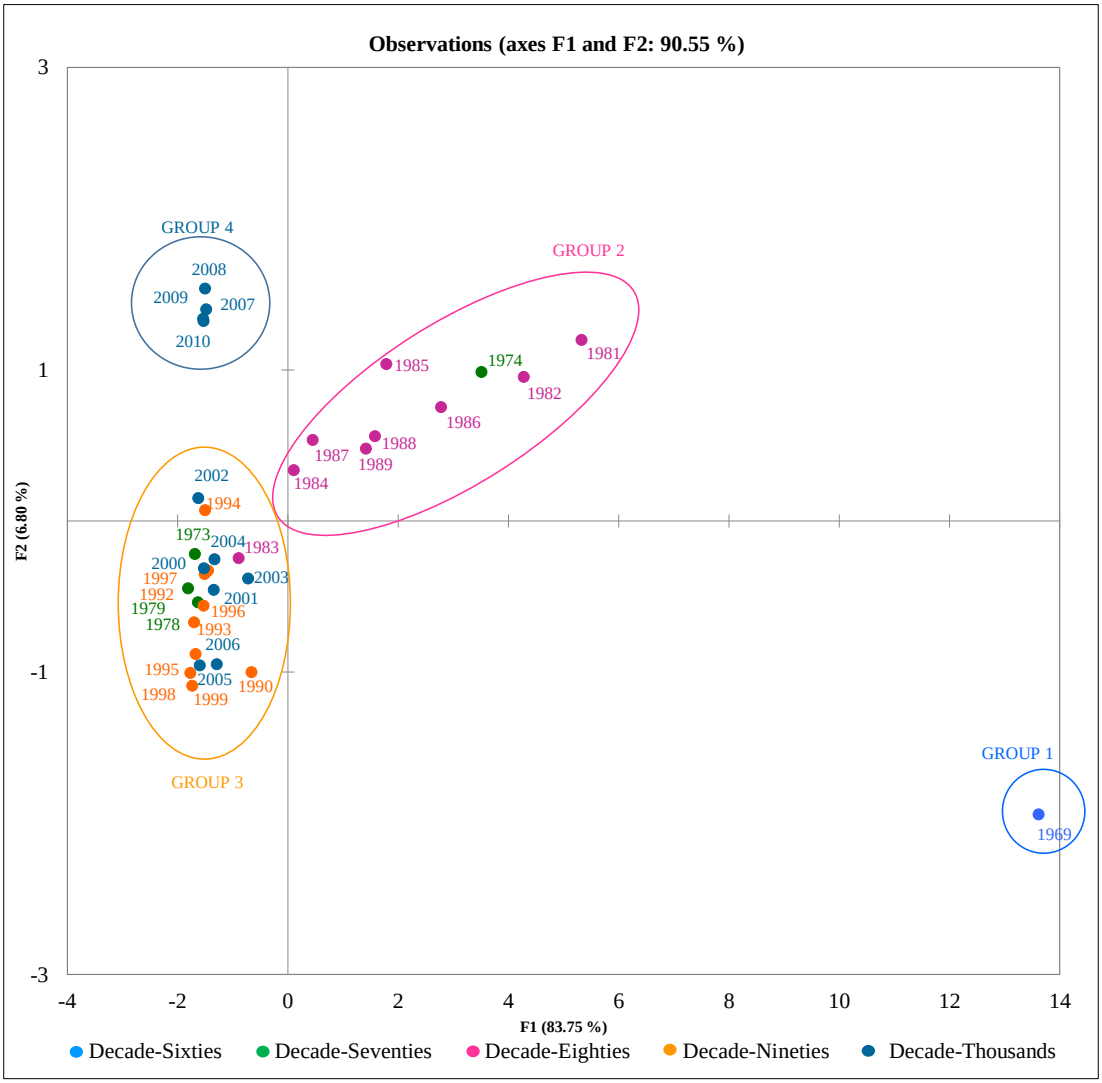


**Figure 25** PCA (PC1 vs. PC2) for the 34 samples coming from the same winery but different vintage (label paper).

In this case, the discrimination between vintage is not as clear as the discrimination performed with the glass analysis, in which bottles could be chronologically classified. However, it can be said that there are four different groups. First of all, bottle from 1969 is completely different from the other vintages, rare earths, Ba and W having a greater influence (Figure 26). The second group mainly corresponds to the bottles belonging to the decade of the eighties in which the Sr has the biggest influence, whose concentration ranges from 11,0 ng·mm$^{-2}$ (1981) to 2.9 ng·mm$^{-2}$ (1984). The third group mainly represents decades of nineties and early two thousands with however 3 bottles from the seventies (1973, 1978, 1979). It is characterized for having a low concentration of Sr (≈ 1.3 ng·mm$^{-2}$) but in which is not possible to perform a further discrimination, which indicates that during this period the paper composition remained almost constant without any considerable change. Finally, the forth group comprising vintages 2007, 2008, 2009 and 2010 is clearly differentiated, indicating a big change in label paper composition. They are characterized

for having a higher concentration of $^{88}Sr$ (≈ 10.3 ng·mm$^{-2}$) and lower concentration of rare earths. This change in label paper composition will be later explained in Chapter 7. The seventies do not make a group as they are distributed in groups 2 and 3.

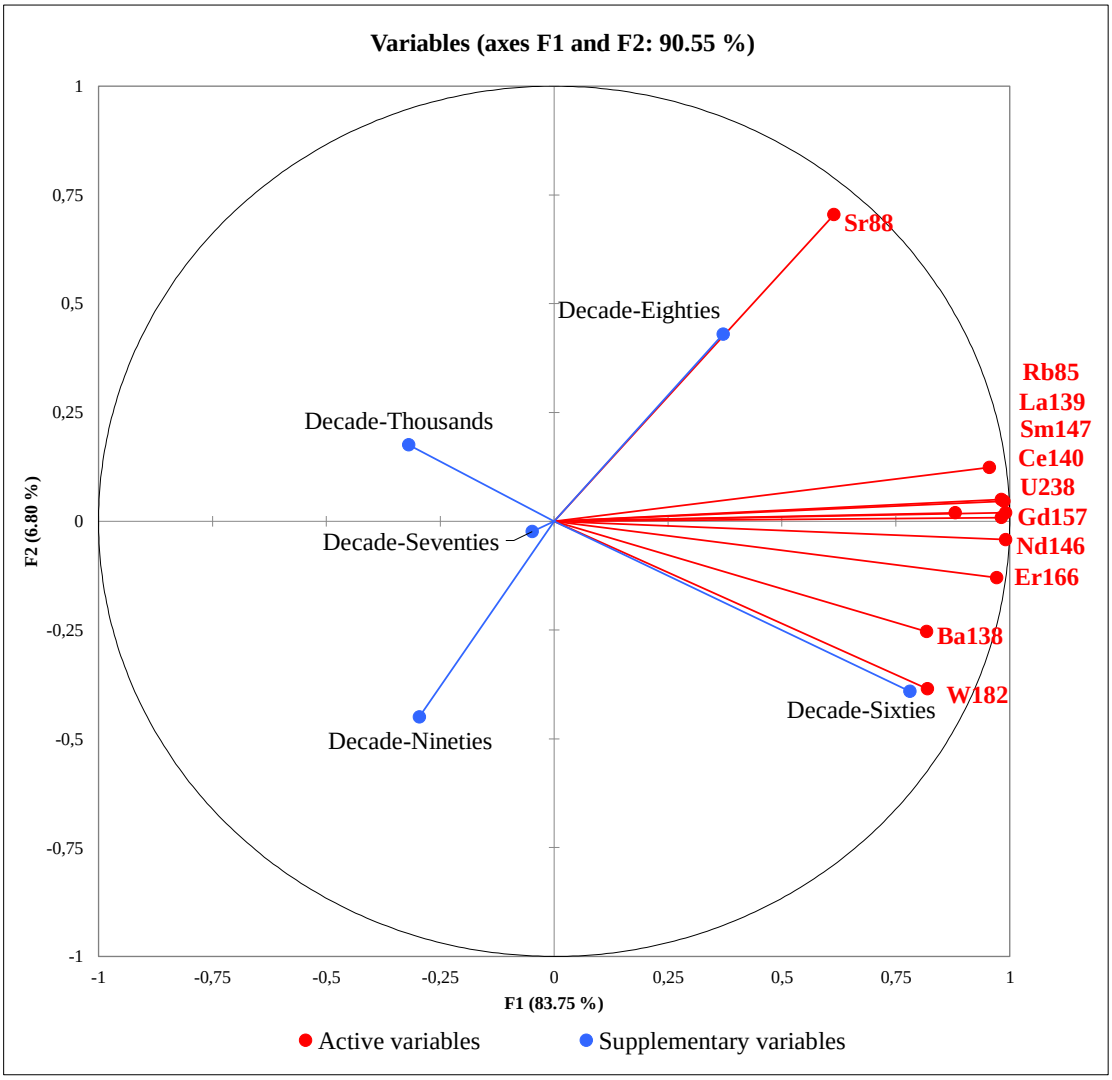


**Figure 26** Distribution of the selected variables in PC1 and PC2 for samples of same winery but different vintage (label paper).

***Black ink***

A PCA model with two PCs explains 86.80% of the variation in the data for the original and counterfeited wine bottles, being the residuals < 1 for all the scores, was developed. The PCA (PCA1 vs. PCA2) (Figure 27) reveals that separation along PC1 accounts for the 69.60% of the variation in the sample set, while separation along PC2 accounts for the 17.19%. Among the monitored elements, eight of them (Ga, Rb, Mo, La, Ce, Nd, Sm and Gd respectively) were found to be the best variables for discrimination. The same procedure previously described was followed for variable reduction.

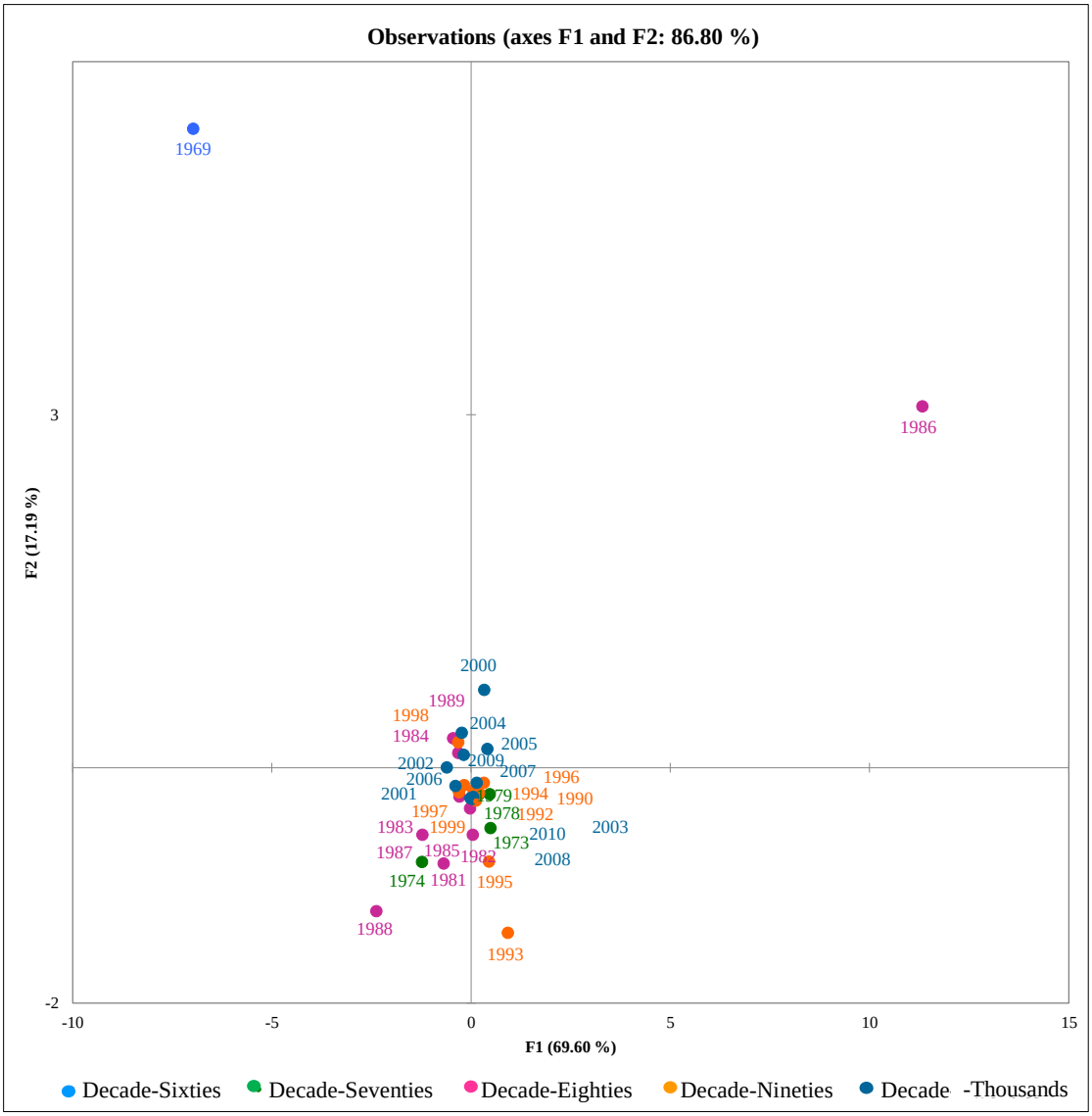


**Figure 27** PCA (PC1 vs. PC2) for the 34 samples coming from the same winery but different vintage (black ink).

As it is possible to observe in Figure 27 there is no differentiation of samples. Only vintages 1969 and 1986 are separated, due to the presence of higher amount of Mo (2.3 μg · $mm^{-2}$) and rare earths, Ga (0.31 μg · $mm^{-2}$) and Rb (0.15 μg · $mm^{-2}$), respectively (Figure28). These concentrations are slightly higher to those found in the paper but they do not show variability from sample to sample as happens for Sr in the case of label matrix.

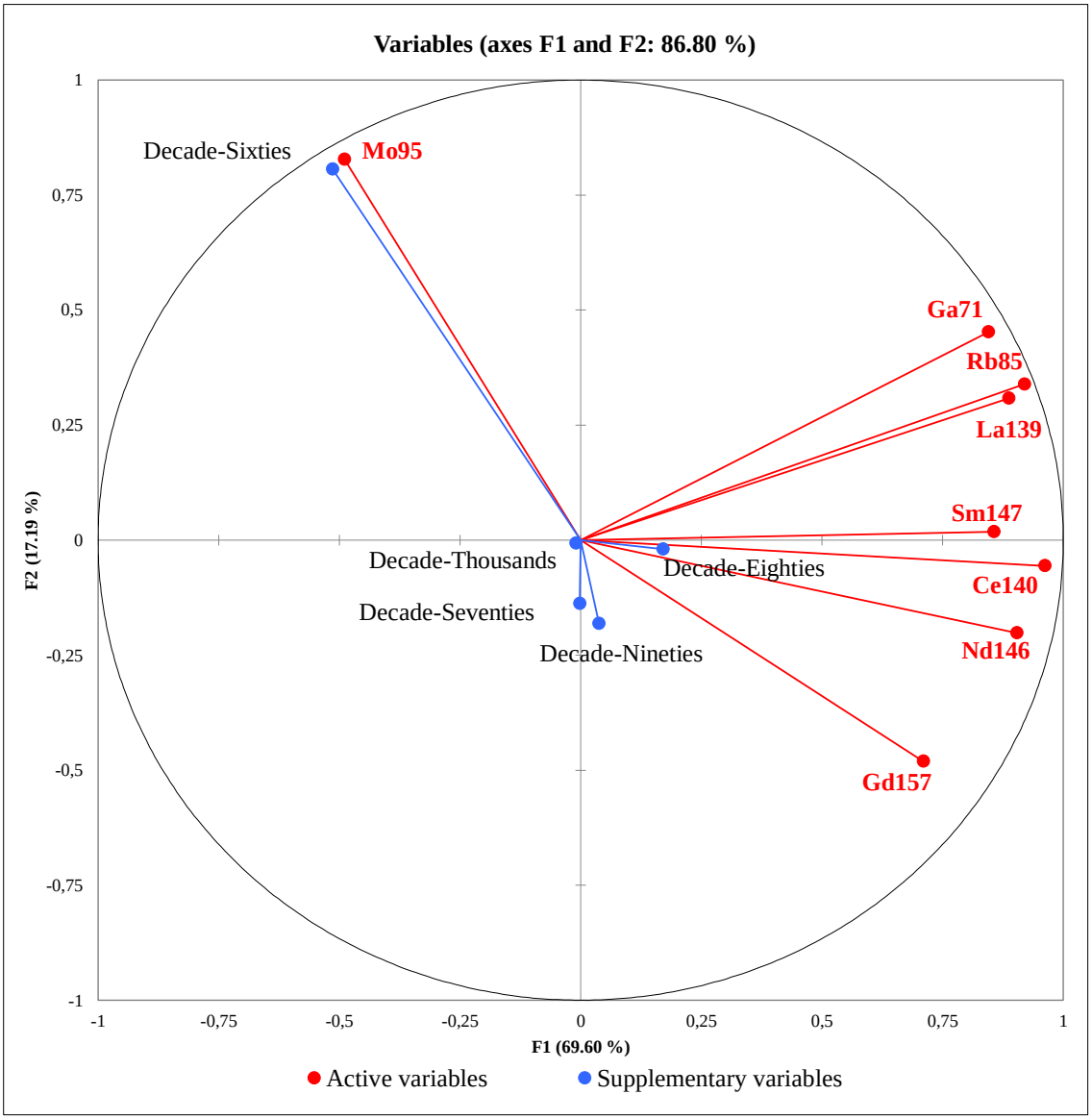


**Figure 28** Distribution of the selected variables in PC1 and PC2 for samples of same winery but different vintage (black ink).

***Red ink***

A PCA model with two PCs explains 84.55% of the variation in the data for the original and counterfeited wine bottles, being the residuals < 1 for all the scores, was developed. The PCA (PCA1 vs. PCA2) (Figure 27) reveals that separation along PC1 accounts for the 71.52% of the variation in the sample set, while separation along PC2 accounts for the 13.02%. Among the monitored elements, eight of them (Rb, Nb, Mo, Ba, La, Nd, Gd and W, respectively) were found to be the most discriminant variables. The same procedure previously described was followed for variable reduction. However, as it is possible to observe in Figure 29, and similarly to the black ink, a lack of sample differentiation, except for vintages 1969, 1986 and 1988.

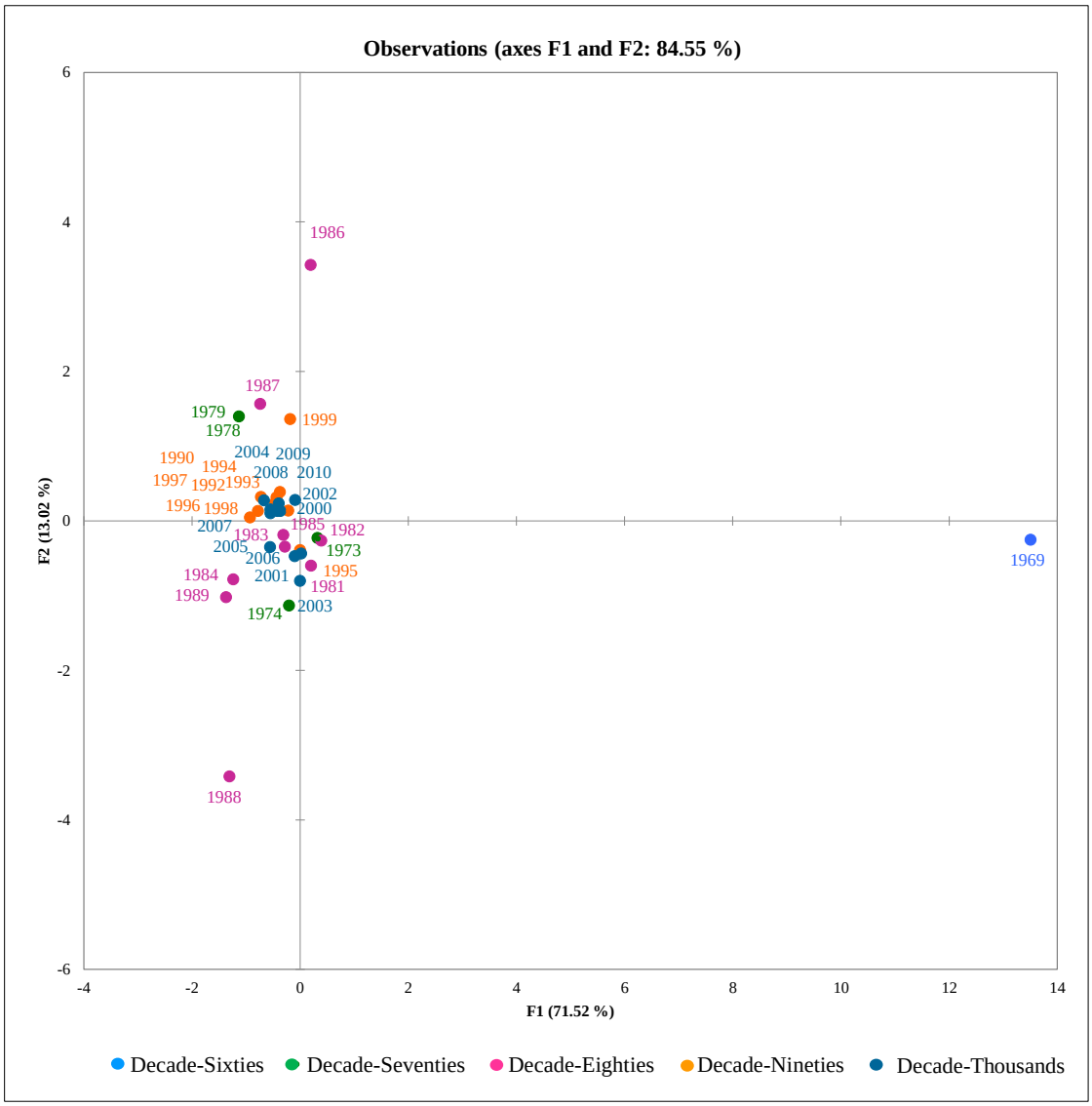


**Figure 29** PCA (PC1 vs. PC2) for the 34 samples coming from the same winery but different vintage (red ink).

Figure 30 indicates that the variables having influence in vintage 1969 are Rb, Mo, Gd, Nd and Ba whereas for the other vintages the most meaningful isotopes are Nb, La and W, concretely. It must be point out that the most discriminant isotope is Ba which has a concentration of 1.2 μg · $mm^{-2}$ for the vintage 1969 while for the other sample has an average of 0.45 μg · $mm^{-2}$.

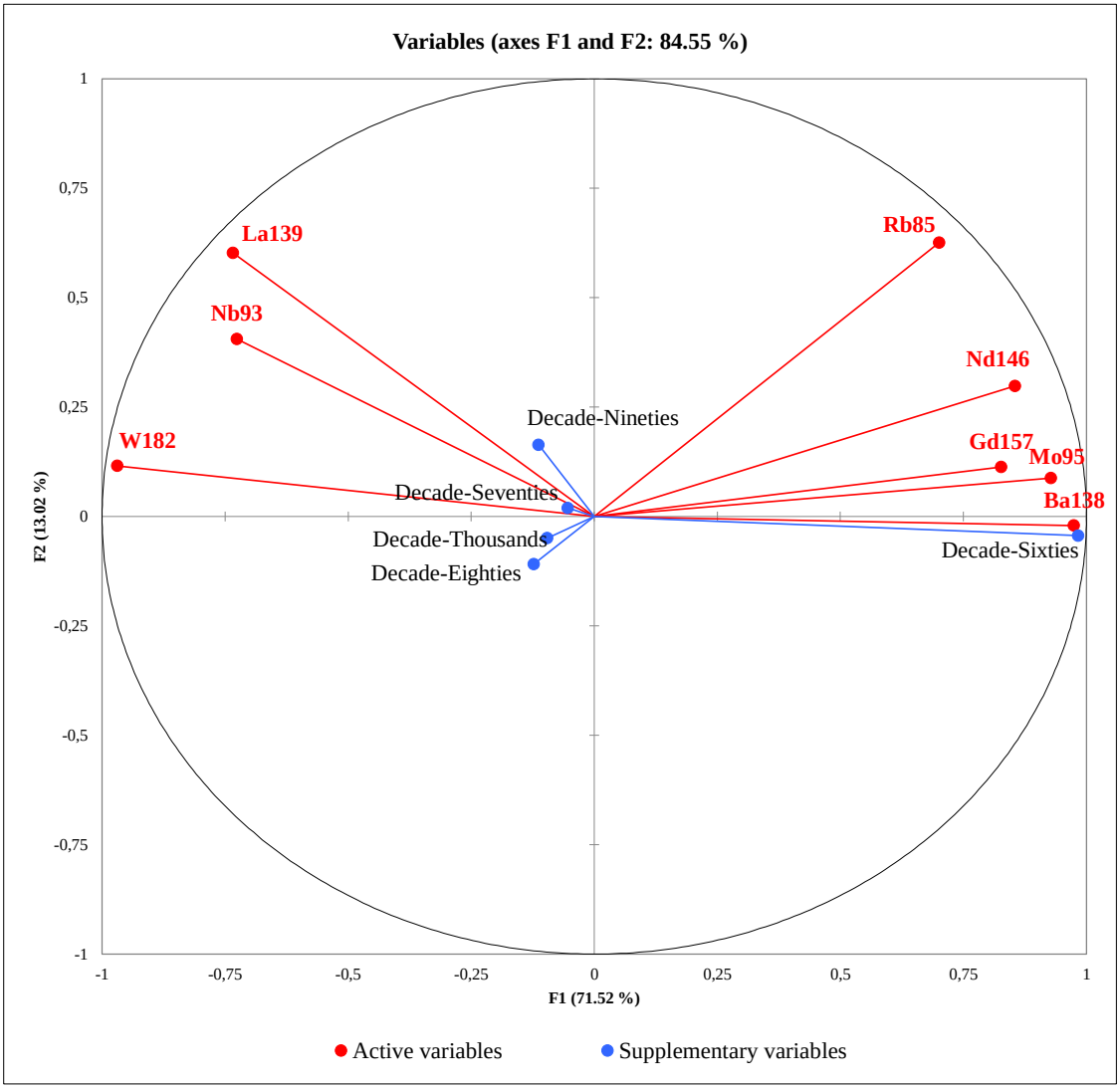


**Figure 30** Distribution of the selected variables in PC1 and PC2 for samples of same winery but different vintage (red ink).

As conclusion, it could be said that the ink (black or red) is not useful for sample classification within a group according to their vintage. Label paper, however, could be used as an approximate indicator of the vintage within the decades of the eighties, nineties and two thousands. Nevertheless, a better separation within the decades in the PCA and more samples for each decade would be desirable to perform a possible classification via SIMCA modelling in order to construct separate PCA models for each group in the training set.

### 3.5.3 Casework 3: collection of worldwide bottles

A total of 49 bottles coming from all continents were analyzed. Non-colored label paper and black ink were selected for analysis as they are most widespread kind of label and the most employed ink color, which can be found easily. Bottles coming from Oceania (2 samples) and Africa (1 sample) were removed from the statistical data analysis due to the lack of representativeness of these few samples and in order to obtain more trustworthy classification.

***Label matrix***

A PCA model with two PCs explains 72.14% of the variation in the data for label paper of worldwide bottles, being the residuals < 1 for all the scores, was developed. The PCA (PCA1 vs. PCA2) (Figure 31) reveals that separation along PC1 accounts for the 51.9% of the variation in the sample set, while separation along PC2 accounts for the 20.3%. Among the monitored elements Y, Sm, Ho and Yb were found to be the most significant for the discrimination of European, American and Asian bottles, having a greater influence in the first group (Figure 32). The same procedure previously described was followed for variable reduction.

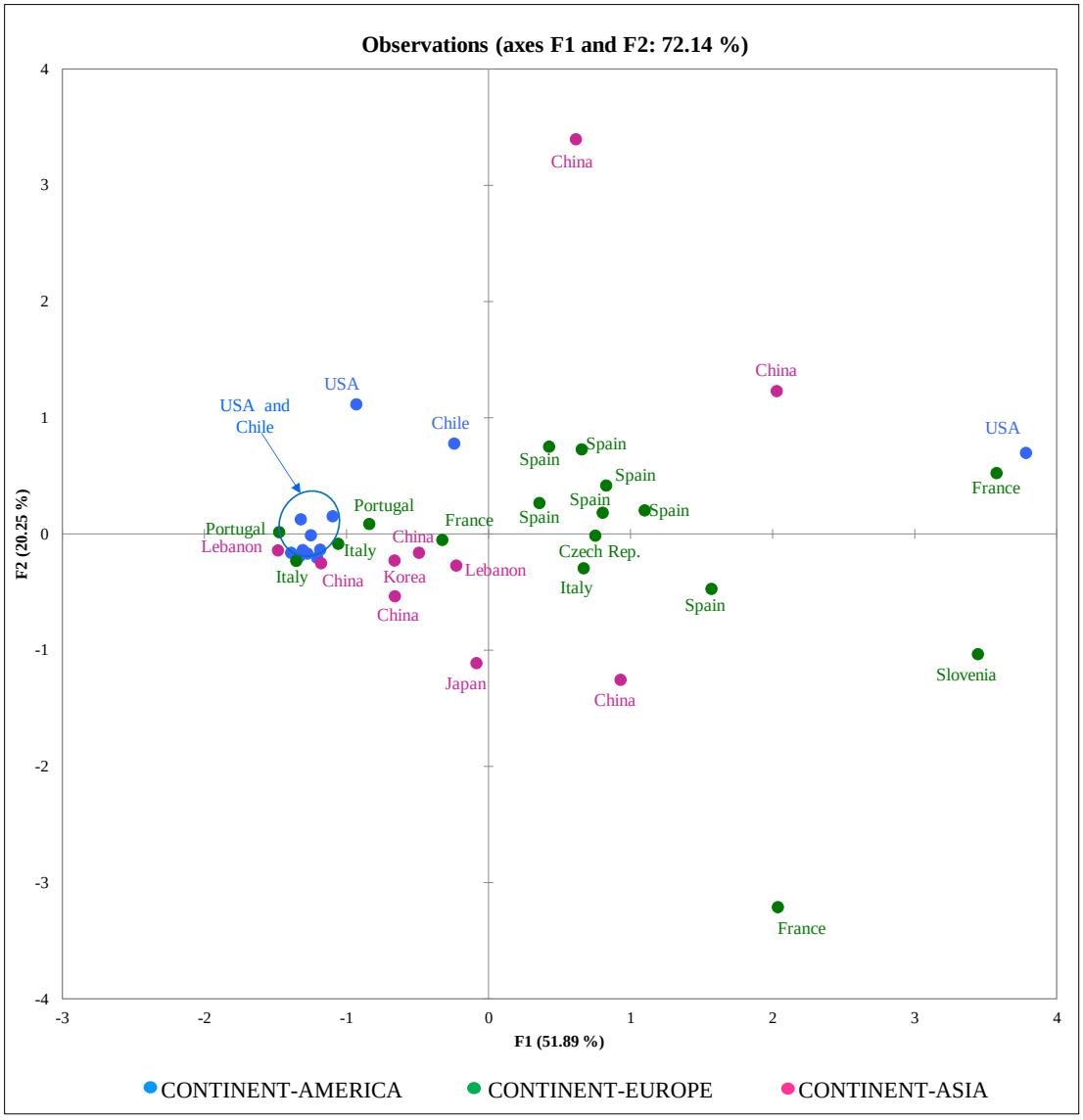


**Figure 31** PCA (PC1 vs. PC2) for the European, American and Asian bottles (label paper).

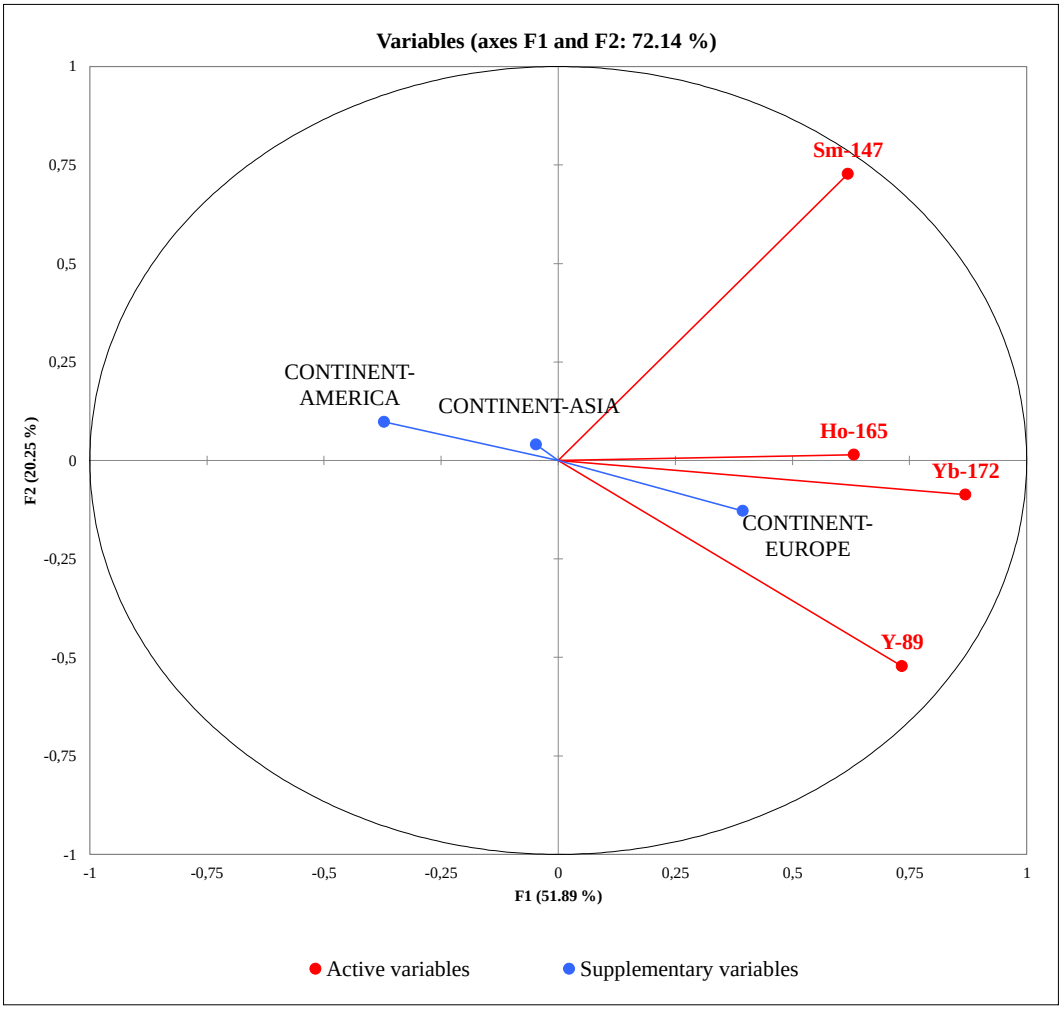


**Figure 32** Distribution of the selected variables in PC1 and PC2 for label paper of worldwide bottles.

It is possible to observe in Figure 31 that European bottles are mostly located in the positive area of the F2 axis while Asian bottle are in the negative area. American bottles, which include bottles from United States and Chile, are indistinguishable from the other continents. Therefore, due to the fact that European and Asian bottles are quite distinguished from each other which is a prerequisite for a possible classification via SIMCA modelling, an attempt to develop a classification model was done. Soft Independent Modelling of Class Analogies (SIMCA) is a classification procedure that makes separate PCA models for each group in the training set. Unknown samples are then compared with the class models and assigned to classes according to their analogy and distance from the category model. American bottles were kept out of the SIMCA model as they are not distinguish neither from the European and Asian bottles.

In this casework, previously centered and scaled data was employed to construct a global PCA excluding eight test samples (4 Asian and 4 European) of each class in the training set. This means that individual PCA were done for European bottles and Asian bottles using the four variables previously selected and randomly chosen eight test samples were extracted from the models. The Cooman's plot (Figure 33) indicated a non-existent class separation. The test samples are distributed according to the distance (similarity) to the model. In this case, EUROPE model is in the X axis while ASIA model is represented in the Y axis. Consequently, the models were not sufficiently different for classification and discrimination of samples. In fact, using a significance level of 5%, there is not classification for samples according to the classification table. Slovenian and one of the French bottles are unclassified while the other test samples are classified both in European model and Asian model.

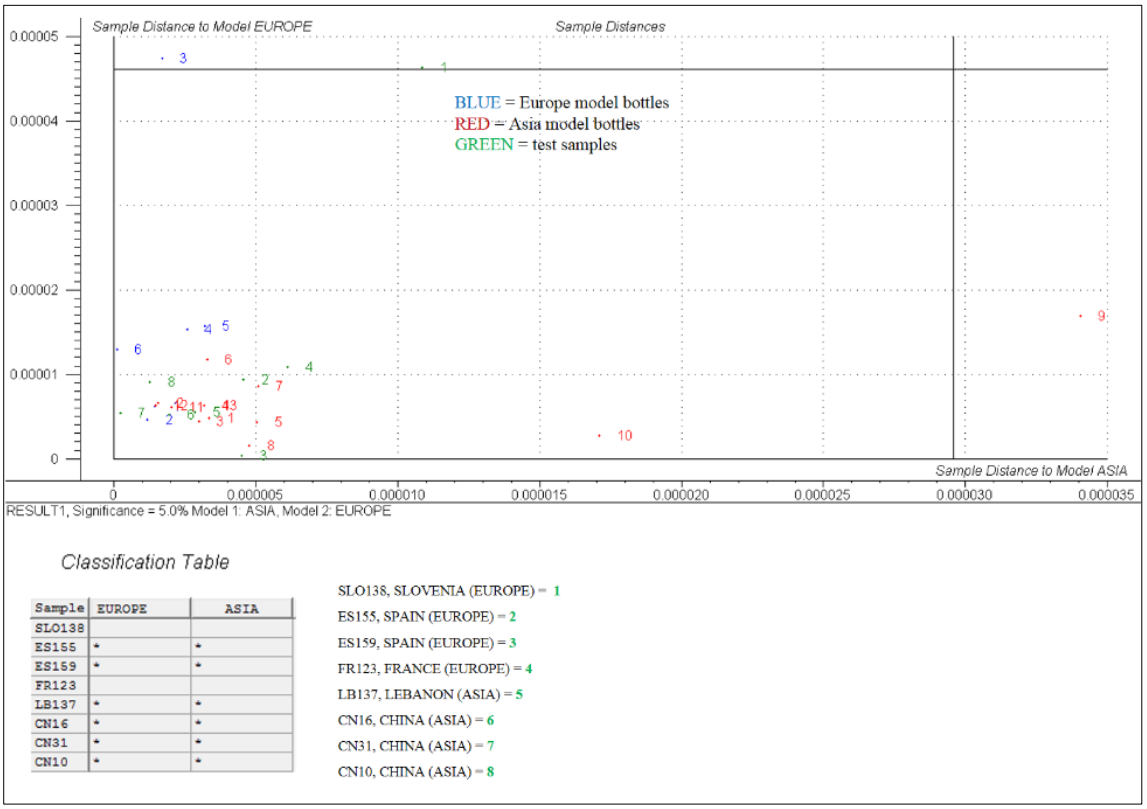


| Sample | EUROPE | ASIA |
|---|---|---|
| SLO138 | | |
| ES155 | * | * |
| ES159 | * | * |
| FR123 | | |
| LB137 | * | * |
| CN16 | * | * |
| CN31 | * | * |
| CN10 | * | * |

**Figure 33** Cooman's plot obtained from SIMCA modelling with its corresponding classification table.

Although SIMCA classification proved to be a suitable classification tool, the small number of samples per continent and even more the absence of two continents (Oceania and Africa), prevented the development of a definitive prediction model for SIMCA to classify bottles of wine according to their continent of origin through the elemental analysis of label paper.

***Black ink***

A PCA model with two PCs explains 69.77% of the variation in the data for the original and counterfeited wine bottles, being the residuals < 1 for all the scores, was developed. The PCA (PCA1 vs. PCA2) (Figure 34) reveals that separation along PC1 accounts for the 50.69% of the variation in the sample set, while separation along PC2 accounts for the 19.08%. Among the monitored elements Y, Nd, Sm, Gd, Tb and Er were found to be the most significant for the discrimination of European, American and Asian bottles, having a greater influence in the first group (Figure 35). The same procedure previously described was followed for variable reduction.

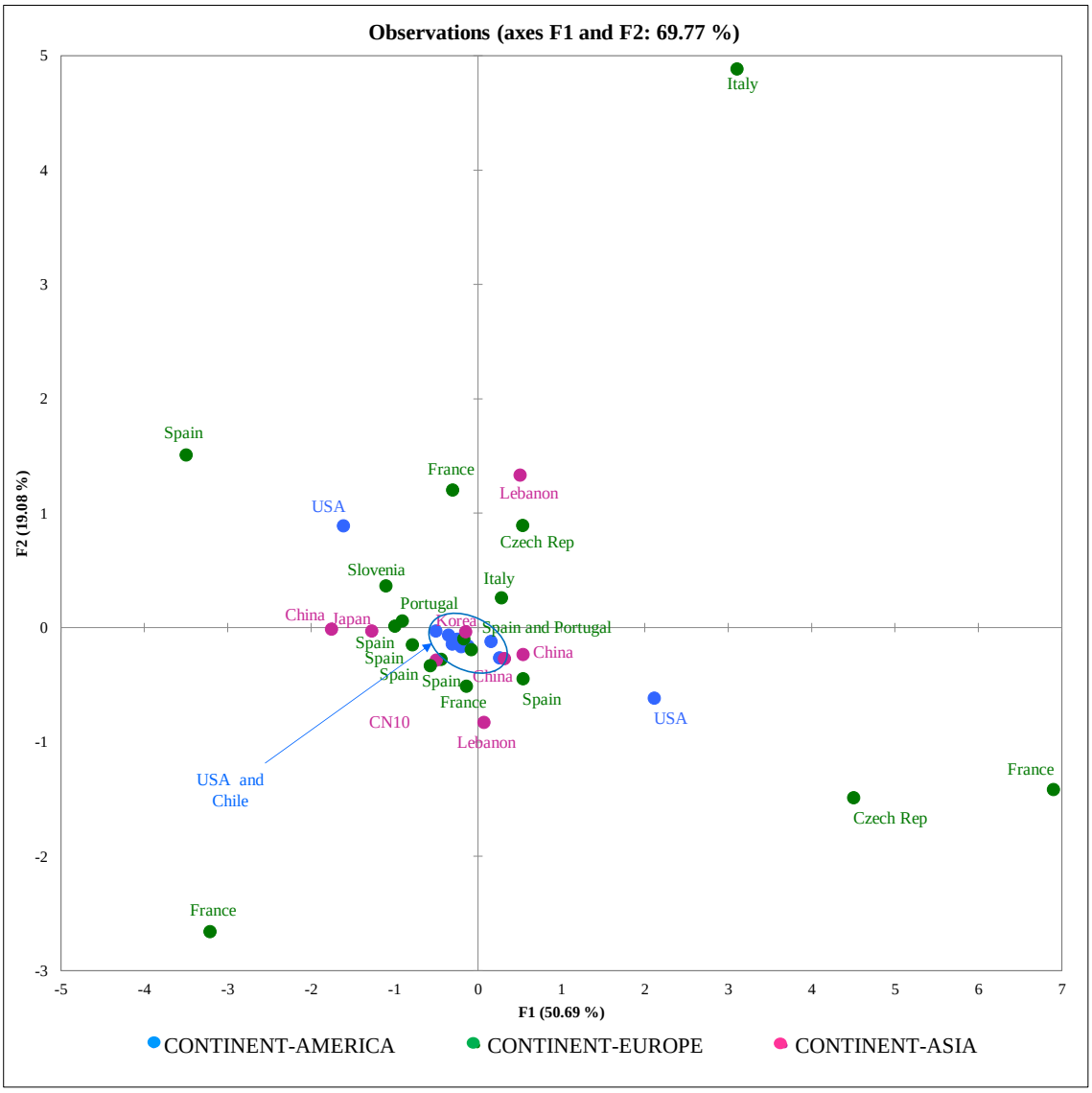


**Figure 34** PCA (PC1 vs. PC2) for the European, American and Asian bottles (black ink).

In this case, as occurs with the black and red ink of previous bottles batches, black ink seems to be not useful at all for sample classification within a group according to their origin. Nevertheless, label paper could be used as an approximate indicator of the continent but according to the results obtained with SIMCA classification, a better separation within the continents in the PCA and

more samples for each continent would be desirable to perform a better classification in order to construct separate PCA models for each group in the training set.

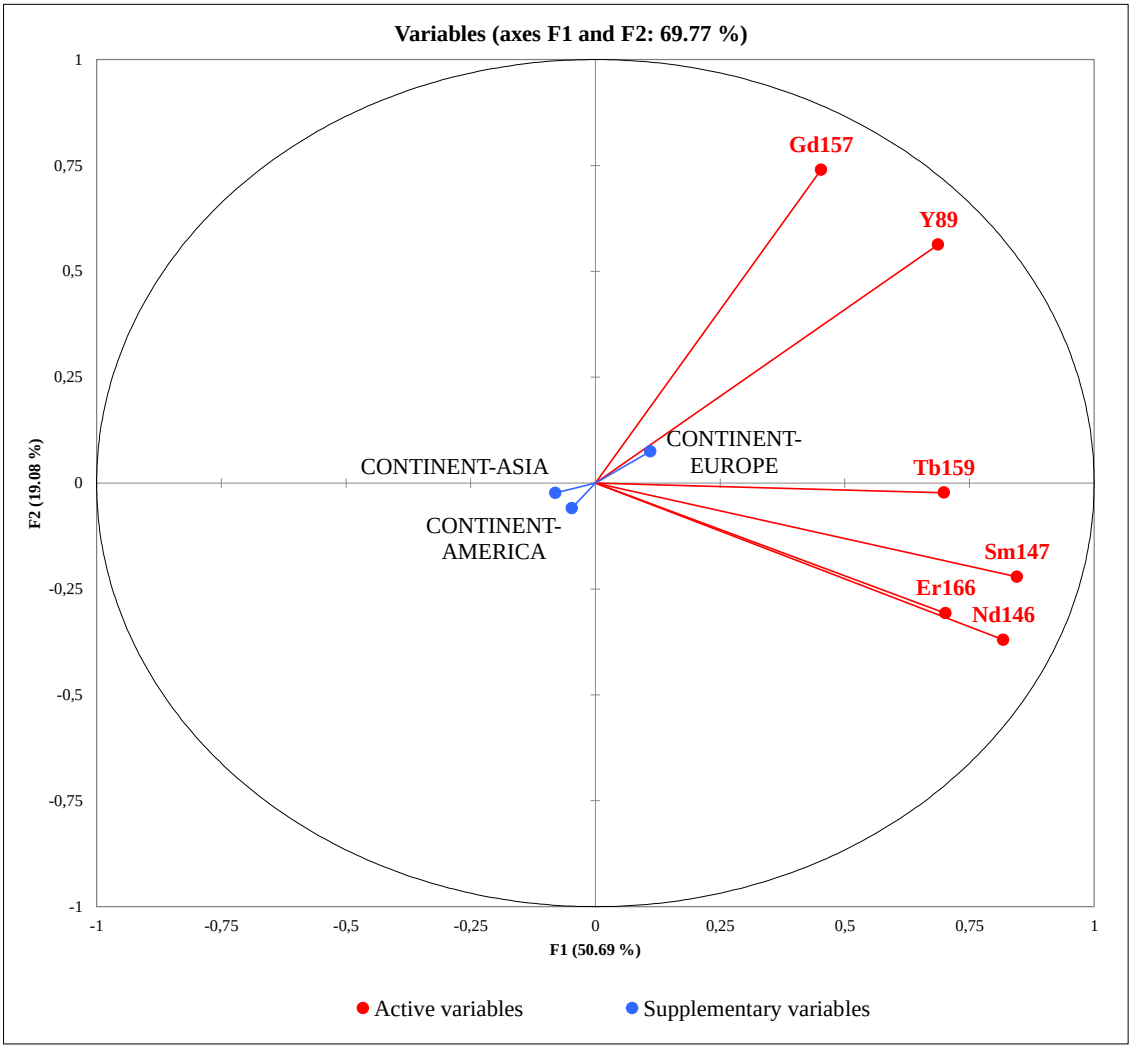


**Figure 35** Distribution of the selected variables in PC1 and PC2 for black ink of worldwide bottles.

## 4. Conclusions

The main objective of this work was to develop a new unambiguous characterization method based on the ultra-trace analysis of label paper and ink of wine packaging by minimally-invasive femtosecond laser ablation ICPMS, which induces no visible degradation of the bottle which could affect its value. Wine relabelling could induce misleading in the consumer which could affects its health and safety due to the possibility of contamination or the use of poor-quality ingredients. Conventional analytical techniques for wine verification are time-consuming, requiring liquid sampling, which irremediably degrade the value of the bottle and even making unattainable its resale.

In this framework, taking into account the previously stated objectives and based on the results derived from this study, the following conclusions can be drawn:

1. A minimally invasive ablation strategy (0.5 x 0.5 mm matrix) have been optimized which cause quasi non-visible damage to the bottle, allowing the analysis of a single bottle in a very competitive time (150 seconds for 3 replicates). The matrix are small enough to be almost invisible to naked eye and thus are virtually non-destructive. Additionally, the proposed ablation strategy have been tested in different types of glossy papers due to the wide range of labels available for wine packaging, finding it appropriate in all the cases.

2. Due to the lack of certified reference materials, matrix-matched standards have been synthesized as external calibrators by using commercially available inkjet printer. The reproducibility between printed droplets, which are on the order of picoliter or less according to the manufactured, is guaranteed by the printing mechanism. Calibration and standardization procedures for LA-ICPMS using a conventional ink jet printer have been already developed mainly focused on biological applications but to authors' knowledge, there are not previous studies in the literature offering a deep insight into the matrix-solution interactions when printers are used as diluting tool, which makes this work pioneer in this topic. The quality assessment of printed standards has been evaluated by imaging of paper's edge by UV-fsLA-ICPMS to study the penetration depth of printed solutions. It highlighted distinct penetration depending on the element of interest, some element being homogenously distributed and some being more concentrated in the surface. As this study was realized at the very end of the thesis, alternative printing approaches to produced perfectly in-depth homogenised standards couldn't be tested due to lack of time. Additional work is then required and alternative double side printing is considered for the next step. Moreover, normalization of the concentration and

signal by ablated area showed to be a valuable approach for accurate quantification of printed ink on label.

3. In addition, the Surface Elemental Concentration (SEC) calculated at different locations of a printout showed good homogeneity over the printed area. Nevertheless, taking into account a single cartridge, the amount of printed solution varied among printouts, which reveals an erratic deposition of solution which is also variable among cartridges. This difference of the inter- and intra-cartridge dependent printing process could be related to a physical defect in the injectors caused by the repetitive printing of acid containing solution or uncontrollable manufacturing modifications, which prevent the printing of the exact amount of solution required for each level.

4. Analytical performance of the fsLA-ICPMS methodology was evaluated for guarantee the consistency of the obtained results which is directly linked to the statistical classification of the samples analyzed among different groups, which is expressly the main objective of this work. Therefore, the analytical performance of the fsLA-ICPMS method was evaluated in terms of long-term reproducibility, in-day repeatability, homogeneity, linearity, and polyatomic interferences.

5. Developed methodology has been successfully applied for the analysis of label paper and ink of 91 bottles which have divided into 3 different batches: i) genuine versus counterfeited bottles, ii) a series of 34 bottles from the same winery and which comprises the vintages from 1969 to 2010 and iii) 49 bottles coming from all around the world. It must take into account that for analysis not-colored label paper and black and/or red ink have been chosen due to the fact that their use is more expanded than other colors.

6. Statistical data analysis based on multivariate analysis including Principal Component Analysis (PCA), Hierarchical Ascendant Classification (HAC) and Soft Independent Modelling of Class Analogy (SIMCA) have allowed:

    6.1 Discrimination between original and counterfeited bottles when label paper is analyzed by the use of the elements Ga, Sr, Zr, Mo, La, Ce, Nd and U. However, one of the original bottles is clearly separated both in the PCA and in the dendrogram. This separation is due to the composition of label paper, which will be detailed in the following Chapter 7. When black ink is analyzed no differentiation between French and Chinese bottle is observed, probably by the use of similar inks. In this case, the last pair of bottles keep far from the other, showing again that in this case a change ink formulation has occurred.

6.2 Distinction of the chemical profile of each bottle according to their vintage and origin.

5.2.1 The series comprising 34 bottles was classified in 4 different groups. However, this differentiation between decades is not as clear as the differentiation done with glass analysis. Rb, Sr, Ba, La, Ce, Nd, Sm, Gd, Er, W and U were found to be the responsible for such group discrimination. The most ancient bottle from 1969 is completely different from the other vintages, having a greater influence the rare earths, W and Ba. The second group corresponds to the bottles belonging to the decade of the eighties in which the Sr has the highest influence, whose concentration range decay from 10.97 $ng \cdot mm^{-2}$ (1981) to 2.87 $ng \cdot mm^{-2}$ (1984). The third group belongs to decades of nineties and two thousands. It is characterized for having a low concentration of Sr (≈ 1.30 $ng \cdot mm^{-2}$) but in which is not possible to perform a further discrimination, which indicates that during these decades the paper composition remained almost constant without any considerable change. Finally, the forth group comprising vintages 2007, 2008, 2009 and 2010 is clearly differentiated, indicating a big change in label paper composition. They are characterized for having a higher concentration of Sr (≈ 10.35 $ng \cdot mm^{-2}$) and lower concentration of rare earths. This change in label paper composition will be later explained in Chapter 7. The analysis and posterior statistical data treatment of black and red inks used in label do not give any valuable information about the vintage. In conclusion, it could be said that the ink (black or red) is not useful, in our case, for sample classification within a group according to their vintage. Label paper, however, could be used as an approximate indicator of the vintage within the decades of the eighties, nineties and 2000s.

5.2.2 An attempt to classify wine bottles coming from all around the world was done. Label paper and black ink were analyzed, finding once again that the black ink not useful for discrimination purposes.

The computed PCA for European, American and Asian bottles shows two major groups, Europe and Asia. American bottles, which include bottles from United States and Chile, are indistinguishable from the other continents. Among the monitored isotopes Y, Sm, Ho and Yb were found to be the most significant for the discrimination of European, American and Asian bottles, having a greater influence in the European group. Therefore, due to the fact that European and Asian bottles are quite distinguished from each other which is a prerequisite for a possible classification via SIMCA modelling, an attempt to develop a classification model

was done. American bottles were kept out of the SIMCA model as they are not distinguish neither from the European and Asian bottles. The constructed models were not sufficiently different for classification and discrimination of samples, using a significance level of 5%. Although SIMCA classification proved to be a suitable classification tool, the small number of samples representing each continent prevented the development of a more accurate prediction model for SIMCA.

Therefore, taking into account the drawn conclusions, it can be stated that a new calibration method has been successfully applied for the analysis of paper and ink found in wine labels with the aim of studying the authenticity and traceability of wine, based on the direct analysis of the wine packaging by the non-destructive technique of femtosecond laser ablation coupled to ICPMS. However, and in comparison with the results obtained from the analysis of glass, paper and ink have less discrimination capabilities but their analysis could be complementary to glass analysis and cannot be discarded to assess wine authenticity.

## 6. Bibliography


1. Zięba-Palus J, Wesełucha-Birczyńska A, Trzcińska B, Kowalski R, Moskal P. Analysis of degraded papers by infrared and Raman spectroscopy for forensic purposes. Journal of Molecular Structure. 2017;1140:154-62.
2. Bellis DJ, Santamaria-Fernandez R. Ink jet patterns as model samples for the development of LA-ICP-SFMS methodology for mapping of elemental distribution with reference to biological samples. Journal of Analytical Atomic Spectroscopy. 2010;25(7):957-63.
3. Orellana FA, Gálvez CG, Roldán MT, García-Ruiz C. Applications of laser-ablation-inductively-coupled plasma-mass spectrometry in chemical analysis of forensic evidence. TrAC Trends in Analytical Chemistry. 2013;42:1-34.
4. Manso M, Carvalho ML. Application of spectroscopic techniques for the study of paper documents: A survey. Spectrochimica Acta Part B: Atomic Spectroscopy. 2009;64(6):482-90.
5. Bajpai P. Basic Overview of Pulp and Paper Manufacturing Process. In: Green Chemistry and Sustainability in Pulp and Paper Industry . Cham: Springer International publishing; 2015. p. 11-39.
6. Aboul-Enein Y, Bunaciu AA, UdriŞTioiu FM, Tanase IG. Application of Micro-Raman and FT - IR Spectroscopy in Forensic Analysis of Questioned Documents. Gazi University Journal of Science. 2012;25(2).
7. Hubbe M. Acidic and Alkaline Sizings for Printing, Writing and Drawing Paper. The Book and Paper Group Annual. 2004;23.
8. Harrison WF. Manufacture of Printing Ink. Industrial and Engineering Chemistry. 1933;25(4):378-81.
9. Calcerrada M, García-Ruiz C. Analysis of questioned documents: A review. Analytica Chimica Acta. 2015;853(0):143-66.
10. Ezcurra M, Góngora JMG, Maguregui I, Alonso R. Analytical methods for dating modern writing instrument inks on paper. Forensic Science International. 2010;197(1):1-20.
11. Neumann C, Margot P. New perspectives in the use of ink evidence in forensic science: Part I. Development of a quality assurance process for forensic ink analysis by HPTLC. Forensic Science International. 2009;185(1):29-37.
12. Braz A, López-López M, García-Ruiz C. Raman spectroscopy for forensic analysis of inks in questioned documents. Forensic Science International. 2013;232(1):206-12.
13. Cantu AA. Analytical methods for detecting fraudulent documents. Analytical Chemistry. 1991;63(17):847A-54A.
14. Grant J. The Rôle of Paper in Questioned Document Work. Journal of the Forensic Science Society. 1973;13(2):91-5.

15. Schlesinger HL, Settle DM. A large-scale study of paper by neutron activation analysis. Journal of Forensic Science. 1971;16(3):309-30.
16. Brunelle RL, Washington WD, Hoffman CM, Pro MJ. Use of neutron activation analysis for the characterization of paper. Journal of Association of Official Analytical Chemist. 1971;54(4):920-4.
17. Blanchard D, Harrison S. Trace Element Profiles and Ratios Determined by Instrumental Neutron Activation Analysis for Fine Paper Identification. Journal of Forensic Science. 1978;23(4):679-86.
18. Langmyhr FJ, Thomassen Y, Massoumi A. Atomic-absorption spectrometric determination of copper, lead, cadmium and manganese in pulp and paper by the direct-atomization technique. Analytica Chimica Acta. 1974;68(2):305-9.
19. Simon PJ, Giessen BC, Copeland TR. Categorization of papers by trace metal content using atomic absorption spectrometric and pattern recognition techniques. Analytical Chemistry. 1977;49(14):2285-8.
20. Wagner B, Garboś S, Bulska E, Hulanicki A. Determination of iron and copper in old manuscripts by slurry sampling graphite furnace atomic absorption spectrometry and laser ablation inductively coupled plasma mass spectrometry. Spectrochimica Acta Part B: Atomic Spectroscopy. 1999;54(5):797-804.
21. Polk D, Attard A, Giessen B. Forensic Characterization of Papers. II: Determination of Batch Differences by Scanning Electron Microscopic Elemental Analysis of the Inorganic Components. Journal of Forensic Science. 1977;22(3):524-33.
22. Rožić M, Mačefat MR, Oreščanin V. Elemental analysis of ashes of office papers by EDXRF spectrometry. Nuclear Instruments and Methods in Physics Research Section B: Beam Interactions with Materials and Atoms. 2005;229(1):117-22.
23. Manso M, Pessanha S, Carvalho ML. Artificial aging processes in modern papers: X-ray spectrometry studies. Spectrochimica Acta Part B: Atomic Spectroscopy. 2006;61(8):922-8.
24. Manso M, Costa M, Carvalho ML. From papyrus to paper: Elemental characterization by X-ray fluorescence spectrometry. Nuclear Instruments and Methods in Physics Research Section A: Accelerators, Spectrometers, Detectors and Associated Equipment. 2007;580(1):732-4.
25. Manso M, Costa M, Carvalho ML. Comparison of elemental content on modern and ancient papers by EDXRF. Applied Physics A. 2008;90(1):43-8.
26. van Es A, de Koeijer J, van der Peijl G. Discrimination of document paper by XRF, LA–ICP–MS and IRMS using multivariate statistical techniques. Science and Justice. 2009;49(2):120-6.
27. Trejos T, Flores A, Almirall JR. Micro-spectrochemical analysis of document paper and gel inks by laser ablation inductively coupled plasma mass spectrometry and laser induced

breakdown spectroscopy. Spectrochimica Acta Part B: Atomic Spectroscopy. 2010;65(11):884-95.

28. Sarkar A, Aggarwal SK, Alamelu D. Laser induced breakdown spectroscopy for rapid identification of different types of paper for forensic application. Analytical Methods. 2010;2(1):32-6.
29. Spence LD, Baker AT, Byrne JP. Characterization of document paper using elemental compositions determined by inductively coupled plasma mass spectrometry. Journal of Analytical Atomic Spectrometry. 2000;15(7):813-9.
30. Spence LD, Francis RB, Tinggi U. Comparison of the elemental composition of office document paper: evidence in a homicide case. Journal of Forensic Sciences. 2002;47(3):648-51.
31. McGaw EA, Szymanski DW, Smith RW. Determination of trace elemental concentrations in document papers for forensic comparison using inductively coupled plasma-mass spectrometry. Journal of Forensic Science. 2009;54(5):1163-70.
32. Tanase IG, Popa DE, Udristioiu GE, Bunaciu AA, Aboul-Enein HY. Validation and quality control of an ICP-MS method for the quantification and discrimination of trace metals and application in paper analysis: an overview. Critical Reviews in Analytical Chemistry. 2014;44(4):311-27.
33. Wagner B, Bulska E. On the use of laser ablation inductively coupled plasma mass spectrometry for the investigation of the written heritage. Journal of Analytical Atomic Spectrometry. 2004;19(10):1325-9.
34. Kaminska A, Sawczak M, Komar K, Śliwiński G. Application of the laser ablation for conservation of historical paper documents. Applied Surface Science. 2007;253(19):7860-4.
35. Wagner B, Bulska E, Sobucki W. Magnesium distribution in paper subjected to deacidification investigated by means of Laser Ablation Inductively Coupled Plasma Mass Spectroscopy. Journal of Cultural Heritage. 2008;9(1):60-5.
36. Adams J. Analysis of printing and writing papers by using direct analysis in real time mass spectrometry. International Journal of Mass Spectrometry. 2011;301(1):109-26.
37. Proietti N, Capitani D, Pedemonte E, Blümich B, Segre AL. Monitoring degradation in paper: non-invasive analysis by unilateral NMR. Part II. Journal of Magnetic Resonance. 2004;170(1):113-20.
38. Casieri C, Bubici S, Viola I, De Luca F. A low-resolution non-invasive NMR characterization of ancient paper. Solid State Nuclear Magnetic Resonance. 2004;26(2):65-73.
39. Brai M, Camaiti M, Casieri C, De Luca F, Fantazzini P. Nuclear magnetic resonance for cultural heritage. Magnetic Resonance Imaging. 2007;25(4):461-5.

40. Workman JJ. Infrared and Raman Spectroscopy in paper and pulp analysis. Applied Spectroscopy Reviews. 2001;36(2-3):139-68.
41. Bitossi G, Giorgi R, Mauro M, Salvadori B, Dei L. Spectroscopic Techniques in Cultural Heritage Conservation: A Survey. Applied Spectroscopy Reviews. 2005;40(3):187-228.
42. Łojewska J, Lubańska A, Miśkowiec P, Łojewski T, Proniewicz LM. FTIR in situ transmission studies on the kinetics of paper degradation via hydrolytic and oxidative reaction paths. Applied Physics A. 2006;83(4):597.
43. Łojewska J, Rabin I, Pawcenis D, Bagniuk J, Aksamit-Koperska MA, Sitarz M, et al. Recognizing ancient papyri by a combination of spectroscopic, diffractional and chromatographic analytical tools. Scientific Reports. 2017;7:46236.
44. Chen S. A survey of methods used for the identification and characterization of inks. Forensic Science Journal. 2002:1-14.
45. LaPorte GM. The use of an electrostatic detection device to identify individual and class characteristics on documents produced by printers and copiers--a preliminary study. Journal of Forensic Science. 2004;49(3):610-20.
46. Tchan J. Forensic Examination of Laser Printers and Photocopiers Using Digital Image Analysis to Assess Print Characteristics. Journal of Imaging Science and Technology. 2007;51(4):299-309.
47. Brown JF. Colour and Colour Matching. In: The Printing Ink Manual. Boston:Springer US; 1988. p. 69-108.
48. Subedi K, Trejos T, Almirall J. Forensic analysis of printing inks using tandem Laser Induced Breakdown Spectroscopy and Laser Ablation Inductively Coupled Plasma Mass Spectrometry. Spectrochimica Acta Part B: Atomic Spectroscopy. 2015;103:76-83.
49. Trzcinska BM. Classification of black powder toners on the basis of integrated analytical information provided by Fourier transform infrared spectrometry and X-ray fluorescence spectrometry. Journal of Forensic Science. 2006;51(4):919-24.
50. Zięba-Palus J, Trzcińska BM. Establishing of Chemical Composition of Printing Ink. Journal of Forensic Science. 2011;56(3):819-21.
51. Chu P-C, Cai BY, Tsoi YK, Yuen R, Leung KSY, Cheung N-H. Forensic Analysis of Laser Printed Ink by X-ray Fluorescence and Laser-Excited Plume Fluorescence. Analytical Chemistry. 2013;85(9):4311-5.
52. Egan WJ, Galipo RC, Kochanowski BK, Morgan SL, Bartick EG, Miller ML, et al. Forensic discrimination of photocopy and printer toners. III. Multivariate statistics applied to scanning electron microscopy and pyrolysis gas chromatography/mass spectrometry. Analytical and Bionalytical Chemistry. 2003;376(8):1286-97.

53. Trejos T, Corzo R, Subedi K, Almirall J. Characterization of toners and inkjets by laser ablation spectrochemical methods and Scanning Electron Microscopy-Energy Dispersive X-ray Spectroscopy. Spectrochimica Acta Part B: Atomic Spectroscopy. 2014;92(0):9-22.
54. Corzo R, Subedi K, Trejos T, Almirall JR. Evaluation of the Forensic Utility of Scanning Electron Microscopy-Energy Dispersive Spectroscopy and Laser Ablation-Inductively Coupled Plasma-Mass Spectrometry for Printing Ink Examinations. Journal of Forensic Science. 2016;61(3):725-34.
55. Joseph D, Saxena A, Choudhury RK, Maind SD. Characterization of offset printing ink tagged with rare-earth taggants by X-ray emission techniques. International Journal of PIXE. 2007;17(3-4):183-91.
56. Szynkowska MI, Czerski K, Paryjczak T, Parczewski A. Ablative analysis of black and colored toners using LA-ICP-TOF-MS for the forensic discrimination of photocopy and printer toners. Surface and Interface Analysis. 2010;42(5):429-37.
57. Aginsky V. Forensic examination of slightly soluble ink pigments using thin-layer chromatography. Journal of Forensic Science. 1993;38(5):1131-3.
58. Tandon G, Jasuja OP, Sehgal VN. Thin layer chromatography analysis of photocopy toners. Forensic Science International. 1995;73(2):149-54.
59. Poon NL, Ho SS, Li CK. Differentiation of coloured inks of inkjet printer cartridges by thin layer chromatography and high performance liquid chromatography. Science and Justice. 2005;45(4):187-94.
60. Szafarska M, Wietecha-Posłuszny R, Woźniakiewicz M, Kościelniak P. Examination of colour inkjet printing inks by capillary electrophoresis. Talanta. 2011;84(5):1234-43.
61. Szafarska M, Wietecha-Posłuszny R, Woźniakiewicz M, Kościelniak P. Application of capillary electrophoresis to examination of color inkjet printing inks for forensic purposes. Forensic Science International. 2011;212(1):78-85.
62. Król M, Kula A, Wietecha-Posłuszny R, Woźniakiewicz M, Kościelniak P. Examination of black inkjet printing inks by capillary electrophoresis. Talanta. 2012;96:236-42.
63. Kula A, Krol M, Wietecha-Posluszny R, Wozniakiewicz M, Koscielniak P. Application of CE-MS to examination of black inkjet printing inks for forensic purposes. Talanta. 2014;128:92-101.
64. Gabriela Udrităioiu E, Bunaciu AA, Aboul-Enein HY, Gh. Tănase I. Infrared Spectrometry in Discriminant Analysis of Laser Printer and Photocopy Toner on Questioned Documents. Instrumentation Science and Technology. 2009;37(2):230-40.
65. Armitage S, Saywell S, Roux C, Lennard C, Greenwood P. The Analysis of Forensic Samples Using Laser Micro-Pyrolysis Gas Chromatography Mass Spectrometry. Journal of Forensic Science. 2001;46(5):1043-52.

66. Egan WJ, Galipo RC, Kochanowski BK, Morgan SL, Bartick EG, Miller ML, et al. Forensic discrimination of photocopy and printer toners. III. Multivariate statistics applied to scanning electron microscopy and pyrolysis gas chromatography/mass spectrometry. Analytical and Bioanalytical Chemistry. 2003;376(8):1286-97.
67. Almeida Assis AC, Barbosa MF, Valente Nabais JM, Custódio AF, Tropecelo P. Diamond cell Fourier transform infrared spectroscopy transmittance analysis of black toners on questioned documents. Forensic Science International. 2012;214(1):59-66.
68. Merrill RA, Bartick EG, Taylor JH, 3rd. Forensic discrimination of photocopy and printer toners I. The development of an infrared spectral library. Analytical and Bioanalytical Chemistry. 2003;376(8):1272-8.
69. Tănase IG, Gabriela Udriştioiu E, Bunaciu AA, Aboul-Enein HY. Infrared Spectroscopy in Qualitative Analysis of Laser Printer and Photocopy Toner on Questioned Documents. Instrumentation Science and Technology. 2009;37(1):30-9.
70. Heudt L, Debois D, Zimmerman TA, Kohler L, Bano F, Partouche F, et al. Raman spectroscopy and laser desorption mass spectrometry for minimal destructive forensic analysis of black and color inkjet printed documents. Forensic Science International. 2012;219(1-3):64-75.
71. de Almeida MR, Correa DN, Rocha WFC, Scafi FJO, Poppi RJ. Discrimination between authentic and counterfeit banknotes using Raman spectroscopy and PLS-DA with uncertainty estimation. Microchemical Journal. 2013;109:170-7.
72. Imperio E, Giancane G, Valli L. Spectral characterization of postage stamp printing inks by means of Raman spectroscopy. Analyst. 2015;140(5):1702-10.
73. Johnson CE, Martin P, Roberts KA, Trejos T, Corzo R, Almirall JR, et al. The Capability of Raman Microspectroscopy to Differentiate Printing Inks. Journal of Forensic Science. 2017.
74. Donnelly S, Marrero JE, Cornell T, Fowler K, Allison J. Analysis of pigmented inkjet printer inks and printed documents by laser desorption/mass spectrometry. Journal of Forensic Science. 2010;55(1):129-35.
75. Houlgrave S, LaPorte GM, Stephens JC, Wilson JL. The Classification of Inkjet Inks Using AccuTOF™DART™ (Direct Analysis in Real Time) Mass Spectrometry—A Preliminary Study. Journal of Forensic Science. 2013;58(3):813-21.
76. Williamson R, Raeva A, Almirall JR. Characterization of Printing Inks Using DART-Q-TOF-MS and Attenuated Total Reflectance (ATR) FTIR. Journal of Forensic Science. 2016;61(3):706-14.
77. Weis P. The transparent witness: forensic examination of glass evidence at the Bundeskriminalamt. Spectroscopy Europe. 2016;28:6-9.

78. Jantzi SC, Almirall JR. Elemental analysis of soils using laser ablation inductively coupled plasma mass spectrometry (LA-ICP-MS) and laser-induced breakdown spectroscopy (LIBS) with multivariate discrimination: tape mounting as an alternative to pellets for small forensic transfer specimens. Applied Spectroscopy. 2014;68(9):963-74.
79. Art T, Gary P. The Importance of Wine Label Information. International Journal of Wine Marketing. 2003;15(2):58-74.
80. Mitch F. Right Bottle, Wrong Wine. Wine Spectator. 2016 [cited 6 July 2017]. Available from: http://www.winespectator.com/webfeature/show/id/Right-Bottle-Wrong-Wine_3325.
81. Venkatachalam A, Koehler CU, Feldmann I, Lampen P, Manz A, Roos PH, et al. Detection of phosphorylated proteins blotted onto membranes using laser ablation inductively coupled plasma mass spectrometry Part 1: Optimisation of a calibration procedure. Journal of Analytical Atomic Spectrometry. 2007;22(9):1023-32.
82. Hoesl S, Neumann B, Techritz S, Linscheid M, Theuring F, Scheler C, et al. Development of a calibration and standardization procedure for LA-ICP-MS using a conventional ink-jet printer for quantification of proteins in electro- and Western-blot assays. Journal of Analytical Atomic Spectrometry. 2014;29(7):1282-91.
83. Feldmann I, Koehler CU, Roos PH, Jakubowski N. Optimisation of a laser ablation cell for detection of hetero-elements in proteins blotted onto membranes by use of inductively coupled plasma mass spectrometry. Journal of Analytical Atomic Spectrometry. 2006;21(10):1006-15.
84. Bonta M, Lohninger H, Laszlo V, Hegedus B, Limbeck A. Quantitative LA-ICP-MS imaging of platinum in chemotherapy treated human malignant pleural mesothelioma samples using printed patterns as standard. Journal of Analytical Atomic Spectrometry. 2014;29(11):2159-67.
85. Moraleja I, Esteban-Fernandez D, Lazaro A, Humanes B, Neumann B, Tejedor A, et al. Printing metal-spiked inks for LA-ICP-MS bioimaging internal standardization: comparison of the different nephrotoxic behavior of cisplatin, carboplatin, and oxaliplatin. Analytical and Bioanalytical Chemistry. 2016;408(9):2309-18.
86. Shelley JT, Ray SJ, Hieftje GM. Laser Ablation Coupled to a Flowing Atmospheric Pressure Afterglow for Ambient Mass Spectral Imaging. Analytical Chemistry. 2008;80(21):8308-13.
87. Fittschen UEA, Bings NH, Hauschild S, Förster S, Kiera AF, Karavani E, et al. Characteristics of Picoliter Droplet Dried Residues as Standards for Direct Analysis Techniques. Analytical Chemistry. 2008;80(6):1967-77.
88. McGaw EA, Szymanski DW, Smith RW. Characterization of undigested particulate material following microwave digestion of recycled document papers. Journal of Forensic Science. 2009;54(5):1171-5.

89. Fernández B, Claverie F, Pécheyran C, Donard OFX. Direct analysis of solid samples by fs-LA-ICP-MS. TrAC Trends in Analytical Chemistry. 2007;26(10):951-66.
90. Miliszkiewicz N, Walas S, Tobiasz A. Current approaches to calibration of LA-ICP-MS analysis. Journal of Analytical Atomic Spectrometry. 2015;30(2):327-38.
91. Bonta M, Limbeck A, Quarles Jr CD, Oropeza D, Russo RE, Gonzalez JJ. A metric for evaluation of the image quality of chemical maps derived from LA-ICP-MS experiments. Journal of Analytical Atomic Spectrometry. 2015;30(8):1809-15.
92. Myllys M, Häkkänen H, Korppi-Tommola J, Backfolk K, Sirviö P, Timonen J. X-ray microtomography and laser ablation in the analysis of ink distribution in coated paper. Journal of Applied Physics. 2015;117(14):144902.
93. Souguir Z, Dupont AL, de la Rie ER. Formation of brown lines in paper: characterization of cellulose degradation at the wet-dry interface. Biomacromolecules. 2008;9(9):2546-52.
94. Adel AM, Dupont A-L, Abou-Yousef H, El-Gendy A, Paris S, El-Shinnawy N. A study of wet and dry strength properties of unaged and hygrothermally aged paper sheets reinforced with biopolymer composites. Journal of Applied Polymer Science. 2014;131(18):n/a-n/a.
95. Jeong M-J, Dupont A-L, de la Rie ER. Degradation of cellulose at the wet-dry interface: I—study of the depolymerization. Cellulose. 2012;19(4):1135-47.
96. Sladkevich S, Dupont A-L, Sablier M, Seghouane D, Cole RB. Understanding paper degradation: identification of products of cellulosic paper decomposition at the wet-dry "tideline" interface using GC-MS. Analytical and Bioanalytical Chemistry. 2016;408(28):8133-47.
97. Schaffer R, Appel W, Forziati F. Reactions at Wet-Dry Interfaces on Fibrous Materials. Journal of Research of the National Bureau of Standards. 1955;54:103-6.
98. Frick DA, Gunther D. Fundamental studies on the ablation behaviour of carbon in LA-ICP-MS with respect to the suitability as internal standard. Journal of Analytical Atomic Spectrometry. 2012;27(8):1294-303.

# CHAPTER 7:

# Analysis of packaging for wine authentication:

## Part 2.2: Molecular analysis of paper and ink by Raman and Infrared spectroscopy

## 1. Introduction

Examination of suspicious documents in the forensic field plays a major role in the investigation of numerous cases involving counterfeiting and forgery. Wine labels have also been targeted by counterfeiters who relabel inferior or cheaper wines into more expensive brands. The wines most often counterfeited are those from the top French and Spanish producers, especially from highly coveted older vintages, stocks of which are nowadays limited. Some counterfeited wines have been revealed simply by noticing typographic errors in the label. Spelling mistakes, missing accent marks and font discrepancies are a strong indication of counterfeit. In addition, the paper used for the label itself should reflect the wine's age, for example, a bright label on a very old vintage is cause of suspicion. Nonetheless, the easy access to high-quality printing technology and skilled counterfeiters have led to create more sophisticated counterfeited labels that closely resemble the authentic. Therefore, the noticeable rise in wine counterfeiting combined with the *savoir faire* of forgers is causing wine collectors, sommeliers, auction houses and law enforcement to take a second look at the wine label. Consequently, chemical analysis of writing materials like paper and inks is a very important part of forensic examinations of questioned documents.

One way to analyze a document is to focus on the composition of the ink used or the materials from which documents are produced (1). With the aim of authenticating the wine without opening the bottle, the research work described in this manuscript aims to develop a new irrefutable diagnostic tool based on the direct molecular analysis of paper and printed ink on the wine label by non-invasive Raman spectroscopy and Infrared spectroscopy, which induce no visible degradation of the bottle.

Both Raman and Infrared spectroscopies are one of the most important techniques for the identification and characterization of paper. They have shown being essential analytical tools for the structural analysis of paper and pulp. The studies of cellulose, hemicellulose, lignin, thermal- and photo-induced oxidation and various chemical treatments of pulp and paper products as well as colorants have been all made possible using these forms of molecular spectroscopies (2). Raman spectroscopy has been proven to show some important advantages in the study of materials that strongly scatter light, such as cellulose and colorants. In fact, Raman spectroscopy makes it possible to identify the black inks, which is often the most difficult task (3). Raman spectroscopy is a simple, rapid, direct and non-destructive method to provide molecular information on a sample with good sensitivity and specificity. The laser beam and optical microscope allow focusing on a microscopic sample area of a few micron in diameter. The ease of use and the fact that it is not affected by the presence of water in a sample makes Raman

spectroscopy an increasingly important tool for getting information about the presence of fillers in the cellulose and the identification of used colorants (4-7). Additionally, the development of handheld and portable Raman spectrometers has radically opened the way to new innovative in-situ applications. These instruments are usually equipped with intuitive onboard software which make easier the acquisition of measurements. However, the most time-consuming task is the interpretation of Raman spectra. When the surface or sample under study is completely unknown, a previous expertise of the user is mandatory to extract correct and complete information from the spectral acquisitions. Similarly, Infrared spectroscopy is of major importance in paper characterization as it allows the identification of chemical functional groups linked with their vibrational modes. It permits to stablish the origin of fibers and the determination of the chemical composition of additives used in papermaking and the identification of impurities distributed on the surface of the paper (5). Moreover, it is a valuable tool for evaluating the ageing process of paper which is linked to the oxidation processes (presence of carbonyl and carboxyl groups on the cellulose chain) (8). Therefore, Raman and Infrared spectroscopies are two complementary and non-destructive techniques that allow fast and efficient analysis of paper and ink of doubtful documents.

In this study, the composition of several wine labels are directly analyzed by means of Raman spectroscopy and Diffuse Reflectance Infrared Fourier Transform Spectroscopy (DRIFTS) with the aim of discriminating among genuine and counterfeited labels and vintage identifying the main components of the label and black and red inks. The significance of the current study is to offer practical, easy-to-apply and robust laser-based spectrochemical methods for the molecular analysis and comparison of paper and printing inks as a means of improving the discrimination capabilities currently available in forensic laboratories. Different caseworks have been studied which comprises 42 wine bottles of controlled origin and bottles originating from the same winery but different millesime. To the authors knowledge this is the first study that evaluates the complementarity of Raman and Infrared spectroscopies for the analysis of paper and ink used in wine labels in order to assess their authenticity.

## 2. Material and methods

### 2.1 Description of the sample set

A total of 42 wine bottle samples were analyzed which include: i) 8 green bottles among which 5 are original French bottles and 3 counterfeited Chinese bottles and ii) a series of 34 green bottles belonging to the same winery which comprises the vintages from 1969 to 2010. There is not sample preparation requirement for the direct analysis of bottle samples by Raman and Infrared spectroscopy, only visually clean label surfaces were selected for analysis.

## 2.2 Instrumentation and methods

In this work two Raman spectrometers were used in order to obtain the best spectral response for each analyzed material (label and/or ink). On the one hand, a portable RA100 Raman spectrometer (Renishaw, Gloucestershire, UK) which implements a 785 nm excitation laser (diode laser) and a CCD detector (Peltier cooled) was used. The nominal laser power is 150 mW at the source. Neutral filters allow to work at 1% (5mW at source, 1mW at the sample), 10% (50 mW at source, 10 mW at the sample) or 100 % (150 mW at the source, 30 mW at the sample) of the total power. The control of the laser power was used, especially, on the analysis of pigments in order to avoid possible thermal decompositions. For the measurements, long-distance lenses of 20x and 50x (laser focus on approximately 20-150 μm spots, depending on the lens used) were employed. The microprobe has a micro-camera, which allows focusing the different grains of the matrix, and the positioning is controlled by a micrometric stage. The instrument was calibrated daily using the 520 $cm^{-1}$ silicon Raman peak. The spectra were collected with a resolution of 1 $cm^{-1}$ and they were taken in the 200-4000 $cm^{-1}$ spectral range. In those cases in which no Raman bands were detectable at highest wavenumbers, spectra were taken in shorter ranges. The integration time and accumulations were set depending on the spectral response (higher or lower signal-to-noise ratio) for each label under 5-10 s and 5-17 accumulations. All the spectra were acquired with the Renishaw WIRE 3.2 software (Renishaw, Gloucestershire, UK).

On the other hand, the second portable Raman spectrometer used was the innoRam™ Raman spectrometer ($B_{\&}WTEK_{INC.}$, Newark, EEUU) provided with a CleanLaze® technology 785 nm excitation laser (< 300 mW laser output power). The instrument implements a controller of the laser power (a scale from 0 to 100% of the total power of the laser). It also includes a two dimensional charge coupled device (CCD) to detect the dispersed Raman signal, which is Thermoelectric Cooled (TC) to -20ºC to maximize dynamic range by reducing dark current. A back-thinned CCD is used to obtain 90% quantum efficiency via collection of incoming photons at wavelengths that would not pass through a front illuminated CCD. A spectral resolution (FWHM) of 3.4 $cm^{-1}$ can be achieved with a double pass transmission optic. The spectral range of the Raman instrument is 65-2500 $cm^{-1}$. The instrument is provided with a Raman probe based on optic fibre (1.5 m of fibre length). The working distance is 5.90 mm and the measured spot size in each case was 85 μm. The probe was mounted on a video-camera (MICROBEAM S.A, Barcelona, Spain) where different objectives can be coupled to perform micro-Raman measurements. Different tests were performed with a 20x (8.8 mm working distance and 105 μm laser beam spot size) and a 50x (3.68 mm working distance and 42 mm laser beam spot size) objective lens. The spectra were acquired between 5-15 seconds and 1-20 accumulations. Spectral acquisition was performed using the BWSpec™ 3.26 software ($B_{\&}WTEK_{INC}$). With both portable Raman spectrometers the spectral data treatment was carried out using OMNIC 7.2 software.

Finally, to complement the molecular characterization, a 4100 Exoscan handheld FTIR spectrometer ($A_2$Technologies, Danbury, CT, USA, nowadays Agilent Technologies) provided with a diffuse reflectance sampling interface (DRIFT) was used. The used handheld FTIR spectrometer is designed to minimize the contribution of the specular reflection on the diffuse reflection. However, this contribution is not always avoided and a little contribution of specular reflection can be collected in the Diffuse Reflection spectra, causing the appearance of so-called Reststrahlen bands. The spectra were accumulated 128 times and the spectral range acquired was set between 4000 and 700 $cm^{-1}$. The Michaelson interferometer has a minimum resolution of 4 $cm^{-1}$. All the spectral information was saved in a PDA using the $A_2$Technologies MicroLabMobile Software™ and transferred to a PC. In this case the DRIFT spectra were also treated using OMNIC 7.2 software.

The interpretation and the assignation of the unknown spectra was carried out by comparison with the collected Raman and Infrared spectra of pure standards compounds inside the free available RUFF (9) and IRUG (10) Raman and Infrared spectral databases and with spectra collected in the e-VISART (11) and e-VISNICH (12) databases.

## Results and discussion

In this work qualitative comparative studies were carried out, which have given satisfactory results suitable for forensic document examination. Although identification of compounds is not usual, because comparison of spectra is enough to discriminate among samples, a successful attempt was carried out to identify the basic composition of label and inks. Finally, the discriminating power and complementarity of both techniques for the analysis of label paper and inks was compared in this work**.**

### 3.1 Casework 1: *in situ* and non-destructive analysis of genuine and counterfeited bottles

The first sample set analyzed in this work consist of 8 green bottles coming from the French region of Pauillac belonging to a private enterprise, divided into original (5 samples) and counterfeited (3 samples). These samples are peer- correlated (Table 1) according to their vintage and origin. Thereby, obtained results will be discussed per type of matrix (label paper and red/black ink) and peer. Figure 1 shows the augmented image (x50) of the samples under examination.

**Table 1** Peer-correlated samples used in this work.

| Peer | Sample code | Year | Origin |
|---|---|---|---|
| 1 | S205 | 2004 | France |
| | S206 | 2004 | China |
| 2 | S207 | 2005 | France |
| | S208 | 2005 | China |
| 3 | S209 | 2006 | France |
| | S210 | 2006 | France |
| 4 | S211 | 2007 | France |
| | S212 | 2007 | China |

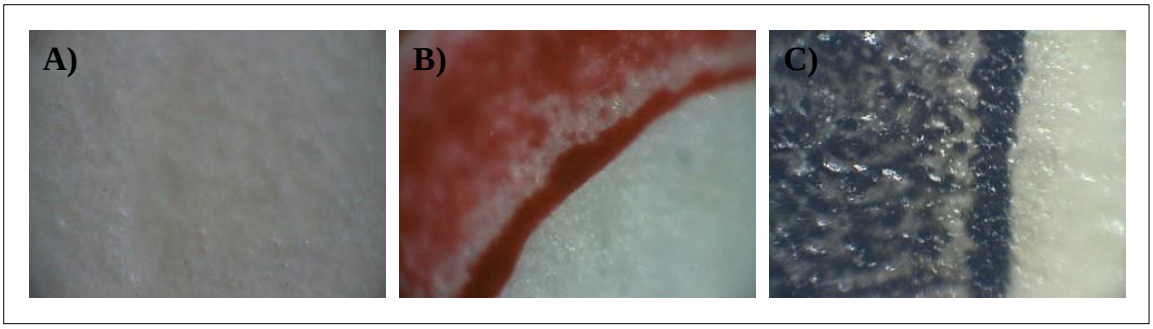


**Figure 1** Analyzed matrix: A) label matrix, B) red ink and C) black ink observed with the long-distance lens of x50 (Renishaw RA100 spectrometer, Gloucestershire, UK).

### 3.1.1 Analysis of label matrix

***Peer 1: S205 (France) vs. S206 (China)***

In order to extract representative conclusions, more than 25 Raman spectra were acquired on each label from each sample. In all the measurements repetitive Raman spectra were obtained. Thanks to that, it was possible to identify polypropylene (PP) as the main component of the label in both French and Chinese bottles (13, 14). Figure 2 shows a representative Raman spectrum of the labels from S205 and S206 samples respectively and Table 2 shows the bands of PP identified in the Raman spectra of both samples.

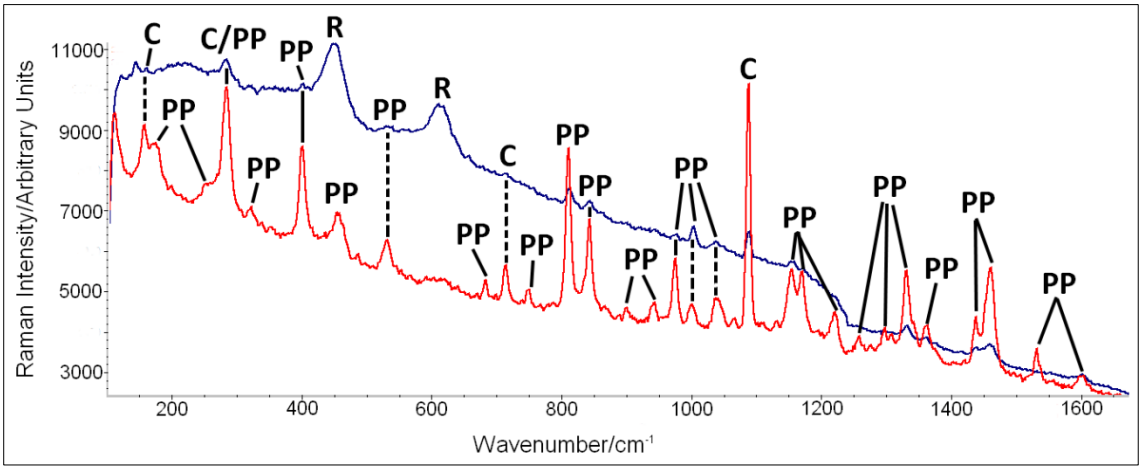


**Figure 2** Raman spectra of sample S205 (red) and S206 (blue) label. PP = Polypropylene, C = Calcite and R = Rutile.

**Table 2** Raman bands of polypropylene identified in the Raman spectra of sample S205 and S206.

| **Raman frequency ($cm^{-1}$)** |
|---|
| 110m, 155m, 172m-sh, 250w-sh, 282m, 320w, 399s, 458m, 530m, 681w, 746w 809vs, 842s, 898w, 941w, 974s, 998m, 1036m, 1152s, 1169s, 1219m, 1258w, 1297w, 1306vw, 1330s, 1360m, 1371sh, 1437m, 1460s, 1531m and 1596w |

vs= very strong, s = strong, m = medium, w = weak, v = very weak, sh = shoulder

In addition, IR spectroscopy confirmed the use of polypropylene as the main component of the label from both, S205 and S206 (Figure 3 and Table 3) and allowed the visualization of an extra band at around 1730-1736 $cm^{-1}$ corresponding to a carbonyl group (15). To extract conclusions based on DRIFTS' results, five DRIFT spectra were acquired from each label. IR spectroscopy is one of the most common methods for studying the degradation of polypropylene (16). Polypropylene is a material that is susceptible to oxidative degradation when exposed to UV radiation in the presence of air. The exact degradation mechanism depends on the condition (temperature, stress, UV light, etc.). Nonetheless, the same chemical species are involved, that is, hydroxyl (OH) groups, carbonyl (C=O) groups and unsaturated (C=C) groups. Carbonyl Index (CI) is probably the most commonly used indicator to measure the chemical oxidation of polyolefins such as polyethylene and polypropylene, and it is generally considered to reflect the degradation of the mechanical properties of these polymers. Although it is well accepted as a relevant criterion, it is often said that measurement of oxidative degradation of PP by the IR absorbance of the carbonyls is not appropriate to the early detection of the degradation (17). However, as the samples analyzed during this work have a degradation period larger than 10 years, CI seems to be an adequate parameter to take into account for the evaluation of the oxidizing process.

It is possible to observe in the spectra that the intensity of the carbonyl peak is much higher in the Chinese bottle, indicating that the polypropylene is much more oxidized. In addition, peak location at these wavelengths indicates the presence of lactones and esters in the degradation process (17, 18). The normalization of the area of the carbonyl peak against non-interfered polypropylene band (973 $cm^{-1}$) in the Chinese bottle shows an increased ratio (around 3 units) compared to the ratio obtained for the French bottle (Table 4). Moreover, it must be pointed out that from the direct visual observation of the bottles, the Chinese bottle has a more marked yellowish hue than the French bottle, which can be attributed to the higher oxidation state of the polypropylene.

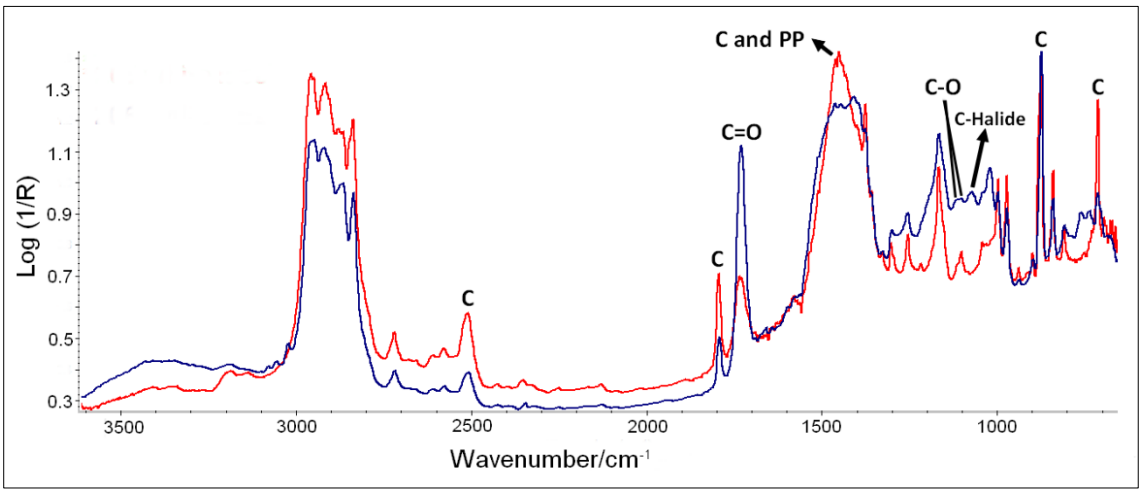


**Figure 3** DRIFT spectra of sample S205 (red) and S206 (blue) label. C=O = Carbonyl, C = Calcite, PP = Polypropylene and C-Halide = Carbon-halide bond vibration. The bands not market in the DRIFT spectra are assigned to PP.

**Table 3** IR bands of polypropylene identified in the DRIFT Raman spectra of sample S205 and S206.

| Raman frequency (cm-1) |
|---|
| 809w, 842m, 900w, 974m, 998m, 1033vw, 1104w, 1168m, 1212vw, 1256w, 1304w, 1330vw, 1358sh, 1378s, 1460s, 2583w, 2614w, 2724w, 2842vs, 2882vs, 2991vs, 2920vs and 2955vs |

vs= very strong, s = strong, m = medium, w = weak, v = very weak, sh = shoulder

**Table 4** Average areas of carbonyl band normalized against PP band for S205, S206, S207 and S208 samples.

| Sample code | Normalized average area |
|---|---|
| S205 | 3.1 ± 0.4 |
| S206 | 10.2 ± 0.8 |
| S207 | 2.2± 0.3 |
| S208 | 27.8 ± 0.8 |

Raman spectroscopy also shows bands corresponding to the mineral filler calcium carbonate (calcite, $CaCO_3$) at 282 $cm^{-1}$, 712 $cm^{-1}$ and 1086 $cm^{-1}$ both, in the French and Chinese bottles. Mineral fillers have been longer used in polymer manufacture to improve the properties and reduce the cost. Incorporating inorganic mineral fillers improves various physical properties of the thermoplastic materials such as mechanical strength, rigidity, hardness, crystallinity, dimensional stability, electrical and thermal conductivity, etc. (19). In general, the effects of a filler on the mechanical and other properties of the polymers depend strongly on its shape, particle size, aggregate size, surface characteristics and degree of dispersion (20). Calcium carbonate-filled PP composites possess very high impact strength because they are poorly bonded to the matrix which allows the formation of microscopic cavities. This leads to local microplastic deformation and an increase in the overall toughness of the composite (21, 22). In this case, the normalized ratios of the calcium carbonate (1797 $cm^{-1}$) against the non-interfered band of polypropylene (973 $cm^{-1}$) were calculated too but the difference is not significant for discrimination purposes.

Chinese bottle shows the two characteristic Raman bands of rutile ($TiO_2$) at 446 and 611 $cm^{-1}$ whereas the French bottle does not (Figure 1). Pigment grade titanium dioxide or rutile ($TiO_2$) is also used as mineral filler in polymer manufacturing for the modification of structural, elastic and thermal properties of thermoplastics (23, 24). Additionally, rutile is a widely used mineral pigment in papermaking process used as filler within the sheet and as the main component of paper coatings. Of all papermaking pigments, $TiO_2$ has the highest brightness and opacifying power, due to its unmatched high refractive index and high light scattering potential even at very low addition levels. Because of its high refractive index, $TiO_2$ is the only pigment which provides high opacity when the paper is wet, which is an extremely positive property when it comes to label paper (25). This compound is not observable in Infrared spectroscopy as its band comes up in lower wavelengths.

***Peer 2: S207 (France) vs. S208 (China)***

As for the peer S205 and S206, Raman (Figure 4) and DRIFT (Figure 5) spectroscopies determined that the main component of the label is also polypropylene. In this case, the counterfeited bottle has also a higher oxidation degree (12 units higher than the French botte), according to the calculated CI ratio, which gives a yellowish hue to Chinese label.

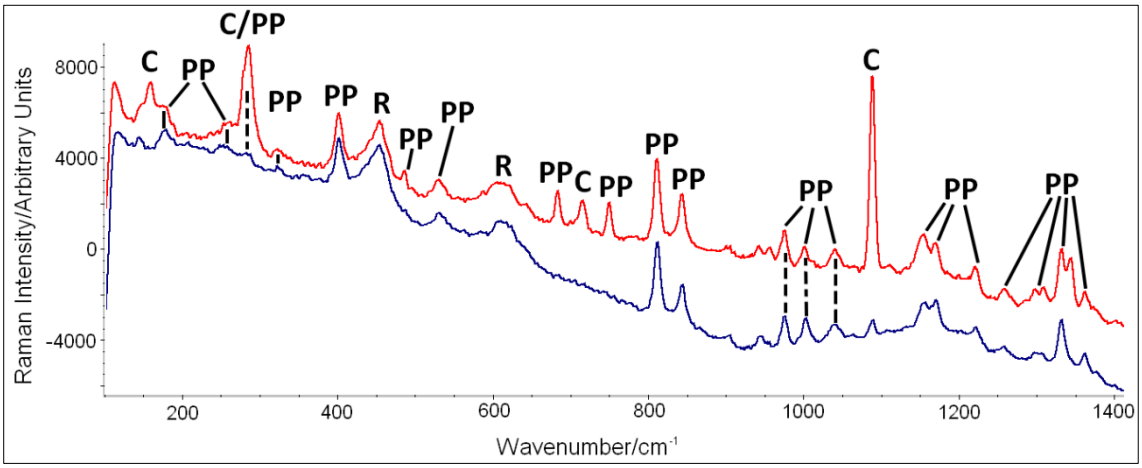


**Figure 4** Raman spectra of sample S207 (red) and S208 (blue) label. PP = Polypropylene, C = Calcite and R = Rutile.

Unlike the S207 label, the DRIFT spectra obtained from the measurements performed in the Chinese label (S208) show a carbonyl band centred at 1750 $cm^{-1}$ with a shoulder at 1720 $cm^{-1}$ (Figure 5). The movement of these bands with respect to S205 and S206 peer suggests the presence of saturated aliphatic cycles involved in the degradation process (26). To calculate the normalized areas of carbonyl against PP band at 973 $cm^{-1}$, the band at 1735 and 1750 $cm^{-1}$ together with the shoulder at 1720 $cm^{-1}$ were used in the S207 (French) and S208 (Chinese) samples respectively (Table 4).

In addition, in the DRIFT spectra of the counterfeited bottle (S208) there are some extra bands observable at 1603 and 1509 $cm^{-1}$ (C=C, aromatic), 1272 $cm^{-1}$ (C-O, phenol) and 1079 $cm^{-1}$ (C-halide) which can be assigned to the use of a halogen-containing flame retardant (Figure 5). Polypropylene is a flammable organic polymer which leads to greater fire risks. Ignition occurs spontaneously or from an external source if the concentration of volatile combustible products evolved by pyrolysis or thermo-oxidative degradation of the polymer is within the flammability limits. Due to its wholly aliphatic hydrocarbon structure, polypropylene by itself burns very rapidly with a relatively smoke-free flame and without leaving a char residue. Therefore, flame retardant formulations of polypropylene are incorporated to the polymer chain. In this case, it could be suggested that an aromatic halogen-containing retardant has been added to the label

(decabromodiphenyl oxide (DBDPO) or bis(2,3-dibromopropyl ether of tetrabromobisphenol A), for example). Due to the release of halogenated acid during decomposition, halogen-containing compounds interrupt the chain reaction of combustion by replacing the highly reactive OH and H radicals by the less reactive halogen X (27, 28).

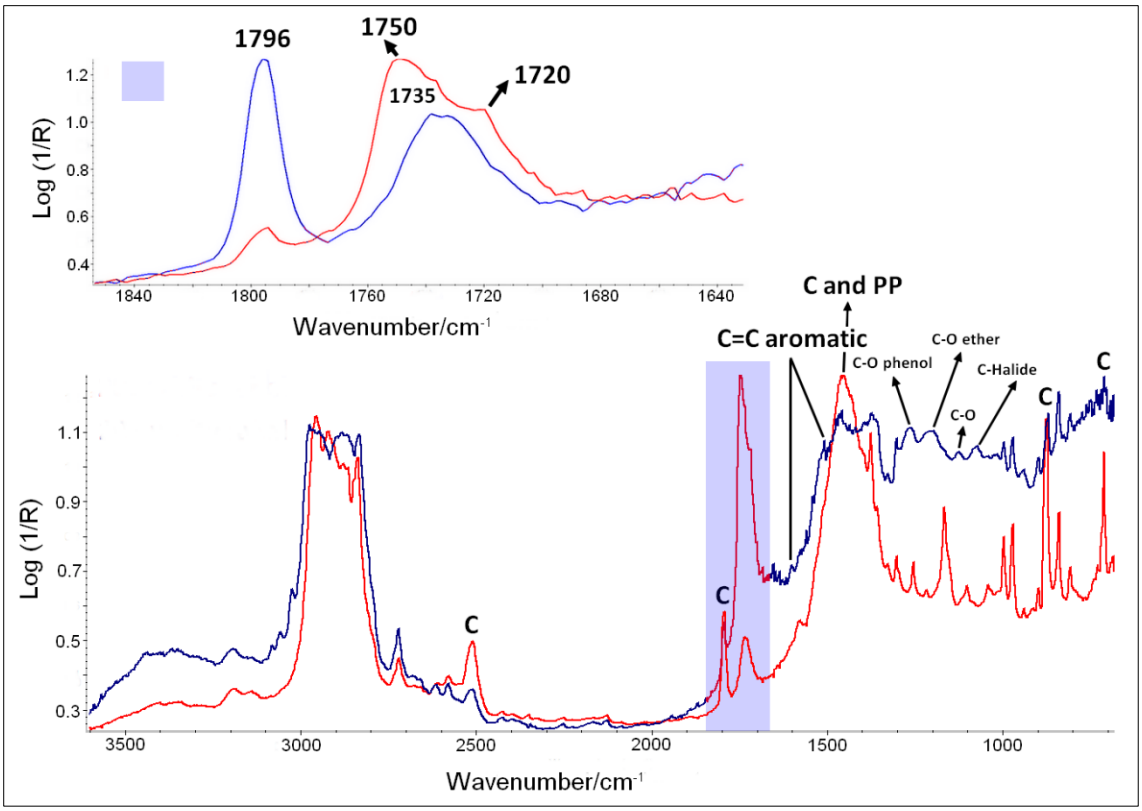


**Figure 5** DRIFT spectra of sample S207 (red) and S208 (blue) label. PP = Polypropylene, C = Calcite, aromatic C=C stretching (C=C), C-O bands and C-Halide band. The bands not market in the DRIFT spectra are assigned to PP. At the top of the Figure a zoom of the 1850-1650 $cm^{-1}$ area showing the position of calcite band at 1796 $cm^{-1}$ and C=O bands (1735 $cm^{-1}$ for S207 label and 1750 and 1720 $cm^{-1}$) are observable.

In this case, both samples show rutile ($TiO_2$) bands at 446 and 611 $cm^{-1}$ in the Raman spectra (Figure 4). Therefore, the presence of this compound could not be used as discriminator between genuine and counterfeited bottles. Similarly, the mineral filler calcium carbonate (calcite, $CaCO_3$) is also observable at 282 $cm^{-1}$, 712 $cm^{-1}$ and 1086 $cm^{-1}$ both in the genuine and counterfeited bottles too. The calculated normalized ratio of calcite using DRIFT results is not significant for discrimination purposes.

***Peer 3: S209 (France) vs. S210 (France)***

In this case both bottles are original and show same spectra both in Raman (Figure 6) and Infrared spectroscopies (Figure 7). Main label component is polypropylene filled with calcium carbonate.

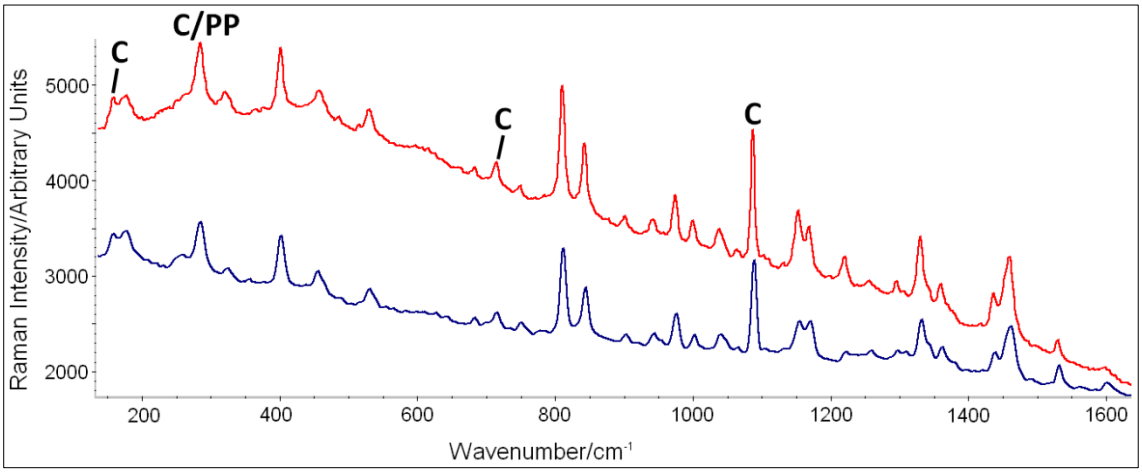


**Figure 6** Raman spectra of the label for pair S209 (red)-S210 (blue). PP = Polypropylene and C = Calcite. Bands not marked in the spectra are assigned to PP.

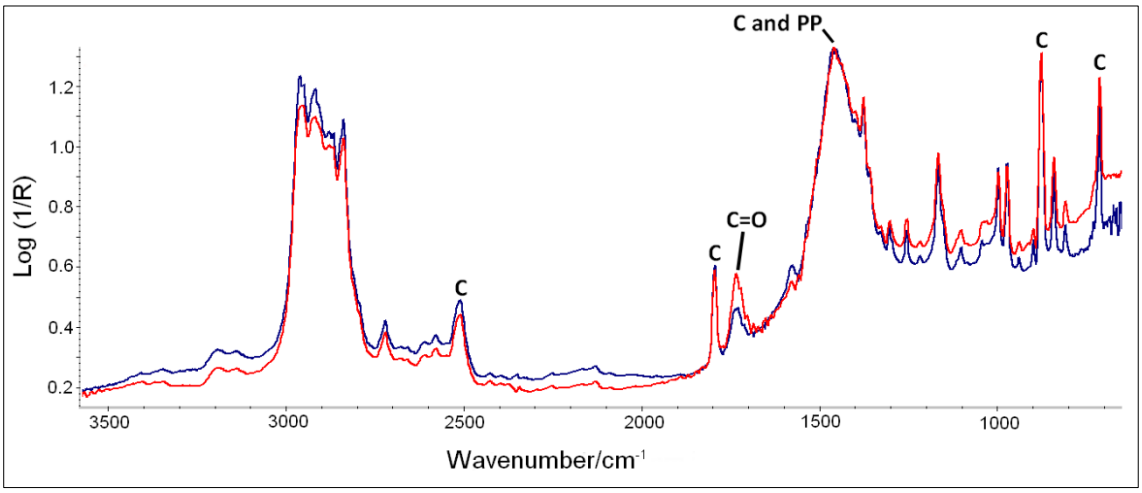


**Figure 7** DRIFT spectra of sample S209 (red) and S210 (blue) label. C=O = Carbonyl, C = Calcite, PP = Polypropylene.The bands not market in the DRIFT spectra are assigned to PP.

***Peer 4: S211 (France) vs. S212 (China)***

In this peer it was not possible to identify the presence of PP in the label of both bottles by both spectroscopic techniques. Instead of that, the presence of polystyrene (PS) was identified. The repetitive Raman spectra obtained for both type of labels show a high fluorescence. In Figure 7 a representative spectra of both labels is presented. As can be observed with this technique PS (bands at 682, 750, 1001, 1036, 1344, 1454 and 1602 $cm^{-1}$) was identified in both labels (29).

Polystyrene is similar to polypropylene, since both are saturated hydrocarbon polymers, they differ in some significant properties. In fact, even it protects against moisture and it maintains its strength and shape after long periods of time, it is not as resistant against chemicals as polypropylene. In this case, only counterfeited bottle label showed the presence of rutile ($TiO_2$) (Figure 8), being possible to differentiate Chinese label from French one using the presence or absence of this compound. As is the rest of the peers analyzed, the mineral filler calcium carbonate (calcite, $CaCO_3$) was also identified in the genuine and counterfeited bottles too (Figure 8) (30).

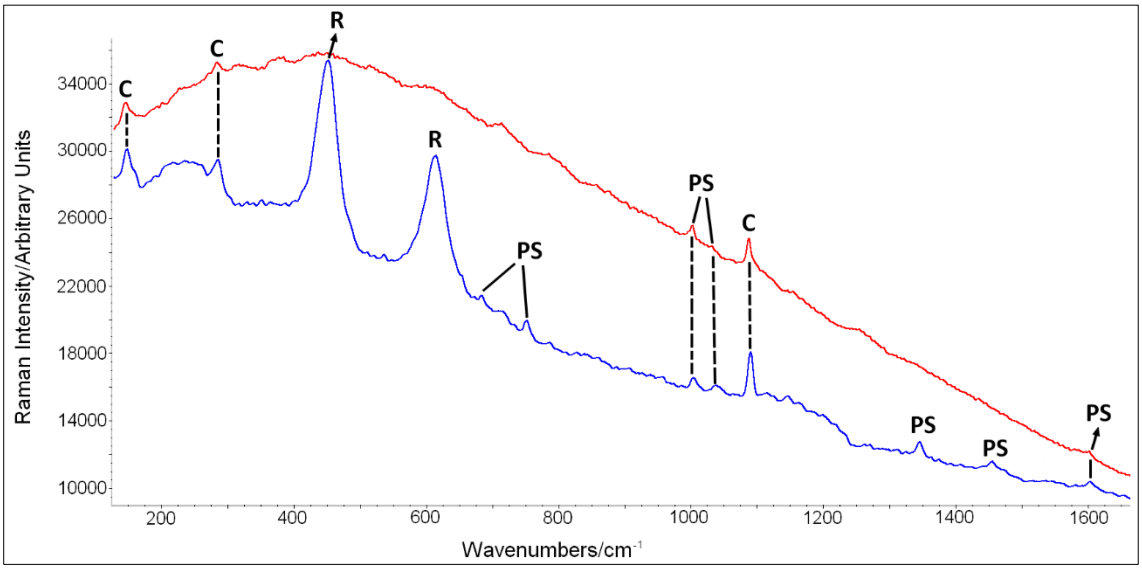


**Figure 8** Raman spectra of the label for pair S211 (red) S212 (blue). PS = Polystyrene, C = Calcite and R = Rutile.

The DRIFT analyses performed on the labels from S211 and S212 bottles showed the repetitive spectra presented in Figure 9. In this case, the bands of a possible polymer placed in the fingerprint area (1100-1700 $cm^{-1}$) are marked by the presence of clays in both labels. In spite of that, it was possible to identify the presence of aromatic C-H stretching vibrations at 3030, 2931 and 2855 $cm^{-1}$ in both labels (31), suggesting the use of a polymeric matrix in the label of the bottle. Apart from that, around 1738 $cm^{-1}$, the carbonyl band was identified in the label of both bottles which can be related to the oxidation process of the polymer. In this case, as specific bands of polystyrene have not been identify in the fingerprint region of the DRIFT spectra, it was not possible to normalize the area of C=O band to compare its signal in the S211 and S212 labels. In spite of that, it can be clearly observed (see Figure 9) that C=O band intensity/area is higher in the representative spectrum of S212.

Raman results regarding the presence of calcite in both labels were also confirmed by DRIFT. Regarding the presence of clay, kaolinite infrared bands are distinguishable in the representative

DRIFT spectra of both labels (32). This layered silicate has been added as mineral filler together with calcium carbonate. The presence of kaolinite in the label of both bottles was the responsible of the high fluorescence observed by Raman spectroscopy (Figure 8). In the representative DRIFT spectrum of S211 label, bands at 1009 and 1034 $cm^{-1}$ appear inverted in the spectrum. These bands inversion is caused by the Reststrahlen effect (33). This effect is a reflectance phenomenon in which the incident beam cannot propagate within a given medium due to change in refractive index concurrent with the specific absorbance band of the medium. As a result of this inability to propagate, Reststrahlen bands experience strong or total reflection from the medium. This effect does not only cause bands inversion, it also distorts the wavenumbers area where it takes place (1480-950 $cm^{-1}$ in this case, Figure 9) making this area of S211 label spectrum quite different to the one of S212 label. Kaolin, or china clay, is found in many parts of the world and it is an important commercial product. It is used as a mineral additive in a range of polymer composite materials. Calcined kaolin is added to polymer films to improve their infrared barrier properties. However, addition of such minerals may reduce the lifetime of the polymer films by catalyzing photo-oxidation and degradation or by inhibiting the action of stabilizer systems (34).

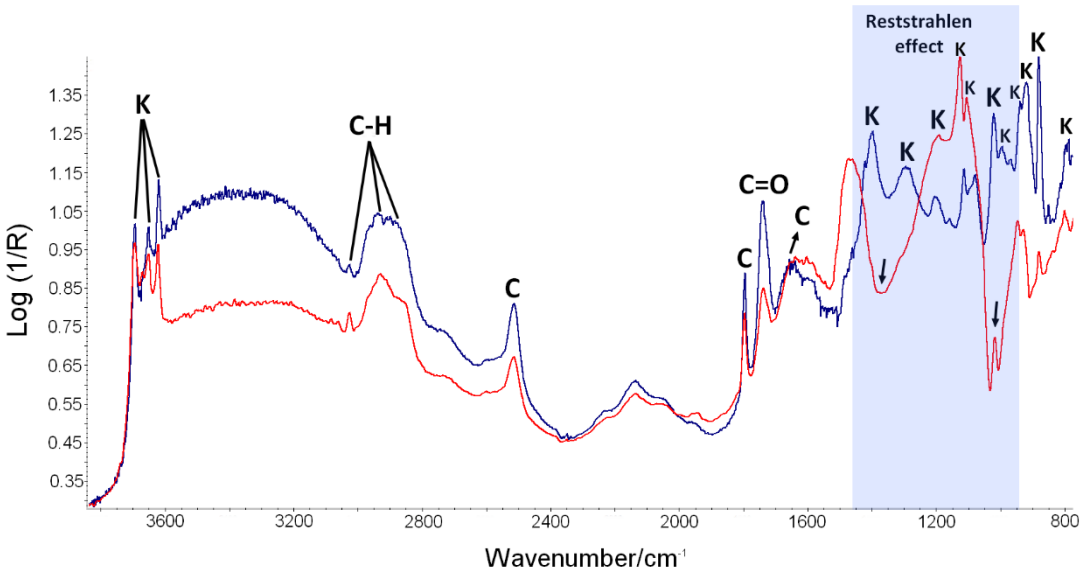


**Figure 9** DRIFT spectra of sample S211 (red) and S212 (blue) label. C=O = Carbonyl, C = Calcite, C-H = aromatic C-H stretching vibrations, PS = Polystyrene, K = Kaolinite.

### 3.1.2 Analysis of ink matrix

***Red ink***

The identification of the red pigment in Chinese and original bottles has been done based on its Raman spectra. In the red inks used in all the samples, the red mono-azo lake pigment PR57:1 was identified (Figure 10), which indicates that red ink cannot be used as discriminant label item. The azo pigments comprise the oldest and largest group of synthetic organic pigments whose use has dramatically increased in the last century. Azo pigments form a large class of synthetic compounds which are characterized by the presence of one or more azo linkage groups (-N-N-) consisting of two nitrogen atoms which are also linked to carbon atoms. In general they are structurally based on the formula Ar-N-N-R, where Ar is an aromatic or heteroaromatic group and R is either an aromatic unit or represents the function $R^1$-(C=O)-C= (C-OH)-$R^2$, where $R^1$ is an alkyl or aryl group and $R^2$ is typically –HN-Ar group (35-37). Table 5 shows the chemical structure of the azo pigment and its Raman bands (36).

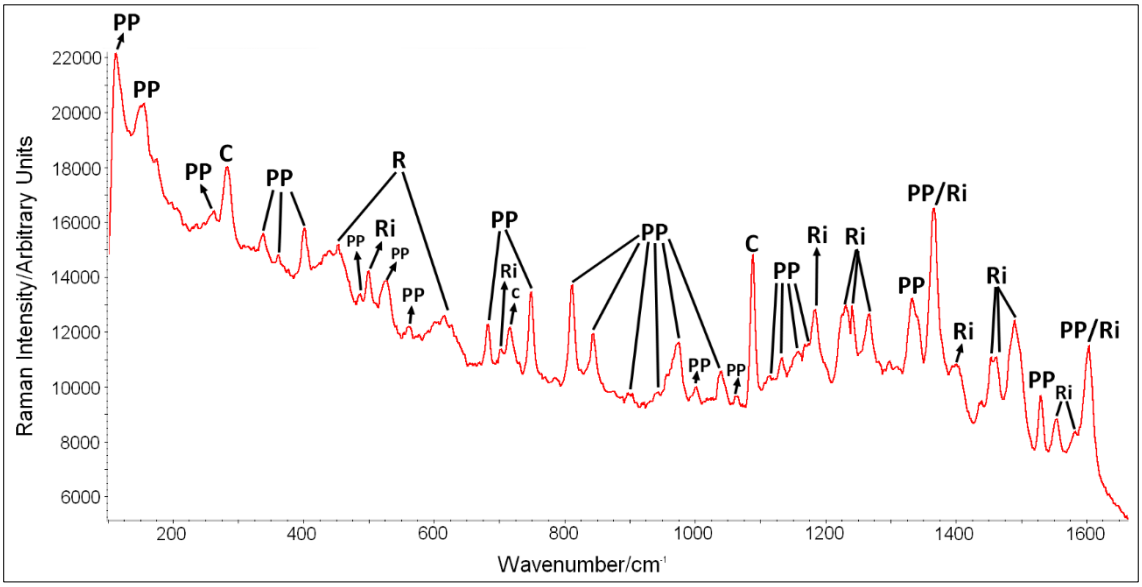


**Figure 10** Raman spectrum of red pigment of bottle S209. PP = Polypropylene, C = Calcite, R = Rutile, Ri = Red ink.

**Table 5** Chemical structure of the BON red mono-azo lake pigment PR57:1 and the identified Raman bands. Abbreviations: vs = very strong, s = strong, m = medium, w = weak, vw = very weak.

| Type of azo compound | General structure | Specific structure | Generic name/ Color Index Number/ CAS Number | Raman band wavenumbers $cm^{-1}$ (between 1800 and 100 $cm^{-1}$) |
|---|---|---|---|---|
| Azo lake pigment:<br><br>type 2-hydroxy-3-naphthoic acid pigment lakes (BON pigments) | 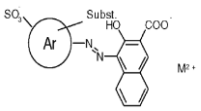 <br>**Ar** = benzene or naphtalene<br><br>**Subst** = $CH_3$, $OCH_3$, $OC_2H_5$, Cl, Br, $COO^-$ or $NO_2$<br><br>**$M^{2+}$** = $Ca^{2+}$, $Mn^{2+}$, $Ba^{2+}$,… | 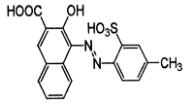 <br>$C_{18}H_{12}N_2Na_2O_6S$<br>2-Naphthalenecarboxylic acid, 3-hydroxy-4-[(4-methyl-2-sulfophenyl) azo]-, calcium salt (1:1)<br><br>**Ar** = benzene<br><br>**Subst** = $CH_3$<br><br>**$M^{2+}$** = $Ca^{2+}$ | Lithol Rubine<br>CI No. 15850.1<br>CAS No. 5281-04-09 | 500m, 701m, 1183m, 1230m, 1240m, 1266, 1365w, 1399s, 1453w, 1466w, 1490m, 1554s, 1582m and 1603s. |

Lake pigment group derive its name from 2-hydroxy-3-naphthioc acid (BON acid) which is used as the coupling component. It is a large class of azo-type pigments made by combining BON acid with diazotized amines. BON pigments were first synthesized in 1887 and although both yellow and red azo lakes can be made, it is only the red color which has any commercial significance with varying shades from red to violet. Lithol Rubine (PR 57) was produced by coupling 2-amino-5-methylbenzenesulfonic acid with BON, firstly synthesized by the chemists Richard Gley and Otto Siebert at Aktien-Gesellschaft für Anilin-Fabrikation (AGFA) in 1903. It is a calcium salt, bluish red (tint pale reddish violet) pigment with excellent brightness, color purity, tinting strength and chroma for color printing processes with aqueous inks. It has good heat stability for use in various plastics applications such as in rigid PVC, polystyrene, polypropylene and polyurethane foams (38).

### *Black ink*

According to Heudt et al., most manufacturers use the same black pigment to produce the black color and consequently, the discrimination of these inks based on the pigment is *a priori* impossible (1). Actually, the analysis of black inks is not widespread in the literature compared to blue and red inks due to the intrinsic nature of black pigments (39). Nonetheless, the identification of the pigments used in this set of bottles has been carried out based on the Raman spectra but it has been proven not to be useful for discrimination purposes. On the one hand, Cu phthalocyanine has been identified as the principal component of black pigment of the labels' ink for the bottles S205, S206, S207, S208, S209, 2S11 and S212, by comparison of the obtained experimental spectra with a Raman spectra included in e-VISART (11) and e-VISNICH (12) databases (Figure 11).

Copper phthalocyanine was first developed in 1930s. Its color ranges from blue to black and is the most commonly used organic pigment in the coatings, paint and printing inks industry due to its fastness properties, especially regarding light fastness and weather fastness (40, 41). Table 6 shows the molecular formula and observed Raman bands for the black ink of label paper of samples S205, S206, S207, S208, S209, S211 and S212.

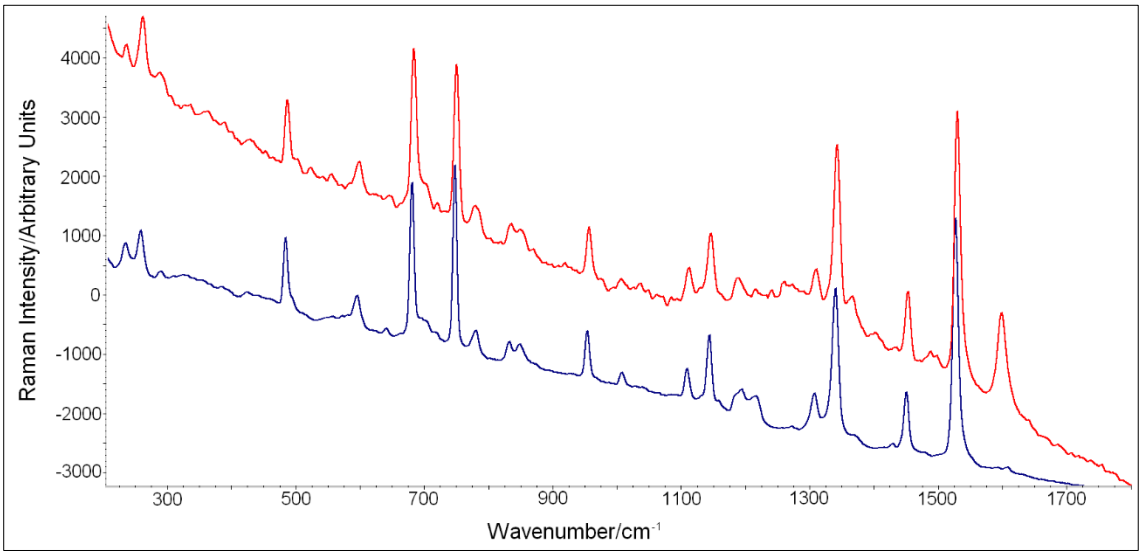


**Figure 11** Representative Raman spectrum acquired on the black pigment of bottle S211 (red) and Raman spectrum of Cu phthalocyanine blue pigment standard (blue).

**Table 6** Chemical structure of the Cu phthalocyanine pigment PB15 and the identified Raman bands. Abbreviations: vs = very strong, s = strong, m = medium, w = weak.

| Type of compound | General structure | Specific structure | Generic name/ Color Index Number/ CAS Number | Raman band wavenumbers $cm^{-1}$ (between 1800 and 100$cm^{-1}$) |
|---|---|---|---|---|
| Phthalocyanine | 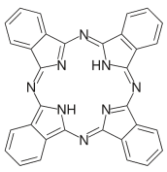 $C_{32}H_{18}N_8$ CAS No. 574-93-6 | 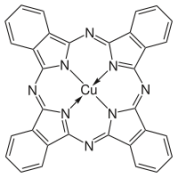 $C_{32}H_{16}CuN_8$ Copper, (29H,31H-phthalocyaninato(2-)-N29,N30,N31,N32)-, (SP-4- 1) | Cu phthalocyanine, CuPc, PB15 CI No. 74160 CAS No. 147-14-8 | 234m, 257m, 288vw, 421vw, 483s, 594m,639w, 680vs, 702w-sh, 747vs, 779m, 831m, 847m, 953m, 1006w, 1108m, 1143s, 1193m, 1216m, 1272vw, 1307m, 1340vs, 1428w, 1450m, 1487w, 1497w, 1527vs, and 1607vw |

For the bottle S210, ultramarine blue has been identified in the black ink of label paper by comparison of the obtained spectra with an internal laboratory standard (11, 12) (Figure 12).

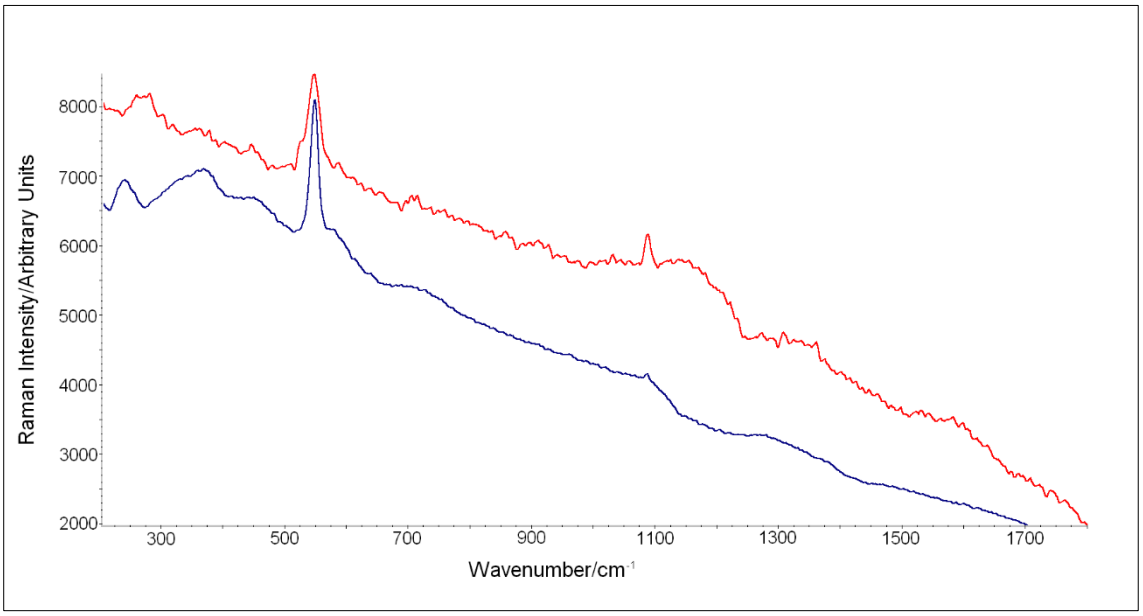


**Figure 12** Representative Raman spectrum acquired on black pigment of bottle S210 (red) and Raman spectrum of ultramarine blue pigment standard (blue).

The sulfur containing aluminosilicate mineral lazurite, called lapis lazuli, is prized as a valuable semi-precious gem for the production of the brilliant blue ultramarine pigment. Lapis lazuli mines in the Badakhshan region of Afghanistan have been exploited since ancient times due to the high purity of the extracted mineral. In the 13th century, the method used to prepare ultramarine pigment was based on the mixture of powdered lapis lazuli with wax, resin and oils. Then the mixture was kneaked in a diluted lye solution which allowed the blue particles to disperse into the alkaline water while the extraneous minerals, such as calcite, pyrite and silicates, were retained in the putty. This time consuming process was responsible for varying shades of blue. In European countries, the stone itself has been widely used in its powdered form up to the thirteenth century. However, the natural pigment began to decline in popularity in the early decades of the nineteenth century due to the industrial production of the less expensive artificial pigment ultramarine blue, whose hue can be modulated by changing the ratio of the species it contains, or by adding different impurities. Nowadays, ultramarine blue is used as a pigment in paints, wallpaper, soap, textile printing and laundry bluing agents. Both natural and synthetic ultramarines are aluminosilicates sodalites that contain anion radicals encapsulated inside the $\beta$-cages. The sulfur anion radicals combined with sodium cations behave as chromophores. The blue color in the ultramarine is caused by the unpaired electron in the sulfur radical anions $S^{-3}$ (42-44). Table 7 shows the molecular formula and observed Raman bands for the black ink of label paper of sample S210.

**Table 7** Chemical structure of the ultramarine blue pigment PB29 and the identified Raman bands. Abbreviations: s = strong, m = medium.

| Type of compound | Specific structure | Generic name/ Color Index Number/ CAS Number | Raman band wavenumbers $cm^{-1}$ (between 1800 and 100 $cm^{-1}$) |
|---|---|---|---|
| Lapis lazuli | 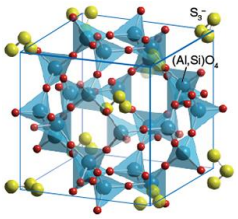  $Na_6Al_4Si_6S_4O_{20}$ | Ultramarine blue PB29 CI No. 77007 CAS No. 57455-37-5 | 549s and 1090m |

### 3.2 Casework 2: *in situ* and non-destructive analysis of a bottle series from same winery

The second sample set comprises 34 *bordelaise* bottles belonging to a French Château and which are classified according to their vintage: *60s* (1969), *70s* (1973, 1974, 1978, 1979), *80s* (1981, 1982, 1983, 1984, 1985, 1986, 1987, 1988, 1989), *90s* (1990, 1992, 1993, 1994, 1995, 1996, 1997, 1998, 1999), *00s* (2000, 2001, 2002, 2003, 2004, 2005, 2006, 2007, 2008, 2009) and *10s* (2010). For these samples analysis the same procedure was followed as for the previous sample batch.

#### 3.2.1 Analysis of label matrix

According to the Raman analysis, the main component of label matrix has changed and evolved over years, showing a composition change from 2007 onwards. Cellulose seems to be the principal component of the label paper from 1969 to 2006 and it has been after replaced by polystyrene (PS) (45) for the last four years. The Raman spectra of the earliest paper labels show a broad fluorescence which mask any band and makes difficult its assignation to cellulose. This could be attributed to the presence of poly-electronic conjugated compounds, indicating an advanced state of oxidation (46). Figure 13 shows the a representative Raman spectrum acquired on the labels of 1969, 1974 and 1998 bottles showing the characteristic bands of cellulose (Raman bands in Table 8, (47)). Even 1969 sample has great fluorescence background which does not allow band assignation, the spectrum background remains similar in all of them.

**Figure 13** Representative Raman spectra of label of vintages 1969 in blue (oxidized cellulose), 1974 in red (partially oxidized cellulose) and 1998 in green (non-oxidized cellulose).

**Table 8** Raman bands of cellulose identified in the spectra acquired from the sample 1998. Bands have been assigned according to the work carried out by Willey and Atalla.

| **Raman frequency ($cm^{-1}$)** |
|---|
| 385s, 439m, 462w, 510 m, 1097s, 1117w-sh, 1123s, 1342m, 1384m |

s = strong, m = medium, w = weak, vw = very weak, sh = shoulder

Polystyrene (PS) , which is the main label component of the last four vintages (48), is one of the most widely used classes of polymers with relative low cost, but its mechanical properties such as low toughness, weather resistance and environmental stress cracking resistance are poor compared to engineering polymers. Polymer/inorganic nanocomposites are known for the tremendous potential in improving polymer properties (49).

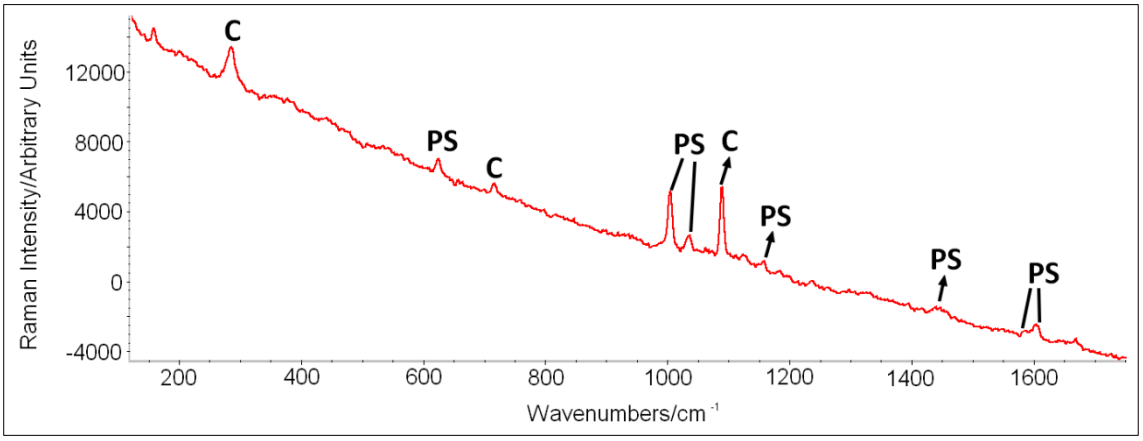


**Figure 14** Representative Raman spectrum of calcium carbonate (C) filled polystyrene (PS) label of the 2009 vintage.

Figure 14 shows the Raman spectra of calcium carbonate filled polystyrene label whose bands are located at 624 $cm^{-1}$ (m), 1003 $cm^{-1}$ (s), 1035 $cm^{-1}$ (m), 1156 $cm^{-1}$ (m), 1447 $cm^{-1}$ (w), 1583 $cm^{-1}$ (w) and 1602 $cm^{-1}$ (m) for the bottle belonging to the 2009 vintage (50, 51). Despite its dimensional stability, opacity and barrier properties, polystyrene is reinforced by filling with mineral particles of calcium carbonate (Raman bands at 282 $cm^{-1}$, 712 $cm^{-1}$ and 1086 $cm^{-1}$) (52).

### 3.2.2 Analysis of ink matrix

***Red ink***

Regarding the red ink of the label, according to the Raman analysis, the pigment employed for label printing has been continuously modified, being able to stablish four different groups which are the followings (Figures 15 and 16): 1) the first group corresponds to the 1969, 1973 and 1974 vintages, 2) the second group includes 1978, 1979, 1981, 1982, 1983, 1984, 1985, 1986, 1987, 1988, 1989, 1990, 1992, 1993, 1994, 1995, 1996, 1997, 1998 and 1999 vintages, 3) the third group comprises the vintages from 2000, 2001, 2002, 2003, 2004, 2005, 2006, 2007, 2008 and 2009 and 4) last group is only composed by the 2010 vintage. Therefore, the identification of the red pigment used in a suspect sample label could be useful to classify it in a determined period of time, which can match to what is determined in the label (authentic) or not (forgery).

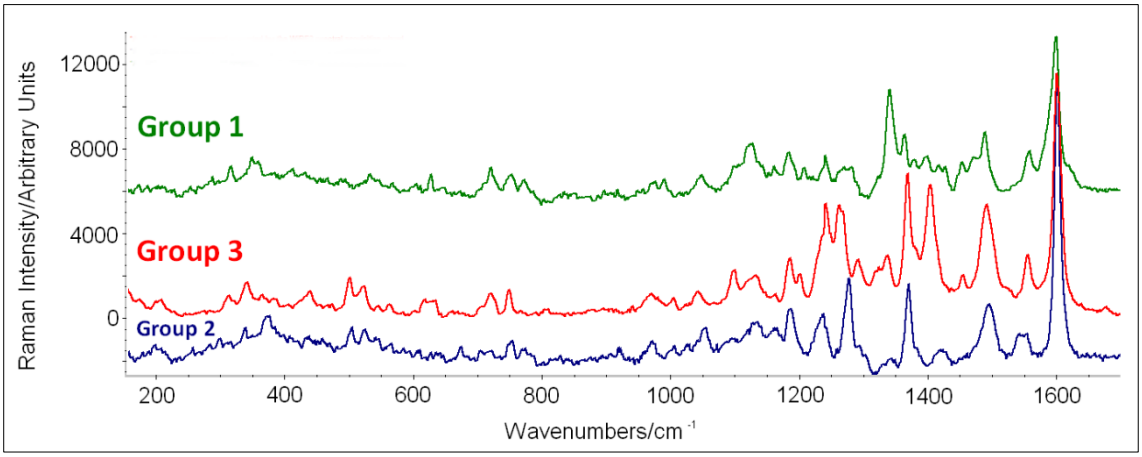


**Figure 15** Representative Raman spectra of red inks from groups 1 (sample 1969), 2 (sample 1993) and 3 (sample 2004).

The azo pigment PR112 (CI 12370, CAS No. 6535-46-2) has been identified as a possible candidate for the pigment present in the red ink of the first group of samples (Table 9). However, the assignation of the pigment to this concrete compound is not definitive as the relative intensity of the experimentally obtained Raman bands is much higher than the intensity shown in the literature (37).

**Table 9** Chemical structure of the Napthol AS pigment PR112 and the identified Raman bands. Abbreviations: s = strong, m = medium, w = weak.

| Type of compound | General structure | Specific structure | Generic name/ Color Index Number/ CAS Number | Raman band wavenumbers $cm^{-1}$ (between 1800 and 100 $cm^{-1}$) |
|---|---|---|---|---|
| Napthol AS pigment | 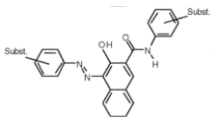 **Subst** = $CH_3$, $OCH_3$, $OC_2H_5$, Cl, Br, $NO_2$, $NHOCH_3$, $COOCH_3$, $CONHC_6H_5$ | 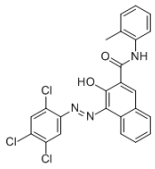 $C_{24}H_{16}Cl_3N_3O_2$ 3-hydroxy-n-(2-methylphenyl)-4-((2,4,5-trichlorophenyl)azo)naphthalene-2-carboxamide;3-hydroxy-N-(o-tolyl)-4-[(2,4,5-trichlorophenyl)azo]naphthalene-2-carboxamide | Pigment Red 112, PR112 CI No. 12370 CAS No. 6335-45-2 | 315m, 349m, 357m, 718m, 752m, 773m, 1183m, 1241m, 1341s, 1365m, 1379w, 1397w, 1416w, 1426w, 1452w, 1469w, 1487m,1558m, 1598s |

For the second group of samples, the pigment PR 57:1 has been identified. This pigment has already been characterized in the red ink of the previous casework bottles (Table 5).

The red pigment employed in the third group of samples corresponds to a B-naphthol lake mono-azo red pigment (PR53:1) (37) (Table 10). B-naphthol lake pigments are monoazo compounds, which contain sulfo and/or carboxy groups, derived from 2-naphthol as coupling component. They are characterized by good fastness to light and weather resistance and their own shades from yellowish to very bluish reds (35, 53). Due to its high tinting strength and solvent fastness, the pigment is used on a large scale in printing processes. It was also approved for cosmetic use in the 1970s as permitted coloring agent for drugs and cosmetics. However, its application use was prohibited in 1988 in the US and in 1992 in the EU based on concerns about the safety of the compound because its carcinogenetic risk (54).

**Table 10** Chemical structure of the B-Naphthol lake red pigment PR53:1 and the identified Raman bands. Abbreviations: vs = very strong, s = strong, m = medium, w = weak, vw = very, sh = shoulder.

| Type of compound | General structure | Specific structure | Generic name/ Color Index Number/ CAS Number | Raman band wavenumbers $cm^{-1}$ (between 1800 and 100 $cm^{-1}$) |
|---|---|---|---|---|
| B-naphthol lake | 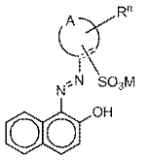 <br>**Ar** = benzene or naphtalene<br>**Subst** = $CH_3$, $OCH_3$, $OC_2H_5$<br>**M** = Alkaline earth metal | 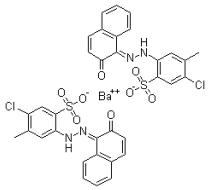 <br>$C_{34}H_{24}BaCl_2N_4O_8S_2$<br>Benzenesulfonic acid, 5-chlro-2-((2-hydroxy-1-naphthalenyl)azo)-4-methyl-, barium salt | Pigment Red 53, Barium salt<br>PR53:1<br>CI No. 15585:1<br>CAS No. 5160-02-01 | 312w, 340w, 365w, 501m, 523m, 544w, 561w, 615m, 718m, 750m, 971w, 1041w, 1186m, 1201m, 1240s, 1263s, 1293m, 1338m, 1369s, 1404s,1454 m, 1492s, 1555m and 1601vs |

In the latter group of samples, iron phthalocyanine (FePc) (Iron (II) phthalocyanine, CAS No. 132-15-1) has been identified as the responsible pigment of the red color of the ink, with Raman bands centered around 680 $cm^{-1}$ (m), 732 $cm^{-1}$ (w), 759 $cm^{-1}$ (m), 1150 $cm^{-1}$ (vw, br) 1209 $cm^{-1}$ (w) 1320 $cm^{-1}$ (w) and 1536 $cm^{-1}$ (m) (55) (Figure 16). Phthalocyanines general molecular formula is described in Table 6. Thus, the same chromophore is involved but the color properties are different, determined by the substituents present in the structure, as in this case an iron atom is located in the molecule. For this substance, it has not been possible to attribute any Color Index (CI) number. It must be point out that the configuration of the phthalocyanines metal complexes shows different polymorphic modifications which can slightly affect the position and the relative intensity of the Raman bands, making difficult the identification of the exact polymorph according to the Raman standard available in the literature (56).

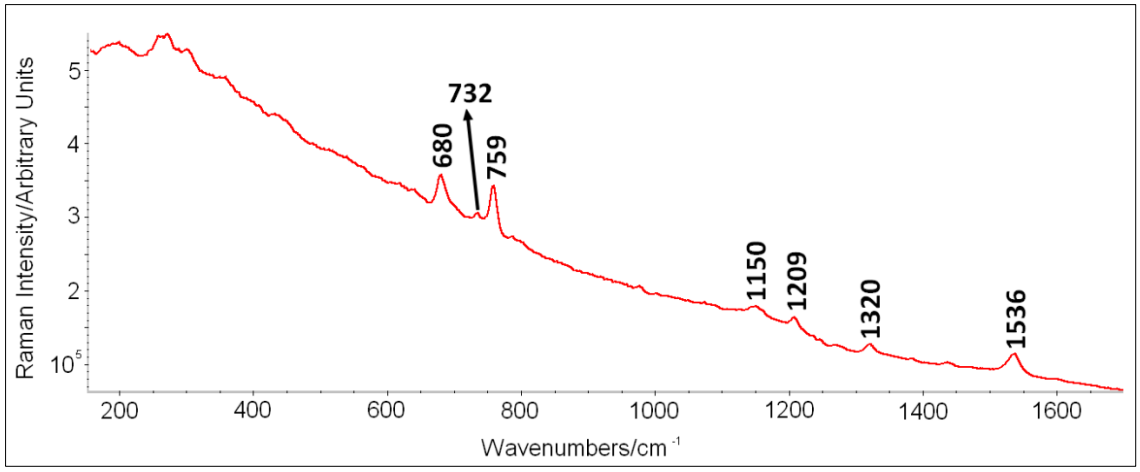


**Figure 16** Representative Raman spectrum of red ink from group 4 (2010 vintage).

## 4. Conclusion

The objective of the present work was to develop a novel method for the qualitative molecular analysis of packaging that would provide complementary information to elementary analysis carried out by fsLA-ICPMS. Therefore, the composition of several wine labels were directly analyzed by means of non-destructive Raman spectroscopy and Diffuse Reflectance Infrared Fourier Transform Spectroscopy (DRIFT) in order to identify the main components of the label and the inks (black and red) used with the aim of discriminating among genuine and counterfeited labels and among vintage. Thus, taking into account the previously stated objectives and in compliance with the results derived from this study, the following conclusions are subtracted:

1. Regarding the samples belonging to the first casework, it must be highlighted that there are subtle dissimilarities between authentic and counterfeited bottles. In fact, the main component of the label and the inks (red and black) are identical both for the genuine bottles and for the falsified ones: i) polypropylene (PP) has been identified as the main component of label for the first 3 pairs, whereas polystyrene (PS) is the main component of the most recent pair, ii) the same azo red pigment (PR57:1) has been employed in all the samples and iii) copper phthalocyanine has been identified in the black pigment with the exception of sample S210, in which ultramarine blue has been detected. Therefore, it can be concluded that from a molecular point of view, none of the pigments could be useful for discrimination purposes. However, subtle differences allow the discrimination among the samples if the composition of label is considered. On the one hand, Chinese bottles tend to have an increase amount of titanium oxide in comparison with French bottles, which has been intentionally added for the bleaching of the label. On the other hand, the oxidation rate of the polymer is significantly higher in the counterfeited labels, which is also a visually striking fact due to their yellowish hue. This fact has been attributed to the use of lesser quality manufacturing materials with a greater ease to oxidize.

2. In respect of the series of 34 bottles belonging to the same wine cellar comprising the vintages from 1969 to 2010, two different groups can be distinguished according to the label main component. Cellulose has been found to be the major compound of the label from the years 1969 to 2006, which has been replaced by PS from 2007 to 2010. In addition, the cellulose of the older labels reported an increased oxidation level. Therefore, this assessment could provide an indication of the approximate manufacturing date although it could not be conclusive. With regard to the inks, three different red pigments have been identified (PR57:1, PR53:1 and

FePc), showing an evolutive process from the ancient bottles to the newest ones that could be a valuable tool for a rough estimation of the date of manufacture.

3. Raman spectroscopy and Infrared spectroscopy have been conjointly employed for the identification of the main components of both label paper and inks, showing a great complementarity for the stated purpose. For example, the identification of the PS could not have been possible based only on Infrared spectroscopy in the pair S211-S12 due to the masking effect that kaolinite bands exert on the fingerprint region were PS bands appear.However, it offers enough information to conclude that it is a polymeric material. Therefore, even if the Raman spectra of the sample S211 has high fluorescence, the identified bands together with the information given by IR allow to confirm that the main label matrix component is PS.

The overall conclusions need to highlight how the current study offers a new practical, easy-to-apply and robust method, by the use of complementary Raman and Infrared spectroscopies, for the molecular analysis of paper and printing inks, with the aim of comparing and discriminating between different sources and date of manufacture. Despite the limited number of samples, mainly due to their uniqueness, the developed method has been applied to two different caseworks comprising 42 wine bottles of controlled origin and bottles originating from the same winery but different millesime, yielding promising results and, thereby clearing the way to further investigations in this topic.

## 5. Bibliography


1. Heudt L, Debois D, Zimmerman TA, Kohler L, Bano F, Partouche F, et al. Raman spectroscopy and laser desorption mass spectrometry for minimal destructive forensic analysis of black and color inkjet printed documents. Forensic Science International. 2012;219(1-3):64-75.
2. Aboul-Enein Y, Bunaciu AA, UdriŞTioiu FM, Tanase IG. Application of Micro-Raman and FT - IR Spectroscopy in Forensic Analysis of Questioned Documents. Gazi University Journal of Science. 2012;25(2).
3. Zięba-Palus J, Trzcińska BM. Establishing of Chemical Composition of Printing Ink. Journal of Forensic Science. 2011;56(3):819-21.
4. Schimid T, Schafer N, Abou-Ras D. Raman microspectroscopy provides access to compositional and microstructural details of polycrystalline materials. Spectroscopy Europe. 2016.
5. Workman JJ. Infrared and Raman Spectroscopy in paper and pulp analysis. Applied Spectroscopy Reviews. 2001;36(2-3):139-68.
6. Zięba-Palus J, Wesełucha-Birczyńska A, Trzcińska B, Kowalski R, Moskal P. Analysis of degraded papers by infrared and Raman spectroscopy for forensic purposes. Journal of Molecular Structure. 2017;1140:154-62.
7. Łojewska J, Rabin I, Pawcenis D, Bagniuk J, Aksamit-Koperska MA, Sitarz M, et al. Recognizing ancient papyri by a combination of spectroscopic, diffractional and chromatographic analytical tools. Scientific Reports. 2017;7:46236.
8. Manso M, Carvalho ML. Application of spectroscopic techniques for the study of paper documents: A survey. Spectrochimica Acta Part B: Atomic Spectroscopy. 2009;64(6):482-90.
9. RUFF™ Integrated database of Raman spectra, X-ray diffraction and chemistry data for minerals.Lafuente B, Downs R T, Yang H, Stone N. The power of databases: the RRUFF project. In: Highlights in Mineralogical Crystallography, T Armbruster and R M Danisi, eds. Berlin, Germany, W. De Gruyter; 2015. pp 1-30.
10. Price, Beth A., and Boris Pretzel, eds. Infrared and Raman Users Group Spectral Database. 2007 ed. Vol. 1 and 2. Philadelphia: IRUG, 2009. Infrared and Raman Users Group Spectral Database. Web. 20 June 2014. www.irug.org.
11. Castro K, Pérez-Alonso M, Rodríguez-Laso MD, Fernández LA, Madariaga JM. On-line FT-Raman and dispersive Raman spectra database of artists' materials (e-VISART database). Analytical and Bioanalytical Chemistry. 2005;382(2):248-58.
12. Maguregui M, Prieto-Taboada N, Trebolazabala J, Goienaga N, Arrieta N, Aramendia J, Gomez-Nubla L, Sarmiento A, Olivares M, Carrero JA, Martinez-Arkarazo I, Castro

K, Arana G, Olazabal MA, Fernandez LA and Madariaga JM. Dispersive Raman spectra database of original and decayed materials belonging to the Natural, Industrial and Cultural Heritage (e-VISNICH database), 1st International Congress on Chemistry for Cultural Heritage, ChemCH , Ravenna (Italy), 2010.

13. Indianapolis Museum of Art. "RSR00021 Polypropylene (PP)". Ed. Beth A. Price and Boris Pretzel. Infrared and Raman Users Group Spectral Database. Infrared and Raman Users Group, 2007. Web: www.irug.org.
14. Andreassen E. Infrared and Raman spectroscopy of polypropylene. In: Polypropylene: An A-Z reference. Dordrecht:Springer Netherlands; 1999. p. 320-328.
15. Philadelphia Museum of Art. "ISR00051 Polypropylene (PP)". Ed. Beth A. Price and Boris Pretzel. Infrared and Raman Users Group Spectral Database. Infrared and Raman Users Group, 2007. Web: www. irug .org.
16. Blais P, Carlsson DJ, Wiles DM. Surface changes during polypropylene photo-oxidation: A study by infrared spectroscopy and electron microscopy. Journal of Polymer Science Part A-1: Polymer Chemistry. 1972;10(4):1077-92.
17. Rouillon C, Bussiere PO, Desnoux E, Collin S, Vial C, Therias S, et al. Is carbonyl index a quantitative probe to monitor polypropylene photodegradation? Polymer Degradation and Stability. 2016;128:200-8.
18. García-Montelongo XL, Martínez-de la Cruz A, Vázquez-Rodríguez S, Torres-Martínez LM. Photo-oxidative degradation of TiO2/polypropylene films. Materials Research Bulletin. 2014;51:56-62.
19. Leong YW, Ishak ZAM, Ariffin A. Mechanical and thermal properties of talc and calcium carbonate filled polypropylene hybrid composites. Journal of Applied Polymer Science. 2004;91(5):3327-36.
20. Chan C-M, Wu J, Li J-X, Cheung Y-K. Polypropylene/calcium carbonate nanocomposites. Polymer. 2002;43(10):2981-92.
21. Zuiderduin WCJ, Westzaan C, Huétink J, Gaymans RJ. Toughening of polypropylene with calcium carbonate particles. Polymer. 2003;44(1):261-75.
22. Leong YW, Abu Bakar MB, Ishak ZAM, Ariffin A, Pukanszky B. Comparison of the mechanical properties and interfacial interactions between talc, kaolin, and calcium carbonate filled polypropylene composites. Journal of Applied Polymer Science. 2004;91(5):3315-26.
23. Burke M, Young RJ, Stanford JL. The relationship between structure and properties in titanium dioxide filled polypropylene. Polymer Bulletin. 1993;30(3):361-8.

24. Bhuiyan AH, Mina MF, Seema S, Khan MM, Rahman MJ, Gafur MA. Structural, elastic and thermal properties of titanium dioxide filled isotactic polypropylene. Journal of Polymer Research. 2011;18(5):1073-9.
25. Bajpai P. Pulp and Paper Chemicals. In: Pulp and paper industry. Amsterdam: Elsevier; 2015. p. 25-273.
26. Singh B, Sharma N. Mechanistic implications of plastic degradation. Polymer Degradation and Stability. 2008;93(3):561-84.
27. Bourbigot S, Bras M, Delobel R. Flame-retardant polypropylene compositions. In: Polypropylene: An A-Z reference. Dordrecht:Springer Netherlands; 1999. p. 254-263.
28. Zhang S, Horrocks AR. A review of flame retardant polypropylene fibres. Progress in Polymer Science. 2003;28(11):1517-38.
29. González-Rodríguez J, Sissons N, Robinson S. Fire debris analysis by Raman spectroscopy and chemometrics. Journal of Analytical and Applied Pyrolysis. 2011;91(1):210-8.
30. Wypych G. Physical properties of filler and filled materials. In: Handbook of Fillers (Fourth Edition). ChemTec Publishing. 2016. p. 303-371.
31. Noda I, Dowrey AE, Marcott C. Two dimensional Infrared (2D IR) Spectroscopy. In: Modern Polymer Spectroscopy. Wiley-VCH Verlag GmbH. 1999. p. 1-32.
32. Guessoum M, Nekkaa S, Fenouillot-Rimlinger F, Haddaoui N. Effects of Kaolin Surface Treatments on the Thermomechanical Properties and on the Degradation of Polypropylene. International Journal of Polymer Science. vol. 2012.
33. Arrizabalaga I, Gomez-Laserna O, Carrero JA, Bustamante J, Rodriguez A, Arana G, et al. Diffuse reflectance FTIR database for the interpretation of the spectra obtained with a handheld device on built heritage materials. Analytical Methods. 2015;7(3):1061-70.
34. Ansari DM, Price GJ. Chromatographic estimation of filler surface energies and correlation with photodegradation of kaolin filled polyethylene. Polymer. 2004;45(6):1823-31.
35. Bamfield P. Phenomena Involving the Absorption and Reflectance of Light. In: Chromic Phenomena: Technological Applications of Colour Chemistry. The Royal Society of Chemistry; 2010. p. 141-233.
36. Vandenabeele P, Moens L, Edwards H, Dams R. Raman spectroscopic database of azo pigments and application to modern art studies. Journal of Raman Spectrometry. 2000;31:509-17.
37. Scherrer NC, Stefan Z, Francoise D, Annette F, Renate K. Synthetic organic pigments of the 20th and 21st century relevant to artist's paints: Raman spectra reference collection. Spectrochimica Acta Part A: Molecular and Biomolecular Spectroscopy. 2009;73(3):505-24.

38. de Keijzer M. The Delight of Modern Organic Pigment Creations. In: Issues in Contemporary Oil Paint. Cham:Springer International Publishing; 2014. p. 45-73.
39. Papson K, Stachura S, Boralsky L, Allison J. Identification of colorants in pigmented pen inks by laser desorption mass spectrometry. Journal of Forensic Science. 2008;53(1):100-6.
40. Loebbert Gerd. Phthalocyanine Compounds. In: Kirk-Othmer Encyclopedia of Chemical Technology. John Wiley & Sons, Inc. 2000.
41. Erk P, Hengelsber H. Phthalocyanine Dyes and Pigments. In: The Porphyrin Handbook. Amsterdan:Academic Press; 2003. p. 105-149.
42. Seel F. Sulfur in Artwork: Lapiz Lazuli and Ultramarine pigments, In: Sulfur, its Significance for Chemistry, for the Geo-, Bio-, and Cosmosphere and Technology. Amsterdam:Elsevier Science Publishers. 1984. p. 67- 89.
43. Kowalak S, Jankowska A, Zeidler S, Wie¸ckowski AB. Sulfur radicals embedded in various cages of ultramarine analogs prepared from zeolites. Journal of Solid State Chemistry. 2007;180(3):1119-24.
44. Favaro M, Guastoni A, Marini F, Bianchin S, Gambirasi A. Characterization of lapis lazuli and corresponding purified pigments for a provenance study of ultramarine pigments used in works of art. Analytical and Bioanalytical Chemistry. 2012;402(6):2195-208.
45. Cultural Heritage Agency of the Netherlands. "RSR0000009 Polystyrene (PS) general purpose". Ed. Beth A. Price and Boris Pretzel. Infrared and Raman Users Group Spectral Database. Infrared and Raman Users Group, 2007. Web: www.irug.org.
46. Bicchieri M, Sodo A, Piantanida G, Coluzza C. Analysis of degraded papers by non-destructive spectroscopic techniques. Journal of Raman Spectroscopy. 2006;37(10):1186-92.
47. Wiley JH, Atalla RH. Band assignments in the raman spectra of celluloses. Carbohydrate Research. 1987;160:113-29.
48. Cultural Heritage Agency of the Netherlands. "RSR0000009 Polystyrene (PS) general purpose". Ed. Beth A. Price and Boris Pretzel. Infrared and Raman Users Group Spectral Database. Infrared and Raman Users Group, 2007. Web: www.irug.org.
49. Luo W, Liu X, Sun L. Polystyrene/calcium carbonate nanocomposites prepared by in situ polymerization in the presence of maleic anhydride. Journal of Applied Polymer Science. 2013;127(3):1502-7.
50. Palm A. Raman Spectrum of Polystyrene. The Journal of Physical Chemistry. 1951;55(8):1320-4.
51. Anema JR, Brolo AG, Felten A, Bittencourt C. Surface-enhanced Raman scattering from polystyrene on gold clusters. Journal of Raman Spectroscopy. 2010;41(7):745-51.

52. Wu DY, Svazas A. Micro- and nano-sized calcium carbonate toughened polystyrene. Journal of Nanoscience and Nanotechnology. 2006;6(12):3919-22.
53. Herbst W, Hunger K, Wilker G, Ohleier H, Winter R. Azo Pigments. In: Industrial Organic Pigments. Wiley-VCH Verlag GmbH and Co. KGaA;2004. p. 183.419.
54. Keck-Wilhelm A, Kratz E, Mildau G, Ilse M, Schlee C, Lachenmeier DW. Chemical analysis and risk assessment of prohibited colouring agents in face paint with special regard to CI 15585 (D and C Red No. 9, Pigment Red 53:1). International Journal of Cosmetic Science. 2015;37(2):187-95.
55. Melendres CA, Rios CB, Feng X, McMasters R. In situ laser Raman spectra of iron phthalocyanine adsorbed on copper and gold electrodes. The Journal of Physical Chemistry. 1983;87(18):3526-31.
56. Anghelone M, Jembrih-Simbürger D, Schreiner M. Identification of copper phthalocyanine blue polymorphs in unaged and aged paint systems by means of micro-Raman spectroscopy and Random Forest. Spectrochimica Acta Part A: Molecular and Biomolecular Spectroscopy. 2015;149(Supplement C):419-25.

# CHAPTER 8:

# General conclusions and future perspectives

Counterfeiting is an illicit activity linked to the infringement of the Intellectual Property Rights (IPR) and the alcoholic beverages, especially the wine and spirits, are prime targets for counterfeiters. Therefore, the wine market needs objective and reliable analysis tools for traceability and authentication purposes, for making international trade more transparent. The detection of counterfeited wine is often a difficult task, which requires more sophisticated analytical techniques. Unfortunately, some of these reported methodologies are slow, expensive, time-consuming, laborious and destructive. They are mainly based on liquid sampling, requiring opening the bottle that can be fateful when it comes to great value wines.

Taking into account the results reported in this research work whose main objective is **the authentication of bottled wine via fast and non-destructive analysis of wine packaging (glass, paper, ink and capsule) by laser-based spectrochemical methods together with chemometric data analysis**, it could be concluded that:

As a first step, regarding **the design and development of a new ablation cell adjustable to different bottle shapes**, a new prototype, which is actually under patent process, have been successfully carried out with the Université de Pau et des Pays de l'Adour. As its characteristics are not achievable by conventional micro-machining techniques, it has been built using a commercially available 3D printer and poly (lactic acid) polymer as manufacturing material. The evaluation of the performance in terms of transport efficiency, elemental fractionation and wash-out time has been highly satisfactory and similar to what is obtained with conventional cells.

In a second step, the new ablation cell has been successfully employed for the ultratrace (< 1ng · g-1) analysis of wine bottle components (glass, paper, ink and capsule) by femtosecond laser ablation coupled to ICPMS. Rapid (≈ 5 min) and quasi non-invasive (<0.5 mm) ablation strategies have been developed which cause limited damage on the bottle surface invisible to the naked eye. In addition, the matrix of labels and inks have also been directly analyzed by Raman spectroscopy and Infrared Spectroscopy.

For **the analysis of glass**, a non-invasive ablation strategy consisting on 2D raster of 0,1mm x 0,5 mm has been optimized which allows the analysis of a bottle in 90 seconds. The packaging characterization method has been applied to a large number of bottles (n>200) of controlled origin and bottles originating from other countries. The homogeneity was found to be lower than 15% for the major and trace elements both within a single bottle and within a batch a of bottles, showing a good homogeneity and a good representativeness of the measurements for statistical purposes. Statistical data processing based on multivariate analysis, including Principal Component Analysis (PCA), Hierarchical Ascendant Classification (HAC) and Soft Independent Modelling of Class Analogy (SIMCA), draw clear distinction between genuine and counterfeited

bottles by isolating and prioritizing the most important trace elements. Al, Eu, Ba and W are the most discriminant elements.

Similarly, it has also been possible to distinguish the chemical signature of the bottles according to their origin (continent/country) and their vintage (within a given Château). Green and transparent bottles belonging to the five continents are clearly distinguished, observing that green bottles are characterized for having much more trace elements (impurities) than transparent bottles, which stands out the absence of specific additives in transparent glass. In fact, common soda-lime glass appears colorless to the naked eye but the intentional or non-intentional addition of metal oxides during its manufacture can modify its color. Then, classification of green and transparent bottles has been performed separately.

For the green bottles, the elements As, Rb, Sb, Cs, Ba, Ce, Nd, Ta, W and Pb are the most significant, allowing the distinction between American/European and Asian bottles. However, the discrimination of the European green bottles according to their origin has not been concluding. In fact, being the EU the world's biggest producer of glass, there are only few independent corporate groups dedicated to glass containers manufacturing which considerably reduces the variability needed for such attempt of discrimination. Finally, similar approach has been done with the aim of identifying the country of origin of the European transparent bottles. In this case, French bottles are slightly separated from Portuguese and Spanish bottles, although 3 French bottles remain in the Portuguese/Spanish group. At this point, it must be highlight that a wine bottle is commonly assigned to a given country based on the indication specified in the label, which certainly means that the wine has been produced in this country. Indeed, it would be possible that the packaging is originating from other country/continent.

Finally, the elemental analysis of a bottle series comprising 34 bottles originating from a given Château close to Pomerol (years from 1969 to 2010) has been classified in 4 different groups according to their vintage. Ancient bottles are particularly characterized by the presence of a higher amount of rare earths and major elements while recent bottles own higher amount of trace elements. This fact has been attributed to the recent recycling process in which the use of raw materials is limited and has allows the homogenization of the impurities. Special mention has to be done to the great addition of iron in the most recent samples, which has influence in their darker green color in order to enhance the UV protection to preserve wine during storage.

Similarly, for **the analysis of label paper and printed ink**, a non-invasive ablation strategy (0,5 x 0,5 mm matrix) has been optimized, allowing the analysis of a bottle in a very competitive time (150 seconds). Due to the lack of commercial certified reference materials, matrix-matched standards have been synthesized as external calibrators by using commercially available inkjet

printer and then applied for the characterization of paper and ink in wine labels. Additionally, a novel method for the qualitative molecular analysis of packaging by Raman spectroscopy and Diffuse Reflectance Infrared Fourier Transform (DRIFT) spectroscopy have been developed, what provided complementary information to elementary analysis carried out by fsLA-ICPMS.

Regarding the synthesis of the matrix-matched standard, the quality assessment of printed standards stands up distinct penetration of the elements within the paper depth, being some element homogenously distributed and being others more concentrated in the surface. Therefore, taking into account that this part of the study was carried at the very end of the research period, alternative printing approaches to produced perfectly in-depth homogenised standards could not be tested. Thus, it is our proposal to do additional experiments in the immediate future considering alternative double side printing. Similarly, the spatial homogeneity within a single label and within a batch was evaluated. The homogeneity within a lot ranged from 10 to 15% whereas it was found to be significantly lower within a bottle, ranging from 0,3 to 5,7%. It is worth mentioning that there is no way to know whether the labels are originating from the same paper batch. Then, these slight variations could reflect batches inhomogeneity from the paper manufacturer.

The elemental analysis of label matrix and printed inks and the subsequent statistical data analysis allow the discrimination between the original and counterfeited bottles by the use of the elements Ga, Sr, Zr, Mo, La, Ce, Nd and U. Nevertheless, one of the original bottles is noticeably separated from the original bottles, which is explained by the change of label principal manufacturing material. According to the Raman spectroscopy and Diffuse Reflectance Fourier Transformed Infrared (DRIFT) spectroscopy, the main component of the label matrix is polypropylene (PP) or polystyrene (PS). The spectroscopic analysis of the label has allowed to identify titanium oxide and calcite and to stablish the oxidation grade of the polymer, which has been a valuable information to discriminate among original and counterfeited bottles. The elemental analysis of the black ink leads to no differentiation between original and counterfeited bottles. Spectroscopic techniques also conclude that none of pigments could be useful for discrimination purposes in this batch of bottles.

The suitability of the proposed method was also assessed in the series of bottles comprising 34 bottles from the same winery (from 1969 to 2010), in which 4 different groups have been identified. However, this differentiation between decades is not as clear as the differentiation done with the elemental glass analysis. The most discriminant elements are Rb, Sr, Ba, La, Ce, Nd, Sm, Gd, Er, W and U. The most ancient bottle from 1969 is completely different from the other vintages, having a greater influence the rare earths, Ba and W. The second group corresponds to the bottles belonging to the decade of the 80s in which the Sr has the biggest influence. The third

group belongs to decades of 90s and 2000s. It has a lower concentration of Sr but it is not possible to perform a further discrimination, which indicates that during these years the paper composition remained almost constant without any considerable change. Finally, the forth group comprising vintages 2007, 2008, 2009 and 2010 is clearly differentiated, indicating a big change in label matrix composition. They have a higher concentration of Sr and lower concentration of rare earths. The analysis performed by spectroscopic techniques are in agreement with this finding, indicating that from 1969 to 2006 the cellulose is the main component of the label matrix (oxidation grade of the paper is higher in older vintages) while for the years 2007, 2008, 2009 and 2010 is polystyrene (PS). Therefore, this assessment could provide an indication of the approximate manufacturing date although could not be conclusive. Black and red inks used in label do not give any valuable information about the vintage neither by laser ablation coupled to ICPMS. However, with regard to the Raman analysis of the red ink, three different red pigments have been identified, showing an evolutive process from the ancient bottles to the newest ones that could be a valuable tool for a rough estimation of the date of manufacture. Considering the usefulness of spectroscopic techniques for *in situ* and non-destructive characterization of materials, it would be worthy to firstly perform spectroscopic analysis in order to get a previous knowledge about the composition of the label matrix and ink before the trace elemental analysis by fsLA-ICPMS.

Finally, the trace elemental analysis of wine bottles coming from all around the world have been done (label matrix and black ink), attempting to classify them according to their geographical origin. Once again the black ink is not useful for discrimination purposes. Nevertheless, the analysis of label matrix allows to distinguish Europe and Asia, while American bottles make no differentiation. The most discriminant elements are Y, Sm, Ho and Yb.

Finally, **the preliminary study of the capsules** based on their elemental analysis shows that this packaging element would be complementary to the analysis of glass, paper and ink for wine authentication. It allows unequivocal discrimination of aluminium or tin based capsules and reveals a potential discrimination between capsules of different origin according to the continent. In case of capsule exclusively made of plastic, the elemental analysis by fsLA-ICPMS could be complemented by Raman spectroscopy and Infrared spectroscopy, which would be of great interest as these techniques have shown to be very valuable tools for fast and simple material characterization.

As general conclusion, the research work presented in this manuscript covers a wide field of analytical sciences, starting from the development of new instrumentation, followed by the development and validation of analytical methods in femtosecond laser ablation, Infrared and Raman and finally, the application of statistical tools in order to identify the counterfeited and

original bottles and also to estimate their geographical origin and vintage. To our knowledge, there are no precedents in the literature on this subject and the results presented in this work here are extremely encouraging. These analytical methods offer considerable prospects for the rapid and non-destructive analysis of goods that extend well beyond the traceability of wine, encompassing the agri-food market, the luxury market, the pharmaceutical market, etc.

La contrefaçon est une activité illégale liée à la violation des droits de propriété intellectuelle (DPI) et les boissons alcooliques, en particulier le vin et les spiritueux, représentent une cible privilégiée des faussaires. Il y a par conséquent un besoin de faire émerger des outils d'analyse fiables, rapides et non destructifs pour l'authentification et la traçabilité du vin afin que le commerce international devienne plus transparent. La détection des vins contrefaits est souvent difficile et nécessite la mise en œuvre de techniques sophistiquées. Elle sont cependant souvent coûteuses, laborieuses et invasives. Elles sont basées principalement sur une analyse du contenu et nécessitent donc l'ouverture de la bouteille, ce qui est dommageable lorsqu'il s'agit de vins de grande valeur.

D'après les résultats présentés dans ce travail de recherche, dont **l'objectif principal est l'authentification des bouteilles de vin grâce à une analyse rapide et non destructive des emballages de vin (verre, papier, encre et capsule) par des méthodes spectrochimiques couplées à un rayonnement laser combinées à l'analyse statistique de données**, on peut conclure que:

Dans un premier temps, **une nouvelle cellule d'ablation adaptable à différentes formes de bouteilles a été développée**. Un nouveau prototype, actuellement en cours de brevet, a été mis en œuvre avec succès à l'Université de Pau. Une imprimante 3D a été utilisée pour créer un prototype de cellule d'ablation en utilisant un polymère d'acide poly-lactique (PLA) comme matériau de construction, la fabrication de cette pièce complexe étant techniquement irréalisable au moyen des machines-outils de micro-usinage conventionnelles. Ses performance en termes d'efficacité du transport, de fractionnement élémentaire et de temps de rinçage se sont montrées très satisfaisantes et similaires à celle obtenue avec les cellules conventionnelles.

Dans une deuxième étape, cette cellule d'ablation a été utilisée avec succès pour l'analyse des teneurs en éléments traces ($< 1 ng \cdot g^{-1}$) des composants de la bouteille (verre, papier, encre et capsule) par l'ablation laser femtoseconde couplée à l'ICPMS. Des stratégies d'ablation rapides ($\approx$ 5 min) et quasi non invasives (<0.5 mm) ont été developées, infligeant des dommages à la surface de la bouteille invisibles à l'œil nu. En outre, la matrice des étiquettes et des encres ont également été directement analysés par la spectroscopie Raman et la spectroscopie Infrarouge

Pour **l'analyse du verre**, une stratégie d'ablation en 2D ligne quasi non invasive (0,1 mm x 0,5 mm) a été optimisée, ce qui permet d'analyser une bouteille en 90 secondes. Cette méthode de caractérisation de l'emballage a été appliquée à un grand nombre de bouteilles (n> 200) d'origine contrôlée et des bouteilles issues d'autres pays. Nous avons montré que la reproductibilité des mesures des éléments majeurs et des éléments traces était meilleure que 15% au sein d'une seule

bouteille ainsi que dans un lot de bouteilles identiques, reflétant une bonne homogénéité et une bonne représentativité des mesures à des fins d'études statistiques. Les traitements statistiques multivariés des données basé, notamment sur l'Analyse en Composantes Principales (ACP), la Classification Ascendante Hiérarchique (CAH) et la Modélisation Indépendante Soft de l'Analogie de Classe (SIMCA), établissent une distinction claire entre les bouteilles authentiques et contrefaites en isolant et en priorisant les éléments traces les plus importants. Les éléments Al, Eu, Ba et W se sont montrés les plus discriminants.

De la même façon, il a également été possible de distinguer la signature chimique des bouteilles selon leur origine (continent / pays) et leur millésime (pour un château donné). Les bouteilles en verre coloré (nuances de vert) se distinguent clairement les bouteille en verre blanc, les premières contenant une plus grande quantité d'éléments traces (impuretés), ce qui souligne l'absence d'additifs spécifiques dans le verre blanc. En fait, le verre sodo-calcique apparaît incolore à l'œil nu, mais l'addition intentionnelle ou non intentionnelle d'oxydes métalliques lors de sa fabrication peut modifier sa couleur. Le classement des bouteilles en verre vert et en verre blanc a ensuite été effectué séparément.

Pour les bouteilles vertes, les éléments As, Rb, Sb, Cs, Ba, Ce, Nd, Ta, W et Pb sont les plus significatifs, et permettent de distinguer les bouteilles américaines / européennes et asiatiques. Par contre, la discrimination des bouteilles vertes européennes selon leur pays d'embouteillage n'a pas véritablement été concluante. En fait, étant l'UE le plus grand producteur mondial de verre, il n'y a que peu d'entreprises dédiés à la fabrication de bouteilles en verre, ce qui réduit considérablement la variabilité nécessaire à une telle tentative de discrimination. Enfin, une approche similaire a été faite pour identifier le pays d'origine des bouteilles en verre blanc européennes. Dans ce cas, les bouteilles françaises sont légèrement séparées des bouteilles portugaises et espagnoles, bien que 3 bouteilles françaises restent dans le groupe portugais / espagnol. À ce stade, il faut souligner qu'une bouteille de vin est attribuée à un pays donné en fonction de l'indication indiquée sur l'étiquette car cela signifie que le vin a été produit dans ce pays. Cependant, il est tout à fait possible que l'emballage provienne d'un autre pays ou d'un autre continent.

Finallement, l'analyse du verre appliquée à une série de 34 bouteilles provenant d'un château donné proche de Pomerol (années 1969 à 2010) a permis de les classer en 4 groupes différents en fonction de leur millésime. Les bouteilles anciennes se caractérisent particulièrement par la présence d'une quantité plus grande de terres rares et d'éléments majeurs, tandis que les bouteilles récentes possèdent une plus grande quantité d'éléments traces en général. Cette tendance peut etre due au processus de recyclage, qui a pris une part de plus en plus importante au cours du temps, qui utilise moins de matière première, et qui conduit à l'homogénéisation des impuretés. Nous

avons également observé que le fer était présent en plus grande quantité dans les échantillons récents. Cet élément, donnant une couleur plus foncée au verre, a été ajouté dans le but d'améliorer la protection UV et ainsi préserver le vin pendant le stockage.

Pour **l'analyse du papier et des encres de l'étiquette**, une stratégie d'ablation non invasive (0,5 x 0,5 mm) a été développée permettant d'analyser une bouteille très rapidement (150 secondes). En raison du manque de matériaux de référence certifiés, nous avons développé nos propres étalons de papier par impression jet d'encre à partir de solutions dopées, permettant une analyse quantitative et comparative du papier et des encres des étiquettes. En outre, une nouvelle méthode pour l'analyse moléculaire qualitative de l'emballage par la spectroscopie Raman et la spectroscopie Infrarouge ont été développées, donnant ainsi des informations complémentaires à l'analyse élémentaire réalisée par fsLA-ICPMS.

En ce qui concerne la synthèse des étalons de papier dopé, nous avons montré une imprégnation en profondeur différente en fonction des éléments. Certains étant répartis de manière homogène et d'autres plus concentrés dans la surface. Cette étude ayant été menée à la fin de ce travail de thèse, des méthodes d'impression alternatives pour produire des étalons parfaitement homogènes en profondeur n'ont pas pu être testées. Une impression recto verso permettrait d'homogénéiser la distribution en profondeur. L'homogénéité spatiale des éléments trace au sein d'une étiquette donnée ainsi que sur un lot a été aussi évaluée. Les variations dans un lot de bouteille se situent entre de 10 et 15% alors qu'elles sont significativement moins importantes au sein d'une étiquette d'une même bouteille, allant de 0,3 à 5,7%. Il convient de mentionner qu'il n'existe aucun moyen de savoir si les étiquettes étudiées sont issues du même lot de papier, ces légères variations pouvant refléter la non-homogénéité des lots du fabricant du papier.

L'analyse de la matrice des étiquettes et des encres imprimées sur des bouteilles contrefaites et les bouteilles authentiques correspondantes, ont permis, grâce à des traitements statistiques des données de discriminer les bouteilles originales et les contrefaçons à partir des éléments suivants : Ga, Sr, Zr, Mo, La, Ce, Nd et U. Il a également été observé que l'une des bouteilles authentique était clairement séparée des autres, ce qui s'explique par la nature différente du matériau constituant l'étiquette. Les spectrométries Raman et infrarouge à transformée de Fourier et réflexion diffuse (DRIFT) ont permis d'identifier le constituant principal des étiquettes le polypropylène (PP), ou le polystyrène (PS) selon les cas. L'approche spectroscopique à permis de déterminer la présence d'oxyde de titane, calcite et le niveau d'oxydation du polymère, ces deux paramètres permettant de discriminer les étiquettes authentique des étiquettes de bouteilles contrefaites. En revanche, sur ce lot de bouteille, l'analyse de l'encre noire par fsLA-ICPMS n'a pas permis de différencier les bouteilles authentiques des contrefaçons. D'ailleurs, les techniques

spectroscopiques concluent également qu'aucun pigment ne peut être utile à des fins de discrimination, sur ce lot de bouteilles.

L'analyse élémentaire de l'étiquette a également été évaluée sur la série de bouteilles comprenant 34 bouteilles provenant du même Château (de 1969 à 2010). Quatre groupes différents ont été identifiés. Cependant, cette différenciation n'est pas aussi claire que la différenciation faite avec l'analyse élémentarie du verre. Les éléments les plus déterminants sont Rb, Sr, Ba, La, Ce, Nd, Sm, Gd, Er, W et U. La bouteille la plus ancienne de 1969 est complètement différente des autres millésimes, celle ci plus marquée par la présence de terres rares, de Ba et de W. Le deuxième groupe correspond aux bouteilles des années 80 où le Sr a la plus grande influence. Le troisième groupe appartient aux des années 90 et 2000. Il se caractérise par une faible concentration de Sr, mais il n'est pas possible d'effectuer une autre discrimination, ce qui indique que pendant ces années, la composition du papier est restée presque constante sans changement considérable. Enfin, le quatrième groupe comprenant les millésimes 2007, 2008, 2009 et 2010 est clairement différencié, ce qui indique une grande modification de la composition de la matrice d'étiquettes. Ces bouteilles présentent une concentration plus élevée en Sr et une plus faible concentration en terres rares. L'analyse effectuée par des techniques spectroscopiques est en accord avec cette constatation, indiquant que de 1969 à 2006, la cellulose est le principal composant des étiquettes (le niveau d'oxydation du papier est plus élevée dans les millésimes plus anciens) tandis que pour les années 2007, 2008, 2009 et 2010 c'est le polystyrène (PS). Par conséquent, cette évaluation pourrait fournir une indication de la date de fabrication approximative, bien qu'elle ne puisse pas être absolument déterminante. Les encres noires et rouges de ces étiquettes ne donnent aucune information précieuse sur le millésime par ablation laser couplée à l'ICPMS. Cependant, l'encre rouge analysée en Raman permet de distinguer trois pigments rouges différents, montrant un processus évolutif des bouteilles anciennes aux plus récentes qui pourraient être un outil précieux pour une estimation approximative de la date de fabrication. Compte tenu de l'utilité des techniques spectroscopiques pour la caractérisation *in situ* et non destructive des matériaux, il serait intéressant d'effectuer d'abord une analyse spectroscopique afin d'obtenir une connaissance préalable de la composition de la matrice de l'étiquette et de l'encre avant de procéder à l'analyse des éléments traces par fsLA-ICPMS.

Enfin, les résultats de l'analyse des éléments traces de l'étiquette (matrice et encre noire) des bouteilles de notre collection de différents pays ont été utilisés pour tenter de classer ces dernières en fonction de leur origine géographique. Une nouvelle fois, nous en avons conclu que l'encre, noire, ne permettait pas les discriminer. Par contre a partir de la matrice des étiquettes les bouteilles, nous avons pu distinguer les bouteilles européennes des bouteilles asiatiques mais pas les bouteilles américaines. Y, Sm, Ho et Yb se sont avérés les éléments les plus discriminants.

Enfin, **l'étude préliminaire portant sur l'analyse élémentaire par fsLA-ICPMS dans les capsules** montre que cet élément d'emballage donne des informations complémentaires de celles obtenues sur le verre, l'étiquette papier et les encres pour l'authentification du vin. Il permet une discrimination sans équivoque des capsules à base d'aluminium ou d'étain et révèle une éventuelle discrimination entre les capsules d'origine différente selon le continent. Bien qu'applicable à l'analyse des traces dans les polymères, l'ablation laser femtoseconde/ICPMS pourrait être complétée de manière interessante par la spectroscopie Raman et la spectroscopie Infrarouge, ces dernières étant des outils précieux pour une caractérisation rapide et simple du matériau.

En conclusion générale, le travail de recherche présenté dans ce manuscrit couvre un large champ des sciences analytiques, partant du développement d'instrumentation, suivi du développement et de la validation de méthodes en ablation laser femtoseconde, Infrarouge et Raman, pour enfin appliquer des outils statistiques permettant d'une part d'identifier les bouteilles contrefaites des bouteilles authentiques et d'autre part d'en estimer la provenance géographique et millésime. A notre connaissance, il n'y a pas de précédents dans la litterature sur ce sujet et les résultats présentés dans ce travail ici sont extrêmement encourageants. Ces méthodes d'analyse offre des perspectives considérables pour l'analyse rapide et non destructive des marchandises qui s'étendent bien au delà de la traçabilité du vin, englobant le marché de l'agroalimentaire en général, le marché du luxe, le marché pharmaceutique, etc.

La falsificación y la piratería son actividades ilícitas relacionadas con la infracción de los Derechos de Propiedad Intelectual (DPI) y las bebidas alcohólicas, especialmente el vino y las bebidas espirituosas, constituyen uno los principales objetivos de los falsificadores. Por ello, se requieren herramientas analíticas objetivas y fiables que garanticen la autenticidad y trazabilidad del vino para hacer más transparente el comercio internacional. Los parámetros individuales son a menudo insuficientes para detectar el vino falsificado, requiriendo técnicas analíticas más sofisticadas. Sin embargo, algunas de estas técnicas son lentas, laboriosas, costosas y destructivas. Las técnicas para la verificación de vino se basan en el muestreo del propio líquido. Por lo tanto, se trata de técnicas invasivas que requieren la apertura de la botella, lo que resulta inviable cuando se trata de vinos de gran valor.

Por lo tanto, teniendo en cuenta que el objetivo principal del presente trabajo es **la autenticación del vino embotellado mediante el análisis rápido y no destructivo de los envases (vidrio, papel, tinta y cápsula) por métodos espectroquímicos acoplados a un haz de láser y el posterior tratamiento estadístico de los datos** y de acuerdo con los resultados presentados a lo largo de este manuscrito, se puede concluir lo siguiente:

Con respecto al **diseño y desarrollo de una nueva cámara de ablación adaptable a las diferentes formas de las botellas**, se ha construido con éxito un nuevo prototipo junto con el taller de física de la *Université de Pau et des Pays de l'Adour* y está actualmente en proceso de patente. Su fabricación se basa en la simplicidad, la rentabilidad y la facilidad de construcción. Se trata de una cámara de ablación abierta cuya geometría asegura un ensamblaje completo entre la cámara y la botella. Su fabricación se ha llevado a cabo mediante impresión 3D empleando ácido poliláctico (PLA) como material, ya que sus características no son alcanzables mediante técnicas de micro-mecanizado convencional de alta precisión. Cabe destacar que la evaluación del rendimiento en términos de eficiencia de transporte, fraccionamiento elemental y tiempo de lavado ha sido satisfactoria y similar a la obtenida con cámaras convencionales.

En la segunda parte de este trabajo, la cámara de ablación desarrollada se ha empleado con éxito para el análisis a nivel ultra-traza ($< 1$ ng·g$^{-1}$) nivel ultra-traza de los componentes de las botellas de vino (vidrio, papel, tinta y cápsula) mediante la ablación láser femtosegundo acoplada a ICPMS. Se han desarrollado estrategias de ablación rápidas ($\approx 5$ min) y no invasivas (<0.5 mm) que no inducen ninguna degradación visible en la botella. Además, la matriz de las etiquetas y las tintas impresas en las etiquetas también han sido directamente analizadas mediante espectroscopia Raman y espectroscopia Infrarroja.

Para el **análisis de vidrio** se ha optimizado una estrategia de ablación 2D en línea (0,1mm x 0,5 mm) que permite el análisis de una sola botella en 90 segundos. El método de caracterización del vidrio se ha aplicado a un gran número de botellas (n> 200) de origen controlado y botellas procedentes de otros países. La homogeneidad de los elementos mayoritarios como la de los elementos traza es inferior al 15% tanto en una botella como en un lote de botellas, lo que refleja una buena homogeneidad y representatividad de las medidas para el posterior análisis quimiométrico. El procesamiento estadístico de datos basado en el análisis multivariante, el cual incluye el Análisis de Componentes Principales (PCA), la Clasificación Ascendente Jerárquica (HAC) y el Modelado Suave Independiente de Analogía de Clases (SIMCA), establecen una clara distinción entre botellas originales y falsificadas aislando y priorizando los elementos traza más importantes. En este caso, se establece que los elementos Al, Eu, Ba y W son los responsables de tal discriminación.

Además, también fue posible distinguir la firma química de las botellas de acuerdo con su país de origen (continente/país) y cosecha (botellas pertenecientes a una misma bodega). Por un lado, se han podido distinguir claramente las botellas verdes y transparentes, observando que las botellas verdes se caracterizan por tener un mayor número de elementos traza (impurezas) que las botellas transparentes, lo que destaca la ausencia de aditivos específicos en el vidrio transparente. De hecho, el vidrio de soda-cálcica es incoloro a simple vista, pero la adición intencional o no intencional de óxidos metálicos durante su fabricación puede modificar su color. En consecuencia, el análisis estadístico para la clasificación de las botellas verdes y transparentes se ha realizado por separado.

En el caso de las botellas verdes, los elementos As, Rb, Sb, Cs, Ba, Ce, Nd, Ta, W y Pb son los más significativos, permitiendo la distinción entre las botellas americanas / europeas y las asiáticas. Sin embargo, la discriminación de las botellas verdes europeas según su país de origen no ha tenido el mismo éxito. De hecho, siendo la UE el mayor productor de vidrio del mundo, hay pocos grupos empresariales independientes dedicados a la fabricación de botellas de vidrio, lo que reduce considerablemente la variabilidad necesaria para tal intento de discriminación. Por último, se ha llevado a cabo un estudio similar con el fin de dilucidar el país de origen de las botellas transparentes europeas. En este caso, las botellas francesas se encuentran levemente separadas de las botellas portuguesas y españolas, aunque 3 botellas francesas permanecen en el grupo portugués/español. Llegados a este punto es necesario destacar que una botella de vino se asigna comúnmente a un país determinado en base a lo especificado en la etiqueta, lo que significa que el vino se ha producido en este país. Sin embargo, no se puede asumir que el envase también sea originario del mismo país/continente.

Finalmente, la serie que comprende 34 botellas provenientes de una misma bodega cercana a la región de Pomerol y que comprende los años de 1969 a 2010 se ha clasificado en 4 grupos diferentes según la cosecha. Las botellas antiguas se caracterizan particularmente por la presencia de una mayor cantidad de tierras raras y elementos mayoritarios, mientras que las botellas más recientes poseen una mayor cantidad de elementos traza. Este hecho se ha atribuido al reciente proceso de reciclado en el que el uso de materias primas, que son más abundantes en elementos mayoritarios, es limitado y fomenta la homogenización de las impurezas. Se debe hacer una mención especial a la adición de hierro en las botellas más recientes, lo que influye en una tonalidad verde más oscura de las botellas con el fin de incrementar la protección UV para mejorar la conservación del vino durante el almacenamiento.

Para el **análisis del papel y de la tinta** se ha optimizado una estrategia de ablación no invasiva (0,5 x 0,5 mm) que permite el análisis de una sola botella en un tiempo muy competitivo (150 segundos). Además, debido a la falta de materiales de referencia certificados, se han sintetizado nuevos estándares *"matrix-matching"* utilizando para ello una impresora de inyección de tinta para su posterior aplicación para el análisis cuantitativo y la comparación de etiquetas de papel y tinta impresa. También se ha desarrollado un nuevo método para el análisis molecular cualitativo de las botellas mediante espectroscopia Raman y espectroscopia Infrarroja de Reflectancia Difusa por Transformada Fourier (DRIFT), lo que ha proporcionado información complementaria al análisis elemental llevado a cabo por fsLA-ICPMS.

La evaluación de la calidad de los nuevos estándares "matrix-matching" ha permitido concluir que la absorción de los elementos es diferente de unos a otros, estando algunos homogéneamente distribuidos y otros más concentrados en la superficie. Por lo tanto, teniendo en cuenta que esta parte del estudio se llevó a cabo al final del período de investigación, no se pudieron probar técnicas de impresión alternativas para producir estándares perfectamente homogeneizados en profundidad. Por lo tanto, es nuestra propuesta hacer experimentos adicionales considerando la impresión alternativa en ambas caras del papel. De forma similar, se estudió la homogeneidad espacial de una única etiqueta y de las etiquetas de un mismo lote. La homogeneidad dentro de un lote varió entre el 10 y el 15%, mientras que es significativamente menor dentro de una misma etiqueta, con una variación entre el 0,3% y el 5,7%. Cabe mencionar que no hay forma de saber si las etiquetas provienen del mismo lote de papel, por lo que estas ligeras variaciones podrían reflejar la heterogeneidad de los lotes un mismo fabricante de papel.

El análisis de la matriz de las etiquetas y de las tintas impresas y el posterior análisis estadístico de los datos ha permitido la discriminación entre las botellas originales y falsas, destacando los elementos Ga, Sr, Zr, Mo, La, Ce, Nd y U como responsables de dicha diferenciación. Sin embargo, se aprecia que una de las botellas originales está notablemente separada del resto de las

botellas originales, lo que se explica por el cambio del material principal de fabricación de la etiqueta. De acuerdo con los resultados obtenidos mediante la espectroscopia Raman y DRIFT espectroscopia Infrarroja de reflectancia difusa por transformada Fourier (DRIFT), el componente principal de las etiquetas es el polipropileno (PP) o poliestireno (PS). Según el análisis espectroscópico de la etiqueta ha permitido identificar óxido de titanio y calcita, así como determinar el grado de oxidación del polímero, permitiendo diferencias las botellas auténticas de las falsificadas. El análisis elemental de la tinta negra no permite hacer ninguna diferenciación entre las botellas originales y falsas. Las técnicas espectroscópicas también concluyen que ninguno de los pigmentos podría ser útil para propósitos de discriminación en este lote de botellas.

La idoneidad del método propuesto para el análisis elemental también se evaluó en la serie de 34 botellas de una misma bodega (1969 a 2010), permitiendo diferenciar 4 grupos. Sin embargo, esta diferenciación entre décadas no es tan evidente como la diferenciación realizada mediante el análisis elemental del vidrio. Los elementos Rb, Sr, Ba, La, Ce, Nd, Sm, Gd, Er, W y U son los responsables de tal discriminación. La botella más antigua (1969) es completamente diferente a las otras añadas, teniendo una mayor influencia las tierras raras, Ba y W. El segundo grupo corresponde a las botellas pertenecientes a la década de los ochenta, en las cuales el Sr tiene mayor influencia. El tercer grupo pertenece a los años 90 y 2000. Se caracteriza por tener una baja concentración de Sr, aunque no es posible realizar una discriminación adicional, lo que indica que durante estas décadas la composición del papel permaneció invariable. Finalmente, el cuarto grupo lo componen los años 2007, 2008, 2009 y 2010 y está claramente diferenciado, lo que indica un gran cambio en la composición de la matriz de las etiquetas. Se caracterizan por tener una mayor concentración de Sr y una menor concentración de tierras raras. El análisis realizado por las técnicas espectroscópicas está en consonancia con este hallazgo, indicando que la celulosa es el componente principal de la matriz de etiquetas desde el año 1969 al 2006 (el grado de oxidación del papel es mayor en las botellas más antiguas), mientras que el poliestireno (PS) es el material de fabricación de las etiquetas de los años 2007, 2008 y 2009 y 2010. Por lo tanto, el análisis del componente principal de la etiqueta mediante técnicas espectroscópicas podría proporcionar una fecha aproximada de fabricación, aunque no pudiera ser concluyente. El análisis elemental de las tintas negras y rojas utilizadas en la etiqueta no ofrecen ninguna información adicional. Sin embargo, el análisis mediante espectroscopia Raman de la tinta roja ha permitido identificar tres pigmentos rojos diferentes, mostrando un proceso evolutivo desde las botellas más antiguas a las más nuevas, lo que podría ser una herramienta valiosa para una estimación aproximada de la fecha de fabricación. Teniendo en cuenta la utilidad de las técnicas espectroscópicas para la caracterización *in situ* y no destructiva de los materiales, sería recomendable realizar en primer lugar el análisis espectroscópico de la matriz de la etiqueta con

el fin de obtener un conocimiento previo sobre su composición antes de proceder al análisis elemental por fsLA-ICPMS.

En último término, se ha tratado de clasificar las botellas de vino procedentes de todo el mundo mediante el análisis elemental la matriz de la etiqueta y la tinta negra, concluyendo una vez más que la tinta negra no es útil para propósitos de discriminación. El análisis elemental de la matriz de la etiqueta permite distinguir entre Europa y Asia mientras que las botellas americanas no hacen ninguna diferenciación. Entre los elementos analizados Y, Sm, Ho y Yb son los más significativos para la discriminación de las botellas europeas, americanas y asiáticas, teniendo un mayor peso en el grupo europeo.

Finalmente, el **análisis preliminar de las cápsulas** por ablación láser de femtosegundo acoplado a ICMPS concluye que el análisis de este componente del embalaje del vino sería de utilidad, junto con el análisis del vidrio, del papel y de la tinta, para la autenticación del vino, ya que permite la discriminación inequívoca de cápsulas de aluminio o de estaño y revela una posible discriminación entre las cápsulas de diferente origen. En el caso de las cápsulas exclusivamente de plástico, sería de gran interés el desarrollo de un método de análisis basado en la espectroscopia Raman y la espectroscopia Infrarroja para completar el análisis elemental por fsLA-ICPMS, ya que estas técnicas han demostrado ser herramientas muy valiosas para la caracterización rápida y sencilla de los materiales de fabricación.

En general, la investigación presentada en este manuscrito abarca un amplio campo de las ciencias analíticas, partiendo del desarrollo de nueva instrumentación, seguido por el desarrollo y validación de métodos analíticos basados en la ablación láser de femtosegundo y las espectroscopias Raman e Infrarroja, y finalmente, la aplicación de las herramientas estadísticas que permitan identificar las botellas falsificadas de las botellas auténticas y estimar su origen geográfico y cosecha. A nuestro entender, no hay precedentes en la literatura sobre este tema y los resultados presentados en este trabajo resultan muy alentadores. Estos métodos analíticos ofrecen perspectivas considerables para el análisis rápido y no destructivo de los bienes que van más allá de la trazabilidad del vino, abarcando el mercado agroalimentario en general, el mercado del lujo, el mercado farmacéutico, etc.

# ANNEX I:

# Preliminary analysis of capsules for wine authentication

## 1. Introduction

The wine packaging is the primary element of communication towards the consumer as the inscriptions on the different parts of the bottle allow the purchaser to identify a wine. However, if the labels and the capsule are sources of information for the consumer, they are also used to identify fraud. For the French wines, the *Capsules Représentative de Droits* (CRD) contains much information about the origin of the wine. Bottles containing spirits, which are subjected to a specific taxation (excise duties), must be provided with CRD, meaning that the taxes have been paid. A bottle without a CRD cannot be marketed on French territory. The information that must be covered in 15 mm diameter capsules is the following: 1) the Marianne emblem and the terms "French Republic" and the acronym "DGDDI" (*Direction Générale des Douanes et Droits*), 2) the number of bottling responsible, for example: 83 E 503. 83 refers to the department number of the bottler's headquarters; the letter is the first letter of his qualification (harvester, trader or Certified Warehouseman) and the number 503 corresponds to the administrative number of the bottler, 3) the brand of the capsule manufacturer, 4) the indication of the capacity and 5) alcoholic graduation in volume. Moreover, the capsule must be of a precise color, which is determined according to the type of alcohol contained (Figure 1) (1).

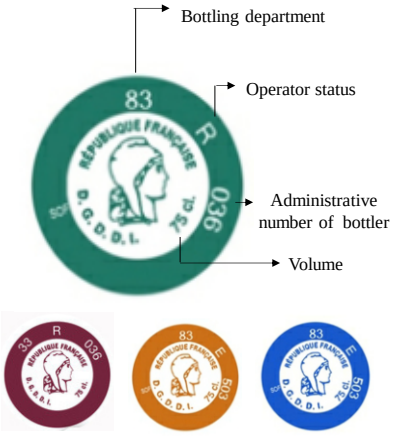


| Type of alcohol | Color of the capsule |
|---|---|
| • Still or sparkling wine with controlled designation of origin (AOC = Appellation d'Origine Contrôlée)<br>• AOC sweet wines | Green (Pantone 340 C)<br>Red (Pantone 209 C) |
| Other wines, table wine or local wines | Blue (Pantone 285 C)<br>Red (Pantone 209 C) |
| Intermediate product with AOC: liqueurs and *vin speciaux* | Orange (Pantone 021 C) |
| Other intermediate products | Gris (Pantone 402 C) |
| Cognac and armagnac | Golden Yellow (Pantone 1225 C) |
| Other alcohols | White (Pantone Gris 1 C) |

**Figure 1** Information given by French capsules according to the French legislation.

The capacity of accurately analyzing, without sampling or destruction, the chemical composition of a micrometric region of the material has been widely exploited by the use of molecular spectroscopic techniques, for example to identify pigments of heritage objects or works of art, to assist in their authentication and even the detection of counterfeits (2-4). A successful way to invalidate a work of art or reveal a counterfeit is to demonstrate that its component parts are anachronistic. Because the palette of pigments used in art and industry have evolved over time,

and because such pigments have tended to be derived from stable minerals and metals, the spectroscopic analysis of colors and pigments has proved a valuable tool for the detection of forgeries (5). This principle is applicable to packaging of wine bottles, especially if the vintage is earlier than the date of appearance of the pigment used.

Lead was widely used in ancient times for wine storage due to its malleability and resistance to corrosion (6). It was first used on the cap covering the cork back in the 18$^{th}$ century, when it was useful to cover the cork to protect it from vermin and insects, as a barrier to oxygen, and for decorative purposes. Nevertheless, concerns over lead poisoning meant they were phased out by the 1990s, as they were lead decanters through old or defective corks (7-9). Nowadays, the use of aluminium is widespread and tin capsules have replaced lead capsules for expensive wines. In some cases, polyethylene and polyethylene terephthalate (PET) can be added between two-layer aluminium foil that are stuck together through adhesive (polylaminated capsules). These capsules are a two-piece construction. The "skirt" is made from a multi-layer lamination of aluminium-polyethylene-aluminium and the top disk is made from a single layer of aluminium. Other plastics, such as polyvinyl chloride (PVC), can be used for entire manufacturing. Therefore, the composition of the alloy is specific and cannot easily be imitated as well as the inks employed to color the capsules, which could be useful for counterfeiting detection as the include anti-falsification measures through fluorescent, invisible, color changing and electronic pigments (10). Thus, the chemical characterization of capsule manufacturing material as well as the identification of employed pigments conceal a great deal of information to reveal a possible counterfeiting.

Solution techniques, such as atomic absorption spectrometry (AAS), optical emission spectroscopy (ICPOES) or inductively coupled plasma mass spectrometry (ICPMS) have been largely used for alloy analysis, which require destructive sampling of the component to be analyzed. X-ray fluorescence (XRF) has been also commonly applied in the metals industry for identifying and checking alloy specifications. However, conventional application of this technique demands a relatively large and well-polished sample, making the process analysis longer and laborious. Thus, laser ablation coupled to inductively coupled plasma mass spectrometry (LA-ICPMS) resurges as an alternative analytical technique essentially due to its non-destructiveness, its adaptability to samples' shape or size and its simplicity as there is no sample preparation step, which considerably reduce the analysis time (11). However, metal alloys are considered as intensively critical and fractionating matrices due to the heat affected zone and thermal relaxation, which takes place on a time-scale of few hundred femtoseconds. In order to restrain these effects, the laser pulse duration needs to fall below the material-specific thermal

relaxation time. Reducing the pulse duration down to this region has been suggested to improve the ablation characteristics and to get closer to the ideal concept of matrix independent laser ablation (12, 13). Gonzalez et al. found a clear trend indicating advantages of femtosecond over nanosecond laser ablation for the ablation of metallic samples. The combination of the appropriate conditions (pulse length and wavelength), which influence light absorption and thermal diffusion, can be optimized to improve ablation efficiency. Indeed, more mass was removed from the sample with femtosecond laser pulses reducing thermal damage caused to the sample and greater number of particles with suitable sizes to be transported and measured were ejected from the sample (14, 15).

Therefore, taking into account the valuable information that could be extracted from chemical characterization of capsule manufacturing material and pigments for wine verification purposes, this preliminary work aims to demonstrate that the analysis of capsules by fsLA-ICPMS could be a good choice for wine authentication purposes and complements the results already obtained for the other wine packaging elements (glass, paper and ink).

## 2. Analytical strategy

Laser ablation of the paper and the ink was performed using ALFAMET laser ablation device (KGW-Yb, 1030 nm) working at 100 Hz, pulse duration of 360 fs and with an energy density of 65% (3.7 J·cm$^2$). For this preliminary study, a fit for purpose open cell was not developed in contrast to the approach used for glass, paper and ink analysis. Instead, a closed ablation cell was used for the analysis, as the developed open cell does not fit to the curvature of the bottleneck. Therefore, a small area of the capsule was removed prior to the analysis. The laser beam was operated with a scan speed of 30 mm·s$^{-1}$ and a 50 mm focal length objective was used for laser beam focusing, producing a spot size diameter of 15 µm at the sample surface. A matrix template (1 x 1 mm, 60 spots per line with 5 pulses per spot, 60 lines) on capsule was used as ablation pattern (Figure 2).

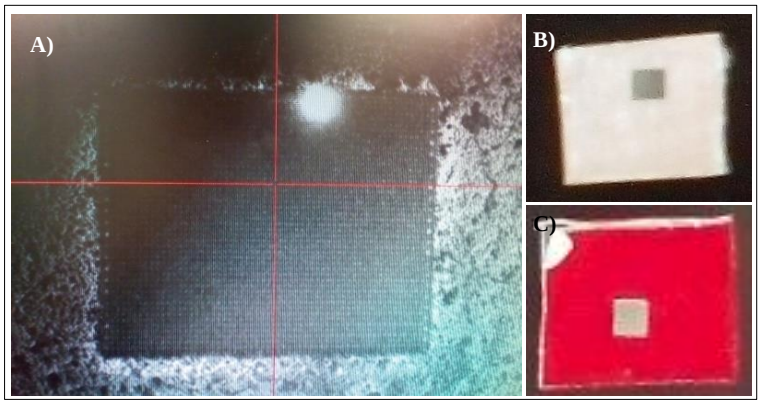


**Figure 2** Ablation matrix on capsule alloy: A) view of ablation process, B) alloy ablation and C) red ink ablation.

The ablated material was transported through a 1 m-long polyurethane tube (i.d. 4 mm) by an argon gas stream (500 $ml \cdot min^{-1}$) to the ICPMS. During the laser ablation analyses, the stability of the plasma was monitored by continuously nebulizing a 1 $\mu g \cdot L^{-1}$ rhodium standard solution. An ELAN DRC II ICPMS instrument was used to acquire ion-signal intensities. A 1.8 $mL \cdot min^{-1}$ $H_2$ (Parker Balston) gas flow was introduced in the cell reaction system.

A list of 68 isotopes were reordered similarly to glass and label analysis: $^{7}Li$, $^{9}Be$, $^{11}B$, $^{13}C$, $^{23}Na$, $^{24}Mg$, $^{25}Mg$, $^{27}Al$, $^{28}Si$, $^{45}Sc$, $^{47}Ti$, $^{51}V$, $^{52}Cr$, $^{53}Cr$, $^{55}Mn$, $^{56}Fe$, $^{59}Co$, $^{60}Ni$, $^{63}Cu$, $^{66}Zn$, $^{71}Ga$, $^{74}Ge$, $^{75}As$, $^{82}Se$, $^{85}Rb$, $^{88}Sr$, $^{89}Y$, $^{90}Zr$, $^{93}Nb$, $^{98}Mb$, $^{101}Ru$, $^{103}Rh$, $^{104}Pd$, $^{105}Pd$, $^{107}Ag$, $^{111}Cd$, $^{115}In$, $^{118}Sn$, $^{121}Sb$, $^{133}Cs$, $^{138}Ba$, $^{139}La$, $^{140}Ce$, $^{141}Pr$, $^{142}Nd$, $^{152}Sm$, $^{153}Eu$, $^{157}Gd$, $^{159}Tb$, $^{163}Dy$, $^{165}Ho$, $^{166}Er$, $^{169}Tm$, $^{172}Yb$, $^{175}Lu$, $^{178}Hf$, $^{180}Hf$, $^{181}Ta$, $^{182}W$, $^{187}Re$, $^{193}Ir$, $^{195}Pt$, $^{197}Au$, $^{205}Tl$, $^{208}Pb$, $^{209}Bi$, $^{232}Th$ and $^{238}U$.

Since the first objective of this preliminary study was to identify the most discriminant elements, the use of CRMs with large number of analytes was required. As aluminum and tin CRM with such a high number of elements were not available in the laboratory, NIST glass series (NIST SRM 600 series) was used for calibration purpose. This non-matrix matched calibration must be considered as semiquantitative as laser-matter interactions depart significantly from conductive samples like metal to glass samples. Some authors have reported the use of the NIST glass series with some success for non-matrix-matched calibration of ilmenite ($FeTiO_3$) by femtosecond LA-ICPMS working at low energy density (3.27 $J \cdot cm^{-2}$) (16) and Bian et al. conclude that samples which are optically transparent for the laser wavelength need the application of high fluence whereas samples with relatively high thermal conductivity and low melting points require low fluence ablation (17).

CRM NIST 612 and 610 were then used for calibration, all calibration curves used showed correlation coefficients better than 0.995. Data was acquired as raw counts per second (cps) for 240 seconds. First, data was recorded for 20 seconds before the laser was fired to establish a background level. Then, the laser was fired for 200 seconds followed by 20 seconds time frame without firing to confirm that values returned to its blank values (Figure 3).

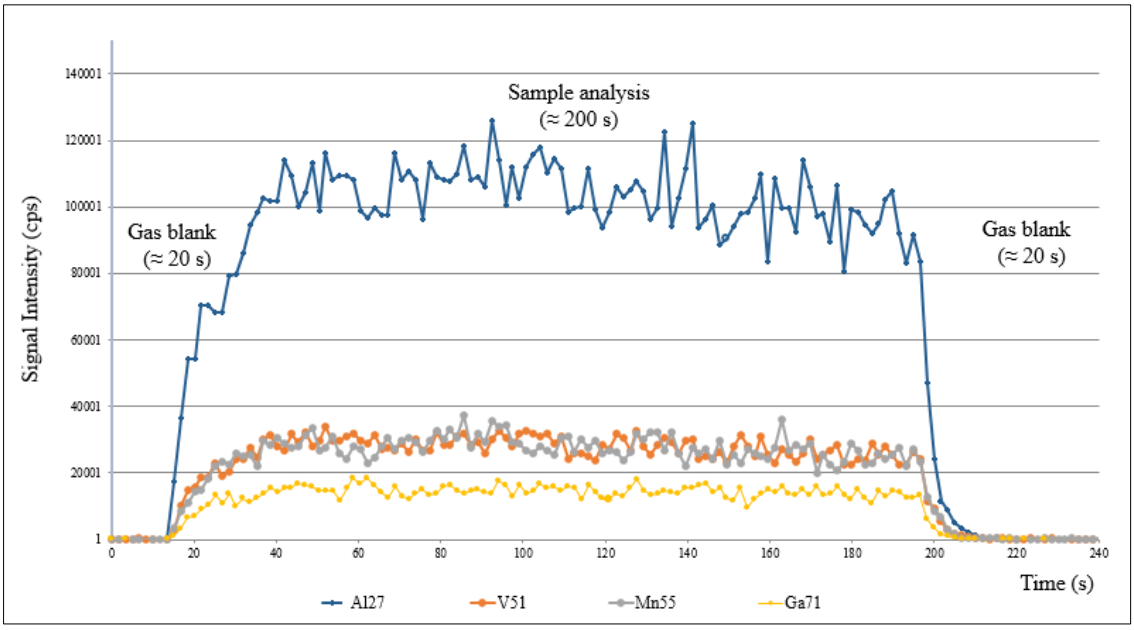


**Figure 3** A typical laser ablation signal for selected isotopes for capsule analysis.

Data preprocessing consisted of peak-area integration, background subtraction, and arranging the data in a form suitable for multivariate analysis. The baseline estimated by the average signal measured during the 20 s prior to the ablation was subtracted point by point from the signals measured for each isotope in the ablation peak. The intensity was after normalized relative to the intensity of the internal standard. As the use of aluminium is widespread for capsule manufacturing, $^{27}$Al was selected as an internal standard ($^{27}$Al, 100%). In order to avoid saturation of the detector Rpq and Rpa values from quadrupole mass filter were modified to attenuate the registered signal. Qualitative data can be used easily and effectively with all chemometrical and statistical interpretation techniques to achieve reliable conclusions. Therefore, in this study, interpretation is based on the comparison of the elemental ratios within a spectral profile. Only analytes giving count rates that were consistently above background signal (10 σ) were used for statistical data analysis.

17 capsules were analyzed which were randomly selected from the worldwide bottle collection, all of them red colored. Concretely, 13 capsules are European (9 French, 2 Spanish and 2 Italian) and 4 Asian (all Chinese). In this case, as bottles belonging to private collections are highly valuable and taking into account that a small sample must be cut from the capsule to make it fit into a close ablation cell, these bottles were not considered for this preliminary study.

## 3. Results and discussion

From the PCA derived from the statistical data analysis (XLSTAT ®, 2016), for which the same procedure as in the previous chapters has been followed for finding the most discriminant isotopes, it is possible to clearly distinguish the aluminium alloy and tin alloy capsules. It is a PCA model with two PCs explaining 99.04% of the variation in the data for the capsules, being the residuals < 1 for all the scores. The biplot (Figure 4) reveals that separation along PC1 accounts for the 83.49% of the variation in the sample set, while separation along PC2 accounts for the 14.55%.

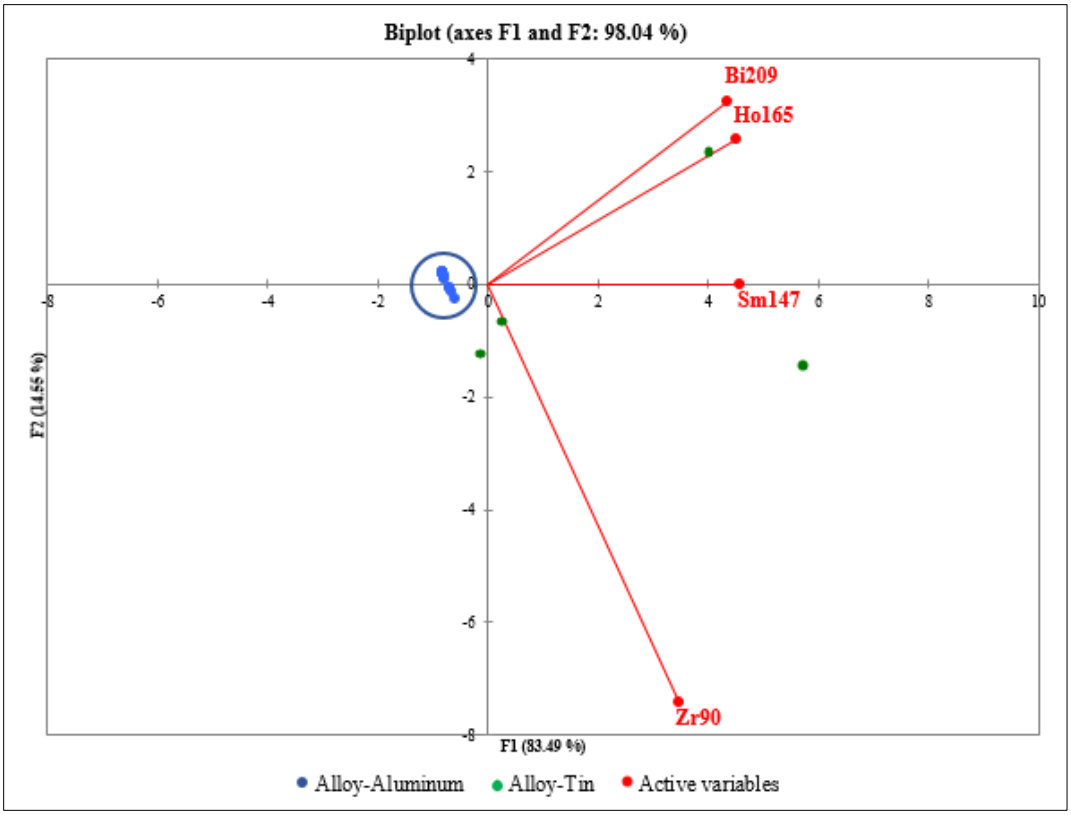


**Figure 4** Biplot (PC1 vs PC2) representing aluminum alloy capsules (in blue) and tin alloy capsules (in green) with the loadings (variables) responsible of such discrimination.

Therefore, taking into account that different alloy capsules can be discriminated, a further essay was done among aluminium capsules to discriminate them according to their origin. This approach was not performed in tin capsules due to the few analyzed samples. Figure 5 shows the biplot (PC1 vs. PC2) for aluminium capsules from different countries. PCA model with two PCs explains 91.65% of the variation in the data for the capsules, being the residuals < 1 for all the scores. Separation along PC1 accounts for the 69.38% of the variation in the sample set, while separation along PC2 accounts for the 22.26%. It can be concluded that Asian (China) and European capsules can be differentiated, being the dysprosium the most representative element

of the first group. Among European capsules (France, Spain and Italy) there is no differentiation, being zirconium and thallium the most significant elements for this group.

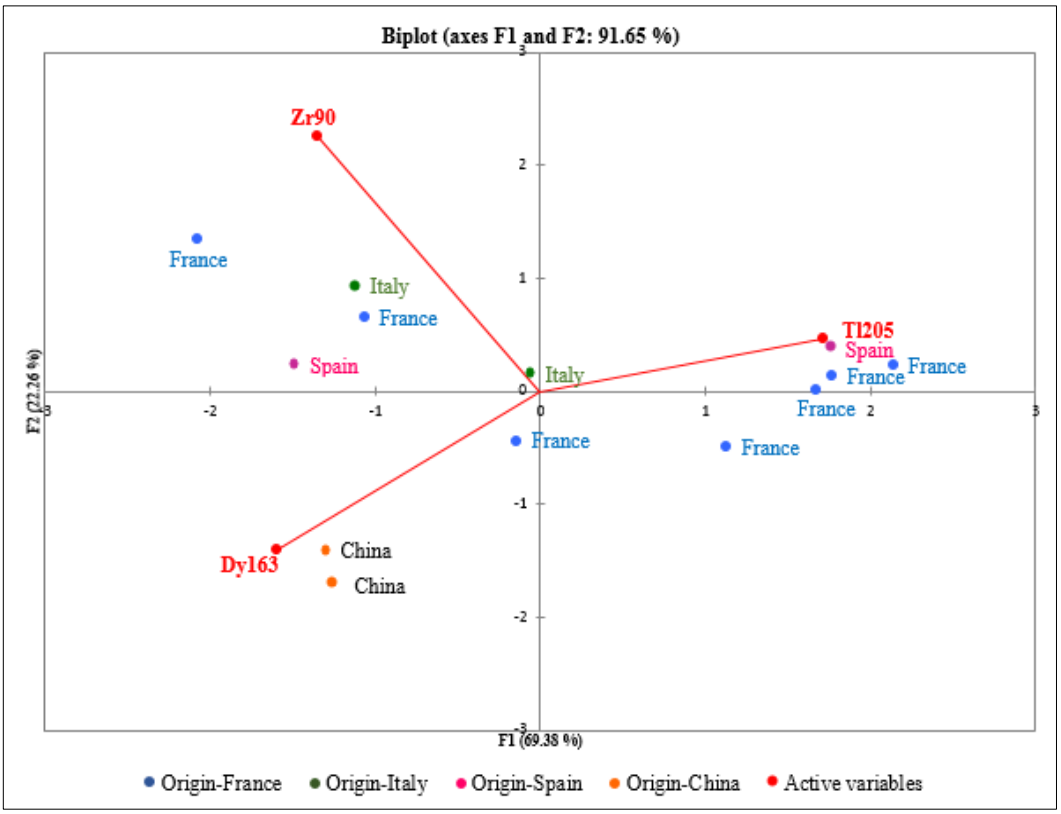


**Figure 5** Biplot (PC1 vs PC2) representing aluminum alloy capsules of different origin with the loadings (variables) responsible of such discrimination.

Similar approach was done with the red ink of aluminium alloy capsules. In this case, Asian capsules were distinguished from European capsules while among these last ones, there is no differentiation. In this case zinc and yttrium are the most discriminant isotopes for the Chinese capsules whereas for the European bottles nickel and rubidium are the most significant, being more significative for French bottles. Figure 6 shows the biplot (PC1 vs. PC2) for aluminium capsules from different countries. PCA model with two PCs explains 86.74% of the variation in the data for the capsules, being the residuals < 1 for all the scores. Separation along PC1 accounts for the 59.42% of the variation in the sample set, while separation along PC2 accounts for the 27.32%.

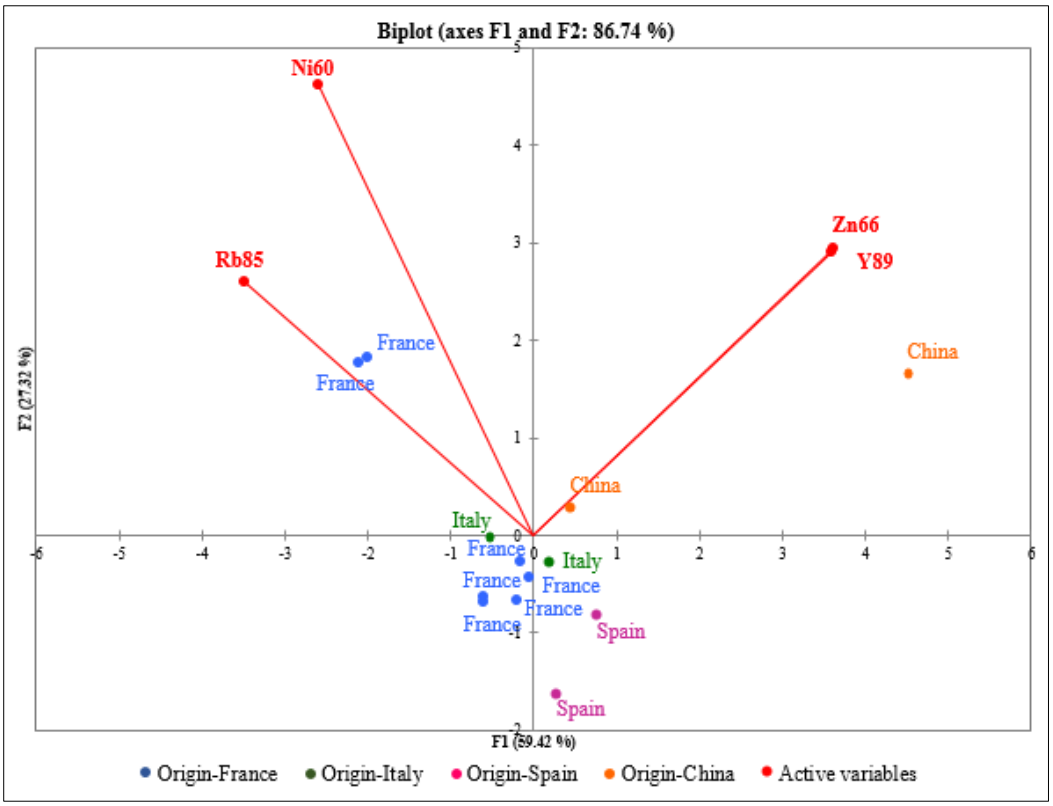


**Figure 6** Biplot (PC1 vs PC2) representing red ink of aluminum alloy capsules of different origin with the loadings (variables) responsible of such discrimination.

## 4. Conclusions

The preliminary results found for the analysis of the capsules show that this packaging element would be helpful together with the analysis of glass, paper and ink for wine authentication. The fast analysis by femtosecond laser ablation coupled to inductively coupled plasma mass spectrometry allows unequivocal discrimination of aluminium or tin based capsules and reveals a potential discrimination between capsules of different origin according to the continent. However, before stablish any tentative conclusions, the small number of samples per continent and even more the absence of three continents (America, Oceania and Africa), prevented the formulation of a definitive conclusion but was still sufficient to enable a preliminary assessment of the potential of this packaging element to classify bottles of wine according to their continent of origin.

It must be pointed out that even in some cases, polyethylene and polyethylene terephthalate (PET) can be added between two-layer aluminium foil, the analysis performed with the laser ablation would guarantee the surface analysis without reaching the plastic. In addition, if other plastics, such as polyvinyl chloride (PVC), are employed for entire manufacturing femtosecond LA/ICPMS would certainly provide valuable information, though it was not tested in this study. In case of capsule exclusively made of plastic, a complementary (or alternative) way of analysis

like Raman spectroscopy and Infrared spectroscopy would be of great interest as these techniques have shown to be very valuable tools for fast and simple material characterization .

Therefore, taking into account the fact that there are no bibliographical precedents on this topic, the initial results presented in this preliminary work are extremely encouraging and this sampling method shows considerable promise for rapid non-destructive sampling on metals and alloys, becoming a valuable new alternative tool to perform authentication and traceability analysis on wine and opening a new horizon based on the direct analysis of the packaging by the non-destructive technique of femtosecond laser ablation coupled to ICPMS. For this new research line, some points must be considered: 1) rapid verification of the capsule manufacturing material by portable Raman or Infrared spectroscopy, 2) synthesis of *homemade* calibration standards for accurate quantification of capsule components. This approach could be performed similarly to the development of paper and ink standards by using stock solutions and a commercial printer. Different printing materials (CDs, aluminum or tin foils) must be considered as well as the best printing option and 3) the development of a new ablation cell which would be capable to adapt somehow to the curvature of the bottleneck to avoid sample extraction and bottle damaging that could render the wine no longer storable and thus worthless for future resale.

## *5.* Bibliography


1. À quoi correspondent les capsules sur les bouchons de bouteilles d'alcool? Site officiel de l'admistration français, direction de l'informatio légale et administrative. 2016 [cited 17 August 2017]. Available from: https://www.service-public.fr/professionnels-entreprises/vosdroits/F33677.
2. de Almeida MR, Correa DN, Rocha WFC, Scafi FJO, Poppi RJ. Discrimination between authentic and counterfeit banknotes using Raman spectroscopy and PLS-DA with uncertainty estimation. Microchemical Journal. 2013;109:170-7.
3. Maguregui M, Knuutinen U, Trebolazabala J, Morillas H, Castro K, Martinez-Arkarazo I, et al. Use of in situ and confocal Raman spectroscopy to study the nature and distribution of carotenoids in brown patinas from a deteriorated wall painting in Marcus Lucretius House (Pompeii). Analytical and Bionalytical Chemistry. 2012;402(4):1529-39.
4. Nielsen SE, Scaffidi JP, Yezierski EJ. Detecting Art Forgeries: A Problem-Based Raman Spectroscopy Lab. Journal of Chemical Education. 2014;91(3):446-50.
5. Saverwyns S. Russian avant-garde… or not? A micro-Raman spectroscopy study of six paintings attributed to Liubov Popova. Journal of Raman Spectroscopy. 2010;41(11):1525-32.
6. Kaufmann A. Lead in wine. Food Additives and Contaminants. 1998;15(4):437-45.
7. Médina B, Guimberteau G, Sudraud P. Dosage du plomb dans les vins, une cause d'enrichissement : les capsules de surbouchage. Journal international des sciences de la vigne et du vin. 1977;11.
8. Gulson BL, Lee TH, Mizon KJ, Korsch MJ, Eschnauer HR. The Application of Lead Isotope Ratios to the Determine the Contribution of the Tin-Lead to the Lead Content of Wine. American Journal of Enology and Viticulture. 1992;43(2):180.
9. Kaufmann A. Lead in wine. Food Additives and Contaminants. 1998;15(4):437-45.
10. Médina B, Salagoïty M, Guyon F, Gaye J, Hubert P, Guillaume F, Using new analytical approaches to verify the origin of wine. In: New Analytical Approaches for Verifying the Origin of Food. Woodhead Publishing: Paul Brereton; 2013. p. 149-188.
11. Raith A, Hutton RC, Abell ID, Crighton J. Non-destructive sampling method of metals and alloys for laser ablation-inductively coupled plasma mass spectrometry. Journal of Analytical Atomic Spectrometry. 1995;10(9):591-4.
12. Koch J, Gunther D. Femtosecond laser ablation inductively coupled plasma mass spectrometry: achievements and remaining problems. Analytical and Bionalytical Chemistry. 2007;387(1):149-53.
13. Wiltsche H, Günther D. Capabilities of femtosecond laser ablation ICP-MS for the major, minor, and trace element analysis of high alloyed steels and super alloys. Analytical and Bioanalytical Chemistry. 2011;399(6):2167-74.

14. Gonzalez JJ, Liu C, Wen S, Mao X, Russo RE. Metal particles produced by laser ablation for ICP–MS measurements. Talanta. 2007;73(3):567-76.
15. Gonzalez JJ, Liu C, Wen S, Mao X, Russo RE. Glass particles produced by laser ablation for ICP-MS measurements. Talanta. 2007;73(3):577-82.
16. Li Z, Hu Z, Günther D, Zong K, Liu Y, Luo T, et al. Ablation Characteristic of Ilmenite using UV Nanosecond and Femtosecond Lasers: Implications for Non-Matrix-Matched Quantification. Geostandards and Geoanalytical Research. 2016;40(4):477-91.
17. Bian Q, Garcia CC, Koch J, Niemax K. Non-matrix matched calibration of major and minor concentrations of Zn and Cu in brass, aluminium and silicate glass using NIR femtosecond laser ablation inductively coupled plasma mass spectrometry. Journal of Analytical Atomic Spectrometry. 2006;21(2):187-91.

# ANNEX II:

# Scientific achievements

## PATENTS

Patent of new ablation cell (In progress) Authors: Christophe Pécheyran – Nagore Grijalba. Owner: Université de Pau et des Pays de l'Adour.

## ARTICLES*

Grijalba, N., Claverie, F., Donard, A., Tabouret, H., Pécheyran, C., Unceta, N., Goicolea, M.A., Barrio, R.J. Laser bidezko ablazioaren egungo egoera eta aplikazioak. *Ekaia* **31,** 50-65 (2017).

Already in preparation the articles concerning the analysis of glass by fsLA-ICPMS, the analysis of label matrix and printed ink by fsLA-ICPMS and the molecular analysis of paper and ink by Raman spectroscopy and Infrared spectroscopy for wine authentication.

* *The publication of scientific articles have been restricted by the patent acceptance process*

## PARTICIPATION IN INTERNATIONAL CONGRESSES

**Authors: Grijalba, N., Claverie, F., Médina, B., Unceta, N., Pécheyran, C.**

Title: Wine Counterfeiting: Non-destructive wine authentication via ultratrace spectrochemical analysis of bottles by fs-LAICPMS

Type of participation: Oral communication

Congress: EUROANALYSIS XVIII

Location: Bordeaux Country: France

Starting date: 06/09/2015 Closing date: 10/09/2015

Abstract: Grape growing and wine production have valuable economic activities and have had important consequences on culture and socio-economic development of many countries. Fine wines are prestigious and consequently, expensive business. Therefore, it is not surprising the appearance of an emerging market of fakes, mostly originating from Asian countries, which represents a huge yearly loss of income for wineries. Obviously, many safeguards have been established against trademark infringement but they generally require time-consuming chemical analysis of the wine and irremediably degrade the value of the bottle. Thus, the current study aims at developing a new and unambiguous diagnosis tool in the fight contrary to wine counterfeiting by the multifactorial trace analysis of the packaging (glass, paper, ink and capsule) with no or very limited degradation that would not alter the value of the bottle. For that purpose, non-invasive technology based on femtosecond laser ablation coupled with inductively coupled plasma mass spectrometry (fs-LA-ICP-MS) has been employed for the analysis of trace elements and isotopes in the different components of the packaging. Moreover, regarding to instrumentation engineering a new ablation cell adjustable to different bottle shapes has been successfully developed. This is an open ablation cell which is directly placed onto the sample surface allowing the minimization of the dead volume and increasing flexibility in sample size. The developed instrumentation and method was applied to the analysis of French and counterfeited bottles which made clear differences between them in terms of presence or absence of trace element, its concentration and isotopic distribution.

**Authors: Grijalba, N., Médina, B., Brü, N., Unceta, N., Pécheyran, C.**

Title: Contrefaçon des vins: authentification non destructive par analyses multifactorielles du contenant

Type of participation: Oral communication

Congress: SPECTR'ATOM 2016

Location: Pau Country: France

Starting date: 24/05/2016 Closing date: 27/05/2016

Abstract: Les grands vins, associés par certains à des produits de luxe empreints d'un terroir et d'un savoir faire millénaire, sont particulièrement exposés à la contrefaçon se développant notamment sur le marché asiatique. A l'échelle mondiale, la contrefaçon représente une perte financière de plusieurs milliards de dollars que les techniques antifraude (marquage par exemple) ne peuvent contenir. Actuellement, les techniques de détection de ces contrefaçons se fondent sur un prélèvement du liquide. Elles sont donc invasives, et impliquent le « sacrifice » d'un échantillon, ce qui peut s'avérer rédhibitoire quand il s'agit de vins de très grande valeur. Un nouvel outil de diagnostic irréfutable dans la lutte contre la contrefaçon de vins a été développé par notre équipe basé sur une analyse multifactorielle de l'emballage (verre, papier, encre et capsule), utilisant la technologie non invasive de l'ablation laser femtoseconde couplée à la spectrométrie de masse à plasma inductif (fs-LA-ICP-MS). Elle permet de mesurer les teneurs de 63 éléments traces (70 isotopes) dans les différents constituants de l'emballage. Cette technique induit très peu ou pas de dégradation qui pourrait modifier la valeur de la bouteille. Par ailleurs, une nouvelle cellule d'ablation ajustable aux différentes formes de bouteilles a également été développée. L'instrumentation et la méthode ont été appliquées à l'analyse de différentes bouteilles d'origine contrôlée et d'autres issues de la contrefaçon sur un échantillon de grands crus de différents pays (à voir). Les traitements statistiques basés sur des analyses multi variées (ACP, PLS, classement hiérarchique) permettent d'aboutir à une discrimination très nette des bouteilles contrefaites en isolant et hiérarchisant les éléments traces importants à l'origine de cette discrimination. Il a par ailleurs été possible de différencier la signature chimique des bouteilles selon leur origine (par pays).

**Authors: Grijalba, N., Médina, B., Unceta, N., Pécheyran, C.**

Title: On the warpath against counterfeiting: wine authentication through non-destructive analysis of bottles by fs-LA-ICPMS

Type of participation: Poster

Congress: EWLA 2016

Location: Ljubliana Country: Slovenia

Starting date: 12/07/2016 Closing date: 15/07/2016

Abstract: The great wines, related by some to luxury products linked to a *terroir* and a thousand-year knowledge, are particularly vulnerable to counterfeiting mostly originating from Asian market. The estimated financial loss is roughly a billion euros per year for the French wineries as a whole. Nowadays, counterfeited wine detection techniques are based on liquid sampling. They are therefore invasive techniques, requiring opening the bottle, which can be fateful when it comes to great value wines. Thus, a new irrefutable diagnostic tool has been developed based on ultratrace analysis of packaging (glass, paper, and ink) by non-invasive femtosecond laser ablation ICPMS, which induces no visible degradation of the bottle that could affect its value. It allows simultaneous monitoring of 63 trace elements (70 isotopes) in the different components of packaging. Moreover, regarding to instrumentation engineering, a new ablation cell adjustable to different bottle shapes has also been developed. It consists of an open ablation cell directly placed onto the bottle surface allowing fast wash-out times and increasing flexibility in sample size. NIST glass series was used for glass calibration, whereas for ink and paper matrix-matched standards were synthetized due to the lack of certified reference materials. This packaging characterization method was successfully applied to a large number of bottles (n>100) of controlled origin and bottles originating from other countries. Statistical data processing based on multivariate analysis (PCA, PLS, hierarchical classification) draw clear distinction between genuine and counterfeited bottles by isolating and prioritizing the most important trace elements. In addition, it was also possible to distinguish the chemical signature of bottles according to their origin country and vintage.

**Authors: Grijalba, N., Médina, B., Unceta, N., Pécheyran, C.**

Title: Autentificación de vinos a través del análisis no destructivo de las botellas for fsLA-ICPMS

Type of participation: Oral communication

Congress: WineTrack 2016

Location: Logroño Country: Spain

Starting date: 24/11/2016 Closing date: 24/11/2016

Abstract: Los grandes vinos están particularmente expuestos a su falsificación, principalmente procedente del mercado asiático. De hecho, según la Oficina de Propiedad Intelectual de la Unión Europea[1], las industrias legítimas pierden aproximadamente 1.300 millones de euros de ingresos anuales debido a la presencia de bebidas espirituosas (740 millones de euros) y vinos (530 millones de euros) falsos en el mercado de la UE y que representan el 3.3% de las ventas del sector. Hasta la actualidad, las técnicas para la detección de vino falsificado se basan en el muestreo del propio líquido. Por lo tanto, se trata de técnicas invasivas que requieren la apertura de la botella, lo que resulta inviable cuando se trata de vinos de gran valor. En esta ponencia se presenta el desarrollo de una nueva herramienta de diagnóstico irrefutable basada en el análisis de elementos presentes solamente en los envases (vidrio, papel y tinta) a nivel de ultratraza (p.e. Cr, Cu, Sc, Y, Gd, La) por ablación láser de femtosegundo acoplado a ICPMS, técnica que no induce degradación o alteración visible de la botella. Para ello ha sido necesario el desarrollo y diseño de una nueva cámara de ablación abierta que se adapta a las diferentes formas de las botellas. Las características de esta nueva cámara permiten tiempos de lavado rápidos y aumentando la flexibilidad en la superficie a muestrear. Este método para la caracterización del envase se ha aplicado con éxito a un gran número de botellas (n> 100) de origen controlado y botellas procedentes de otros países. El procesamiento estadístico de datos, basado en el análisis multivariante (PCA, PLS, clasificación jerárquica), establece una distinción clara entre las botellas originales y las falsificadas permitiendo aislar y priorizar los elementos más importantes. Además, también fue posible distinguir el perfil químico de las botellas de acuerdo a su país de origen y cosecha.

**Authors: Grijalba, N., Médina, B., Unceta, N., Pécheyran, C.**

Title: Wine authentication via fast and non-destructive analysis of packaging by fsLA-ICPMS

Type of participation: Oral communication

Congress: 40th OIV Congress

Location: Sofia Country: Bulgaria

Starting date: 29/05/2017 Closing date: 02/07/2017

Abstract: The knowledge of grape and wine is as old as the cultural history of mankind. Grape growing and wine production are valuable economic activities which represent an important economic activity in the frame of the total agricultural production. The great wines are a prime target for counterfeiters because of their brand value, mostly originating from the Asian market. In fact, according to the European Union Intellectual Property Office[1], the legitimate industries losses approximately €1.3 billion of revenue annually due to the presence of counterfeit spirits (€740 million) and wine (€530 million) in the EU marketplace, 3.3% of the sector's sales. Wine fraud may be categorized in several forms and anti-counterfeiting measures have shown lack of effectiveness. Unfortunately, invasive techniques are used for wine verification purposes which are mainly based on liquid sampling, requiring opening the bottle which can be fateful when it comes to great value wines. This work aims to develop a new unambiguous diagnostic tool based on ultratrace analysis of packaging (glass, paper, and ink) by non-invasive femtosecond laser ablation ICPMS, which induces no visible degradation of the bottle. In addition, regarding to instrumentation development, a new ablation cell adjustable to different bottle shapes has also been designed. Moreover, for the analysis of paper and ink and owing to the lack of certified reference materials, matrix-matched standards have been synthesized as external calibrators by using commercially available printer. This packaging characterization method was successfully applied to a large number of bottles (n>200) of controlled origin and bottles originating from other countries. Statistical data processing based on multivariate analysis (PCA, PLS, hierarchical classification) draw clear distinction between genuine and counterfeited bottles by isolating and prioritizing the most important trace elements. In addition, it was also possible to distinguish the chemical signature of bottles according to their origin country and vintage.

## COLLABORATION IN INTERNATIONAL CONGRESSES

**Authors: Pécheyran C., Claverie F., Donard, A., Tabouret, H., Bareille, G., Bérail, B., Barre, J., Baltron, O., Pointurier, F., Grijalba, N., Unceta, N., Aramendia, FM, Resano, M.**

Title: L'ablation Laser ICPMS: de l'élémentaire à l'isotopie, de l'environnement à la lutte contre la contrefaçon

Type of participation: Oral communication (Invited talk)

Congress: ISOTRACE 2017

Location: Clermont Ferrand Country: France

Starting date: 12/09/2017 Closing date: 14/09/2107

**Authors: Médina, B., Grijalba N., Epova, E., Péchyran, C., Donard, O.**

Title: Utilisation des éléments minéraux pour garantir l'authenticité et la traçabilité des vins

Type of participation: Oral communication

Congress: 15$^{e}$ matinée des oenologues de Bordeaux

Location: Bordeaux Country: France

Starting date: 14/04/2017 Closing date: 14/04/2017

**Authors: Pécheyran C., Claverie F., Donard, A., Grijalba, N.**

Title: Ablation laser et spectrométrie ICPMS : imagerie ultra trace et isotopie

Type of participation: Oral communication (Invited talk)

Congress: J'EXCEL 2016 – Les laser dans le monde analytique

Location: Lyon Country: France

Starting date: 24/11/2016 Closing date: 24/11/2016

**Authors: Pécheyran C., Claverie F., Barbotin, G., Donard, A., Pointurier, F., Grijalba, N., Unceta, N., Martin, L., Trobolo, C., Mercier, N.**

Title: Ablation laser et spectrométrie ICPMS : imagerie ultra trace et isotopie

Type of participation: Oral communication (Invited talk)

Congress: LIBS2016

Location: Chamonix Country: France

Starting date: 12/09/2016 Closing date: 16/09/2016

**Authors: Pécheyran C., Claverie F., Donard, A., Barbotin, G., Grijalba, N., Bareille, G., Tabouret, H., Pointurier, F., Hubert, A., Martin, L., Trobolo, C., Mercier, N.**

Title: Le 21eme siècle sera-t-il celui de l'ablation laser ?

Type of participation: Oral communication (Invited talk)

Congress: Spectr'Atom 2016

Location: Pau Country: France

Starting date: 24/05/2016 Closing date: 27/05/2016

**Authors: Médina, B., Epova, E., Bérail, S., Pécheyran, C., Grijalba, N., Donard, O.**

Title: Analyse multi-élémentaire, isotopique et ablation laser pour la traçabilité et l'authenticité des vins

Type of participation: Oral communication

Congress: XV Congreso Latino-Americano de Viticultura y Enología

Location: Bento Gonçalves Country: Brazil

Starting date: 03/11/2015 Closing date: 07/11/2015

**Authors: Claverie F., Donard, A., Hubert, A., Pointurier, F., Grijalba, N., Unceta, N., Becker, S., Pécheyran, C.**

Title: Advances in high repetition rate femtosecond laser ablation

Type of participation: Oral communication (Invited talk)

Congress: Scix 2015

Location: Providence Country: USA

Starting date: 27/09/2015 Closing date: 02/10/2015

# ANNEX III:

# Supplementary information

| | Element | LQ (ng·cm2) | Paper blank | | | LVL1 | | | LVL2 | | | LVL3 | | | LVL4 | | | LVL5 | | | LVL6 | | |
|---|---|---|---|---|---|---|---|---|---|---|---|---|---|---|---|---|---|---|---|---|---|---|---|
| | | | Measured printed conc. (ng·cm2) | RSD % (n=3) | Recovery (%) | Measured printed conc. (ng·cm2) | RSD % (n=3) | Recovery (%) | Measured printed conc. (ng·cm2) | RSD % (n=3) | Recovery (%) | Measured printed conc. (ng·cm2) | RSD % (n=3) | Recovery (%) | Measured printed conc. (ng·cm2) | RSD % (n=3) | Recovery (%) | Measured printed conc. (ng·cm2) | RSD % (n=3) | Recovery (%) | Measured printed conc. (ng·cm2) | RSD % (n=3) | Recovery (%) |
| CCS-1 | Ce | 7,90E-06 | 1,1 | 2,8 | * | 1,5 | 1,7 | 1205,6 | 2,9 | 0,6 | 586,4 | 7,3 | 0,2 | 235,5 | 18,2 | 1,0 | 145,3 | 0,0 | 65,0 | 0,1 | 0,1 | 1,9 | 0,1 |
| | Er | 6,90E-08 | <LQ | * | * | 1,1 | 1,7 | 872,0 | 2,5 | 0,3 | 500,9 | 6,8 | 0,4 | 219,2 | 17,3 | 1,4 | 138,7 | <LQ | * | * | <LQ | * | * |
| | Gd | 8,00E-07 | <LQ | * | * | 1,2 | 1,3 | 943,4 | 2,6 | 0,02 | 511,5 | 6,8 | 0,6 | 217,9 | 17,5 | 1,3 | 140,3 | <LQ | * | * | <LQ | * | * |
| | La | 5,00E-06 | 0,5 | 9,8 | * | 1,5 | 1,6 | 1176,9 | 2,9 | 1,1 | 578,2 | 7,3 | 0,6 | 233,9 | 17,9 | 1,1 | 142,9 | 0,0 | 0,6 | 0,1 | 0,0 | 3,7 | 0,1 |
| | Nd | 1,90E-05 | 0,5 | 6,9 | * | 1,4 | 2,8 | 1142,1 | 2,9 | 0,6 | 570,6 | 7,1 | 0,1 | 227,3 | 17,8 | 1,2 | 142,7 | 0,0 | 2,1 | 0,1 | 0,0 | 7,6 | 0,1 |
| | Sm | 1,30E-05 | <LQ | * | * | 1,1 | 2,6 | 919,8 | 2,5 | 0,3 | 504,5 | 6,7 | 0,3 | 215,7 | 17,3 | 1,2 | 138,1 | <LQ | * | * | <LQ | * | * |
| | Tb | 3,60E-06 | <LQ | * | * | 0,8 | 1,3 | 649,0 | 2,3 | 1,6 | 451,1 | 6,7 | 0,4 | 214,5 | 17,2 | 1,1 | 137,2 | <LQ | * | * | <LQ | * | * |
| | Tm | 4,10E-06 | <LQ | * | * | 0,8 | 1,4 | 627,5 | 2,2 | 1,0 | 4449,7 | 6,7 | 0,1 | 214,6 | 17,2 | 1,1 | 137,7 | <LQ | * | * | <LQ | * | * |
| | Yb | 9,60E-04 | <LQ | * | * | 1,1 | 0,6 | 855,5 | 2,5 | 1,1 | 499,8 | 6,8 | 0,3 | 217,8 | 17,0 | 1,1 | 136,1 | <LQ | * | * | <LQ | * | * |
| | Dy | 8,20E-04 | <LQ | * | * | 1,2 | 1,9 | 932,0 | 2,6 | 0,5 | 519,3 | 6,9 | 0,5 | 222,0 | 17,3 | 0,7 | 138,6 | <LQ | * | * | <LQ | * | * |
| | Eu | 9,10E-06 | <LQ | * | * | 0,9 | 1,9 | 719,9 | 2,3 | 1,5 | 463,9 | 6,6 | 0,6 | 212,7 | 17,1 | 0,9 | 136,4 | <LQ | * | * | <LQ | * | * |
| | Ho | 4,80E-06 | <LQ | * | * | 0,8 | 2,5 | 667,5 | 2,3 | 0,4 | 458,7 | 6,7 | 0,4 | 216,0 | 17,2 | 0,8 | 137,7 | <LQ | * | * | <LQ | * | * |
| | Lu | 1,30E-06 | <LQ | * | * | 0,8 | 2,4 | 652,5 | 2,3 | 0,7 | 455,3 | 6,7 | 0,8 | 215,9 | 17,1 | 1,0 | 137,2 | <LQ | * | * | <LQ | * | * |
| | Pr | 1,70E-06 | <LQ | * | * | 1,0 | 1,1 | 795,6 | 2,9 | 0,7 | 487,8 | 6,9 | 0,9 | 220,2 | 17,6 | 1,3 | 140,6 | <LQ | * | * | <LQ | * | * |
| | Sc | 6,40E-04 | 0,6 | 7,2 | * | 1,5 | 3,6 | 1214,8 | 3,4 | 4,3 | 677,1 | 6,9 | 0,6 | 220,2 | 11,9 | 2,7 | 94,9 | 0,5 | 21,2 | 2,1 | 0,5 | 12,3 | 0,8 |
| | Th | 2,80E-06 | <LQ | * | * | 0,9 | 2,4 | 708,3 | 2,3 | 0,3 | 461,7 | 6,7 | 0,3 | 215,3 | 16,7 | 1,3 | 133,3 | <LQ | * | * | <LQ | * | * |
| | U | 4,10E-06 | 1,6 | 3,6 | * | 1,5 | 0,3 | 1230,4 | 3,0 | 1,2 | 595,8 | 7,4 | 0,4 | 236,9 | 17,8 | 1,3 | 142,1 | 1,6 | 0,3 | 6,3 | 1,6 | 3,1 | 2,6 |
| | Yb | 1,50E-05 | 2,5 | 4,3 | * | 1,5 | 0,6 | 1222,7 | 3,0 | 0,0 | 598,7 | 7,5 | 0,4 | 239,0 | 13,9 | 0,4 | 111,3 | 0,1 | 0,4 | 0,3 | 0,1 | 2,4 | 0,1 |
| CCS-2 | Pt | 7,10E-05 | <LQ | * | * | <LQ | * | * | <LQ | * | * | 0,7 | 2,4 | 22,3 | 1,9 | 3,2 | 15,2 | <LQ | * | * | 11,7 | 3,1 | 18,9 |
| | Ir | 1,90E-04 | <LQ | * | * | <LQ | * | * | <LQ | * | * | 3,9 | 0,8 | 125,5 | 10,4 | 102,0 | 83,5 | <LQ | * | * | 17,4 | 3,2 | 53,6 |
| | Ru | 2,20E-05 | <LQ | * | * | <LQ | * | * | <LQ | * | * | 5,2 | 0,8 | 165,4 | 11,3 | 0,8 | 90,5 | <LQ | * | * | 10,8 | 2,9 | 17,14 |
| CCS-4 | Ba | 5,30E-05 | 34,2 | 1,3 | * | 0,2 | 1,1 | 151,0 | 4,9 | 0,2 | 986,7 | 4,3 | 1,7 | 136,9 | 23,2 | 1,5 | 185,6 | 26,3 | 1,5 | 105,2 | 66,1 | 3,3 | 106,5 |
| | Bi | 1,60E-05 | <LQ | * | * | <LQ | * | * | 3,8 | 0,2 | 750,1 | 3,4 | 6,2 | 108,5 | 12,7 | 1,4 | 101,7 | 23,8 | 1,1 | 95,2 | 61,2 | 3,4 | 98,7 |
| | Cs | 4,10E-06 | <LQ | * | * | <LQ | * | * | 4,5 | 0,4 | 896,3 | 3,8 | 6,4 | 121,6 | 15,3 | 1,3 | 122,4 | 27,2 | 0,7 | 108,8 | 68,9 | 3,0 | 111,2 |
| | In | 8,70E-06 | <LQ | * | * | <LQ | * | * | 4,1 | 14,7 | 812,3 | 4,1 | 5,7 | 130,3 | 13,7 | 1,1 | 109,7 | 26,5 | 0,8 | 106,1 | 66,8 | 3,6 | 107,7 |
| | Rb | 5,10E-05 | <LQ | * | * | <LQ | * | * | 5,0 | 1,5 | 1006,6 | 4,4 | 6,2 | 139,7 | 12,1 | 0,6 | 97,0 | 28,1 | 0,6 | 112,5 | 70,7 | 3,1 | 114,1 |
| | As | 2,60E-04 | <LQ | * | * | <LQ | * | * | 4,6 | 13,0 | 920,5 | 4,5 | 4,3 | 142,8 | 3,5 | 1,4 | 27,9 | 27,6 | 0,2 | 110,6 | 68,4 | 3,4 | 110,3 |
| | Be | 1,20E-04 | <LQ | * | * | <LQ | * | * | 4,1 | 11,4 | 817,3 | 4,1 | 5,9 | 131,6 | 10,4 | 3,1 | 83,5 | 27,2 | 0,5 | 108,7 | 69,4 | 2,8 | 111,9 |
| | Ga | 2,90E-05 | <LQ | * | * | <LQ | * | * | 4,4 | 13,8 | 872,9 | 4,4 | 5,0 | 140,5 | 10,0 | 0,9 | 80,8 | 26,0 | 0,6 | 104,1 | 65,5 | 2,9 | 105,7 |
| | Li | 6,90E-02 | <LQ | * | * | 0,1 | 23,9 | 42,7 | 4,6 | 14,5 | 925,0 | 4,8 | 5,7 | 150,3 | 10,0 | 3,2 | 80,2 | 28,0 | 0,9 | 112,1 | 71,0 | 3,4 | 114,5 |
| | Se | 2,50E-03 | <LQ | * | * | <LQ | * | | 5,4 | 14,0 | 1076,1 | 5,5 | 8,5 | 174,8 | 10,6 | 9,3 | 85,0 | 27,4 | 8,2 | 109,6 | 70,3 | 6,0 | 113,3 |
| CCS-5 | Sb | 3,40E+05 | <LQ | * | * | <LQ | * | * | <LQ | * | * | 6,6 | 3,3 | 212,6 | 14,1 | 1,5 | 112,8 | 26,2 | 1,2 | 104,7 | 68,6 | 2,7 | 110,6 |
| | Ge | 2,40E-04 | <LQ | * | * | <LQ | * | * | <LQ | * | * | 6,7 | 0,9 | 213,8 | 9,5 | 2,1 | 76,1 | 24,9 | 0,8 | 99,5 | 64,8 | 3,2 | 104,6 |
| | Mo | 3,20E-04 | 68,5 | 3,8 | * | <LQ | * | * | <LQ | * | * | 9,1 | 0,4 | 292,1 | 7,8 | 0,2 | 62,1 | 22,1 | 0,5 | 88,6 | 65,3 | 2,6 | 105,4 |
| | Ta | 6,50E-05 | <LQ | * | * | <LQ | * | * | <LQ | * | * | 1,0 | 12,8 | 32,1 | 1,3 | 13,3 | 10,0 | 4,1 | 6,4 | 16,5 | 13,2 | 4,9 | 21,3 |
| | Ti | 1,90E-04 | 31,1 | 3,7 | * | <LQ | * | * | <LQ | * | * | 5,8 | 3,0 | 186,1 | 7,0 | 6,2 | 55,7 | 23,5 | 1,3 | 93,9 | 62,7 | 0,8 | 101,1 |
| | Zr | 3,10E-05 | 1,7 | 4,6 | * | 0,1 | 5,3 | 80,3 | <LQ | * | * | 7,3 | 4,0 | 234,1 | 12,9 | 4,4 | 102,8 | 27,9 | 0,3 | 111,5 | 72,0 | 3,0 | 116,2 |
| | B | 6,80E-06 | 5,5 | 7,3 | * | 0,2 | 13,9 | 128,0 | 0,8 | 6,2 | 159,5 | 7,6 | 2,0 | 243,2 | 8,9 | 3,0 | 70,8 | 26,4 | 2,7 | 105,5 | 67,4 | 4,7 | 108,6 |
| | Hf | 1,14E-06 | <LQ | * | * | <LQ | * | * | <LQ | * | * | 1,2 | 2,0 | 38,0 | 14,9 | 1,8 | 119,5 | 6,8 | 0,8 | 27,0 | 18,7 | 3,3 | 30,2 |
| | Nb | 3,40E-05 | <LQ | * | * | <LQ | * | * | <LQ | * | * | 6,5 | 0,4 | 208,8 | 12,0 | 2,0 | 95,6 | 26,9 | 1,8 | 107,6 | 70,0 | 3,7 | 112,9 |
| | Sn | 3,90E-04 | <LQ | * | * | <LQ | * | * | <LQ | * | * | 7,2 | 8,4 | 230,1 | 14,1 | 3,1 | 112,6 | 26,5 | 1,4 | 105,9 | 68,7 | 5,3 | 110,8 |
| | W | 1,30E-04 | <LQ | * | * | <LQ | * | * | <LQ | * | * | 4,5 | 5,5 | 144,1 | 13,4 | 3,9 | 107,0 | 23,8 | 2,7 | 95,2 | 66,6 | 3,8 | 107,4 |